

Phosphite Catalysed Enantioselective Radical Reactions

by

Asish Bera
10CC17J26012

A thesis submitted to the
Academy of Scientific & Innovative Research
For the Award of the Degree of
DOCTOR OF PHILOSOPHY
in
SCIENCE

Under the supervision of
Dr. Pradip Maity



CSIR-National Chemical Laboratory, Pune



Academy of Scientific and Innovative Research
AcSIR Headquarters, CSIR-HRDC campus
Sector 19, Kamla Nehru Nagar,
Ghaziabad, U.P.–201 002, India
March-2023

Certificate

This is to certify that the work incorporated in this Ph.D. thesis entitled, “*Phosphite Catalysed Enantioselective Radical Reactions*”, submitted by *Asish Bera* to the Academy of Scientific and Innovative Research (AcSIR), in partial fulfillment of the requirements for the award of the Degree of *Doctor of Philosophy in Science*, embodies original research work carried-out by the student. We, further certify that this work has not been submitted to any other University or Institution in part or full for the award of any degree or diploma. Research material(s) obtained from other source(s) and used in this research work has/have been duly acknowledged in the thesis. Image(s), illustration(s), figure(s), table(s) etc., used in the thesis from other source(s), have also been duly cited and acknowledged.

Asish Bera

(Signature of Student)

Asish bera

Date: 16-02-2023

Pradip Maity

(Signature of Supervisor)

Supervisor: Dr. Pradip Maity

Date: 16-02-2023

STATEMENTS OF ACADEMIC INTEGRITY

I, Asish Bera a Ph.D. student of the Academy of Scientific and Innovative Research (AcSIR) with Registration No. 10CC17J26012 hereby undertake that, the thesis entitled “Phosphite Catalysed Enantioselective Radical Reactions” has been prepared by me and that the document reports original work carried out by me and is free of any plagiarism in compliance with the UGC Regulations on “*Promotion of Academic Integrity and Prevention of Plagiarism in Higher Educational Institutions (2018)*” and the CSIR Guidelines for “*Ethics in Research and in Governance (2020)*”.

Asish Bera

Signature of the Student

Date : 16-02-2023

Place : CSIR-NCL, Pune

It is hereby certified that the work done by the student, under my/our supervision, is plagiarism-free in accordance with the UGC Regulations on “*Promotion of Academic Integrity and Prevention of Plagiarism in Higher Educational Institutions (2018)*” and the CSIR Guidelines for “*Ethics in Research and in Governance (2020)*”.

NA

Signature of the Co-supervisor (if any)

Name :

Date :

Place :

Pradip Maity

Signature of the Supervisor

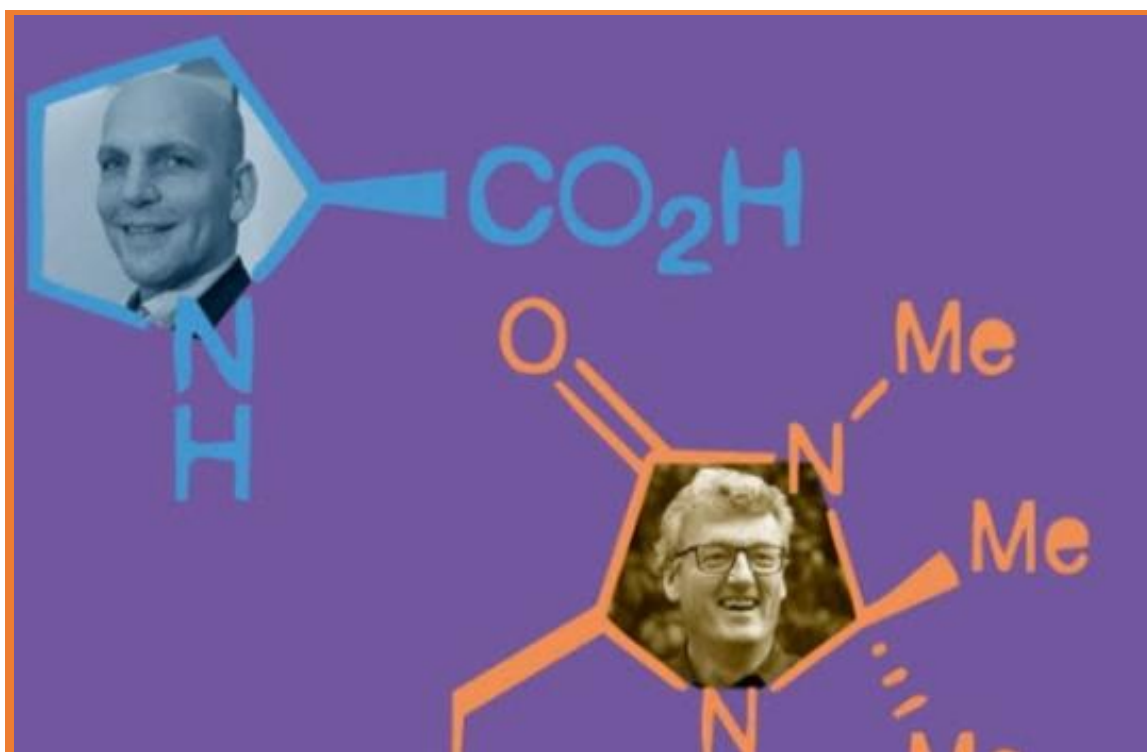
Name : Dr. Pradip Maity

Date : 16-02-2023

Place : CSIR-NCL, Pune

*Dedicated to
My All Respected Teachers, Beloved Family
Members & Bosom friends....*

“Making Molecules is Like Creating Something Beautiful”



Nobel Prize in Chemistry 2021: Asymmetric Organocatalysis

<https://www.chemistryworld.com/features/how-organocatalysis-won-the-nobel-prize/4014582.article>

ACKNOWLEDGEMENT

Once the moments come, I take this opportunity & try to do my best to extend my great appreciation to everyone who helped me scientifically and emotionally throughout my whole Ph. D journey.

First of all, I want to express my sincere gratitude to my research supervisor Dr. Pradip Maity. My heartfelt thanks go to him for introducing me to the wonders of scientific research, for his persistent guidance followed by encouragement, motivation, inspiration, scolding and support during every stage of my doctoral research work. Again I warmly thank him for his precious advice, analysis, criticism and discussions on my research work.

I would also like to sincerely thank my DAC members Dr. Utpal Das, Dr. J. Nithyanandhan, current DAC chairperson Dr. Benudhar punji and emeritus DAC chairperson Dr. E. Balaran for their constructive, innovative suggestion and logical comments throughout my Ph.D. work period at CSIR-NCL, Pune.

I extend my sincere thanks to the current and former Director of CSIR-NCL, Chair of Organic Chemistry Division (OCD) for their kind help and support during the course of this work. I must earnestly acknowledge Dr. Arup sir, Dr. Sakya sir, Dr. Sayan sir, Dr. Kinage sir, Dr. Paul sir, Dr. santhoshbabu sir, Dr. Dinesh sir, Dr. Asish sir and Dr. ramesh sir for their supports during my journey in NCL.

I am very grateful to UGC, New Delhi for economical support by providing fellowship to carry out my research work. I thank all the non-teaching staff of CSIR-NCL for their assistance on various occasions.

I wish to thank all my friendly and cooperative labmates Abdul, Nirshad, Chandrakant, Soniya, Subal, Ratnamala, Nilofar di, Moni, and piku for creating a cheerful and enjoyable working atmosphere in the lab. I would also like to thank project students Anu, Laxmi, Anirban, Debasish, Pratiksha, Sagar, Hariharan, upala, sandeep and Nikhil, who helped in various projects. Apart from, I would like to say thanks to my many new labmates, Abhishek, Devendra, Shekhar, Ashfaq, Rajesh, Ayantika, Arthika and susmita for spending such a beautiful time with them.

I am thankful to Suvendu, Debranjana, Subrata, Tapasda, Anirban (comrade), Tamal da, Subhrashis da, Abhijit da, Siba da, Manjur, Pranab da, Shanti da, Arunava da, Koushik, Indradweep, Joga da, Pankaj, Sutanu, Basudeb, Sanjukta, Pronay, Anagh, Sayantan, Moumita, Gargi, Naru, Rahul, Milan, lakshmi, Suryakant, Baliram, Amardipsing, Balasaheb (Balu), Madhukar, Priyanka (pinkie), Sagar, Nitin, Nitian (mama), Ambaji, Kailash and many others for their support. The moments spent with them will always cherish me and be remembered forever.

I would also like to thank to all my seniors Krishanu da, Atanu da, Anup da, Kheria da, Chini da, Arghya da, Ganesh via, Tarun via, koushik da, Munmun di, for their support during my tenure.

I would not forget Sujit (meso), Chotu (vipo), Bharat (mote), Subhas (mama), sankar da from HR-II, HR (IV) & GJ hostel to making the hostel premises special.

I am grateful to all my teachers and I expressed my gratitude for their encouragement in different part of my life. I thank the entire members of my family, and my friends for their constant care and wishes. Last but not least, I would like to pay high regards to my parents for their constant encouragement and inspiration.

Above all as well as blessing of Lord Krishna (ISKCON) granted me the wisdom, health, and strength to undertake this research task and enabled me to its completion.

-Asish Bera

List of Abrrivation

ACN : Acetonitrile
Ar : Aryl
Bn : Benzyl
bs : Broad singlet
t-Bu : Tertiary butyl
n-BuLi : n-Butyllithium
Cy : Cyclohexyl
CAT : Catalyst
d : Doublet
DABCO : 1,4-Diazabicyclo[2.2.2]octane
DBU : 1,8-Diazabicyclo 5.4.0 undec-7-ene
DCE : 1,2-Dichloroethane
DCM : Dichloromethane
dd : Doublet of doublet
DMHP : Dimethyl Hydrogenphosphite
DMSO : Dimethyl sulfoxide
dt : Doublet of triplet
ee : Enantiomeric excess
Et ₃ N : Triethyl amine
Et : Ethyl
g : gram(s)
h : hour(s)
HFIP : Hexafluoro-2-propanol
HOD: Head of the division
HPLC : High Performance Liquid Chromatography
HRMS : High-resolution mass spectrometry
Hz : Hertz
IR : Infrared
UV : Ultra violet

J : Coupling constant in NMR
LiHMDS : Lithium bis(trimethylsilyl)amide
LDA : Lithium diisopropylamide
KHMDS : Potassium bis(trimethylsilyl)amide
m : Multiplet
Me : Methyl
MeCN : Acetonitrile
min : Minute(s)
mp : Melting point
MTBE : Methyl tert-Butyl Ether
mL : Milliliter(s)
mmol : Millimole(s)
μM : Micromole(s)
μL : Microliter(s)
MW : Microwave
NMR : Nuclear magnetic resonance
Nu : Nucleophile
OCD : Organic Chemistry Division
ORTEP : Oak Ridge Thermal Ellipsoid Plot
Ph : Phenyl
ⁱ Pr : Isopropyl
q: Quartet
R _f : Retention factor
r.t. : Room temperature
S : Singlet
TADDOL : $\alpha,\alpha,\alpha',\alpha'$ -tetraaryl-2,2-disubstituted 1,3-dioxolane-4,5-dimethanol
THF : Tetrahydrofuran
TLC : Thin layer chromatography
tt : Triplet of triplet

Table of contents

Chapter 1

Introduction: Catalytic asymmetric functionalization of imine embedded in N-heteroaromatic compounds.....	1
1.1 Abstract.....	2
1.2 Introduction of Six-Member N-Heteroaromatics Containing α -Carbonyl/Alkyl Functional Unit	
1.2.A Occurrence.....	2
1.2. B A literature precedent Synthetic Approaches.....	9
1.2.B.1 Synthesis of Pyridone Derivatives: A Literature Review.....	9
1.2.B.2 Synthesis of Chiral Pyridines: A Literature Review.....	11
1.3 “Aza-acyl” anion and radical equivalent approach for umpolung imine functionalization:A literature review.....	16
1.3.A “Aza-acyl” anion equivalent approach: A literature review	16
1.3.B “Aza-acyl” radical equivalent approach: A literature review.....	19
1.4 Conclusion.....	22

Chapter 2

Preparation of chiral phosphites as nucleophilic organocatalysts.....	23
2.1 Abstract	24
2.2 Introduction.....	24
2.3 Background of phosphite catalysis.....	25
2.4 Result and discussion.....	28
2.5 Conclusion.....	33
2.6 Experimental procedure.....	34
2.7 Spectral Data.....	37
2.8 NMR spectra (^1H & ^{13}C).....	57
2.9 P^{31} NMR of phosphites.....	82

Chapter 3

Phosphite “aza-acyl” radical intermediate for catalyst-controlled aerobic oxidation of iminium ions..	90
3.1: Abstract.....	91
3.2 Introduction.....	91
3.3: General Research Goal.....	92
3.4 Preparation of Substrate.....	93
3.5: Screening of Catalyst.....	93
3.6: Result and Discussion.....	94
3.7 Oxidative Kinetic Resolution.....	98
3.8: Mechanistic Study and proposed Mechanism.....	98
3.9: One-Pot Synthesis of Lactam.....	100
3.10: Conclusion.....	104
3.11: Experimental Procedure.....	105
3.12 General Procedure for the Synthesis of Salts.....	107
3.13 Oxidation of salts.....	109
3.14: Compounds characterization data.....	113
3.15 NMR Spectra of Characterized Compounds.....	125
3.16 HPLC for oxidative kinetic resolution of 1m with chiral catalyst 9e.....	165

Chapter 4

Synthesis of chiral N-alkylpyridinium salts and their phosphite catalyzed oxidation and rearrangements.....	166
4.1 Abstract.....	167
4.2 Introduction.....	167
4.3 N-alkylpyridinium as alkyl source.....	169
4.4 Research Goal.....	171
4.5 Preparation of chiral amine.....	172
4.6 Preparation of Substrate.....	173
4.7 Oxidation of salt.....	177
4.8 Conclusion.....	178
4.9 Experimental Procedure.....	179
4.10 Compound Characterization Data.....	182
4.11 Spectral data.....	202
4.12 HPLC data.....	246

Chapter 5

Summary and Outlook.....	276
--------------------------	-----

.Synopsis Report



Synopsis of the Thesis was submitted to the Academy of Scientific and Innovative Research for Award of the Degree of Doctor of Philosophy in Chemical Science

Name of the Candidate	Mr. Asish Bera
Degree	Ph. D. in Chemical Science
Enrollment No. & Date	10CC17J26012; 1 st January, 2017
Laboratory	CSIR-National Chemical Laboratory (CSIR-NCL)
Title of the Thesis	Phosphite Catalysed Enantioselective Radical Reactions
Research Supervisor	Dr. Pradip Maity

1. Introduction:

The thesis title is "**Phosphite Catalysed Enantioselective Radical Reactions.**" The thesis describes our efforts to functionalize N-heteroaromatic compounds via nucleophilic phosphite organocatalysis. This thesis is organized into four different chapters. **The first chapter**, Part I, briefly describes the importance of N-heteroaromatic molecules having chiral pyridine, and pyridone moieties in their core structures and their literature-reported synthesis. In Part II, we discussed the "aza-acyl" anion and the radical equivalent approach for umpolung imine reactivity in nucleophilic catalysis. The last part chronicles the literature reporting phosphite catalysis. **In the second chapter**, we discussed the synthesis of chiral phosphite catalysts for the enantioselective functionalization of imines embedded in pyridines to explore the catalyst structure-activity relationship. **The third chapter** describes an auto-photo redox path with the combination of a phosphite catalyst and household light for imine-embedded pyridine oxidation via catalyst-bound "aza-acyl" radical equivalent. The catalyst bound to the radical intermediate led to catalyst control regioselectivity and kinetic resolution for the first time in the aerobic oxidation of iminium. **In chapter four**, we discussed the synthesis of both racemic and chiral amines for the preparation of racemic and chiral N-alkyl pyridinium salts. The enantiopurity of those salts was determined via their mild aerobic auto-oxidation developed in the third chapter. The chiral N-alkyl pyridinium salts were utilized for the phosphite-catalysed asymmetric N-to-C migration to synthesize chiral heterocycles from primary amines via both stereoretentive and enantioselective pathways.

2. Statement of the problem:

Given the importance of chiral pyridines¹ in drugs, APIs, and other bioactive molecules, chiral catalysts and ligands, and functional materials, we set out to establish a sustainable catalysis platform for their direct functionalization.

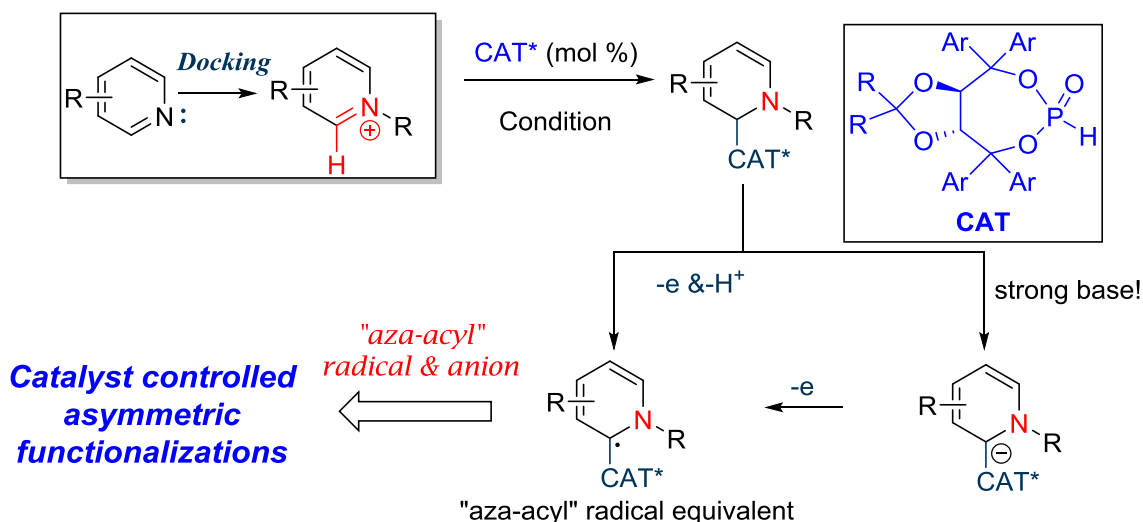
Although transition metal-catalyzed C-H functionalization found some recent successes,² only one single chiral Sc (III) catalyst was reported for pyridine C-H functionalization at the time of our beginning.³ Presumably, the electron-poor nature of pyridines, along with the strong coordinating power of pyridines to transition metal complicates the direct C-H functionalizations. On the other hand, although umpolung of C=O found great success with nucleophilic organocatalysts,⁴ the functionalization of C=N was not reported when we started. During our explorations, Biju and Suresh's group reported the first C=N umpolung functionalization with intramolecular electrophiles.⁵ Subsequently, a few other highly specific imine umpolung via NHC have recently been reported.⁶ But none of these approaches are applied to the functionalization of pyridines.

The radical functionalization of C=N embedded in N-heteroaromatic compounds was known for decades (minisci reaction),⁷ which was realized asymmetrically very recently for specific electrophiles only.

Hence, the development of a general sustainable catalytic system for the umpolung of imine embedded in pyridines remains an unmet challenge for the synthesis of N-heterocyclic compounds. We sought to establish a catalyst that could facilitate both ionic and radical functionalization for complementary and broad functionalizations.

3. Objective:

We sought to find a nucleophile catalyst that could add to the imine or iminium embedded in pyridines to form a catalyst-substrate adduct that could lead to the "aza-acyl" radical and anion equivalents. Since the imine or iminium in pyridinium salt is part of an aromatic system, it is more stable than acyclic imine or iminium. The nucleophilic adduct would form at the cost of aromaticity. Therefore, the nucleophilicity of the catalyst was crucial. We also wanted the catalyst to stabilize both the radical and anion formed in the proposed "aza-acyl" intermediate (Scheme 1). Our initial screening with most of the known nucleophile catalyst types with stable N-alkyl pyridinium salts failed to satisfy all the requirements. Our search for a suitable nucleophilic organocatalyst led us to establish organophosphites as a successful catalyst. Since we focused on the asymmetric functionalization of pyridines, we set out to synthesize stable chiral organophosphites first and then use those catalysts for asymmetric transformations of pyridine derivatives.

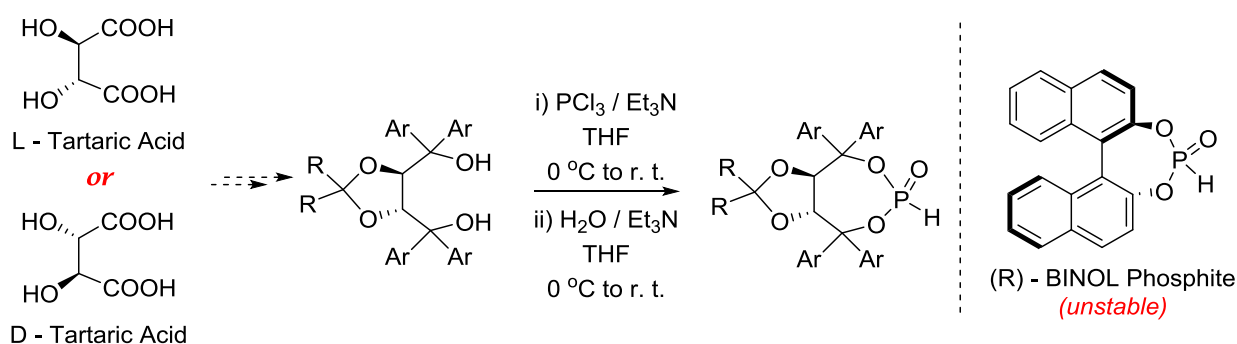


Scheme 1: Nucleophilic catalyst controlled radical reactivity for Asymmetric transformation

4. Methodology & Results:

Chapter 2: Preparation of chiral phosphites as nucleophilic organocatalysts

Our understanding and initial screening suggest phosphite could be a suitable nucleophilic catalyst. We started the preparation of chiral phosphite catalysts using different chiral scaffolds reported in the literature.⁸ We initially chose to synthesize chiral BINOL-based phosphites since BINOLs are privileged chiral backbones for asymmetric induction and are easy to access.⁹ The corresponding phosphites turned out to be labile and hydrolyze easily under the isolation, storage, and reaction conditions in our hands. We then focused on the synthesis of TADDOL-based chiral phosphites since those are reported for catalysis and started with tartaric acid as the inexpensive natural chiral source.¹⁰ We reoptimize the reaction sequence to synthesize numerous known and new chiral phosphites (Scheme 2) and set to use them for the asymmetric functionalization of pyridines.

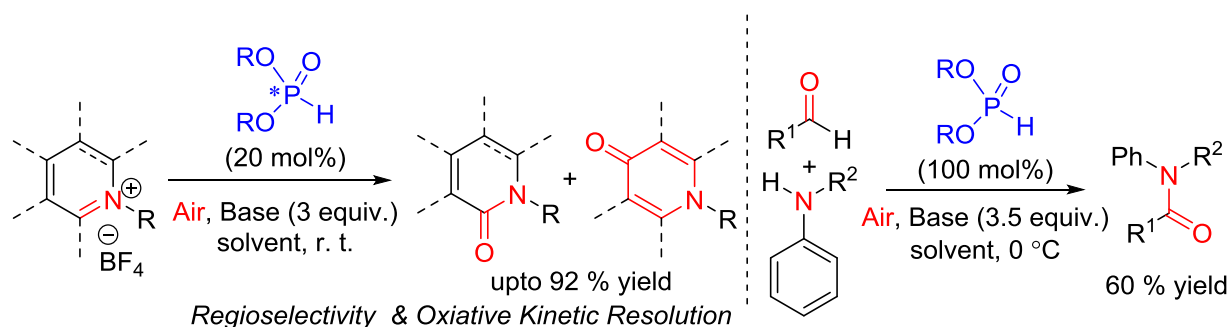


Scheme 2: Preparation of chiral phosphite catalysts

Chapter 3: Phosphite “aza-acyl” radical intermediate for catalyst-controlled aerobic oxidation of iminium ions

Here, we developed an organocatalyst bound α -aminoalkyl radical approach for the aerobic oxidation of pyridinium and iminium without any external radical-generating catalyst. N-Alkyl

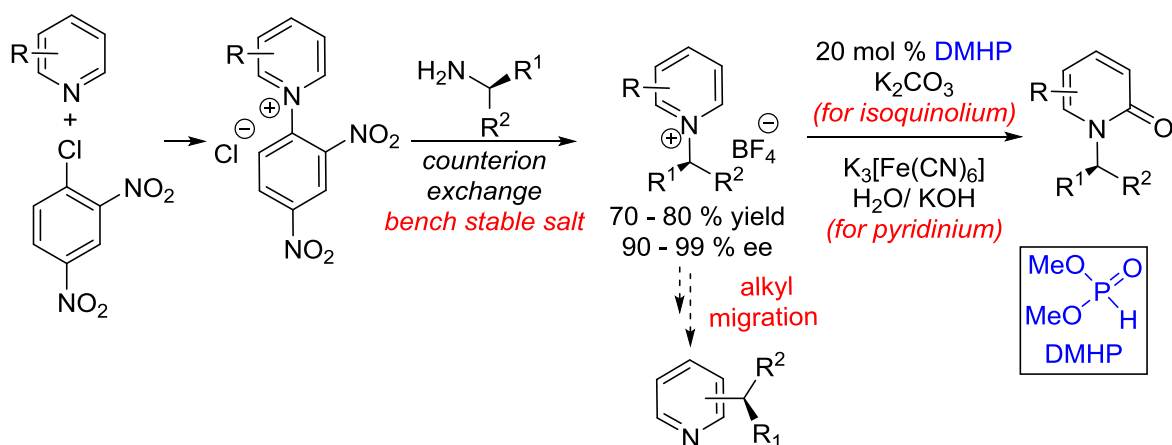
salts of a variety of heteroaromatic compounds were oxidized successfully in the presence of household light (Scheme 3). The regioselective catalyst addition to pyridinium led to regioselective pyridone formation. The catalyst bound α -radical was utilized successfully for an unprecedented oxidative kinetic resolution with racemic isoquinolinium salts with chiral phosphite catalysts synthesized. Cyclic and acyclic iminium salts were oxidized via a strong alternative base-mediated aerobic auto-oxidation. The strong base method presumably formed the "aza-acyl" anion equivalent first and, consequently, the corresponding radical for its aerobic oxidation. Although this reaction was performed with stoichiometric phosphite, it has the potential to be used as a sub-stoichiometric catalyst.



Scheme 3: Phosphite-catalysed controlled aerobic oxidation of iminium ions

Chapter 4: Synthesis of N-alkylpyridinium salts and their phosphite-catalysed oxidation and rearrangements

This chapter describes the synthesis of chiral and achiral primary amines and their corresponding pyridinium salts. The pyridinium salt synthesis was modified to achieve chiral pyridinium salts without the racemization of chiral amines. The enantioselectivities of both primary amines and their corresponding pyridinium salts were determined. The enantiomeric excess of pyridinium salts was not reported, and we failed to find a suitable chiral HPLC method to separate enantiomers. We utilized our phosphite-catalyzed aerobic auto-oxidation for the synthesis of corresponding pyridines. The mild reaction condition avoids any racemizations during the oxidation, and the determination of enantiomeric excess of corresponding pyridones provides us with the % ee of starting N-alkyl pyridines. These N-alkyl pyridines were used for achiral phosphite-catalysed stereoretentive chiral pyridines from the chiral amine-derived salts, as well as chiral phosphite-catalysed asymmetric pyridine synthesis from racemic N-alkyl pyridinium salts.



Scheme-4: Synthesis of chiral and achiral primary amines, corresponding pyridinium salts & their oxidation

5. Conclusions & future direction:

In conclusion, the thesis describes the synthesis of BINOL and TADDOL-based chiral phosphites. These chiral phosphites were successfully utilized for the radical and anionic functionalizations of N-alkylpyridinium salts. The work established an organocatalytic activation of C=N embedded in pyridine via “aza-acyl” radical and anionic pathways. The screening of chiral phosphites synthesized led to moderate to high enantioselection. I believe the establishment of phosphite-catalyzed radical and anion paths for pyridine functionalization has the potential for broader applications.

6. References:

- ¹ Forbis, R. M.; Jr. Rinehart, K. L. *J. Am. Chem. Soc.*, **1973**, *95*, 5003.; Claassen, G.; Brin, E.; Crogan-Grundy, C.; Vaillancourt, M. T.; Zhang, H. Z.; Cai, S. X.; Drewe, J.; Tseng, B.; Kasibhatla, S. *Cancer Lett.*, **2009**, *274*, 243.; Ramanathan, S.; Mathias, A. A.; German, P.; Kearney, P. B.; *Clin. Pharmacokinet.*, **2011**, *50*, 229.; McTavish, D.; Sorkin, E. M. *Azelastine. Drugs*, **1989**, *38*, 778.; Vitaku, E.; Smith, T. D.; Njardarson, T. J. *J. Med. Chem.* **2014**, *57*, 10257.; S. Varga, P. Angyal, G. Martin, O. Egyed, T. Holczbauer and T. Soos, *Angew. Chem., Int. Ed.*, **2020**, *59*, 13547.; L. Mengozzi, L.; Gualandi, A.; Cozzi, G. P. *Chem. Sci.* **2014**, *5*, 3915.
- ² Maryanoff, B. E.; Zhang, H.-C.; Cohen, J. H.; Turchi, I. J.; Maryanoff, C. A. *Chem. Rev.* **2004**, *104*, 1431-1628.; V Farina, V.; Reeves, J. T.; Senanayake, C. H.; J. Song, J. J. *Chem. Rev.*, **2006**, *106*, 2734-2793.; Baumann, M.; Baxendale, I. R. *Beilstein J. Org. Chem.*, **2013**, *9*, 2265-2319.; Li, L.; Wang, C.-Y.; Huang, R.; Biscoe, M. R. *Nat. Chem.* **2013**, *5*, 607-612.
- ³ Song, G.; O, W. W. N.; Hou, Z. *J. Am. Chem. Soc.* **2014**, *136*, 12209-12212.

- ⁴ Linghu, X.; Potnick, R. J.; Johnson, S. J. *J. Am. Chem. Soc.* **2004**, *126*, 3070.; Garrett, R. M.; Tarr, C. J.; Johnson, S. J. *J. Am. Chem. Soc.* **2007**, *129*, 12944-12945.; Nahm, R. M.; Linghu, X.; Potnick, R. J.; Yates, M. C.; White, S. P.; Johnson, S. J. *Angew. Chem. Int. Ed.* **2005**, *44*, 2377-2379; Nahm, R. M.; Potnick, R. J.; White, S. P.; Johnson, S. J. *J. Am. Chem. Soc.* **2006**, *128*, 2751-2756.; White, A. N.; Rovis, T. *J. Am. Chem. Soc.* **2014**, *136*, 14674-14677.
- ⁵ Patra, A.; Mukherjee, S.; Das, K. T.; Jain, S.; Gonnade, G. R.; Biju, T. A. *Angew. Chem. Int. Ed.* **2017**, *56*, 2730-2734.; Harish, B.; Subbireddy, M.; Suresh, S. *Chem. Commun.* **2017**, *53*, 3338-3341.
- ⁶ Akulov, A. A.; Varaksin, V. M.; Charushin, N. V.; Chupakhin, N. O. *Russ. Chem. Rev.* **2021**, *90*, 374-394.; Wang, G.; Zhang, C. Q.; Wei, C.; Zhang, Y.; Zhang, L.; Huang, J.; Wei, D.; Fu, Z.; Huang, W.; *Angew. Chem. Int. Ed.* **2021**, *60*, 7913-7919.; Yang, X.; Xie, Y.; Xu, J.; Ren, S.; Mondal, B.; Zhou, L.; Tian, W.; Zhang, X.; Hao, L.; Jin, Z.; Chi, R. Y. *Angew. Chem. Int. Ed.* **2021**, *60*, 7906-7912.; T. Wu, M. R. Tatton, M. F. Greaney, *Angew. Chem. Int. Ed.* **2022**, *61*, e202117524.
- ⁷ Jack, J. L. "Minisci reaction". **2009**, 361–362. DOI: 10.1007/978-3-642-01053-8_163.
- ⁸ Pizzano, A. *Chem. Rec.* **2016**, *16*, 2599–2622.; Alexakis, A.; Burton, J.; Vastra, J.; Benhaim, C.; Fournioux, X.; Heuvel, V. D. A.; Leveque, J.; Maze, R. F.; Rosset, S. *Eur. J. Org. Chem.* **2000**, 4011-4027.
- ⁹ Parmar, D.; Sugiono, E.; Raja, S.; Rueping, M. *Chem. Rev.* **2014**, *114*, 9047–9153.
- ¹⁰ Linghu, X.; Potnick, R. J.; Johnson, S. J. *J. Am. Chem. Soc.* **2004**, *126*, 3070-3071.

7. Publications & patents:

1. Motaleb, A.; **Bera, A.**; Maity, P. *Org. Biomol. Chem.* **2018**, *16*, 5081
2. Rani, S.; Dash, R. S.; **Bera, A.**; Alam, N. M.; Vanka, K.; Maity P. *Chem. Sci.* **2021**, *12*, 8996
3. A catalyst bound α -radical and synthesis of oxo compound using the same. A. Motaleb, **A. Bera**, P. Maity. *PCT/IN2018/05013*.
4. Phosphite-mediated asymmetric N to C migration for the synthesis of chiral heterocycles from primary amines. S. Rani, **A. Bera**, P. Maity. Patent filed

Asish Bera

Asish Bera

Student Name and signature

Dr. Pradip Maity (Supervisor)

Pradip Maity

Dr. Pradip Maity

Guide Name and Signature

Asish Bera (Candidate)

Chapter 1

Introduction:

Catalytic asymmetric functionalization of imine
embedded in N-heteroaromatic compounds

1.1 Abstract

Here in Part I, we briefly describe the importance of N-heteroaromatic molecules having chiral pyridine, and pyridone moieties in their core structures and their literature-reported synthesis (sections 1.1 and 1.2). In Part II, we discussed the "aza-acyl" anion and the radical equivalent approach for umpolung imine reactivity in nucleophilic catalysis (section 1.3).

1.2 Introduction of Six-Member N-Heteroaromatics Containing α -Carbonyl/Alkyl Functional Unit

Nitrogen is prevalent in >80% of FDA-approved drugs and pharmaceuticals. Among them, six-membered amino cycles piperidine and pyridines are respectively number one and two among heterocyclic scaffolds present in FDA-approved drugs.¹ Its polarity, basicity, and ability to form H-bonding are pivotal for desirable medicinal properties. Substituted pyridones and (thio)pyridones also exist widely in other bioactive molecules,² agrochemicals, and functional materials. Among those, chiral amino cycles are becoming important features for bioactive and functional materials. For example, a 2006 survey found 56% of all drugs used are chiral and a vast majority of newly approved drugs are single enantiomers of the chiral molecules. The nitrogen and N-oxide of chiral heteroarene also found widespread use as organocatalysts and ligands to transition metals and Lewis acids.³ Therefore, the enantioselective generation of chiral centers around nitrogen has received significant interest from chemists in recent times.

1.2.A Occurrence

Among different N-heterocyclic scaffolds, Pyridone, Isoquinolone, quinolone, and phthalazinone scaffolds are common structural motifs found in natural products and synthetic bioactive molecules. For instance, isoquinolone has been shown to exhibit melatonergic,⁴ antitumor,⁵ antimetastasis,⁶ antivirulence,⁷ anti-inflammatory,⁸ JNK,⁹ and topoisomerase I

¹Chrzanowska, M.; Grajewska, A.; Rozwadowska, M. D. *Chem. Rev.*, **2016**, *116*, 12369-12465.

²Ahmed, A.; Daneshtalab, M. *J. Pharm. Pharmaceut. Sci.*, **2012**, *15*, 52-72.

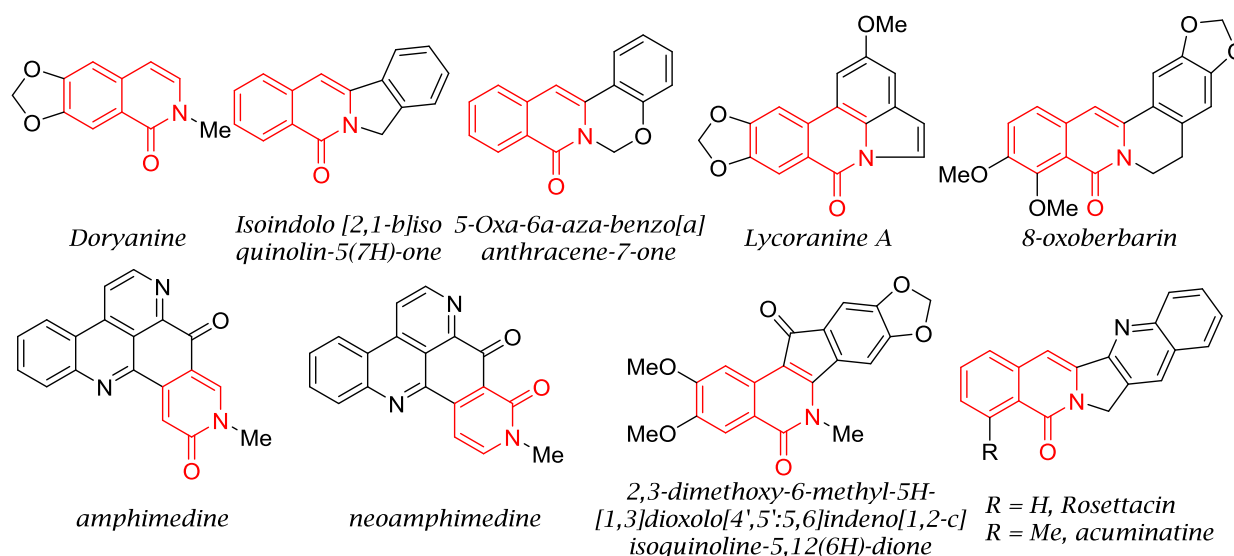
³Vitaku, E.; Smith, D. T.; Njardarson, T. *J. Med. Chem.* **2014**, *57*, 10257-10274, C. Giorgio.; *Chem. Soc. Rev.*, **2006**, *35*, 1230-1243)

⁴Hu, Y.; Chan, H. K.; He, X.; Ho, C. K. M.; Wong, H. Y. *PLoS One*, **2014**, *9*, e113638.

⁵Khadka, B. D.; Cho, J. W. *Bioorg. Med. Chem.*, **2011**, *19*, 724.

⁶Francis, S.; Croft, D.; Schüttelkopf, W. A.; Parry, C.; Pugliese, A.; Cameron, K.; Claydon, S.; Drysdale, M.; Gardner, C.; Gohlke, A.; Goodwin, G.; Gray, H. C.; Konczal, J.; McDonald,

(Top I) inhibitor's activities.¹⁰ The alkaloids doryamine and sarcomejine, containing isoquinolone skeleton, have been isolated from *Cryptocarya chinensis* (Lauraceae) and *Sarcomelicope megistophylla* (Rutaceae) respectively.¹¹



Pyridone or Isoquinolone Natural Products and Alkaloids Motif

L.; Mezna, M.; Pannifer, A.; Paul, R. N.; Machesky, L.; McKinnon, H.; Bower, J. *Bioorg. Med. Chem. Lett.*, **2019**, 29, 1023.

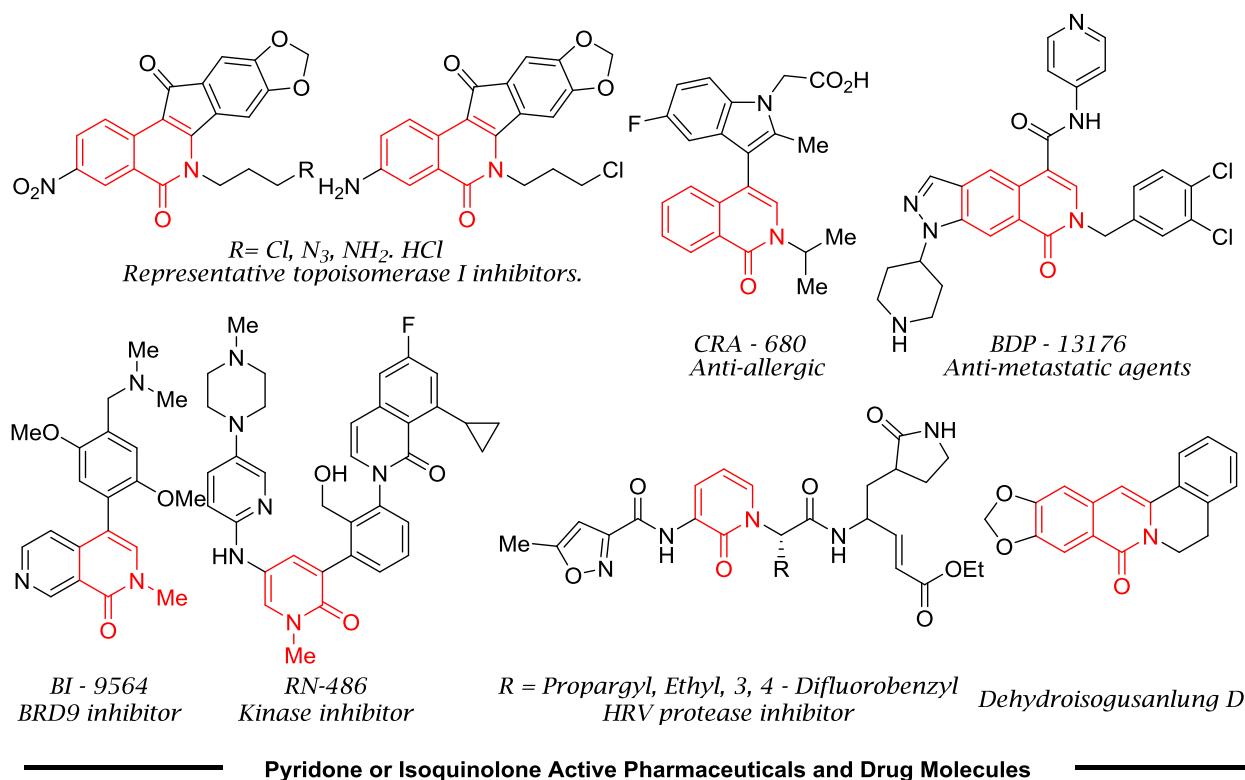
⁷Jarvis, C.; Han, Z.; Kalas, V.; Klein, R.; Pinkner, S. J.; Ford, B.; Binkley, J.; Cusumano, K. C.; Cusumano, Z.; MydockMcGrane, L.; Hultgren, J.; Janetka, W. *J. Chem. Med. Chem.*, **2016**, 11, 367.

⁸Kaila, N.; Follows, B.; Leung, L.; Thomason, J.; Huang, A.; Moretto, A.; Janz, K.; Lowe, M.; Mansour, S. T.; Hubeau, C.; Page, K.; Morgan, P.; Fish, S.; Xu, X.; Williams, C.; Saiah, E. *J. Med. Chem.*, **2014**, 57, 1299.

⁹Asano, A.; Kitamura, S.; Ohra, T.; Itoh, F.; Kajino, M.; Tamura, T.; Kaneko, M.; Ikeda, S.; Igata, H.; Kawamoto, T.; Sogabe, S.; Tanaka, T.; Yamaguchi, M.; Kimura, H.; Fukumoto, S. *Bioorg. Med. Chem.*, **2008**, 16, 4699.

¹⁰Morrell, A.; Antony, S.; Pommier, Y.; Cushman, M. *J. Med. Chem.*, **2006**, 49, 7740.; MyVan, T. H.; Cho, J. W. *Bioorg. Med. Chem.*, **2009**, 19, 2551.; Glushkov, V. A.; Shklyayev, Y. V. *Chem. Heterocycl. Compd.* **2001**, 37, 663.

¹¹Fokialakis, N.; Magiatis, P.; Skaltsounis, L. A.; Tillequin, F.; S'évenet, T. *J. Nat. Prod.*, **2000**, 63, 1004.; Wu, S. T.; Lin, W. F. *J. Nat. Prod.*, **2001**, 64, 1404.; Mitaku, S.; Fokialakis, N.; Magiatis, P.; Tillequin, F. *Fitoterapia*, **2007**, 78, 169.; Coombes, H. P.; Mwangi, M. E.; Peters, K. B.; Crouch, R. N.; Mulholland, A. D. *Biochem. Syst. Ecol.*, **2009**, 37, 494.; Cho, -Y. J.; Bae, -H. S.; Kim, -K. H.; Lee, -L. M.; Choi, -S. Y.; Jin, -R. B.; Lee, J. H.; Jeong, Y. H.; Lee, G. Y.; Moon, -H. J. *J. Agric. Food Chem.*, **2015**, 63, 3587.



Scheme 1.1: Biological active isoquinolone scaffold having common Pyridone motif

On the other hand, quinolone shows anticancer,¹² antibiotic,¹³ antiviral, and antihypertensive activities. They are used as cannabinoid CB2 receptor inverse agonists¹⁴, neuronal maxi-K channel activators,¹⁵ and AMPA/kainate and glycine antagonists.¹⁶ Elvitegravir (EVG), which contains the elementary unit of the corresponding quinolone, is a potent inhibitor of human immunodeficiency virus type 1 (HIV-1) integrase.¹⁷

¹²Claassen, G.; Brin, E.; Crogan-Grundy, C.; Vaillancourt, M. T.; Zhang, H. Z.; Cai, S. X.; Drewe, J.; Tseng, B.; Kasibhatla, S. *Cancer Lett.*, **2009**, 274, 243.; Ni, Z.-J.; Barsanti, P.; Brammeier, N.; Diebes, A.; Poon, D. J.; Ng, S.; Pecchi, S.; Pfister, K.; Renhowe, P. A.; Ramurthy, S.; Wagman, A. S.; Bussiere, D. E.; Le, V.; Zhou, Y.; Jansen, J. M.; Ma, S.; Gesner, T. G. *Bioorg. Med. Chem. Lett.*, **2006**, 16, 3121.

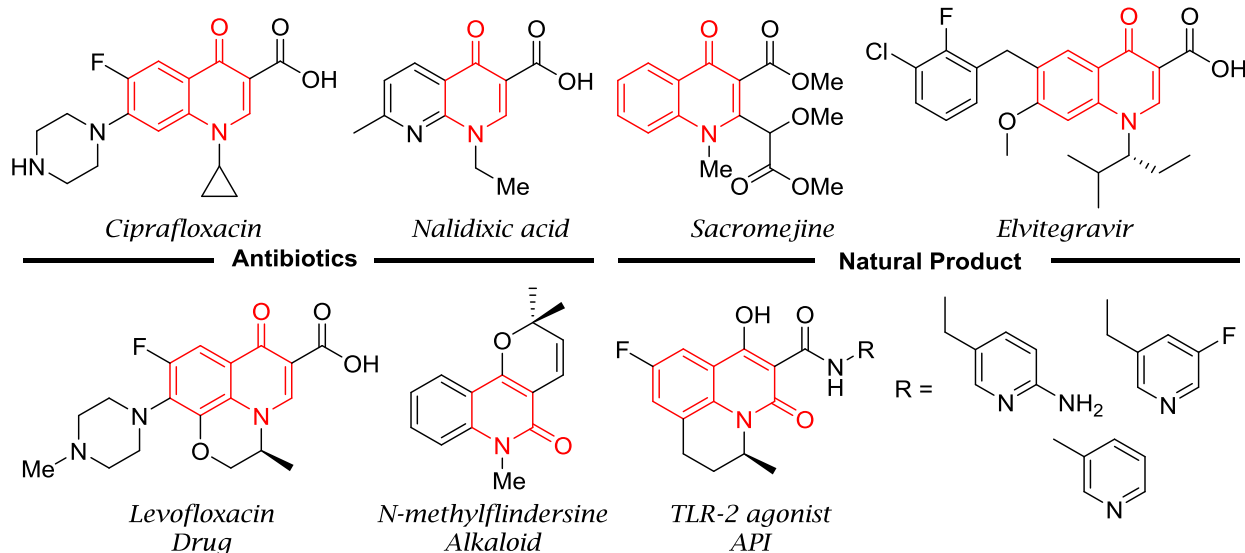
¹³Forbis, R. M.; Jr. Rinehart, K. L. *J. Am. Chem. Soc.*, **1973**, 95, 5003.

¹⁴Raitio, K. H.; Savinainen, J. R.; Vepsäläinen, J.; Laitinen, J. T.; Poso, A.; Järvinen, T.; Nevalainen, T. *J. Med. Chem.*, **2006**, 49, 2022.

¹⁵Hewawasam, P.; Fan, W.; Knipe, J.; Moon, S. L.; Boissard, V. C. G.; Gribkoff, K.; Starrett, J. E. *Bioorg. Med. Chem. Lett.*, **2002**, 12, 1779.

¹⁶Cordi, A. A.; Desos, P.; Randle, J. C. R.; Lepagnol, J. *Bioorg. Med. Chem.*, **1995**, 3, 129.; Desos, P.; Lepagnol, J. M.; Morain, P.; Lestage, P.; Cordi, A. A. *J. Med. Chem.*, **1996**, 39, 197.

¹⁷Sato, M.; Kawakami, H.; Motomura, T.; Aramaki, H.; Matsuda, T.; Yamashita, M.; Ito, Y.; Matsuzaki, Y.; Yamataka, K.; Ikeda, S.; Shinkai, H. *J. Med. Chem.*, **2009**, 52, 4869.;



Scheme 1.2: Biological active quinolone scaffold having common Pyridone motif

Other than Isoquinolone and quinolones, phthalazinones, a condensed heterocycle, have significant biological activities which show great potential in the treatment of various pathological processes, including diabetes,¹⁸ hepatitis B,¹⁹ vascular hypertension,²⁰ and arrhythmia.²¹ Azelastine, a phthalazinones derivative, is a well-known antiallergic and antihistaminic drug that sold worth \$0.24 billion in 2008.²²

Ramanathan, S.; Mathias, A. A.; German, P.; Kearney, P. B.; *Clin. Pharmacokinet.*, **2011**, *50*, 229.

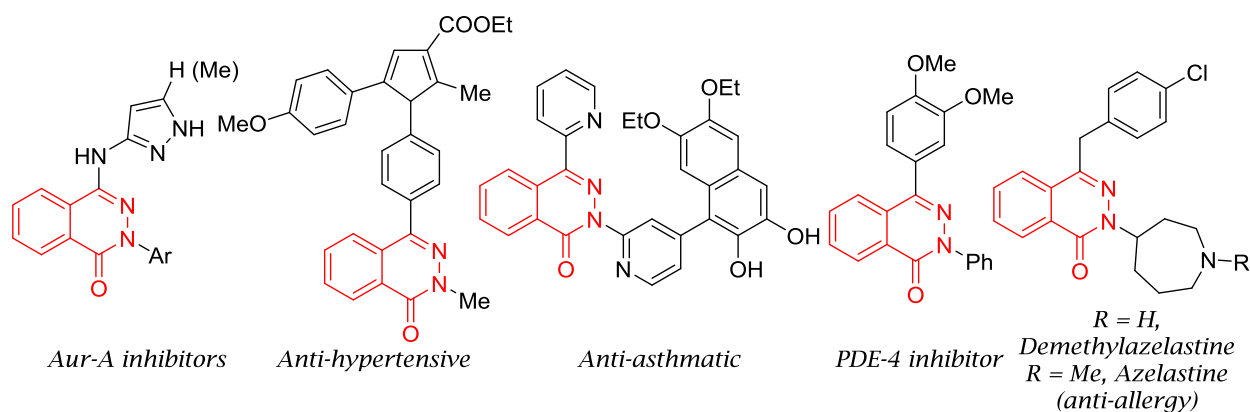
¹⁸Mylari, B. L.; Larson, E. R.; Beyer, T. A.; Zembrowski, W. J.; Aldinger, C. E.; Dee, M. F.; Siegel, T. W.; Singleton, D. H. *J. Med. Chem.*, **1991**, *34*, 108.; Madhavan, G. R.; Chakrabarti, R.; Kumar, S. K. B.; Misra, P.; Mamidi, R. N. V. S.; Balraju, V.; Kasiram, K.; Babu, R. K.; Suresh, J.; Lohray, B. B.; Lohray, V. B.; Iqbal, J.; Rajagopalan, R. *Eur. J. Med. Chem.*, **2001**, *36*, 627.

¹⁹El Ashry, E. S. H.; Abdel-Rahman, A. A. H.; Rashed, N.; Rasheed, H. A. *Pharmazie*, **1999**, *54*, 893.

²⁰García-Cadenas, A. E.; del Olmoa, E. L.; López, J.; Ferro, A.; Authib, K.; San Feliciano, A. *Abstracts of Papers, Joint Meeting on Medicinal Chemistry, Vienna, Austria, June 20–23*, **2005**, PO-80.; Demirayak, S.; Karaburun, C.; Beis, R. *Eur. J. Med. Chem.*, **2004**, *39*, 1089.; Nakajima, M.; Ohyama, K.; Nakamura, S.; Shimada, N.; Yamazaki, H.; Yokoi et. *Drug. Metab. Dispos.*, **1999**, *27*, 792.

²¹Engel, J.; Kutscher, B.; Fleischhauer, I.; Szeleny, S.; Metzmaener, U. *Eur. Patent*, EP 590551, **1994**.

²²Nakajima, M.; Ohyama, K.; Nakamura, S.; Shimada, N.; Yamazaki, H.; Yokoi et. *Drug. Metab. Dispos.*, **1999**, *27*, 792–797.; McTavish, D.; Sorkin, E. M. *Azelastine. Drugs*, **1989**, *38*, 778.; Huestis, P. M. *J. Org. Chem.*, **2016**, *81*, 12545.; Outerbridge, M. V.; Landge, M. S.; Tamaki, H.; Török, B. *Synthesis*, **2009**, *11*, 1801.



Scheme 1.3: Biological active phthalazinones scaffold

Apart from this, dihydroisoquinolones represent useful synthetic precursors of various organic molecules and bioactive compounds.²³

In addition, these compounds exhibit numerous important biological activities such as antimalarial,²⁴ antitussive,²⁵ and antiparkinsonian properties²⁶ and display a mitochondrial branched-chain aminotransferase (BCATm) inhibition effect.²⁷

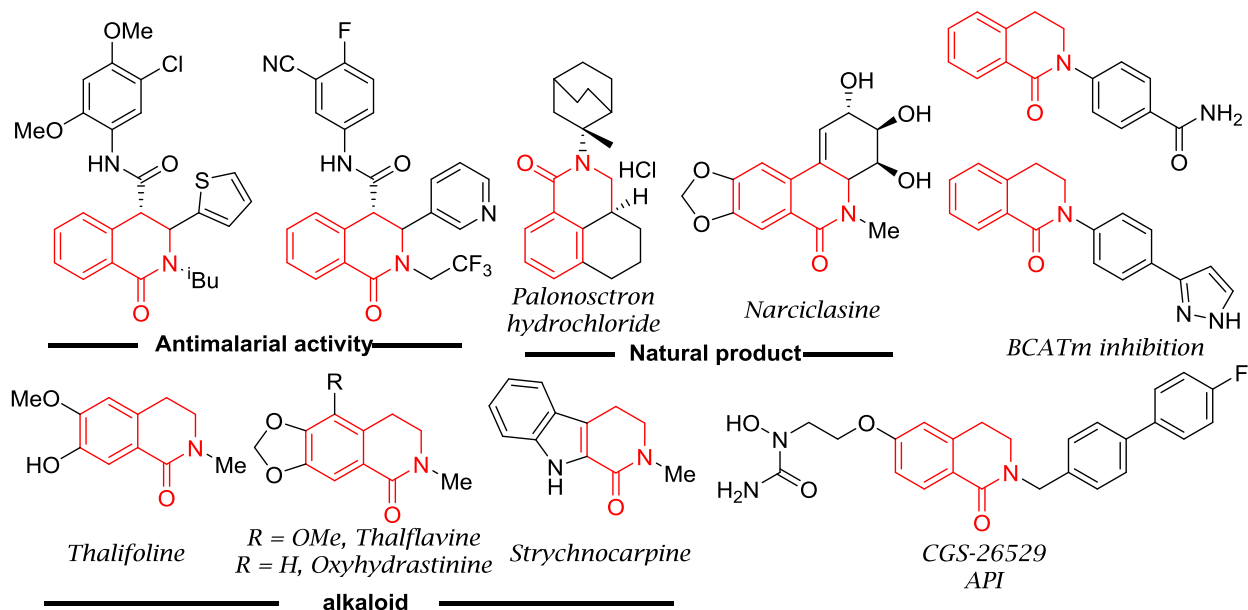
²³Briet, N.; Brookes, H. M.; Davenport, J. R.; Galvin, A. C. F.; Gilbert, J. P.; Mack, R. D.; Sabin, V. *Tetrahedron*, **2002**, 58, 5761.; Chrzanowska, M.; Rozwadowska, D. M. *Chem. Rev.*, **2004**, 104, 3341.; Kim, J.; Jo, M.; So, W.; No, Z. *Tetrahedron Lett.*, **2009**, 50, 1229.; Burks, E. H.; Abrams, T.; Kirby, A. C.; Baird, J.; Fekete, A.; Hamann, G. L.; S. Kim, S.; Lombardo, F.; Loo, A.; Lubicka, D.; Macchi, K.; McDonnell, P. D.; Mishina, Y.; Norris, D. J.; Nunez, J.; Saran, C.; Sun, Y.; Thomsen, M. N.; Wang, C.; Wang, J.; Peukert, S. *J. Med. Chem.*, **2017**, 60, 2790.

²⁴Liu, J.; Wang, Z.; Levin, A.; Emge, J. T.; Rablen, R. P.; Floyd, M. D.; Knapp, S. *J. Org. Chem.* **2014**, 79, 7593.

²⁵Kneko, H.; Kinugasa, H. *Vol. JP 42001295 B 19670123*, **1967**.

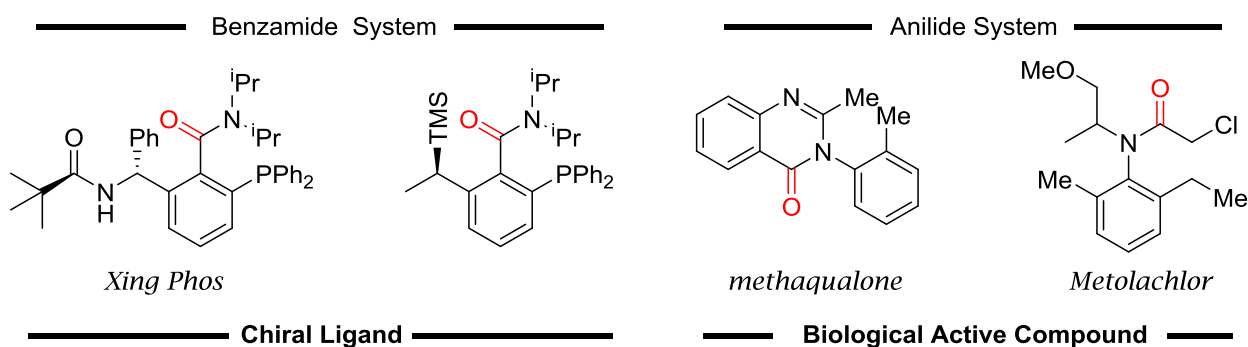
²⁶Lorenc-Koci, E.; Sokolowska, M.; Kwiecien, I.; Włodek, L. *Brain Res.*, **2005**, 1049, 133.

²⁷Borthwick, A. J.; Ancellin, N.; Bertrand, M. S.; Bingham, P. R.; Carter, S. P.; Chung, C.; Churcher, I.; Dodic, N.; Fournier, C.; Francis, L. P.; Hobbs, A.; Jamieson, C.; Pickett, D. S.; Smith, E. S.; Somers, N. O. D.; Spitzfaden, C.; Suckling, J. C.; Young, J. R. *J. Med. Chem.* **2016**, 59, 2452.



Scheme 1.4: Biological active dihydro-isoquinolone scaffold

Interestingly acyclic amides are studied in atroposelective synthesis. Among them atroposelective Xing Phos, which belong to the benzamide system used as a chiral ligand for enantioselective transformation.²⁸ Other than atroposelective anilides, methaqualone, and metolachlor are shown to have biological activity.²⁹

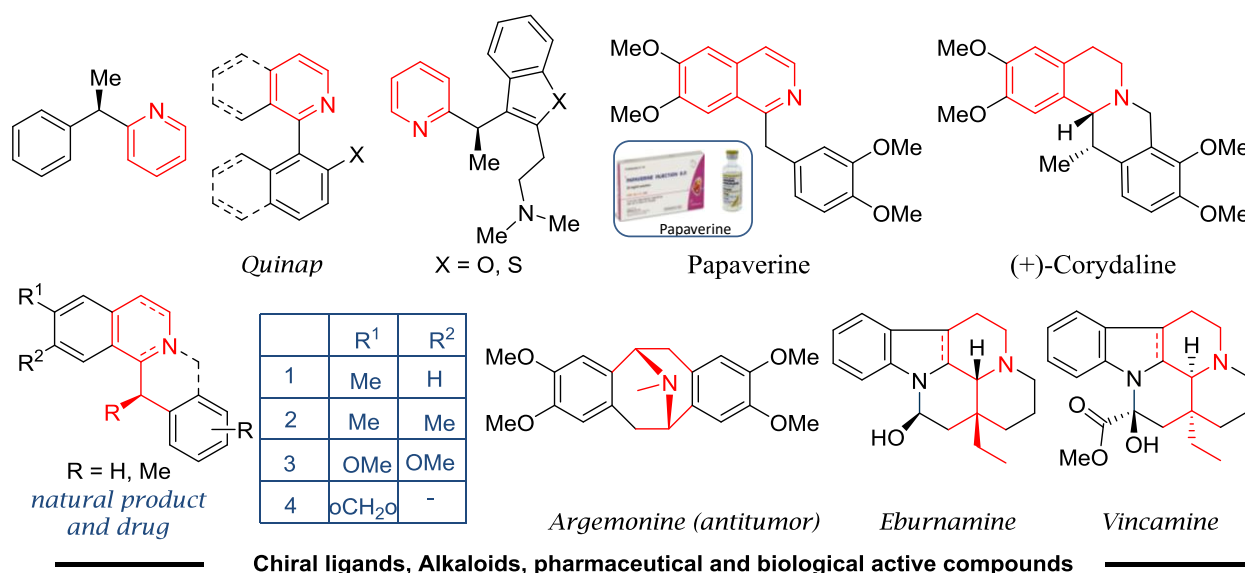


Scheme 1.5: Valuable acyclic amide scaffold

²⁸Bai, F. X.; Song, T.; Xu, Z.; Gu Xia, G. C; Huang, S. W; Xu, W. L. *Angew. Chem.*, **2015**, *127*, 5344.; Clayden, J.; Johnson, P.; Pink, H. J.; Helliwell, M. *J. Org. Chem.*, **2000**, *65*, 7033.

²⁹Shirakawa, S.; Liu, K.; Maruoka, K. *J. Am. Chem.Soc.*, **2012**, *134*, 916.; Mannschreck, A.; Koller, H.; Stühler, G.; Davies, M. A.; Traber, J. *Eur. J. Med. Chem. Chim. Ther.*, **1984**, *19*, 381.; Blaser, H.-U.; Pugin, B.; Spindler, F.; Thommen, M. *Acc. Chem. Res.* **2007**, *40*,1240.; Blaser, H. U. *Adv. Synth. Catal.*, **2002**, *344*, 17.

In terms of chiral alkyl six-member N-heterocycles, numerous scaffolds include substituted pyridines, isoquinolines, 3, 4- dihydro isoquinoline are known as drugs and shown pharmaceutical and other biological activities.³⁰ Papaverine is a benzylisoquinoline alkaloid found in the latex of the opium poppy (*Papaver somniferum* L.). It is a direct-acting smooth muscle relaxant, used in the treatment of impotence and as a vasodilator, especially for cerebral vasodilation.³¹ There is a numerous isoquinoline alkaloid that shows significant cytotoxicities and therapeutic effect, allevating pain and promoting blood circulation, and anti-allergic effect.³² Eburnamine, Vincamine, and Argemone alkaloids exert shows, pharmacological activities on cell multiplication, cardiovascular system, brain functions, and anti-proliferative.³³ Interestingly brown *et. al.* introduce quinap as a chiral ligand for asymmetric synthesis.³⁴



³⁰E. Vitaku, D. T. Smith and J. T. Njardarson, *J. Med. Chem.*, **2014**, *57*, 10257.; H. Yang, E. Wang, P. Yang, H. Lv and X. Zhang, *Org. Lett.*, **2017**, *19*, 5062.; K.-S. Zhou, P. Yi, T. Yang, F.-M. Yanf, K.-H. Lee, B.-Y. Zhao, Y.-H. Wang and C.-J. Tan, *Org. Lett.*, **2019**, *21*, 5051.; S. Varga, P. Angyal, G. Martin, O. Egyed, T. Holczbauer and T. Soos, *Angew. Chem., Int. Ed.*, **2020**, *59*, 13547.; K. M. Lambert, J. B. Cox, L. Liu, A. C. Jackson, S. Yruegas, K. B. Wiberg and J. L. Wood, *Angew. Chem., Int. Ed.*, **2020**, *59*, 9757.

³¹L. Mengozzi, L.; Gualandi, A.; Cozzi, G. P. *Chem. Sci.* **2014**, *5*, 3915.

³²Saito, Y. S.; Tanaka, M.; Matsunaga, K.; Li, Y.; Ohizumi, Y. *Biol. Pharm. Bull.* **2004**, *27*, 1270.

³³Vas, A.; Gulyas, B. *Med. Res. Rev.*, **2005**, *25*, 587 - 757. DOI: 10.1002/med.20043.; Wang, J.; Lv, X.; Xu, J.; Liu, X.; Du, T.; Sun, G.; Chen, J.; Shen, X.; Wang, J.; Hu, L. *Eur. J. Med. Chem.* **2020**, *188*, 111976. doi: 10.1016/j.ejmech. 2019.111976.; Stermitz, R. F.; Lwo, Y. S.; Kallos, G. *J. Am. Chem. Soc.* **1963**, *85*, 10, 1551–1552.

³⁴Vitaku, E.; Smith, T. D.; Njardarson, T. J. *J. Med. Chem.* **2014**, *57*, 10257.; Elena Fernandez, E.; Guiry, J. P.; Connole, P. T. K.; Brown, M. J. *J. Org. Chem.* **2014**, *79*, 539.

Scheme 1.6: Valuable chiral pyridine, isoquinoline, and dihydroisoquine scaffold

1.2. B A literature precedent Synthetic Approaches

Aza-arenes scaffolds, especially for six-member N-heterocycles are found in applications in synthetic chemistry, medicinal chemistry, and pharmaceuticals and are also present in various natural products and bioactive molecules (section 1.1 A). Hence, the synthesis of these structural scaffolds is very important. Here, we will discuss briefly the synthesis of aza-arenes.

1.2.B.1 Synthesis of Pyridone Derivatives: A Literature Review

The multi-step synthesis from highly functionalized units to construct poly-substituted bioactive compounds and alkaloids of N-heterocycles remains a well-established approach.³⁵ In the 19th century, Pyridone rings were synthesized from pyrone rings in the presence of ammonia and primary amines (a).³⁶ The base-promoted cyclization of ester or Michael acceptor was reported by several groups to construct pyridone rings (b).³⁷ Later on, metal-catalyzed pyridone ring synthesis is known by many other groups (c).³⁸ Both base promoted and base-free solid phase polymers supported the efficient synthesis of Pyridone from 2-hydroxy pyridine also known (d).³⁹ Bicyclic Pyridones were synthesized either by cyclo

³⁵Ali, T. El. S.; Ibrahim, M. A. *J. Braz. Chem. Soc.*, **2010**, *21*(6), 1007-1016.; Jessen, H. J.; Gademann, K. *Nat. Prod. Rep.*, **2010**, *27*, 168-1185.; He, X.; Shang, Y.; Yu, Z.; Fang, M.; Zhou, Y.; Han, G.; Wu, F. *J. Org. Chem.*, **2014**, *79*, 8882-8888.

³⁶Cavalieri, L. F. *Chem. Rev.*, **1947**, *41*, 525.; Staunton, J. *Comprehensive Organic Chemistry; Pergamon: Oxford, U.K.*, **1979**, *4*, 629.; Ellis, G. P. *Comprehensive Heterocyclic Chemistry; Pergamon: Oxford, U.K.*, **1984**, *3*, 675.; Shusharina, N. P.; Lapteva, V. L. *J. Org. Chem., USSR*, **1974**, *10*, 852.

³⁷Overman, L. E.; Tsuboi, S.; Roos, J. P.; Taylor, G. F. *J. Am. Chem. Soc.*, **1979**, *102*, 747.; Shine, M.; Shibanuma, T.; Mukaiyama, T. *Chem. Lett.*, **1976**, 1041.; Quick, J. *Tetrahedron Lett.*, **1977**, 327.; Carles, L.; Narkunan, K.; Penlou, S.; Rousset, L.; Bouchu, D.; Ciufolini, M. A. *J. Org. Chem.*, **2002**, *67*, 4304.; Hachiya, I.; Ogura, K.; Shimizu, M. *Org. Lett.*, **2002**, *4*, 2755.; Fujii, M.; Nishimura, T.; Koshiba, T.; Yokoshima, S.; Fukuyama, T. *Org. Lett.*, **2013**, *15*, 232.

³⁸Ackermann, L.; Lygin, A. V.; Hofmaan, N. *Org. Lett.*, **2011**, *13*, 3278.; Thrimurtulu, N.; Dey, A.; Maiti, D.; Volla, C. M. R. *Angew. Chem. Int. Ed.*, **2016**, *55*, 12361.; R. Zeng, C. Fu, S. Ma, *J. Am. Chem. Soc.*, **2012**, *134*, 9597.; R. Zeng, S. Wu, C. Fu, S. Ma, *J. Am. Chem. Soc.*, **2013**, *135*, 18284.; Wang, H.; Glorius, F. *Angew. Chem. Int. Ed.*, **2012**, *51*, 7318.; Wang, H.; Glorius, F. *Angew. Chem.* **2012**, *124*, 7430.

³⁹Dragovich, P. S.; Zhou, R.; Prins, T. J. *J. Org. Chem.*, **2002**, *67*, 741-746.; Zhu, T.; Yan, Z.; Chucholowski, A.; Webb, T. R.; Li, R. *J. Comb. Chem.*, **2006**, *8*, 401-409.; Ando, M.; Wada,

condensation of the corresponding scaffold(e).⁴⁰ Similarly, microwave-assisted intramolecular Mitsunobu reaction of substituted pyridines gives corresponding bicyclic pyridinium salts, which further hydrolysis provides pyridones derivatives (f).⁴¹ Traditionally, the most used method to obtain isoquinolone and quinolones derivatives are the oxidation of isoquinolinium and quinolinium salts by using $K_3[Fe(CN)_6]$ as oxidant (g).⁴² In contrast, oxidation in the presence of oxygen is an environmentally friendly green method. Recently, some achievements have been made to obtain Pyridones by using oxygen as an oxidant in the presence of metal-based photocatalysts, organophotocatalyst, and photocatalyst-free conditions (h).⁴³

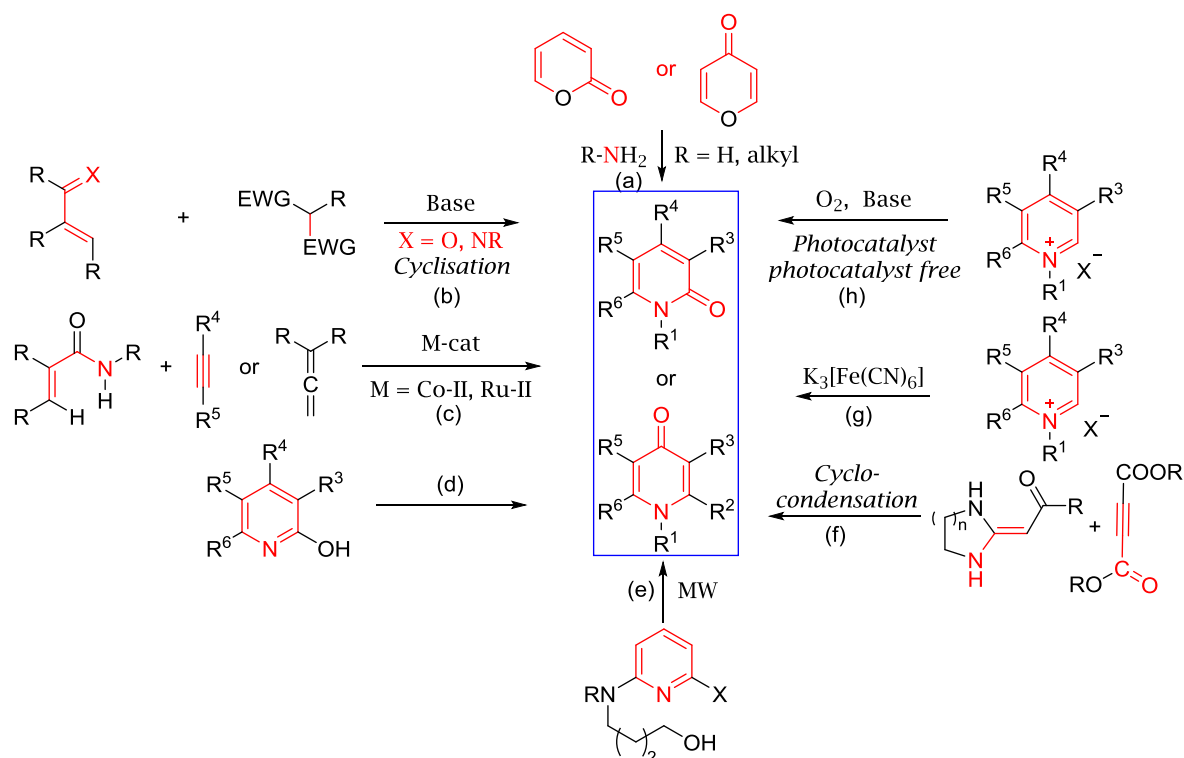
T.; Sato, N. *Org. Lett.*, **2006**, 8(17), 3805-3808.; Feng, B.; Li, Y.; Zhang, X.; Xie, H.; Cao, H.; Yu, L.; Xu, Q. *J. Org. Chem.*, **2018**, 83, 6769-6775.

⁴⁰Zhao, M. X.; Wang, M. X.; Huang, Z. T. *Tetrahedron*, **2002**, 58, 1309.; Hehemann, D. G.; Winnik, W. *J. Heterocycl. Chem.*, **1994**, 31, 393.; Chanu, G. L.; Singh, P. T.; Jang, J. Y.; Yoon, J. Y.; Singh, M. O.; Lee, G. S. *Bull. Korean Chem. Soc.*, **2014**, 35, 994.

⁴¹Cheng, D.; C, Laura.; Abdi, M.; Lightfoot, A.; Gallagher, T. *Org. Lett.*, **2007**, 9, 5175.

⁴²Khalil, M. I.; Barker, D.; Copp, R. B.; *J. Org. Chem.*, **2016**, 81, 282.; Ishi-i, T.; Hirashima, R.; Tsutsumi, N.; Amemori, S.; Matsuki, S.; Teshima, Y.; Kuwahara, R.; Mataka, S.; *J. Org. Chem.*, **2010**, 75, 6858.; Fan-Chiang, -T. T.; Wang, -K. H.; Hsieh, -C. J. *Tetrahedron*, **2016**, 72, 5640.

⁴³Bai, -G. L.; Zhou, Y.; Zhuang, X.; Zhang, L.; Xue, J.; Lin, -L. X.; Cai, T.; Luo, -L. Q. *Green Chem.*, **2020**, 22, 197.; Wang, G.; Hu, W.; Hu, Z.; Zhang, Y.; Yao, W.; Li, L.; Fu, Z.; Huang, W. *Green Chem.*, **2018**, 20, 3302.; Jin, Y.; Ou, L.; Yang, H.; Fu, H. *J. Am. Chem. Soc.*, **2017**, 139, 14237.; Fang, Z.; Wang, Y. *Org. Lett.*, **2019**, 21, 434.; Sun, Q.; Zhang, -Y. Y.; Sun, J.; Han, Y.; Jia, X.; Yan, G. C. *Org. Lett.*, **2018**, 20, 987.; Zhou, Y.; Liu, W.; Xing, Z.; Guan, J.; Song, Z.; Peng, Y. *Org. Chem. Front.*, **2020**, 7, 2405.; Zhou, M.; Yu, K.; Liu, J.; Shi, W.; Pan, Y.; Tang, H.; Peng, X.; Liu, Q.; Wang, H. *RSC Adv.*, **2021**, 11, 16246.



Scheme 1.7: Several Synthetic routes for Pyridone synthesis

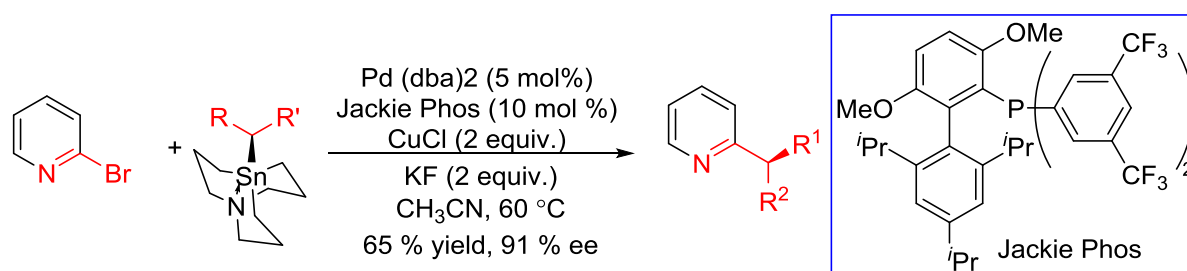
1.2.B.2 Synthesis of Chiral Pyridines: A Literature Review

Six-membered N-heteroaromatic chiral derivatives are prevalent structural motifs for bioactive molecules, drugs, and drug-like molecules. Therefore, their synthesis remained an important field of research. Until recently, mostly the racemic functionalization of N-heteroaromatic compounds is reported.⁴⁴

The initial success of C2-functionalised asymmetric synthesis was achieved in 2013 by developing the first general stereoretentive method by prof. M. R. Biscoe and coworkers via Pd-catalysed Stille cross-coupling of pre-functionalized pyridine with stoichiometric chiral alkylstannane reagents having 94 % ee.⁴⁵

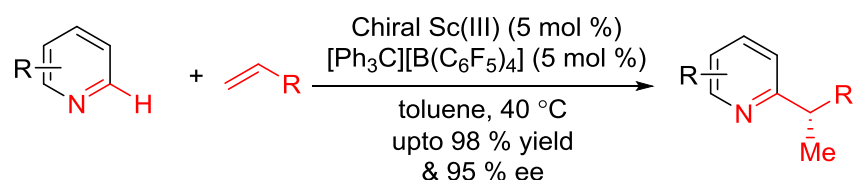
⁴⁴Maryanoff, B. E.; Zhang, H.-C.; Cohen, J. H.; Turchi, I. J.; Maryanoff, C. A. *Chem. Rev.* **2004**, *104*, 1431-1628.; V Farina, V.; Reeves, J. T.; Senanayake, C. H.; J. Song, J. J. *Chem. Rev.*, **2006**, *106*, 2734-2793.; Baumann, M.; Baxendale, I. R. *Beilstein J. Org. Chem.*, **2013**, *9*, 2265-2319.

⁴⁵Li, L.; Wang, C.-Y.; Huang, R.; Biscoe, M. R. *Nat. Chem.* **2013**, *5*, 607-612.



Scheme 1.8: Stereoretentive Pd-catalysed Stille cross-coupling reaction

Although transition metal catalyzed⁴⁶ C-H alkylation of pyridine represents a direct and waste-free approach, the electron-poor nature of pyridines poses challenges for C-H activation. The strong coordinating nature of pyridine complicates things further, as strong substrate coordination either deactivates the transition metal catalyst or inhibits the coordination of chiral ligands. Hence, asymmetric pyridine C-H activation remains severely underdeveloped. When we started our exploration of catalytic asymmetric pyridine functionalizations, only one single chiral scandium-catalyzed alkylation with terminal alkenes by prof. Hou and co-workers reported in 2014 the formation of a variety of enantioenriched alkylated pyridine derivatives with high yields, and good functional group compatibility.⁴⁷ This breakthrough report is shown to be successful with 2-substituted pyridines, while quinolines failed to undergo this transformation. The reason speculated was the strong coordination of non-C2-blocked pyridines and quinolones.



Scheme 1.9: Scandium catalysed enantioselective addition of substituted pyridines to various olefins

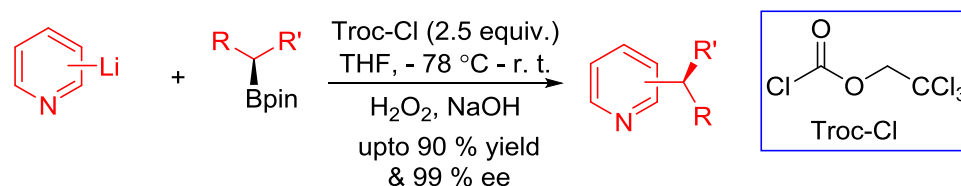
In 2015, Aggarwal et. al. developed a novel method for the stereospecific coupling of chiral boronic esters with lithiated six-membered N-heterocycles.⁴⁸ This approach consists first formation of a boronate complex and the Subsequent addition of Troc-Cl results in the acylation of the nitrogen heterocycle which triggers alkyl migration for C2 and C4

⁴⁶Wang, D.; Wu, L.; Wang, F.; Wan, X.; Chen, P.; Lin, Z.; Liu, G. *J. Am. Chem. Soc.* **2017**, *139*, 6811-6814.; Friis, S. D.; Pirnot, M. T.; Dupuis, L. N.; and Stephen L. Buchwald, S. L. *Angew. Chem. Int. Ed.* **2017**, *56*, 7242-7246.; Yin, Y.; Dai, Y.; Jia, H.; Li, J.; Bu, L.; Qiao, B.; Zhao, X.; Jiang, Z. *J. Am. Chem. Soc.* **2018**, *140*, 6083–6087.; Jiang, X.; Boehm, P.; Hartwig, J. F. *J. Am. Chem. Soc.* **2018**, *140*, 1239-1242.; Panda, S.; Coffin, A.; Nguyen Q. N.; Tantillo, D. J.; Ready, J. M. *Angew. Chem. Int. Ed.* **2016**, *55*, 2205-2209.

⁴⁷Song, G.; O, W.W. N.; Hou, Z. *J. Am. Chem. Soc.* **2014**, *136*, 12209-12212.

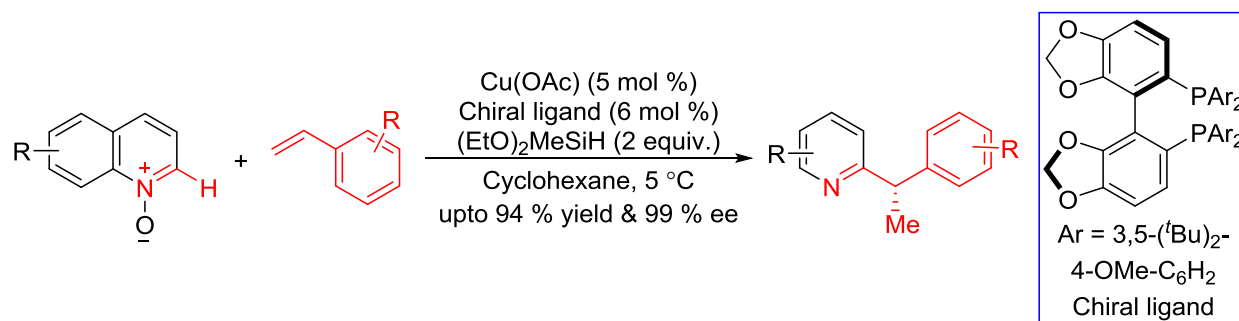
⁴⁸Llaveria, J.; Leonori, D.; Aggarwal, K. V. *J. Am. Chem. Soc.* **2015**, *137*, 10958.

functionalization. Finally, Oxidative workup gives the coupled product with good yield and excellent enantioselectivity.



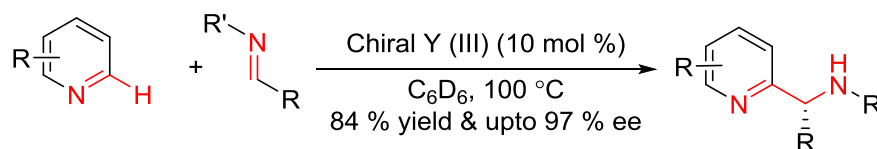
Scheme 1.10: Stereospecific coupling of a boronic ester with N-Heteroaromatic compound

In 2017, Ge and co-workers developed a copper-catalyzed 2-alkylation of quinoline N-oxide with vinyl arenes to prepare C2-functionalised chiral quinolines in high yield with good to excellent enantioselectivity.⁴⁹ In terms of gram scale synthesis reducing Cu-catalyst to 1.5 mol % also works well.



Scheme 1.11: Enantioselective copper catalysed alkylation of quinoline N-oxide with vinylarenes

Later on, in 2018 enantioselective aminoalkylation was reported by Mashima and Tsurugi group in the presence of chiral yttrium catalyst with a good yield and similarly with C2 blocked limited substrate scope.⁵⁰



Scheme 1.12: Enantioselective Aminoalkylation of ortho-substituted pyridines via yttrium catalyst

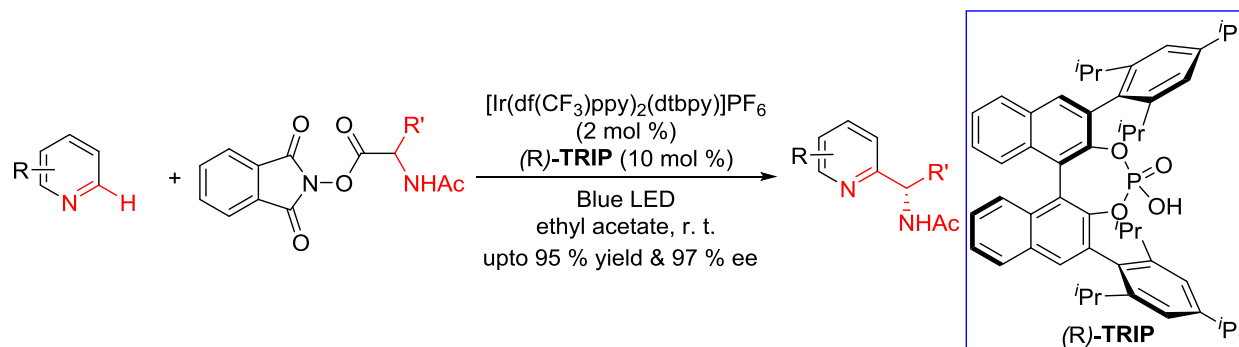
At the same time, Phipps and Jiang's group independently reported an efficient dual photoredox-chiral phosphoric acid-catalyzed aminoalkylation of azaarenes.⁵¹ According to

⁴⁹Songjie Yu, S.; Hui Leng Sang, H. L.; Ge, S. *Angew. Chem. Int. Ed.* **2017**, *56*, 15896-15900.

⁵⁰Kundu, A.; Inoue, M.; Nagae, H.; Tsurugi, H.; Mashima, K. *J. Am. Chem. Soc.* **2018**, *140*, 7332-7342.

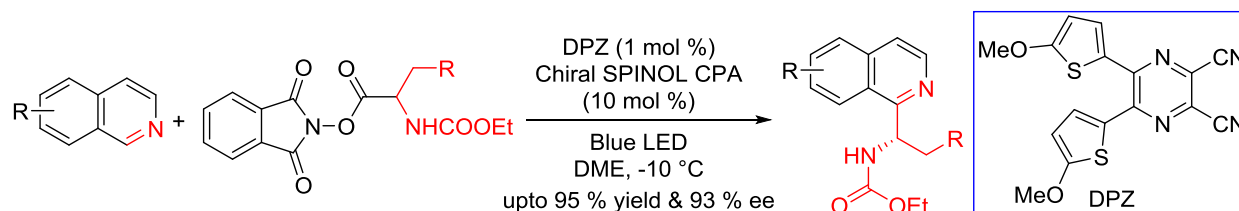
⁵¹Proctor, R. S. J.; Davis, H. J.; Phipps, R. J. *Science* **2018**, *360*, 419-422.; Liu, X.; Liu, Y.; Chai, G.; Qiao, B.; Zhao, X.; Jiang, Z. *Org. Lett.* **2018**, *20*, 6298-6301

Phipps *et. al.*, an iridium photocatalyst involved in the SET process to generate radicals from amino acid derivatives and radical addition to pyridines and quinolines provides a functionalized product with excellent control of both enantioselectivity and regioselectivity. For this, An enantiopure chiral Brønsted acid catalyst serves both to activate the substrate and induce asymmetry.



Scheme 1.13: Asymmetric radical addition to Heteroarenes via dual catalysis path.

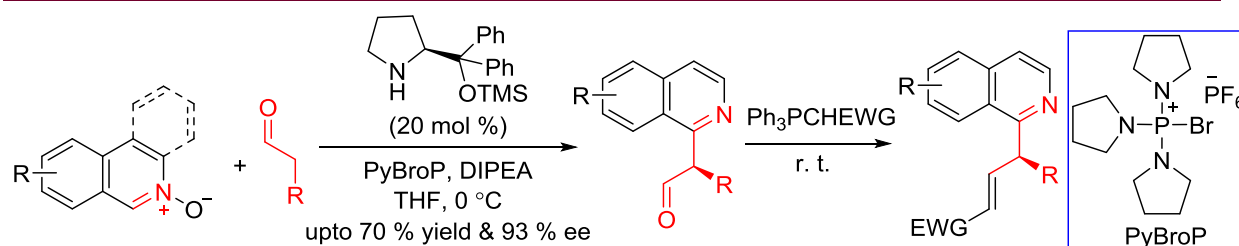
Jiang *et. al.* replaced an Ir-photo catalyst with DPZ as a photosensitizer to develop a dual organocatalytic cycle in the presence of chiral phosphoric acid (CPA). By this method, a variety of α -aminoalkyl radicals generated from redox-active esters efficiently react with various isoquinolines to produce several valuable α -isoquinoline substituted secondary amines in high yields with good to excellent enantioselectivities.



Scheme 1.14: Enantioselective addition of α -aminoalkyl radical to Isoquinolines via transition metal-free dual catalysis

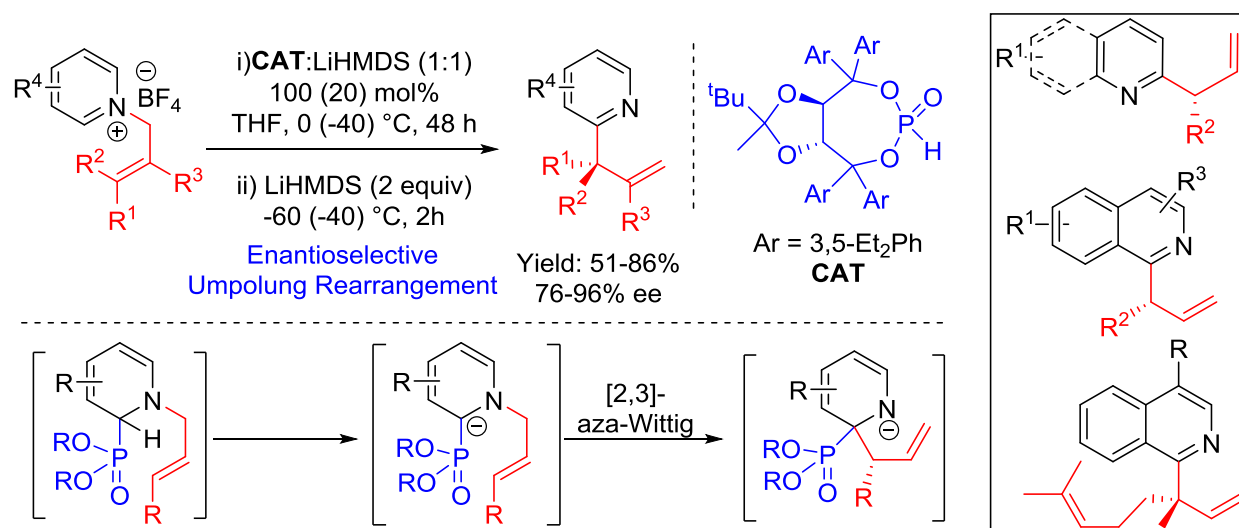
In 2018, Fochi *et. al.* successfully developed a new protocol for enantioselective α – heteroarylation with isoquinoline N-oxides, via chiral enamine catalysis by using a chiral amine catalyst and pyBroP as a chemoselective activating agent.⁵² By this method, a variety of α – heteroarylated products are formed with high ee and moderate to good yield.

⁵² Bertuzzi, G.; Pecorari, D.; Bernardi, L.; Fochi, M. *Chem. Commun.* **2018**, *54*, 3977-3980.



Scheme 1.15: Enantioselective α -arylation of aldehyde via chiral enamine catalysis.

In 2019 our group achieved successfully a base-mediated enantioselective aza-[2, 3] Wittig rearrangement to the synthesis of chiral *N*-heterocyclic compounds with good enantioselectivity by using the chiral phosphites.⁵³ All isoquinoline, quinoline, and 4-substituted pyridine substrates were remain successful for this branched allylation product formation.

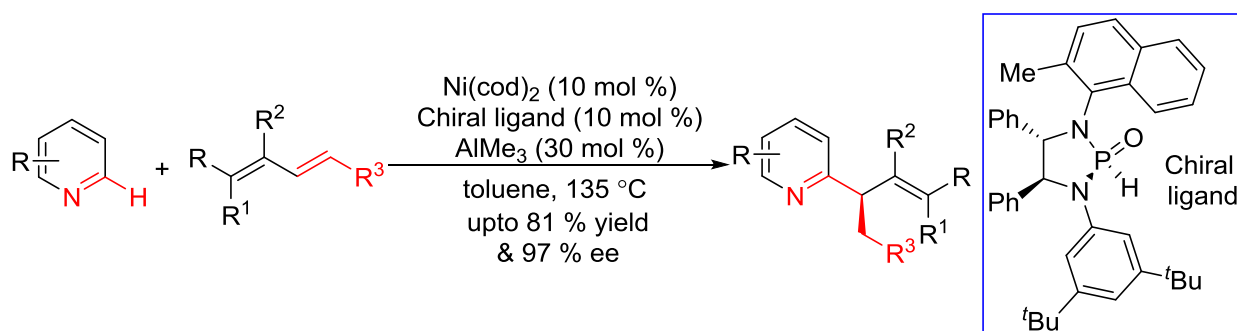


Scheme 1.16: Phosphite-catalysed asymmetric branched allylation of pyridines.

In 2022, Huang, Ye, and coworkers reported a Ni-Al bimetallic catalyst system with chiral phosphine oxide ligands for asymmetric C2 allylation with 1,3-dienes without the need for a C2-block.⁵⁴ This efficient method provides a C2-alkylated chiral derivatives pyridines, including unsubstituted pyridine, C3, C4, or C2-substituted pyridines, and even complex pyridine-containing bioactive molecules in 54–81% yield and 60–97% ee.

⁵³ Motaleb, A.; Rani, S.; Das, T.; Gonnade, G. R.; Maity, P. *Angew. Chem. Int. Ed.* **2019**, *58*, 14104.

⁵⁴ Li, J.; Pan, D.; Wang, H.; Zhang, T.; Li, Y.; Huang, G.; Ye, M. *J. Am. Chem. Soc.* **2022**, *144*, 18810–18816.



Scheme 1.17: Enantioselective alkylation of pyridines with various olefins via Ni-Al bimetallic catalysis

With the potential difficulties in the transition metal-catalyzed asymmetric functionalization of pyridines, we plan to develop an organocatalytic functionalization of imine embedded in pyridines. Unfortunately, asymmetric aza-functionalization was not developed when we started, while oxa-versions are one of the most successful substrates for asymmetric functionalizations. Asymmetric reduction and nucleophile addition to C=N are the only two types that are well developed but led to chiral amine products rather than the regeneration of C=N. Installing chiral centers away from C-1 of nitrogen remains a desirable but largely unsolved problem.

1.3 “Aza-acyl” anion and radical equivalent approach for umpolung imine functionalization: A literature review

For enantioselective nucleophilic catalysis reactions, there are several catalysts, like chiral amine, DMAP, isothioureia, NHC, phosphines, and cyano were developed well to establish an organocatalysis field through. Apart from NHC catalysis one of the major field for umpolung C(H)=N functionalization where phosphite is not known for that when we start work. To talk about phosphite catalysis, firstly in 2004, the Johnson group reported the enantioselective cross silyl benzoin reaction with chiral phosphites.⁵⁵ The success of phosphite catalysis remained limited to the activation of acylsilanes and rather than its expansion, they collaborated with the Ooi group to use phosphite as a stoichiometric reagent for “umpolung” via the phospho-Brook rearrangement strategy.⁵⁶ So, catalytic use of phosphites remains

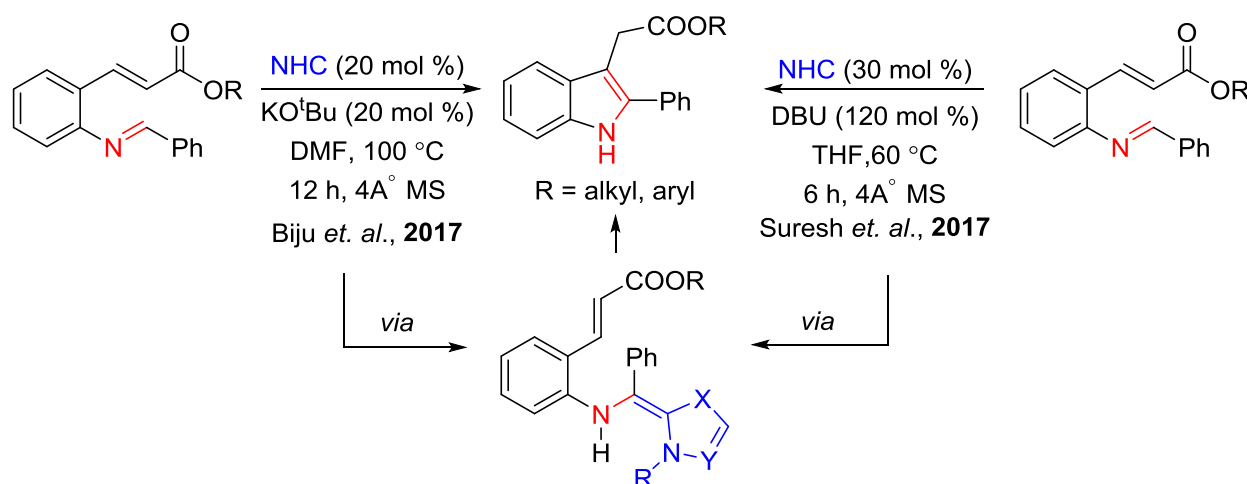
⁵⁵Linghu, X.; Potnick, R. J.; Johnson, S. J. *J. Am. Chem. Soc.* **2004**, *126*, 3070-3071.

⁵⁶Corbett, T. M.; Uraguchi, D.; Ooi, T.; Johnson, S. J. *Angew. Chem., Int. Ed.* **2012**, *51*, 4685-4689.; Horwitz, A. M.; Tanaka, N.; Yokosaka, T.; Uraguchi, D.; Johnson, S. J.; Ooi, T. *Chem. Sci.* **2015**, *6*, 6086-6090.

challenging. Particularly for umpolung imine functionalization of aldimine via “aza-acyl” anion & radical” equivalent from aldimine remains unsolved to the best of knowledge.

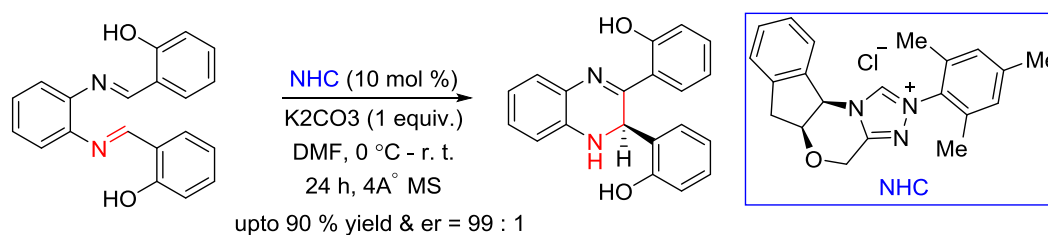
1.3.A “Aza-acyl” anion equivalent approach: A literature review

To focus on NHC catalysis, in 2017, Biju and Suresh's group came up with an approach for umpolung imines functionalization and achieved success by intramolecular functionalization of aldimine with Michael acceptor via aza-Breslow intermediates for racemic synthesis.⁵⁷



Scheme 1.18: NHC catalysis for umpolung imines functionalization

Later on, in 2019 Biju *et. al.* reported the asymmetric intramolecular cyclization of Bisimines under NHC catalysis provided the desired product in moderate to good yield and enantioselectivity. The reaction proceeds via the generation of aza Breslow intermediate.⁵⁸

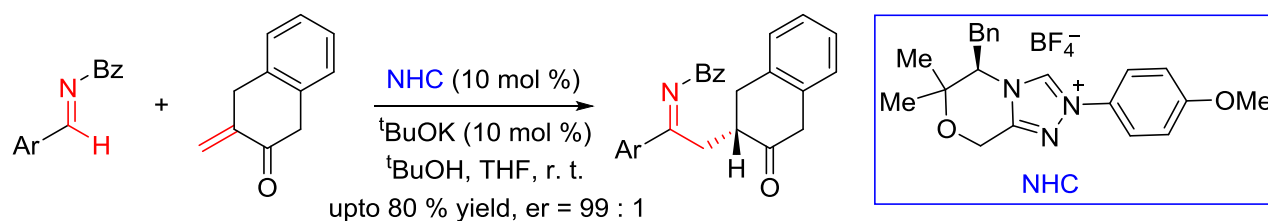


Scheme 1.19: Asymmetric NHC catalysis for umpolung imines functionalization

In 2019, Lupton and coworkers reported asymmetric intermolecular enantioselective aza-stetter reaction that proceeds via imine umpolung NHC catalysis with good to high enantioselectivity.⁵⁹

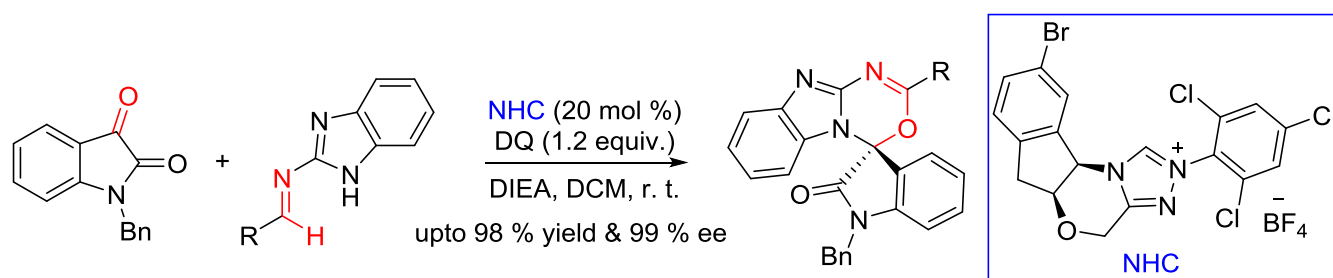
⁵⁷A. Patra, S. Mukherjee, T. K. Das, S. Jain, R. G. Gonnade, A. T. Biju, *Angew. Chem. Int. Ed.* **2017**, 56, 2730–2734; *Angew. Chem.* **2017**, 129, 2774–2778.; B. Harish, M. Subbireddy, S. Suresh, *Chem. Commun.* **2017**, 53, 3338–3341.

⁵⁸T. K. Das, A. Ghosh, K. Balanna, P. Behera, R. G. Gonnade, U. K. Marelli, A. K. Das, A. T. Biju, *ACS Catal.* **2019**, 9, 4065–4071.



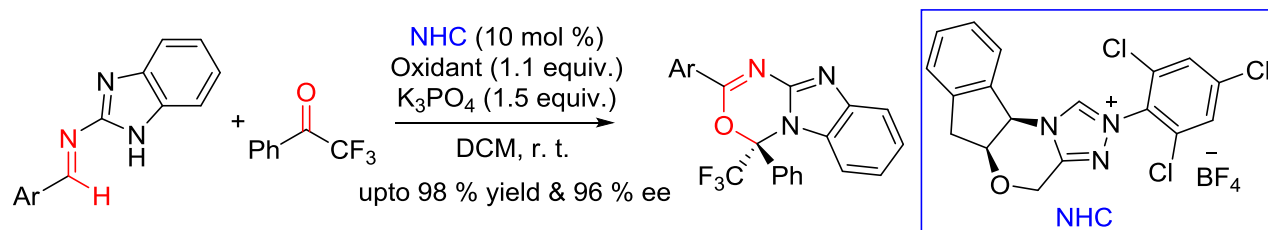
Scheme 1.20: Asymmetric NHC catalysis for umpolung imines functionalization

In 2021, Chi et. al. developed an NHC-catalyzed enantioselective synthesis of heterocycles with (Benz) imidazole-derived imines and activated ketones in the presence of an oxidant.⁶⁰



Scheme 1.21: Carbene catalysed intermolecular enantioselective synthesis for heterocycles

Subsequently, Fu et. al. successfully developed asymmetric intermolecular NHC - catalysed oxidative reaction of functionalized aldimines, as 1,4-dipole precursors with electron-deficient ketone.⁶¹ This method consists of mild reaction conditions, broad substrate scope, and a good enantiomeric ratio.



Scheme 1.22: Asymmetric carbene catalysed oxidation of aldimines with activated ketone

In 2022, prof. M. F. Greaney offers a new path for umpolung N-heterocyclic carbene (NHC) catalysis beyond the aldimine to form a C-C bond.⁶² For that, by taking of pyridinium ion, it

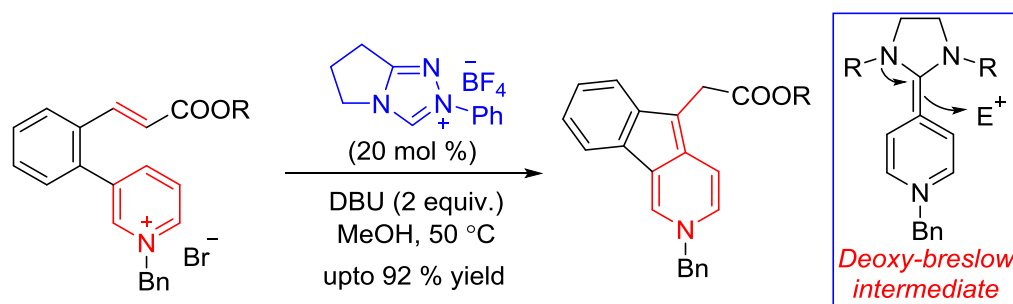
⁵⁹ J. E. M. Fernando, Y. Nakano, C. Zhang, D. W. Lupton, *Angew. Chem. Int. Ed.* **2019**, *58*, 4007–4011.; *Angew. Chem.* **2019**, *131*, 4047–4051.

⁶⁰ X. Yang, Y. Xie, J. Xu, S. Ren, B. Mondal, L. Zhou, W. Tian, X. Zhang, L. Hao, Z. Jin, Y. R. Chi, *Angew. Chem. Int. Ed.* **2021**, *60*, 7906–7912.; *Angew. Chem.* **2021**, *133*, 7985–7991.

⁶¹ G. Wang, Q. C. Zhang, C. Wei, Y. Zhang, L. Zhang, J. Huang, D. Wei, Z. Fu, W. Huang, *Angew. Chem. Int. Ed.* **2021**, *60*, 7913–7919.; *Angew. Chem.* **2021**, *133*, 7992–7998.

⁶² T. Wu, M. R. Tatton, M. F. Greaney, *Angew. Chem. Int. Ed.* **2022**, *61*, e202117524.

undergoes NHC catalysis to form an intramolecular C-C bond via a deoxy-Breslow intermediate. But, this strategy is limited to racemic synthesis only.



Scheme 1.23: Umpolung pyridinium alkylation under NHC catalysis

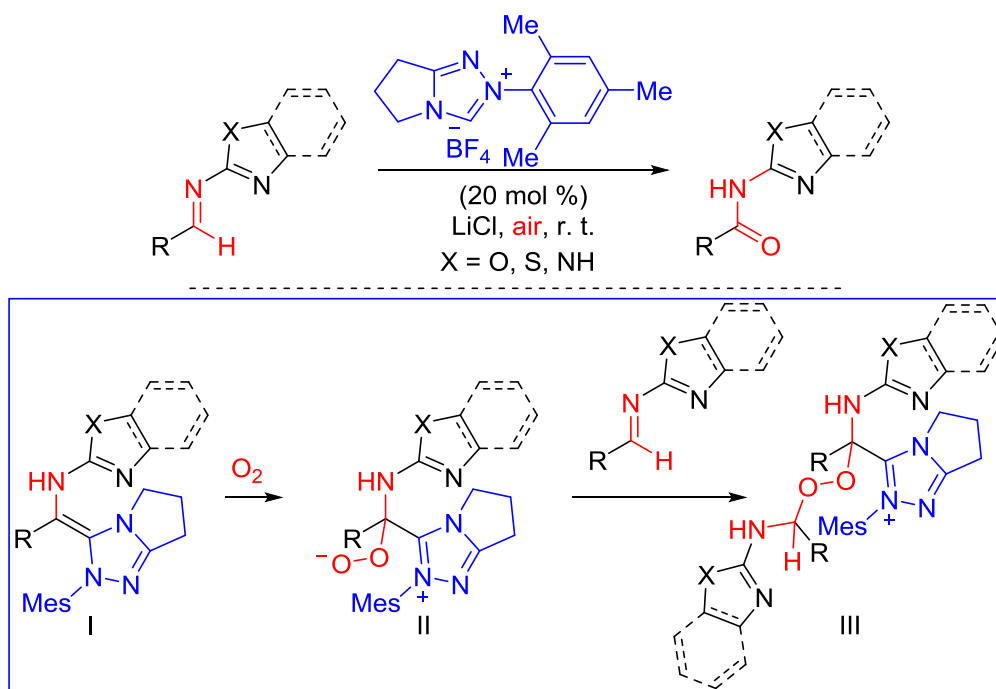
1.3.B “Aza-acyl” radical equivalent approach: A literature review

The recent exploration of nucleophilic catalysis in the field of radical chemistry is known for the case of both cyanide and thiazolium adduct of aldehydes to undergo aerobic oxidation via single electron transfer processes but the radical path remains unclear.⁶³ Later on, the radical oxidation of imine was also developed but the asymmetric version via chiral NHC is not yet achieved.

In this context, in 2017 Huang et. al. developed a mild and efficient method for the synthesis of amides from aldimines via aerobic oxidative NHC catalysis where NHC activates the aldimines with the assistance of LiCl to afford aza-Breslow intermediates.⁶⁴ To look at the mechanism, the aza-Breslow intermediate II then adds to O₂ to form another reactive intermediate II containing oxygen anion. Further, the addition of oxygen anion in intermediate II to activated aldimine substrate gives intermediate III and subsequent O-O bond cleavage under basic conditions provides two molecules of the amide with the regeneration of NHC.

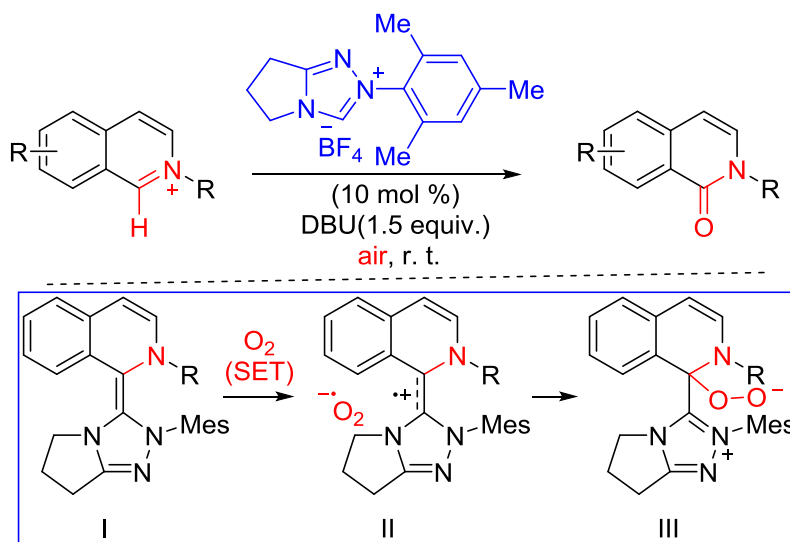
⁶³D. Kieslich, J. Christoffers, *Synthesis*. **2021**, 53, 3485–3496.; C. C. Chiu, K. Pan, F. Jordan, *J. Am. Chem. Soc.* **1995**, 117, 7027–7028.; L. Delfau, S. Nichilo, F. Molton, J. Broggi, E. T. Mendivil, D. Martin, *Angew. Chem. Int. Ed.* **2021**, 60, 26783–26789.; *Angew. Chem.* **2021**, 133, 26987–26993.

⁶⁴ Wang, G.; Fu, Z.; Huang, W. *Org. Lett.* **2017**, 19, 3362–3365.



Scheme 1.24: Formation of amide from aldimine via umpolung imine NHC catalysis

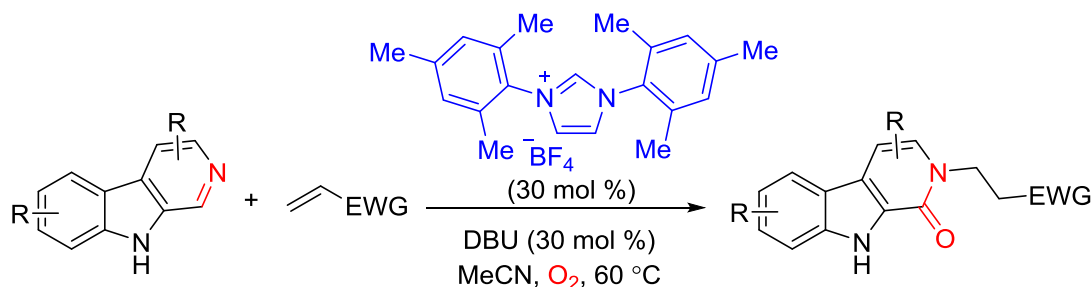
Next year, the same group reported a similar strategy of aerobic oxidation method for umpolung of isoquinolinium salt enabled by NHC to synthesize isoquinolinones derivatives with good to excellent yields.⁶⁵ Here, they clearly stated the single electron transfer (SET) transfer of the aza-Breslow intermediate II to O_2 generates radical cation intermediate II and superoxide radical anion. Further, radical recombination gives intermediate III followed by O-O bond cleavage and release of NHC-formed amide. The phthalazinium, pyridinium, and quinolinium salts are also suitable substrates for this transformation.



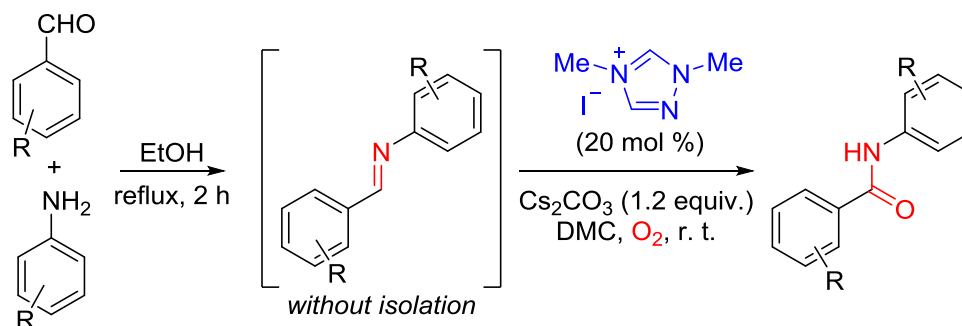
⁶⁵ Wang, G.; Hu, W.; Hu, Z.; Zhang, Y.; Yao, W.; Li, L.; Fu, Z.; Huang, W. *Green Chem.*, **2018**, *20*, 3302–3307.; Bortolini, O.; Chiappe, C.; Fogagnolo, M.; Massi, A.; Pomelli, S. *C. J. Org. Chem.*, **2017**, *82*, 302.

Scheme 1.25: NHC catalysed aerobic oxidation of isoquinolium salt

Later on, in 2020 Suresh *et. al.* developed an NHC organocatalyzed umpolung imines oxidation, that proceeds via a similar aza-Breslow intermediate by taking β -carboline based cyclic imines and molecular oxygen as a sole oxidant for the synthesis of the corresponding N-substituted cyclic amides.⁶⁶

**Scheme 1.26:** NHC catalyzed tandem imine umpolung aza-Michael addition and oxidation of β -carboline based cyclic imines

Recently, in 2022 Suresh *et. al.* reported an efficient and environmentally friendly method for the oxidation of unactivated aldimines to amides under NHC catalysis aerobic oxidation.⁶⁷ Similarly, this method developed a umpolung imine oxidation through the aza-Breslow intermediate. This method that a green solvent such as dimethyl carbonate and molecular oxygen in the air to act as the sole oxidant under mild conditions without using any additive.

**Scheme 1.27:** NHC catalysis for aerobic oxidation of unactivated aldimines to amide

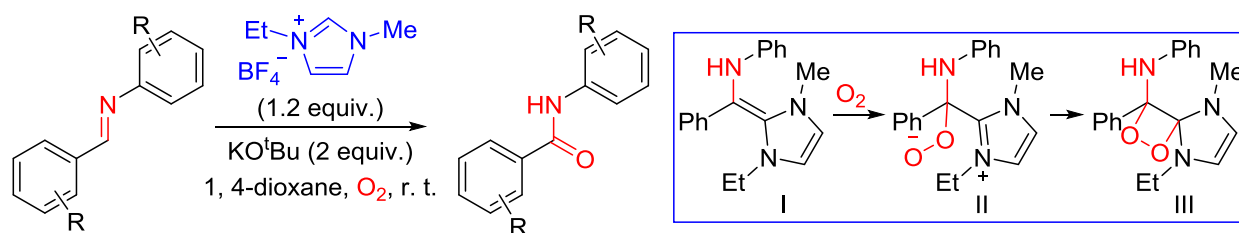
In 2022, wang *et. al.* also reported NHC-mediated aerobic oxidation of imines to amide in good to high yield.⁶⁸ The reaction proceeds via the first formation of aza-Breslow intermediate and then O₂ insertion formed 1,2-dioxetane intermediate. Finally O-O bond cleavage generates expected amide with stoichiometry waste of NHC amide. The application

⁶⁶ Satyam, K.; Harish, B.; Nanubolu, B. J.; Suresh, S. *Chem. Commun.*, **2020**, 56, 2803-2806.

⁶⁷ J. Ramarao, S. Yadav, K. Satyam, S. Suresh, *RSC Adv.* **2022**, 12, 7621–7625.

⁶⁸ S. Sun, D. Guo, F. Li, J. Wang, *Org. Chem. Front.* **2022**, 9, 356–363.

of this method is also found in a gram-scale one-pot aerobic oxidative amidation directly starting from aldehyde and amine.



Scheme 1.28: NHC mediated oxidation of imines to amide via aza-Breslow dioxetane intermediate

1.4 Conclusion

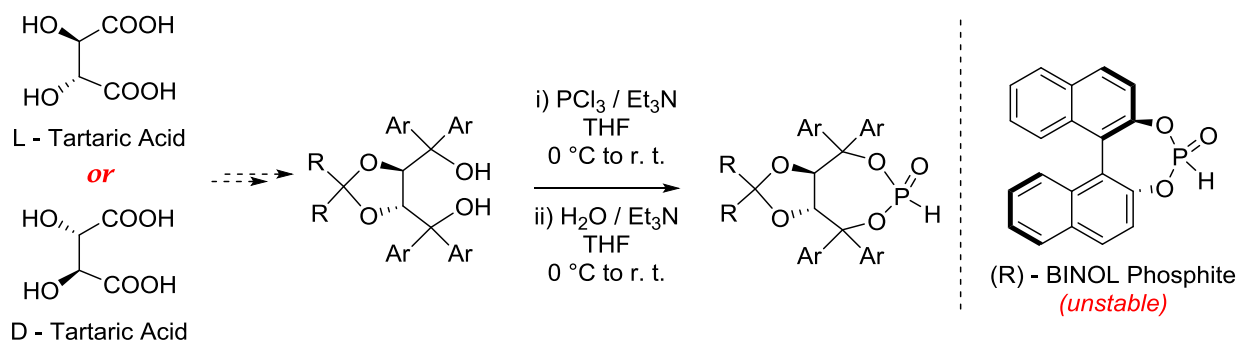
In conclusion, we discussed various bioactive molecules having chiral pyridine and pyridone moiety in their core structure, and their literature reported synthesis in the first section. In the last section, we discussed the “aza-acyl” anion and radical equivalent approach for umpolung imine reactivity in several transformations. The first success of phosphite catalysis from our lab in aza-[2,3] Wittig rearrangement.

Chapter 2

Preparation of chiral phosphites as nucleophilic organocatalysts

2.1 Abstract

In this chapter, we discussed the synthesis of chiral phosphite catalysts for the enantioselective functionalization of imines embedded in pyridines to explore the catalyst structure-activity relationship.



Scheme 2.1: General scheme for the preparation of chiral phosphite catalysts

2.2 Introduction

Over the past few decades, asymmetric catalysis is one of the most attractive approaches due to its very high reactivity, selectivity, and environmentally friendly nature.¹ In terms of the application of asymmetric synthesis, one enantiomer has the desired properties while the other enantiomer is either inactive or has undesirable side effects. Of the various ways of creating enantiomerically enriched compounds, catalytic methods are considered the most appealing. Besides the enzymatic and metal-catalyzed asymmetric transformations, the use of organocatalysts has proved to have enormous potential for the catalysis of stereoselective reactions¹ and reflected the Nobel Prize award 2021 to B. List and David W. C. MacMillan.

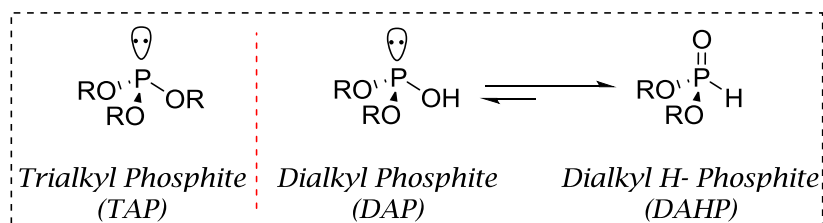
In this context, to reach the highest levels of reactivity and selectivity in catalytic enantioselective reactions, several reaction parameters must be optimized and among them, the selection and design of the chiral ligands are one of the more crucial steps. In this regard,

¹Asymmetric catalysis in an industrial scale: Challenges, approaches, and solution; Blased, H. U.; Schmidt, E.; Eds.; Wiley: Weinheim, **2003**.; Comprehensive asymmetric catalysis; Jacobsen, E. N.; Pfaltz, A.; Yamamoto, H.; Eds.; Springer-verlag: Berlin, **1999**.; Asymmetric catalysis in organic synthesis; Noyori, R.; Eds.; Wiley: New York, **1994**.; For comprehensive reviews on organocatalysis, see a) A. Berkessel, H. Gröger, *Asymmetric Organocatalysis: From Biomimetic Concepts to Applications in Asymmetric Synthesis* Wiley-VCH, Weinheim, Germany, **2005**; b) I. Dalko, *Enantioselective Organocatalysis*, Wiley-VCH, Weinheim, Germany, **2007**; c) M. Waser, in *Prog. Chem. Org. Nat. Prod.* vol. 96 (Eds.: A.-D. Kinghorn, H. Falk, J. Kobayashi), Springer, Wien, Austria, **2012**.; The advent and development of organic catalysis; David W. C. MacMillan, *Nature*, **2008**, 455, 304–308.

BINOL² (α, α' -Bi-2-naphthol) and TADDOLs³ ($\alpha, \alpha, \alpha', \alpha'$ -tetraphenyl-1,3-dioxolane-4,5-dimethanol) derivatives are a well-known family of compounds that have been used as chiral ligands in several relevant stereoselective transformations. On the other hand, chiral phosphites derivatives are extremely important for asymmetric catalytic reactions as a nucleophilic chiral catalyst, reported by Johnson *et. al.* and found its application in asymmetric cross-silyl benzoin,⁴ Stetter reaction,⁵ etc.

2.3 Background of phosphite catalysis

In general, phosphorous compounds exist in two oxidation states, P (III) and P (V) where P (V) is more stable. The general formula of the phosphorous reagents is PX_3 , where X is alkyl, aryl, alkyl amine, alkoxy, aryloxy, alkylthio, halogen, etc. Having a lone pair of electrons of these reagents shows the endowed basicity and nucleophilic properties of the molecule.⁶ Generally, dialkyl phosphites (DAP) are less nucleophilic and less reactive than trialkyl phosphites (TAP). This is due to the equilibrium exit between DAP and DAHP (Scheme 2.2) and the presence of the P atom in DAPs in a penta rather than a trivalent state. Also, the presence of acid and base enhances the equilibrium toward the formation of active phosphite tautomer.⁶



Scheme 2.2: Existence of equilibrium between DAP and DAHP.

Based on, the chemistry of TAP/ DAP, a successful tool for phosphorylation of $C=X$ electrophile ($X = C, O, N$) was developed well.⁶ Since, our target is the development of a phosphite catalyst (DAHP) library as a chiral nucleophilic catalyst for asymmetric imine functionalization, we initially focus on the background of phosphite.

² Chen, Y.; Yekta, S.; Yudin, K. A. *Chem. Rev.* **2003**, *103*, 3155–3211.

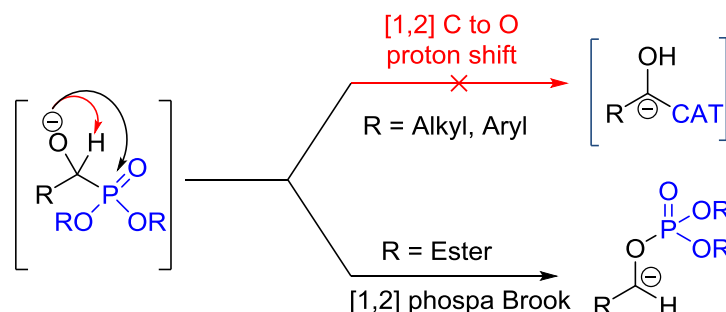
³ Seebach, D.; Beck, K. A.; Heckel, A. *Angew. Chem. Int. Ed.* **2001**, *40*, 92 – 138.

⁴ Linghu, X.; Potnick, R. J.; Johnson, S. J.; *J. Am. Chem. Soc.* **2004**, *126*, 3070.; Garrett, R. M.; Tarr, C. J.; Johnson, S. J. *J. Am. Chem. Soc.* **2007**, *129*, 12944-12945.

⁵ Nahm, R.; Linghu, X.; Potnick, R. J.; Yates, M. C.; White, S. P.; Johnson, S. J. *Angew. Chem. Int. Ed.* **2005**, *44*, 2377-2379; Nahm, R. M.; Potnick, R. J.; White, S. P.; Johnson, S. J. *J. Am. Chem. Soc.* **2006**, *128*, 2751-2756.

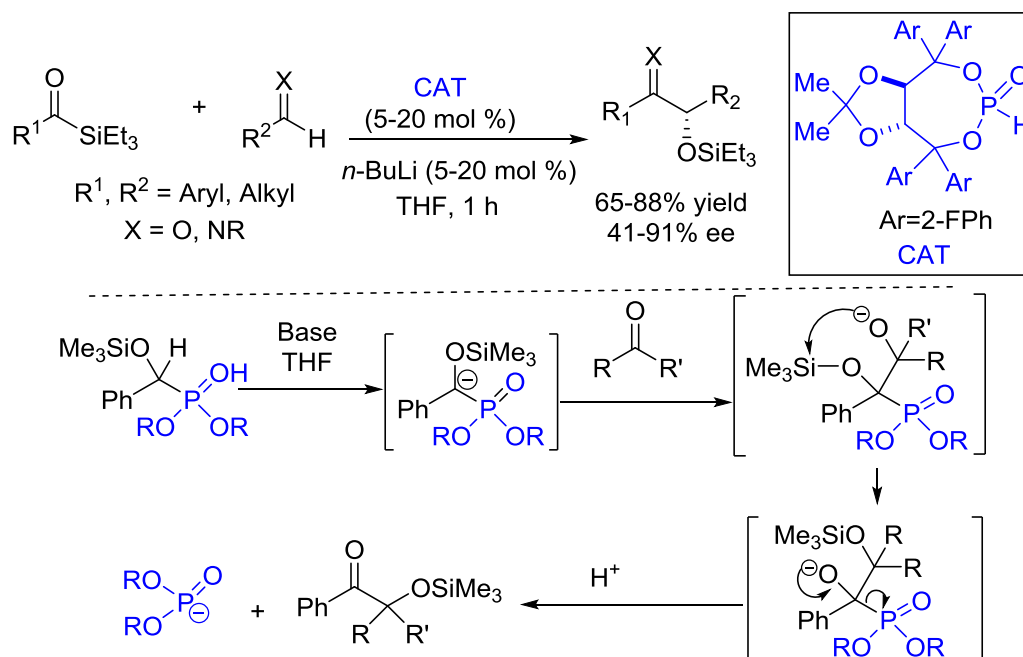
⁶ Ganoub, N. A.; Sabry, E.; Abdou, M. W. *Synth. Commun.* **2007**, *47*, 1631.

Initial screening of phosphite for umpolung reactivity of aldehyde as an acyl anion equivalent shows, instead of requiring [1, 2] C to O proton shift, a phospha-Brook rearrangement happened.⁷ This factor discouraged the chemists to consider phosphite as a "umpolung" catalyst for the development of the catalysis path.



Scheme 2.3: Reactivity of aldehyde-phosphite adduct

In 2004, the Johnson group introduced phosphite anion as the nucleophilic umpolung catalyst for enantioselective cross-silyl benzoin reaction with chiral phosphites.⁴ After that, dialkyl hydrogen phosphites (DAHP) take more attention for organonucleophilic catalysis reaction.

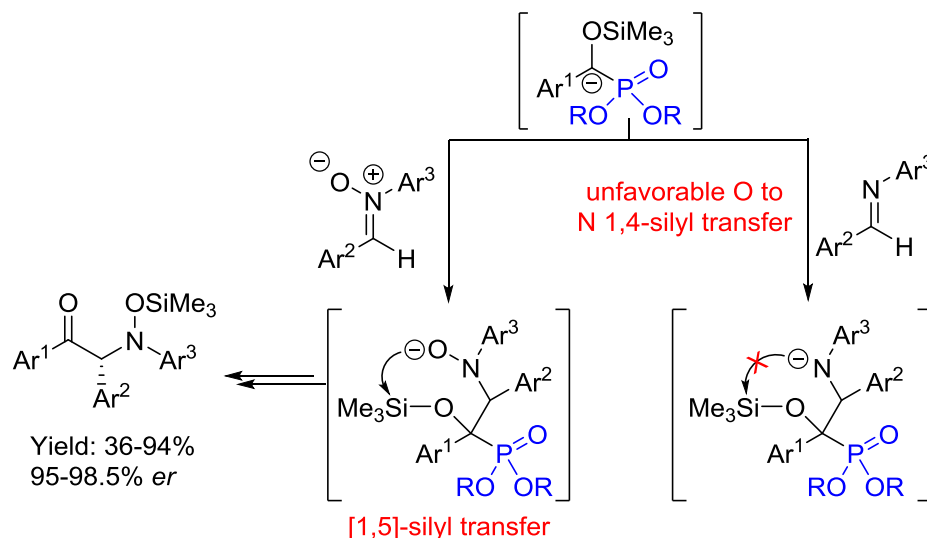


Scheme 2.4: Chiral phosphite-catalysed enantioselective cross-benzoin reaction

Next, the same group explored the application of cross silyl benzoin reaction with other electrophiles, beyond an aldehyde. Initial screening with imine as the electrophilic partner failed to produce the desired product, presumably due to the unfavorable O to N 1,4-silyl

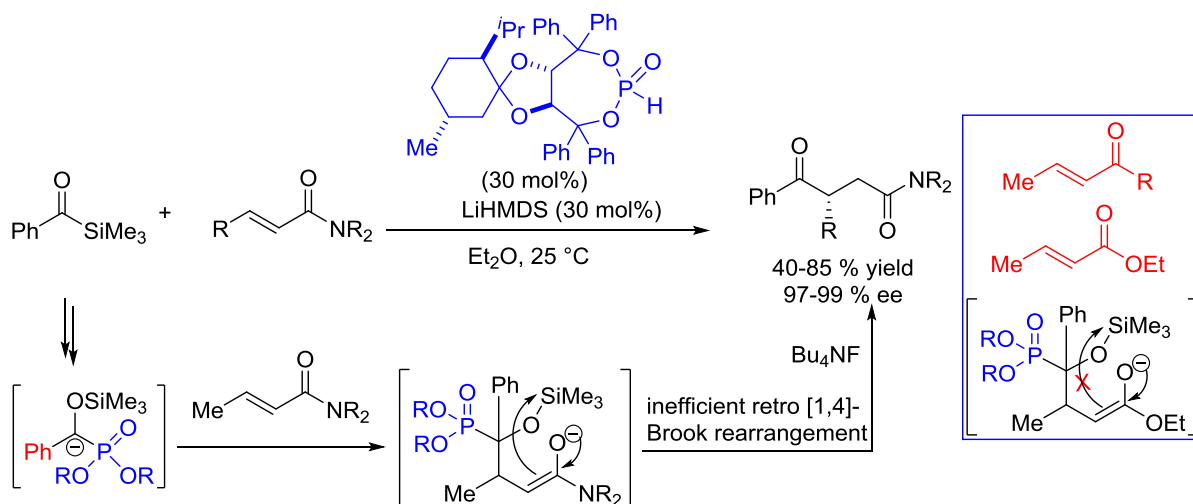
⁷ Kondoh, A.; Terada, M. *Org. Lett.* **2013**, *15*, 4568–4571.; Quesada, E.; Taylor, K. J. R. *Synthesis*, **2005**, *19*, 3193–3195.

transfer. On the other hand, N-aryl nitrones produce a corresponding product with the regeneration of the catalyst through an O to O 1,5-silyl transfer.⁴



Scheme 2.5: Chiral phosphite-catalysed enantioselective cross-benzoin reaction with Imine and aryl nitron

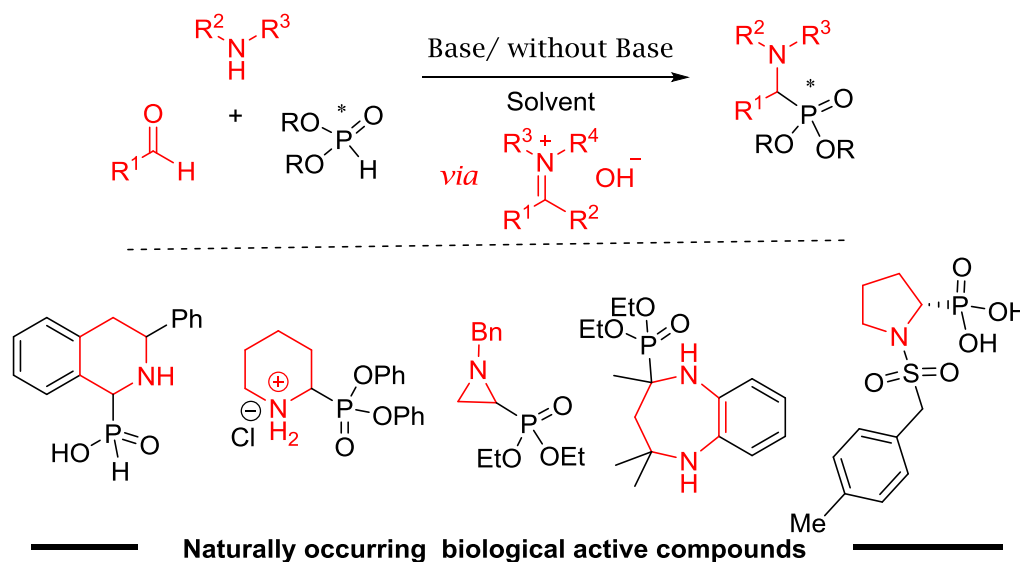
Later on, an enantioselective stetter reaction is also developed by the same group with suitable Michael acceptor.⁵ Here, only α , β -unsaturated amide works well and the other two having ketone and ester group containing Michael acceptor remain unsuccessful.



Scheme 2.6: metallophosphite-catalysed enantioselective Stetter reaction

Overall, by the Johnson group, different BINOL and TADDOL-based chiral phosphites were successfully screened for several reactions (mention above) to achieve high enantioselectivity and it shows TADDOL derives phosphites significantly participate to attain excellent selectivity.

Apart from this, phosphites addition to imines is also one of the well-known reactions to generate α -amino phosphonates which are biologically active compound⁸ and possess a diverse range of biological activities because they are structurally analogous to many enzyme inhibitors, antitumors, and antibiotic agents.⁹



Scheme 2.7: Biologically active amino phosphonate

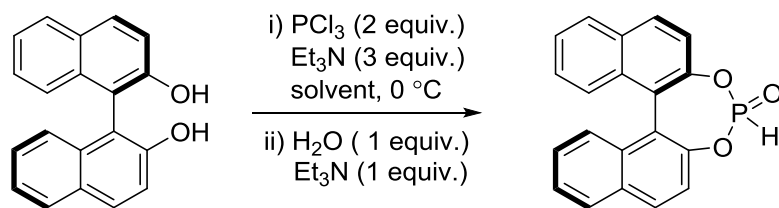
Although phosphite's addition to imines is well known, its catalytic asymmetric application on organic transformation is not known to the best of our knowledge. So, we focused on enantioselective synthesis to imine embedded in pyridines, by using a chiral phosphite catalyst. For that in this section, we discussed the preparation of several chiral phosphites catalysts. Although the chiral phosphite catalyst was invented by the Johnson group, here we are representing various new chiral phosphite scaffolds for umpolung imine functionalization run by our lab.

2.4 Result and discussion

For chiral phosphite preparation, we initially chose to synthesize chiral BINOL-based phosphites since BINOLs are privileged chiral backbones for asymmetric induction and are easy to access. The corresponding phosphites are formed by a reaction between BINOL with PCl_3 in the presence of toluene under basic conditions. Later on, changing solvent and temperature shows, THF at 0 °C works well. But, in terms of stability, BINOL-derived phosphites turned out to be labile and hydrolyze easily under isolation and storage.

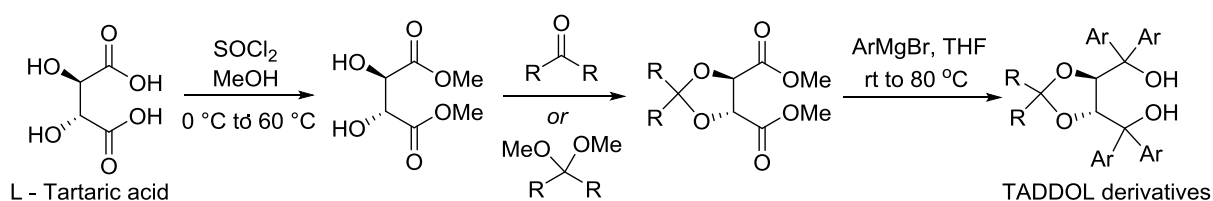
⁸ Choudhury, R. A.; Mukherjee, S. *Chem. Sci.*, **2016**, 7, 6940.

⁹ Lim, T.; Kim, M. B. *J. Org. Chem.* **2020**, 85, 13246-13255.



Scheme 2.8: Preparation of binaphthyl phosphite.

To overcome such instability, next to choosing a chiral ligand, TADDOL derivatives got priorities as a similar chiral diol scaffold, due to its easy synthesis from inexpensive and commercially available natural chiral source, D- or L-tartaric acid.^{3,4} Here, first etherification tartaric acid gives corresponding tartrate ester, then 1,3-dioxolane ring formed by the reaction with acetals or ketals under acid catalysis, and finally reaction with aliphatic or aromatic Grignard reagents produce corresponding TADDOLs. In terms of properties, TADDOLs are generally nonvolatile solids, having a strong tendency to crystallize, showing high optical rotation values (for chiral), nonpolar, and stable enough to store. Even though the dioxolane ring, having R = Me (acetonide) are extraordinarily stable, and also survive in acidic workup condition with no problems.³

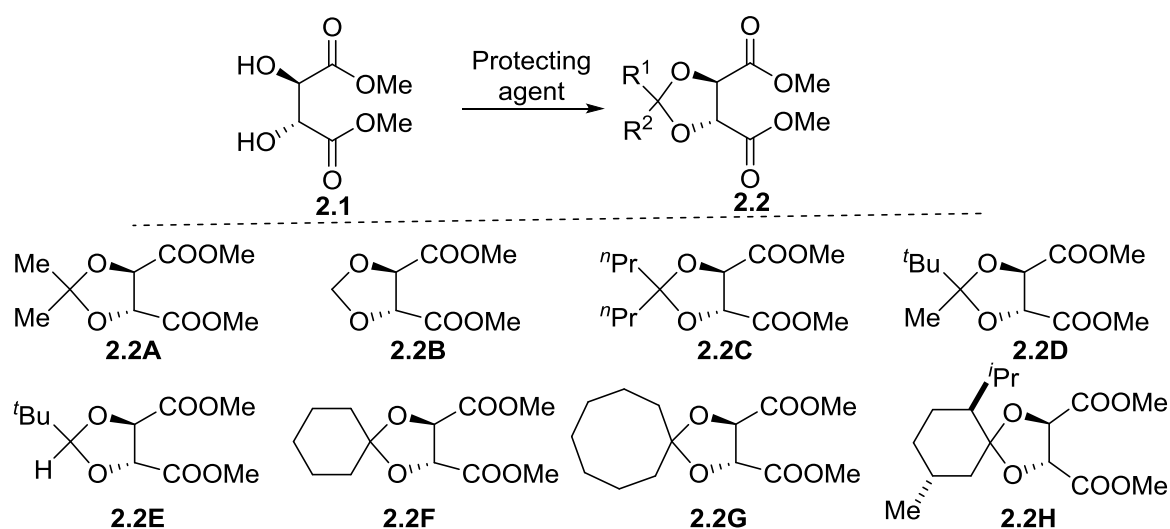


Scheme 2.9: General scheme for the preparation of TADDOL derivatives from tartaric acid.

Based on the literature reported synthesis and stability, we initially focused to get different dioxolane scaffolds by changing the R group. First, we protect the diol part of a tartrate ester by using 2, 2-dimethoxy propane in the presence of a catalytic amount of p-toluene sulfonic acid (PTSA) in DCM at room temperature and it results in 85 % acetonide formation (R = Me) (A).¹⁰ Treatment of dimethyl L-tartrate with 2, 2-dimethoxy propane in the presence of $\text{BF}_3 \cdot \text{Et}_2\text{O}$ in ethyl acetate at 90 °C gives Dimethyl 2,3-O-methylene-L-tartrate with 55% yield

¹⁰ Kim, M. B.; Bae, J. S.; So, M. S.; Yoo, T. Y.; Chang, K. S.; Lee, H. J.; Kang, J. *Org. Lett.* **2001**, 3, 2349.

(B).¹¹ The reaction of tartrate ester with 4-heptanone in the presence of trimethyl orthoformate and a catalytic amount of p-toluenesulfonic acid in toluene at 80 °C gives colorless oil of 2,2-dipropyl-1,3-dioxolane derivative in 65 % yield (C).¹² Similarly, the reaction of tartrate ester with pinacolone in the presence of trimethyl orthoformate and p-toluenesulfonic acid in methanol at 70 °C provides an expected 1, 3-dioxolane derivative with 85% yield (D).¹² A similar method does not work for dioxolane E. Then to focus on dioxolane (E), tartrate ester was treated with pivalaldehyde in the presence of TsOH in pentane at 60 °C giving 55 % yield of expected dioxolane.¹³ After that, focus on the cyclic system, the reaction of tartrate ester with cyclohexanone in the presence of p-toluenesulfonic acid and ZnCl₂ in benzene at 120 °C gives 50 % of dioxolane (F).¹³ A similar process work with the cyclooctene system with a very low yield. Next, to improve yield tartrate ester was treated with cyclopentanone in the presence of trimethyl orthoformate and TsOH in toluene at 120 °C to provide 62 % yield (G).¹² Later, to protect with menthyl group, we react tartrate ester with (-) –menthone in the presence of trimethyl orthoformate and methane sulphonic acid in benzene at 90 C gives dioxolane in 20 % yield (H).



Scheme 2.10: Preparation of several protected dioxolane ester derivatives

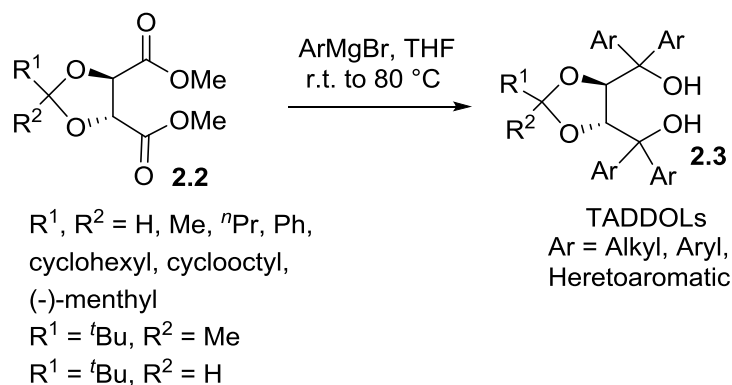
These 1, 3-dioxolane ester derivatives are used with a variety of in situ-formed Grignard reagents containing aliphatic, aromatic, heteroaromatic, and other groups to make several TADDOL motifs. For this to happen, we make Grignard first and then added a corresponding ester solution to it. Initially, screening of several aliphatic and aromatic Grignard reagent

¹¹ Gerard, B.; Sangji, S.; OLeary, J. D.; Porco, A. J. *J. Am. Chem. Soc.*, **2006**, *128*, 7754-7755

¹² Jozak, T.; Sun, Y.; Thiel, R. W. *New J. Chem.*, **2011**, *35*, 2114.

¹³ Seebach, D.; Beck, K. A.; Imwinkelried, R.; Roggo, S.; Wonnacott, A. *Helv. Chim. Acta.* **1987**, *70*, 954 – 974.

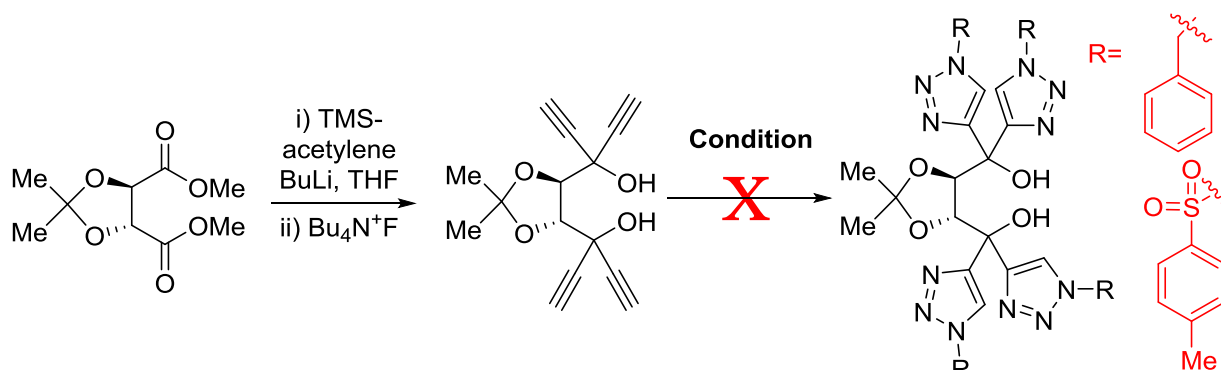
provide different TADDOLs scaffold. The presence of EWG and WDG at different positions of the benzene ring was well tolerated for TADDOL formation, except for ortho-fluoro substitution probably due to competitive benzyne intermediate formation. Further, Grignard reagents from polyaromatic hydrocarbons, like naphthalene, anthracene, and perylene work well for TADDOLs formation. Similarly, protective dioxolane tartrate with different acyclic ($R = H, Me, ^nPr, ^tBu, aryl$) as well as cyclic group ($R = cyclohexyl, octyl, (-)-menthyl$) also successfully gives a variety of TADDOL derivatives.



Scheme 2.11: Preparation of Taddol derivatives

Later on, with Movement to heteroaromatic substituents, the Grignard reagent from 2-bromothiophene successively provides corresponding TADDOL derivatives. To focus on another type of TADDOL (Scheme), we synthesized an alkyne TADDOL derivative with 81 % yield and use it further in click chemistry with several azide derivatives in different literature-known procedures,¹⁴ but remain unsuccessful.

¹⁴ Yoo, J. E.; Ahlquist, M.; Kim, H. S.; Bae, I.; Fokin, V. V.; Sharpless, B.; Chang, S. *Angew. Chem. Int. Ed.* **2007**, *46*, 1730–1733.; Andrew J. McCarroll, J. A.; Charles S. Matthews, S. C.; Geoffrey Wells, G.; Tracey D. Bradshaw, D. T.; Stevens, G. F. M. *Org. Biomol. Chem.* **2010**, *8*, 2078–2084.; Wang, F.; Fu, H.; Jiang, Y.; Zhao, Y. *Adv. Synth. Catal.* **2008**, *350*, 1830 – 1834.; Liu, Y.; Wang, X.; Xu, J.; Zhang, Q.; Zhao, Y.; Hu, Y. *Tetrahedron.* **2011**, *67*, 6294-6299.

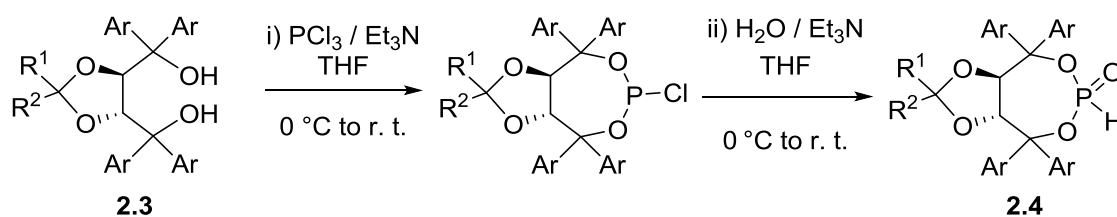


Condition: i) azide, 2,6-lutidine, CuI, CHCl₃, 0 °C-r.t.; **or** ii) azide, CuSO₄·5H₂O, sodium ascorbate, ^tBuOH/ H₂O, r.t.; **or** iii) azide, CuBr, PhSMc, H₂O, r.t.; **or** iv) azide, Cu(OAc)₂·H₂O, 2-aminophenol, MeCN, r.t.

Scheme 2.12: Preparation of triazole ring containing TADDOL derivatives

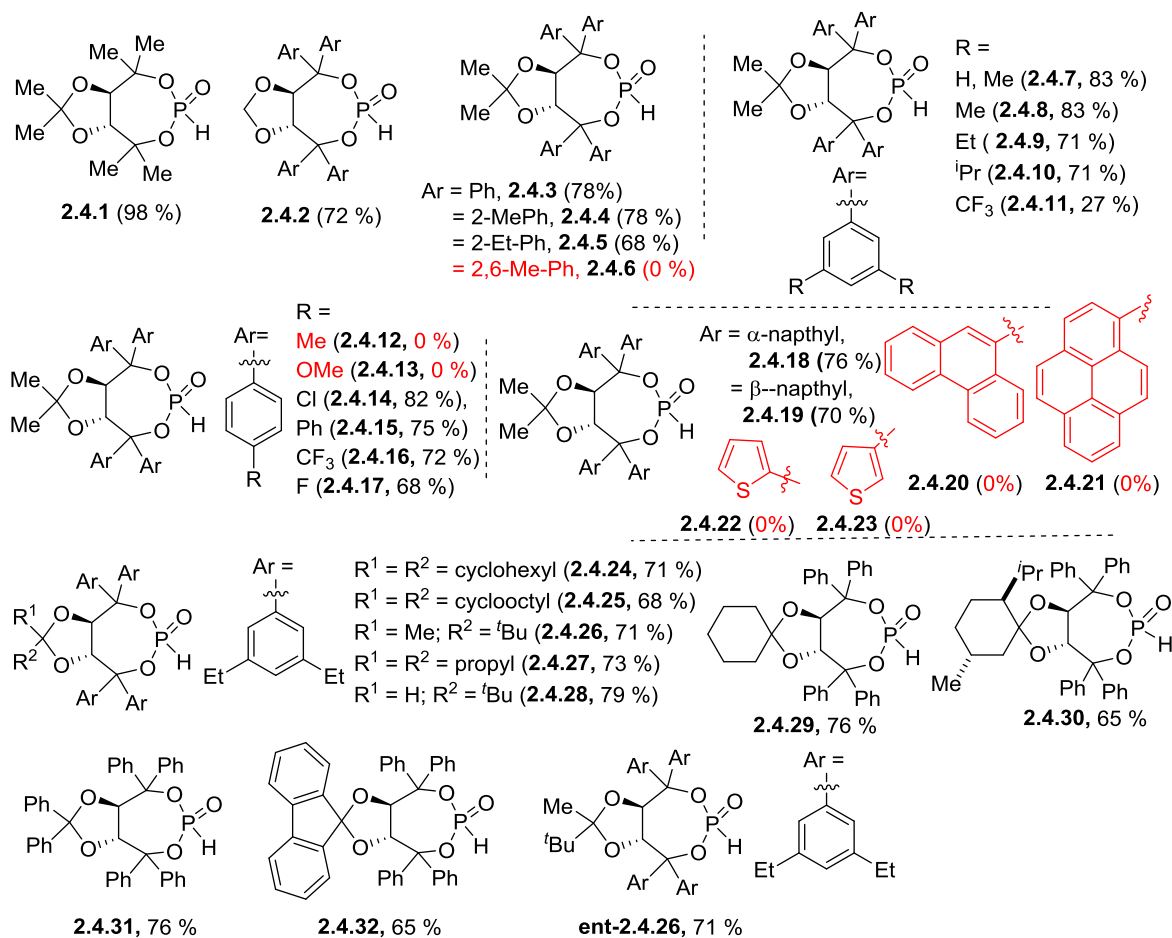
As the TADDOLs are Bench stable to handle, we store these compounds in sufficient quantity and further use them for phosphite preparation depending upon the requirement.

After getting numerous TADDOLs chiral diol in hand, we focus on the synthesis of the corresponding phosphites by following the modified Johnson scheme.¹⁵ Modification is done only in operating procedures only for easy to handle. The involvement of these TADDOLs in phosphite formation explores the chiral phosphite catalysts library. The phosphite formation, having a methyl group at both the ortho position (compound-2.4.6) and methyl, methoxy at the para position (compound-2.4.12, 2.4.13) remains unsuccessful due to column instability. Moving from the substituted aromatic to a poly-aromatic group, α - and β - naphthyl provide phosphites, but, anthracenyl and pyrenyl do not work probably due to the steric hindrance being more predominant here. Further changing to a heteroaromatic group, 2- and 3-thiophenyl also not works.



Scheme 2.13: Preparation of phosphites derivatives

¹⁵ Linghu, X.; Potnick, R. J.; Johnson, S. J. *J. Am. Chem. Soc.* **2004**, *126*, 3070.



Scheme 2.13: Several number of chiral phosphite derivatives

2.5 Conclusion

Although the reaction sequence is known, by modifying it to an operational simple method we synthesize numerous known and new chiral phosphites. In terms of stability of phosphites, except for a few, the maximum numbers of synthesis TDDOL-derived phosphites are bench stable and easy to store. Finally, These Phosphites are ready to use for the asymmetric functionalization of pyridines.

2.6 Experimental Procedures

2.6.1 General Information

The rearrangement reactions were carried out with anhydrous solvents in flame-dried glass wares under anhydrous argon and oxygen free conditions. All other reactions were carried out under anhydrous and argon atmosphere. THF was used from MBRAUN (MB-SPS-COMPACT) solvent purification system. All other solvents were purchased anhydrous and stored under argon over 4 Å molecular sieves. Analytical thin-layer chromatography was performed on glass plates pre-coated with silica gel (Silica Gel 60 F254; Merck). Plates were visualized using UV light ($\lambda = 254$ nm) and then stained with either aqueous basic potassium permanganate (KMnO₄) or p-anisaldehyde and developed upon heating in Hitachi heat gun. Flash chromatography was performed using silica gel (Merck and Spectrochem, 230-400 mesh), eluting with solvents as indicated. Flash column was performed using Sebo aquarium air pump (SB-548A). ¹H, ¹³C and ³¹P spectrum were acquired in deuterated solvents at room temperature on Bruker: Ultrashield 400 MHz, Ultrashield 500 MHz and JEOL 400 spectrometer. Chemical shifts (δ) are reported for ¹H NMR in ppm from TMS as internal standard and ¹³C from the residual solvent peak. ¹H NMR spectra are reported as follows: chemical shift (δ ppm), multiplicity, coupling constant (Hz), and integration. Data for ¹³C NMR spectra are reported in terms of chemical shift (δ ppm). Melting points were recorded in Buchi Melting Point B-540 instrument and reported in °C. FT-IR were analyzed in Bruker ALPHA instrument and reported as cm⁻¹. High resolution (HRMS) mass spectral analyses were recorded by High-resolution mass spectrometry using ESI TOF mass analyzer.

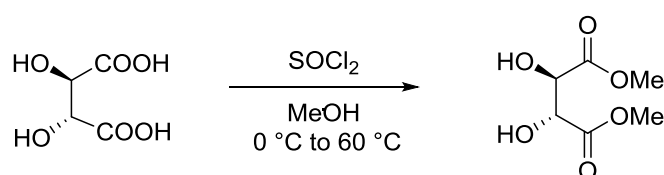
2.6.2 Materials

Commercially available reagents were purchased and used as obtained. Generally, Grignard solution was prepared to use in situ by following literature procedure. The literature reported spectral data were compared favorably with our ¹H NMR spectra of these compounds.

2.6.3 General scheme for the synthesis of chiral phosphite

TADDOLs and phosphites were prepared by following the modified literature procedures.¹⁶

2.6.3.1 Preparation of (2S,3S)-dimethyl-2,3-dihydroxysuccinate (2.1)¹⁷

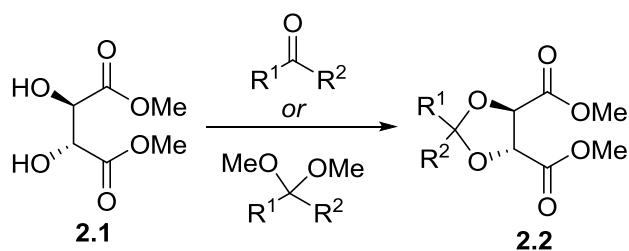


¹⁶ Linghu, X.; Potnick, R. J.; Johnson, S. J. *J. Am. Chem. Soc.* **2004**, *126*, 3070-3071.

¹⁷ Xing Gao, X.; Han, J.; Wang, L. *Org. Lett.* **2015**, *17*, 4596-4599.

A flame dried two neck round bottomed flask with magnetic stir bar and condenser was charged with (R,R)- tartaric acid (30.0 g, 0.199 mol). The apparatus was purged with Ar, and methanol (95 mL) was added. The reaction flask was fitted with an outlet at the top of a condenser, which was connected to a bubbler containing a saturated aqueous solution of NaHCO₃. The reaction flask and the bubbler were both cooled to 0 °C and SOCl₂ (74.3 mL, 1.02 mol) was added drop wise to the reaction. Once the evolution of HCl (g) slowed, the reaction was removed from the ice bath and heated to reflux for 4 hours. The reaction was then cooled to room temperature and condensed in vacuo until only a viscous oil remained. The crude material was then diluted with distilled H₂O (50 mL) and EtOAc (50 mL). The layers were separated and the aqueous layer was then further extracted with EtOAc (10 x 50 mL). The combined organics were dried over Na₂SO₄, filtered and condensed in vacuo. The resulting crude was purified via silica column chromatography by using 20-25 % EtOAc/ pet ether as eluent to obtain pure (2R,3R)-dimethyl 2,3-dihydroxysuccinate (**2.1**) in 65 % Yield.

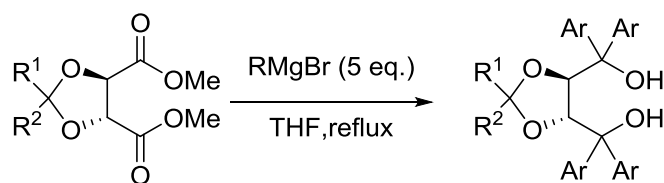
2.6.3.2 Preparation of 1,3-dioxolane-tartrate ester derivatives¹⁸



A two neck round-bottomed flask with magnetic stir bar and condenser was charged with (R,R)-dimethyl tartrate (20-50 mmol) and catalytic amount of acid and/or others (mentioned from literature¹⁸). The apparatus was purged with Argon gas, and added required solvent. Protecting agent was added, and the reaction was brought to reflux and stirred for 4 hours (depends on literature reported reaction condition). The reaction was then cooled to room temperature and condensed in vacuo. The crude residue was then diluted with distilled H₂O (50 mL) and EtOAc (50 mL). The layers were separated and the aqueous layer was then extracted with EtOAc (3 x 50 mL). The combined organics were dried over Na₂SO₄, filtered and condensed in vacuo. The crude material was purified via silica column chromatography by using 15-20 % EtOAc/ pet ether as eluent to obtain pure title compound (upto 85% yield).

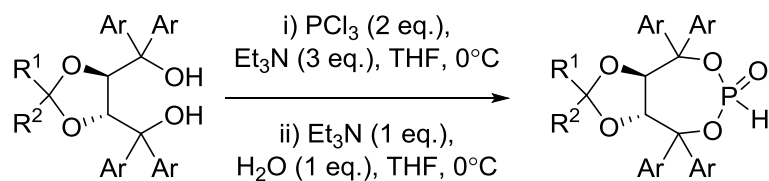
2.6.3.3 Preparation of TADDOL derivatives (2.3)

¹⁸ Kim, M. B.; Bae, J. S.; So, M. S.; Yoo, T. Y.; Chang, K. S.; Lee, H. J.; Kang, J. *Org. Lett.* **2001**, 3, 2349.; Gerard, B.; Sangji, S.; OLeary, J. D.; Porco, A. J. *J. Am. Chem. Soc.*, **2006**, 128, 7754-7755.; Jozak, T.; Sun, Y.; Thiel, R. W. *New J. Chem.*, **2011**, 35, 2114.; Seebach, D.; Beck, K. A.; Imwinkelried, R.; Roggo, S.; Wonnacott, A. *Helv. Chim. Acta.* **1987**, 70, 954 – 974.



A 250 ml two neck round-bottom flask with a magnetic stir bar and condenser was charged with Magnesium turnings (576 mg, 24 mmol, 1.2 equiv.) under argon atmosphere. Then, an anhydrous THF (20 mL), and a grain of iodine was taken. Initially, RB was placed at a optimum temperature, 0 °C- r.t.. The corresponding Bromo derivatives (20 mmol) was taken in THF (5-10 mL) and then added dropwise to start grignard reaction. Then complete consumption of magnesium was observed at room temperature to reflux at 80 °C. After complete formation of Grignard reagent, the reaction mixture is allowed to cool to room temperature. Finally, maintain 0 °C by an ice bath and a solution of TADDOL-based dicarboxylate (**2.2**, 4 mmol.) in THF (5-10 ml) was slowly added to the grignard solution by a syringe at 0 °C over 30 min. After completion of the addition, the reaction mixture was heated at reflux for 8-14 h and also monitor by TLC analysis. After complete conversion, reaction mixture was cooled to room temperature and carefully added an aqueous saturated ammonium chloride solution (5-10 mL), water (50 mL) to quench the reaction. After that, the total reaction mixture was extracted with ethyl acetate (3 times) and the combined organic layer was washed with brine (10 mL). Finally, Collect the total organic layer, dry over Na₂SO₄ and concentrated under reduced pressure to give yellowish foam. Further, crude residue was purified by silica gel column chromatography by using ethyl acetate and pet ether combination as eluent to provide pure TADDOL derivatives (**2.3**) in 70-90% yield.

2.6.3.4 Preparation of TADDOLs derived phosphite catalyst (**2.4**)



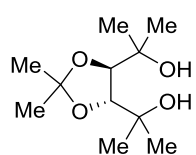
To a dry round-bottom flask with magnetic stir bar was added 10 mL dry THF, PCl₃ (2.0 eq.), and tri-ethylamine (3.0 eq.) at 0 °C via an ice bath. The mixture was stir for 15-20 min and to this solution was added a solution of diol **2.3** (1 equiv.) in 4 mL THF via syringe, drop wise, under argon at 0 °C. The reaction was allowed to stir at the same temperature for 1 h. To the resulting solution was added tri-ethylamine (1.0 eq.) and H₂O (1.0 eq.) via a syringe at 0 °C. The reaction mixture was allowed to warm to ambient temperature and stir for 1 h. Solid tri-ethyl ammonium chloride was removed by filtration through crucible and the solvent was

removed with a rotary evaporator. The crude product was purified through silica gel flash column chromatography by eluting EtOAc-pet ether solvent system to afford the pure phosphites (**2.4**) in 65-98% yield.

2.7 Spectral data

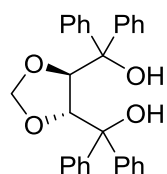
2.7.1 Spectral Data of Alcohols

(4*R*, 5*R*)-2, 2-dimethyl-tetramethyl-TADDOL (2.3.1)



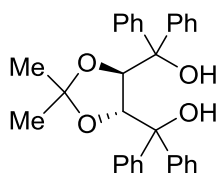
The titled compound was prepared by following the literature procedure,¹⁹ obtained as a white solid (600 mg, 76 %). R_f (Ethyl acetate/Pet. ether = 30:70) = 0.3. The spectral values were matched favorably with literature values.

((4*R*,5*R*)-5-(ethoxydiphenylmethyl)-1,3-dioxolan-4-yl)diphenylmethanol (2.3.2)



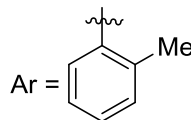
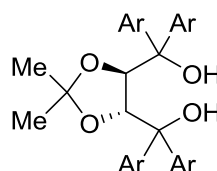
The titled compound was prepared by following the literature procedure,²⁰ obtained as a white solid. R_f (Ethyl acetate/Pet. ether = 30:70) = 0.5. The spectral values were matched favorably with literature values.

((4*R*,5*R*)-2,2-dimethyl-1,3-dioxolane-4,5-diyl)bis(diphenylmethanol) (3.2.3)



The titled compound was prepared by following the literature procedure,¹⁸ obtained as a white solid. R_f (Ethyl acetate/Pet. ether = 30:70) = 0.4. The spectral values were matched favorably with literature values.

((4*R*,5*R*)-2,2-dimethyl-1,3-dioxolane-4,5-diyl)bis(di-*o*-tolylmethanol) (2.3.4)

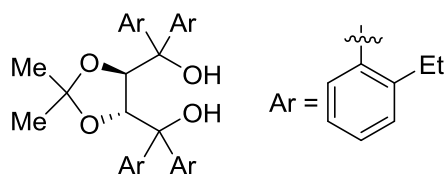


The titled compound was prepared by following the literature procedure,²¹ obtained as a white solid. R_f (Ethyl acetate/Pet. ether = 30:70) = 0.4. The spectral values were matched favorably with literature values.

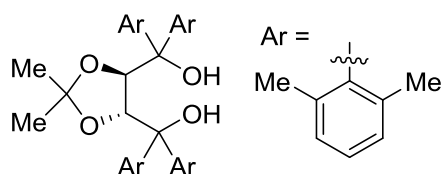
¹⁹ Linghu, X.; Potnick, R. J.; Johnson, S. J. *J. Am. Chem. Soc.* **2004**, *126*, 3070-3071

²⁰ Seebach, D.; Beck, A. K.; Imwinkelried, R.; Roggo, S.; Wonnacott, A. *Helvetica. Chemica. Acta.* **1987**, *70*, 954-974.

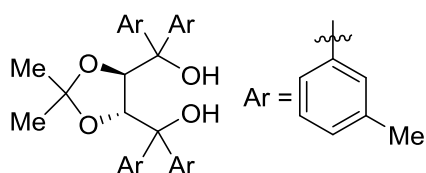
²¹ Gao, X.; Han, J.; Wang, L. *Org. Lett.* **2015**, *17*, 4596-4599.

((4R,5R)-2,2-dimethyl-1,3-dioxolane-4,5-diyl)bis(bis(o-ethylphenyl)methanol) (2.3.5)

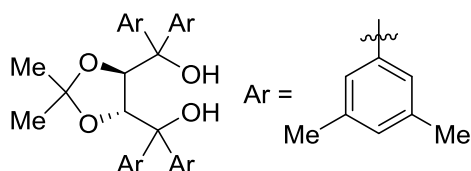
The titled compound was prepared by following the literature procedure,²² obtained as a white solid. R_f (Ethyl acetate/Pet. ether = 30:70) = 0.4. The spectral values were matched favorably with literature values

((4R,5R)-2,2-dimethyl-1,3-dioxolane-4,5-diyl)bis(bis(2,6-dimethylphenyl)methanol) (2.3.6)**(2.3.6)**

The titled compound was prepared by following the literature procedure, obtained as a white solid with very low yield and complex NMR. R_f (Ethyl acetate/Pet. ether = 30:70) = 0.45.

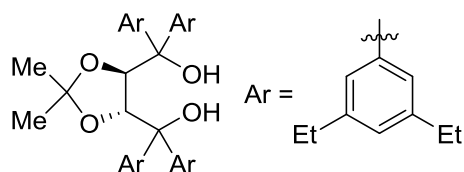
((4R,5R)-2,2-dimethyl-1,3-dioxolane-4,5-diyl)bis(di-m-tolylmethanol) (2.3.7)

The titled compound was prepared by following the literature procedure,²⁰ obtained as a white solid. R_f (Ethyl acetate/Pet. ether = 30:70) = 0.4. The spectral values were matched favorably with literature values.

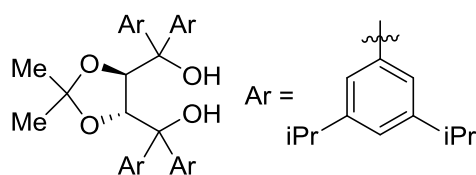
((4R,5R)-2,2-dimethyl-1,3-dioxolane-4,5-diyl)bis(bis(3,5-dimethylphenyl)methanol) (2.3.8)**(2.3.8)**

The titled compound was prepared by following the literature procedure,²⁰ obtained as a white solid. R_f (Ethyl acetate/Pet. ether = 30:70) = 0.45. The spectral values were matched favorably with literature values.

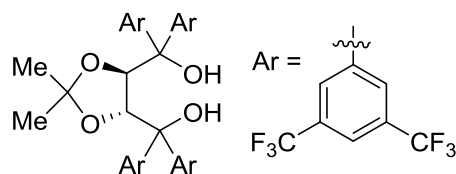
²² Schmitz, C.; Leitner, W.; Franciò, G. *Chem. Eur. J.* **2015**, *21*,10696–1070.

((4R,5R)-2,2-dimethyl-1,3-dioxolane-4,5-diyl)bis(bis(3,5-diethylphenyl)methanol) (2.3.9)

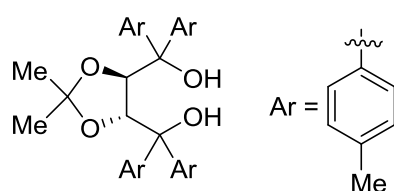
The titled compound was prepared by following the literature procedure,²³ obtained as a white solid. R_f (Ethyl acetate/Pet. ether = 30:70) = 0.5. The spectral values were matched favorably with literature values.

((4R,5R)-2,2-dimethyl-1,3-dioxolane-4,5-diyl)bis(bis(3,5-diisopropylphenyl)methanol) (2.3.10)

The titled compound was prepared by following the literature procedure,²⁴ obtained as a white solid. R_f (Ethyl acetate/Pet. ether = 30:70) = 0.5. The spectral values were matched favorably with literature values.

((4R,5R)-2,2-dimethyl-1,3-dioxolane-4,5-diyl)bis(bis(3,5-di(trifluoromethyl)phenyl)methanol) (2.3.11)

The titled compound was prepared by following the literature procedure,²⁵ obtained as a white solid. R_f (Ethyl acetate/Pet. ether = 30:70) = 0.55. The spectral values were matched favorably with literature values.

((4R, 5R)- 5-(bis(4 -chlorophenyl)(ethoxy)methyl)-2, 2-dimethyl-1, 3-dioxolan- 4-yl)bis(4 -methylphenyl)methanol (2.3.12)

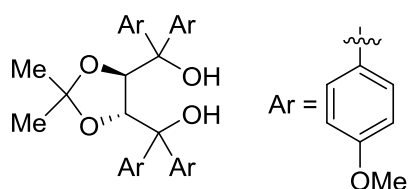
The titled compound was prepared by following the literature procedure,²⁰ obtained as a white solid. R_f (Ethyl acetate/Pet. ether = 30:70) = 0.5. The spectral values were matched favorably with literature values.

((4R, 5R)- 5-(bis(4 -chlorophenyl)(ethoxy)methyl)-2, 2-dimethyl-1, 3-dioxolan- 4-yl)bis(4 -methoxyphenyl)methanol (2.3.13)

²³ Kliman, L.T.; Mlynarski, S.N.; Morken, J.P. *J. Am. Chem. Soc.* **2009**, *131*, 13210-13211.

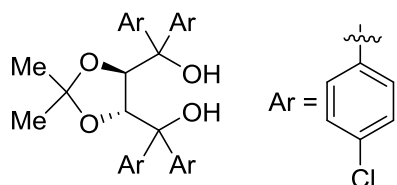
²⁴ Coombs, J. R.; Haeffner, F.; Kliman, L.T.; Morken, J. P. *J. Am. Chem. Soc.* **2013**, *135*, 11222-11231.

²⁵ Hintermann, L.; Perssghini, M.; Togni, A. *Beilstein J. Org. Chem.* **2011**, *7*, 1421-1435.



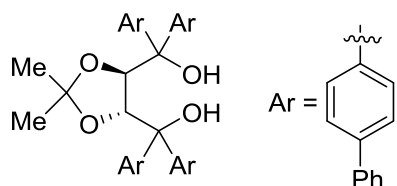
The titled compound was prepared by following the literature procedure,²⁶ obtained as a white solid. R_f (Ethyl acetate/Pet. ether = 30:70) = 0.5. The spectral values were matched favorably with literature values.

((4R, 5R)- 5-(bis(4 -chlorophenyl)(ethoxy)methyl)-2, 2-dimethyl-1, 3-dioxolan- 4-yl)bis(4 -chlorophenyl)methanol (2.3.14)



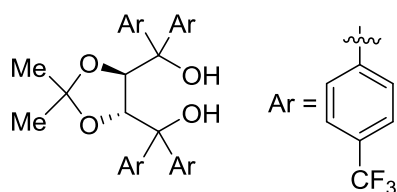
The titled compound was prepared by following the literature procedure,²⁰ obtained as a white solid. R_f (Ethyl acetate/Pet. ether = 30:70) = 0.5. The spectral values were matched favorably with literature values.

((4R, 5R)- 5-(bis(4 -chlorophenyl)(ethoxy)methyl)-2, 2-dimethyl-1, 3-dioxolan- 4-yl)bis(4 -biphenyl)methanol (2.3.15)



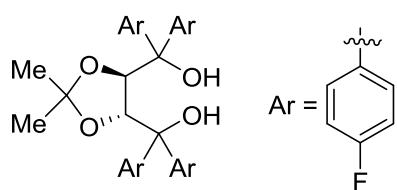
The titled compound was prepared by following the literature procedure,²⁰ obtained as a white solid. R_f (Ethyl acetate/Pet. ether = 30:70) = 0.6. The spectral values were matched favorably with literature values.

((4R, 5R)- 5-(bis(4 -chlorophenyl)(ethoxy)methyl)-2, 2-dimethyl-1, 3-dioxolan- 4-yl)bis(4 -trifluorophenyl)methanol (2.3.16)



The titled compound was prepared by following the literature procedure,²⁷ obtained as a white solid. R_f (Ethyl acetate/Pet. ether = 30:70) = 0.6. The spectral values were matched favorably with literature values.

((4R, 5R)- 5-(bis(4 -chlorophenyl)(ethoxy)methyl)-2, 2-dimethyl-1, 3-dioxolan- 4-yl)bis(4 -fluoro phenyl)methanol (2.3.17)



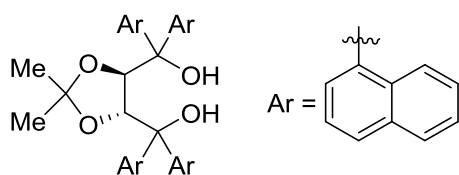
The titled compound was prepared by following the literature procedure,²⁰ obtained as a white solid. R_f (Ethyl acetate/Pet.

²⁶ Teller, H.; Flugge, S.; Goddard, R.; Furstner, A. *Angew. Chem. Int. Ed.* **2010**, *49*, 1949-1953.

²⁷ Allmendinger, S.; Kinuta, H.; Breit, B. *Adv. Synth. Catal.* **2015**, *357*, 41 – 45.

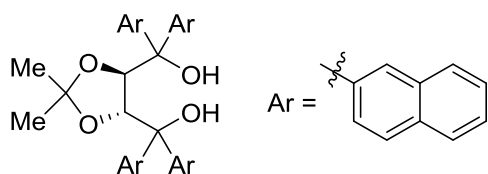
ether = 30:70) = 0.5. The spectral values were matched favorably with literature values.

((4R,5R)-2,2-dimethyl-1,3-dioxolane-4,5-diyl)bis(di(naphthalen-1-yl)methanol) (2.3.18)



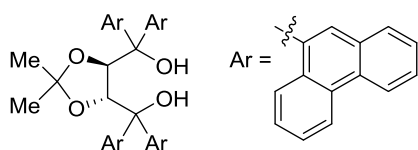
The titled compound was prepared by following the literature procedure,²⁸ obtained as a white solid. R_f (Ethyl acetate/Pet. ether = 30:70) = 0.45. The spectral values were matched favorably with literature values.

((4R,5R)-2,2-dimethyl-1,3-dioxolane-4,5-diyl)bis(di(naphthalen-2-yl)methanol) (2.3.19)



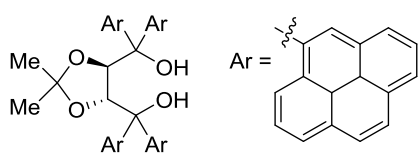
The titled compound was prepared by following the literature procedure,²⁷ obtained as a white solid. R_f (Ethyl acetate/Pet. ether = 30:70) = 0.45. The spectral values were matched favorably with literature values.

((4R,5R)-2,2-dimethyl-1,3-dioxolane-4,5-diyl)bis(di(phenanthren-2-yl)methanol) (2.3.20)



The titled compound was prepared by following the literature procedure,²⁹ obtained as a white solid. R_f (Ethyl acetate/Pet. ether = 30:70) = 0.5. The spectral values were matched favorably with literature values.

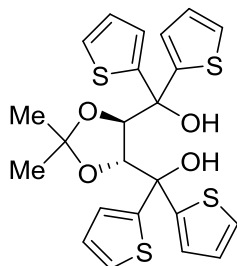
((4R,5R)-2,2-dimethyl-1,3-dioxolane-4,5-diyl)bis(di(pyren-1-yl)methanol) (2.3.21)



The titled compound was prepared by following the literature procedure,²⁸ obtained as a white solid. R_f (Ethyl acetate/Pet. ether = 30:70) = 0.6. The spectral values were matched favorably with literature values.

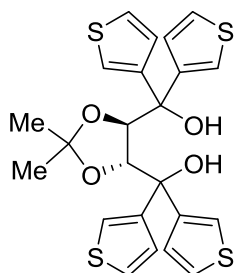
²⁸ Linghu, X.; Potnick, R. J.; Johnson, S. J. *J. Am. Chem. Soc.* **2004**, *126*, 3070-3071.; Allmendinger, S.; Kinuta, H.; Breit, B. *Adv. Synth. Catal.* **2015**, *357*, 41 – 45.

²⁹ Gerard, B.; Sangji, S.; O'Leary, J. D.; Jr. Porco, A. J. *J. Am. Chem. Soc.* **2006**, *128*, 7754-7755.

((4R,5R)-2,2-dimethyl-1,3-dioxolane-4,5-diyl)bis(di(thiophen-2-yl)methanol) (2.3.22)

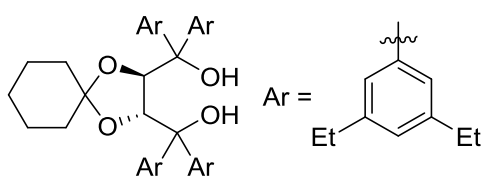
The titled compound was prepared by following the literature procedure,³⁰ obtained as a white solid. R_f (Ethyl acetate/Pet. ether = 40:60) = 0.5. The spectral values were matched favorably with literature values.

$^1\text{H NMR}$ (400 MHz, CDCl_3) δ 1.25 (s, 6 H), 4.42 (s, 2 H), 4.97 (s, 2 H), 6.91 (dd, $J = 5.07, 3.69$ Hz, 2 H), 7.04 (dd, $J = 5.13, 3.63$ Hz, 2 H), 7.08 (dd, $J = 3.63, 1.25$ Hz, 2 H), 7.23 (dd, $J = 5.07, 1.19$ Hz, 2 H), 7.27 (dd, $J = 3.56, 1.19$ Hz, 2 H), 7.31 (dd, $J = 5.07, 1.19$ Hz, 2 H); $^{13}\text{C NMR}$ (101 MHz, CDCl_3) δ 27.11, 75.72, 82.90, 110.02, 125.41, 125.65, 125.81, 126.53, 126.57, 126.60, 145.74, 149.83. LCMS (ESI) m/z Calculated for $\text{C}_{23}\text{H}_{22}\text{O}_4\text{S}_4\text{Na}$ $[\text{M}+\text{Na}]^+$: 513.02; found: 513.

((4R,5R)-2,2-dimethyl-1,3-dioxolane-4,5-diyl)bis(di(thiophen-3-yl)methanol) (2.3.23)

The titled compound was prepared by following the literature procedure, obtained as a white solid. R_f (Ethyl acetate/Pet. ether = 40:60) = 0.5.

$^1\text{H NMR}$ (400 MHz, CDCl_3) δ 1.15 (s, 6 H) 4.24 (s, 2 H) 4.60 (br. s., 2 H) 6.99 (dd, $J = 4.94, 1.44$ Hz, 2 H) 7.18 (dd, $J = 5.00, 1.25$ Hz, 2 H) 7.20 - 7.24 (m, 4 H) 7.27 (dd, $J = 5.00, 3.13$ Hz, 2 H) 7.40 (dd, $J = 3.06, 1.31$ Hz, 2 H); $^{13}\text{C NMR}$ (101 MHz, CDCl_3) δ 26.97, 75.15, 82.09, 109.16, 122.81, 123.00, 124.66, 125.43, 126.86, 128.27, 143.92, 146.43.; LCMS (ESI) m/z Calculated for $\text{C}_{23}\text{H}_{22}\text{O}_4\text{S}_4\text{Na}$ $[\text{M}+\text{Na}]^+$: 513.02; found: 513.

((2R,3R)-1,4-dioxaspiro[4.5]decane-2,3-diyl)bis(bis(3,5-diethylphenyl)methanol) (2.3.24)

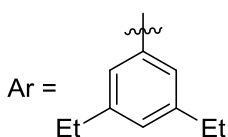
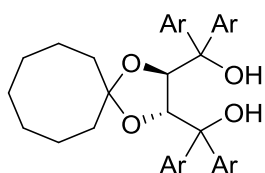
The titled compound was prepared by following the literature procedure, obtained as a white solid. R_f (Ethyl acetate/Pet. ether = 30:70) = 0.6. MP = 60.4 – 61.8 °C. $^1\text{H NMR}$ (400 MHz, CDCl_3) δ 1.08 - 1.17

(m, 15H), 1.18 - 1.25 (m, 15H), 1.39 (dt, $J = 12.78, 6.39$ Hz, 4H), 2.50 - 2.64 (m, 16H), 3.91 (br. s., 2H), 4.60 (s, 2H), 6.95 (s, 2H), 6.91 (s, 2H), 6.99 - 7.10 (m, 4H), 7.12 - 7.23 (m, 4H); $^{13}\text{C NMR}$ (100 MHz, CDCl_3) δ 15.53, 15.86, 24.00, 25.09, 28.93, 29.02, 36.56, 80.57, 109.58, 124.67, 125.85, 126.04, 126.45, 142.69, 142.73, 143.61, 146.24. FTIR (cm^{-1}): 3014,

³⁰ He, C.; Hou, M.; Zhu, Z.; Gu, Z. *ACS Catal.* **2017**, 7, 5316–5320.

2970, 2930, 2873, 1600, 1520, 1325, 1164, 1012, 923, 876, 734, 704. **LCMS** (ESI) m/z Calculated for $C_{50}H_{66}O_4$ $[M+Na]^+$: 753.4; found: 753.3

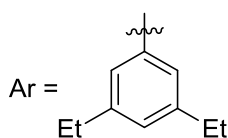
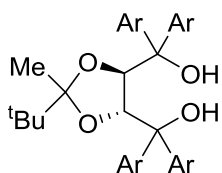
((2R, 3R)-3-(bis(3, 5-diethylphenyl)(ethoxy)methyl)-1, 4-dioxaspiro[4. 7]dodecan-2-yl)bis(3, 5-diethylphenyl)methanol (2.3.25)



The titled compound was prepared by following the literature procedure, obtained as a white solid. R_f (Ethyl acetate/Pet. ether = 30:70) = 0.65. MP = 85.3 – 87.1 °C. 1H NMR (400 MHz, $CDCl_3$) δ 1.14 (t, J

= 7.52 Hz, 12H), 1.21 (t, J = 7.89 Hz, 12 H), 1.37 - 1.45 (m, 14H), 2.54 (q, J = 7.52 Hz, 8H), 2.64 (q, J = 7.52 Hz, 8H), 4.01 (br. s., 2H), 4.49 (s, 2H), 6.90 (s, 2H), 6.95 (s, 2H), 7.01 (s, 4H), 7.18 (s, 4H); ^{13}C NMR (100 MHz, $CDCl_3$) δ 15.50, 15.95, 21.76, 24.04, 27.76, 28.91, 29.06, 29.69, 35.56, 78.29, 80.43, 112.05, 124.68, 125.84, 126.03, 126.43, 142.70, 143.55, 146.20. **FTIR** (cm^{-1}): 3322, 2962, 2927, 2869, 1599, 1457, 1373, 1262, 1151m 874, 743. **LCMS** (ESI) m/z Calculated for $C_{52}H_{70}O_4Na$ $[M+Na]^+$: 781.5; found: 781.3.

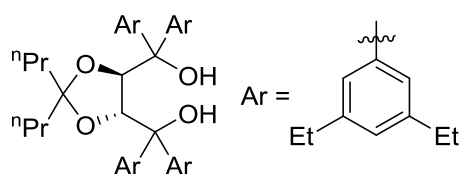
((4R,5R)-2-(tert-butyl)-2-methyl-1,3-dioxolane-4,5-diyl)bis(bis(3,5-diethylphenyl) methanol) (2.3.26)



The titled compound was prepared by following the literature procedure, obtained as a white solid. R_f (Ethyl acetate/Pet. ether = 30:70) = 0.52. MP = 78.5 – 81.1 °C. $[\alpha]_D^{25}$ +22.8 (c = 3.0 CH_2Cl_2). 1H NMR (500 MHz,

$CDCl_3$) δ 0.62 (s, 9H), 0.78 (s, 3H), 1.16 (q, J = 7.63 Hz, 12H), 1.15 (q, J = 7.63 Hz, 12H), 2.52 - 2.61 (m, 16H), 4.42 - 4.47 (m, 3H), 4.56 (s, 1H), 6.90 - 6.96 (m, 4H), 7.06 (s, 6H), 7.13 (s, 2H); ^{13}C NMR (126 MHz, $CDCl_3$) δ 15.42, 15.51, 15.92, 19.64, 24.85, 28.88, 28.94, 28.98, 38.91, 78.21, 78.84, 79.02, 80.84, 112.61, 124.40, 124.77, 126.03, 126.10, 126.19, 126.41, 126.46, 126.48, 142.48, 142.60, 142.66, 143.54, 146.64, 146.70. **FTIR** (cm^{-1}): 3013, 2967, 2932, 2873, 1600, 1520, 1325, 1164, 1002, 922, 876. **LCMS** (ESI) m/z Calculated for $C_{50}H_{38}O_4$ $[M+Na]^+$: 755.5; found: 755.3.

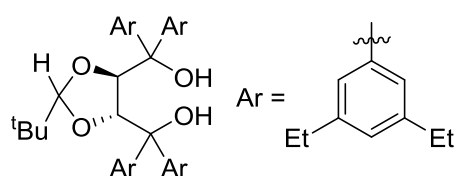
((4R,5R)-5-(bis(3,5-diethylphenyl)(ethoxy)methyl)-2,2-dipropyl-1,3-dioxolan-4-yl)bis(3,5-diethylphenyl)methanol (2.3.27)



The titled compound was prepared by following the literature procedure, obtained as a white solid. R_f (Ethyl acetate/Pet. ether = 30:70) = 0.62. MP = 63.5 – 64.8 °C.

$^1\text{H NMR}$ (500 MHz, CDCl_3) δ 0.68 - 0.73 (m, 6H), 0.95 - 1.03 (m, 4H), 1.14 (t, $J = 7.63$ Hz, 12H), 1.17 - 1.24 (m, 15H), 1.24 - 1.27 (m, 1H), 2.54 (q, $J = 7.50$ Hz, 8H), 2.62 (q, $J = 7.50$ Hz, 8H), 4.09 (s, 2H), 4.52 (s, 2H), 6.91 (s, 2H), 6.95 (s, 2H), 7.03 (s, 4H), 7.15 (s, 4H); $^{13}\text{C NMR}$ (125 MHz, CDCl_3) δ 14.30, 15.46, 16.01, 17.05, 28.91, 29.02, 39.85, 78.45, 80.27, 111.31, 124.64, 126.05, 126.52, 142.60, 142.74, 143.61, 146.27. **FTIR** (cm^{-1}): 3231, 2962, 2929, 2872, 1730, 1600, 1457, 1373, 1169, 1073, 966, 873. **LCMS** (ESI) m/z Calculated for $\text{C}_{51}\text{H}_{70}\text{O}_4\text{Na}$ $[\text{M}+\text{Na}]^+$: 769.5; found: 769.3

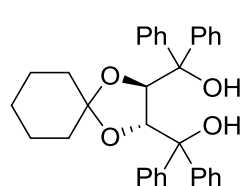
((4R, 5R)-5-(bis(3, 5-diethylphenyl)(ethoxy)methyl)-2-(tert-butyl)-1, 3-dioxolan-4-yl)bis(3, 5-diethylphenyl)methanol (2.3.28)



The titled compound was prepared by following the literature procedure, obtained as a white solid. R_f (Ethyl acetate/Pet. ether = 30:70) = 0.55. MP = 58.2 – 60.1 °C.

$^1\text{H NMR}$ (400 MHz, CDCl_3) δ 0.70 (s, 9H), 0.92 (s, 1H), 1.07 (t, $J = 7.63$ Hz, 6H), 1.15 (s, 1H), 1.17 (s, 4H), 1.18 (s, 2H), 1.19 (s, 4H), 1.20 (s, 3H), 1.21 (s, 2H), 1.22 (s, 2H), 2.49 - 2.56 (m, 8H), 2.57 - 2.62 (m, 8H), 3.54 (s, 1H), 3.78 (s, 1H), 4.82 (d, $J = 6.10$ Hz, 1H), 4.86 (d, $J = 6.10$ Hz, 1H), 6.85 (s, 1H), 6.91 (d, $J = 9.16$ Hz, 3H), 7.04 (s, 2H), 7.07 (s, 2H), 7.13 (s, 2H), 7.18 (s, 2H). $^{13}\text{C NMR}$ (100 MHz, CDCl_3) δ 15.57, 15.65, 15.78, 24.26, 25.99, 28.91, 28.96, 33.58, 78.06, 78.50, 79.80, 81.41, 109.32, 124.17, 124.29, 125.22, 125.55, 125.97, 126.14, 126.32, 142.36, 143.03, 143.09, 143.68, 144.50, 145.03, 147.33. **FTIR** (cm^{-1}): 3353, 2964, 2930, 2870, 1729, 1599, 1456, 1109, 906, 741.

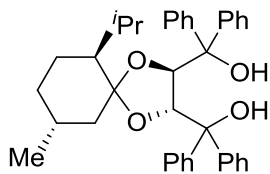
((2R,3R)-1,4-dioxaspiro[4.5]decane-2,3-diyl)bis(diphenylmethanol) (2.3.29)



The titled compound was prepared by following the literature procedure,³¹ obtained as a white solid. R_f (Ethyl acetate/Pet. ether = 30:70) = 0.6. The spectral values were matched favorably with literature values.

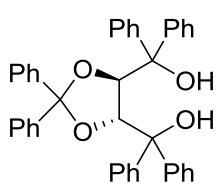
³¹ Gao, X.; Han, J.; Wang, L. *Org. Chem. Front.* **2016**, 3, 656-660.

((2R,3R,6S,9R)-3-(ethoxydiphenylmethyl)-6-isopropyl-9-methyl-1,4-dioxaspiro[4.5]decan-2-yl)diphenylmethanol (2.3.30)



The titled compound was prepared by following the literature procedure,³² obtained as a white solid. R_f (Ethyl acetate/Pet. ether = 30:70) = 0.6. The spectral values were matched favorably with literature values.

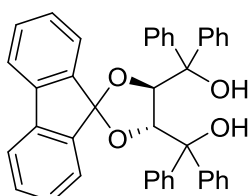
((4R,5R)-2,2-diphenyl-1,3-dioxolane-4,5-diyl)bis(diphenylmethanol) (2.3.31)



The titled compound was prepared by following the literature procedure,³³ obtained as a white solid. R_f (Ethyl acetate/Pet. ether = 30:70) = 0.5. The spectral values were matched favorably with literature values.

$^1\text{H NMR}$ (400 MHz, CDCl_3) δ 1.97 (s, 2 H), 5.46 (s, 2 H), 6.80 - 6.89 (m, 6 H), 6.93 - 6.98 (m, 4 H), 7.10 - 7.12 (m, 6 H), 7.14 - 7.16 (m, 3 H), 7.17 - 7.20 (m, 4 H), 7.22 - 7.26 (m, 4 H), 7.38 - 7.44 (m, 4 H). **LCMS** (ESI) m/z . Calculated for $\text{C}_{41}\text{H}_{34}\text{O}_4\text{Na}$ $[\text{M}+\text{Na}]^+$: 613.23; found: 613.

((4'R,5'R)-4'-(ethoxydiphenylmethyl)spiro[fluorene-9,2'-[1,3]dioxolan]-5'-yl)diphenylmethanol (2.3.32)



The titled compound was prepared by following the literature procedure,³⁴ obtained as a white solid. R_f (Ethyl acetate/Pet. ether = 30:70) = 0.6. The spectral values were matched favorably with literature values.

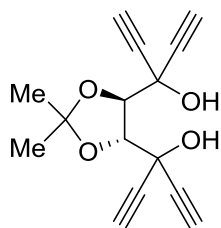
$^1\text{H NMR}$ (400 MHz, CDCl_3) δ 4.64 (s, 2 H) 4.96 (s, 2 H) 6.44 (d, $J=7.50$ Hz, 2 H) 7.05 (td, $J=7.50$, 1.00 Hz, 2 H) 7.15 - 7.23 (m, 6 H) 7.24 - 7.30 (m, 3 H) 7.31 - 7.45 (m, 12 H) 7.48 - 7.55 (m, 4 H)

3,3'-((4R,5R)-2,2-dimethyl-1,3-dioxolane-4,5-diyl)bis(penta-1,4-diyne-3-ol) (2.3.33)

³² Nahm, R. M.; Potnick, R. J.; White, S. P.; Johnson, S. J. *J. Am. Chem. Soc.* **2006**, *128*, 2751-2756.

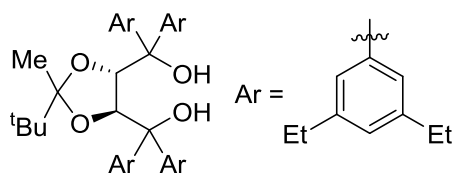
³³ Iurre, J.; Alonso-Alija, C.; Piniella, F. J.; Alvarez-Larena, A. *Tetrahedron: Asymmetry*, **1992**, *3*, 1531.

³⁴ Budragchaa, T.; Abraham, M.; Schöfberger, W.; Roller, A.; Widhalm, M. *Asymmetric Catalysis*. **2016**, *3*, 1-14.



The titled compound was prepared by following the literature procedure, obtained as a white solid. R_f (Ethyl acetate/Pet. ether = 30:70) = 0.6. The spectral values were matched favorably with literature values.³⁵

((4S, 5S)-5-(bis(3, 5-diethylphenyl)(ethoxy)methyl)-2-(tert-butyl)-2-methyl-1, 3-dioxolan-4-yl)bis(3, 5-diethylphenyl)methanol (ent-2.3.26)

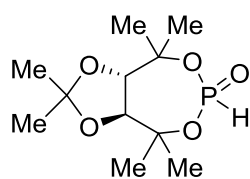


The titled compound was prepared starting from D-(+)-tartaric acid, obtained as a white solid. R_f (Ethyl acetate/Pet. ether = 30:70) = 0.5. MP = 78.3 – 79.8 °C. $[\alpha]_D^{25} +21.2$ (c = 3.0 CH₂Cl₂). ¹H NMR (500 MHz, CDCl₃)

δ 0.62 (s, 9H), 0.78 (s, 3H), 1.16 (q, $J = 7.63$ Hz, 12H), 1.15 (q, $J = 7.63$ Hz, 12H), 2.52 - 2.61 (m, 16H), 4.42 - 4.47 (m, 3H), 4.56 (s, 1H), 6.90 - 6.96 (m, 4H), 7.06 (s, 6H), 7.13 (s, 2H); ¹³C NMR (126 MHz, CDCl₃) δ 15.42, 15.51, 15.92, 19.64, 24.85, 28.88, 28.94, 28.98, 38.91, 78.21, 78.84, 79.02, 80.84, 112.61, 124.40, 124.77, 126.03, 126.10, 126.19, 126.41, 126.46, 126.48, 142.48, 142.60, 142.66, 143.54, 146.64, 146.70. FTIR (cm⁻¹) 3013, 2967, 2932, 2873, 1600, 1520, 1325, 1164, 1002, 922, 876. LCMS (ESI) m/z Calculated for C₅₀H₆₈O₄ [M+H]⁺: 755.5; found: 755.3.

2.7.2 Spectral data of Phosphites

(1R, 7R)-9, 9-dimethyl-4-hydrido-4-oxo-2, 2, 6, 6-tetramethyl-3, 5, 8, 10 tetraoxa-4-phosphabicyclo[5.3.0]decane (2.4.1)



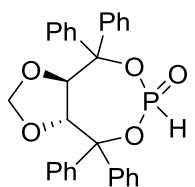
The titled compound was prepared by following the literature procedure, with the corresponding 2,75 mmol of TADDOL (2.3.1) in 10 ml THF, which afforded 712 mg (98%) of the product as white crystals. R_f (Ethyl acetate/Pet. ether = 50:50) = 0.6. MP = 91.3 °C. ¹H NMR (500 MHz, CDCl₃)

δ 1.40 - 1.43 (m, 9 H) 1.47 (s, 3 H) 1.62 (s, 3 H) 1.65 (s, 3 H) 3.98 (d, $J = 9.54$ Hz, 1 H) 4.47 (d, $J = 8.17$ Hz, 1 H) 6.73 (d, $J_{H-P} = 732$ Hz, 1H). ¹³C NMR (125 MHz, CDCl₃) δ 21.96, 21.99, 22.04, 27.00, 27.04, 28.97, 28.99, 29.66, 29.73, 80.37, 80.38, 81.65, 82.04, 82.12, 82.19, 110.40. ³¹P NMR (200 MHz, CDCl₃): δ 1.15. FTIR (cm⁻¹): 2979, 1597, 1445,

³⁵ Gangadhar, P.; Reddy, S. A.; Srihari, P. Tetrahedron. **2016**, 72, 5807-5817.

1371, 1243, 1164, 1076, 929, 847, 745. **HRMS:** Calculated for $C_{22}H_{42}O_{10}NaP_2[M]^+$: 551.2151, found: 551.2145.

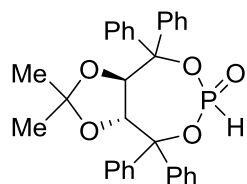
(3aR, 8aR)-4, 4, 8, 8-tetraphenyltetrahydro-[1, 3]dioxolo[4,5-e][1, 3, 2]dioxaphosphepine 6-oxide (2.4.2)



The titled compound was prepared by following the literature procedure, with the corresponding 1 mmol of TADDOL (**2.3.2**) in 10 ml THF, which afforded 315 mg (72 %) of the product as white solid. MP = 70.6 – 71.8 °C.

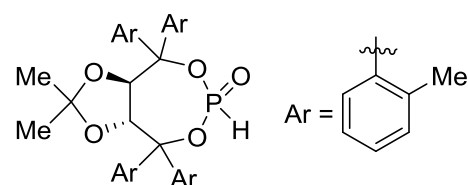
R_f (Ethyl acetate/Pet. ether = 20:80) = 0.6. 1H NMR (500 MHz, $CDCl_3$) δ 4.22 - 4.27 (m, 1H), 4.52 - 4.57 (m, 1H), 5.02 - 5.08 (m, 1H), 5.15 - 5.21 (m, 1H), 6.38 (d, J = 720 Hz, 1H), 7.27 - 7.41 (m, 12H), 7.49 - 7.60 (m, 8H); ^{13}C NMR (100 MHz, $CDCl_3$) δ 80.29, 80.33, 80.41, 87.14, 87.23, 87.59, 87.68, 96.52, 126.63, 126.69, 127.41, 127.84, 127.91, 128.23, 128.30, 128.41, 128.46, 128.61, 128.66, 137.92, 137.98, 138.50, 138.56, 142.53, 142.57, 143.11, 143.16; ^{31}P NMR (162 MHz, $CDCl_3$) δ -3.90. **FTIR** (cm^{-1}) 3062, 2971, 2873, 2405, 1593, 1494, 1448, 1351, 1164, 1064, 969, 736. **HRMS** (ESI) m/z Calculated for $C_{29}H_{25}O_5P [M+Na]^+$: 507.1332; found: 507.1332.

(3aR, 8aR)-2, 2-dimethyl-4, 4, 8, 8-tetraphenyltetrahydro-[1,3]dioxolo[4, 5-e][1,3,2]dioxaphosphepine 6-oxide (2.4.3)

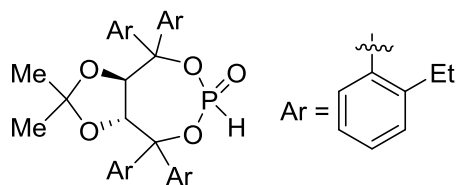


The titled compound was prepared by following the literature procedure, with the corresponding 2.5 mmol of TADDOL (**2.3.3**) in 10 ml THF, which afforded 1100 mg (78%) of the product as white crystals. R_f (Ethyl acetate/Pet. ether = 20:80) = 0.3. The spectral values were matched favorably with literature values.²⁷

(3aR, 8aR)-2, 2-dimethyl-4, 4, 8, 8-tetra-*o*-tolyltetrahydro-[1,3]dioxolo[4,5-e][1,3,2]dioxaphosphepine 6-oxide (2.4.4)

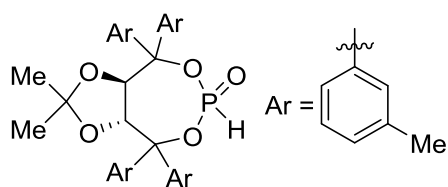


The titled compound was prepared by following the literature procedure, with the corresponding 1.15 mmol of TADDOL (**2.3.4**) in 10 ml THF, which afforded 512 mg (78%) of the product as white crystals. R_f (Ethyl acetate/Pet. ether = 30:70) = 0.6. The spectral values were matched favorably with the literature values.²⁷

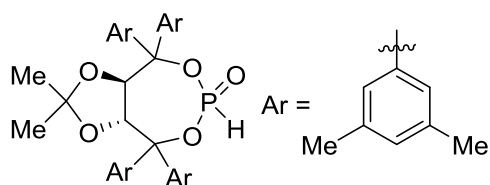
(3aR, 8aR)-2, 2-dimethyl-4, 4, 8, 8-tetra-o-ethylphenyltetrahydro-[1,3]dioxolo[4,5-e][1,3,2]dioxaphosphepine 6-oxide (2.4.5)

literature values.²⁷

The titled compound was prepared by following the literature procedure, with the corresponding 1 mmol of TADDOL (2.3.5) in 10 ml THF, which afforded 512 mg (68%) of the product as white crystals. R_f (Ethyl acetate/Pet. ether = 30:70) = 0.6. The spectral values were matched favorably with the

(3aR, 8aR)-2, 2-dimethyl-4, 4, 8, 8-tetra-m-tolyltetrahydro-[1,3]dioxolo[4,5-e][1,3,2]dioxaphosphepine 6-oxide (2.4.7)

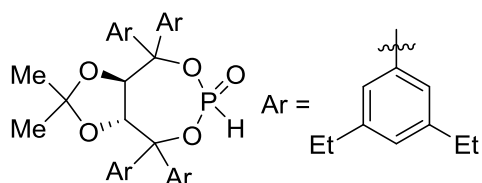
literature procedure, with the corresponding 1 mmol of TADDOL (2.3.7) in 10 ml THF, which afforded 471 mg (83%) of the product as white solid. R_f (Ethyl acetate/Pet. ether = 20:80) = 0.5. MP = 88.3 – 89.6 °C. $^1\text{H NMR}$ (400 MHz, CDCl_3) δ 0.57 (s, 3H), 0.90 (s, 3H), 2.33 (s, 6H), 2.39 (s, 6H), 5.19 (d, $J = 7.93$ Hz, 1H), 5.28 (d, $J = 7.93$ Hz, 1H), 6.19 (d, $J = 7.18$ Hz, 1H), 7.06 - 7.16 (m, 2H), 7.16 - 7.25 (m, 6H), 7.26 - 7.31 (m, 3H), 7.32 - 7.36 (m, 1H), 7.37 - 7.42 (m, 3H) 7.47 (d, $J = 7.93$ Hz, 1H); $^{13}\text{C NMR}$ (100 MHz, CDCl_3) δ 21.50, 21.55, 21.61, 21.70, 26.09, 26.84, 80.05, 80.19, 80.23, 88.25, 88.34, 88.47, 88.57, 114.00, 123.65, 123.85, 124.93, 125.80, 127.19, 127.32, 127.38, 127.54, 127.94, 128.33, 128.53, 128.67, 128.85, 129.15, 129.20, 129.34, 136.71, 137.07, 137.71, 138.44, 138.79, 138.86, 139.06, 139.13, 143.04, 143.07, 143.60; $^{31}\text{P NMR}$ (162 MHz, CDCl_3) δ -4.79. FTIR (cm^{-1}): 3020, 2928, 2434, 2402, 1733, 1668, 1605, 1484, 1430, 1379, 1081, 670. HRMS (ESI) m/z . Calculated for $\text{C}_{35}\text{H}_{37}\text{O}_5\text{P}$ $[\text{M}+\text{Na}]^+$: 591.2271; found: 591.2256.

(3aR, 8aR)-4, 4, 8, 8-tetrakis(3,5-dimethylphenyl)-2, 2-dimethyltetrahydro-[1,3]dioxolo[4,5-e][1,3,2]dioxaphosphepine 6-oxide (2.4.8)

The titled compound was prepared by following the literature procedure, with the corresponding 1 mmol of TADDOL (2.3.8) in 10 ml THF, which afforded 486 mg (83%) of the product as white crystals. R_f

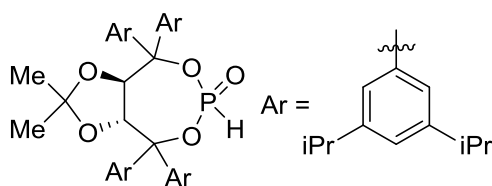
(Ethyl acetate/Pet. ether = 20:80) = 0.2. The spectral values were matched favorably with the literature values.³⁶

(3aR, 8aR)-4, 4, 8, 8-tetrakis(3, 5-diethylphenyl)-2, 2-dimethyltetrahydro-[1,3]dioxolo[4,5-e][1,3,2]dioxaphosphepine 6-oxide (2.4.9)



The titled compound was prepared by following the literature procedure, with the corresponding 1 mmol of TADDOL (**2.3.9**) in 10 ml THF, which afforded 523 mg (71%) of the product as white solid. R_f (Ethyl acetate/Pet. ether = 20:80) = 0.5. MP = 61.3 – 62.0 °C. $^1\text{H NMR}$ (500 MHz, CDCl_3) δ 0.47 (s, 3H), 0.94 (s, 3H), 1.18 - 1.24 (m, 13H), 1.25 - 1.30 (m, 11H), 2.56 - 2.65 (m, 8H), 2.65 - 2.73 (m, 8H), 5.24 - 5.33 (m, 2H), 6.32 (d, $J = 708$ Hz, 1H), 6.96 (s, 1H), 6.99 (s, 1H), 7.03 (s, 1H), 7.07 (s, 3H), 7.12 (s, 2H), 7.21 (s, 2H), 7.29 (s, 2H); $^{13}\text{C NMR}$ (126 MHz, CDCl_3) δ 14.91, 15.42, 15.49, 15.85, 15.98, 25.83, 26.97, 28.63, 28.85, 28.94, 29.06, 80.16, 80.19, 80.31, 88.27, 88.33, 88.82, 88.90, 113.48, 123.47, 123.91, 123.99, 124.33, 125.19, 125.75, 126.90, 127.05, 127.36, 127.48, 139.05, 139.33, 143.07, 143.39, 143.61, 143.74, 144.43; $^{31}\text{P NMR}$ (162 MHz, CDCl_3) δ -4.98. FTIR (cm^{-1}): 3014, 2967, 2933, 2874, 2435, 2402, 1740, 1601, 1377, 958, 825, 769. LCMS (ESI) m/z Calculated for $\text{C}_{47}\text{H}_{61}\text{O}_5\text{PNa}$ $[\text{M}+\text{Na}]^+$: 759.4; found: 759.1.

(3aR, 8aR)-4, 4, 8, 8-tetrakis(3, 5-diisopropylphenyl)-2, 2-dimethyltetrahydro-[1,3]dioxolo[4,5-e][1,3,2]dioxaphosphepine 6-oxide (2.4.10)

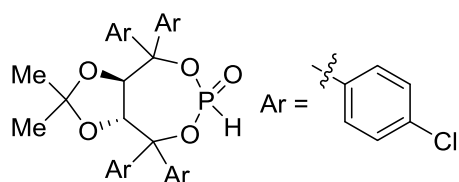


The titled compound was prepared by following the literature procedure, with the corresponding 1 mmol of TADDOL (**2.3.10**) in 10 ml THF, which afforded 611 mg (71%) of the product as white solid. R_f (Ethyl acetate/Pet. ether = 20:80) = 0.6. $^1\text{H NMR}$ (500 MHz, CDCl_3) δ 0.35 (s, 3H), 0.87 (s, 3H), 1.13 - 1.27 (m, 48H), 2.76 - 2.97 (m, 8H), 5.26 (s, 2H), 6.3 (d, $J_{\text{H-P}} = 705$ Hz, 1H), 6.98 (s, 1H), 6.95 (s, 1H), 7.00 - 7.05 (m, 3H), 7.06 - 7.11 (m, 3H), 7.17 (s, 2H), 7.31 (s, 2H); $^{13}\text{C NMR}$ (125 MHz, CDCl_3) δ 23.64, 23.89, 23.92, 24.02, 24.19, 24.34, 25.52, 26.96, 29.66, 34.10, 34.17, 34.21, 34.23, 80.27, 80.50, 88.50, 88.56, 89.01, 89.08, 113.07, 122.80, 122.92, 123.76, 123.97, 124.29, 124.5,

³⁶ Wang, Y. X.; Qi, S. L.; Luan, Y. X.; Han, X. W.; Wang, S.; Chen, H.; Ye, M. *J. Am. Chem. Soc.* **2018**, *140*, 5360-5364.

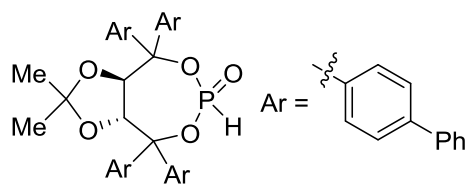
138.92, 138.97, 139.22, 139.28, 142.95, 142.98, 143.47, 147.49, 147.90, 148.09, 149.04; ^{31}P NMR (162 MHz, CDCl_3) δ -4.64. FTIR (cm^{-1}) 3012, 2968, 2940, 2877, 2402, 1742, 1607, 1377, 967, 826, 766.

(3aR, 8aR)-4, 4, 8, 8-tetrakis(4-chlorophenyl)-2, 2-dimethyltetrahydro-[1, 3]dioxolo[4, 5-e][1, 3, 2]dioxaphosphepine 6-oxide (2.4.14)



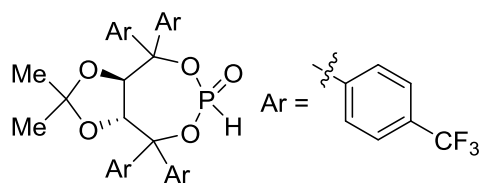
The titled compound was prepared by following the literature procedure, with the corresponding 1 mmol of TADDOL (**2.3.14**) in 10 ml THF, which afforded 560 mg (82%) of the product as white crystals. R_f (Ethyl acetate/Pet. ether = 20:80) = 0.3. The spectral values were matched favorably with the literature values.³⁷

(3aR, 8aR)-4, 4, 8, 8-tetrakis(4-biphenyl)-2, 2-dimethyltetrahydro-[1, 3]dioxolo[4, 5-e][1, 3, 2]dioxaphosphepine 6-oxide (2.4.15)



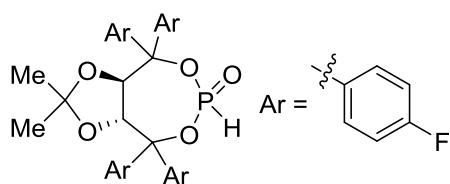
The titled compound was prepared by following the literature procedure, with the corresponding 1 mmol of TADDOL (**2.3.1**) in 10 ml THF, which afforded 612 mg (75%) of the product as white crystals. R_f (Ethyl acetate/Pet. ether = 20:80) = 0.6. The spectral values were matched favorably with the literature values.³⁵

(3aR, 8aR)-4, 4, 8, 8-tetrakis(4-trifluorophenyl)-2, 2-dimethyltetrahydro-[1, 3]dioxolo[4, 5-e][1, 3, 2]dioxaphosphepine 6-oxide (2.4.16)

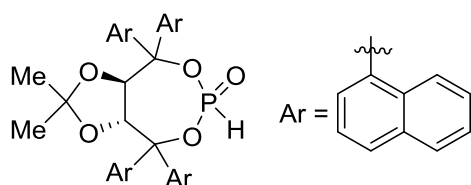


The titled compound was prepared by following the literature procedure, with the corresponding 1 mmol of TADDOL (**2.3.16**) in 10 ml THF, which afforded 564 mg (72%) of the product as white crystals. R_f (Ethyl acetate/Pet. ether = 20:80) = 0.6. The spectral values were matched favorably with the literature values.³⁵

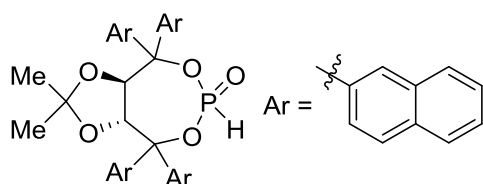
³⁷ Liu, Q. S.; Wang, D. Y.; Yang, Z. J.; Luan, Y. X.; Yang, J. F.; Li, J. F.; Pu, Y. J.; Ye, M. J. *Am. Chem. Soc.* **2017**, *139*, 18150-18153.

(3aR, 8aR)-4, 4, 8, 8-tetrakis(4-fluorophenyl)-2, 2-dimethyltetrahydro-[1, 3]dioxolo[4, 5-e][1, 3, 2]dioxaphosphepine 6-oxide (2.4.17)

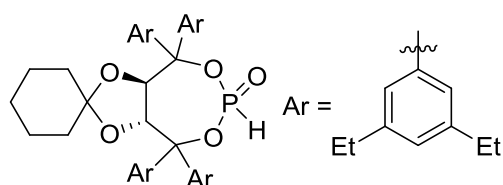
The titled compound was prepared by following the literature procedure, with the corresponding 1 mmol of TADDOL (**2.3.2**) in 10 ml THF, which afforded 397 mg (68%) of the product as white crystals. R_f (Ethyl acetate/Pet. ether = 20:80) = 0.5. The spectral values were matched favorably with the literature values.²⁷

(3aR, 8aR)-2, 2-dimethyl-4, 4, 8, 8-tetra(naphthalen-1-yl)tetrahydro-[1,3]dioxolo[4,5-e][1,3,2]dioxaphosphepine 6-oxide (2.4.18)

The titled compound was prepared by following the literature procedure, with the corresponding 1 mmol of TADDOL (**2.3.18**) in 10 ml THF, which afforded 498 mg (70%) of the product as white crystals. R_f (Ethyl acetate/Pet. ether = 20:80) = 0.3. The spectral values were matched favorably with the literature values.²⁷

(3aR, 8aR)-2, 2-dimethyl-4, 4, 8, 8-tetra(naphthalen-2-yl)tetrahydro-[1,3]dioxolo[4,5-e][1,3,2]dioxaphosphepine 6-oxide (2.4.19)

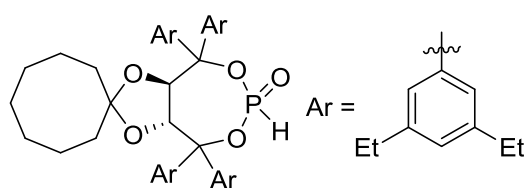
The titled compound was prepared by following the literature procedure, with the corresponding 1 mmol of TADDOL (**2.3.18**) in 10 ml THF, which afforded 541 mg (76%) of the product as white crystals. R_f (Ethyl acetate/Pet. ether = 20:80) = 0.25. The spectral values were matched favorably with the literature values.²⁷

(3a'R, 8a'R)-4', 4', 8', 8'-tetrakis(3, 5-diethylphenyl)tetrahydrospiro[cyclohexane-1, 2'-[1,3]dioxolo[4,5-e][1,3,2]dioxaphosphepine] 6'-oxide (2.4.24)

The titled compound was prepared by following the literature procedure, with the corresponding 1 mmol of TADDOL (**2.3.24**) in 10 ml THF, which afforded 567 mg (73%) of the product as white solid. R_f (Ethyl acetate/Pet. ether = 20:80) = 0.7. MP = 58.9 – 61.2 °C. $^1\text{H NMR}$ (400 MHz, CDCl_3) δ 1.00 - 1.44 (m, 34H), 2.52 - 2.60 (m, 8H), 2.60 - 2.67 (m, 8H), 5.18 (d, J = 7.63 Hz, 1H), 5.22

- 5.26 (d, $J = 8.39$ Hz, 1H), 6.15 (d, $J_{\text{H-P}} = 712$ Hz, 1H), 6.91 (s, 1H), 6.94 (s, 1H), 6.99 (s, 1H), 7.00 - 7.05 (m, 5H), 7.22 (s, 2H), 7.27 (s, 2H); ^{13}C NMR (100 MHz, CDCl_3) δ 15.45, 15.51, 15.80, 23.93, 24.05, 24.83, 28.84, 28.86, 28.92, 35.56, 36.50, 79.62, 79.68, 79.71, 88.51, 88.58, 89.21, 89.31, 114.15, 123.90, 123.95, 125.22, 125.74, 126.76, 126.88, 127.35, 127.49, 139.03, 139.11, 139.34, 139.40, 142.99, 143.23, 143.59, 144.38; ^{31}P NMR (162 MHz, CDCl_3) δ -5.02. FTIR (cm^{-1}): 2964, 2933, 2867, 2435, 1776, 1600, 1456, 1370, 1275, 1074, 960, 742. LCMS: Calculated for $\text{C}_{50}\text{H}_{65}\text{O}_5\text{P}$ $[\text{M}+\text{Na}]^+$: 799.4; found: 799.2.

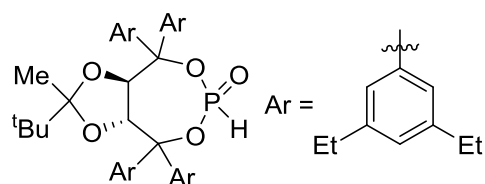
(3a'R, 8a'R)-4', 4', 8', 8'-tetrakis(3, 5-diethylphenyl)tetrahydrospiro[cyclooctane-1, 2'-[1,3]dioxolo[4,5-e][1,3,2]dioxaphosphine] 6'-oxide (2.4.25)



The titled compound was prepared by following the literature procedure, with the corresponding 1 mmol of TADDOL (2.3.25) in 10 ml THF, which afforded 534 mg (68%) of the product as white

solid. R_f (Ethyl acetate/Pet. ether = 20:80) = 0.75. MP = 89.1 – 91.4 °C. ^1H NMR (400 MHz, CDCl_3) δ 1.10 - 1.39 (m, 38H), 2.52 - 2.68 (m, 16H), 5.17 (d, $J = 8.27$ Hz, 1H), 5.24 (d, $J = 8.27$ Hz, 1H), 6.13 (d, $J = 713$, 1H), 6.91 (s, 1H), 6.93 (s, 1H), 6.96 - 7.03 (m, 5H), 7.04 (s, 1H), 7.23 (s, 2H), 7.27 (s, 2H); ^{13}C NMR (125 MHz, CDCl_3) δ 14.89, 15.40, 15.45, 15.79, 15.85, 15.97, 21.71, 21.79, 24.03, 27.50, 27.60, 28.60, 28.83, 28.89, 29.03, 34.59, 35.54, 79.59, 79.71, 88.39, 88.45, 89.26, 89.34, 117.21, 123.46, 123.89, 124.31, 125.20, 125.66, 126.73, 126.83, 127.34, 127.48, 139.31, 139.36, 139.53, 139.60, 142.97, 143.17, 143.21, 143.54, 143.61, 144.37; ^{31}P NMR (162 MHz, CDCl_3) δ -4.78. FTIR (cm^{-1}): 3052, 2964, 2728, 2439, 1776, 1601, 1459, 1376, 1269, 1152, 1076, 981, 738. LCMS: Calculated for $\text{C}_{52}\text{H}_{69}\text{O}_5\text{P}$ $[\text{M}+\text{Na}]^+$; 827.4; found: 827.2.

(3aR, 8aR)-2-(tert-butyl)-4, 4, 8, 8-tetrakis(3, 5-diethylphenyl)-2-methyltetrahydro-[1,3]dioxolo[4,5-e][1,3,2]dioxaphosphine 6-oxide (2.4.26)

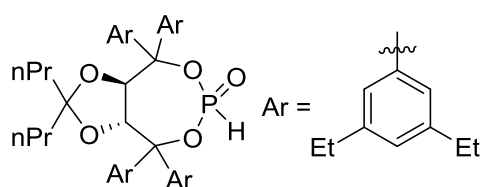


The titled compound was prepared by following the literature procedure, with the corresponding 1 mmol of TADDOL (2.3.26) in 10 ml THF, which afforded 553 mg (71%) of the product as white solid

(diastereomeric ratio 1: 0.75). R_f (Ethyl acetate/Pet. ether = 20:80) = 0.7. MP = 62.3 – 63.8 °C. $[\alpha]_D^{25}$ -182 (c = 3.0 CH_2Cl_2). ^1H NMR (500 MHz, CDCl_3) δ 0.29 (d, $J = 4.20$ Hz, 3H), 0.44 (d, $J = 6.10$ Hz, 9H), 1.16 (q, $J = 7.63$ Hz, 6H), 1.14 (q, $J = 7.25$ Hz, 6H), 1.25 - 1.29 (m,

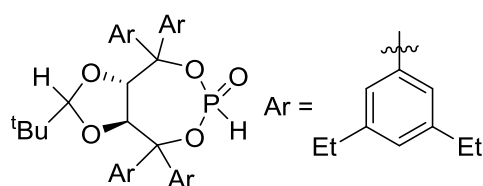
12H), 2.47 - 2.61 (m, 8H), 2.66 - 2.72 (m, 8H), 5.21 (dd, $J = 135$ Hz, 135 Hz, 1H), 6.82 (d, $J = 722$ Hz, 1H), 6.88 (s, 1H) 6.91 (d, $J = 8.77$ Hz, 2H), 6.94 (s, 1H), 7.01 (s, 1H), 7.05 (d, $J = 5.72$ Hz, 1H), 7.09 (d, $J = 5.34$ Hz, 1H), 7.26 (s, 1H), 7.29 (s, 1H), 7.32 (d, $J = 6.87$ Hz, 2H); ^{13}C NMR (126 MHz, CDCl_3) δ 15.26, 15.38, 15.50, 15.77, 15.83, 15.89, 15.98, 17.86, 18.16, 24.36, 28.85, 28.88, 38.32, 38.43, 78.53, 78.58, 79.62, 79.65, 87.53, 87.59, 88.63, 88.69, 89.47, 89.55, 90.70, 90.78, 117.80, 117.90, 123.62, 123.79, 125.31, 125.51, 125.74, 126.79, 126.85, 127.59, 139.62, 139.77, 142.95, 143.01, 143.40, 143.44, 143.54, 143.58, 143.63, 143.85, 144.52, 144.56; ^{31}P NMR (162 MHz, CDCl_3) δ -4.62 (major), -4.79 (minor). FTIR (cm^{-1}): 3017, 2967, 2933, 1741, 1601, 1457, 1373, 1164, 1076, 961, 669. LCMS (ESI) m/z Calculated for $\text{C}_{50}\text{H}_{67}\text{O}_5\text{PNa}$ $[\text{M}+\text{Na}]^+$: 801.4; found: 801.2.

(3aR, 8aR)-4, 4, 8, 8-tetrakis(3, 5-diethylphenyl)-2, 2-dipropyltetrahydro-[1, 3]dioxolo[4, 5-e][1, 3, 2]dioxaphosphepine 6-oxide (2.4.27)



The titled compound was prepared by following the literature procedure, with the corresponding 1 mmol of TADDOL (**2.3.27**) in 10 ml THF, which afforded 567 mg (73%) of the product as white solid. R_f (Ethyl acetate/Pet. ether = 20:80) = 0.7. MP = 135.2 – 137.1 °C. ^1H NMR (400 MHz, CDCl_3) δ 0.50 - 0.57 (m, 4H), 0.59 - 0.66 (m, 4H), 0.75 - 0.99 (m, 6H), 1.12 - 1.22 (m, 12H), 1.24 - 1.28 (m, 12H), 2.51 - 2.62 (m, 8H), 2.63 - 2.71 (m, 8H), 5.18 (d, $J = 8.54$ Hz, 1H), 5.28 (d, $J = 8.55$ Hz, 1H), 6.16 (d, $J = 718$ Hz, 1H), 6.90 (s, 2H), 6.94 (d, $J = 6.71$ Hz, 2H), 6.97 (s, 2H), 7.03 (s, 1H), 7.08 (s, 1H), 7.29 (m, 4H); ^{13}C NMR (100 MHz, CDCl_3) δ 14.08, 14.15, 15.38, 15.46, 15.88, 15.92, 16.29, 16.33, 28.81, 28.85, 28.89, 29.65, 39.25, 39.57, 79.41, 88.27, 88.34, 89.81, 89.91, 116.35, 123.78, 123.88, 125.35, 125.68, 126.77, 126.83, 127.50, 127.56, 139.52, 139.59, 139.79, 139.88, 142.99, 143.06, 143.26, 143.55, 143.64, 144.47; ^{31}P NMR (162 MHz, CDCl_3) δ -4.84. FTIR: 3051, 2965, 2931, 2873, 2440, 1777, 1601, 1376, 1170, 1079, 969, 876, 739. LCMS: Calculated for $\text{C}_{51}\text{H}_{69}\text{O}_5\text{P}$ $[\text{M}+\text{Na}]^+$: 815.4; found: 815.2.

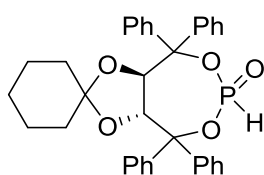
(3aR, 8aR)-2-(tert-butyl)-4, 4, 8, 8-tetrakis(3, 5-diethylphenyl)tetrahydro-[1,3]dioxolo[4,5-e][1, 3, 2]dioxaphosphepine 6-oxide (2.4.28)



The titled compound was prepared by following the literature procedure, with the corresponding 1 mmol of TADDOL (**2.3.28**) in 10 ml THF, which afforded

607 (79 %) of product as white solid (diastereomeric ratio 1:0.9). R_f (Ethyl acetate/Pet. ether = 20:80) = 0.7. MP = 61.0 – 62.9 °C. $^1\text{H NMR}$ of major diastereomer (400 MHz, CDCl_3) δ 0.52 (s, 9H), 1.14 - 1.22 (m, 24 H), 2.53 - 2.63 (m, 16 H), 3.49 (s, 1H), 4.83 (d, $J = 7.32$ Hz, 1H), 5.20 (d, $J = 7.93$ Hz, 1H), 6.08 (d, $J = 694$ Hz, 1H), 6.92 (s, 1H), 6.95 - 7.00 (m, 5H), 7.01 - 7.03 (m, 3H), 7.07 (s, 1H), 7.12 (s, 2H). $^{13}\text{C NMR}$ (100 MHz, CDCl_3) δ 15.33, 15.45, 15.54, 24.25, 28.74, 28.81, 28.84, 28.87, 33.29, 78.49, 80.16, 81.76, 87.29, 87.55, 87.82, 90.04, 110.85, 123.39, 123.52, 123.64, 124.45, 126.79, 127.20, 127.41, 137.98, 138.63, 138.84, 139.10, 142.57, 142.98, 143.25, 143.56, 143.97, 144.37, 144.40; $^{31}\text{P NMR}$ (162 MHz, CDCl_3) δ -5.39 (major), -4.38 (minor). FTIR (cm^{-1}): 2964, 2930, 2871, 2431, 1600, 1457, 1368, 1172, 1072, 983, 876, 743.

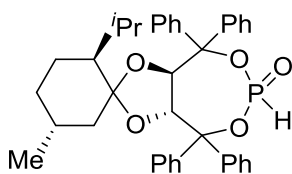
((3a'R, 8a'R)-4', 4', 8', 8'-tetraphenyltetrahydrospiro[cyclohexane-1, 2'-[1,3]dioxolo[4, 5-e][1, 3, 2]dioxaphosphepine] 6'-oxide (2.4.29)



The titled compound was prepared by following the literature procedure, with the corresponding 1 mmol of TADDOL (2.3.29) in 10 ml THF, which afforded 420 mg (76%) of the product as white solid. MP = 63.4 – 64.8 °C. R_f (Ethyl acetate/Pet. ether = 20:80) = 0.55.

$^1\text{H NMR}$ (400 MHz, CDCl_3) δ 0.63 (m, 2H), 0.72 - 0.89 (m, 2H), 1.13 - 1.20 (m, 2H), 1.21 - 1.27 (m, 2H), 1.27 - 1.35 (m, 2H), 5.19 (d, $J = 7.93$ Hz, 1H), 5.35 (d, $J = 7.93$ Hz, 1H), 6.19 (d, $J = 728$ Hz, 1H) 7.23 - 7.30 (m, 6H) 7.30 - 7.36 (m, 3H), 7.36 - 7.47 (m, 7H), 7.62 (t, $J = 6.41$ Hz, 4H); $^1\text{H NMR}$ (400 MHz, CDCl_3) δ 23.91, 23.97, 24.69, 35.94, 36.34, 79.28, 79.63, 88.86, 88.95, 115.16, 126.75, 126.86, 127.21, 127.36, 127.77, 127.86, 128.12, 128.29, 128.43, 128.59, 128.66, 128.70, 138.89, 138.95, 139.09, 139.17, 143.22, 143.66; $^{31}\text{P NMR}$ (162 MHz, CDCl_3) δ -4.48. FTIR: 3061, 2948, 2889, 2426, 1493, 1364, 1160, 1076, 963, 737, 702. HRMS: calculated for $\text{C}_{34}\text{H}_{33}\text{O}_5\text{P}$ $[\text{M}+\text{Na}]^+$: 575.1958, found: 575.1953.

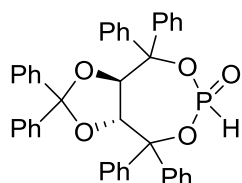
(2S,3a'R,5R,8a'R)-2-isopropyl-5-methyl-4',4',8',8' tetraphenyltetrahydrospiro [cyclohexane-1,2'-[1,3]dioxolo[4,5-e][1,3,2]dioxaphosphepine] 6'-oxide (2.4.30)



The titled compound was prepared by following the literature procedure, with the corresponding 1 mmol of TADDOL (2.3.30) in 10 ml THF, which afforded 541 mg (65%) of the product as white crystals. R_f (Ethyl acetate/Pet. ether = 20:80) = 0.25. The spectral

values were matched favorably with the literature values.³⁸

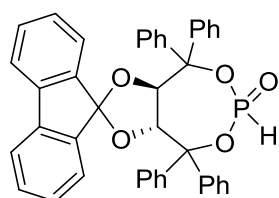
(3aR,8aR)-2,2,4,4,8,8-hexaphenyltetrahydro-[1,3]dioxolo[4,5-e][1,3,2]dioxaphosphepine 6-oxide (2.4.31)



The titled compound was prepared by following the modified literature procedure, with the corresponding 1 mmol of TADDOL (**2.3.31**) in 10 ml THF, which afforded 483 mg (76%) of the product as white crystals.

R_f (Ethyl acetate/Pet. ether = 30:70) = 0.4. $^1\text{H NMR}$ (400 MHz, CDCl_3) δ 5.52 (d, J = 8.38 Hz, 1 H), 5.61 (d, J = 8.38 Hz, 1 H), 6.69 - 6.77 (m, 2 H), 6.82 - 6.90 (m, 2 H), 6.90 - 7.03 (m, 7 H), 7.04 - 7.12 (m, 4 H), 7.12 - 7.23 (m, 5 H), 7.34 - 7.48 (m, 6 H), 7.65 (t, J = 7.57 Hz, 4 H), 7.96 (s, 1 H); $^{13}\text{C NMR}$ (101 MHz, CDCl_3) δ 81.77, 81.86, 81.88, 88.12, 88.21, 88.52, 88.61, 114.24, 125.47, 125.60, 126.79, 126.90, 127.22, 127.51, 127.55, 127.76, 127.82, 127.95, 128.30, 128.36, 128.56, 128.75, 128.78, 138.51, 138.57, 138.64, 138.72, 141.66, 142.06, 143.04, 143.06, 143.45, 143.49; $^{31}\text{P NMR}$ (162 MHz, CDCl_3) δ -4.12.; LCMS (ESI) m/z . Calculated for $\text{C}_{41}\text{H}_{33}\text{O}_5\text{P}$ $[\text{M}+\text{Na}]^+$: 659.19; found: 659.1.

4',4',8',8'-tetraphenyl-3a',4',8',8a'-tetrahydrospiro[fluorene-9,2'-[1,3]dioxolo[4,5-e][1,3,2] dioxaphosphepine] 6'-oxide (2.4.32)



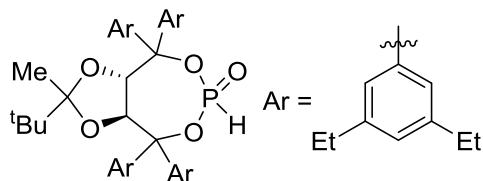
The titled compound was prepared by following the modified literature procedure,²⁷ with the corresponding 1 mmol of TADDOL (**2.3.32**) in THF, which afforded 398 mg (63%) of the product as white crystals. R_f (Ethyl acetate/Pet. ether = 30:70) = 0.45.

$^1\text{H NMR}$ (400 MHz, CDCl_3) δ 5.41 (dd, J = 16.63, 7.50 Hz, 2 H), 5.66 (d, J = 8.38 Hz, 1 H), 5.85 (d, J = 8.51 Hz, 1 H), 6.66 - 6.84 (m, 2 H), 7.15 - 7.20 (m, 2 H), 7.21 - 7.29 (m, 7 H), 7.31 - 7.41 (m, 11 H), 7.45 (d, J = 7.50 Hz, 3 H), 7.59 - 7.65 (m, 4 H), 8.19 (s, 1 H). $^{13}\text{C NMR}$ (101 MHz, CDCl_3) δ 80.08, 80.48, 89.04, 89.14, 89.24, 89.33, 116.71, 119.26, 119.33, 123.71, 123.75, 126.58, 126.63, 127.87, 127.92, 127.97, 128.02, 128.17, 128.45, 128.67, 128.77, 128.83, 129.36, 130.10, 130.17, 138.91, 139.03, 139.07, 139.17, 139.23, 142.54,

³⁸ Nahm, R. M.; Potnick, R. J.; White, S. P.; Johnson, S. J. *J. Am. Chem. Soc.* **2006**, *128*, 2751-2756.

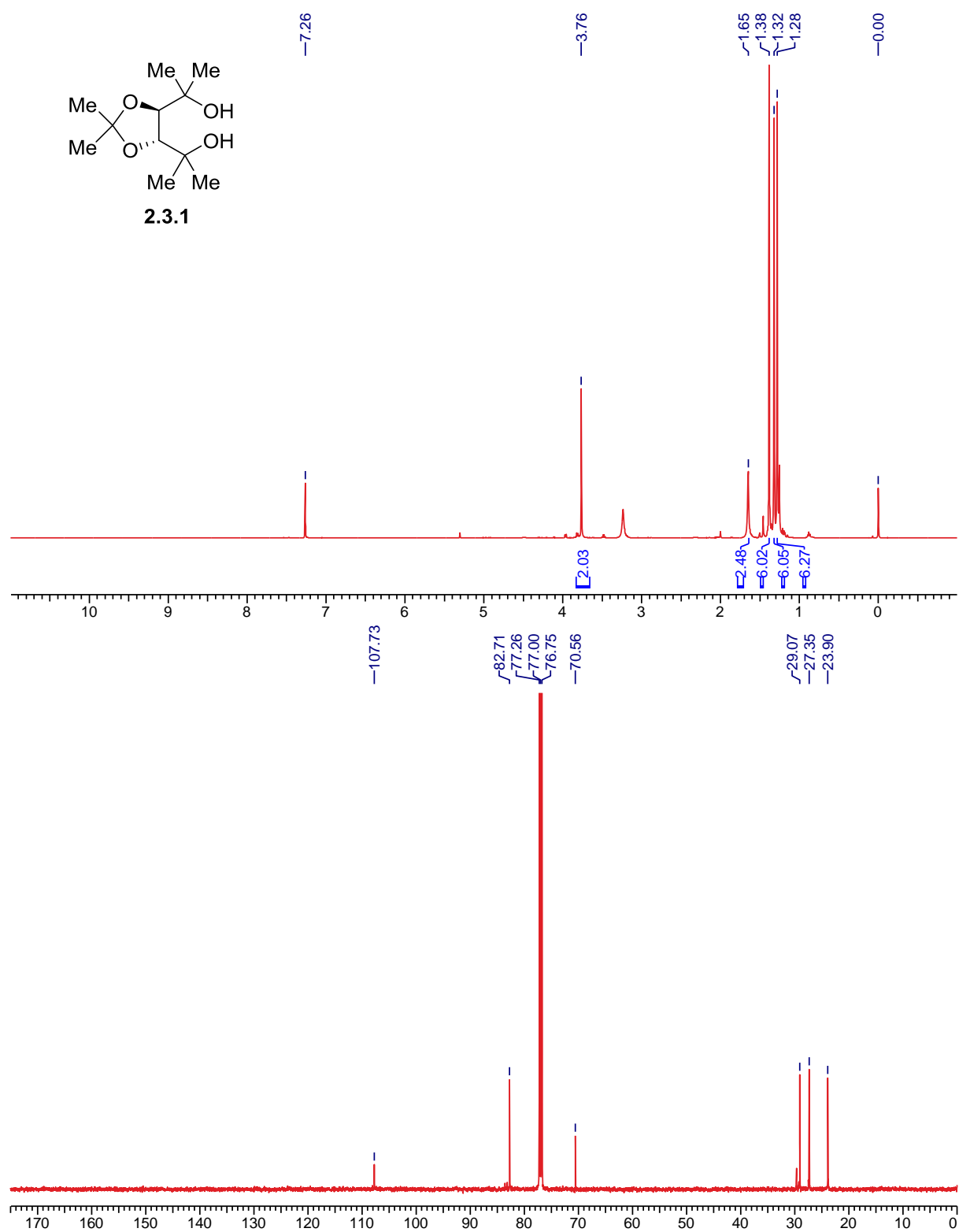
143.19, 143.75. ^{31}P NMR (162 MHz, CDCl_3) δ -4.29.; LCMS (ESI) m/z Calculated for $\text{C}_{41}\text{H}_{33}\text{O}_5\text{P}$ $[\text{M}+\text{Na}]^+$: 657.19; found: 657.1.

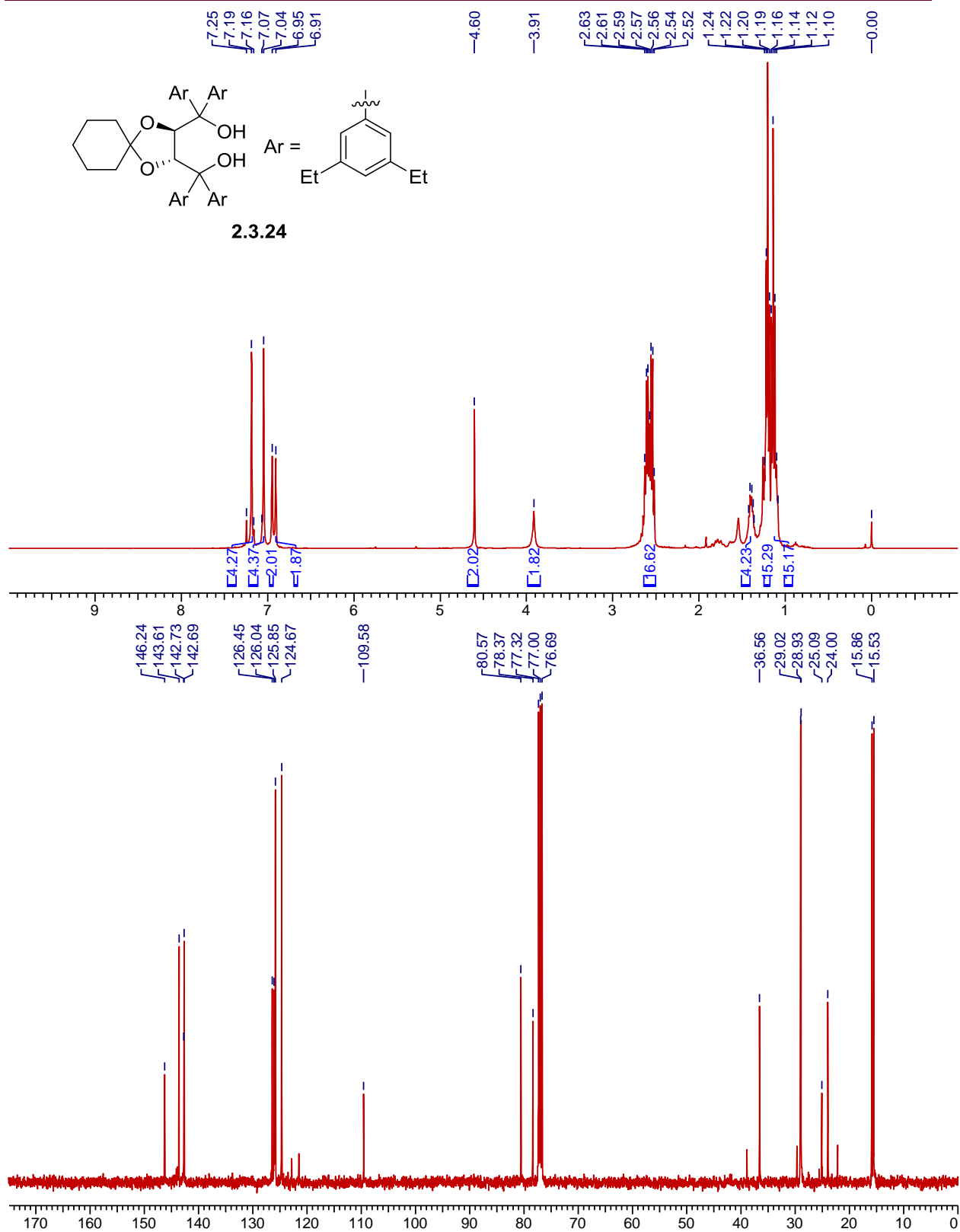
(3aS, 8aS)-2-(tert-butyl)-4, 4, 8, 8-tetrakis(3, 5-diethylphenyl)-2-methyltetrahydro-[1,3]dioxolo[4, 5-e][1, 3, 2]dioxaphosphepine 6-oxide (ent-2.4.26)

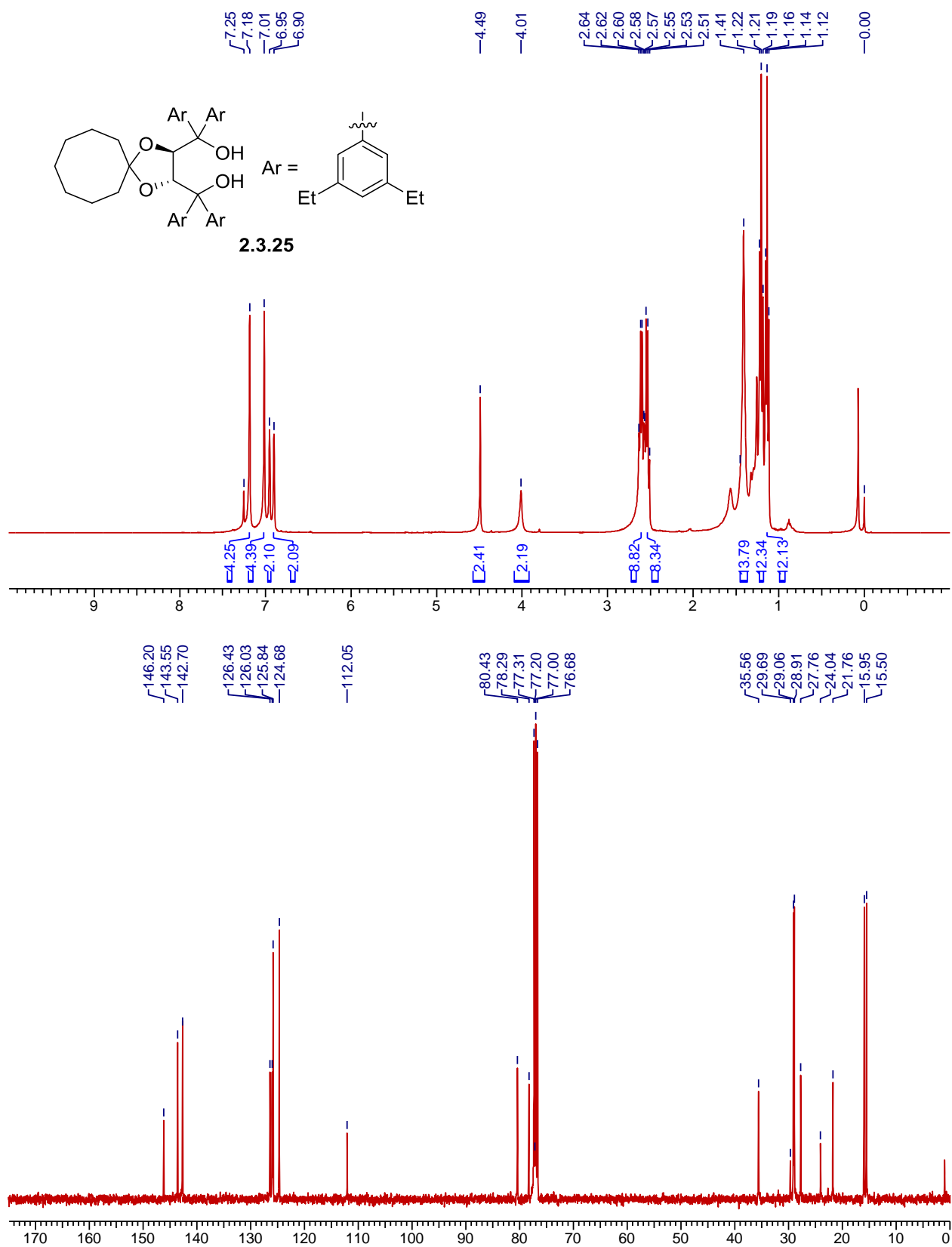


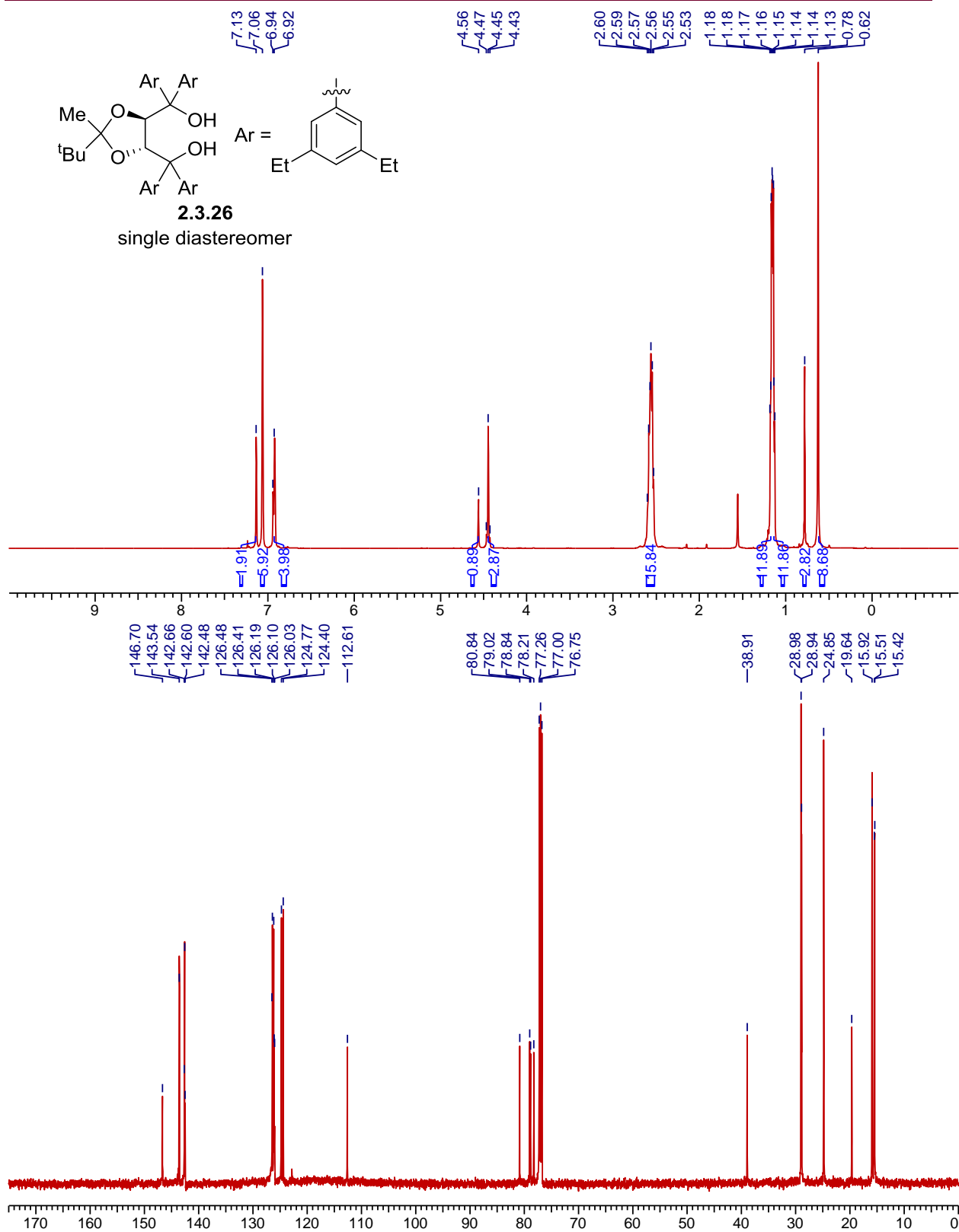
The titled compound was prepared by following the literature procedure, with the corresponding 1 mmol of TADDOL (**ent-2.3.26**) in 10 ml THF, which afforded 553 mg (71%) of the product as white solid

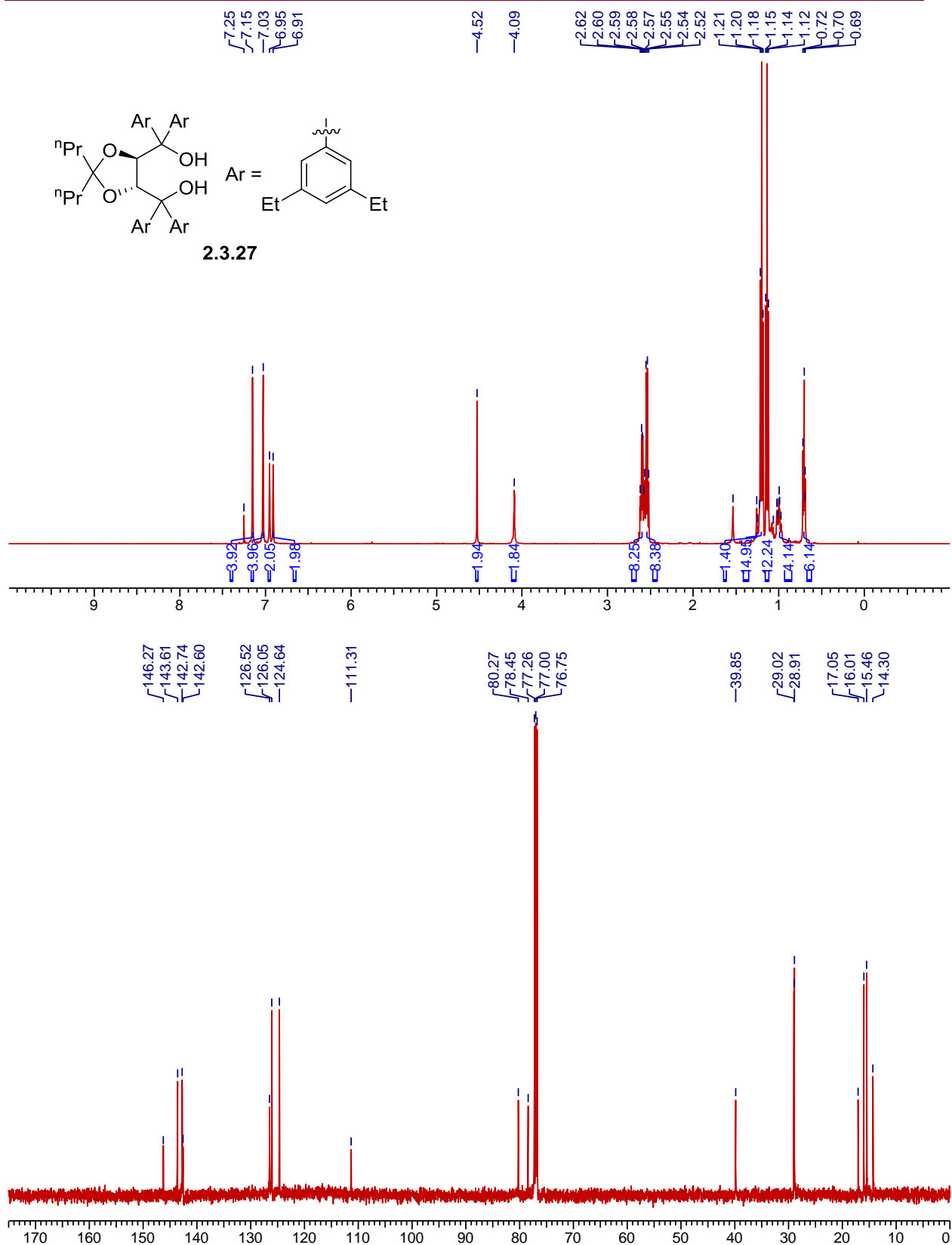
(diastereomeric ratio 1:0.75). R_f (Ethyl acetate/Pet. ether = 20:80) = 0.7. MP = 62.4 – 63.9 °C. $[\alpha]_{\text{D}}^{25} +179$ ($c = 3.0$ CH_2Cl_2). ^1H NMR (500 MHz, CDCl_3) δ 0.29 (d, $J = 4.20$ Hz, 3H), 0.44 (d, $J = 6.10$ Hz, 9H), 1.16 (q, $J = 7.63$ Hz, 6H), 1.14 (q, $J = 7.25$ Hz, 6H), 1.25 - 1.29 (m, 12H), 2.47 - 2.61 (m, 8H), 2.66 - 2.72 (m, 8H), 5.21 (dd, $J = 135$ Hz, 135 Hz, 1H), 6.82 (d, $J = 722$ Hz, 1H), 6.88 (s, 1H) 6.91 (d, $J = 8.77$ Hz, 2H), 6.94 (s, 1H), 7.01 (s, 1H), 7.05 (d, $J = 5.72$ Hz, 1H), 7.09 (d, $J = 5.34$ Hz, 1H), 7.26 (s, 1H), 7.29 (s, 1H), 7.32 (d, $J = 6.87$ Hz, 2H); ^{13}C NMR (126 MHz, CDCl_3) δ 15.26, 15.38, 15.50, 15.77, 15.83, 15.89, 15.98, 17.86, 18.16, 24.36, 28.85, 28.88, 38.32, 38.43, 78.53, 78.58, 79.62, 79.65, 87.53, 87.59, 88.63, 88.69, 89.47, 89.55, 90.70, 90.78, 117.80, 117.90, 123.62, 123.79, 125.31, 125.51, 125.74, 126.79, 126.85, 127.59, 139.62, 139.77, 142.95, 143.01, 143.40, 143.44, 143.54, 143.58, 143.63, 143.85, 144.52, 144.56; ^{31}P NMR (202 MHz, CDCl_3) δ -4.78 (major), -4.62 (minor). FTIR (cm^{-1}): 3018, 2966, 2933, 2975, 1742, 1601, 1457, 1373, 1268, 1077, 877, 669. LCMS (ESI) m/z Calculated for $\text{C}_{50}\text{H}_{67}\text{O}_5\text{P}$ $[\text{M}+\text{Na}]^+$: 801.4; found: 801.2.

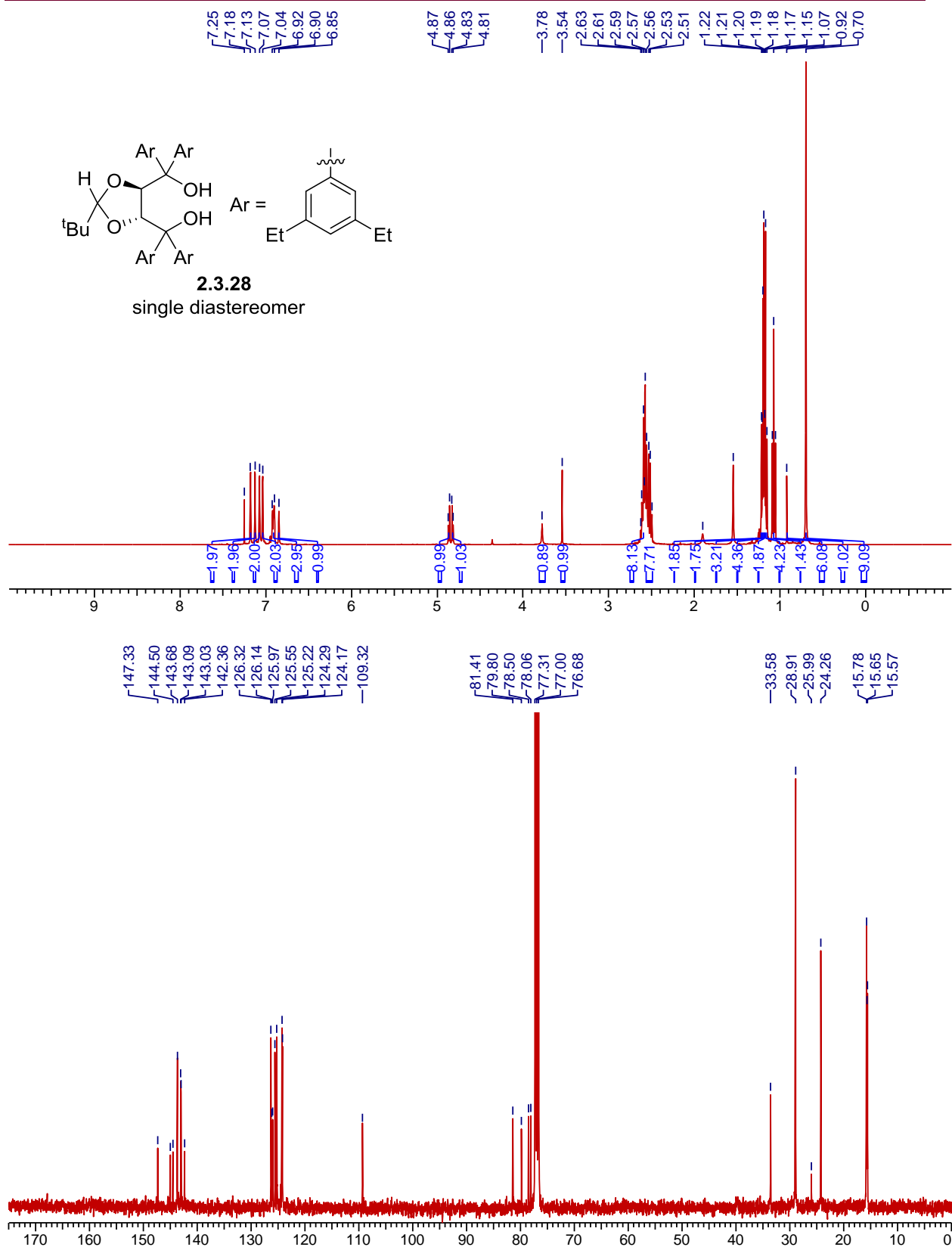
2.8 NMR spectra (^1H & ^{13}C)

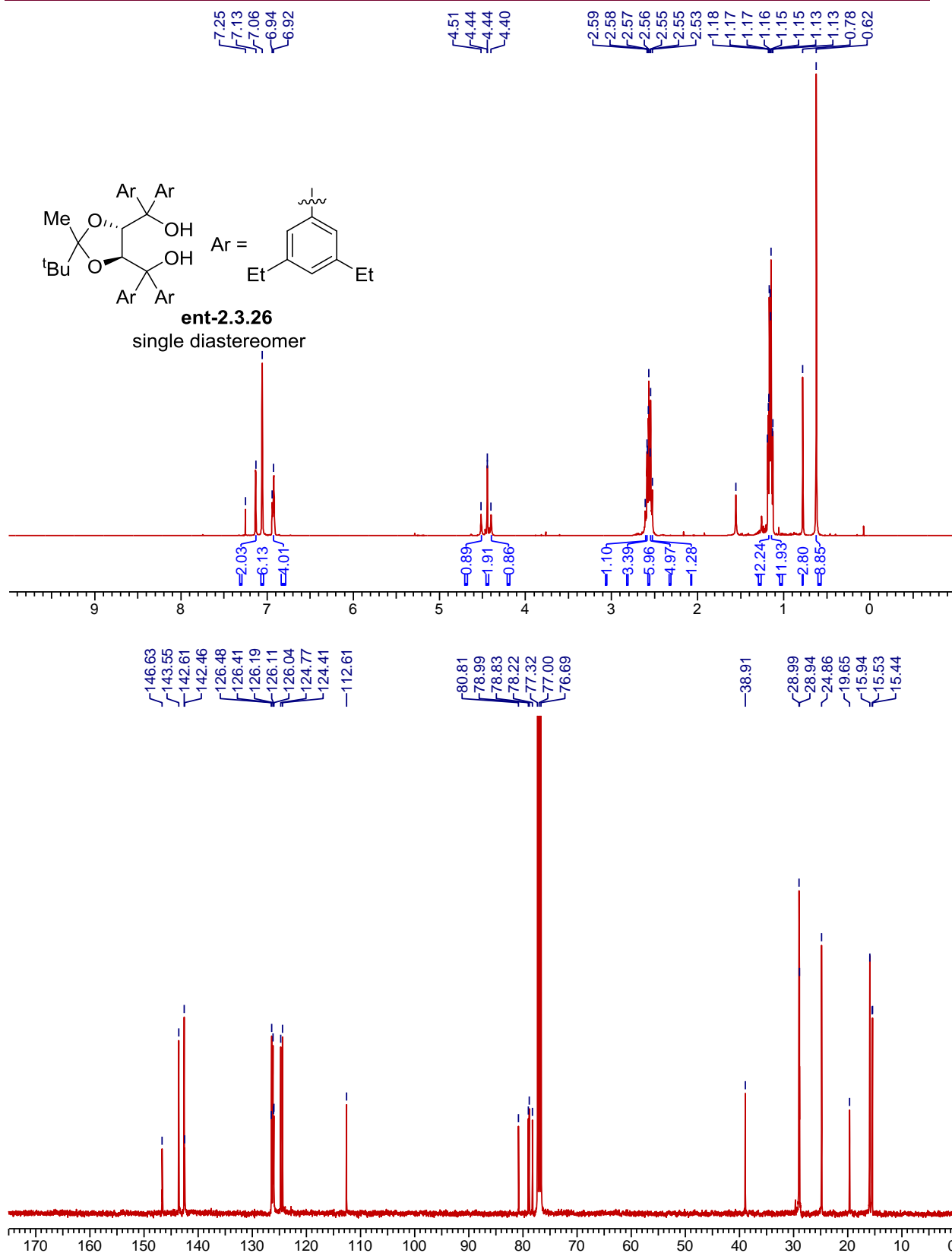


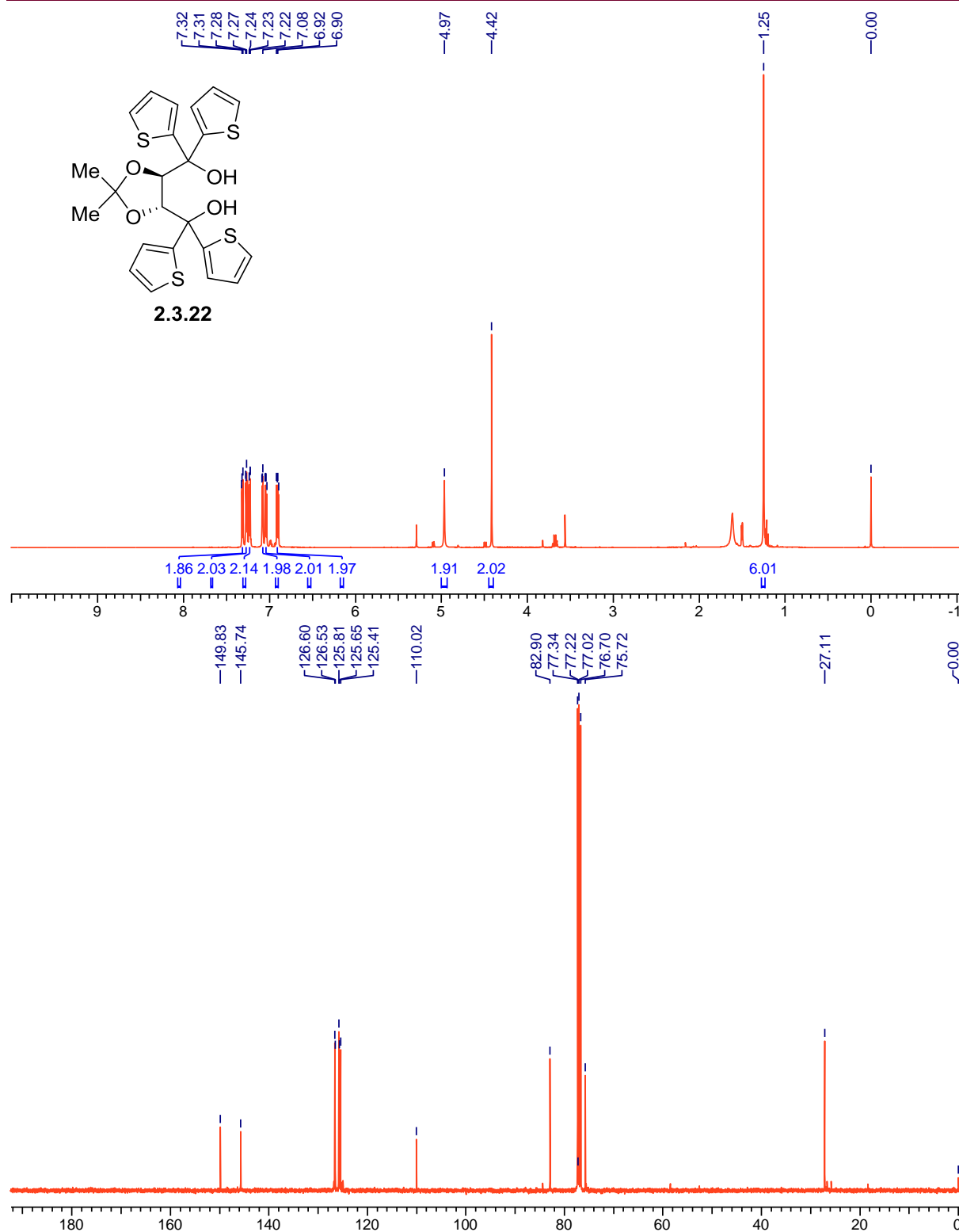


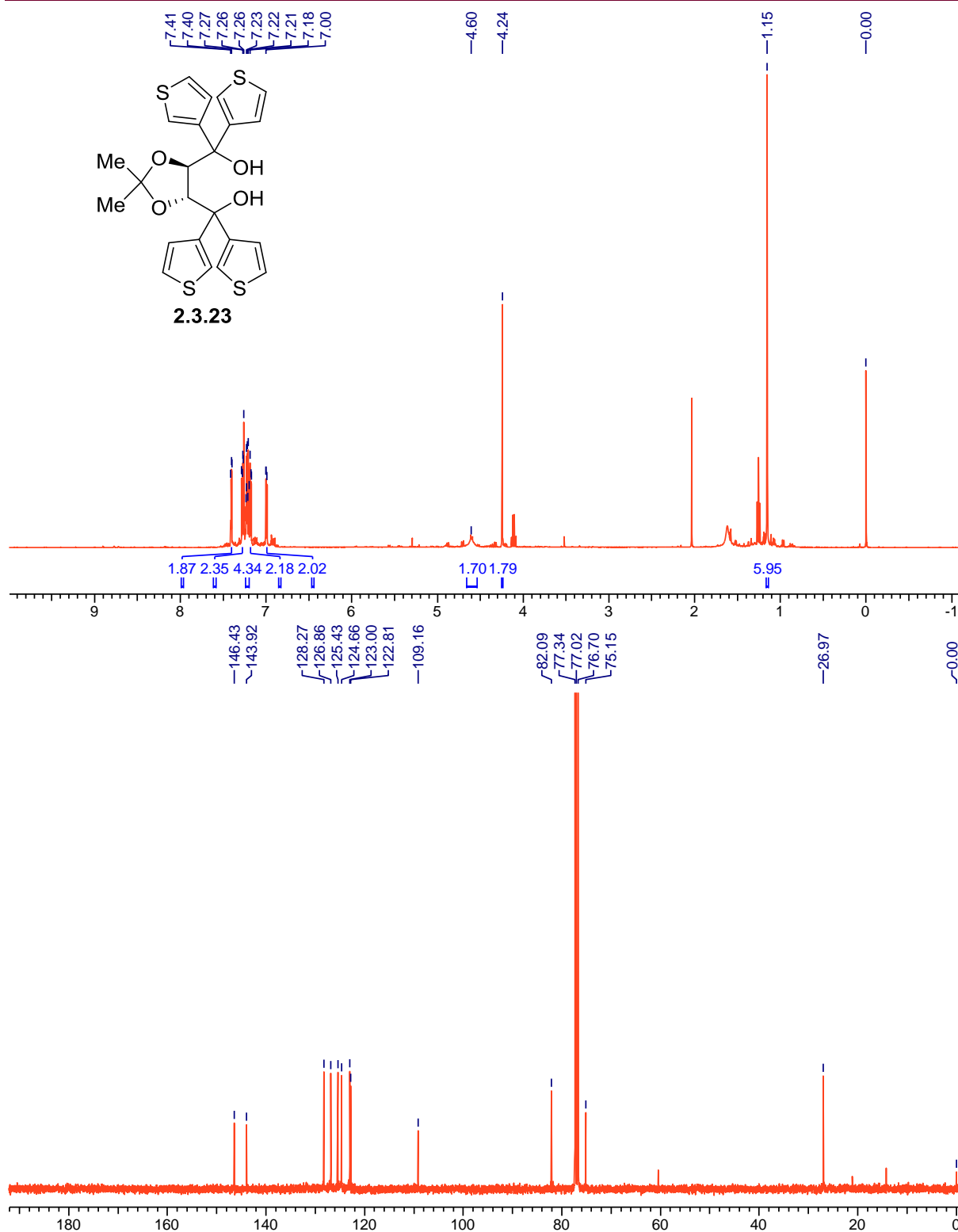


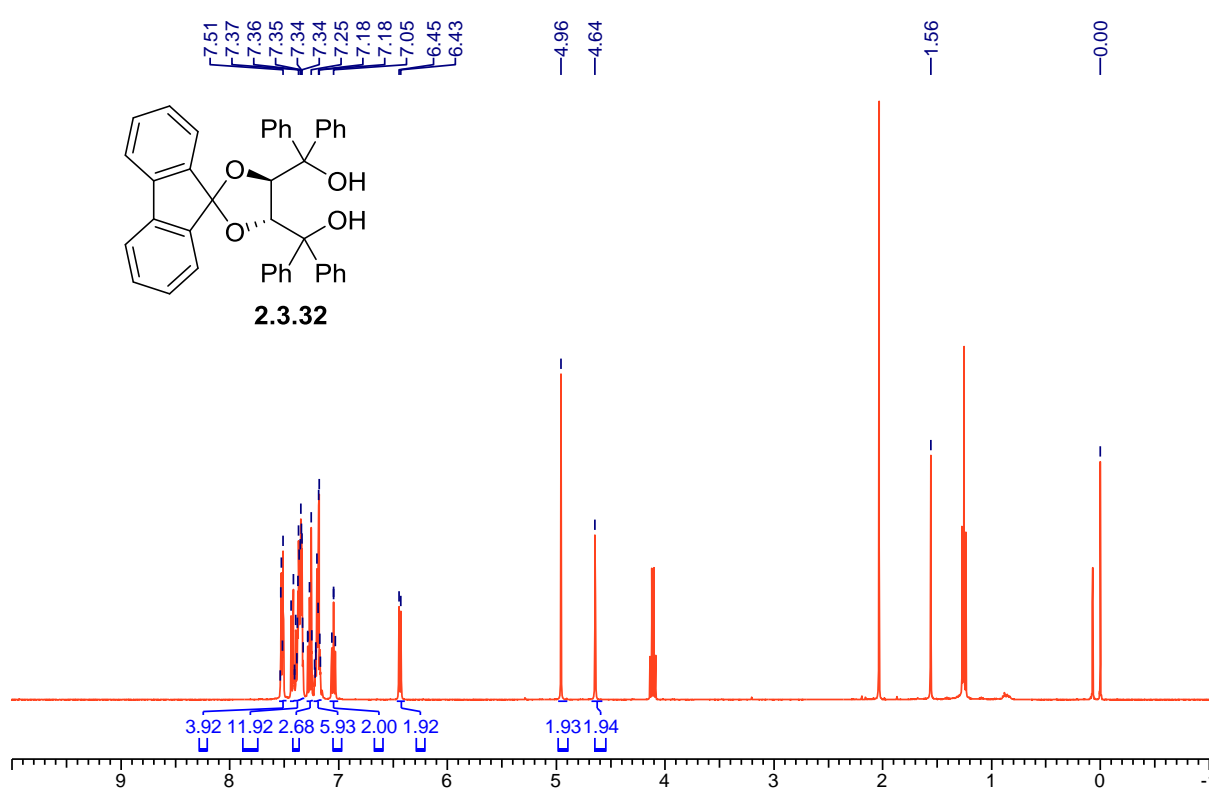
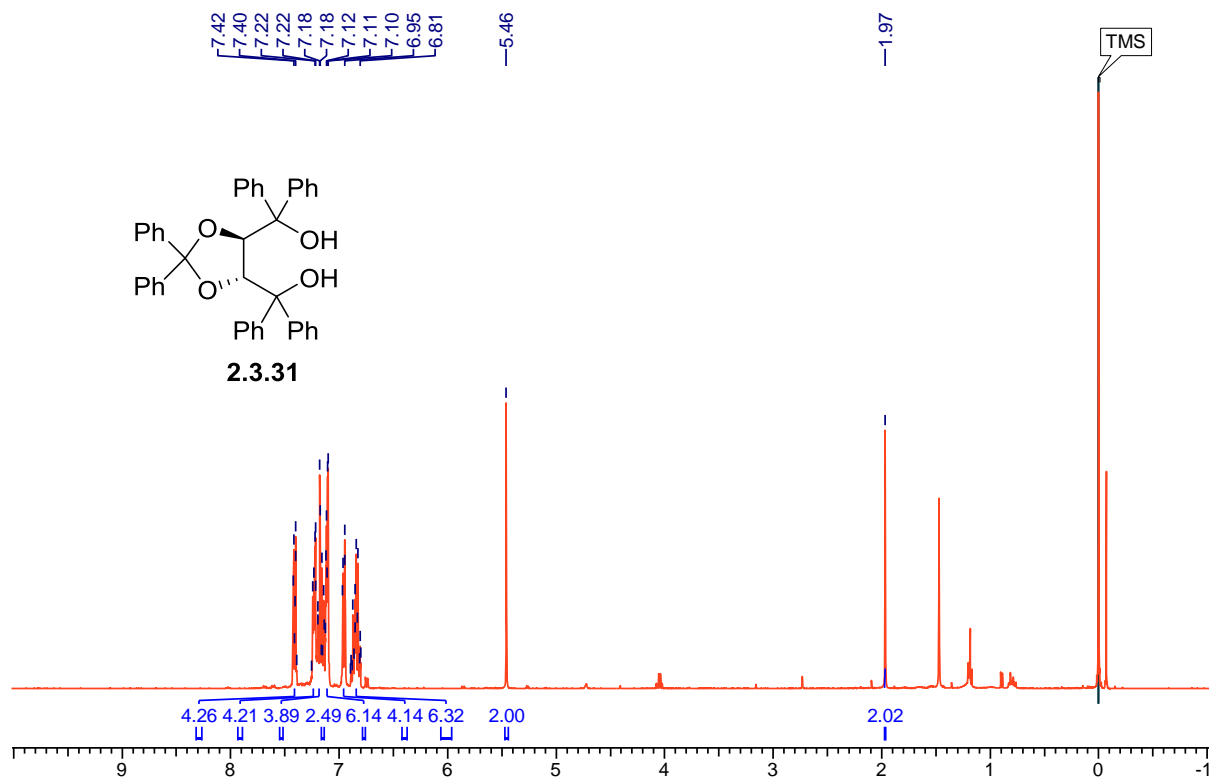


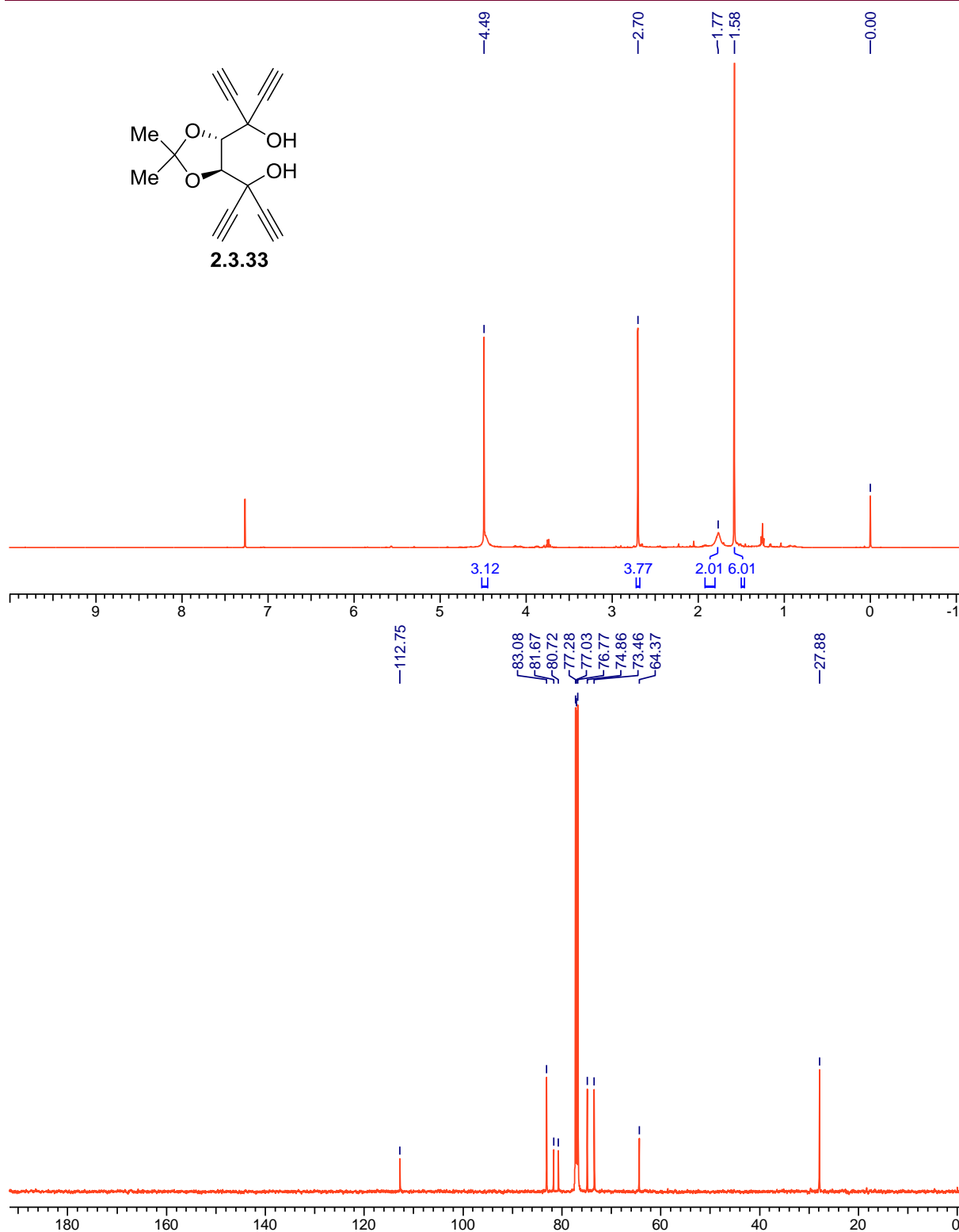


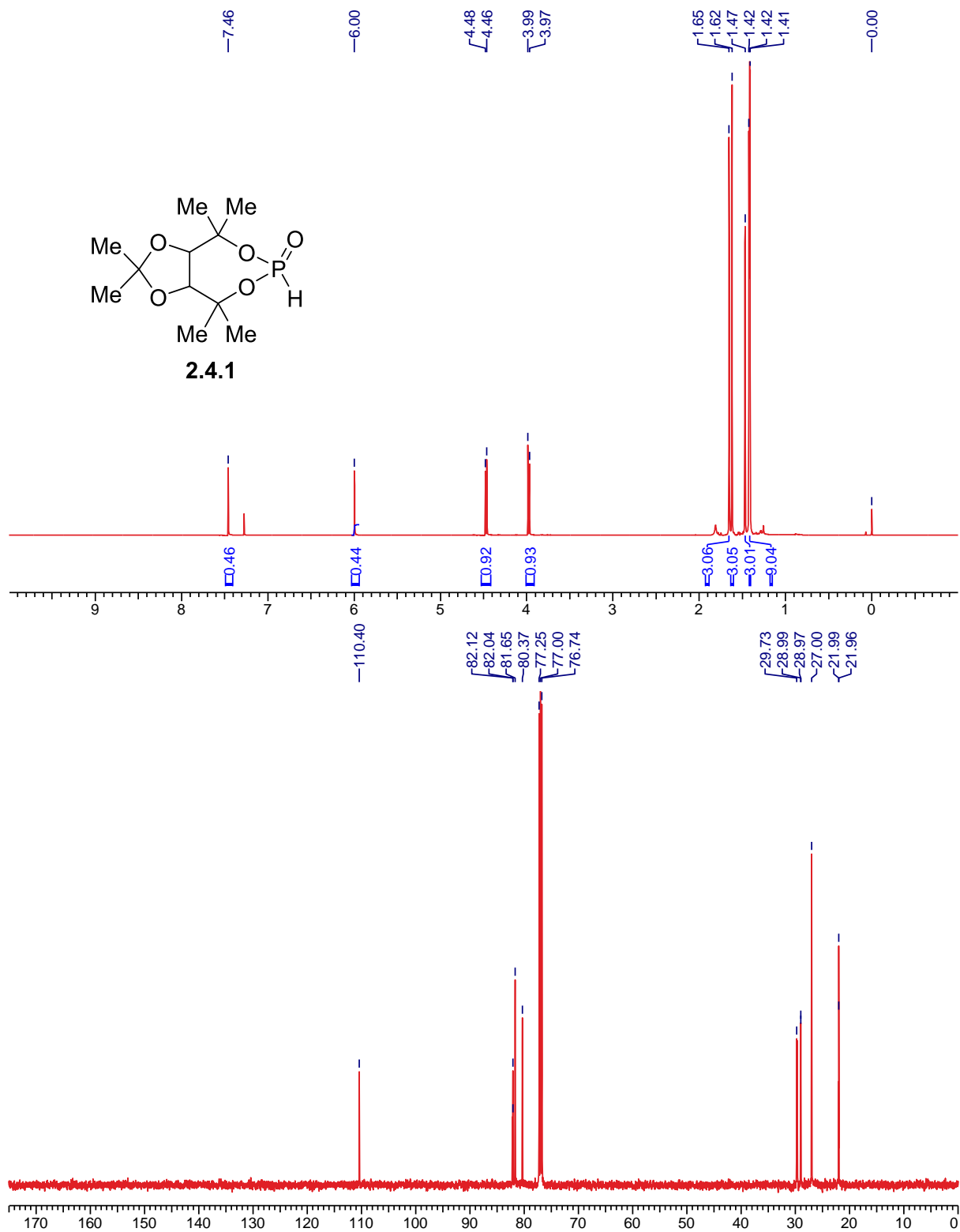


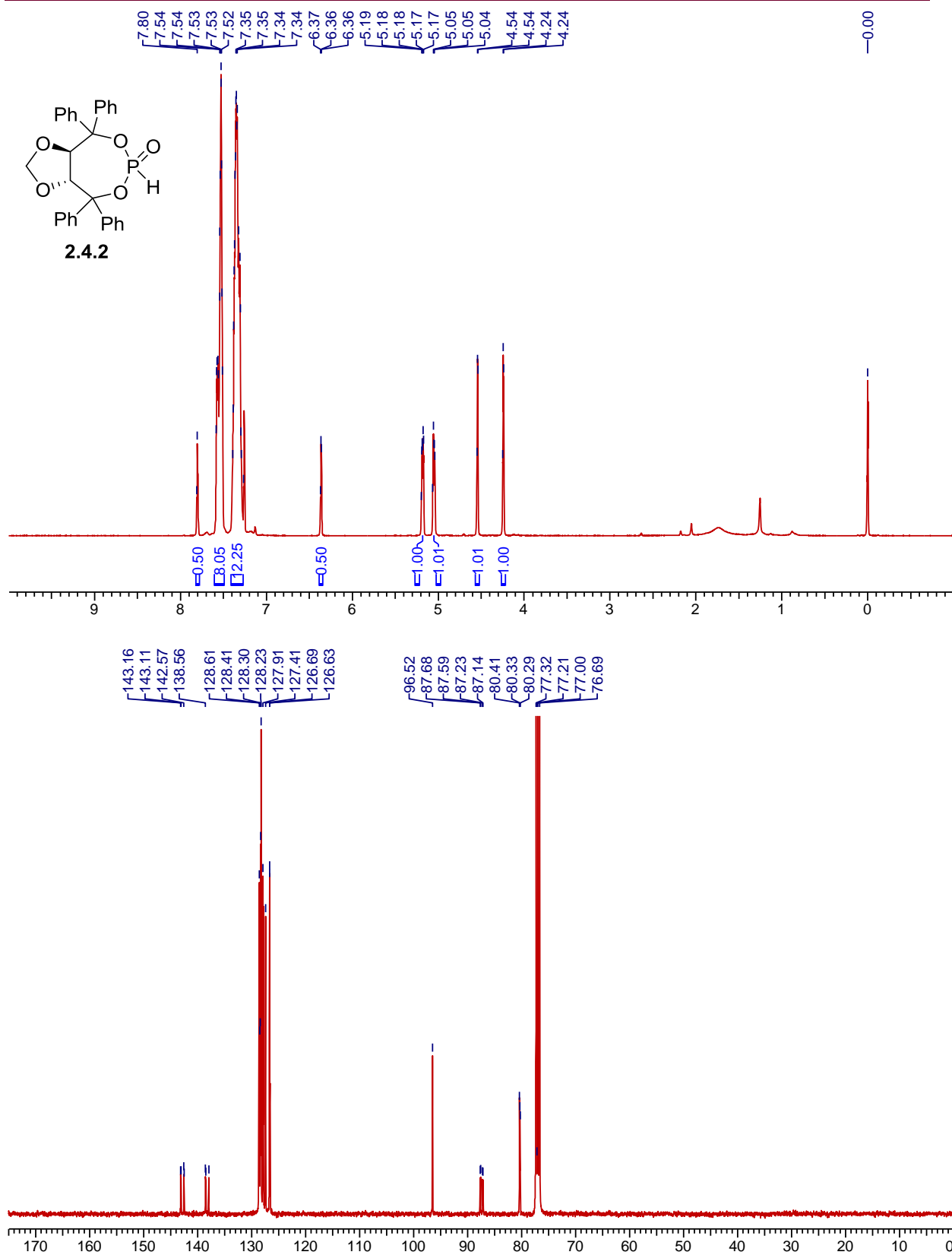


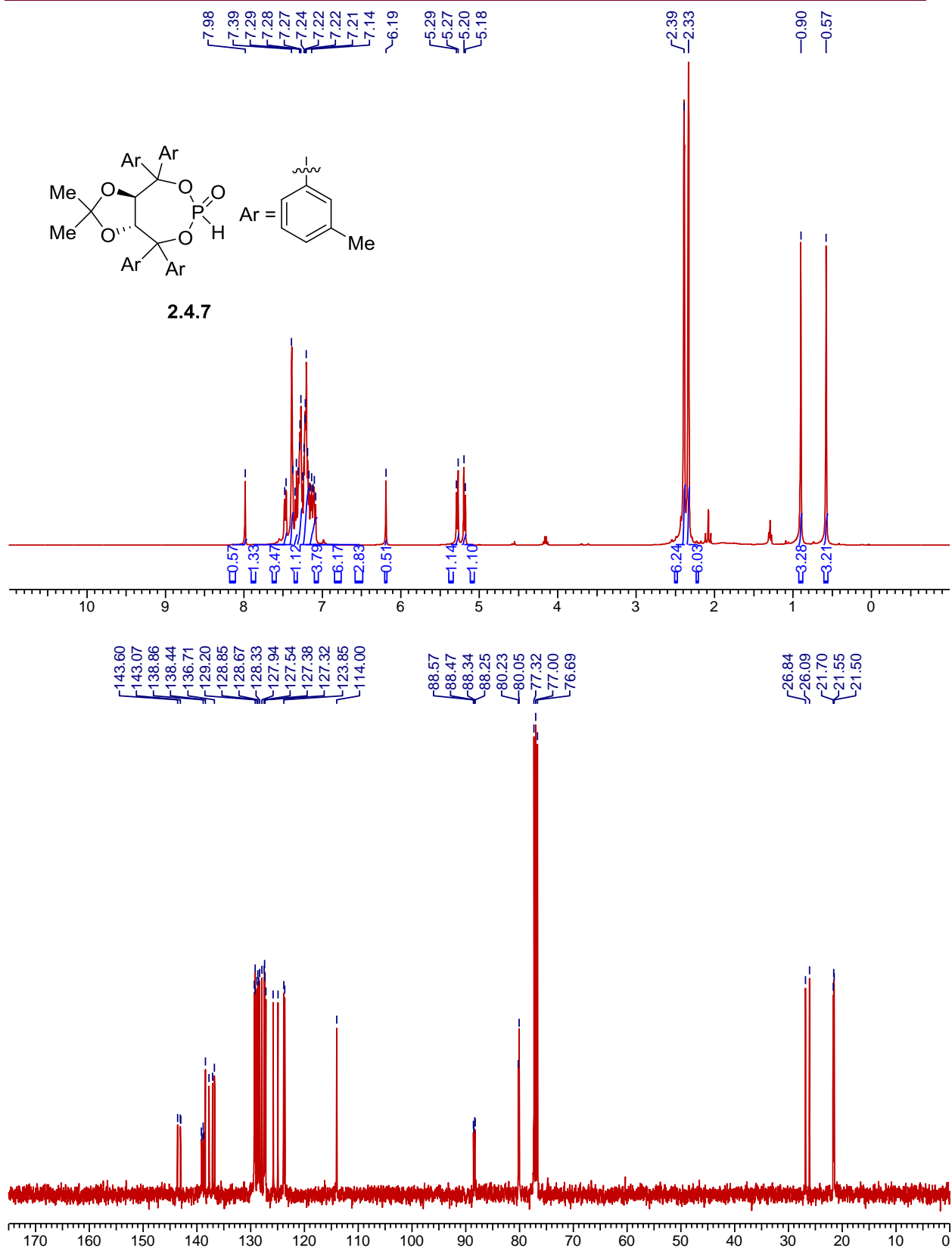


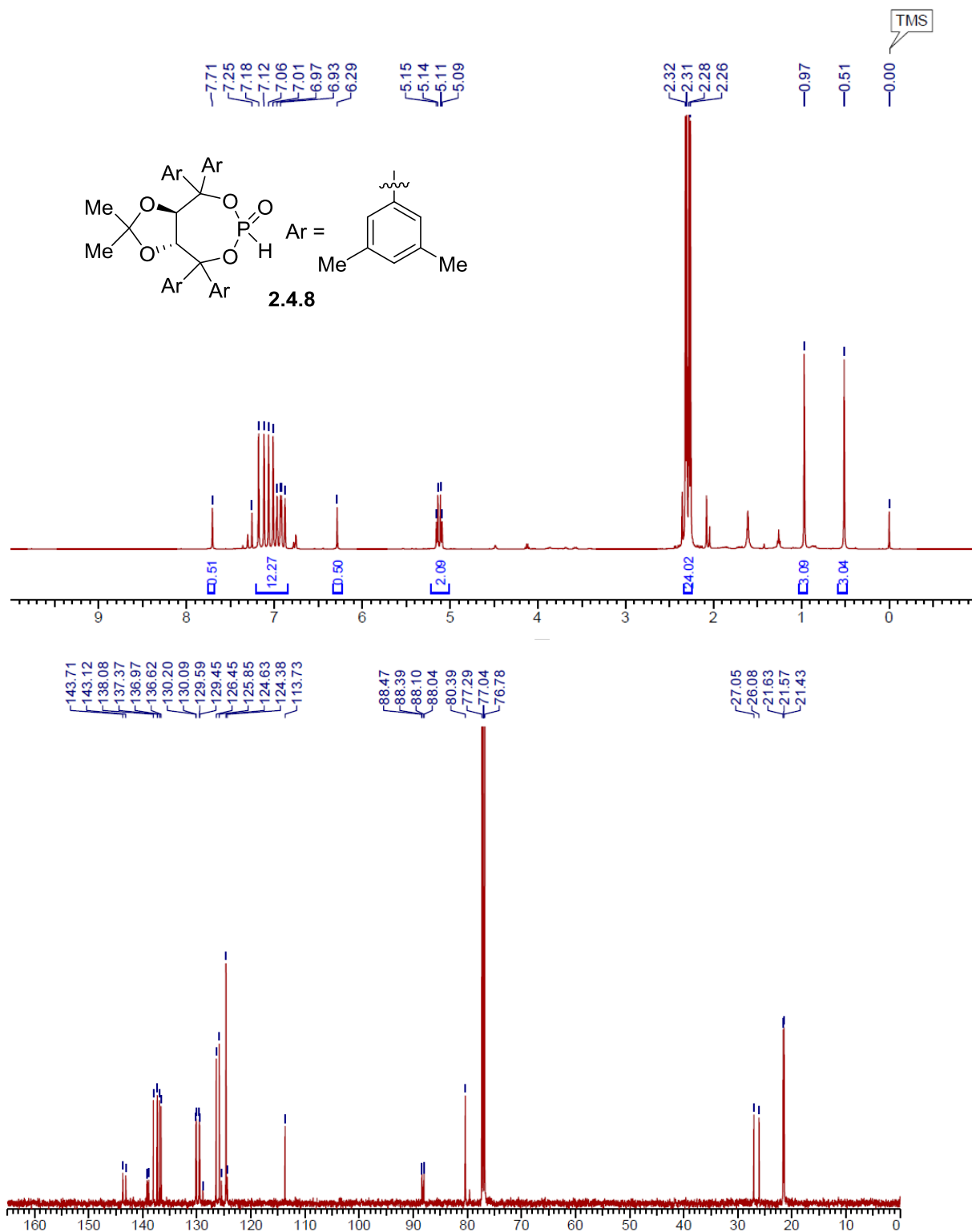


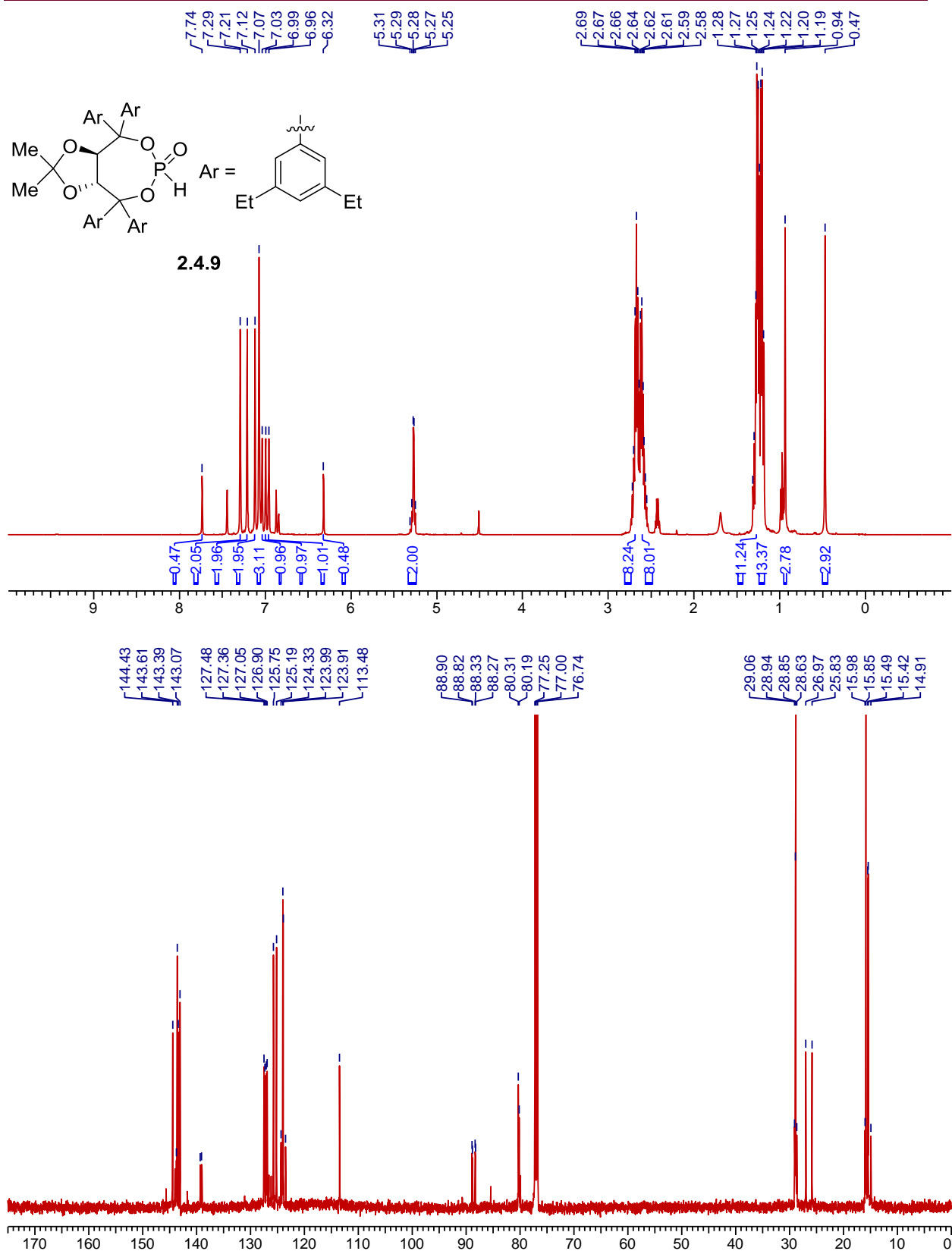


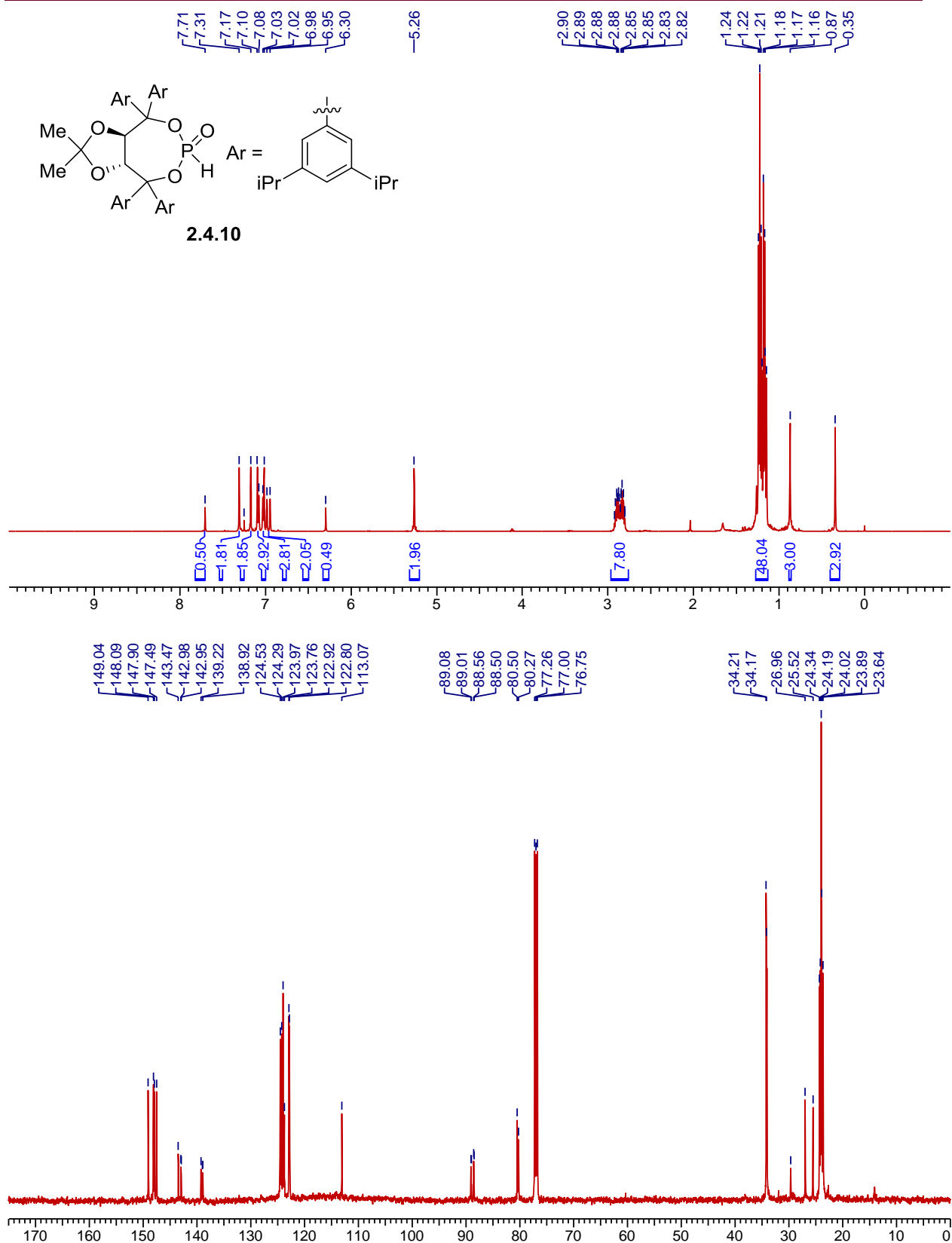


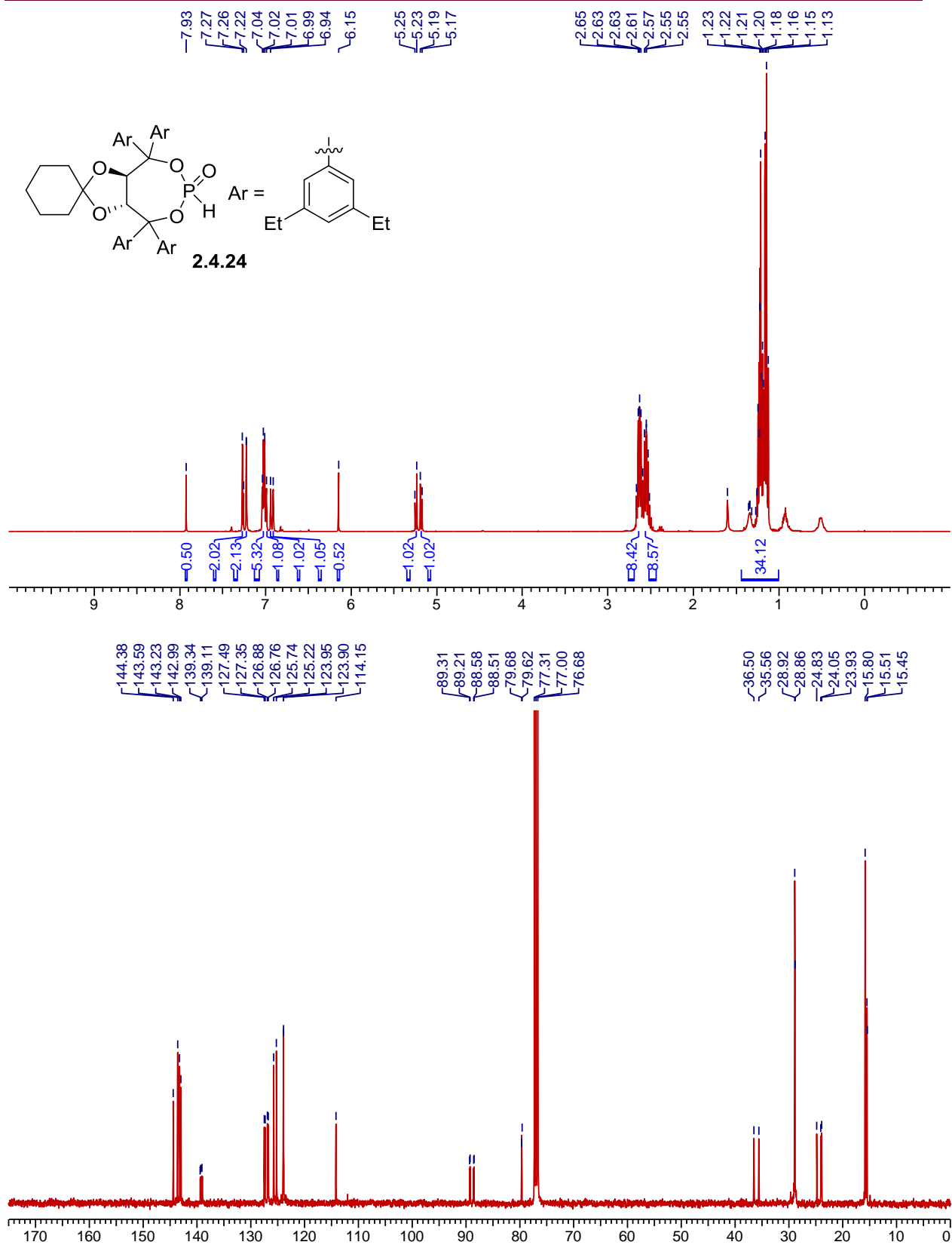


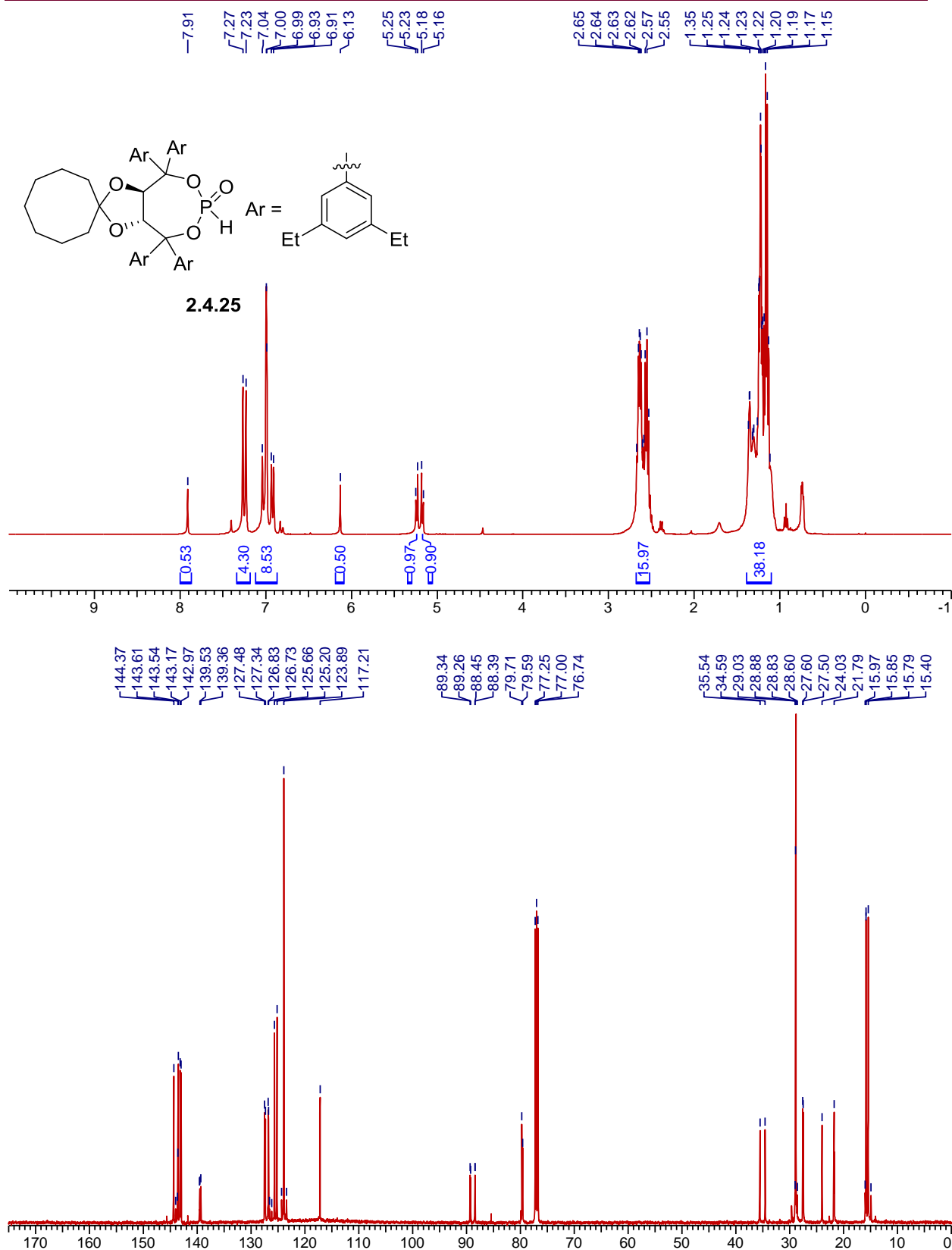


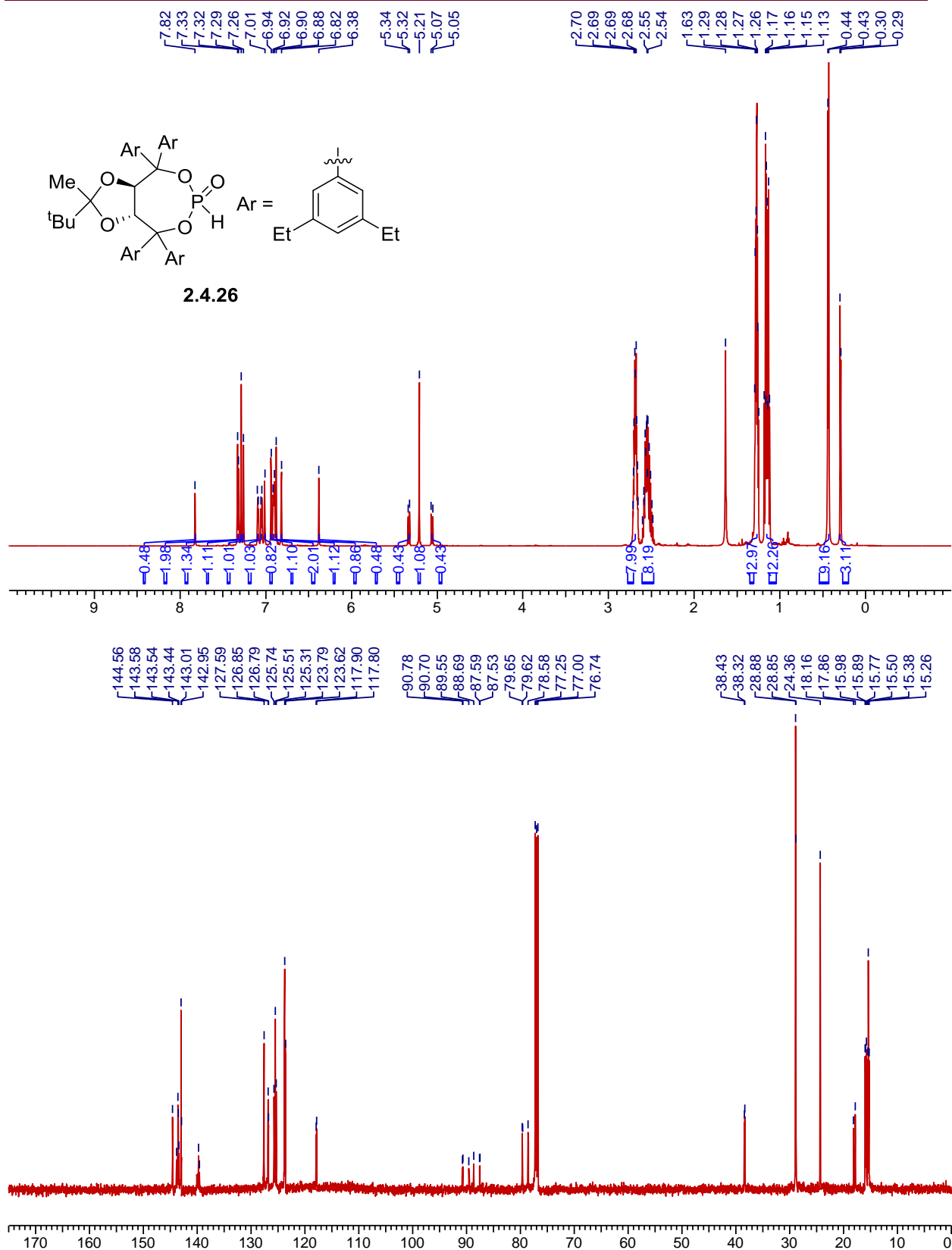


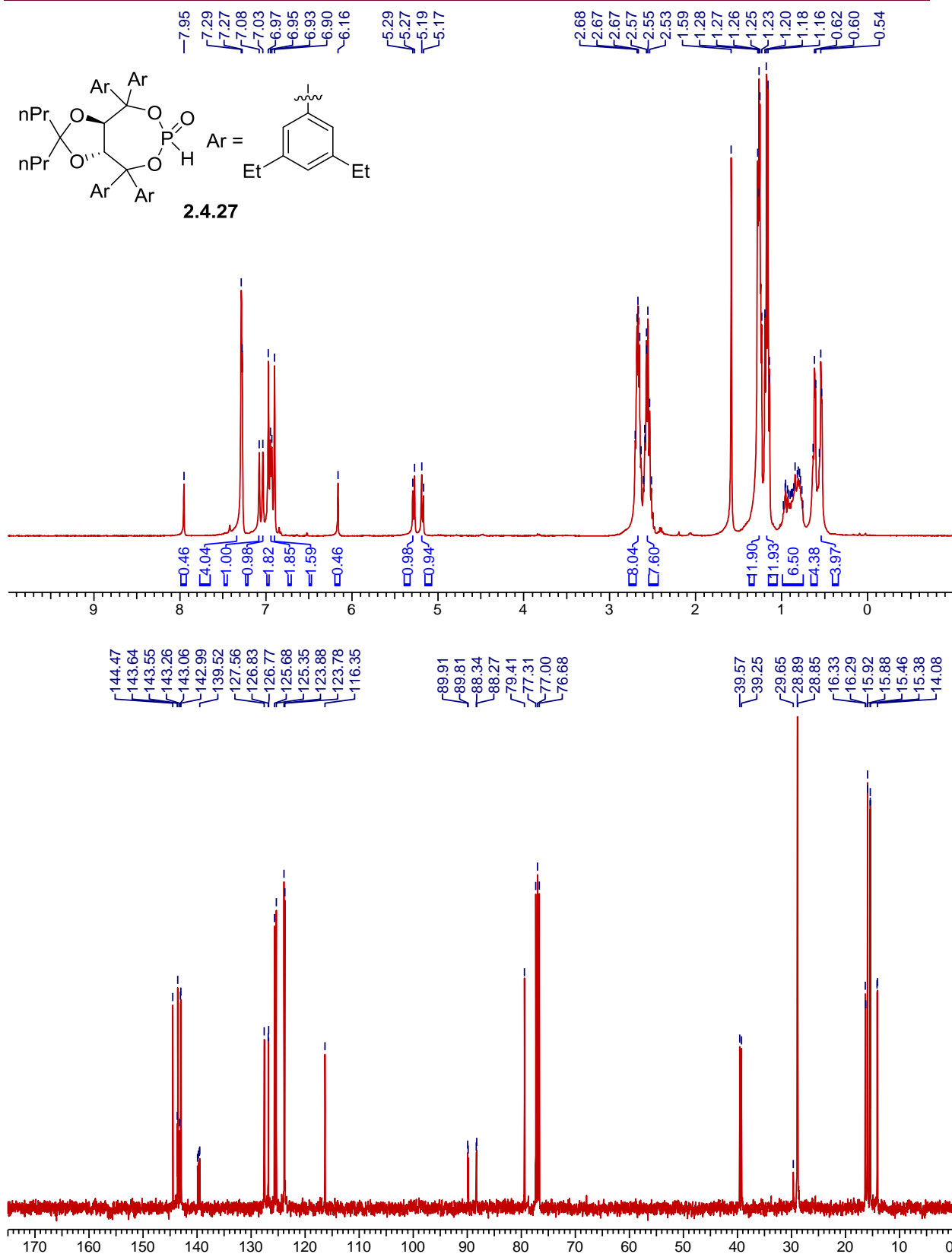


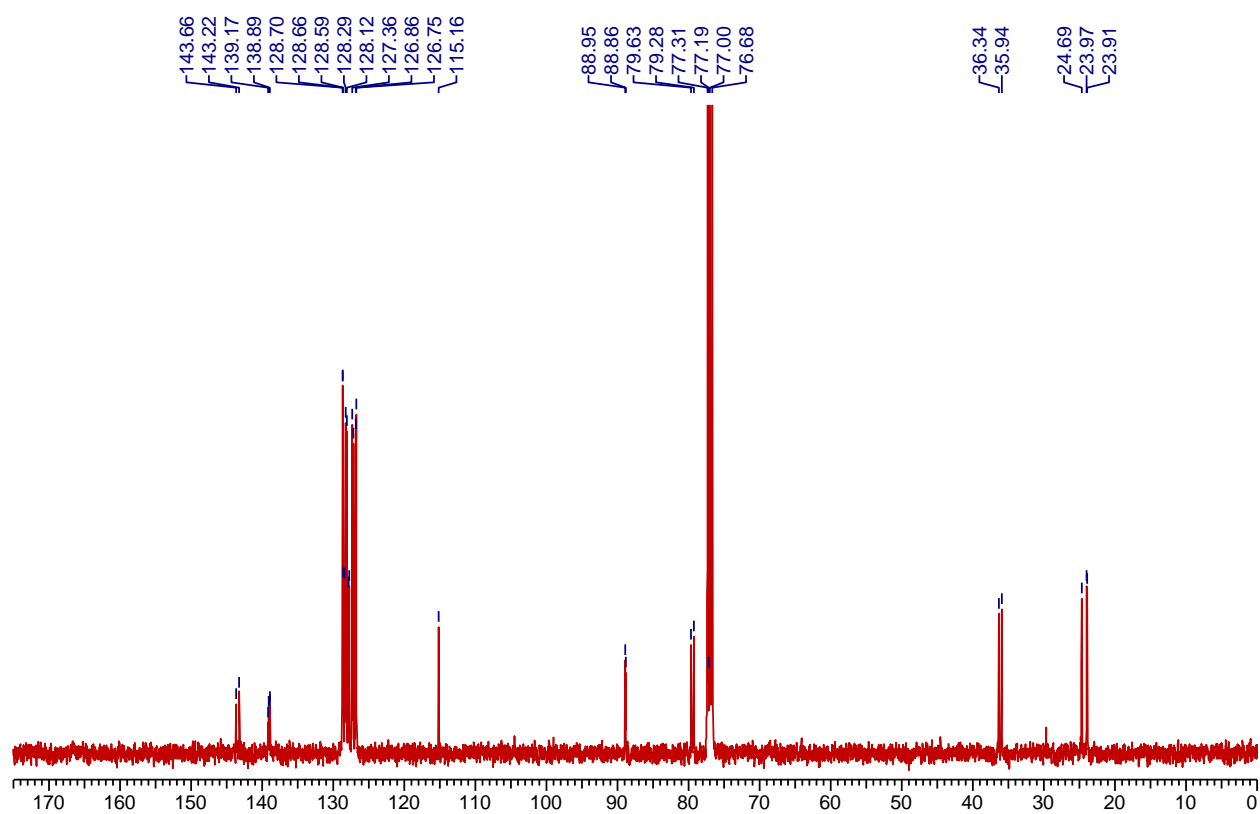
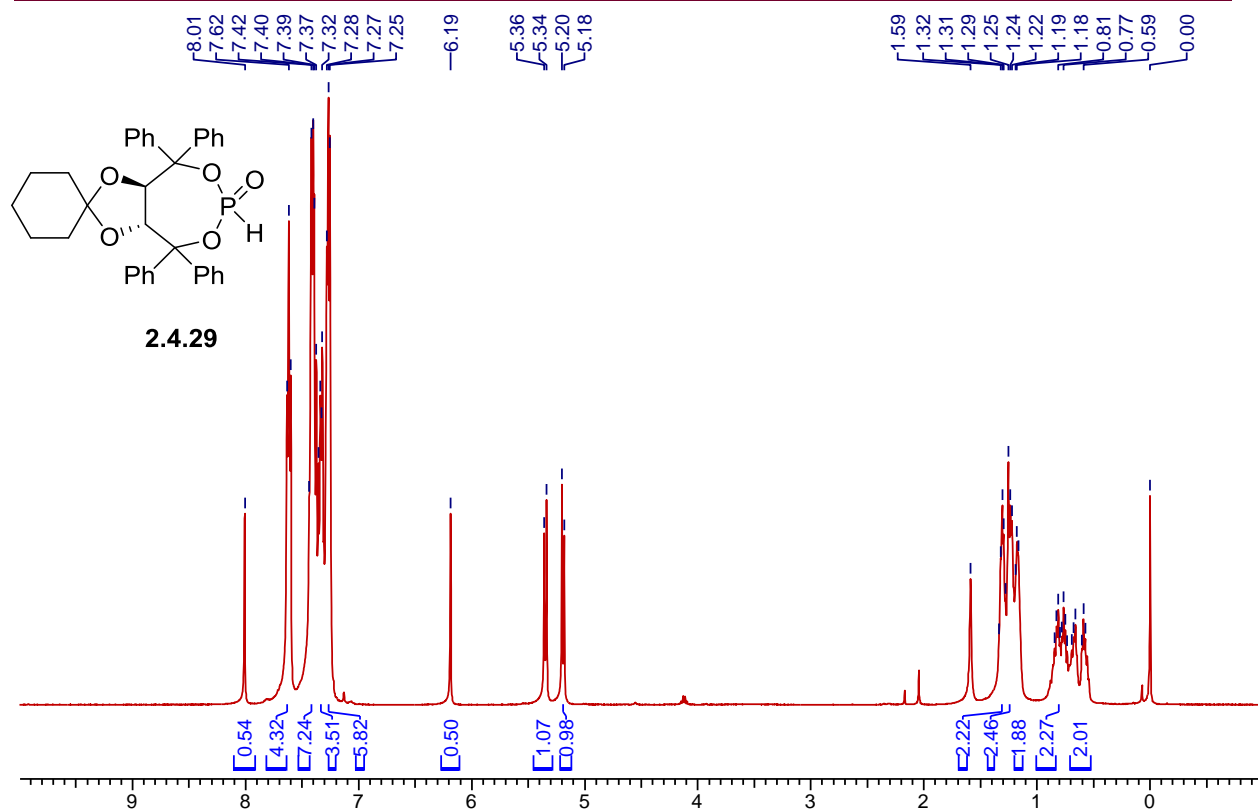


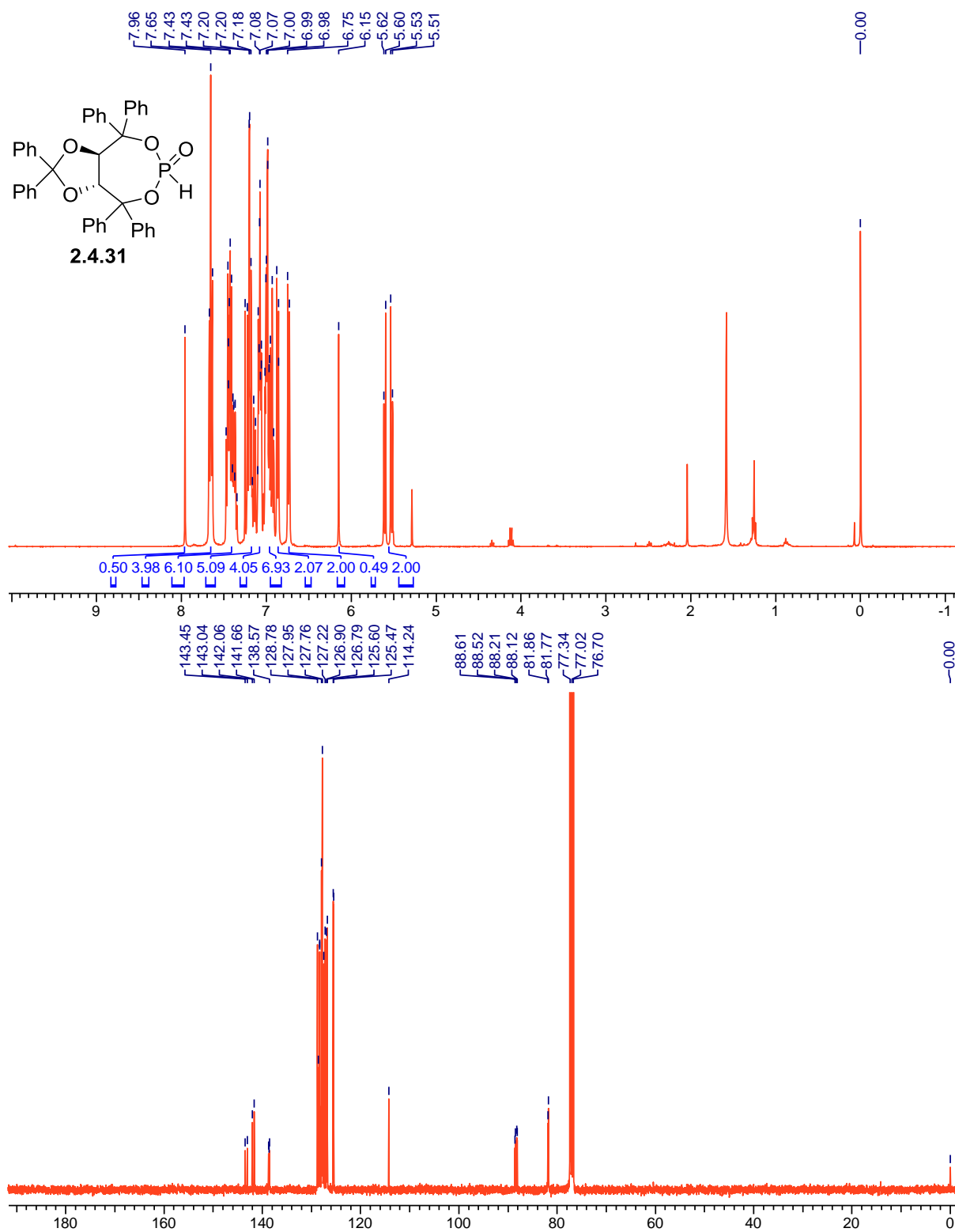


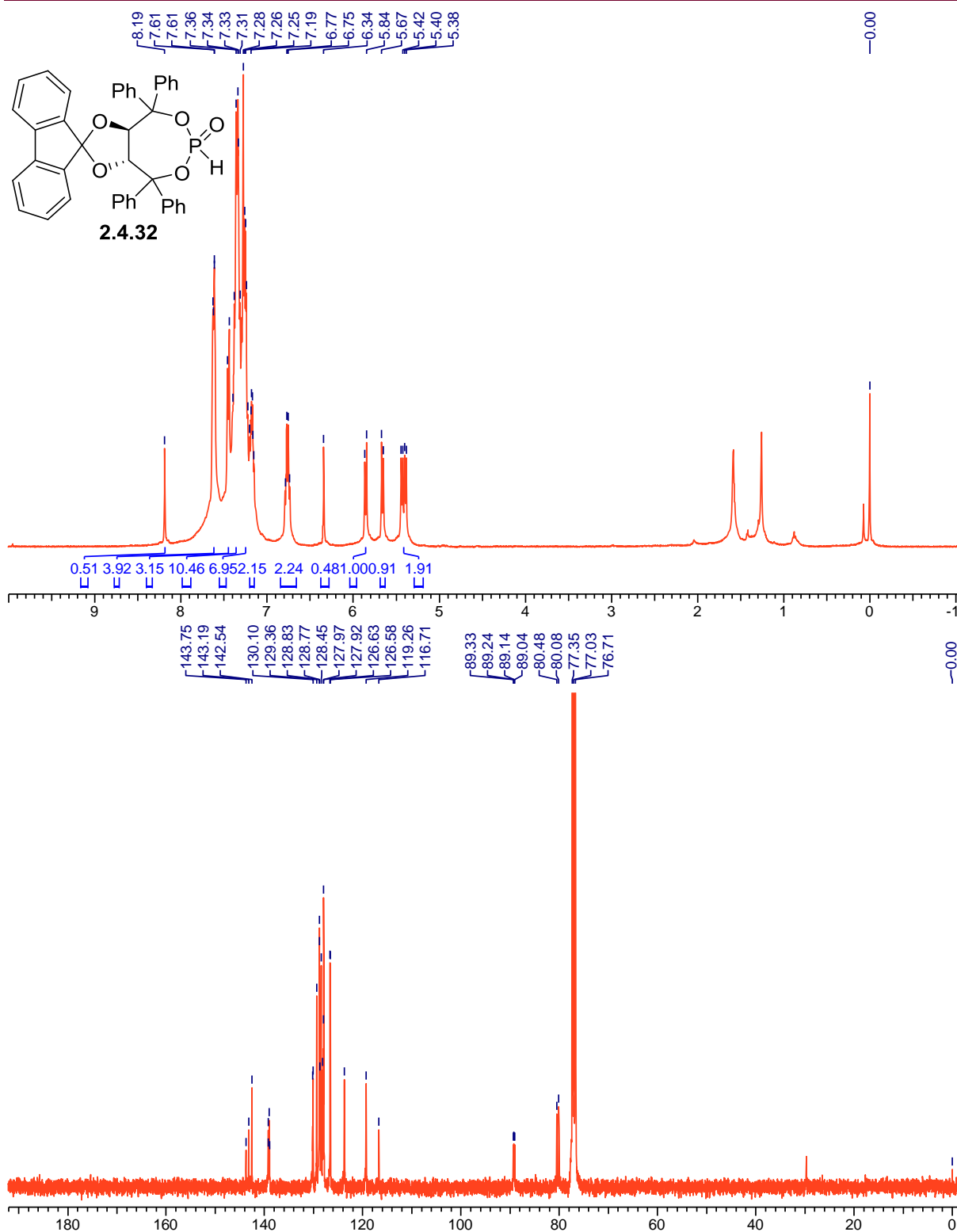


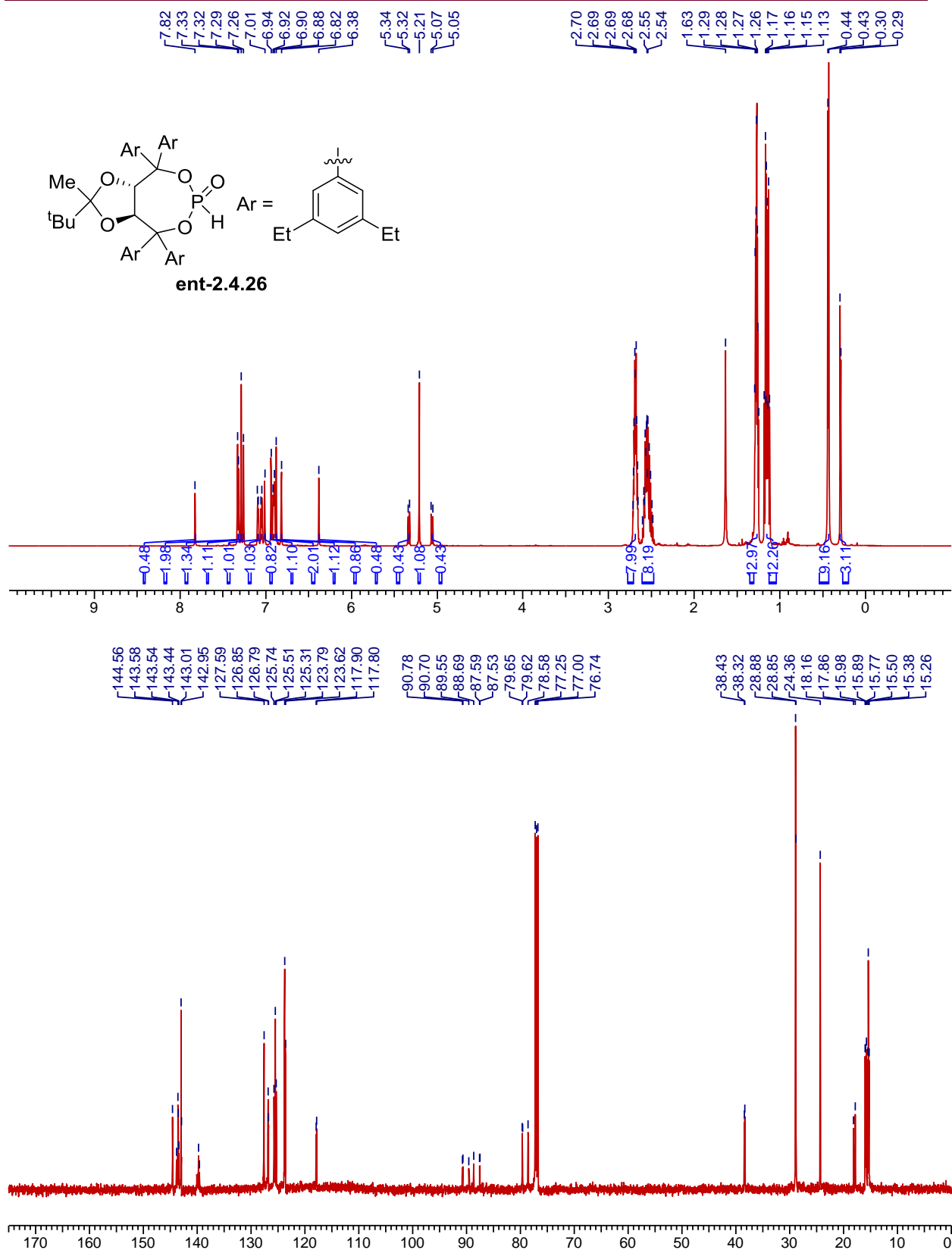


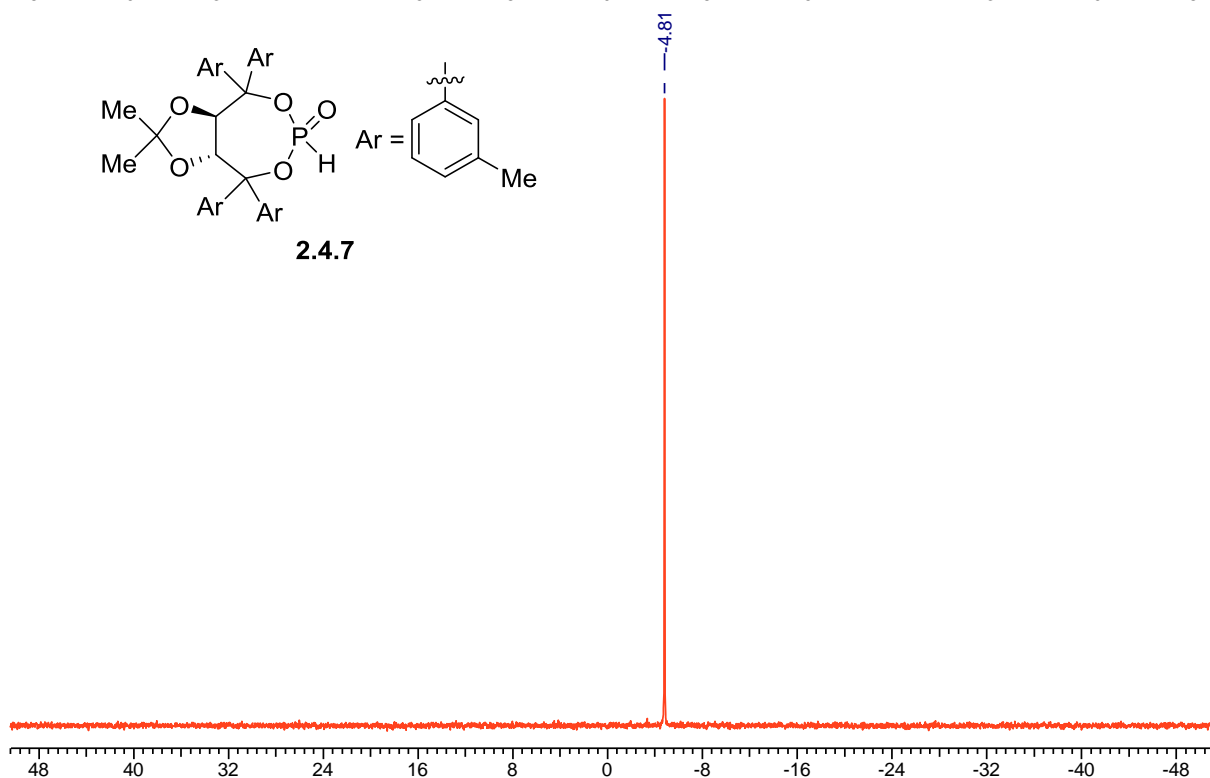
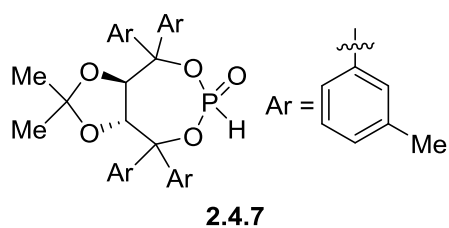
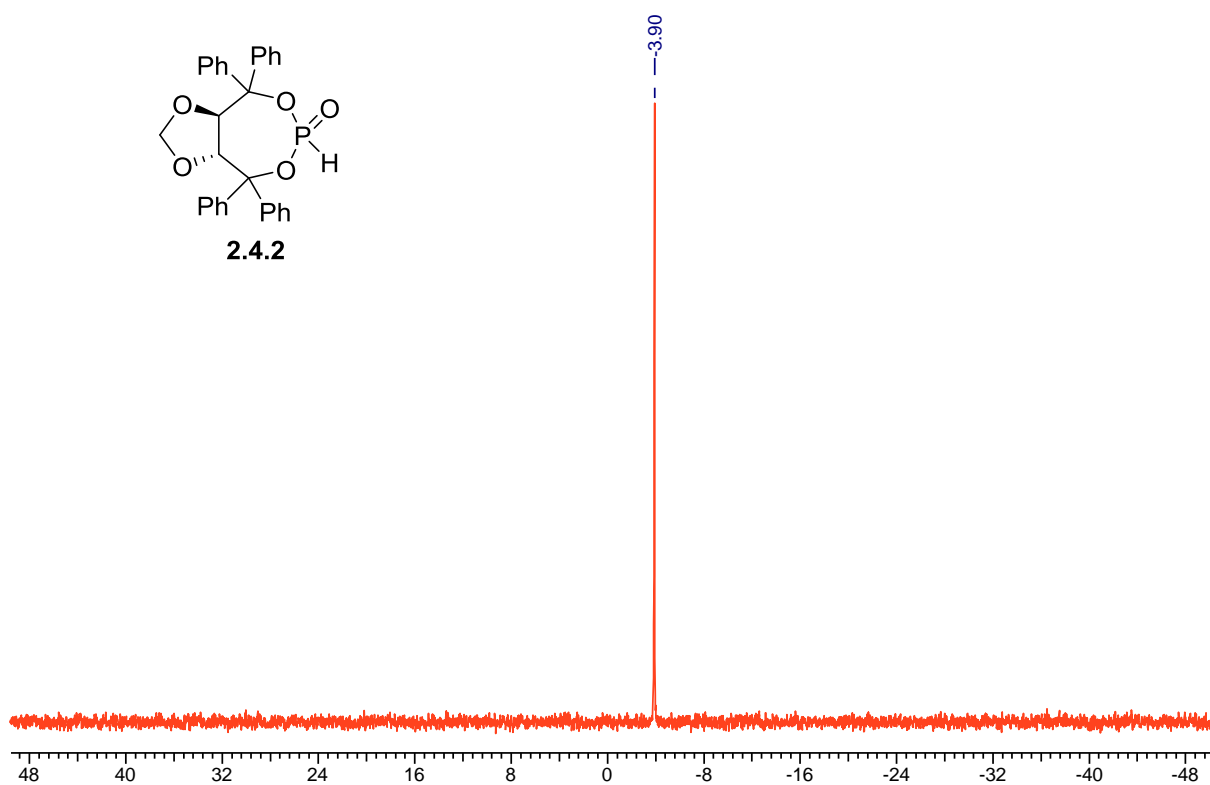
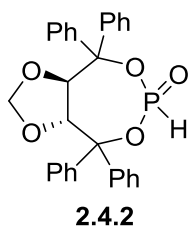


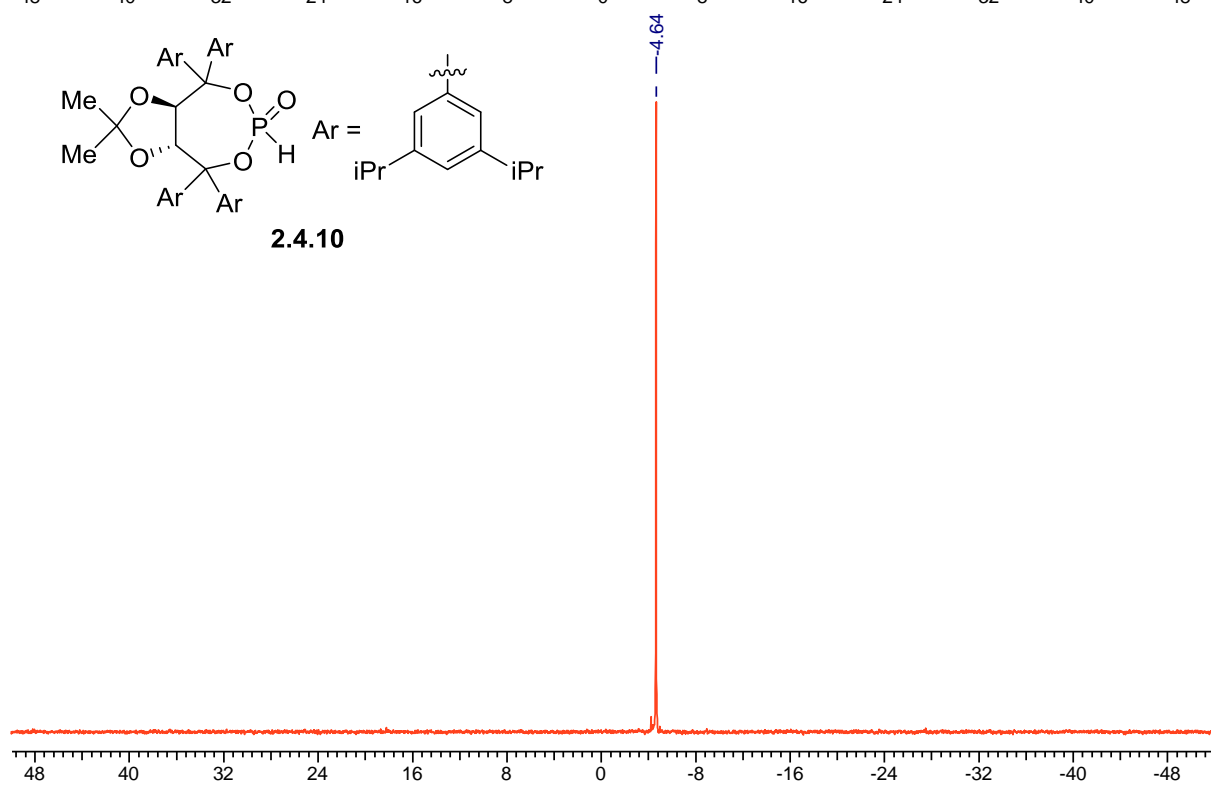
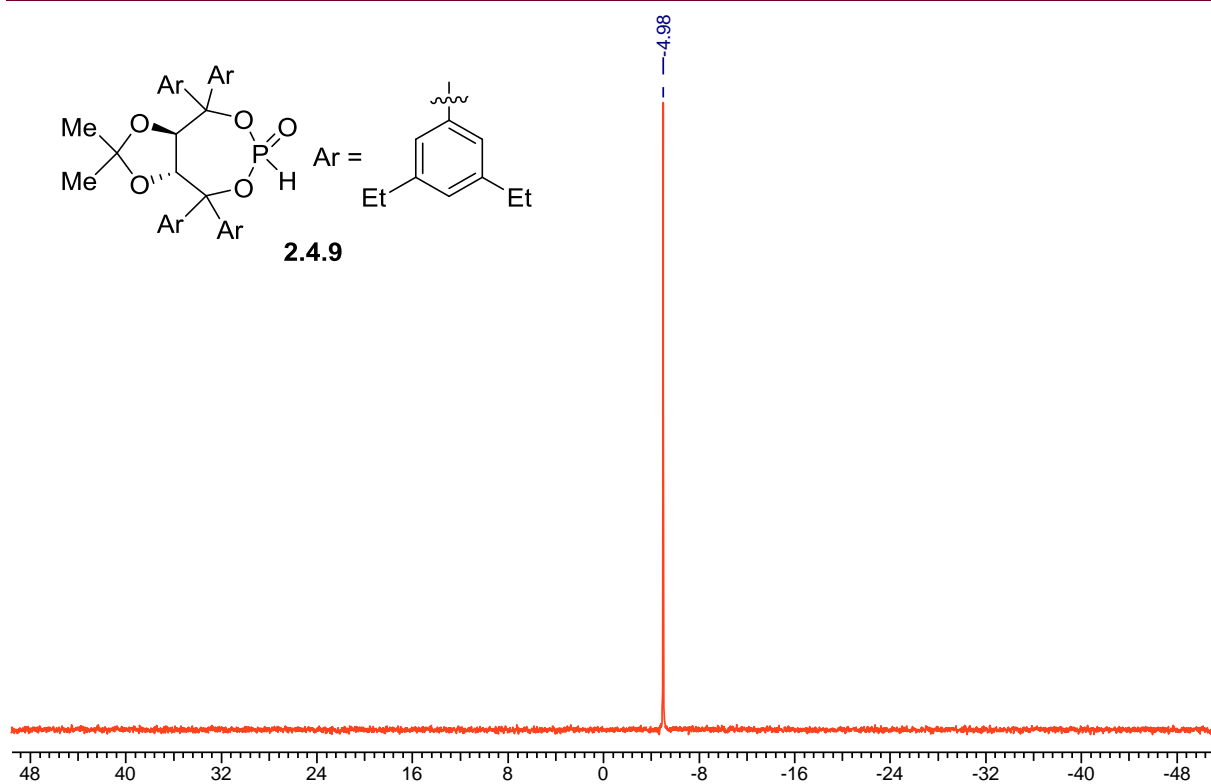


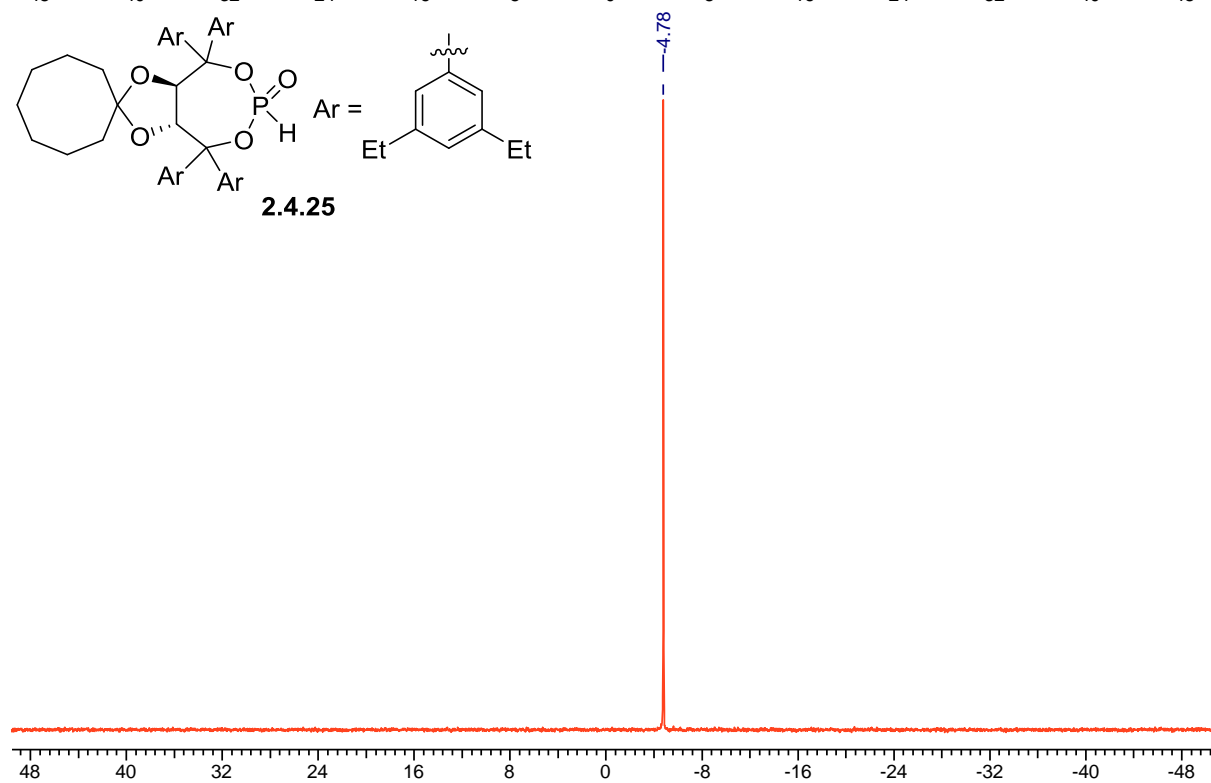
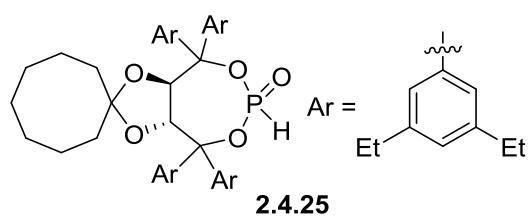
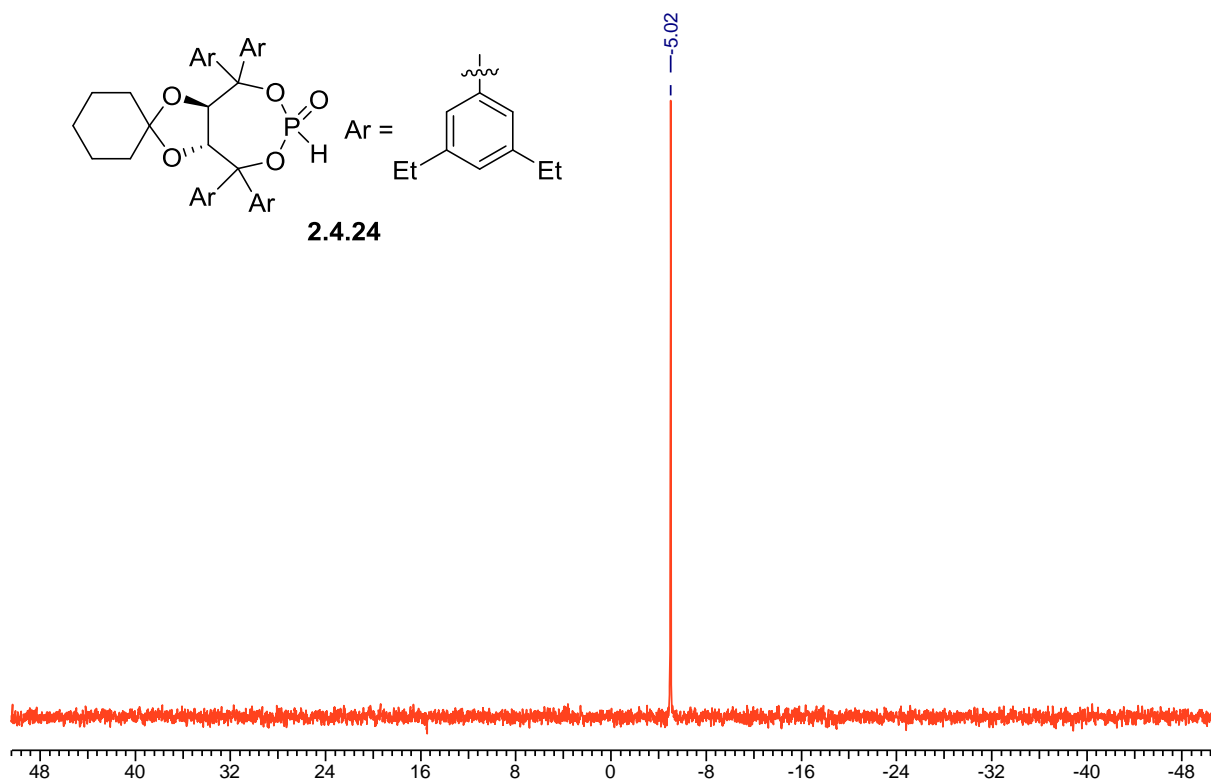
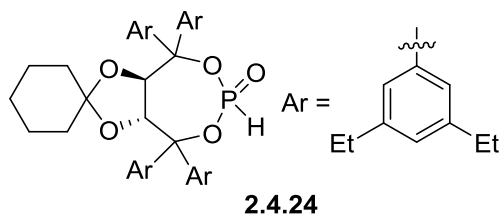


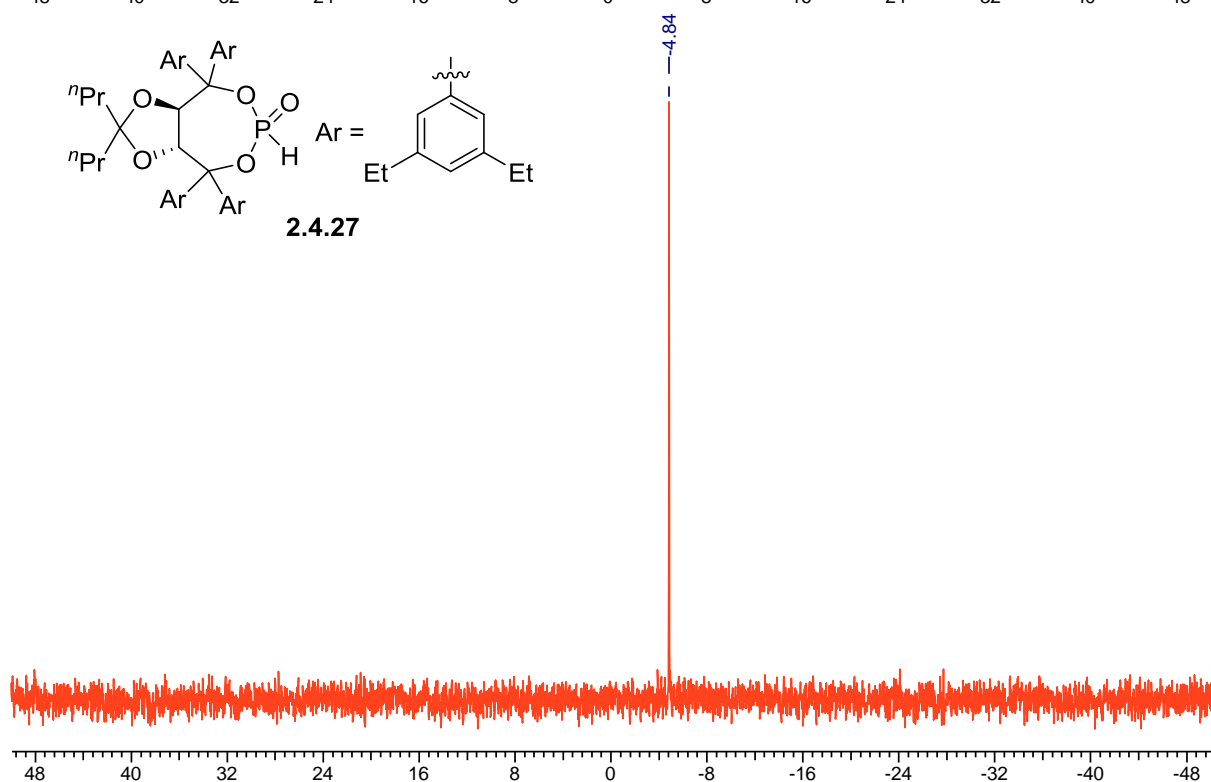
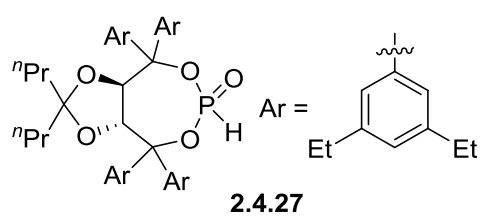
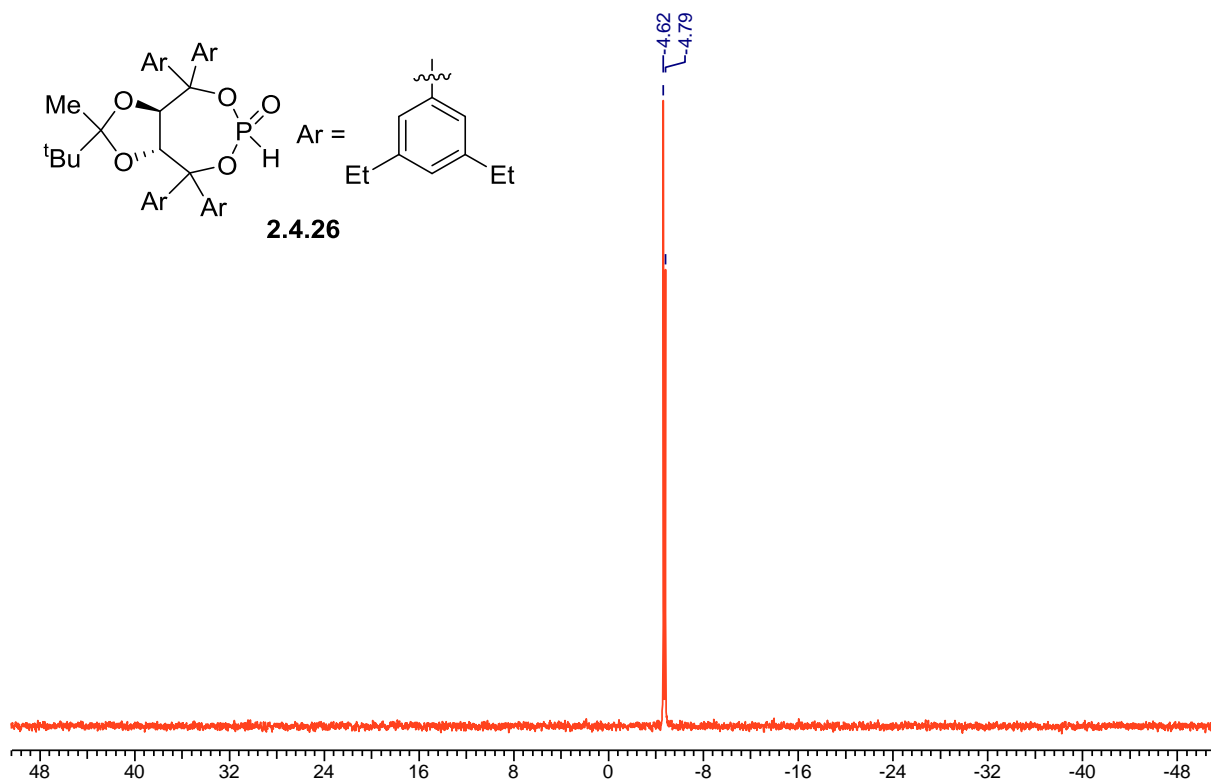
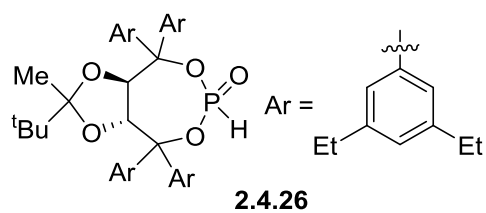


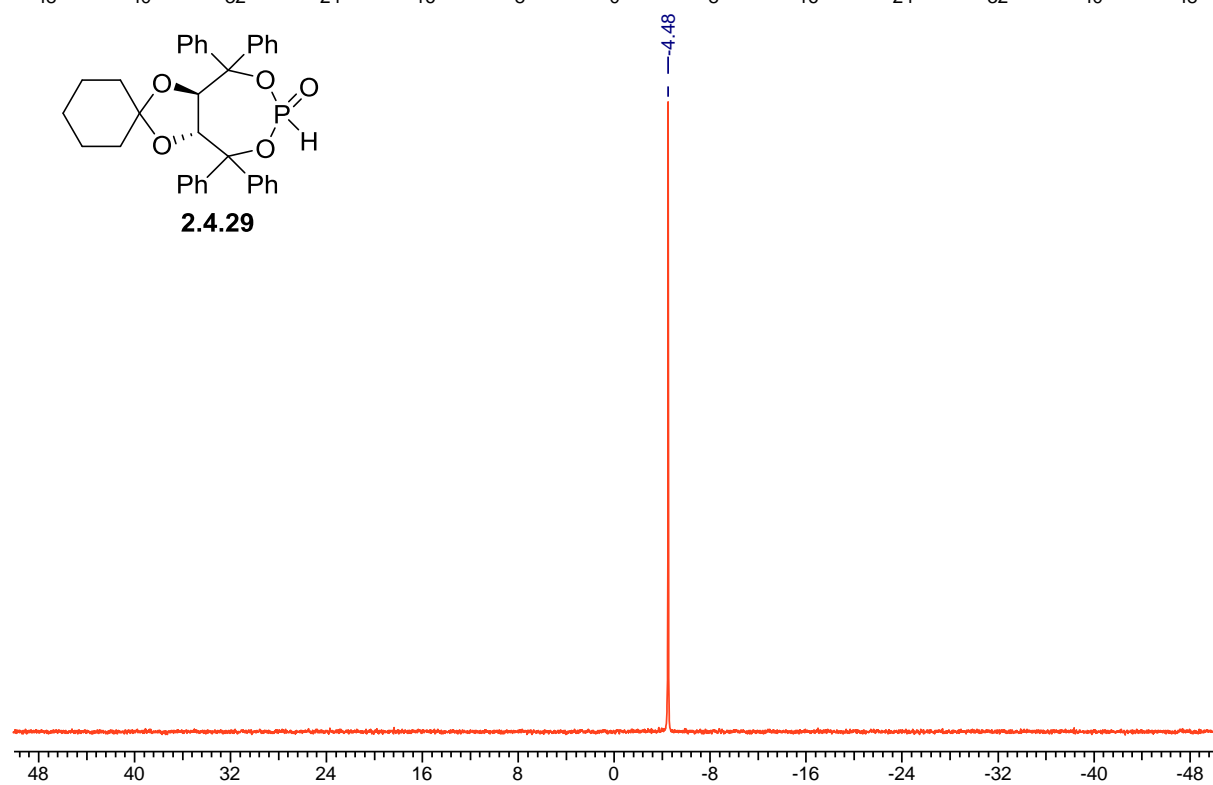
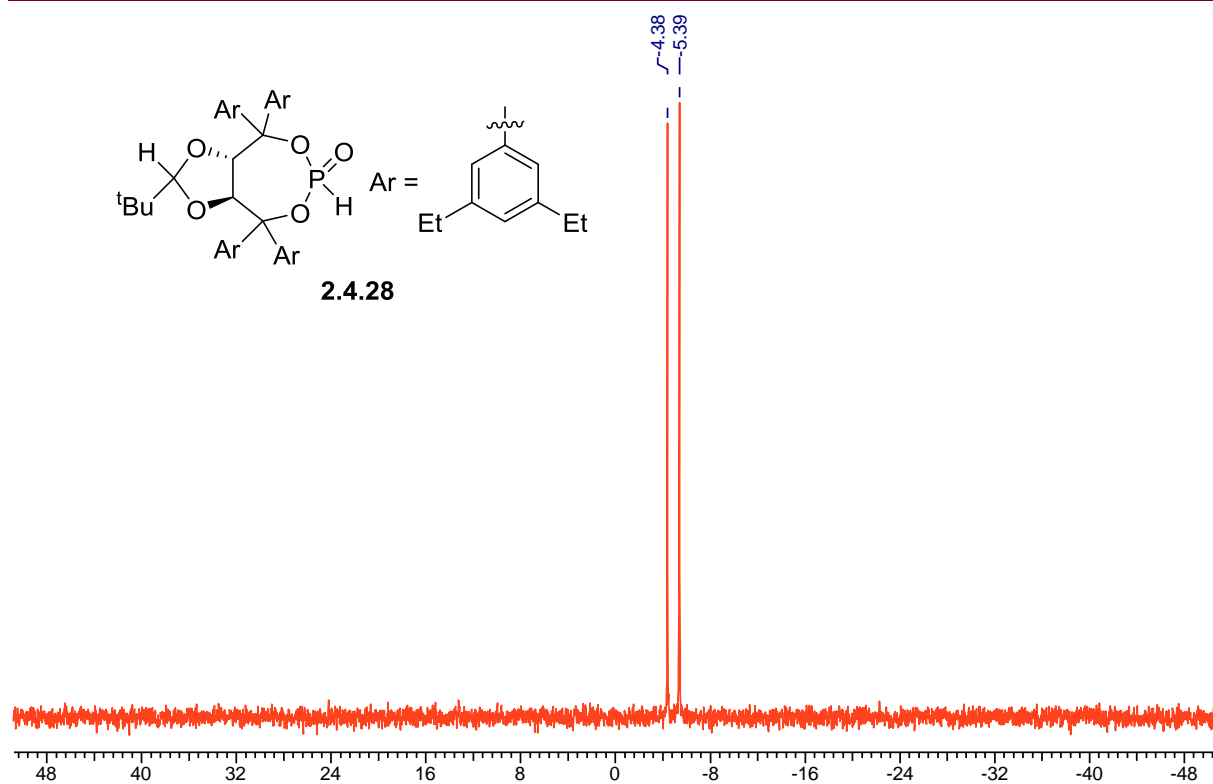


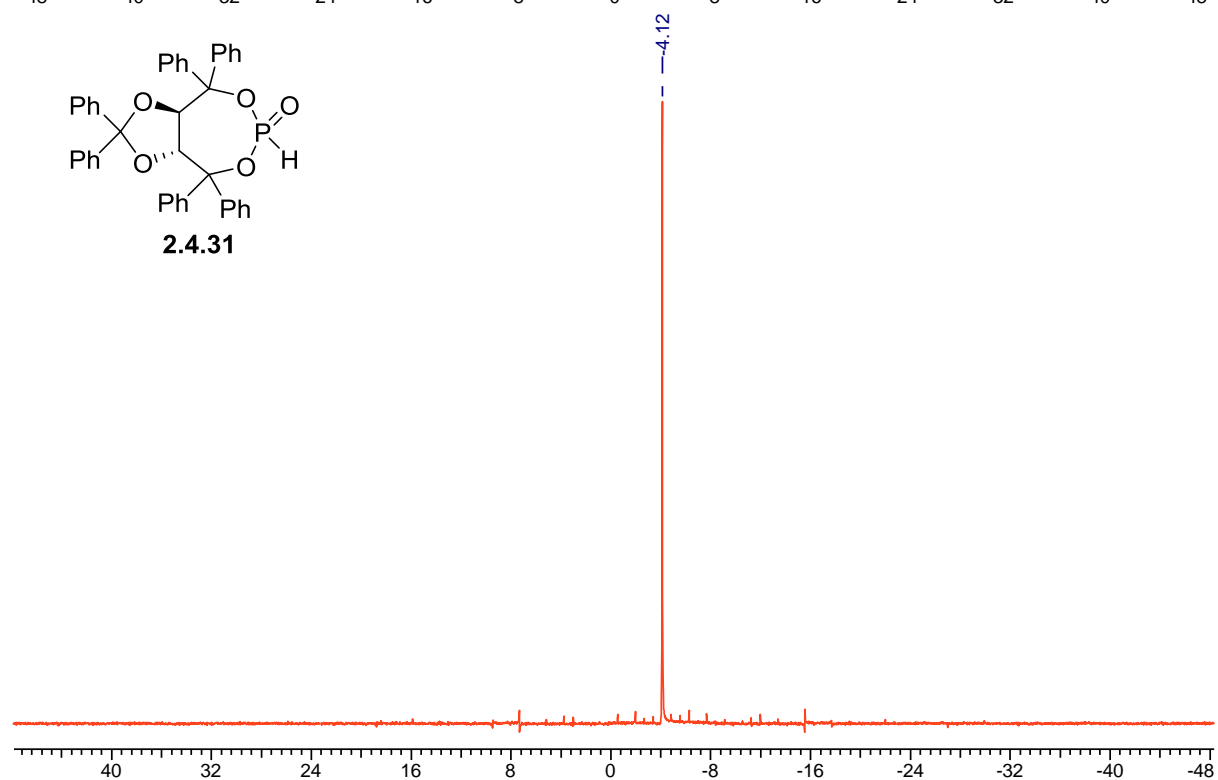
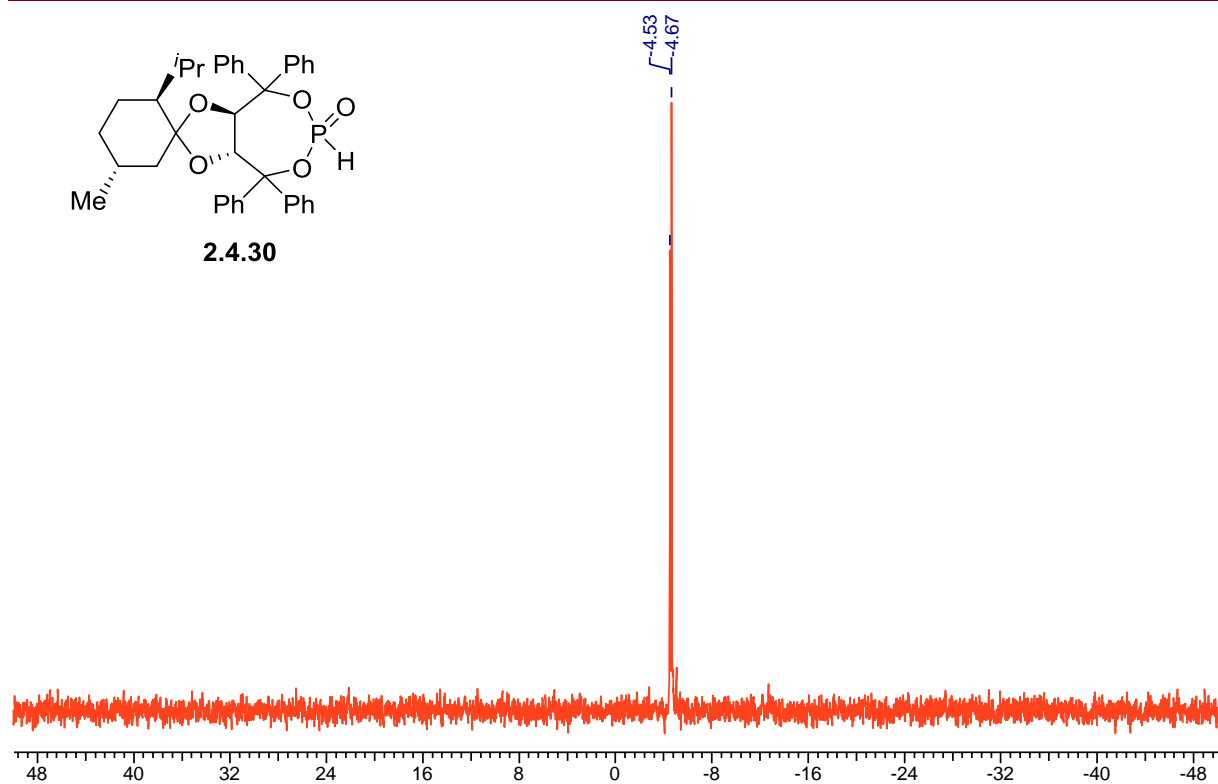
2.9 P^{31} NMR of phosphites

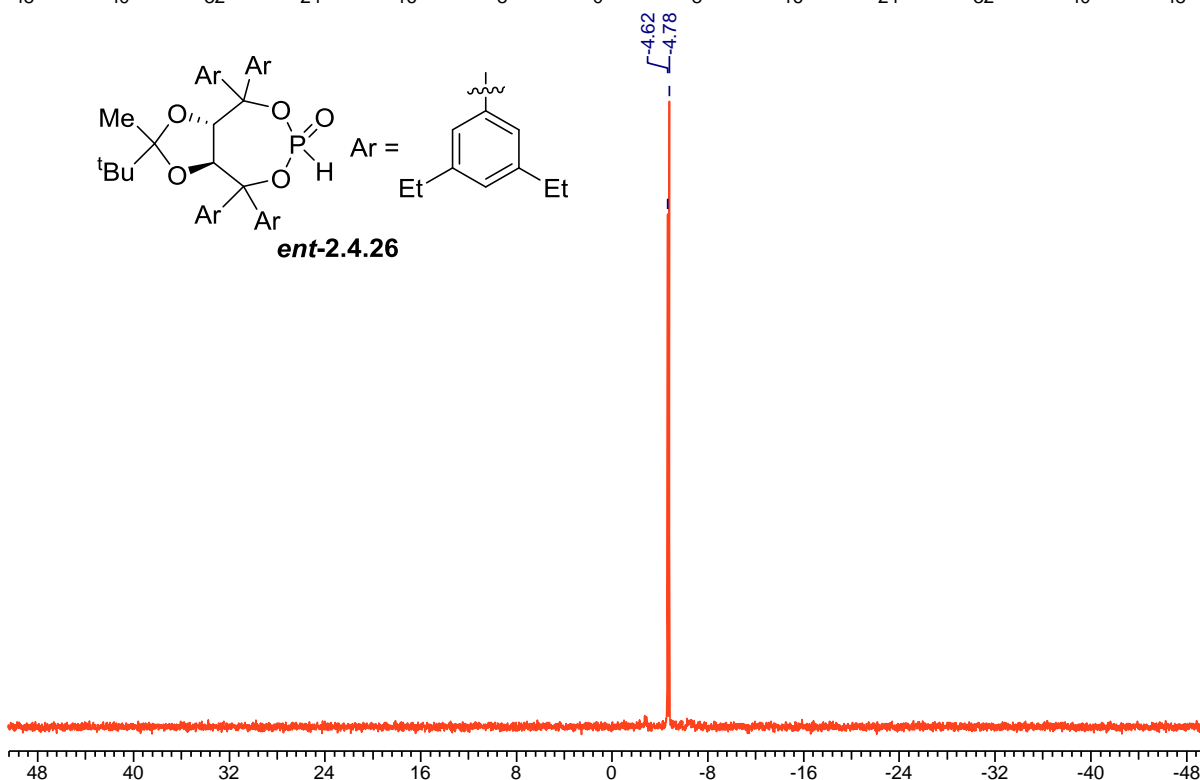
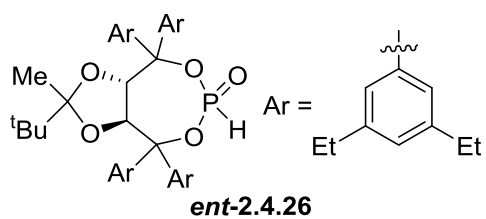
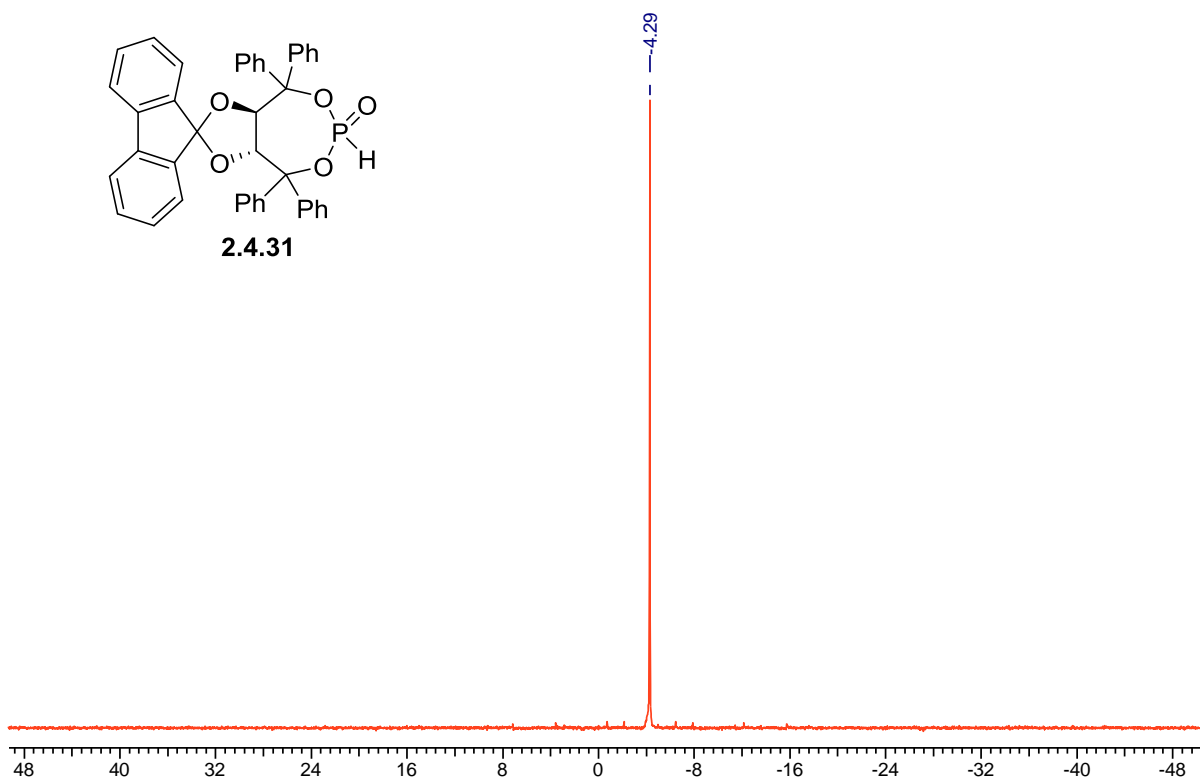
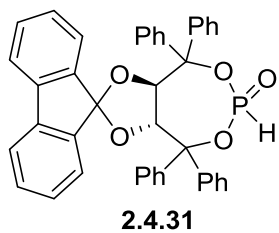


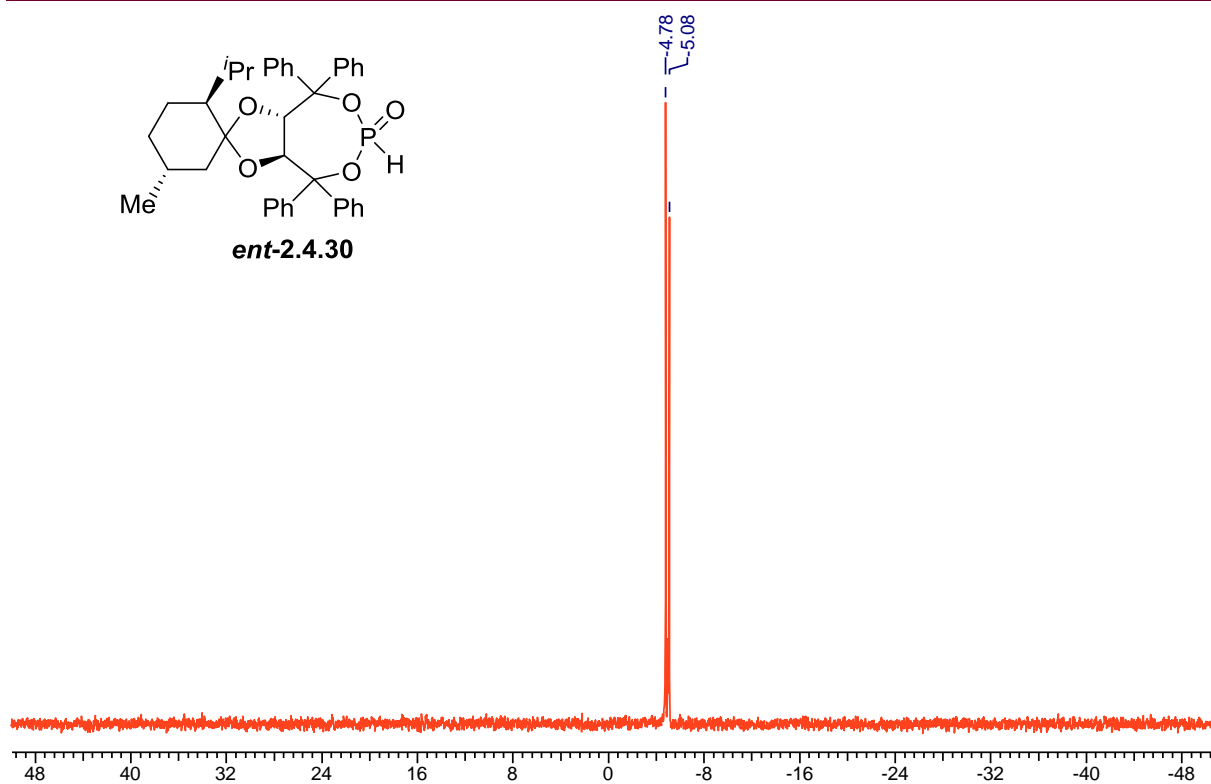










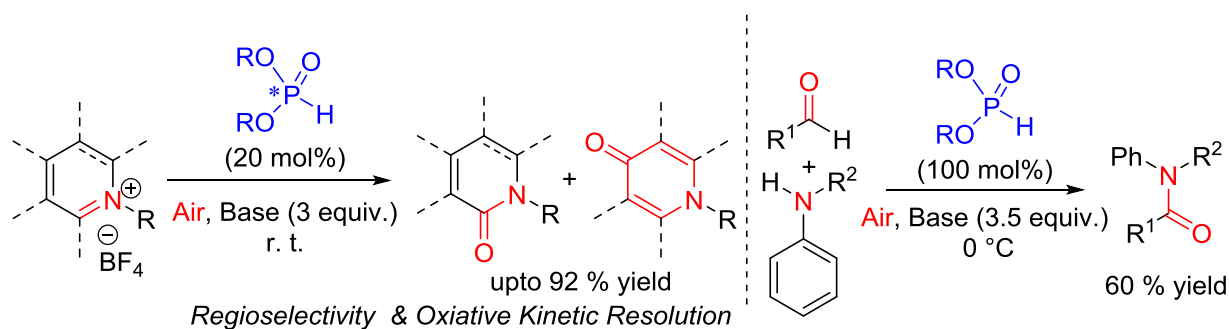


Chapter 3

Phosphite “aza-acyl” radical intermediate for catalyst-controlled aerobic oxidation of iminium ions

3.1 Abstract

In this chapter, we developed an organocatalyst-bound "aza-acyl" radical approach for the aerobic oxidation of pyridinium and iminium without any external radical-generating catalyst. N-alkylsalts of a variety of heteroaromatic compounds were oxidized successfully in the presence of household light (scheme 3.1). The regioselective catalyst addition to pyridinium led to regioselective pyridone formation. The catalyst bound α -radical was utilized successfully for an unprecedented oxidative kinetic resolution with racemic isoquinolinium salts with chiral phosphite catalysts synthesized. Cyclic and acyclic iminium salts were oxidized via a strong alternative base-mediated aerobic auto-oxidation. The strong base method presumably formed the "aza-acyl" anion equivalent first and, consequently, the corresponding radical for its aerobic oxidation. Although this reaction was performed with stoichiometric phosphite, it has the potential to be used as a sub-stoichiometric catalyst.



Scheme 3.1: Phosphite-catalysed controlled aerobic oxidation of iminium ions via “aza-acyl” radical intermediate approach

3.2 Introduction

Based on literature reported survey (chapter 1) for the application and synthesis of chiral pyridone derivatives, the recent research focused on an alternate approach, represented by reductions in cost, waste, energy use, material consumption, risk, hazards, and usage amounts of non-renewable resource with controlling the selectivity. Therefore, attention to green & sustainable chemistry has attracted more frequently in organic synthesis. In this context combination of light and photoredox catalysts explore radical chemistry as a sustainable approach. To talk about the radical oxidation in the presence of O_2 in terms of the "aza-acyl" radical intermediate approach only fewer reports were presented by several research groups mainly in racemic synthesis (chapter 1) through NHC catalysis. To focus on asymmetric synthesis, radical reactivity controlled by a chiral catalyst to radical oxidation under the O_2 atmosphere is still now not reported to the best of our knowledge. So, until recently to

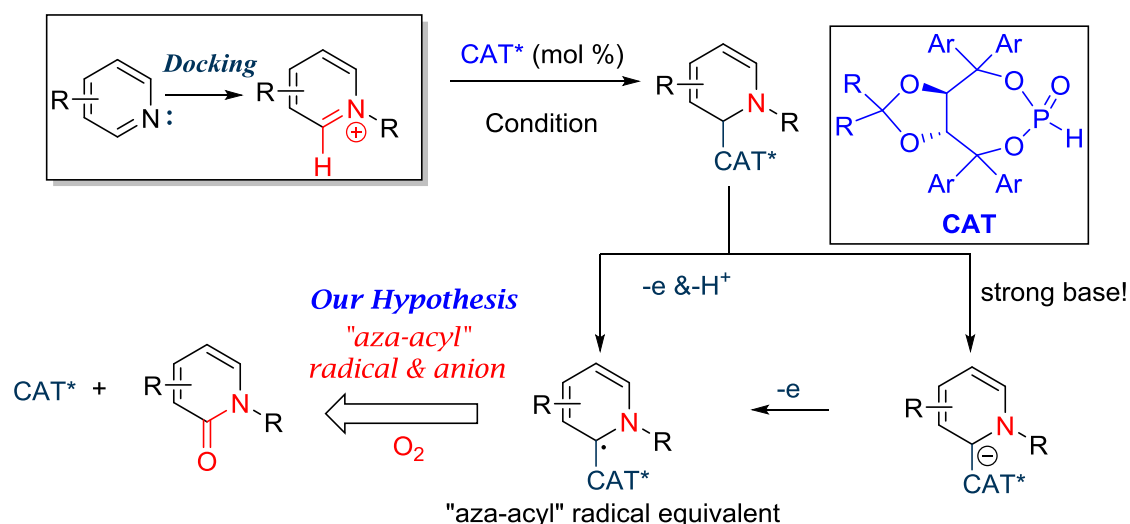
construct the C-C and C-X (X = heteroatom's) bond via reactive free radical pathway under mild reaction conditions remains challenging for asymmetric organic synthesis.

3.3 General Research Goal

In this context, our interest in finding catalyst control for radical reactions led us to explore a possible organocatalyst-bound "aza-acyl" radical formation and its reactivity. In reality, the reactivity of the radical center α - to the catalyst could be controlled by the steric and electronic nature of the catalyst. In terms of acyl cation equivalent and acyl anion equivalent intermediate, The asymmetric transformations are well established,¹ where is acyl radical equivalent not much explored as well as corresponding aza-versions are also rare and proved difficult to achieve. Here, we explored the possibility of an organocatalyst bound α -aminoalkyl radical formation and study their reactivity. As, The nitrogen on N-heteroaromatic compounds is sufficiently nucleophilic and can form stable quaternary nitrogen salts having N-C, N-O, and N-N, etc. bonds. We envision nitrogen to be a docking point to attach various groups on it; and selectively rearrange them catalytically asymmetrically to obtain chiral N-heterocyclic pharmaceuticals, drug intermediates, and chiral ligands. For this, the pyridinium salts can be considered as an iminium embedded in the Heteroaromatics and a development of a phosphite catalytic system for aerobic iminium oxidation obtains substituted pyridones derivative.

For this purpose, we are going to enclose the visible light-promoted self-photoredox process for generating catalyst bound α -aminoalkyl radicals; an aza-acyl radical equivalent approach, and their coupling with molecular triplet oxygen to generate lactams. We also demonstrate the first catalyst-controlled enantioselective aerobic oxidation of isoquinolinium with a chiral TADDOL-based phosphonate catalyst.

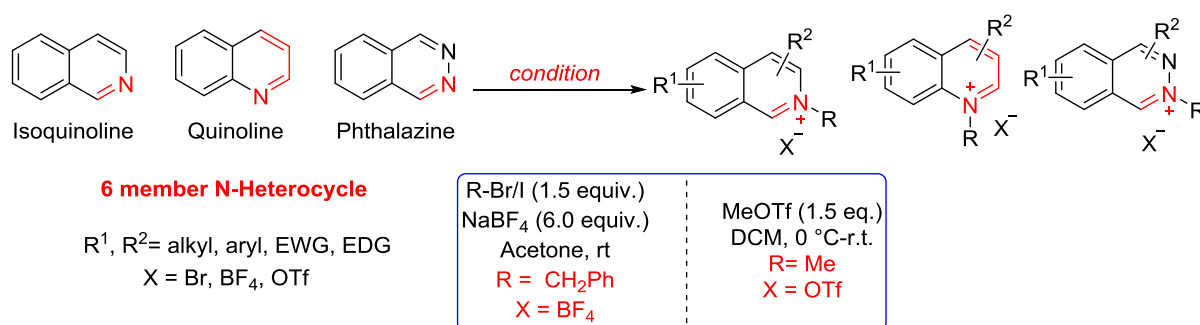
¹ (a) Hashimoto, T.; Hirose, M.; Maruoka, K. *J. Am. Chem. Soc.*, **2008**, *130*, 7556.; Liu, Q.; Perreault, S.; Rovis, T. *J. Am. Chem. Soc.*, **2008**, *130*, 14066.



Scheme 3.2: Generation of catalyst control "aza-acyl" radical and its reactivity towards oxidation

3.4 Preparation of Substrate

As The nitrogen on N-heteroaromatic compounds is sufficiently nucleophilic and can form stable quaternary nitrogen salts having N–C bonds. We initially choose six-member N-heterocycles like isoquinoline, quinoline & so on for the preparation of stable salt. For N-benzyl salt preparation, the first step is the nucleophilic addition of N-heterocycle to benzyl bromide as electrophile led the formation of the expected salt with bromide anion as counterpart. These salts are probably hygroscopic. To think about the stability and long time storage capability, we exchange the counterpart, Br^- with NaBF_4 to get a more stable salt with BF_4^- as a counterpart. These salts are bench stable, and easy to synthesize and isolate. But, for N-methyl salt, we choose MeOTf as methyl source and the reaction happens very fast at 0°C to provide a stable N-methyl salt with OTf⁻ as counterpart.

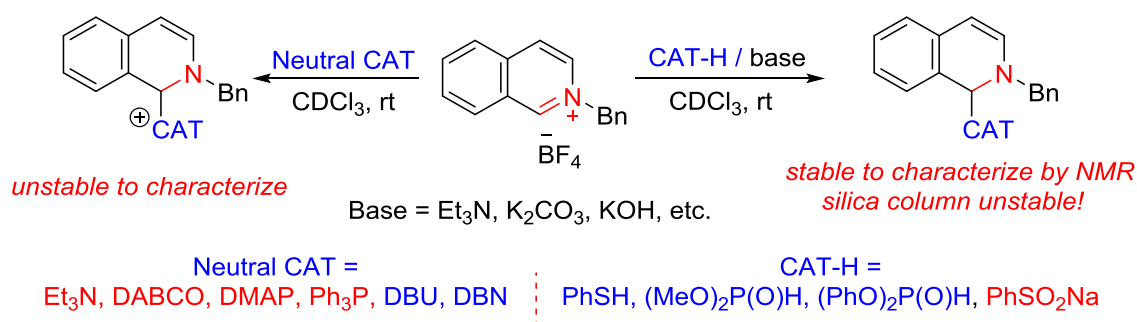


Scheme 3.3: Preparation of N-heteroaromatic salts

3.5 Screening of Catalyst

We started our investigation to find a suitable catalyst capable of forming the intermediate with the stable methyl isoquinolinium triflate and the adduct formation was studied in CDCl_3 .

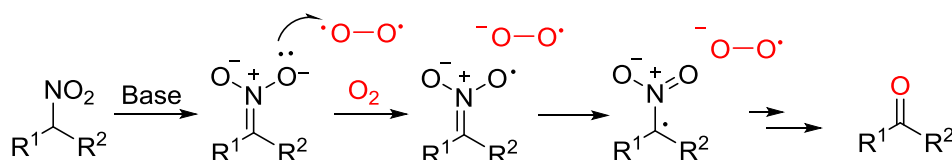
The crude proton NMR is analyzed directly and anticipates its reversible formation and instability. Here we screen both neutral and anionic nucleophiles. Neutral nucleophiles such as PPh₃, DABCO, and DMAP did not form adducts, but DBU led to complex NMR, indicating a possible formation of the unstable cationic adduct. Among anionic nucleophiles, sulfite did not form an adduct, but phosphites (DMHP and DPHP) and thiophenol with K₂CO₃ led to corresponding adducts effectively. After getting the optimization condition, we checked phosphite addition with other scaffold-like, quinolinium, cyclic nonaromatic N-heterocyclic iminium, and acyclic iminium in the presence of K₂CO₃ as a weak base and it results in the successive addition of phosphite to form a reactive intermediate.



Scheme 3.4: Screening for a variety of catalyst

3.6 Result and Discussion

After the successful screening of the catalyst, our next goal is to explore the feasibility of radical intermediate formation from the catalyst-attached adduct. We initially chose phosphites as a nucleophilic catalyst since the corresponding radical intermediate should gain synergistic stability via the captodative effect.² The reactivity of a captodatively stable radical is not well-studied, and it could differ from common α -radicals. As a result, its formation should be facile, and catalyst detachment from the radical intermediate is less likely. To keep in mind Nef oxidation (scheme 3.5),³ we have chosen aerobic oxygen as a suitable coupling partner to release the catalyst.



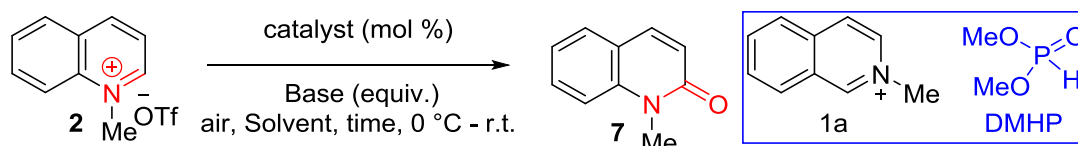
Scheme 3.5: Aerobic oxidation via nef reaction

² Viehe, H.; Anousek, D. Z.; Merenyi, R. *Acc. Chem. Res.*, **1985**, *18*, 148.

³ Umemiya, S.; Nishino, K.; Sato, I.; Hayashi, Y. *Chem. Eur. J.*, **2014**, *20*, 15753.; Li, J.; Lear, M. J.; Kawamoto, Y.; Umemiya, S.; Wong, A. R.; Kwon, E. Sato, I.; Hayashi, Y. *Angew. Chem. Int. Ed.*, **2015**, *54*, 12986.

During catalyst screening under an air atmosphere with a weak base (K_2CO_3), we were pleasantly surprised to observe the oxidation product in 10-20 % yield over 24 h without any radical generating catalyst and specific light. Further unprocessed reaction observation under dark conditions suggests daylight or hood light-mediated self-photo-redox⁴ might be operating.

3.6.1 Optimisation Study



Entry	Catalyst (mol%)	Solvent	Base (equiv.)	Time (h)	Yield (%)
1	DMHP (20)	MTBE	K_2CO_3 (3)	48	<5
2	DMHP (50)	THF	KOH (3)	48	25
3	DMHP (50)	DCM	KOH (3)	48	35
4	DMHP (50)	Toluene	KOH (3)	48	72
5	DMHP (50)	MeCN	KOH (3)	24	88
6	DMHP (50)	MeCN	-	72	NR
7	DMHP (50)	MeCN	KOH (3)	24	NR ^a
8	-	CH ₃ CN	KOH (3)	24	50
9	-	CH ₃ CN	KOH (3)	26	NR ^a
10	DMHP (20)	CH ₃ CN	KOH (3)	24	86
11	DMHP (50)	MeCN	KOH (7)	4	82
12	DMHP (20)	MeCN	KO ^t Bu (3)	16	82
13	DBU (120)	MTBE	-	24	28

Reaction Condition: quinolinium salt, **2** (0.3 mmol), catalyst (mol%), base (3 eq.), solvent (3 ml), 0 °C-r.t., DMHP = dimethyl hydrogen phosphite. ^a reaction in dark.

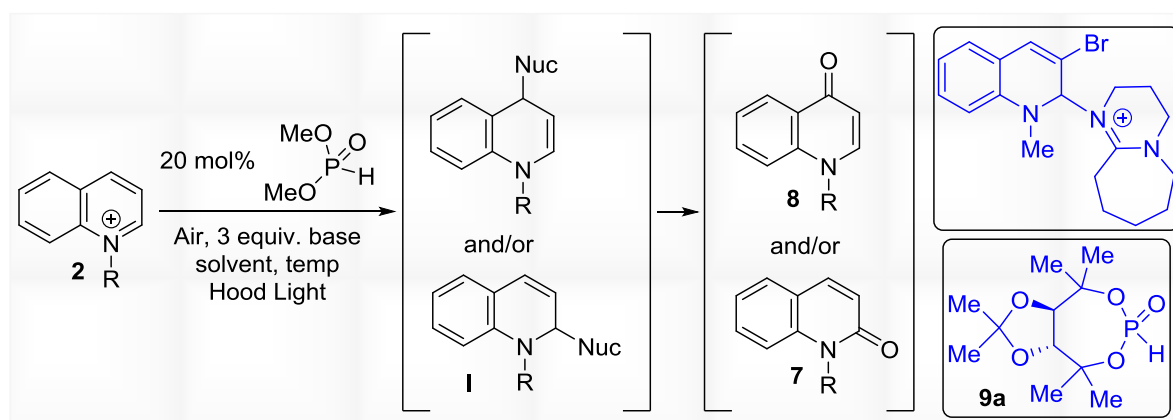
Optimization of reaction temperature, base, and solvent with N-methyl isoquinolinium (**1a**) led to good yield in the presence of 3 equivalent K_2CO_3 bases in MTBE as solvent at 40 °C after 72 h. Carrying the same reaction condition for 48 h at room temperature with N-methyl

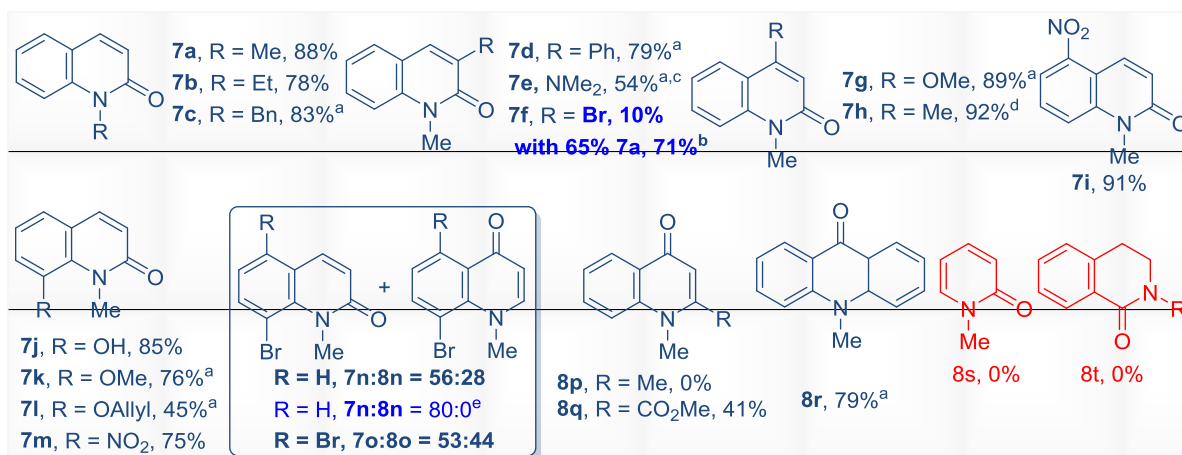
⁴ Romero, N. A.; Nicewicz, D. A. *Chem. Rev.*, **2016**, *116*, 10075. For direct photoexcitation of the catalyst-added substrate (enamine), see (a) Silvi, M.; Arceo, A.; Jurberg, I. D.; Cassani, C.; Melchiorre, P. *J. Am. Chem. Soc.*, **2015**, *137*, 6120. (b) Bahamonde, A. Melchiorre, P. *J. Am. Chem. Soc.*, **2016**, *138*, 8019.

quinoline salt (2a) did not result in any oxidation (entry 1). This suggests the necessity of reoptimization for the case of quinoline salt. Hoping, rather than a variation of temperature, screening of base is ideal probably due to low pKa of DMHP added adduct. In choosing the base, our first choice is KOH a little stronger base but it is nucleophilic. To overcome such complications, initially, THF was used as the solvent instead of MTBE, and 50 mol% of DMHP was added in the presence of KOH at room temperature which results in an improvement in yield (entry 2). Subsequent screening of solvent (entries 3-5) shows acetonitrile (MeCN) is the best choice (entry-5) and the Feasibility of reaction suggests base (entry 6) and light (27 W CFL bulb, entry 7, 9)) is required for this transformations. But, the absence of a catalyst (DMHP) results in an expected thermal product with a 50 % yield (entry 8). This suggests that KOH itself is a nucleophilic base and triggers the reaction. But, reduce of catalyst loading from 50% to 20%, reflect parallel yield (entry 5 & 10) which indicate that the catalyst plays some role in this transformation. Further, an increment of KOH up to 7 equivalent results in a minute drop in yield (entries 5 & 11). Overall, although KOH triggers the reaction, not efficiently work for this transformation and to work efficiently DHMP must be needed. Furthermore, Moving to a stronger base like KO^tBu results in a faster reaction (entry 12) with parallel yield. As, during catalyst screening 1, 8-diazabicyclo(5, 4, 0)undec-7-ene (DBU) was added to iminium, here we used DBU as a nucleophilic base (entry 13) which provides Low yield (entry-13).

3.6.2 Substrates Scope

From the optimization, we choose two optimized conditions (**entry 10 & entry 12**) for screening substrate where the first choice is the use of KOH as a base and the second choice is tBuOK as a base if KOH does not work efficiently. Based on this concept, we start to screen several scaffolds mentioned below.





Conditions: 0.3 mmol scale, for 2 to 7, 2 ml MeCN, KOH base, 16–48 h. ^aKOtBu as a base. ^bDBU (0.36 mmol), 50 °C, 24 h. ^c50 °C. ^d1.5 equiv. dimethyl hydrogen phosphite. catalyst 9a

Scheme 3.6: Substrates scope of quinolinium for self-photoredox aerobic oxidation

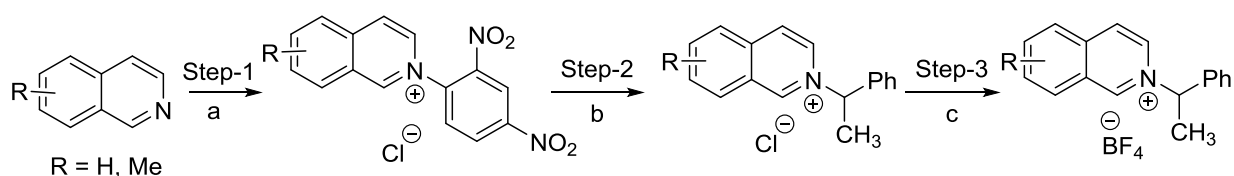
Different N-alkyl substitutions on quinoline derivatives were subjected to the optimized reaction conditions to test the compatibility of our method, where methyl (7a) and ethyl (7b) substitution on nitrogen works well but the KOtBu base results in better yield for benzyl substitution (7c). Phenyl at the 3-position works well with the KOtBu base, but electron-rich NMe₂ substitution led to a very slow reaction. Raising the temperature to 50 °C led to moderate yield (7e, 56%). A major debromination product was obtained along with the minor required product (7f) for 3-bromo substitution. Photoredox debrominations of aryl bromides are known,⁵ which might be operating here. The change in base and reaction temperature did not improve the result. But using DBU result corresponding lactam (7f) at 50 °C. 4-Methoxy substitution works well with KOtBu (7g), but 4-methyl quinolinium gave poor yield (<10%) under standard reaction conditions. We suspect that the possible deprotonation of the 4-methyl proton in starting salt under basic reaction conditions could be a problem. To circumvent this, 1.5 equivalent DMHP was added to convert all the salt to the intermediate before base-mediated oxidation, which led to a 92 % yield (7h). Aryl, electron-withdrawing as well as electron donating groups on other rings were well tolerated, including a free hydroxyl group at C-8 (7j). Surprisingly, the 8-Br substrate gave the required 7n (56%), along with a minor 4-oxo product (23%). A sterically bulky 9a catalyst yielded 7n selectively with a good yield (87%). Again, 5, 8- dibromo produce 7o (55%), along with 8o (44%). Further, C-2 substitution with methyl didn't result in a 4-oxo product (7p), but the presence of the 2-COOMe group generates 7q (41%). Later oxidation of acridinium with KOH results in 50%

⁵ Devery III, J. J.; Nguyen, D. J.; C. Dai, C.; Stephenson, J. R. C. *ACS Catal.*, **2016**, *6*, 5962.

oxo product (7q) with 40% 10-methyl-9,10-dihydro acridine, but in pres KO^tBu base gives 79% of 7q. pyridinium and non-aromatic cyclic iminium salt did not oxidize under our optimized photoredox reaction conditions.

3.7 Oxidative Kinetic Resolution

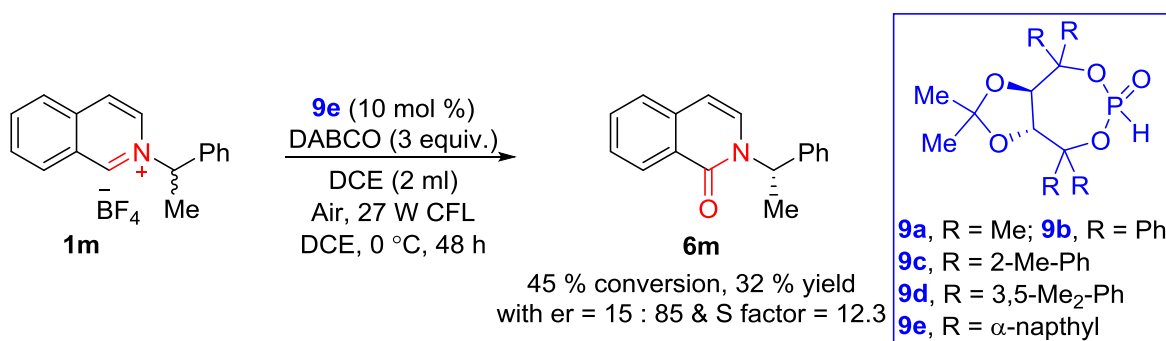
After the successful aerobic oxidation of N-alkyl salts of isoquinoline and quinoline, we utilized this method for catalyst-controlled oxidative kinetic resolution. For that, we choose a racemic 1-Phenylethyl isoquinolium salt as an electrophilic iminium motif and TADDOL-based phosphite (9e) as a chiral catalyst. The preparation of phosphite is mentioned in a previous chapter (chapter 2) and for salt preparation, we follow the below mention procedure (scheme 3.7).



Condition: a) 2,4-dinitrobenzene, Acetone, 80 °C. b) (±)-1-phenylethylamine/(S)-(-)-1-phenylethylamine, diethylamine, rt, 48 h. c) silver tetrafluoroborate, DCM, 0 °C to r.t.

Scheme 3.7: Preparation of salt having α -stereogenic center

After getting salt in hand, we find changing base K_2CO_3 to DABCO works well in the presence of chiral phosphite catalyst 9e at 0 °C in DCE as a solvent to achieve an enantiomeric ratio of 15:85 with 45 % conversion (scheme 3.8).



Scheme 3.8: Oxidative kinetic resolution with chiral phosphites 9e

3.8 Mechanistic Study and proposed Mechanism

To explore the probable mechanistic path, we first checked the UV-vis absorption of isoquinoline salt and catalyst (9a) added adduct. The study shows salt does not absorb light in the visible region, but, catalyst (9a) added adduct absorbs. Further fluorescence quenching study showed a decrease in fluorescence by adding isoquinoline salt (Figure 3.1). It indicates

a light-mediated excitation of the adduct, followed by single electron transfer to starting iminium salt to generate radical cation intermediate.

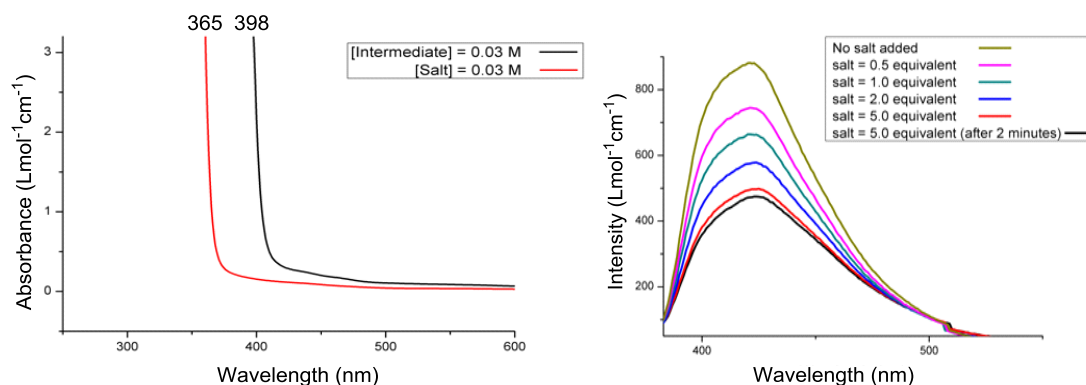


Figure 3.1: UV-vis absorption spectra and fluorescence quenching study

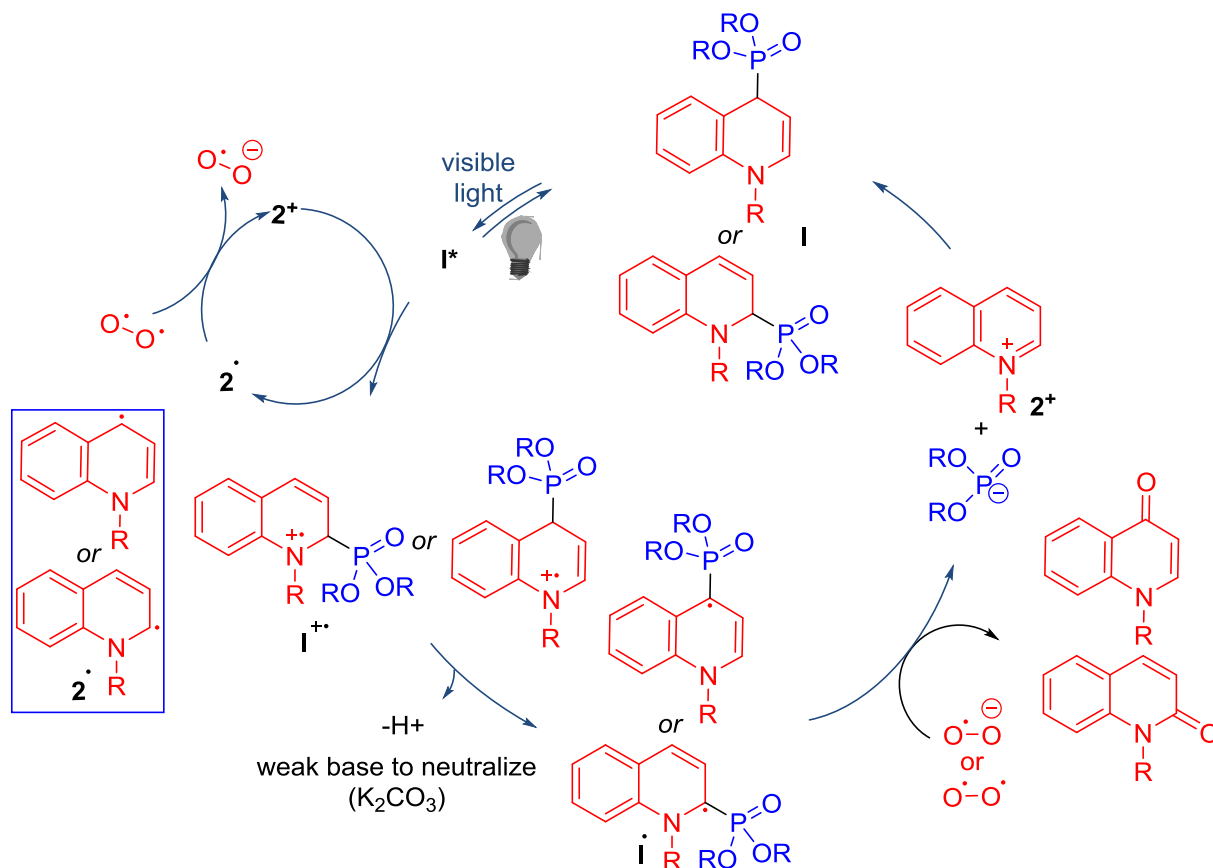
As we did UV and fluorescence study with isoquinolium salt and also, developed an oxidation method with similar kind iminium motif, an quinolinium salt (2^+). So, based on the result and by hoping that quinolinium also can show similar photochemical property, here we proposed a possible reaction pathway with quinolium substrate (2^+). Similarly, a light-mediated excitation happened from quinolinium-phosphite adduct (**I**). Now, α C–H acidity of the radical cation intermediate (\mathbf{I}^+) would increase greatly,⁶ and deprotonation via a base led to our proposed catalyst-bound "aza-acyl" radical equivalent (**F**). On the other hand, the reduced salt (2^\bullet) can transfer one electron to ground state oxygen to regenerate the salt back and superoxide anion ($\text{O}_2^{\bullet-}$). The reaction of radical intermediate (**F**) with either O_2 or $\text{O}_2^{\bullet-}$ can lead to product formation with the removal of the catalyst.⁷ A catalyst detachment and further use, suggest establishing a catalytic cycle. Apart from this, Direct oxidation of the reduced α -aminoalkyl radical (2^\bullet) is also possible with oxygen or $\text{O}_2^{\bullet-}$, but, we are anticipating this is either not operating or is a minor path since we achieved catalyst-controlled kinetic resolution. Further, The involvement of salt (2^+) in the oxidation cycle suggests there were always some intermediates that remained unreacted in the reaction, and also, no reaction occurred with pre-formed intermediate (**I**) in the absence of salt (2^+). This also tells that direct oxidation of adduct (**I**) by oxygen under visible light is not possible. After that, The reaction

⁶ Martin de, A.; Nicholas, P.; Arnold, R. D. *Can. J. Chem.* **1982**, *60*, 2165.

⁷ Jin, Y.; Ou, L.; Yang, H.; Fu, H. *J. Am. Chem. Soc.*, **2017**, *139*, 14237.; Base-mediated aerobic oxidations with very limited substrate scope are known with a different mechanistic rationale: (a) S. Ruchirawat, S.; S. Sunkul, S.; Y. Thebtaranonth, Y.; and Y. Thirasasna, Y. *Tetrahedron Lett.* **1977**, *27*, 2335; (b) Paira, P.; Hazra, A.; Sahu, B. K.; Banerjee, S.; Mondal, B. N.; Sahu, P. N.; Weber, M.; Luger, P. *Tetrahedron*, **2008**, *64*, 4026.

proceeded in the presence of DABCO which is known as a singlet oxygen quencher and it suggests photo-excitation to singlet oxygen is less likely.

Based on the mechanistic study, we propose the possible mechanism cycle mentioned below.



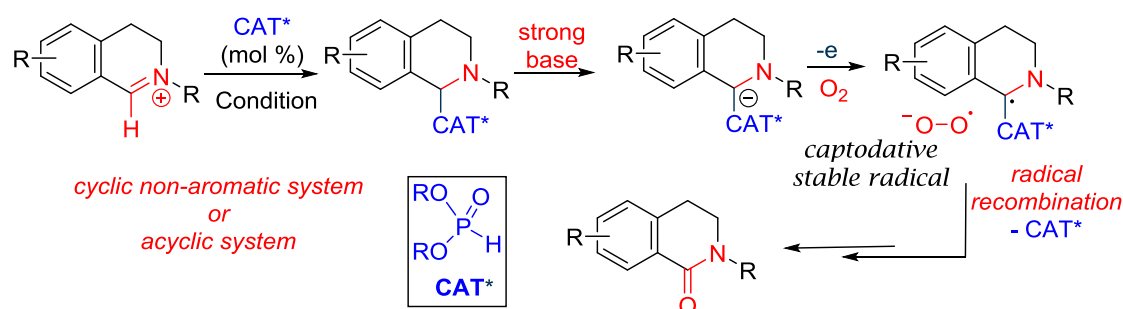
Scheme 3.9: Proposed catalytic cycle for self-photoredox aerobic oxidation

3.9 One-pot Synthesis of Lactam and amide

Here, we aim to develop a general method beyond the N-heteroaromatic aromatic iminium salts like isoquinolinium, 1.; quinolinium, 2.; and so on. As we know, During the substrate scope screening (scheme3.6) the oxidation of a non-aromatic iminium salt (8t) remains unsuccessful and it is expected probably due to the salt, or the corresponding phosphite adduct does not absorb visible light. So, an external photoredox⁸ catalyst can oxidize the adduct to initiate the process. For that to happen, it has to be compatible with the nucleophilic phosphite catalyst. Instead of it, we checked a possible Nef-type anionic auto-oxidation

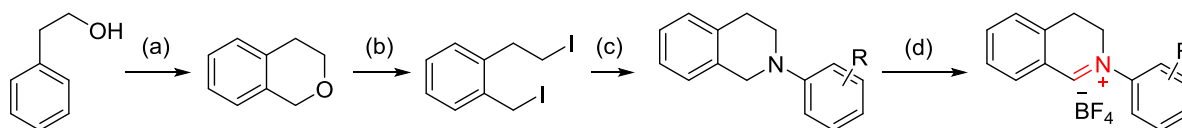
⁸ Pandey, G.; Kumaraswamy, G.; Bhalerao, T. U. *Tetrahedron Lett.*, **1989**, 30, 6059.; Kohls, P.; Jadhav, D.; Pandey, G.; Reiser, O. *Org. Lett.*, **2012**, 14, 672.

(scheme 3.5)⁹ first to avoid external photoredox catalysts. Base-mediated aerobic oxidations with very limited substrate scope are known with different mechanistic pathways.¹⁰ Although no clear understanding is presented for the Nef-type reaction, we presume that the radical (5) stability in comparison to the corresponding carbanion is a key factor. The proposed captodative stability of radical 5 could facilitate this approach.

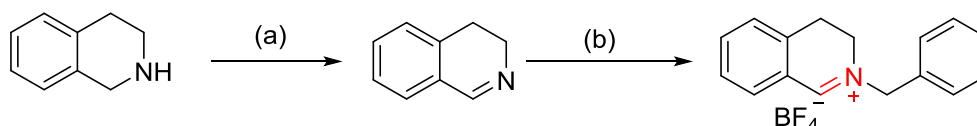


Scheme 3.10: General scheme for oxidation of acyclic & cyclic non-aromatic system

We start to synthesize a cyclic salt by following the below-mentioned procedure for N-phenyl and -naphthyl case (R = Ph, α -naphthyl).¹¹ For N-benzyl salt preparation we used benzyl bromide and follow the below mention method literature procedure.¹² Here, instead of aqueous NaOH used DBU as we know, the salt is not stable enough under free hydroxide ion.



Method A: condition: a) (HCHO)_n, HCl (35 %), 40 °C, 24 h. b) HI (57 %), reflux, dark, 1 h. c) sodium dodecyl sulphate (SDS), NaHCO₃/H₂O, 130 °C, 4 h. d) (i) CBrCl₃, MeCN, blue LED.; (ii) NaBF₄, Acetone, r.t., 12 h.



Method B: Condition: a) NCS, DBU, DCM, -20 °C to r.t., 12 h. b) benzyl bromide, NaBF₄, acetone, r.t., 24 h

Scheme 3.11: Preparation of 3,4-dihydroisoquinolinium salt: Method A for N-aryl & Method B for N-benzyl salt.

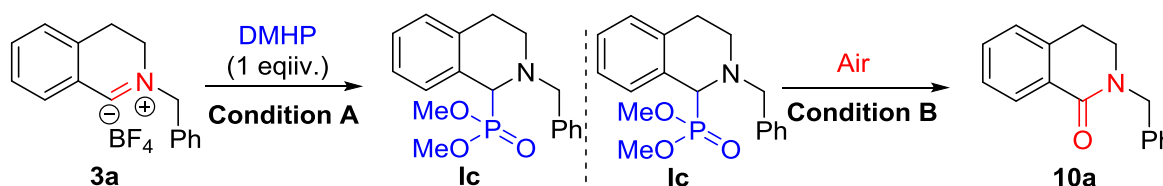
⁹ Umemiya, S.; Nishino, K.; Sato, I.; Hayashi, Y. *Chem. Eur. J.*, **2014**, *20*, 15753.; Li, J.; Lear, J. M.; Kawamoto, Y.; Umemiya, S.; Wong, R. A.; Kwon, E.; Sato, I.; Hayashi, Y. *Angew. Chem. Int. Ed.*, **2015**, *54*, 12986.

¹⁰ Ruchirawat, S.; Sunkul, S.; Thebtaranonth, Y.; Thirasasna, Y. *Tetrahedron Lett.*, **1977**, *27*, 2335.; Paira, P.; Hazra, A.; Sahu, B. K.; Banerjee, S.; Mondal, B. N.; Sahu, P. N.; Weber, M.; Luger, P. *Tetrahedron*, **2008**, *64*, 4026.

¹¹ Aggarwal, K. V.; Bae, I.; Lee, Y. H.; Williams, T. D. *Angew. Chem. Int. Ed.*, **2003**, *42*, 3274.; Franz, F. J.; Krausab, B. W.; Zeitler, K. *Chem. Commun.*, **2015**, *51*, 8280.

¹² Darras, H. F.; Kling, B.; Heilmann, J.; Decker, M. *ACS Med. Chem. Lett.* **2012**, *3*, 914–919.

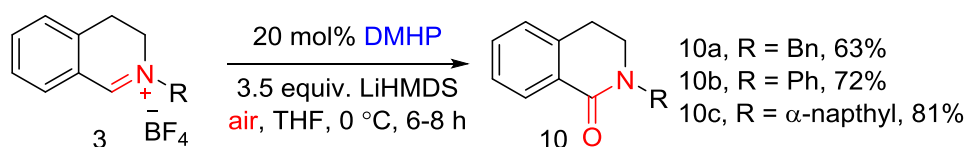
After the preparation of hydrolytically stable salt, initially, we focused on the stepwise oxidation process. Regarding this, we look at the formation of a stable intermediate, first and then their oxidation under certain reaction conditions. So, salt (3a) was subjected to form a stable catalyst attach adduct (**Ic**) with stoichiometry amount DMHP as a catalyst. Screening of several solvents and bases at 0 °C to r.t concludes the formation of the expected intermediate (**Ic**) in the presence of Et₃N in DCM at 0 °C as a sticky solid with 71% isolated yield. Further, oxidation of the same intermediate by changing several bases found, LiHMDS (1.5 equiv.) works efficiently in THF at 0 °C to provide 76% of the corresponding oxo-product.



Condition A: several screening parameter: i) Bases: K₂CO₃, Et₃N, KOH.; ii) Solvent: MeCN, DCM, Toluene, THF, Dioxane.; iii) Temperature: 0 °C, r.t.; **Condition B:** changing of solvent of bases at 0 °C: i) Bases: KOH, ^tBuOK, LiHMDS.; ii) Solvents: MeCN, DCM, THF, DMF, DMA, Toluene.; DMHP = dimethyl hydrogen phosphite

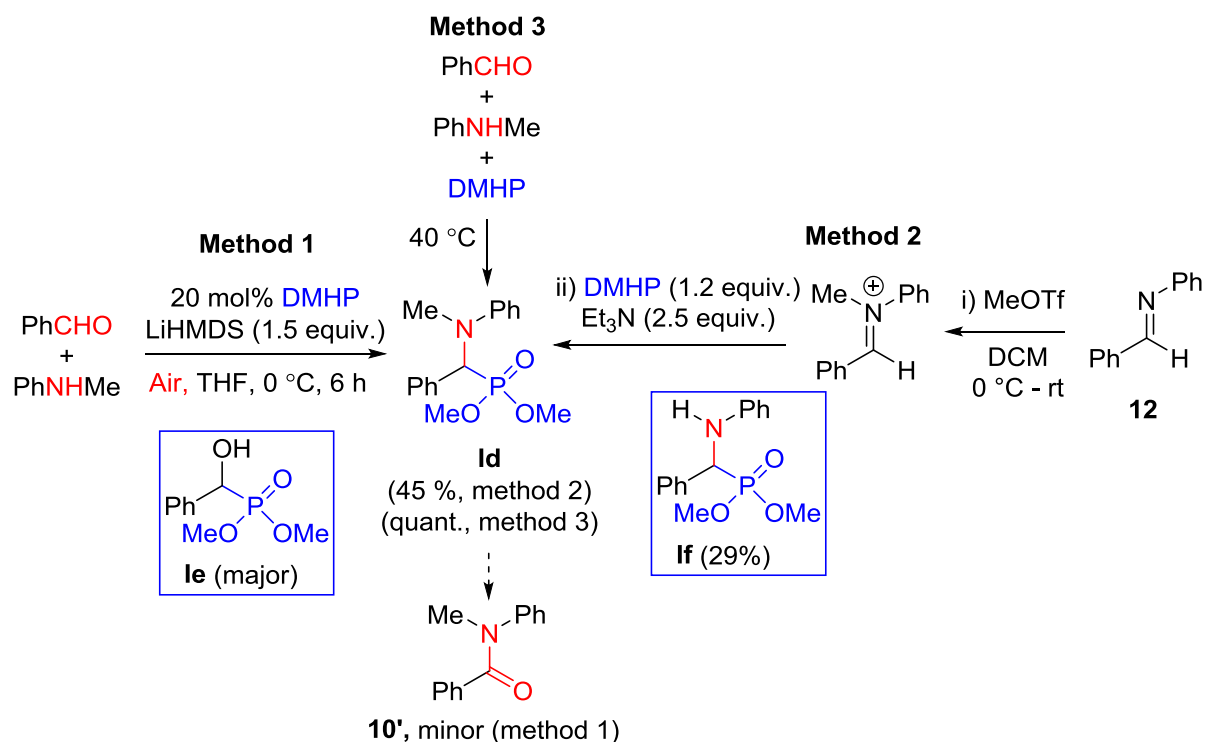
Scheme 3.12A: Stepwise aerobic oxidation of non-aromatic cyclic iminium salt to lactam

To extend the procedure to a catalytic oxidation method, we consider 20 mol% of DMHP as a catalyst and 1.5 equivalent of base. Using base KOH and ^tBuOK did not result in the formation of oxo product, but, LiHMDS gives the expected product in a low yield with some reactive remains at 0 °C. Further, raising the amount of LiHMDS to 3.5 equivalent increases the yield up to 63%. Here, LiHMDS consider a little strong base (pka~26) than ^tBuOK (pka ~18) to deprotonate the α C–H bond of the substrate-catalyst adduct (3-10a). Then, changing the N-alkyl group (Bn) to aryls, phenyl (Ph), and α-naphthyl works well under the standard reaction condition for corresponding lactam formation in moderate to good yields (scheme-3.12B).



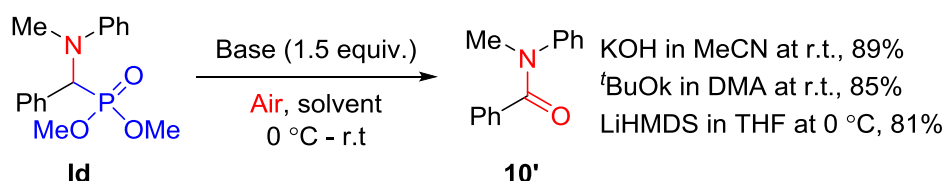
Scheme 3.12B: Catalytic aerobic oxidation of non-aromatic cyclic iminium salt to lactam,

Further, to focus on one pot amide synthesis via the aerobic oxidation method, an in situ formed acyclic iminium salt was subjected to oxidation in the same reaction condition mentioned above (Scheme 3.12B), and this resulted in the expected amide formation in a minor amount. This is due to the competitive formation of corresponding α-hydroxy phosphonate (**Ie**) other than α-amino phosphonate (**Id**) (scheme 3.13A, method 1).



Scheme 3.13A: Catalytic oxidation of iminium to amide (method 1) and reactive intermediate formation (method 2 & 3)

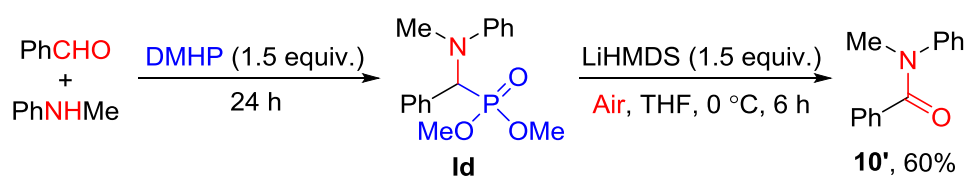
To overcome such a problem, and to check the efficiency of oxidation for the acyclic system, we synthesized a stable α -amino phosphonate intermediate (**Id**) in two possible ways, methods 2 and method 3. In Method 2, an imine (**12**), was treated with MeOTf in DCM form in situ iminium, and then, reaction with DMHP (1.2 equiv.) in the presence Et₃N gives α -amino phosphonate intermediate (**Id**) in 45% yield with 29 % of another phosphonate byproduct (**1f**) (scheme 3.13A, method 2). In method 3, the mixing of benzaldehyde, N-methyl aniline, and dimethyl hydrogen phosphite (DMHP) in a stoichiometric amount under neat reaction condition at 40 °C provide a successive formation of α -amino phosphonate intermediate (**Id**) in quantitative yield (scheme 3.13A, method 3).¹³ This α -amino phosphonate intermediate (**Id**) was stable enough for column purification and stored in freeze to further use it. The same intermediate (**Id**) was treated for oxidation to amide formation with a different solvent-base combination under an air atmosphere and it was found the best possible combination for this transformation to result good yield.



¹³ Keglevich, G.; Bálint, E. *Molecules*, **2012**, *17*, 12821.

Scheme 3.13B: Best solvent-base combination for amide formation from intermediate

Based, on the result in our hand, again we move to the catalytic oxidation process for one pot amide synthesis by using 20 mol% DMHP in the presence of different bases. The result shows KOH and tBuOK form more α -hydroxy phosphonate (**Ie**) intermediate at room temperature where is at 0 °C very slow oxidation, and LiHMDS shows expected intermediate (**3'**) formation with faint byproduct as α -hydroxy phosphonate (**Ie**) and amide (**10'**). Further, DMHP loading up to 1.5 equivalent fully converted to intermediate (**Id**) and then the addition of LiHMDS in THF at 0 °C provide moderate yield. Although it looks like two step process, it perform in one pot one reaction vessel.



Scheme 3.13C: Insitu stepwise oxidation to an amide.

3.10 Conclusion

In conclusion, we developed an organocatalyst bound α -aminoalkyl radical approach for aerobic oxidation without any external radical-generating catalyst. N-Alkyl salts of a variety of heteroaromatic compounds were oxidized successfully in the presence of household light. The catalyst bound α -radical was utilized successfully for an unprecedented oxidative kinetic resolution with racemic isoquinolinium salts. Cyclic and acyclic iminium salts were oxidized via an alternative strong base-mediated aerobic auto-oxidation. Full mechanistic studies and catalyst-controlled stereoselective and regioselective oxidation are underway.

3.11: Experimental Procedure

3.11.1: General Information

The oxidation reactions were carried out with anhydrous solvents in flame-dried glass wares under anhydrous oxygen or air atmosphere. All other reactions were carried out under anhydrous and argon atmosphere. THF was dried over sodium before use. All other solvents were purchased anhydrous and stored under argon over 4 Å molecular sieves. Analytical thin-layer chromatography was performed on glass plates pre-coated with silica gel (Silica Gel 60 F₂₅₄; Merck). Plates were visualized using UV light ($\lambda = 254$ nm) and then stained with either aqueous basic potassium permanganate (KMnO₄) or p-anisaldehyde and developed upon heating in Hitachi heat gun. Flash chromatography was performed using silica gel (Merck and Spectrochem, 230-400 mesh), eluting with solvents as indicated. Flash column was performed using Sebo aquarium air pump (SB-548A). ¹H and ¹³C spectras were acquired in deuterated solvents at room temperature on Bruker: Ultrashield 400 MHz, Ultrashield 500 MHz spectrometer. Chemical shifts (δ) are reported for ¹H NMR in ppm from TMS as internal standard and ¹³C from the residual solvent peak. ¹H NMR spectra are reported as follows: chemical shift (δ ppm), multiplicity, coupling constant (Hz), and integration. Data for ¹³C NMR spectra are reported in terms of chemical shift (δ ppm). Melting points were checked in Buchi Melting Point B-540 instrument and reported in °C. FT-IR were analyzed in Bruker ALPHA instrument and reported as cm⁻¹. High resolution (HRMS) mass spectral analyses were recorded on a Thermo Scientific Q-Exactive, Accela 1250 pump. Chiral HPLC separations were achieved using an Agilent 1260 Infinity series normal phase HPLC unit and HP Chemstation software with Chiralpak[®] IA columns (250 × 4.6 mm). All eluent systems were isocratic.

3.11.2: Preparation of Substituted Analogs

Commercially available reagents were purchased and used as obtained. Substituted analogs of quinoline and chiral phosphite catalysts were synthesized following literature procedures: 3-bromoquinoline,¹⁴ 5, 8-dibromoquinoline,¹⁵ 5-nitroquinoline and 8-nitroquinoline,¹⁶ N, N-dimethylquinolin-3-amine,¹⁷ 8-methoxyquinoline,¹⁸ 4-chloroquinoline and 4-

¹⁴ Shen, B. G.; Xia, K.; Li, T. X.; Li, L. J.; Fu, H. Y.; Yuan, L.; Zhu, Q. X. *J. Phys. Chem. (A)*, **2016**, *120*, 1779.

¹⁵ Brown, D. W.; Goulliaey, H. A. *Synthesis*, **2002**, *1*, 83.

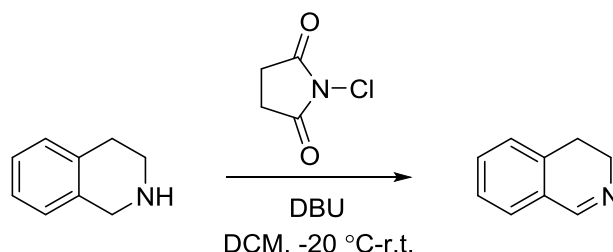
¹⁶ Paloque, L.; Verhaeghe, P.; Casanova, M.; Ducros, C. C.; Dumetre, A.; Mbatchi, L.; Hutter, S.; M'Rabet, K. M.; Laget, M.; Remusat, V.; Sylvain, R.; Rathelot, P.; Azas, N.; Vanelle, P.; *Eur. J. Med. Chem.*, **2012**, *54*, 75.

¹⁷ Ferles, M.; Kocian, O.; Collect, C. *Chem. Commun.*, **1979**, *44*, 3141.

methoxyquinoline,¹⁹ 3-phenylquinoline,²⁰ 8-(allyloxy) quinoline,²¹ and chiral phosphite catalyst.²² The literature reported spectral data were compared favorably with our ¹H NMR spectra of these compounds.

3.11.3: Preparation of Starting Materials

Preparation of 3, 4-dihydroisoquinoline:²³



In an oven dry round bottom flask 1, 2, 3, 4-tetrahydroisoquinoline was taken (5.00 g, 37.6 mmol) in 200 mL of CH₂Cl₂ and stir under Argon atmosphere. To a stirred solution of N-chlorosuccinimide (1.1 equiv.) was added portion wise over 20 min at -20 °C. After the addition was complete, the mixture was stirred for another 30 min at same temperature. Then, DBU (1.5 equiv.) was added, and stirring was continued for 1 hr at 25 °C. The organic layer was separated and washed with water (100 mL). The organic layer was extracted with 10% HCl (2 x 100 mL). The combined acidic extracts were washed with CH₂Cl₂ (100 mL) and made basic with ammonia solution (pH 9). The total solution was further extracted with CH₂Cl₂ (3 x 100 mL), dried over Na₂SO₄, and evaporated to afford a light yellow oil residue. The residue was purified by column chromatography to afford 3,4-Dihydroisoquinoline as colourless oil with 94% yield.

¹H NMR (200 MHz, CDCl₃) δ: 2.77 – 2.61 (m, 2H, CCH₂CH₂), 3.72 (ddt, J = 13.7, 9.7, 4.9 Hz, 2H, CH₂CH₂N), 7.16 – 7.07 (m, 1H, arom.), 7.37 – 7.18 (m, 3H, arom.), 8.30 (t, J = 2.1 Hz, 1H, NCHC) ppm. Spectral data is in accordance with literature data.

¹⁸ Li, K.; Li, Y.; Zhou, D.; Fan, Y.; Guo, H.; Ma, T.; Wen, J.; Liu, D.; Zhao, L. *Bioorg. Med. Chem.*, **2016**, *24*, 1889.

¹⁹ Zurro, M.; Asmus, S.; Beckendorf, S.; Muck-Lichtenfeld, C.; Mancheño, O. C. *J. Am. Chem. Soc.*, **2014**, *136*, 13999.

²⁰ Li, J.; Zhu, Q.; Xie, Y. *Tetrahedron*, **2006**, *62*, 10888.

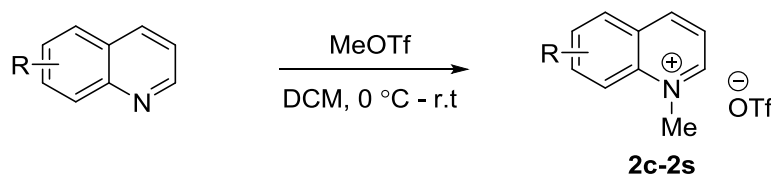
²¹ Vandekerckhove, S.; Tran, H. G.; Desmet, T.; D'hooge, M. *Bioorg. Med. Chem. Lett.*, **2013**, *23*, 4641.

²² Linghu, X.; Potnick, J. R.; Johnson, J. S. *J. Am. Chem. Soc.*, **2004**, *126*, 3070.; Falk, A.; Goderz, A. L.; Schmalz, H. G. *Angew. Chem. Int. Ed.*, **2013**, *52*, 1576.; Mlynarski, N. S.; Schuster, H. C.; Morken, P. J. *Nature*, **2014**, *505*, 386.

²³ Darras, H. F.; Kling, B.; Heilmann, J.; Decker, M. *ACS Med. Chem. Lett.*, **2012**, *3*, 914.

3.12 General Procedure for the Synthesis of Salts

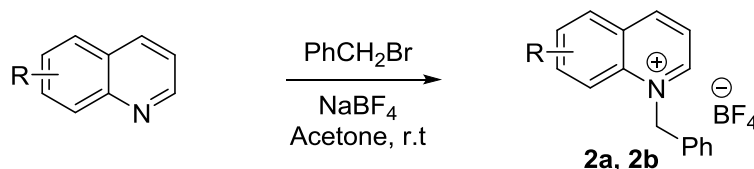
3.12.A N - Methylation of Quinoline derivatives with trifluoromethanesulfonate as counter anion



To a flame dried 50 ml round-bottom flask under argon atmosphere quinoline derivatives (2.0 mmol, 1.0 equiv) was taken followed by dry DCM (10 ml). The solution was cooled to 0 °C, and methyl trifluoromethanesulfonate (3.0 mmol, 1.5 equiv) was added dropwise via syringe. The reaction mixture was slowly warmed to room temperature with TLC monitoring. Upon consumption of starting material, DCM was removed under reduced pressure, and the residue was washed with diethyl ether (3-5 times) to remove low polar impurities to obtain pure salt. In few cases, the ether wash was not sufficient, and the salts were purified by flash column chromatography using 5-10% methanol in DCM as the eluting solvent.

(Caution: Initially, to keep in mind the hygroscopic nature of ammonium salts, we decided, after the preparation of salts use them asap. These salts are stored in a vial and kept at room temperature only. Also, we observe that these salts are bench stable and easy to handle.)

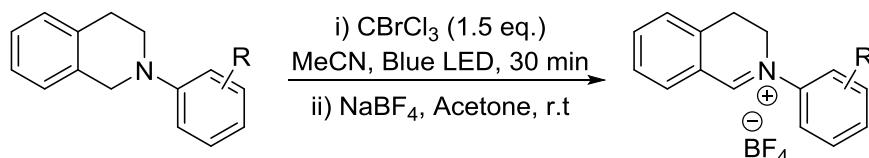
3.12.B N - Benzylation of Quinoline derivatives with tetrafluoroborate as counter anion



To a flame dried 50 ml round-bottom flask under argon atmosphere, quinoline derivatives (5.0 mmol, 1.0 equiv) was dissolved in dry acetone (30 ml) at r.t. To this solution, benzyl bromide (10.0 mmol, 2.0 equiv) was added followed by sodium tetrafluoroborate (30.0 mmol, 6.0 equiv) and stirred at r.t. The TLC analysis shows two polar spots with major low polar one. The reaction stopped after no further change in relative intensities for those polar spots, and the precipitate was removed by filtration. The solvent was removed under reduced pressure, and the residual solid was purified via silica column chromatography by 5:95 MeOH/DCM as eluent to obtain tetrafluoroborate salt as the major product (lower polar) as well as some bromo salt (higher polar spot).

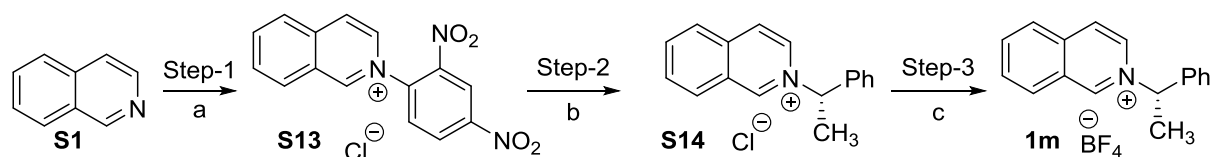
3.12.C N-aryl-3,4-dihydroisoquinolinium derivatives:²⁴

²⁴ Franz, F. J.; Kraus, B. W.; Zeitler, K. *Chem. Commun.*, **2015**, 51, 8280.



In an oven-dried Schlenk tube equipped with a magnetic stir bar the THIQ derivate (0.25 mmol, 1.0 equiv) was dissolved in acetonitrile (0.5 mL). Bromotrichloromethane (0.375 mmol, 1.5 equiv) was added under nitrogen and the tube was then irradiated with blue LEDs for 30 min at room temperature. After completion of reaction, solvent was removed by rotary evaporator and added acetone (2.5 ml) followed by sodium tetrafluoroborate (1.5 mmol, 6.0 equiv) and stirred at r.t. The TLC analysis shows two polar spots with major low polar one. The reaction stopped after no further change in relative intensities for those polar spots, and the precipitate was removed by filtration. The solvent was removed under reduced pressure, and the residual solid was purified via silica column chromatography by 5:95 MeOH/DCM as eluent to obtain tetrafluoroborate salt as the major product (lower polar) as well as some bromo salt (higher polar spot).

3.12.D 2-(1-phenylethyl)isoquinolin-2-ium trifluoromethanesulfonate (**1m**)



Condition: a) 2,4-dinitrobenzene, Acetone, 80 °C. b) (±)-1-phenylethylamine (for racemic)/(S)-(-)-1-phenylethylamine (for chiral), diethylamine, rt, 48 h. c) silver tetrafluoroborate, DCM, 0 °C to r.t.

2-(2,4-dinitrophenyl)isoquinolin-2-ium chloride²⁵ (**S13**) and both racemic and (S)-2-(1-phenylethyl)isoquinolin-2-ium chloride (**S14**) were prepared according to literature procedure, and the analytical data were matched.²⁶

Step-3:

DCM (10 ml) was added to a dry 50 ml round bottom flask containing isoquinolinium salt (**S14**, 1.5 mmol) under argon and stirred at room temperature for 10-15 min until the salt dissolved. Then the mixture was cooled to 0 °C, and silver tetrafluoroborate (439 mg, 2.25 mmol, 1.5 equiv) was added followed by slow warming to r.t. The anion exchange was monitored by TLC with the tetrafluoroborate as lower polar spot. Once the complete

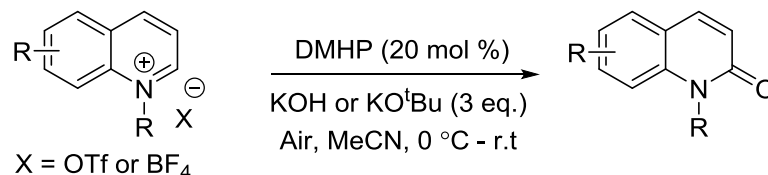
²⁵Vandekerckhove, S., Tran, G. H., Desmet, T. D'hooge, M. *Bioorg. Med. Chem. Lett.* **2013**, *23*, 4641-4643.

²⁶Bujedo, S. G.; Alcarazo, M.; Pichon, C.; Alvarez, E.; Fernandez, R.; Lassaletta, J. M. *Chem. Commun.* **2007**, *11*, 1180-1182.

exchange judged by TLC, the silver chloride was filtered off and the solvent was removed under reduced pressure. The residual solid was purified by small silica pad filtration to obtain pure salt **1m**. Both racemic as well as chiral salt prepared by the above procedure.

3.13 Oxidation of salts

3.13.A General optimized reaction procedure for aerobic oxidation of quinolinium salts



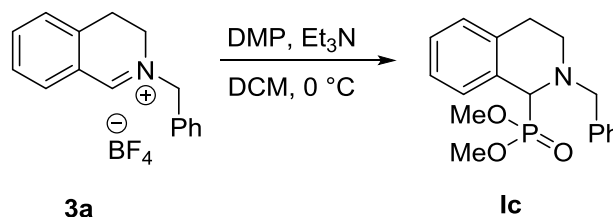
MeCN (2 ml) was added to a dry 10 ml reaction tube containing quinolinium salt (0.3 mmol) under air and stirred at room temperature for 10-15 min until the salt dissolved. The reaction tube was closed via an open top cap with septa and cooled to 0 °C under air balloon. To the above mixture dimethyl hydrogen phosphite (DMHP, 20 mol %) was added followed by appropriate base (3 equiv) and stirred for 2h. Then the reaction tube was slowly brought to room temperature with TLC monitoring for the consumption of starting quinolinium salt. Upon completion, saturated sodium chloride solution (5 ml) was added to quench the reaction, and the organic layer was extracted with ethyl acetate (3 times). The combined organic layer was dried over anhydrous sodium sulfate, and the solvent was removed under reduced pressure to obtain the crude which was filtered through a 6-inch silica column to get the desired product in pure form.

3.13.B Aerobic auto-oxidation of Aromatic Iminium Salt to Lactum:²⁷

1. Stepwise Oxidation of Aromatic Iminium Salt to Lactum

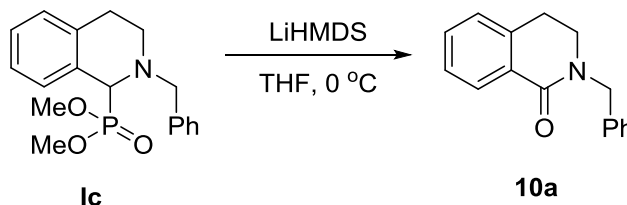
Step-1: Preparation of Dimethyl (2-benzyl-1,2,3,4-tetrahydroisoquinolin-1-yl)phosphonate(3-10a)

²⁷ (a) Franz, F.J.; Krausab, B. W.; Zeitler, K. *Chem. Commun.*, **2015**, 51, 8280. (b) Orito, K.; Horibata, A.; Nakamura, T.; Ushito, H.; Nagasaki, H.; Yuguchi, M.; Yamashita, S.; Tokuda, M. *J. Am. Chem. Soc.*, **2004**, 126, 14342. (c) Liu, Y.; Wang, C.; Xue, D.; Xiao, M.; Liu, J.; Li, C.; Xiao, J. *Chem. Eur. J.*, 2017, **23**, 3062.; Benmekhbi, L.; Loufi, F.; Roisnel, T.; Hurvois, J. P. *J. Org. Chem.* **2016**, 81, 6721-6739.; Lanni, E. L.; Bosscher, M. A.; Ooms, B. D.; Shandro, C. A.; Ellsworth, B. A.; Anderson, C. E.; *J. Org. Chem.* **2008**, 73, 6425-6428.



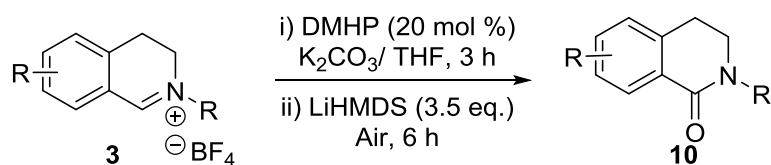
DCM (8 ml) was added to a dry 25 ml rb flask containing 3,4-dihydroquinolinium salt (**3a**, 2.0 mmol, 1.0 equiv.) under argon and stirred at room temperature for 10-15 min until the salt dissolved. The reaction mixture was cooled to 0 °C, and dimethyl phosphite (DMP, 4.4 mmol, 1.2 equiv.) was added followed by Et₃N (3 mmol, 1.5 equiv.) and stirred at the same temperature with TLC monitoring for the consumption of starting salt. Upon completion, the reaction mixture was quenched by the addition of 10 ml of saturated sodium bicarbonate solution and the organic layer was extracted with ethyl acetate (3 times). The combined organic layer was dried over anhydrous sodium sulfate, and the solvent was removed under reduced pressure to obtain the crude which was purified by flash column chromatography to get the desired compound in pure form. R_f (Ethyl acetate/Pet. ether =50:50) = 0.4, yield 71 %.

Step-2: Oxidation of Dimethyl (2-benzyl-1,2,3,4-tetrahydroisoquinolin-1-yl)phosphonate(**10a**)



THF (3 ml) was added to a dry 25 ml round bottom flask containing dimethyl (2-benzyl-1,2,3,4-tetrahydroisoquinolin-1-yl)phosphonate (**3-10a**, 0.2 mmol) and oxygen was purged through the solution via a balloon and long needle for 5 min and cooled it to 0 °C under the O₂ balloon. Then LiHMDS (1.5 equiv.) solution was added to it dropwise over a period of 15-20 mins at 0 °C via gas tight syringe, with TLC monitoring for the consumption of starting intermediate. Upon completion, saturated ammonium chloride solution (5 ml) was added to quench the reaction, and the organic layer was extracted with ethyl acetate (3 times). The combined organic layer was dried over anhydrous sodium sulfate, and the solvent was removed under reduced pressure to obtain the crude which was purified by flash column chromatography to get the desired compound in pure form. R_f (Ethyl acetate/Pet. ether = 20:80) = 0.3, yield 76 %.

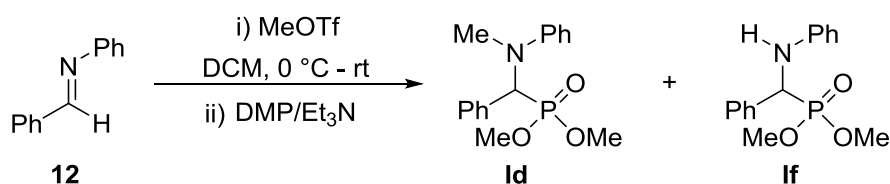
2. One pot Oxidation of Aromatic Iminium Salt to Lactum



THF (3 ml) was added to a dry 25 ml round bottom flask containing salt **3** (0.3 mmol) and stirred at room temperature for 10-15 min until the salt dissolved. The reaction mixture was cooled to 0 °C with an air balloon, and dimethyl phosphite (20 mol%) was added followed by K₂CO₃ (0.15 mmol, 2.5 equiv. to catalyst) and stirred at the same temperature for 1h.17 Then LiHMDS (1M solution in THF, 1.05 mmol, 3.5 equiv.) solution was added to it dropwise over a period of 4h via gastight syringe. The reaction was monitored by TLC for the consumption of isoquinilonium salt. Upon completion, saturated sodium chloride solution (5 ml) was added to quench the reaction, and the organic layer was extracted with ethyl acetate (3 times). The combined organic layer was dried over anhydrous sodium sulfate, and the solvent was removed under reduced pressure to obtain the crude which was filtered through a 6-inch silica column to get the desired product in pure form.

3.13.C Oxidative coupling of aldehyde and amine to Amide:²⁸

1. Method 1 for intermediate formation

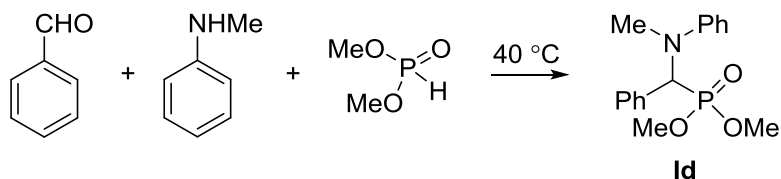


DCM (4 ml) was added to a dry 25 ml round bottom flask containing (E)-N,1-diphenylmethanimine (**12**, 1mmol, 1.0 equiv) and cooled to 0 °C. Methyl trifluoromethanesulfonate (1.5mmol, 1.5 equiv) was added dropwise via syringe. The reaction mixture was slowly warmed to room temperature and stirring for 3h. The mixture was re-cooled to 0 °C, and Et₃N (0.33 ml, 2.5 mmol, 2.5 equiv.) was added followed by dimethylphosphite (0.12 ml, 1.2 mmol, 1.2 equiv.). TLC was monitored with slowly bringing the temperature to r.t. Upon completion, saturated aqueous ammonium chloride solution was added to quench the reaction, and the organic layer was extracted with DCM (3 times). Organic layer dried with Na₂SO₄ and solvent was removed under rotary evaporator. The combined organic layer was dried over anhydrous sodium sulfate, and the solvent was

²⁸ Zhou, S.; Junge, K.; Addis, D.; Das, S.; Beller, M. *Angew. Chem. Int. Ed.*, **2009**, *48*, 9507.; Orito, K.; Horibata, A.; Nakamura, T.; Ushito, H.; Nagasaki, H.; Yuguchi, M.; Yamashita, S.; Tokuda, M. *J. Am. Chem. Soc.* **2004**, *126*, 14342-14343.; Nakao, Y.; Idei, H.; Kanyiva, K. S.; Hiyama, T. *J. Am. Chem. Soc.* **2009**, *131*, 15996-15997.; Outerbridge, V. M.; Landge, S. M.; Tamaki, H.; Torok, B. *Synthesis* **2009**, *11*, 1801-1806.

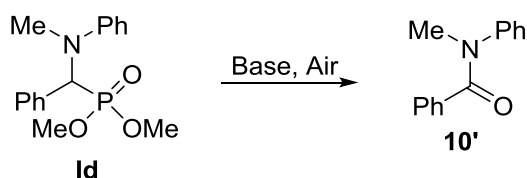
removed under reduced pressure to obtain the crude which was purified by flash column chromatography which gives amino phosphonate **Id** (45 %) and **If** (29 %).

2. Method 2 for intermediate formation



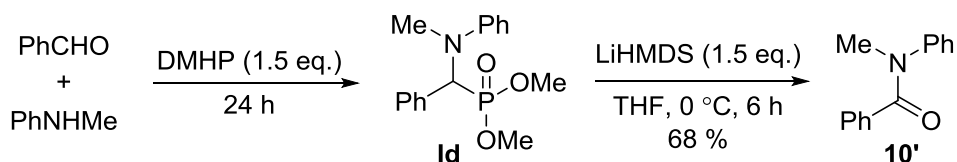
In an oven dry round bottom flask with a magnetic stir taken benzaldehyde (1.06 g, 10 mmol), N-methyl aniline (1.07 g, 10 mmol) and DMHP (1.1 g, 10 mmol) one by one. Then the reaction mixture was stir at 40 °C for 24 h and completion of reaction checked by TLC monitoring. Upon completion of reaction, crude mixture was purified by column chromatography using to obtain pure α -amino phosphite intermediate (**Id**).

3. Oxidation from reactive intermediate (**Id**)



Solvent (3 ml) was added to a dry reaction tube containing **3'** (0.3 mmol) and air was purged through the solution with cooling to 0 °C. Then KOH (1.5 mmol, 5 equiv) was added to it and slowly brought to r.t. with TLC monitoring. After 20 h, the reaction mixture was quenched by the addition of 10 ml of saturated ammonium chloride solution and the organic layer was extracted with ethyl acetate (3 times). The combined organic layer was dried over anhydrous sodium sulfate, and the solvent was removed under reduced pressure to obtain the crude which was purified by flash column chromatography to obtain N-methyl-N-phenyl benzamide **10'**. For base KOH used MeCN as solvent (89%); For base ^tBuOk used DMA as solvent (85%); for base LiHMDS used THF as solvent (81%).

4. One-pot amide synthesis



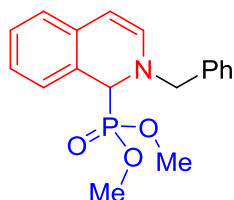
Benzaldehyde (1.0 mmol), N-methyl aniline (1.2 mmol, 1.2 equiv), and dimethylphosphite (1.5 mmol, 1.5 equiv) was taken together and stirred at room temperature (35 °C) with 100 mg 4 Å molecular sieves. Upon complete consumption of aldehyde, the reaction mixture was dissolved in DCM and dried with sodium sulfate, filtered and solvent was removed. 6 ml THF was added to the crude and cooled to 0 °C under air balloon. Then LiHMDS (1.5 mmol, 1.5

equiv) was added to it dropwise over 10 minutes and stirred at that temperature for 6h. The reaction was monitored by TLC for the consumption of isoquinilonium salt. Upon completion, saturated sodium chloride solution (5 ml) was added to quench the reaction, and the organic layer was extracted with ethyl acetate (3 times). The combined organic layer was dried over anhydrous sodium sulfate, and the solvent was removed under reduced pressure to obtain the crude which was filtered through a 6-inch silica column to get the desired product in pure form. *R_f* (Ethyl acetate/Pet. ether = 30:70) = 0.5, yield 60 %.

3.14: Compounds characterization data

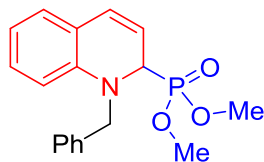
3.14.1 Spectral data for catalyst added intermediate

Dimethyl (2-benzyl-1,2-dihydroisoquinolin-1-yl)phosphonate (Ia)



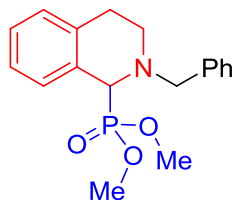
¹H NMR (200 MHz, CDCl₃) δ 3.63 (dd, *J* = 16.23, 10.42 Hz, 6 H) 4.38 (d, *J* = 15.54, 1 H) 4.51 - 4.72 (m, 1 H) 4.84 (dd, *J* = 8.40, 0.44 Hz, 1 H) 5.33 - 5.38 (m, 1 H) 6.20 - 6.24 (m, 1 H) 6.87 - 7.14 (m, 4 H) 7.26 - 7.32 (m, 5 H).

Dimethyl (1-benzyl-1,2-dihydroquinolin-2-yl)phosphonate (Ib)



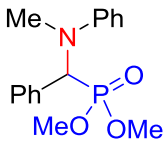
¹H NMR (400 MHz, CDCl₃) δ 3.61 (d, *J* = 10.38 Hz, 3 H), 3.72 (d, *J* = 10.38 Hz, 3 H), 4.12 - 4.24 (m, 1 H), 4.57 - 4.67 (m, 2 H), 4.67 - 4.73 (m, 1 H), 6.24 (dd, *J* = 7.48, 5.95 Hz, 1 H), 6.55 (d, *J* = 8.24 Hz, 1 H), 6.81 - 6.89 (m, 1 H), 6.96 - 7.05 (m, 1 H), 7.18 (d, *J* = 7.63 Hz, 1 H), 7.24 (td, *J* = 5.95, 2.75 Hz, 1 H), 7.29 - 7.33 (m, 4 H). ³¹P NMR (202 MHz, CDCl₃) □ 24.22 (s, 1 P).

dimethyl (2-benzyl-1,2,3,4-tetrahydroisoquinolin-1-yl)phosphonate (Ic)



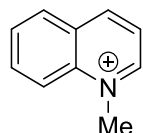
¹H NMR (500 MHz, CDCl₃) δ 2.68 (dd, *J* = 16.48, 3.66 Hz, 1 H), 2.79 - 2.98 (m, 2 H), 3.57 - 3.69 (m, 7 H), 3.80 - 3.86 (m, 1 H), 3.86 - 3.93 (m, 1 H), 4.21 (s, 1 H), 7.09 - 7.21 (m, 3 H), 7.21 - 7.28 (m, 2 H), 7.30 (t, *J* = 7.48 Hz, 2 H), 7.33 - 7.38 (m, 2 H). ¹³C NMR (126 MHz, CDCl₃) δ 23.07, 43.80, 51.30, 51.36, 51.88, 51.94, 57.11, 57.57, 57.67, 58.37, 75.36, 75.61, 75.86, 124.11, 124.14, 125.42, 125.45, 125.63, 126.63, 127.36, 127.43, 127.60, 134.17, 134.21, 136.81. ³¹P NMR (202 MHz, CDCl₃) δ 25.45 (s, 1 P).

Dimethyl ((methyl(phenyl)amino)(phenyl)methyl)phosphonate (Id)


 $^1\text{H NMR}$ (500 MHz, CDCl_3) δ 3.71 (d, $J = 10.68$ Hz, 3 H) 3.79 (d, $J = 10.68$ Hz, 3 H) 5.36 (s, 1 H) 5.41 (s, 1 H) 6.84 (t, $J = 7.25$ Hz, 1 H) 6.92 (m, $J = 8.01$ Hz, 2 H) 7.24 - 7.40 (m, 5 H) 7.52 (m, $J = 7.25$ Hz, 2 H). $^{13}\text{C NMR}$ (126 MHz, CDCl_3) δ 34.62, 52.51, 52.57, 53.64, 53.70, 60.99, 62.27, 113.92, 118.22, 127.99, 128.51, 128.68, 128.75, 129.21, 134.00, 134.06, 149.98, 150.04.

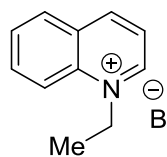
3.14.2: Analytical Data for Salts

1-methylquinolin-1-ium trifluoromethanesulfonate (2a)



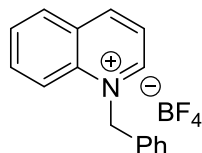
The titled compound was prepared by following the general procedure A, Obtained as a white solid (486 mg, 83 % yield). R_f (MeOH/DCM = 10:90) = 0.45; $\text{MP} = 118.4$ °C. $^1\text{H NMR}$ (400 MHz, $\text{DMSO}-d_6$) δ 4.66 (s, 3 H), 8.00 - 8.14 (m, 1 H), 8.14 - 8.26 (m, 1 H), 8.31 (t, $J = 7.93$ Hz, 1 H), 8.54 (d, $J = 9.16$ Hz, 1 H), 8.51 (d, $J = 8.55$ Hz, 1 H), 9.31 (d, $J = 8.55$ Hz, 1 H), 9.55 (d, $J = 5.49$ Hz, 1 H). $^{13}\text{C NMR}$ (100 MHz, $\text{DMSO}-d_6$) δ 45.91, 119.63, 122.48, 129.63, 130.41, 130.76, 135.92, 138.76, 147.50, 150.64. **FTIR** (cm^{-1}): 2984, 1528, 1268, 1224, 1129, 1023, 837, 778, 630. **HRMS**: Calculated for $\text{C}_{10}\text{H}_{10}\text{N}$ $[\text{M}]^+$: 144.0813, found: 144.0808.

1-ethylquinolin-1-ium tetrafluoroborate (2b)



The titled compound was prepared (7.75 mmol scale) by following the general procedure B, Obtained as a yellow solid (1134 mg, 60 % yield). R_f (MeOH/DCM = 10:90) = 0.5; $\text{MP} = 142.6$ °C. $^1\text{H NMR}$ (500 MHz, $\text{DMSO}-d_6$) δ 1.65 (t, $J = 7.25$ Hz, 3 H), 5.16 (q, $J = 6.99$ Hz, 2 H), 8.09 (t, $J = 7.63$ Hz, 1 H), 8.24 (dd, $J = 8.20, 5.91$ Hz, 1 H), 8.32 (t, $J = 7.63$ Hz, 1 H), 8.54 (d, $J = 8.01$ Hz, 1 H), 8.68 (d, $J = 8.77$ Hz, 1 H), 9.35 (d, $J = 8.39$ Hz, 1 H), 9.66 (d, $J = 5.34$ Hz, 1 H). $^{13}\text{C NMR}$ (125 MHz, $\text{DMSO}-d_6$) δ 15.20, 52.93, 118.81, 122.26, 129.55, 129.79, 130.66, 135.58, 137.13, 147.11, 149.30. **FTIR** (cm^{-1}): 2914, 2845, 1592, 1524, 1434, 1358, 803, 766, 731. **HRMS**: Calculated for $\text{C}_{11}\text{H}_{12}\text{N}$ $[\text{M}]^+$: 158.0970, found: 158.0964.

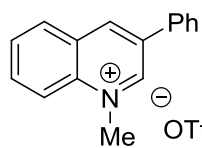
1-benzylquinolin-1-ium tetrafluoroborate (2c)



The titled compound was prepared (10 mmol scale) by following the general procedure B, Obtained as a white powder (2443 mg, 80 % yield). R_f (MeOH/DCM = 05:95) = 0.4; $\text{MP} = 163$ °C. $^1\text{H NMR}$ (400 MHz, $\text{DMSO}-d_6$) δ 6.45 (s, 2 H), 7.29 - 7.49 (m, 5 H), 7.97 - 8.11 (m, 1 H), 8.23 (t, $J = 7.93$ Hz, 1 H), 8.33 (dd, $J = 7.93, 6.10$ Hz, 1 H), 8.47 - 8.62 (m, 2 H), 9.43 (d, $J = 8.55$ Hz, 1 H), 9.86 (d, $J = 5.49$ Hz, 1 H). $^{13}\text{C NMR}$ (100 MHz, $\text{DMSO}-d_6$) δ 59.82, 119.29, 122.46, 127.33, 128.75, 129.07, 129.90, 129.96, 130.85, 133.88, 135.72, 137.51, 148.16, 150.43. **FTIR** (cm^{-1}): 3004, 1585,

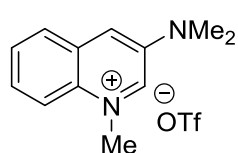
1528, 1360, 1232, 1150, 1043, 811, 767, 717, 645. **HRMS:** Calculated for $C_{16}H_{14}N$ $[M]^+$: 220.1126 found: 220.1121.

1-methyl-3-phenylquinolin-1-ium trifluoromethanesulfonate (2d)



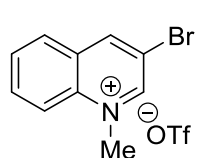
The titled compound was prepared (1 mmol) by following the general procedure **A**, Obtained as a White Solid (199 mg, 54 % yield). R_f (MeOH/DCM = 10:90) = 0.2; **MP** = 181.6 °C. 1H NMR (500 MHz, DMSO- d_6) δ 4.72 (s, 3 H), 7.56 - 7.64 (m, 1 H), 7.64 - 7.71 (m, 2 H), 8.03 (d, J = 7.25 Hz, 2 H), 8.09 (t, J = 7.63 Hz, 1 H), 8.18 - 8.35 (m, 1 H), 8.53 (d, J = 8.77 Hz, 1 H), 8.49 (d, J = 8.01 Hz, 1 H), 9.62 (s, 1 H), 9.91 - 10.02 (m, 1 H). ^{13}C NMR (125 MHz, DMSO- d_6) δ 45.86, 119.42, 127.87, 129.69, 130.03, 130.31, 130.68, 131.00, 133.89, 133.99, 135.64, 137.65, 143.37, 149.82. **FTIR** (cm^{-1}): 2985, 2885, 1538, 1387, 1246, 1142, 1029, 764, 694, 638. **HRMS:** Calculated for $C_{16}H_{14}N$ $[M]^+$: 220.1126, found: 220.1121.

3-(dimethylamino)-1-methylquinolin-1-ium trifluoromethanesulfonate (2e)



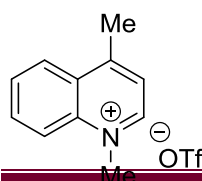
The titled compound was prepared (1.5 mmol) by following the general procedure **A**, Obtained as a yellow Solid (376 mg, 56 % yield). R_f (MeOH/DCM = 10:90) = 0.3; **MP** = 134 °C. 1H NMR (500 MHz, DMSO- d_6) δ 3.17 (s, 6 H), 4.62 (s, 3 H), 7.75 - 7.90 (m, 2 H), 8.08 - 8.17 (m, 1 H), 8.17 - 8.31 (m, 2 H), 9.20 (d, J = 2.67 Hz, 1 H). ^{13}C NMR (125 MHz, DMSO- d_6) δ 28.98, 45.35, 118.42, 121.12, 127.93, 129.53, 129.62, 130.24, 131.22, 139.04, 143.73. **FTIR** (cm^{-1}): 3058, 1619, 1538, 1390, 1267, 1137, 1020, 879, 765, 629. **HRMS:** Calculated for $C_{12}H_{15}N_2$ $[M]^+$: 187.1235, found: 187.1230.

3-bromo-1-methylquinolin-1-ium trifluoromethanesulfonate(2f)



The titled compound was prepared (4 mmol scale) by following the general procedure **A**, Obtained as a yellow solid (1428 mg, 65 % yield). R_f (MeOH/DCM = 10:90) = 0.5; **MP** = 177 °C. 1H NMR (400 MHz, DMSO- d_6) δ 4.62 (s, 3 H), 8.09 (t, J = 7.32 Hz, 1 H), 8.31 (t, J = 7.93 Hz, 1 H), 8.39 (d, J = 8.55 Hz, 1 H), 8.50 (d, J = 8.55 Hz, 1 H), 9.63 (s, 1 H), 9.89 (s, 1 H). ^{13}C NMR (100 MHz, DMSO- d_6) δ 45.74, 114.89, 119.67, 130.04, 131.25, 136.10, 137.65, 148.59, 151.84. **FTIR** (cm^{-1}): 3043, 1524, 1250, 1151, 1023, 896, 776, 757, 624. **HRMS:** Calculated for $C_{10}H_9BrN$ $[M]^+$: 221.9918, found: 221.9913.

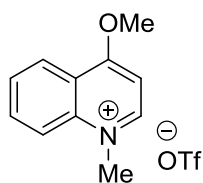
1,4-dimethylquinolin-1-ium trifluoromethanesulfonate (2g)



The titled compound was prepared by following the general procedure **A**, Obtained as a white solid (497 mg, 80 % yield). R_f (MeOH/DCM = 10:90)

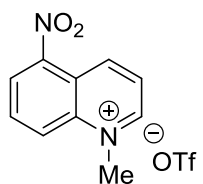
= 0.2; **MP** = 114.6 °C. **¹H NMR (500 MHz, DMSO-*d*₆)** δ 3.01 (s, 3 H), 4.58 (s, 3 H), 8.00 - 8.11 (m, 2 H), 8.27 (t, *J* = 7.63 Hz, 1 H), 8.49 (d, *J* = 8.77 Hz, 1 H), 8.54 (d, *J* = 8.39 Hz, 1 H), 9.33 (d, *J* = 5.72 Hz, 1 H). **¹³C NMR (125 MHz, DMSO-*d*₆)** δ 19.55, 44.95, 119.48, 122.45, 126.77, 128.49, 129.65, 134.93, 137.70, 148.97, 158.22. **FTIR (cm⁻¹)**: 2985, 1589, 1524, 1396, 1243, 1137, 1023, 840, 765, 637. **HRMS**: Calculated for C₁₁H₁₂N [M]⁺: 158.0970, found: 158.0964.

4-methoxy-1-methylquinolin-1-ium trifluoromethanesulfonate (2h)



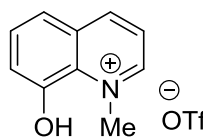
The titled compound was prepared by following the general procedure A. Obtained as a pale yellow solid (338 mg, 52 % yield). **R_f**(MeOH/DCM = 10:90) = 0.2; **MP** = 133.5 °C. **¹H NMR (500 MHz, DMSO-*d*₆)** δ 4.34 (s, 3 H), 4.43 (s, 3 H), 7.65 (d, *J* = 6.87 Hz, 1 H), 7.98 (t, *J* = 7.63 Hz, 1 H), 8.24 (t, *J* = 8.01 Hz, 1 H), 8.37 (d, *J* = 8.77 Hz, 1 H), 8.47 (d, *J* = 8.01 Hz, 1 H), 9.32 (d, *J* = 7.25 Hz, 1 H). **¹³C NMR (125 MHz, DMSO-*d*₆)** δ 44.11, 59.36, 102.82, 119.54, 121.18, 124.07, 129.43, 135.50, 139.57, 151.96, 168.80. **FTIR (cm⁻¹)**: 2967, 1580, 1538, 1400, 1258, 1224, 1132, 1015, 947, 859, 769, 630. **HRMS**: Calculated for C₁₁H₁₂NO [M]⁺: 174.0919, found: 174.0912.

1-methyl-5-nitroquinolin-1-ium trifluoromethanesulfonate (2i)

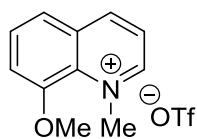


The titled compound was prepared by following the general procedure A. Obtained as a yellow solid (486 mg, 72 % yield). **R_f**(MeOH/DCM = 10:90) = 0.2; **MP** = 158.7 °C. **¹H NMR (500 MHz, DMSO-*d*₆)** δ 4.80 (s, 3 H), 8.34 - 8.57 (m, 2 H), 8.82 (d, *J* = 7.63 Hz, 1 H), 8.99 (d, *J* = 9.16 Hz, 1 H), 9.59 (d, *J* = 9.16 Hz, 1 H), 9.73 (d, *J* = 5.72 Hz, 1 H). **¹³C NMR (125 MHz, DMSO-*d*₆)** δ 47.18, 122.24, 124.91, 125.94, 127.54, 134.29, 138.97, 142.80, 146.68, 152.23. **FTIR (cm⁻¹)**: 3087, 1606, 1535, 1351, 1239, 1145, 1021, 896, 809, 737, 637. **HRMS**: Calculated for C₁₀H₉N₂O₂ [M]⁺: 189.0664, found: 189.0659.

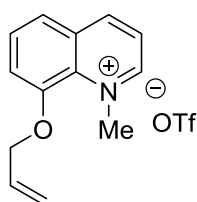
8-hydroxy-1-methylquinolin-1-ium trifluoromethanesulfonate (2j)



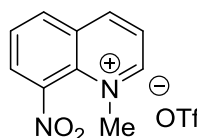
The titled compound was prepared by following the general procedure A. Obtained as a light greenish powder (595 mg, 96 % yield). **R_f**(MeOH/DCM = 10:90) = 0.15; **MP** = 128.8 °C. **¹H NMR (500 MHz, DMSO-*d*₆)** δ 4.83 (s, 3 H), 7.41 - 7.64 (m, 1 H), 7.66 - 7.89 (m, 2 H), 8.01 (dd, *J* = 8.39, 5.72 Hz, 1 H), 9.10 (d, *J* = 8.39 Hz, 1 H), 9.25 (d, *J* = 5.72 Hz, 1 H), 11.74 (s, 1 H). **¹³C NMR (100 MHz, DMSO-*d*₆)** δ 51.78, 120.00, 121.02, 122.09, 122.77, 130.95, 132.37, 147.41, 150.36, 151.67. **FTIR (cm⁻¹)**: 2984, 1587, 1548, 1376, 1237, 1146, 1027, 835, 757, 636. **HRMS**: Calculated for C₁₀H₁₀NO [M]⁺: 160.0762, found: 160.0757.

8-methoxy-1-methylquinolin-1-ium trifluoromethanesulfonate (2k)

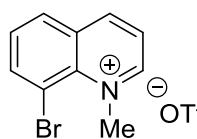
The titled compound was prepared by following the general procedure A, Obtained as a light yellow solid (313 mg, 48 % yield). R_f (MeOH/DCM = 10:90) = 0.5; **MP** = 119.8 °C. $^1\text{H NMR}$ (500 MHz, DMSO- d_6) δ 4.08 (s, 3 H), 4.80 (s, 3 H), 7.68 - 7.86 (m, 1 H), 7.87 - 8.03 (m, 2 H), 8.10 (dd, J = 8.39, 5.72 Hz, 1 H), 9.18 (d, J = 8.01 Hz, 1 H), 9.31 (d, J = 5.72 Hz, 1 H). $^{13}\text{C NMR}$ (125 MHz, DMSO- d_6) δ 52.36, 57.82, 116.75, 122.50, 122.63, 130.84, 132.14, 147.52, 151.78, 152.23. **FTIR** (cm^{-1}): 3071, 1580, 1535, 1406, 1321, 1253, 1226, 1134, 1031, 951, 861, 770, 636. **HRMS**: Calculated for $\text{C}_{11}\text{H}_{12}\text{NO}$ $[\text{M}]^+$: 174.0919, found: 174.0912.

8-(allyloxy)-1-methylquinolin-1-ium trifluoromethanesulfonate(2l)

The titled compound was prepared by following the general procedure A, Obtained as a White powder (500 mg, 71 % yield). R_f (MeOH/DCM = 10:90) = 0.6; **MP** = 108 °C. $^1\text{H NMR}$ (500 MHz, DMSO- d_6) δ 4.83 (s, 3 H), 4.92 (d, J = 5.34 Hz, 2 H), 5.40 (d, J = 10.68 Hz, 1 H), 5.47 - 5.61 (m, 1 H), 6.11 - 6.30 (m, 1 H), 7.78 (d, J = 7.63 Hz, 1 H), 7.92 (t, J = 8.01 Hz, 1 H), 7.98 (d, J = 8.01 Hz, 1 H), 8.09 (dd, J = 8.20, 5.91 Hz, 1 H), 9.18 (d, J = 8.39 Hz, 1 H), 9.32 (d, J = 5.72 Hz, 1 H). $^{13}\text{C NMR}$ (125 MHz, DMSO- d_6) δ 52.46, 71.59, 118.08, 119.64, 122.60, 122.81, 130.75, 130.97, 132.21, 132.85, 147.61, 150.54, 152.37. **FTIR** (cm^{-1}): 3073, 2984, 1603, 1529, 1383, 1244, 1149, 1023, 918, 880, 749, 626. **HRMS**: Calculated for $\text{C}_{13}\text{H}_{14}\text{NO}$ $[\text{M}]^+$: 200.1075, found: 200.1070.

1-methyl-8-nitroquinolin-1-ium trifluoromethanesulfonate (2m)

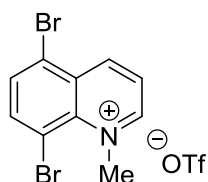
The titled compound was prepared by following the general procedure A, Obtained as a yellow solid (466 mg, 69 % yield). R_f (MeOH/DCM = 10:90) = 0.2; **MP** = 113.6 °C. $^1\text{H NMR}$ (500 MHz, DMSO- d_6) δ 4.42 (s, 3 H), 8.20 (t, J = 7.82 Hz, 1 H), 8.39 (dd, J = 8.20, 5.91 Hz, 1 H), 8.82 (d, J = 7.63 Hz, 1 H), 8.79 (d, J = 8.01 Hz, 1 H), 9.48 (d, J = 8.39 Hz, 1 H), 9.65 (d, J = 5.72 Hz, 1 H). $^{13}\text{C NMR}$ (125 MHz, DMSO- d_6) δ 47.62, 124.38, 129.86, 130.32, 131.35, 132.92, 136.06, 142.11, 148.80, 155.27. **FTIR** (cm^{-1}): 2968, 1598, 1529, 1456, 1358, 1251, 1151, 1029, 967, 835, 756, 623. **HRMS**: Calculated for $\text{C}_{10}\text{H}_9\text{N}_2\text{O}_2$ $[\text{M}]^+$: 189.0664, found: 189.0659.

8-bromo-1-methylquinolin-1-ium trifluoromethanesulfonate(2n)

The titled compound was prepared (1 mmol scale) by following the general procedure A, Obtained as a White solid (175 mg, 47 % yield). R_f (MeOH/DCM = 10:90) = 0.15; **MP** = 140.9 °C. $^1\text{H NMR}$ (500 MHz, DMSO- d_6) δ 4.99 (s, 3 H), 7.87 (br. s, 1 H), 8.08 - 8.28 (m, 1 H), 8.48 (d, J = 7.25 Hz, 1 H),

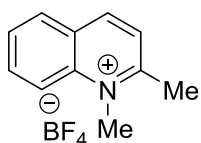
8.53 - 8.72 (m, 1 H), 9.33 (d, $J = 8.39$ Hz, 1 H), 9.51 (d, $J = 5.72$ Hz, 1 H). ^{13}C NMR (125 MHz, DMSO- d_6) δ 52.21, 111.21, 122.98, 130.78, 131.96, 132.85, 137.50, 143.64, 149.48, 154.56. FTIR (cm^{-1}): 2972, 1543, 1243, 1226, 1135, 1029, 845, 757, 629. HRMS: Calculated for $\text{C}_{10}\text{H}_9\text{BrN}$ [M] $^+$: 221.9918, found: 221.9913

5,8-dibromo-1-methylquinolin-1-ium trifluoromethanesulfonate(2o)



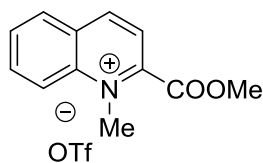
The titled compound was prepared (5.23 mmol) by following the general procedure A, Obtained as a White Solid (1100 mg, 50 % yield). R_f (MeOH/DCM = 10:90) = 0.4; 107.2 °C. ^1H NMR (400 MHz, DMSO- d_6) δ 4.98 (s, 3 H), 8.16 - 8.37 (m, 2 H), 8.52 (d, $J = 8.55$ Hz, 1 H), 9.45 (d, $J = 8.54$ Hz, 1 H), 9.60 (d, $J = 5.49$ Hz, 1 H). ^{13}C NMR (100 MHz, DMSO- d_6) δ 52.53, 111.52, 124.38, 124.61, 131.28, 134.68, 139.17, 143.35, 147.95, 155.20. FTIR (cm^{-1}): 3033, 1576, 1511, 1382, 1252, 1148, 1029, 842, 751, 637. HRMS: Calculated for $\text{C}_{10}\text{H}_8\text{Br}_2\text{N}$ [M] $^+$: 301.9003, found: 301.8998.

2-methyl-1-methylquinolin-1-ium trifluoromethanesulfonate (2p)



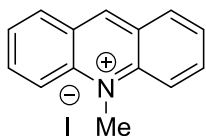
The titled compound was prepared (10 mmol scale) by following the general procedure B, Obtained as a yellowish solid (1764 mg, 72 % yield). R_f (MeOH/DCM = 10:90) = 0.25; MP = 183.3 °C. ^1H NMR (500 MHz, DMSO- d_6) δ 3.10 (s, 3 H), 4.46 (s, 3 H), 8.00 (t, $J = 7.44$ Hz, 1 H), 8.14 (d, $J = 8.39$ Hz, 1 H), 8.23 (t, $J = 7.82$ Hz, 1 H), 8.41 (d, $J = 8.01$ Hz, 1 H), 8.60 (d, $J = 8.77$ Hz, 1 H), 9.11 (d, $J = 8.39$ Hz, 1 H). ^{13}C NMR (125 MHz, DMSO- d_6) δ 22.87, 39.37, 118.66, 118.74, 118.83, 124.88, 128.73, 130.06, 134.80, 145.12, 145.18. FTIR (cm^{-1}): 2919, 2843, 1603, 1515, 1426, 1358, 1220, 1058, 832, 775, 751. HRMS: Calculated for $\text{C}_{11}\text{H}_{12}\text{N}$ [M] $^+$: 158.0970, found: 158.0964.

2-(methoxycarbonyl)-1-methylquinolin-1-ium trifluoromethanesulfonate (2q)



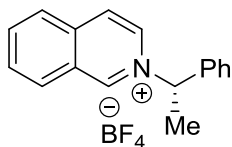
The titled compound was prepared (1 mmol scale) by following the general procedure A, Obtained as a white solid (76 mg, 22 % yield). R_f (MeOH/DCM = 10:90) = 0.25; MP = 143.9 °C. ^1H NMR (500 MHz, DMSO- d_6) δ 4.15 (s, 3 H), 4.67 (s, 3 H), 8.15 (t, $J = 7.44$ Hz, 1 H), 8.40 (t, $J = 8.01$ Hz, 1 H), 8.48 (d, $J = 8.39$ Hz, 1 H), 8.55 (d, $J = 8.01$ Hz, 1 H), 8.69 (d, $J = 9.16$ Hz, 1 H), 9.48 (d, $J = 8.39$ Hz, 1 H). ^{13}C NMR (125 MHz, DMSO- d_6) δ 43.30, 55.56, 120.49, 122.59, 130.41, 131.02, 131.37, 137.52, 139.96, 147.88, 149.14, 161.51. FTIR (cm^{-1}): 2985, 1749, 1442, 1385, 1264, 1151, 1027, 947, 854, 777, 635. HRMS: Calculated for $\text{C}_{12}\text{H}_{12}\text{NO}_2$ [M] $^+$: 202.0868, found: 202.0863.

10-methylacridin-10-ium trifluoromethanesulfonate (2r)



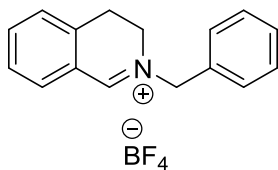
The titled compound was prepared (6 mmol scale) by following the general procedure A. This compound is previously known in literature.²⁹ Obtained as a red solid (1078 mg, 56 % yield).

2-(1-phenylethyl)isoquinolin-2-ium trifluoromethanesulfonate (1m)



Obtained as a white solid (321 mg, 67 % yield). R_f (MeOH/DCM = 05:95) = 0.6; MP = 157.3°C. $^1\text{H NMR}$ (500 MHz, DMSO- d_6) δ 2.17 (d, J = 7.25 Hz, 3 H), 6.33 - 6.37 (m, 1 H), 7.44 - 7.50 (m, 3 H), 7.60 - 7.62 (m, 2 H), 8.12 (t, J = 7.63 Hz, 1 H), 8.28 - 8.31 (m, 1 H), 8.36 (d, J = 8.39 Hz, 1 H), 8.59 (t, J = 8.01 Hz, 2 H), 8.84 - 8.85 (m, 1 H), 10.33 (s, 1 H). $^{13}\text{C NMR}$ (125 MHz, DMSO- d_6) δ 19.79, 69.46, 126.36, 127.30, 127.39, 129.17, 129.27, 129.28, 130.81, 131.30, 133.42, 137.19, 138.16, 148.83. FTIR (cm^{-1}): 3126, 3066, 2160, 1640, 1608, 1156, 1043. HRMS: Calculated for $\text{C}_{17}\text{H}_{16}\text{N}$ $[\text{M}]^+$: 234.1283, found: 234.1282.

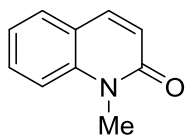
2-benzyl-3,4-dihydroisoquinolin-2-ium tetrafluoroborate (3a)



The titled compound was prepared by following the general procedure B, Obtained as a light yellow solid (565 mg, 85 % yield). R_f (MeOH/DCM = 05:95) = 0.5; MP = 147.2°C. $^1\text{H NMR}$ (500 MHz, DMSO- d_6) δ 3.16 (t, J = 16.78, 2 H), 3.93 (t, J = 16.78, 2 H), 5.24 (s, 2 H), 7.44 - 7.52 (m, 4 H), 7.57 - 7.61 (m, 3 H), 7.83 (t, J = 16.26, 1 H), 7.91 (d, J = 7.63 Hz, 1 H), 9.48 (s, 1 H). $^{13}\text{C NMR}$ (125 MHz, DMSO- d_6) δ 55, 47.42, 62.97, 124.73, 128.18, 128.27, 129.15, 129.37, 131.71, 133.83, 136.62, 137.78, 167.01. FTIR (cm^{-1}): 3074, 3035, 2108, 1820, 1656, 1603, 1291, 1232, 1040. HRMS: Calculated for $\text{C}_{16}\text{H}_{16}\text{N}$ $[\text{M}]^+$: 222.1283, found: 222.1277.

3.14.3: Analytical Data for Quinolones

1-methylquinolin-2(1H)-one (7a)

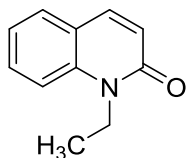


The titled compound was prepared by following the general procedure D and previously known in literature.³⁰ Obtained as a pale yellow solid (43 mg, 90% yield). R_f (Ethyl acetate/Pet. ether = 40:60) = 0.2.

1-ethylquinolin-2(1H)-one (7b)

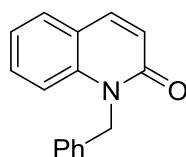
²⁹ Roman, D. S., Takahashi, Y.; Charette, A. B. *Org. Lett.*, **2011**, *13*, 3242.

³⁰ Hartman, T.; Cibulka, R. *Org. Lett.*, **2016**, *18*, 3710.



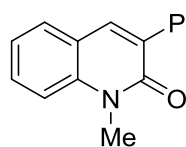
The titled compound was prepared by following the general procedure D. Obtained as a pale yellow viscous oil (41 mg, 78 % yield). R_f (Ethyl acetate/Pet. ether = 50:50) = 0.35; $^1\text{H NMR}$ (500 MHz, CDCl_3) δ 1.37 (t, J = 7.06 Hz, 3 H), 4.37 (q, J = 7.12 Hz, 2 H), 6.70 (d, J = 9.54 Hz, 1 H), 7.22 (t, J = 7.44 Hz, 1 H), 7.39 (d, J = 9.16 Hz, 1 H), 7.54 - 7.60 (m, 2 H), 7.67 (d, J = 9.54 Hz, 1 H). $^{13}\text{C NMR}$ (125 MHz, CDCl_3) δ 12.75, 37.30, 114.04, 121.00, 121.82, 121.90, 129.02, 130.59, 139.00, 161.91. FTIR (cm^{-1}): 2984, 2879, 1638, 1573, 1453, 1161, 833, 752, 619. HRMS: Calculated for $\text{C}_{11}\text{H}_{12}\text{NO}$ $[\text{M}+\text{H}]^+$: 174.0919, found: 174.0913.

1-benzylquinolin-2(1H)-one (7c)



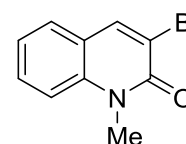
The titled compound was prepared by following the general optimized procedure D and previously known in literature.³¹ Obtained as a white solid (51 mg, 72 % yield). R_f (Ethyl acetate/Pet. ether = 20:80) = 0.4.

1-methyl-3-phenylquinolin-2(1H)-one (7d)



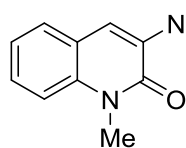
The titled compound was prepared (0.1 mmol scale) by following the general procedure D with KO^tBu as base and previously known in literature.³² Obtained as a white solid (18 mg, 77% yield). R_f (Ethyl acetate/Pet. ether = 50:50) = 0.3.

3-bromo-1-methylquinolin-2(1H)-one (7e)



The titled compound was prepared (0.1 mmol scale) by DBU as catalyst and base in MTBE solvent at 40 °C for 24 h and previously known in literature.³³ Obtained as a white solid (17 mg, 71% yield). R_f (Ethyl acetate/Pet. ether = 20:80) = 0.25.

3-(dimethylamino)-1-methylquinolin-2(1H)-one (7f)



The titled compound was prepared (0.1 mmol scale) by following the general procedure D with KO^tBu as base at 50 °C. Obtained as a white solid (11 mg, 54% yield). R_f (Ethyl acetate/Pet. ether = 50:50) = 0.1; MP = 174 °C. $^1\text{H NMR}$ (500 MHz, CDCl_3) δ 2.95 (s, 6 H), 3.76 (s, 3 H), 6.88 (br. s., 1 H), 7.14 - 7.23 (m, 1 H), 7.30 (d, J = 8.39 Hz, 1 H), 7.34 - 7.42 (m, 1 H), 7.47 (d, J = 7.63 Hz, 1 H). $^{13}\text{C NMR}$ (125 MHz, CDCl_3) δ 29.71, 29.99, 42.00, 113.64, 116.99, 121.06, 121.58, 122.24,

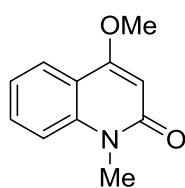
³¹ Nakao, Y.; Idei, H.; Kanyiva, S. K.; Hiyama, T. *J. Am. Chem. Soc.*, **2009**, *131*, 15996.

³² Cao, Y.; Zhao, H.; Negrier, Z. D.; Du, Y.; Zhao, K. *Adv. Synth. Catal.*, **2016**, *358*, 3610.

³³ Franck, P.; Hostyn, S.; Halasz, D. B.; Balint, P. A.; Monsieurs, K.; Matyus, P.; Maes, B. W. U. *Tetrahedron*, **2008**, *64*, 6030.

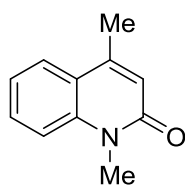
126.84, 135.93, 139.57, 159.71. **FTIR** (cm^{-1}): 2926, 2854, 1655, 1264, 732, 703. **HRMS**: Calculated for $\text{C}_{12}\text{H}_{15}\text{N}_2\text{O}$ $[\text{M}+\text{H}]^+$: 203.1184, found: 203.1179.

4-methoxy-1-methylquinolin-2(1H)-one (7g)



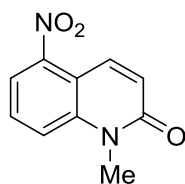
The titled compound was prepared (0.1 mmol scale) by following the general procedure D with KO^tBu as base and previously known in literature.³⁴ Obtained as orange solid (17 mg, 89% yield). R_f (Ethyl acetate/Pet. ether = 50:50) = 0.5.

1,4-dimethylquinolin-2(1H)-one (7h)



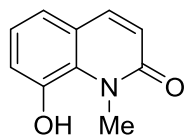
The titled compound was prepared (0.1 mmol scale) by following the general procedure D with 150 mol% DMP catalyst and previously known in literature.³⁵ Obtained as a white solid (16 mg, 92% yield). R_f (Ethyl acetate/Pet. ether = 50:50) = 0.15.

1-methyl-5-nitroquinolin-2(1H)-one (7i)



The titled compound was prepared by following the general procedure D. Obtained as a light yellow solid (56 mg, 92% yield). R_f (Ethyl acetate/Pet. ether = 50:50) = 0.2; **MP** = 134.9 °C. $^1\text{H NMR}$ (500 MHz, CDCl_3) δ 3.79 (s, 3 H), 6.91 (d, J = 9.92 Hz, 1 H), 7.67 (d, J = 7.63 Hz, 2 H), 7.83 (dd, J = 7.25, 1.53 Hz, 1 H), 8.29 (d, J = 9.92 Hz, 1 H). $^{13}\text{C NMR}$ (125 MHz, CDCl_3) δ 30.22, 113.74, 118.39, 119.00, 125.09, 129.78, 132.69, 141.28, 147.65, 160.93. **FTIR** (cm^{-1}): 2972, 2883, 1655, 1518, 1351, 1287, 955, 844, 728, 618. **HRMS**: Calculated for $\text{C}_{10}\text{H}_9\text{N}_2\text{O}_3$ $[\text{M}+\text{H}]^+$: 205.0613, found: 205.0607.

8-hydroxy-1-methylquinolin-2(1H)-one (7j)



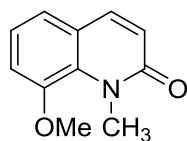
The titled compound was prepared by following the general procedure D. Obtained as a white solid (44 mg, 84 %). R_f (Ethyl acetate/Pet. ether = 50:50) = 0.1; **MP** = 274.5 °C. ($^1\text{H NMR}$ (500 MHz, $\text{DMSO}-d_6 + \text{CDCl}_3$) δ 3.88 (s, 3 H), 6.54 (d, J = 9.54 Hz, 1 H), 6.98 - 7.09 (m, 2 H), 7.09 - 7.15 (m, 1 H), 7.76 (d, J = 9.16 Hz, 1 H), 10.05 (s, 1 H). $^{13}\text{C NMR}$ (125 MHz, $\text{DMSO}-d_6$) δ 34.59, 118.07, 120.42, 121.30,

³⁴ Clarke, S. L.; McGlacken, G. P. *Tetrahedron*, **2015**, *71*, 2906.

³⁵ Yasui, Y.; Kakinokihara, I.; Takeda, H.; Takemoto, Y. *Synthesis*, **2009**, *23*, 3989.

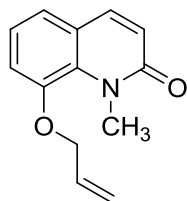
123.18, 123.22, 129.80, 140.04, 146.27, 162.68. **FTIR** (cm^{-1}): 3450, 3066, 1641, 1284, 1049, 990, 826, 757. **HRMS**: Calculated for $\text{C}_{10}\text{H}_{10}\text{NO}_2$ $[\text{M}+\text{H}]^+$: 160.0762, found: 160.0757.

8-methoxy-1-methylquinolin-2(1H)-one (7k)



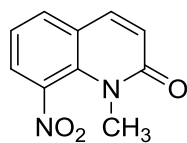
The titled compound was prepared (0.1 mmol scale) by following the general procedure D with KO^tBu as base. Obtained as a white solid (14 mg, 74 % yield). R_f (Ethyl acetate/Pet. ether = 50:50) = 0.5; MP = 139.8 °C. **^1H NMR (500 MHz, CDCl_3)** δ 3.90 (s, 3 H), 3.97 (s, 3 H), 6.69 (d, J = 9.16 Hz, 1 H), 7.06 (dd, J = 6.87, 2.29 Hz, 1 H), 7.09 - 7.21 (m, 2 H), 7.59 (d, J = 9.16 Hz, 1 H). **^{13}C NMR (125 MHz, CDCl_3)** δ 35.22, 56.58, 113.80, 121.60, 121.87, 122.73, 122.94, 131.38, 139.15, 148.63, 16. **FTIR** (cm^{-1}): 2974, 1660, 1457, 1267, 1078, 835, 727. **HRMS**: Calculated for $\text{C}_{11}\text{H}_{12}\text{NO}_2$ $[\text{M}+\text{H}]^+$: 190.0864, found: 190.0861.

8-(allyloxy)-1-methylquinolin-2(1H)-one (7l)



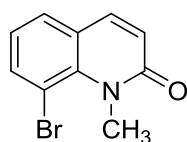
The titled compound was prepared by following the general procedure D with KO^tBu as base. Obtained as a light yellow liquid (30 mg, 47% yield). R_f (Ethyl acetate/Pet. ether = 50:50) = 0.3; MP = 118 °C. **^1H NMR (500 MHz, CDCl_3)** δ 3.99 (s, 3 H), 4.61 (d, J = 5.34 Hz, 2 H), 5.34 (d, J = 10.68 Hz, 1 H), 5.40 - 5.48 (m, 1 H), 6.04 - 6.16 (m, 1 H), 6.70 (d, J = 9.54 Hz, 1 H), 7.04 - 7.10 (m, 1 H), 7.10 - 7.19 (m, 2 H), 7.60 (d, J = 9.54 Hz, 1 H). **^{13}C NMR (126 MHz, CDCl_3)** δ 35.43, 71.21, 115.49, 118.35, 121.83, 121.91, 122.66, 123.04, 131.63, 132.59, 139.15, 147.47, 163.66. **FTIR** (cm^{-1}): 2936, 1638, 1586, 1456, 1269, 1121, 835, 747. **HRMS**: Calculated for $\text{C}_{13}\text{H}_{14}\text{NO}_2$ $[\text{M}+\text{H}]^+$: 216.1025, found: 216.1018.

1-methyl-8-nitroquinolin-2(1H)-one (7m)



The titled compound was prepared by following the general procedure D. Obtained as a light brown solid (40 mg, 65 % yield). R_f (Ethyl acetate/Pet. ether = 50:50) = 0.2; MP = 114.9 °C. **^1H NMR (500 MHz, CDCl_3)** δ 3.48 (s, 3 H), 6.82 (d, J = 9.54 Hz, 1 H), 7.16 - 7.38 (m, 1 H), 7.65 - 7.79 (m, 2 H), 7.80 - 7.91 (m, 1 H). **^{13}C NMR (125 MHz, CDCl_3)** δ 34.31, 121.58, 123.21, 123.36, 127.04, 132.62, 133.69, 138.55, 139.76, 162.60. **FTIR** (cm^{-1}): 2971, 2880, 1653, 1590, 1529, 1453, 1351, 1287, 1122, 1064, 961, 843, 728, 618. **HRMS**: Calculated for $\text{C}_{10}\text{H}_9\text{N}_2\text{O}_3$ $[\text{M}+\text{H}]^+$: 205.0613, found: 205.0606.

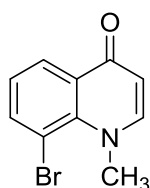
8-bromo-1-methylquinolin-2(1H)-one (7n)



The titled compound was prepared (0.18 mmol scale) by following the general procedure D. Obtained as a light yellow solid (24 mg, 56 % yield). R_f

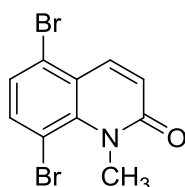
R_f (Ethyl acetate/Pet. ether = 100:0) = 0.6; **MP** = 127.3 °C. **$^1\text{H NMR}$ (500 MHz, CDCl_3)** δ 3.99 (s, 3 H), 6.72 (d, J = 9.54 Hz, 1 H), 6.98 - 7.12 (m, 1 H), 7.39 - 7.53 (m, 1 H), 7.60 (d, J = 9.16 Hz, 1 H), 7.73 - 7.87 (m, 1 H). **$^{13}\text{C NMR}$ (125 MHz, CDCl_3)** δ 37.55, 108.10, 122.18, 123.52, 124.06, 128.52, 137.75, 139.09, 139.80, 164.00. **FTIR** (cm^{-1}): 3411, 2933, 1637, 1575, 1437, 1277, 1120, 1023, 835, 751, 618. **HRMS**: Calculated for $\text{C}_{10}\text{H}_9\text{BrNO}$ $[\text{M}+\text{H}]^+$: 237.9868, found: 237.9862.

8-bromo-1-methylquinolin-4(1H)-one (7n $\hat{}$)



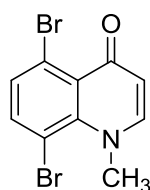
The titled compound was prepared by following the general procedure D and previously known in literature.³⁶ Obtained as a light yellow solid (12 mg, 28 % yield). R_f (Ethyl acetate/Pet. ether = 100:0) = 0.2.

5,8-dibromo-1-methylquinolin-2(1H)-one (7o)



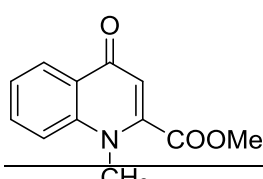
The titled compound was prepared (0.1 mmol scale) by following the general procedure D. Obtained as a light yellow solid (17 mg, 53 % yield). R_f (Ethyl acetate/Pet. ether = 20:80); = 0.3; **MP** 75.1 °C. **$^1\text{H NMR}$ (400 MHz, CDCl_3)** δ 3.94 (s, 3 H), 6.79 (d, J = 9.77 Hz, 1 H), 7.33 (d, J = 8.54 Hz, 1 H), 7.63 (d, J = 8.54 Hz, 1 H), 8.10 (d, J = 9.77 Hz, 1 H). **$^{13}\text{C NMR}$ (100 MHz, CDCl_3)** δ 38.38, 107.46, 122.84, 123.03, 123.27, 127.71, 137.62, 137.80, 141.38, 163.63. **FTIR** (cm^{-1}): 2912, 2858, 1651, 1565, 1437, 1290, 1205, 1130, 1050, 940, 820, 615. **HRMS**: Calculated for $\text{C}_{10}\text{H}_8\text{Br}_2\text{NO}$ $[\text{M}+\text{H}]^+$: 317.8952, found: 317.8947.

5,8-dibromo-1-methylquinolin-4(1H)-one (7o $\hat{}$)



The titled compound was prepared by following the general procedure D. Obtained as a light yellow solid (14 mg, 44% yield). R_f (Ethyl acetate/Pet. ether = 40:60) = 0.2; **MP** = 136.3 °C. **$^1\text{H NMR}$ (400 MHz, CDCl_3)** δ 3.73 (s, 3 H) 6.79 (d, J =9.77 Hz, 1 H) 7.34 (d, J =7.93 Hz, 1 H) 7.49 (d, J =7.32 Hz, 1 H) 8.13 (d, J =9.77 Hz, 1 H). **$^{13}\text{C NMR}$ (100 MHz, CDCl_3)** δ ppm 29.86, 113.84, 114.92, 122.91, 123.84, 126.41, 130.97, 134.36, 137.60, 161.83. **FTIR** (cm^{-1}): 2927, 1657, 1577, 1445, 1361, 1264, 1069, 909, 731, 702. **HRMS**: Calculated for $\text{C}_{10}\text{H}_8\text{Br}_2\text{NO}$ $[\text{M}+\text{H}]^+$: 317.8952, found: 317.8947.

Methyl 1-methyl-4-oxo-1,4-dihydroquinoline-2-carboxylate (7q)

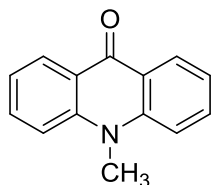


The titled compound was prepared (0.1 mmol scale) by following the general procedure D and previously known in literature.³⁷ Obtained as a

³⁶ Gao, X.; Han, J.; Wang, L. *Org. Lett.*, **2015**, *17*, 4596.

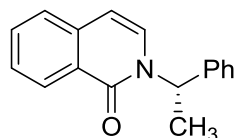
brown solid (9 mg, 41% yield). R_f (Ethyl acetate/Pet. ether = 50:50) = 0.3.

10-methylacridin-9(10H)-one(7r)



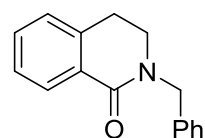
The titled compound was prepared by following the general procedure D with KO^tBu as base and previously known in literature.³⁸ Obtained as light brown crystals (50 mg, 95% yield). R_f (Ethyl acetate/Pet. ether = 20:80) = 0.15.

(S)-2-(1-phenylethyl)isoquinolin-1(2H)-one(6m)



Obtained as a white color solid³⁹ (10 mg, 80 % yield, 98.5 % ee) starting with chiral **1m** (<98% ee). The HPLC analysis was done using Isopropanol: n-Hexane(30:70) in chiralpak[®] IA columns (250 × 4.6 mm).

2-benzyl-3,4-dihydroisoquinolin-1(2H)-one (10'a)



The titled compound was prepared by following the general procedure C. This compound is previously known in literature.⁴⁰ Obtained as a white color solid. R_f (Ethyl acetate/Pet. ether = 20:80) = 0.3, yield 76%.

³⁷ Schmitz, C.; Leitner, W.; Franciý, G. *Chem. Eur. J.*, **2015**, *21*, 10696.

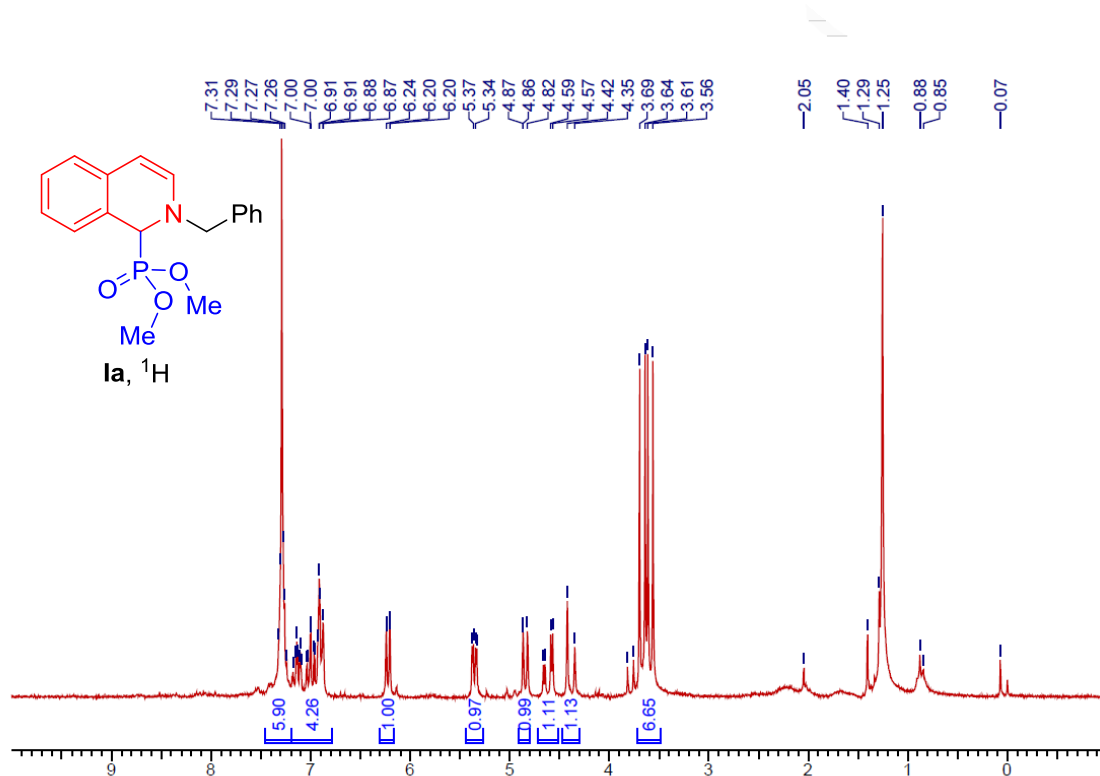
³⁸ Linghu, X.; Potnick, R. J.; Johnson, S. J. *J. Am. Chem. Soc.*, **2004**, *126*, 3070.

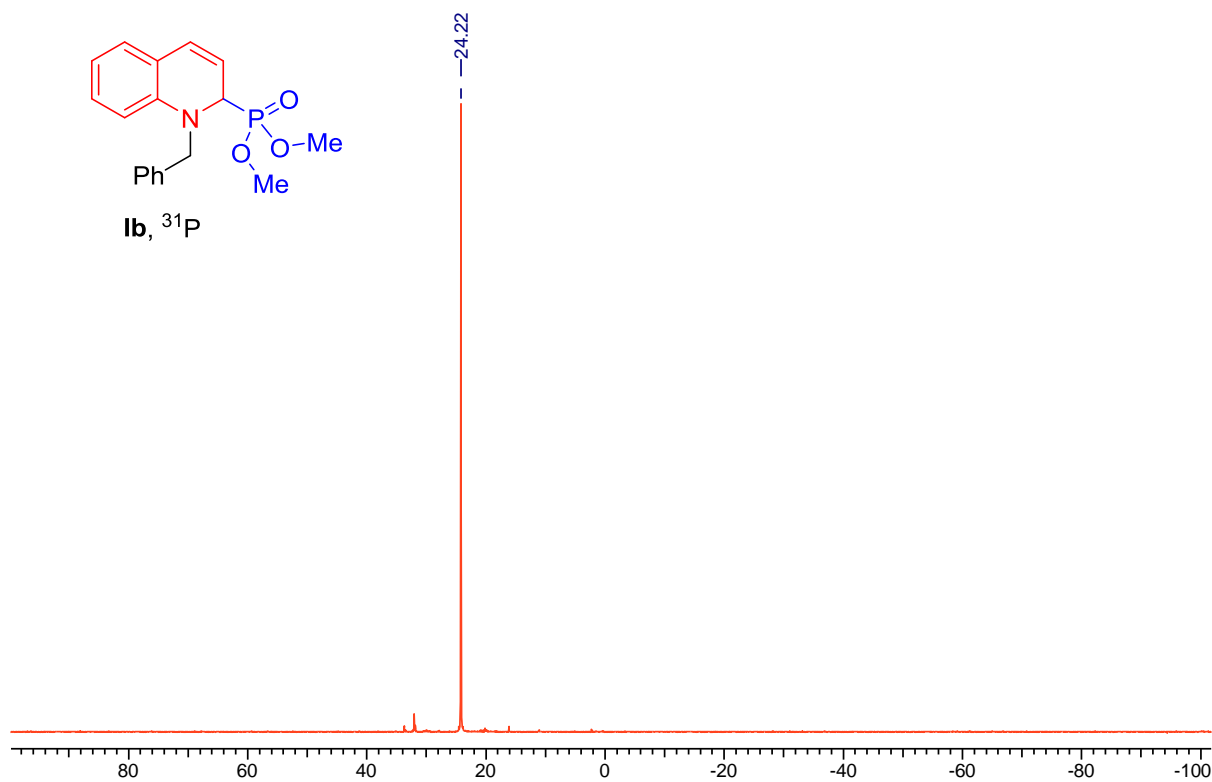
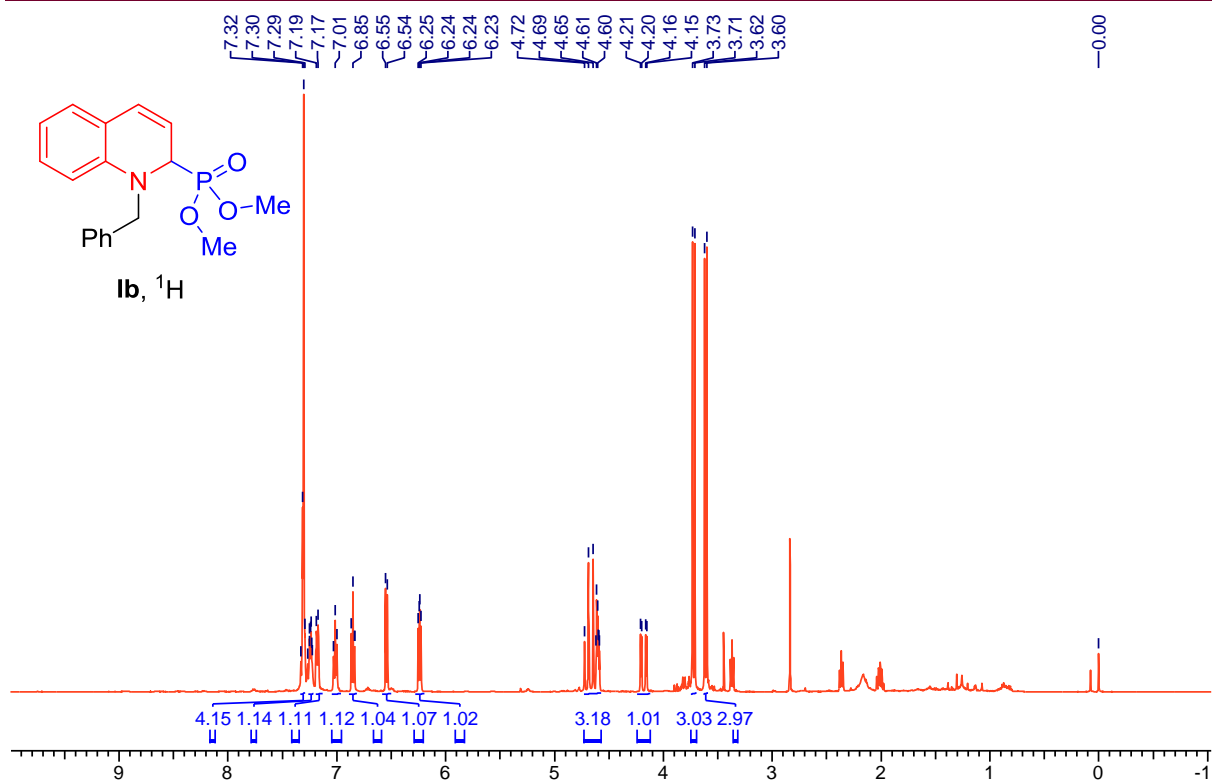
³⁹ Clarke, L. S.; McGlacken, P. *Tetrahedron*. **2015**, *71*, 2906-2913.

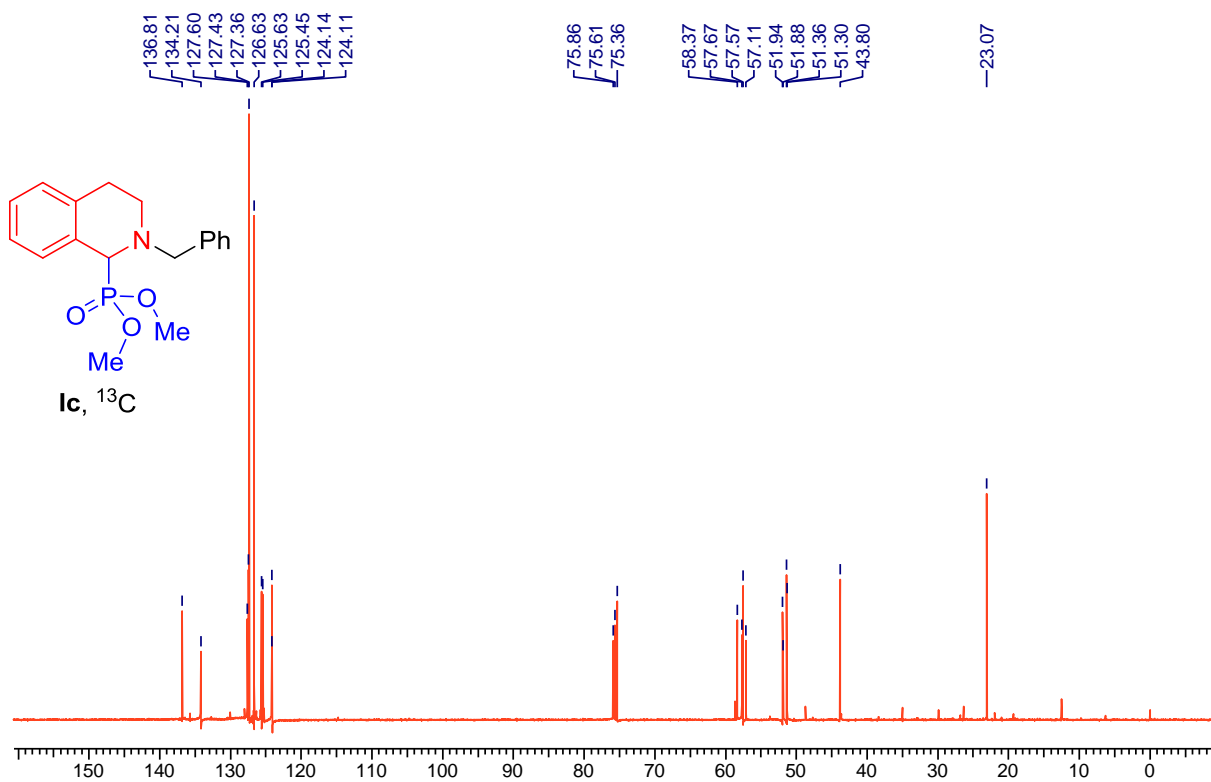
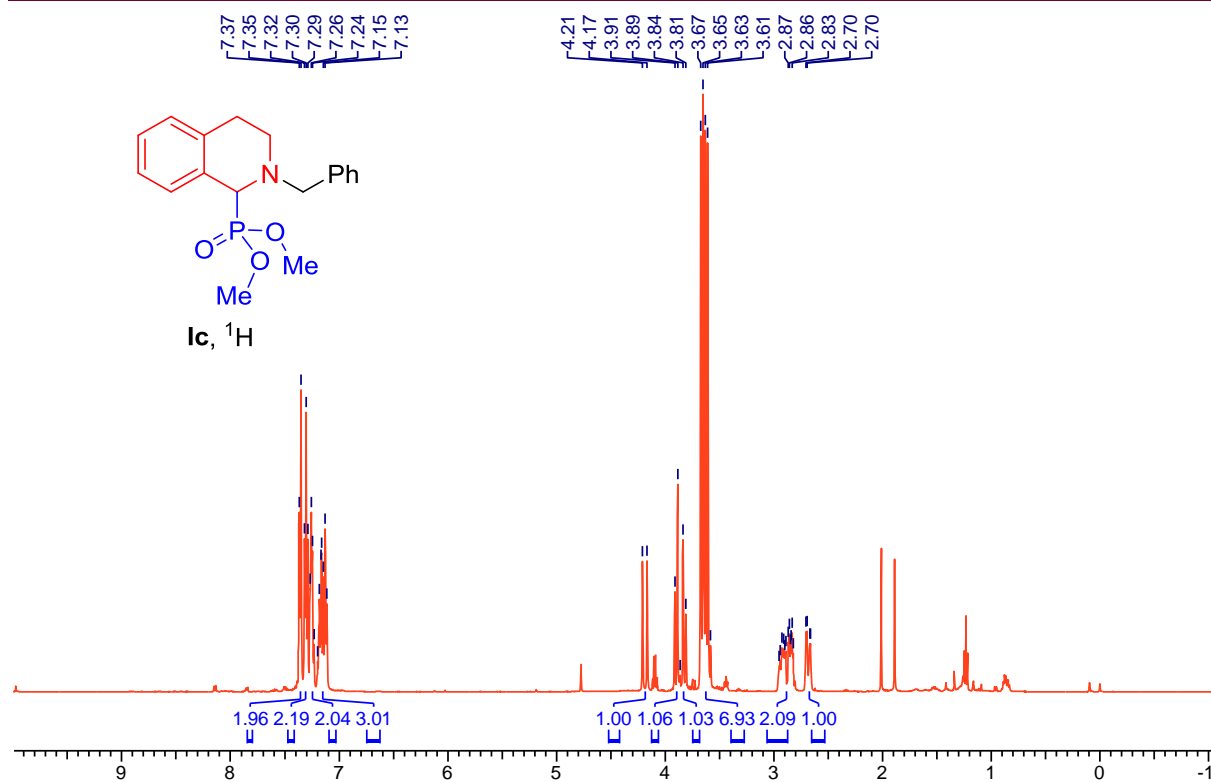
⁴⁰ Griffiths, J. R.; Glenn A. Burley, A. G.; Talbot, A. P. E. *Org. Lett.*, **2017**, *19*, 870.

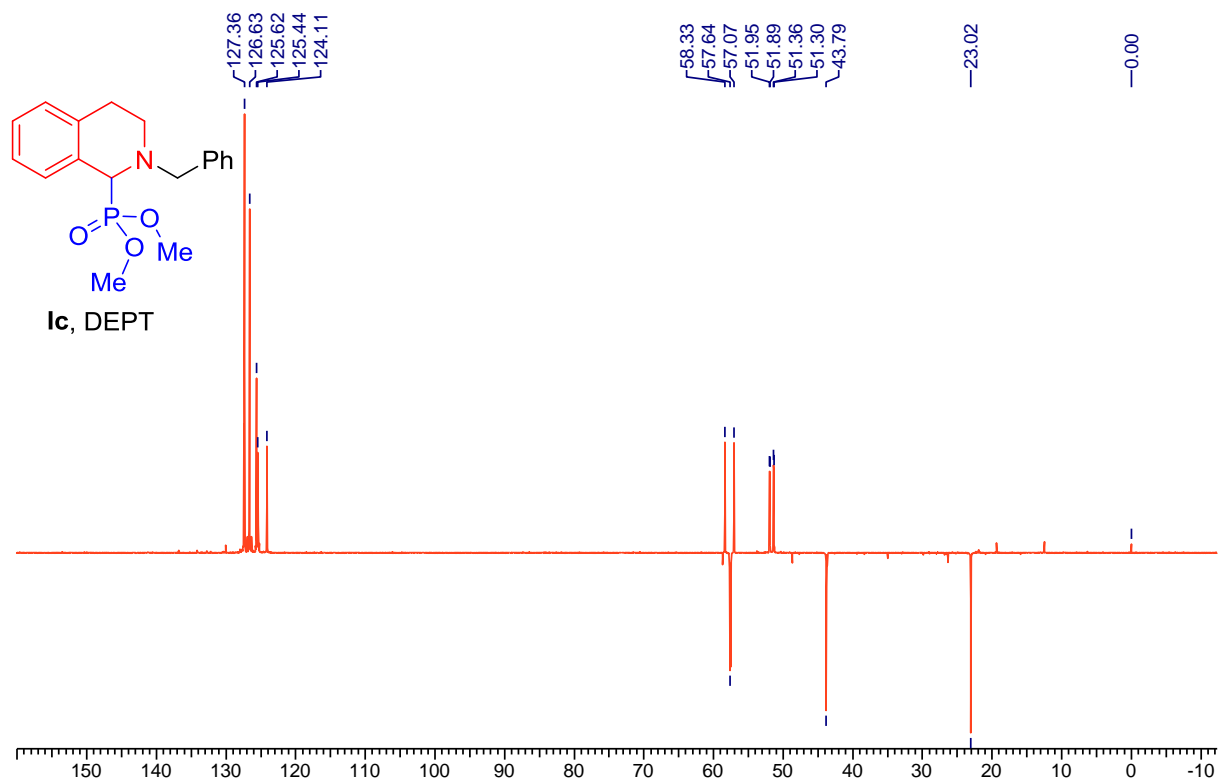
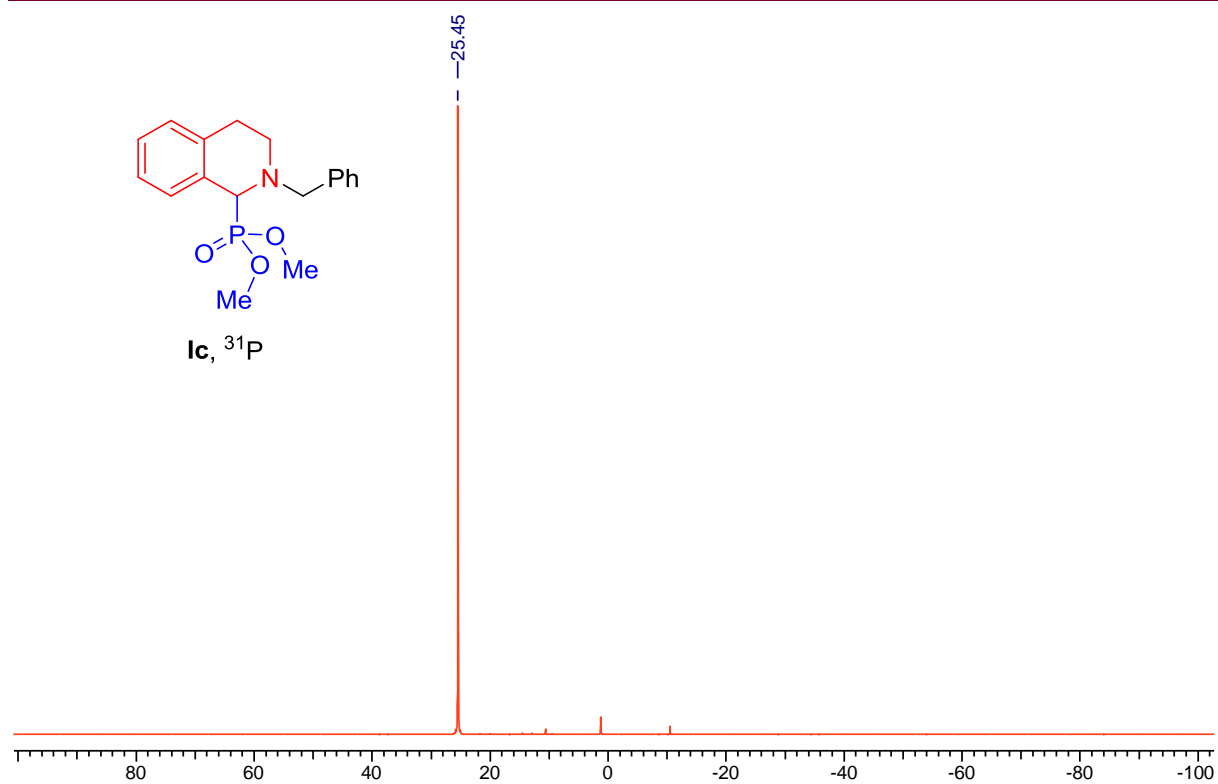
3.15 NMR Spectra of Characterized Compounds

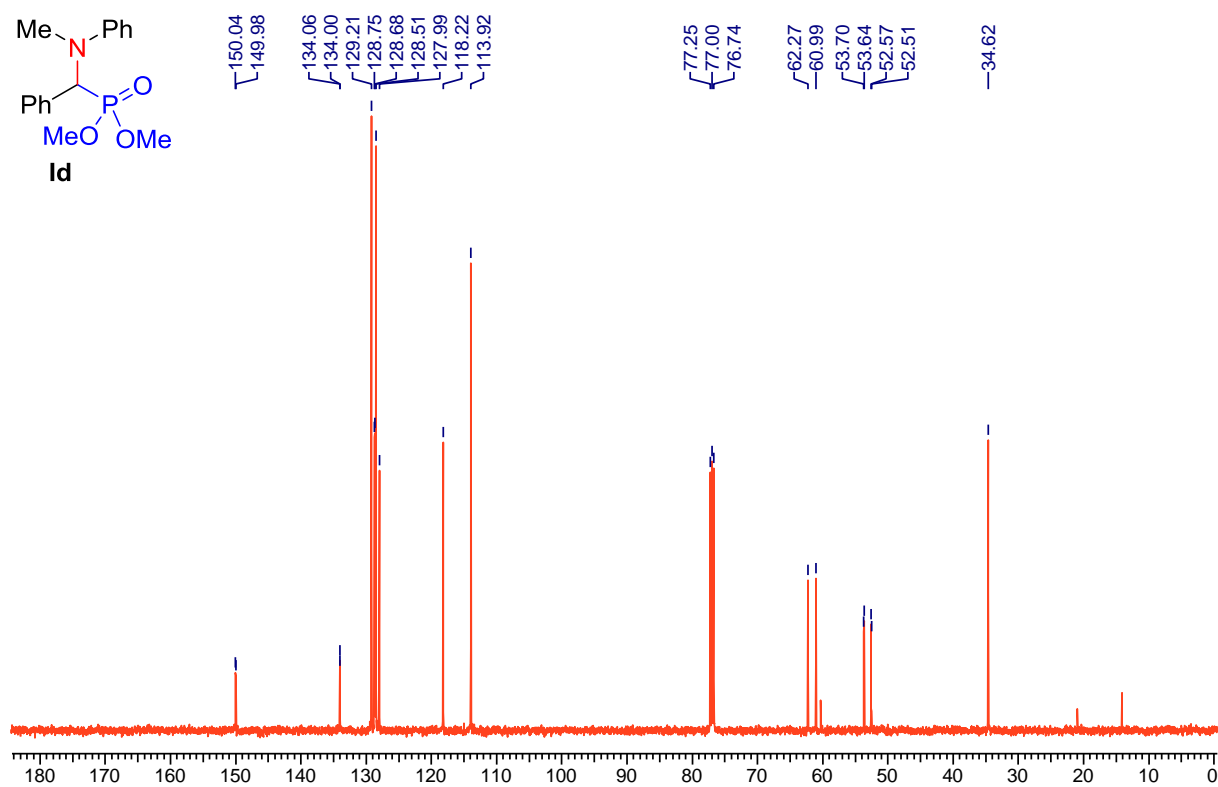
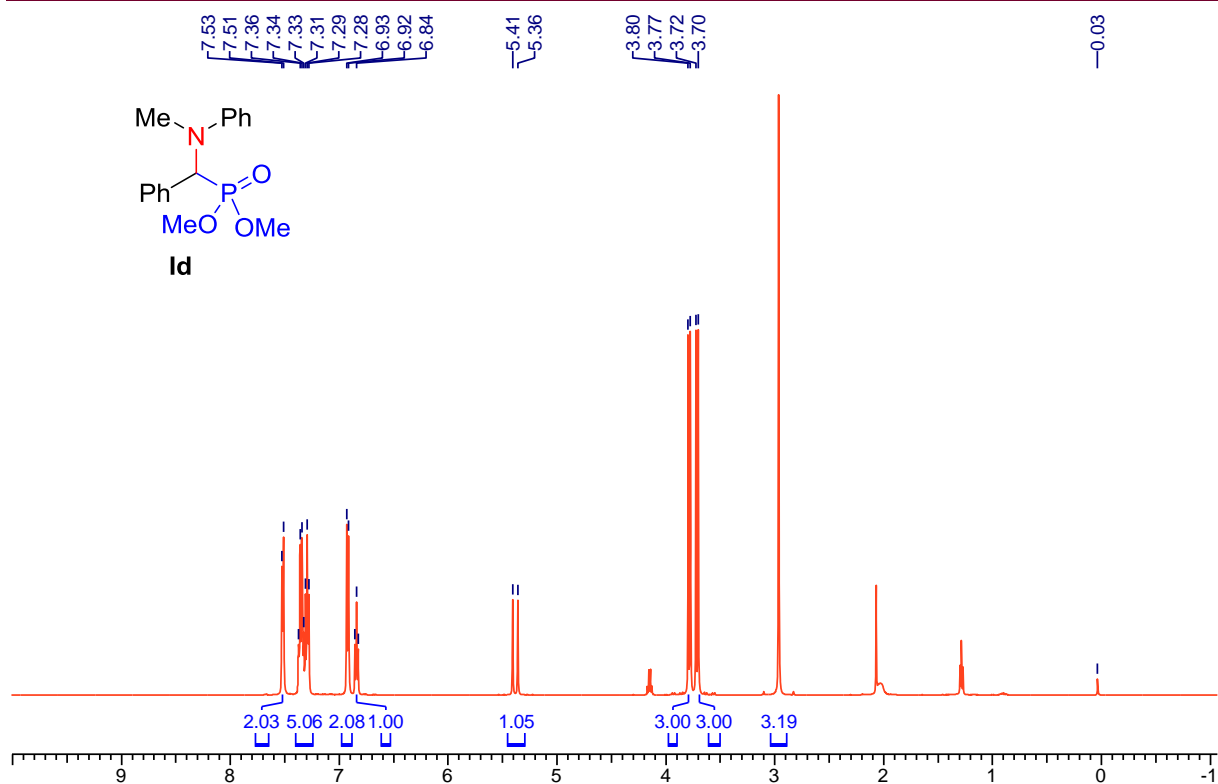
3.15.A NMR of catalyst added intermediate



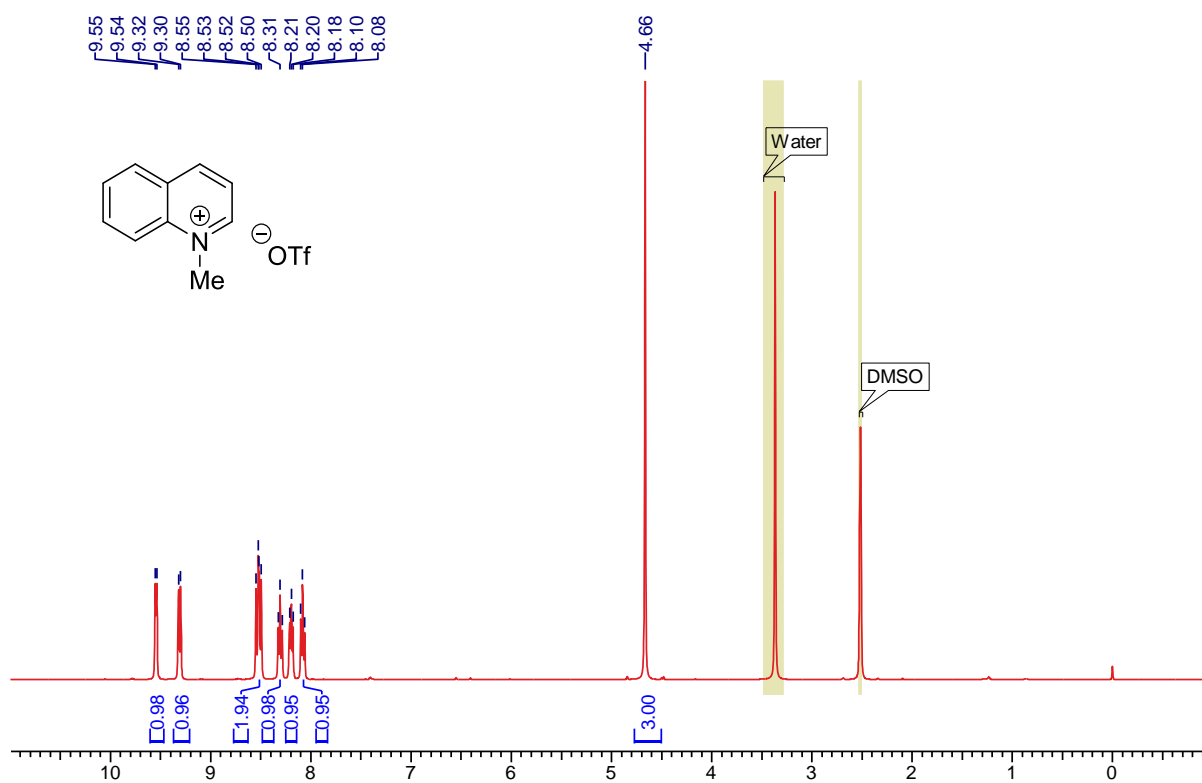


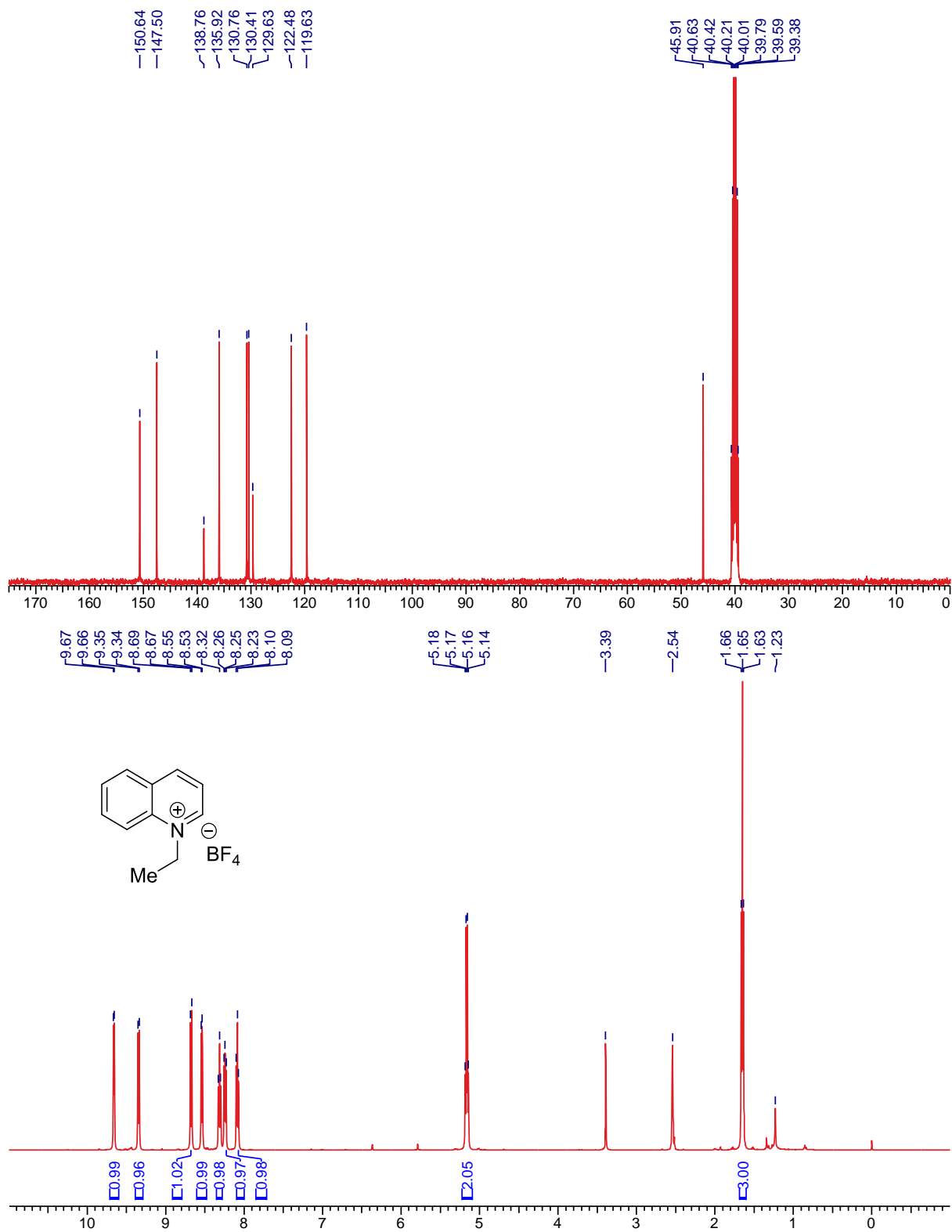


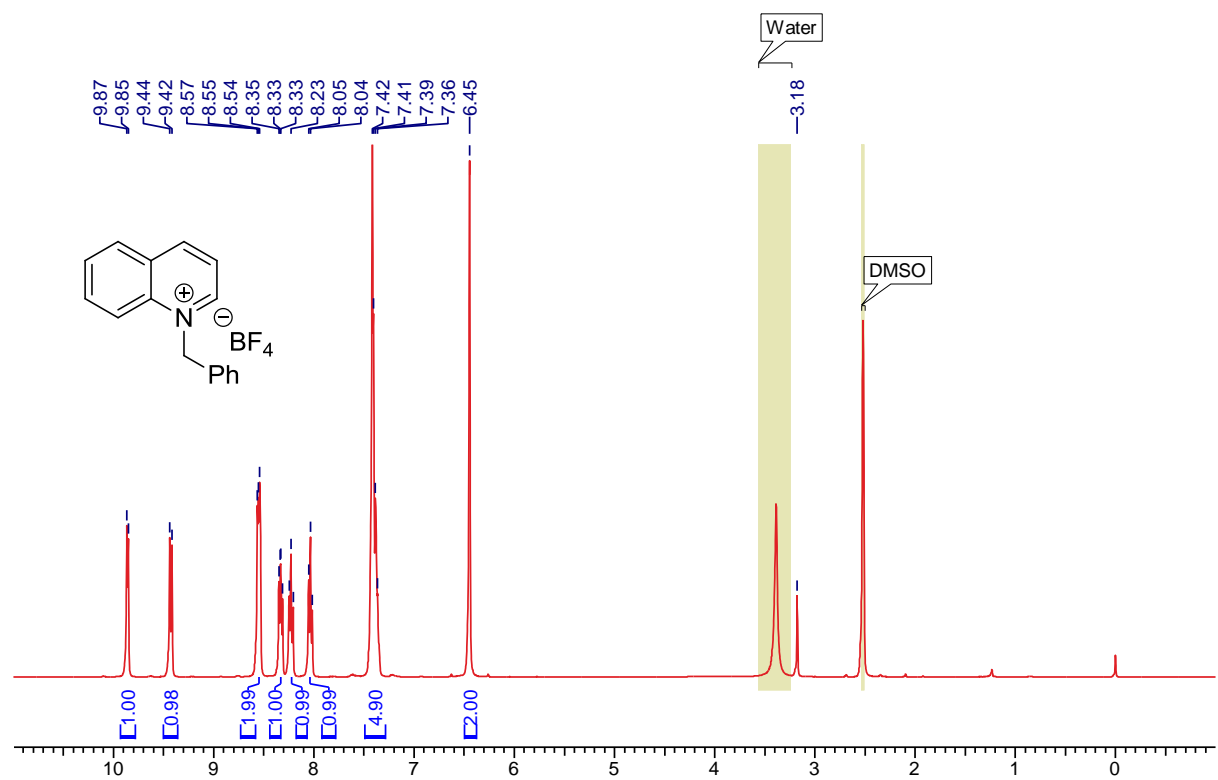
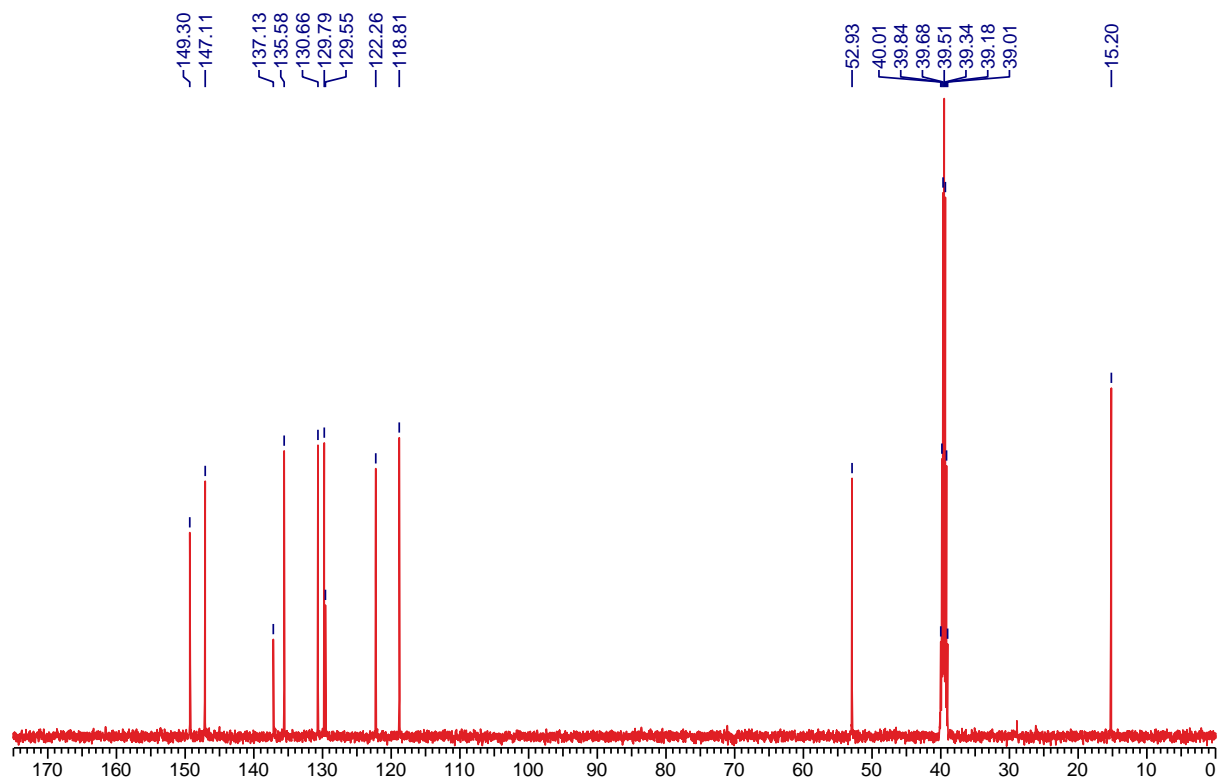


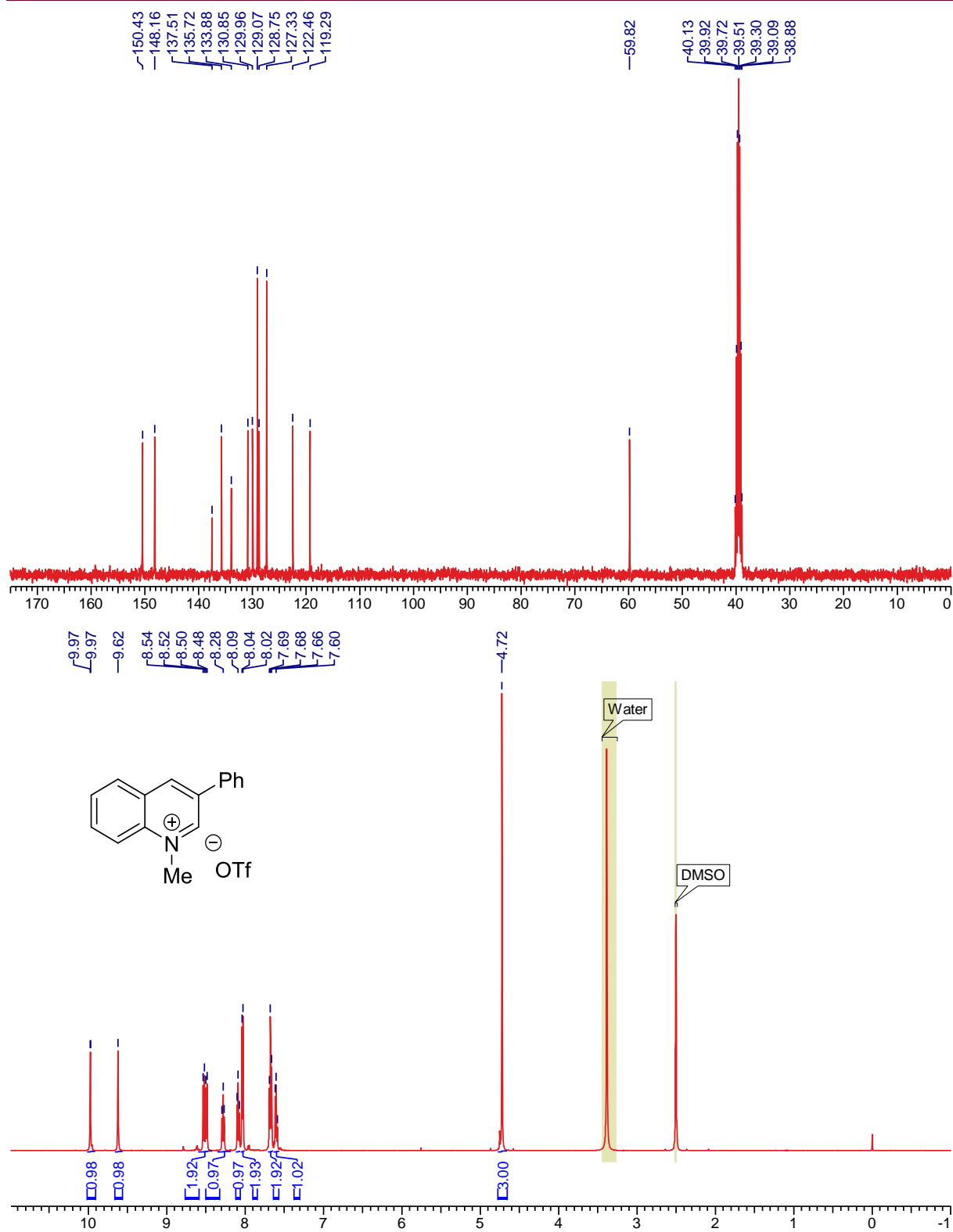


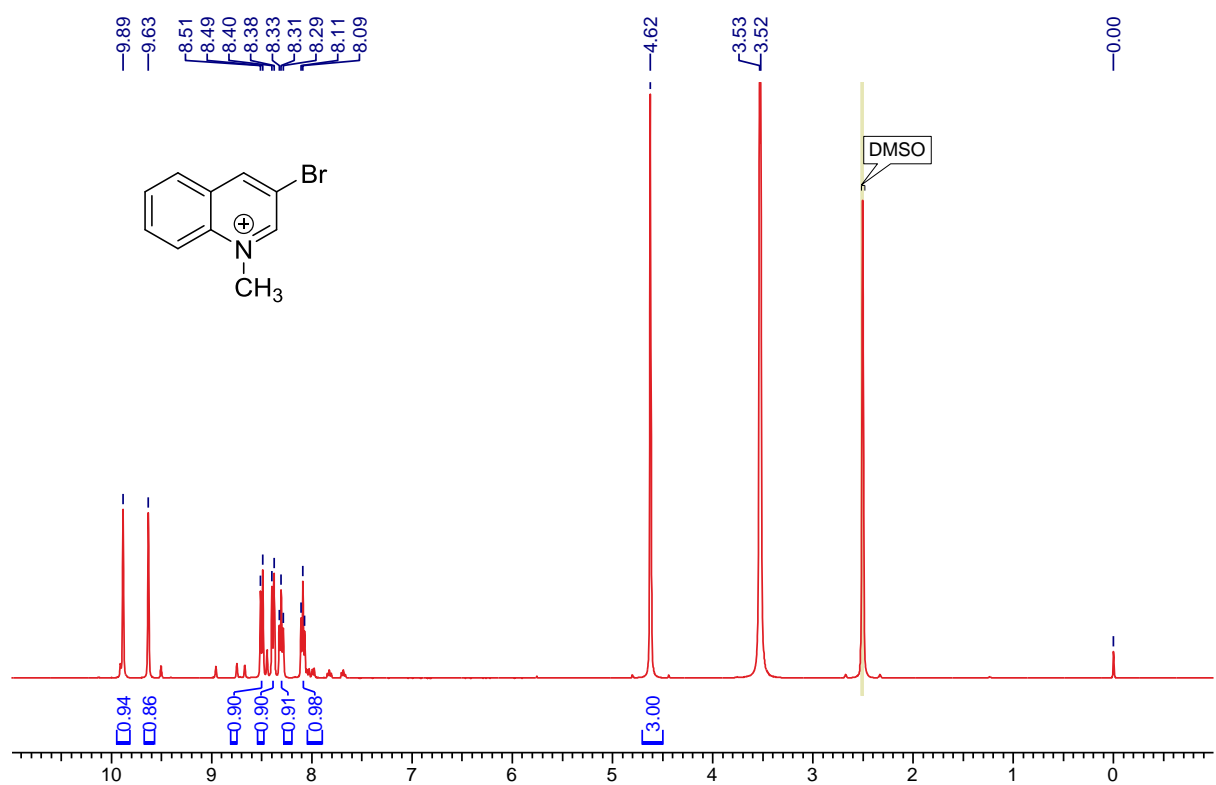
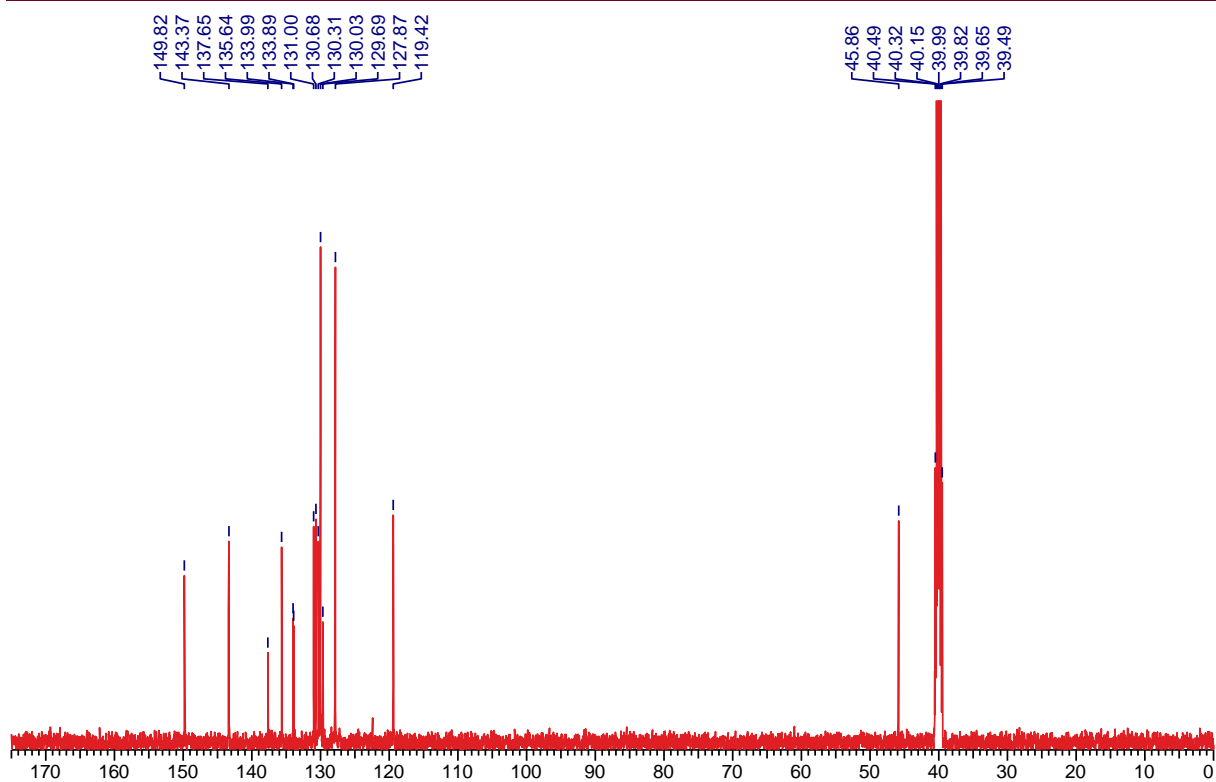
3.15.B NMR of salts

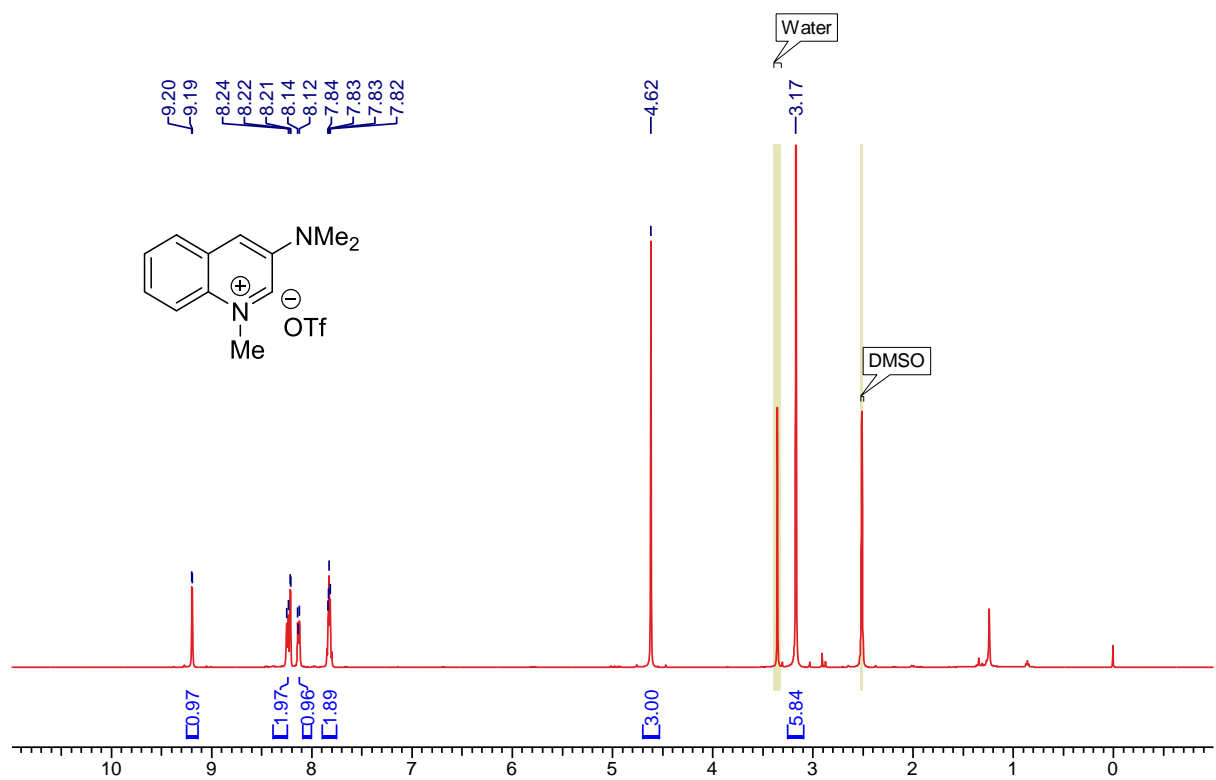
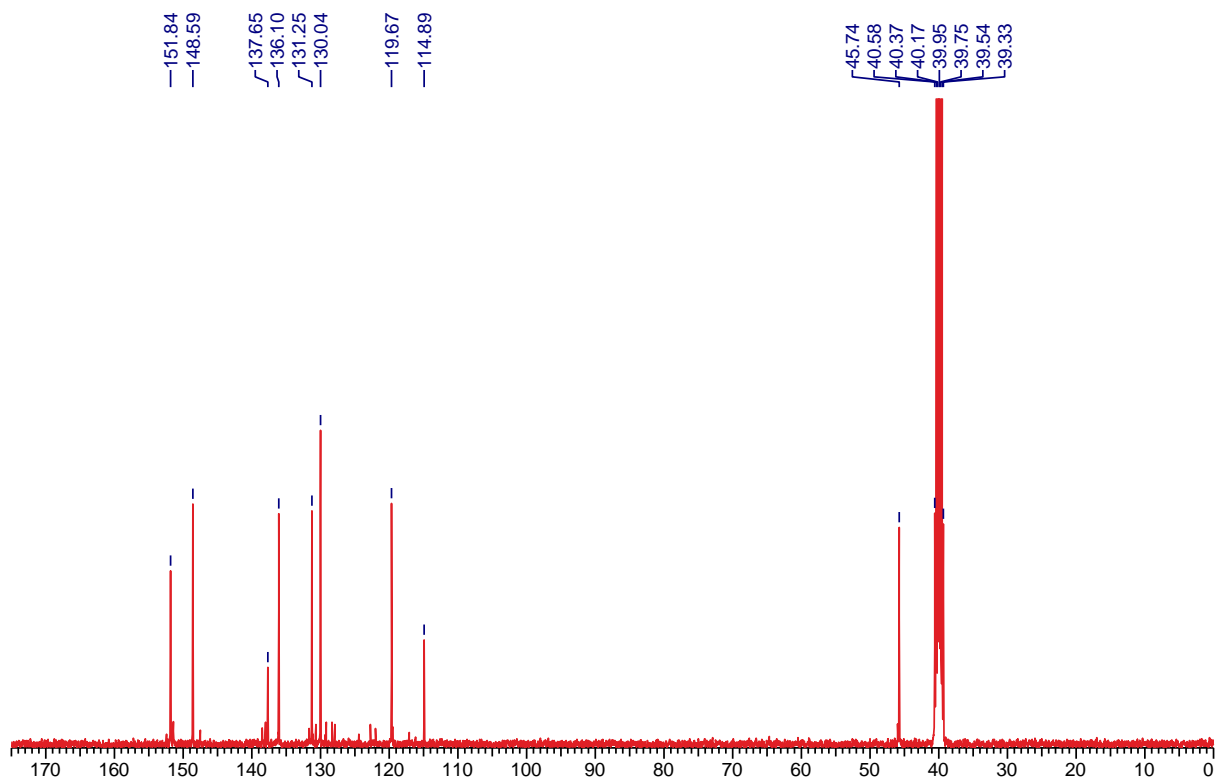


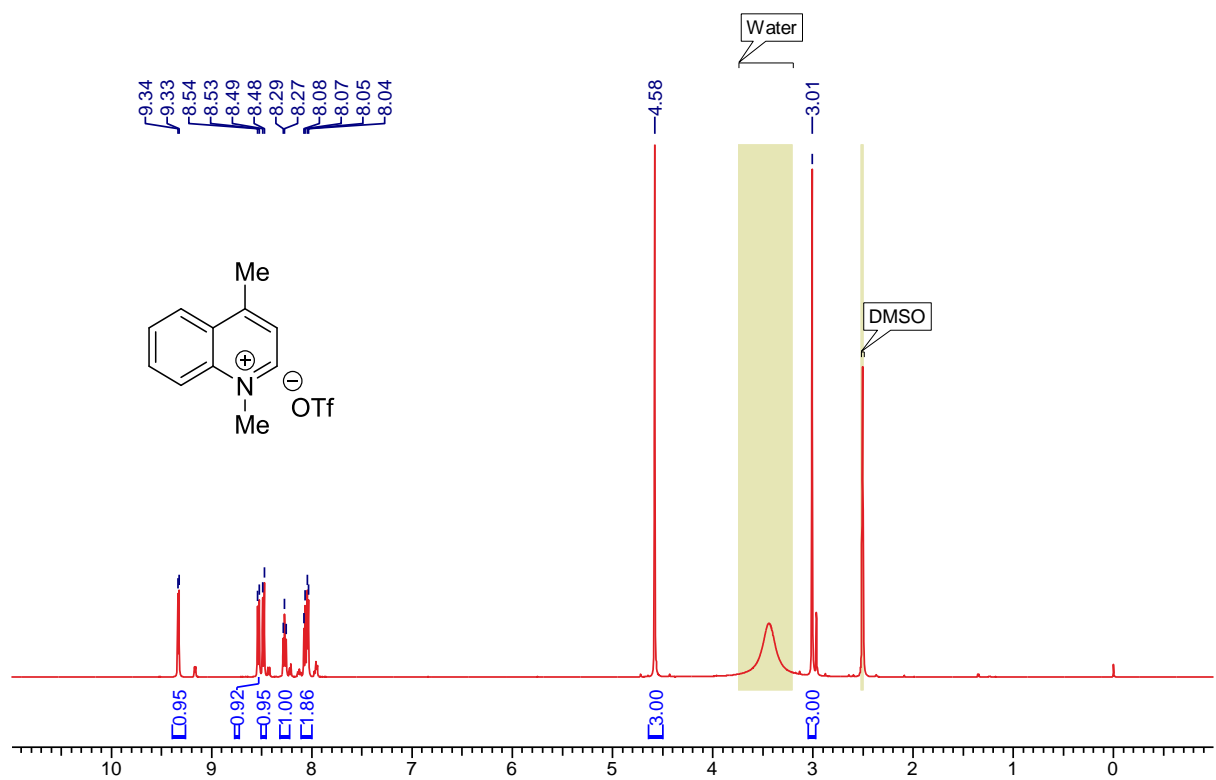
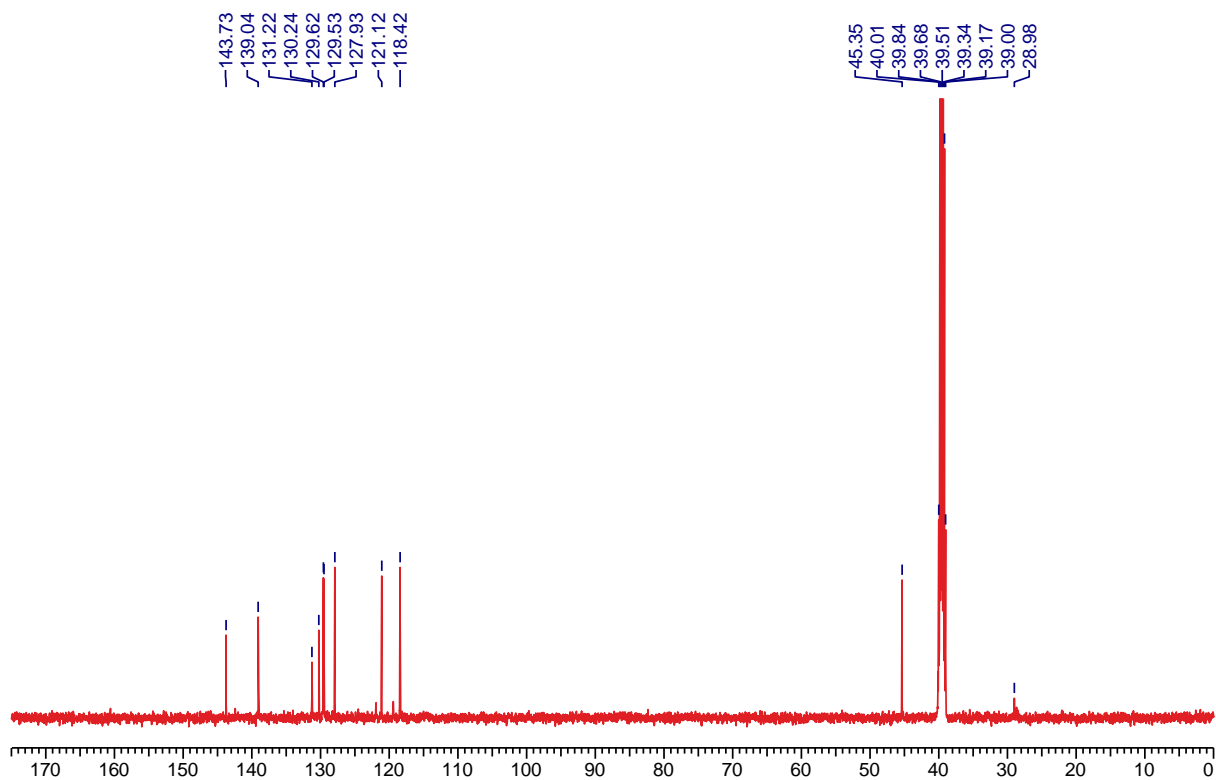


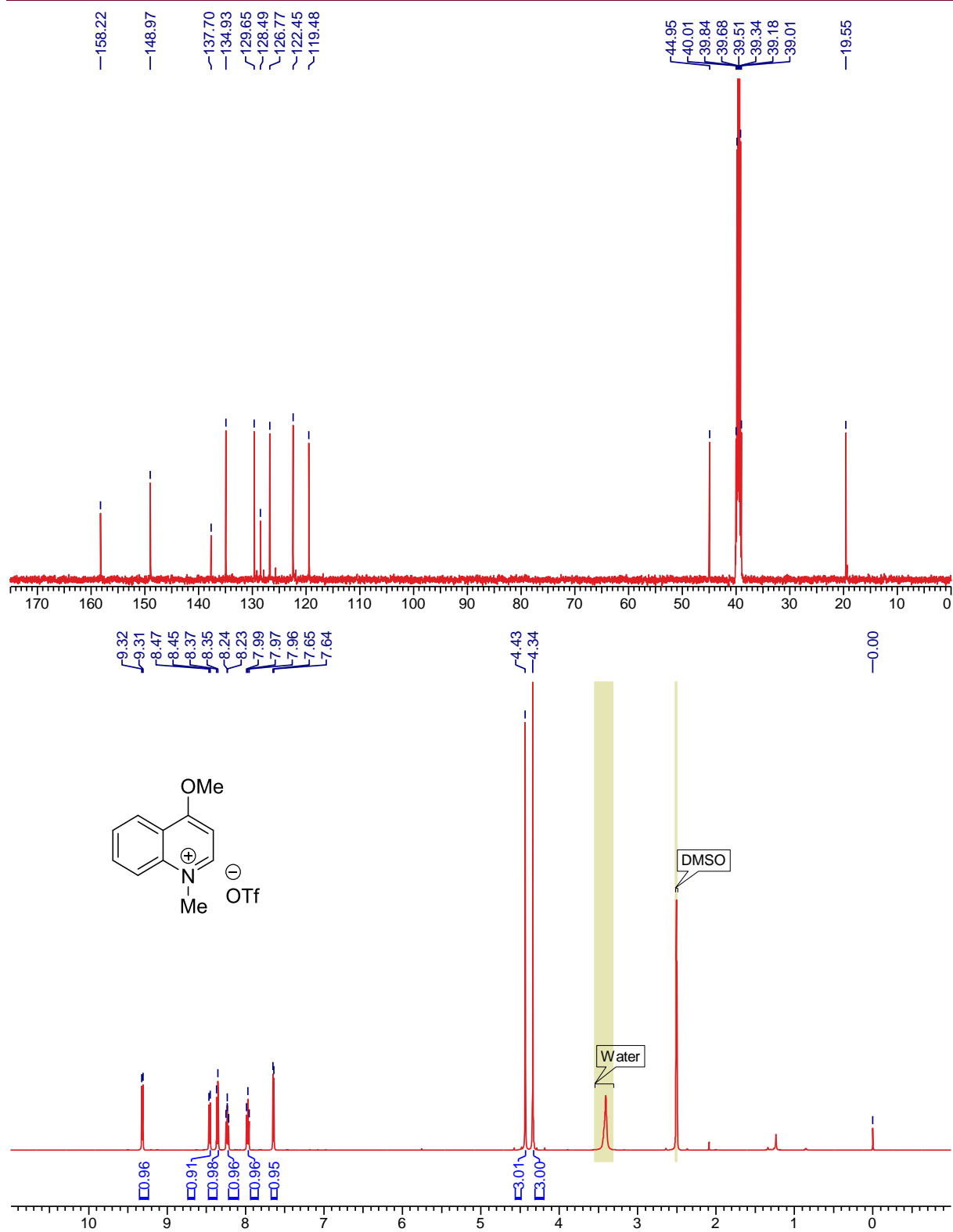


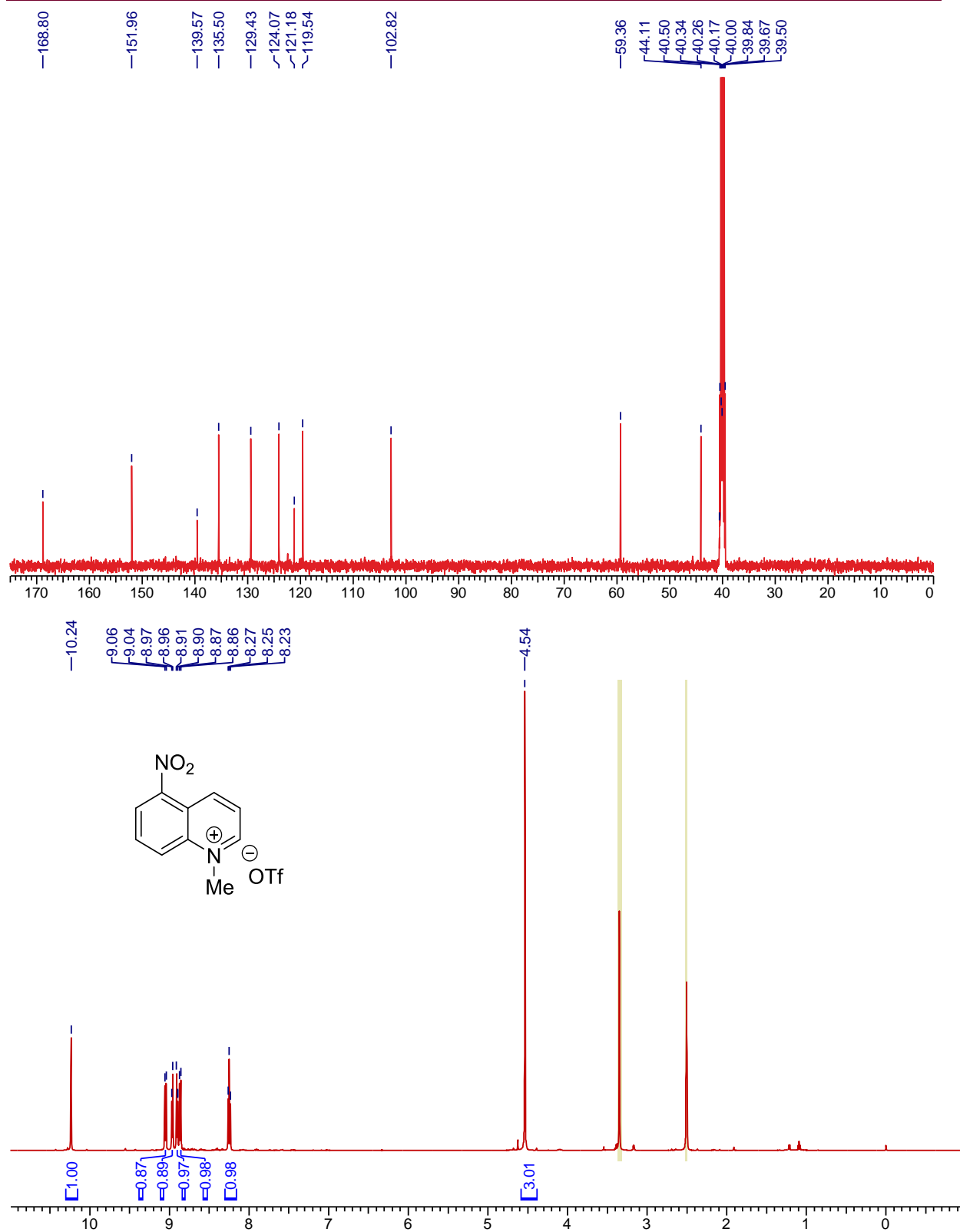


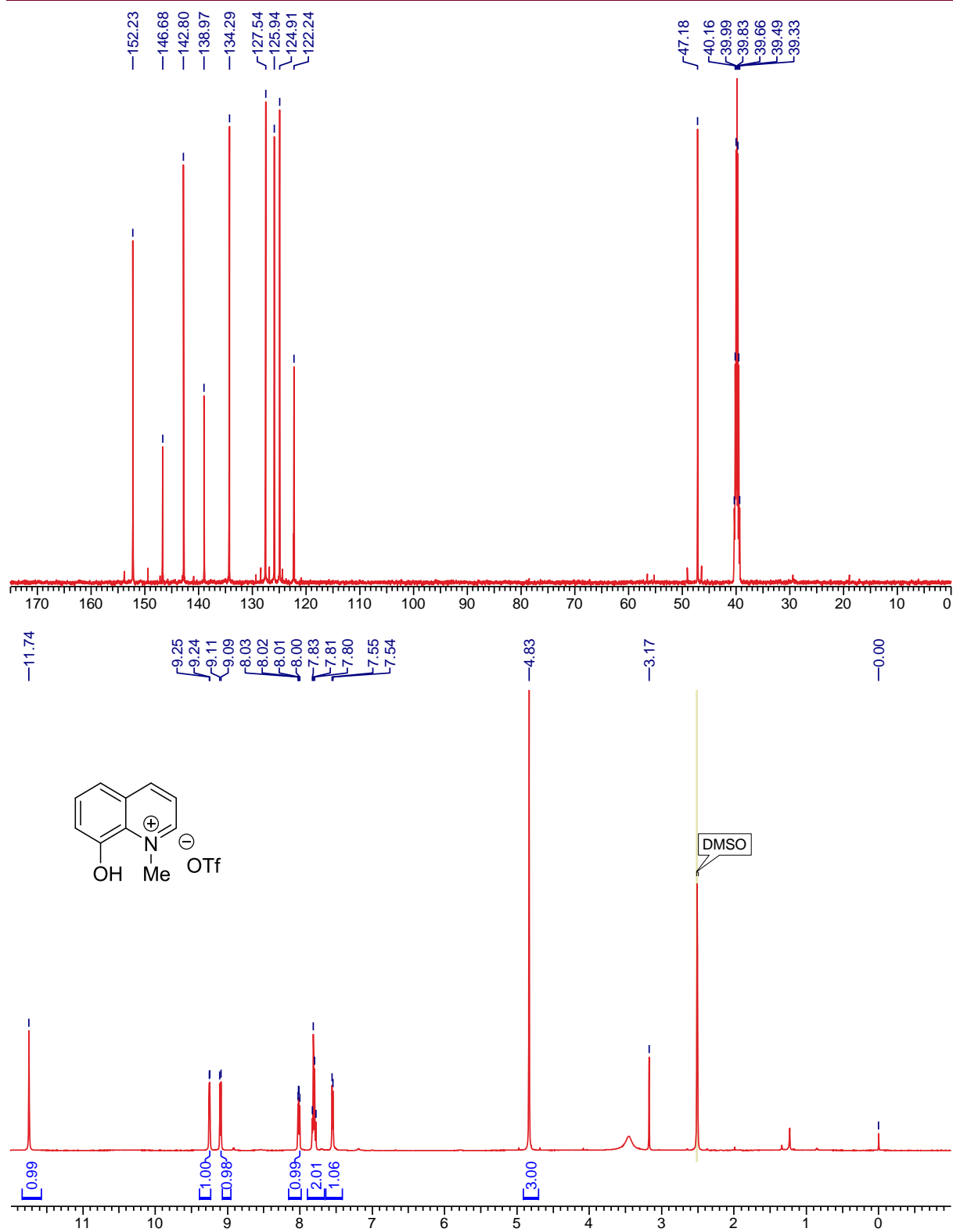


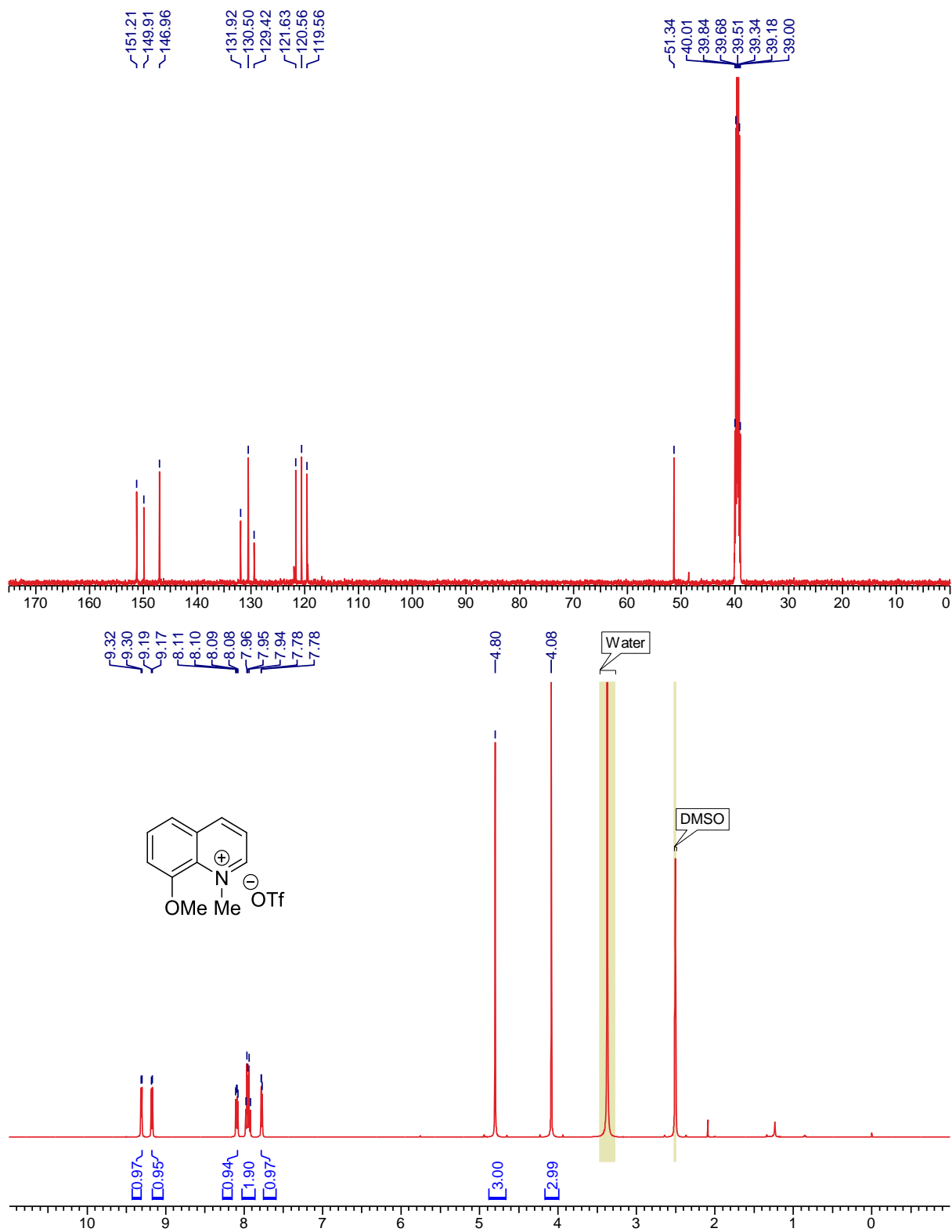


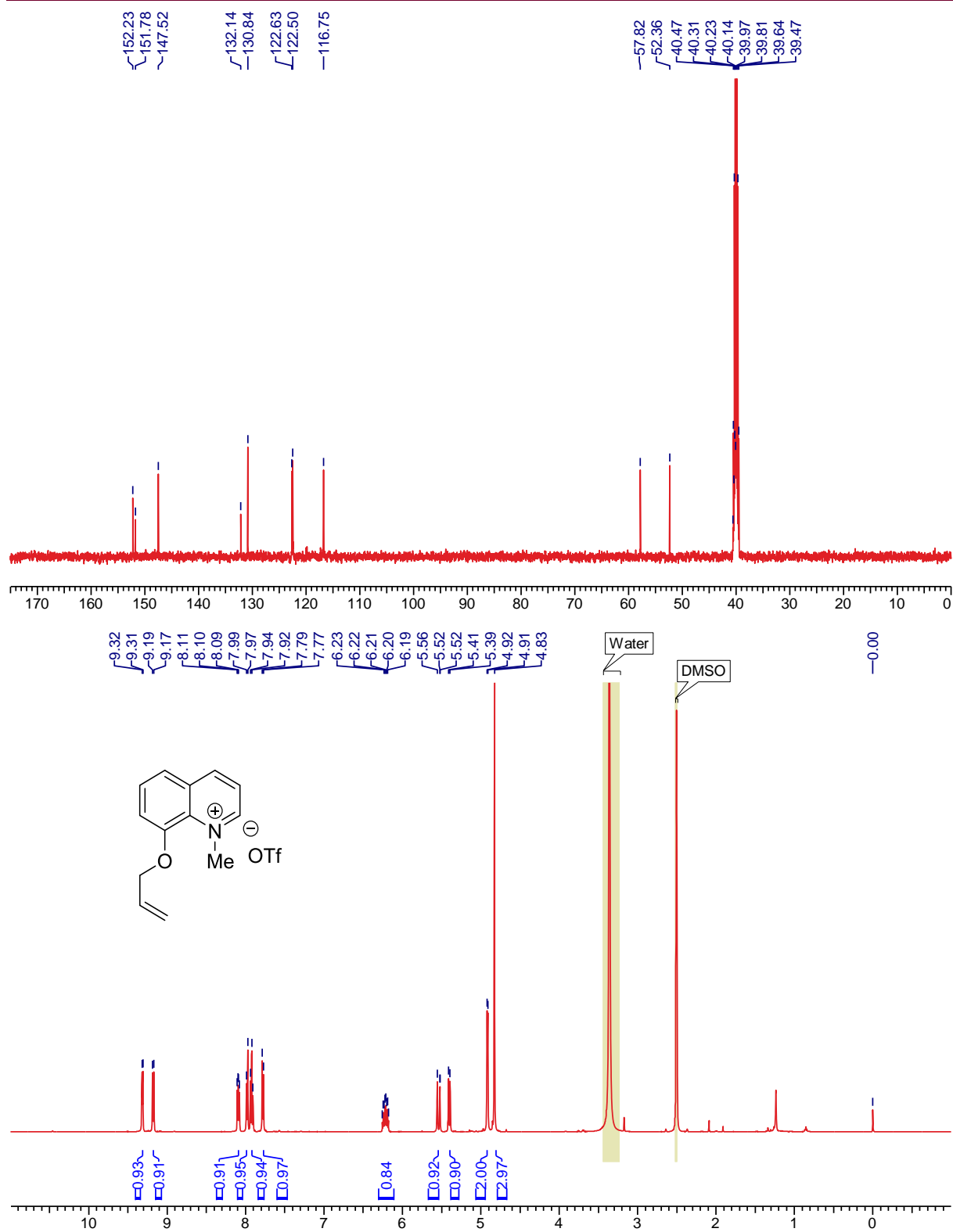


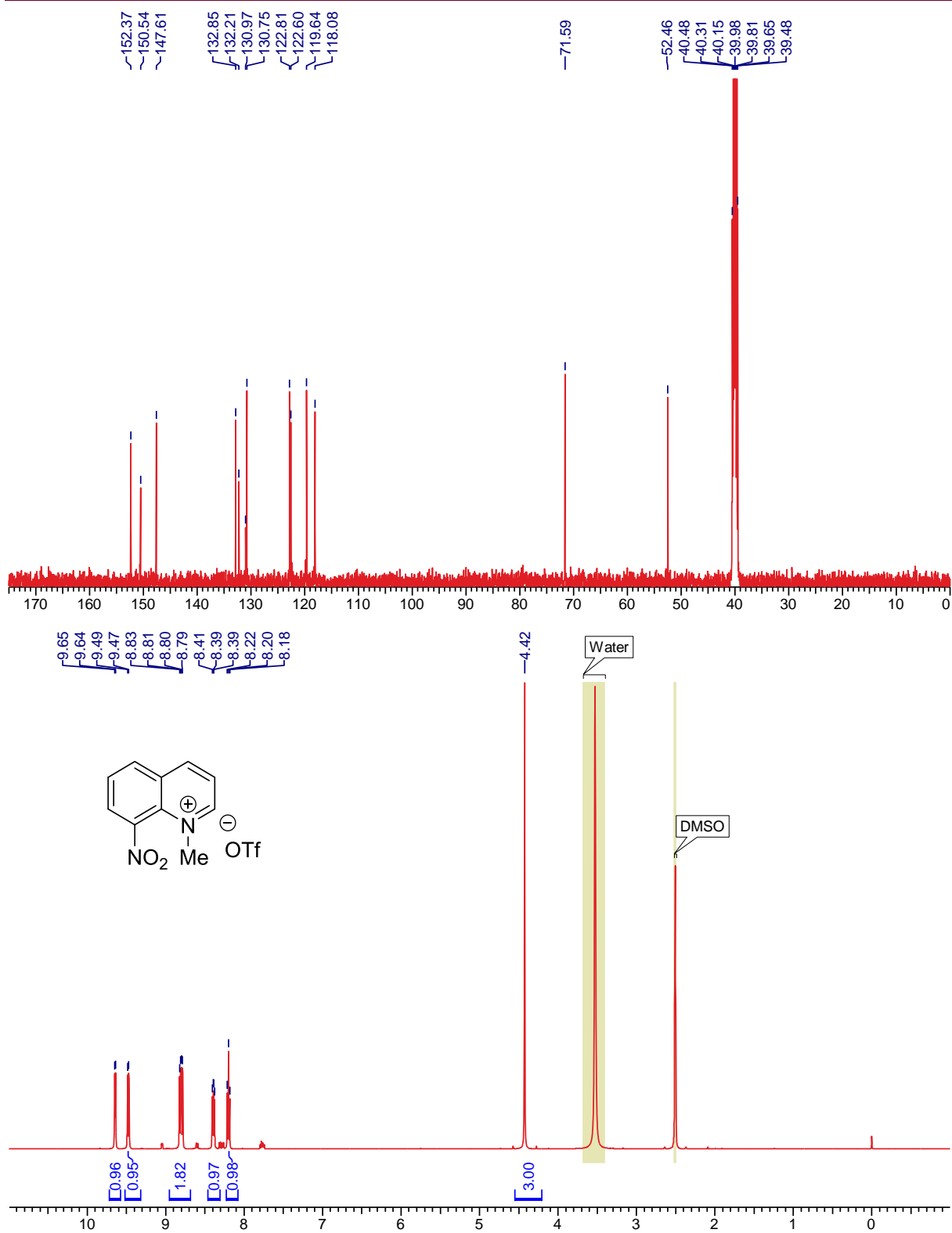


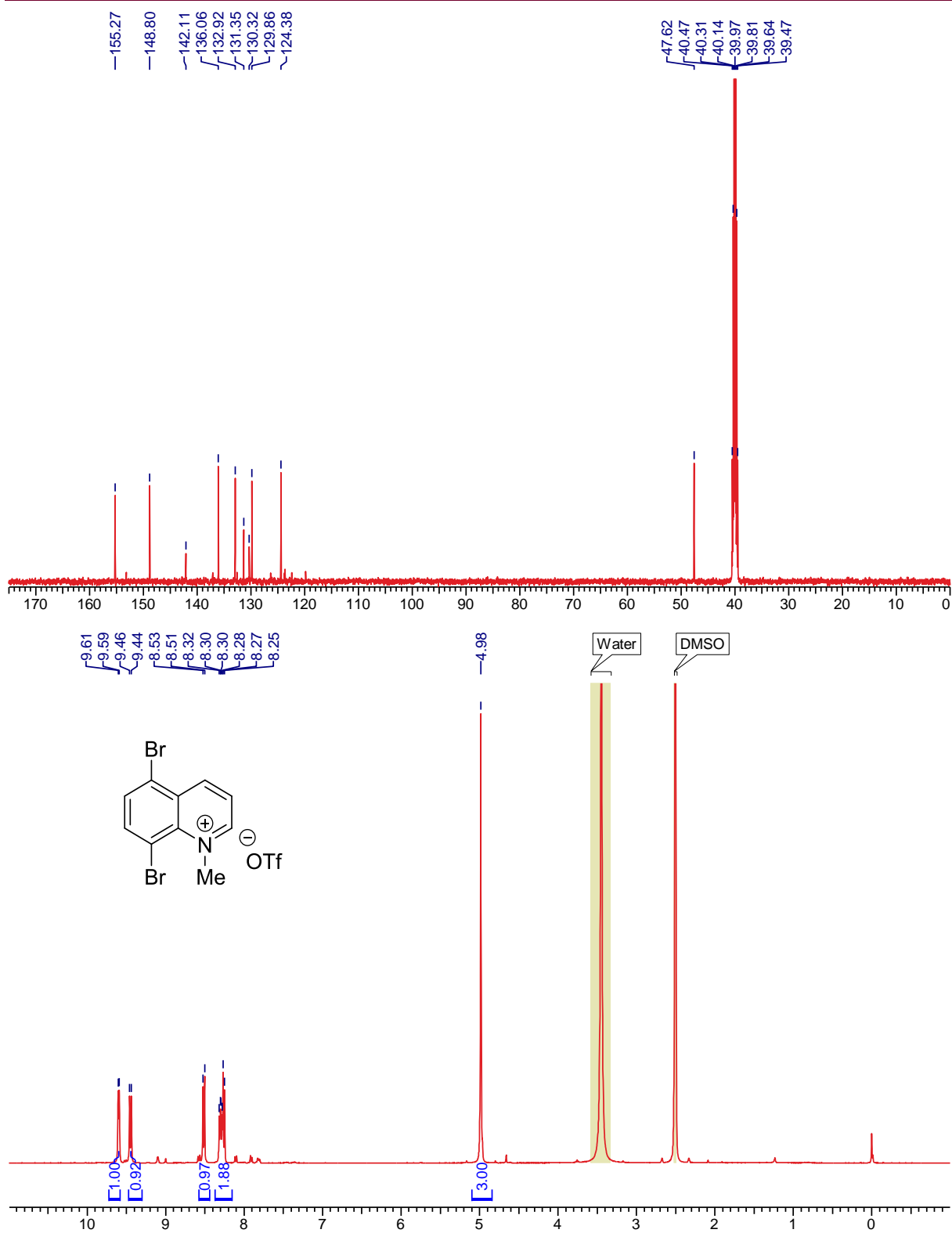


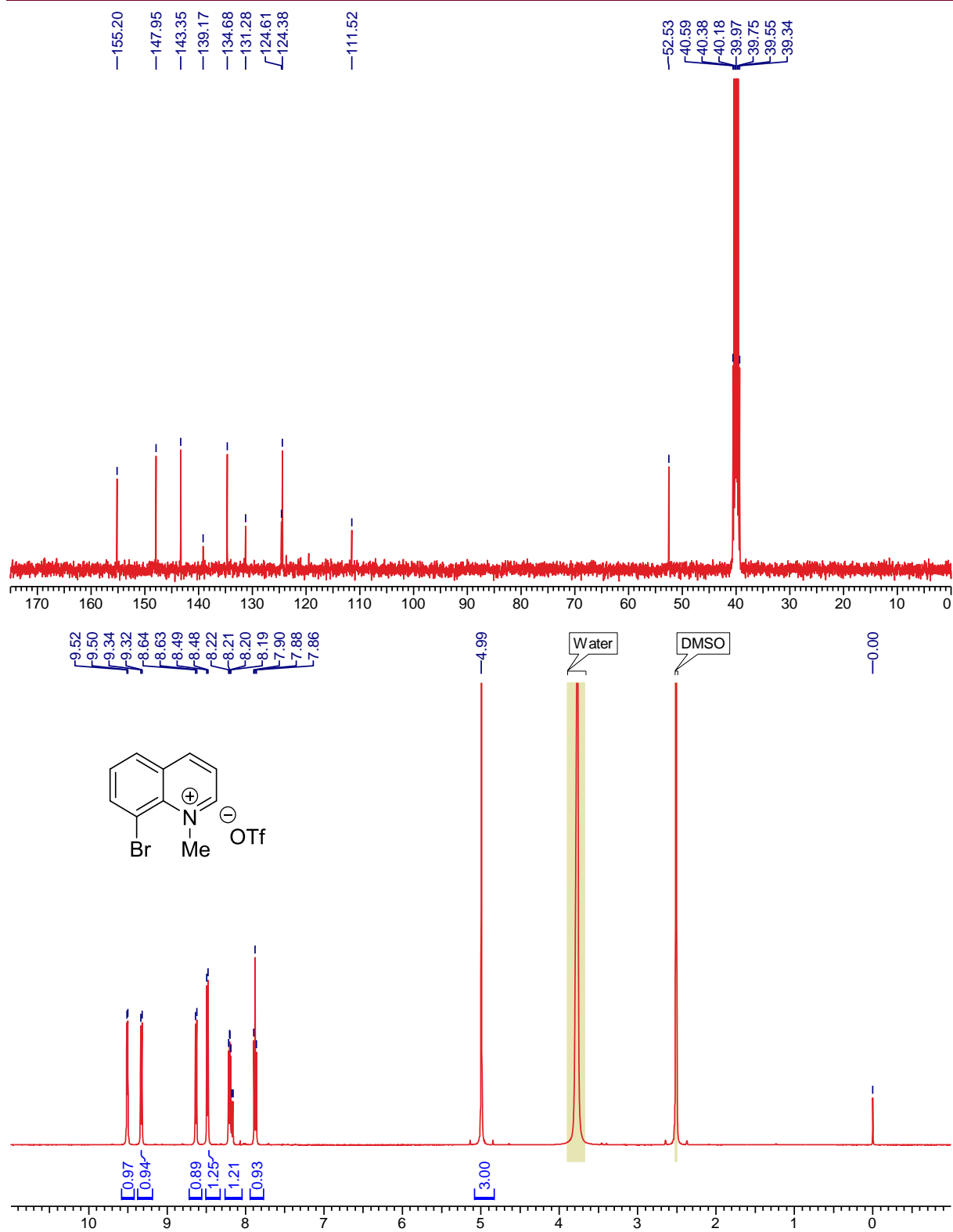


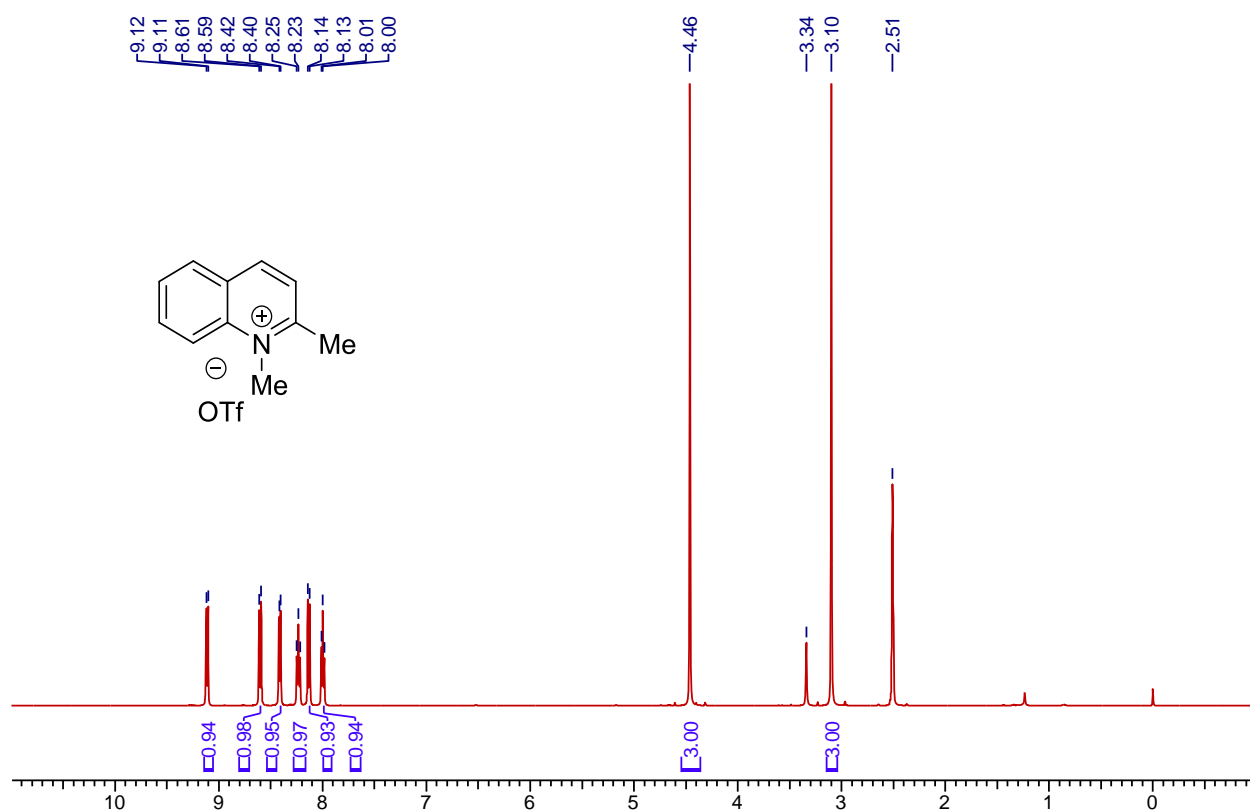
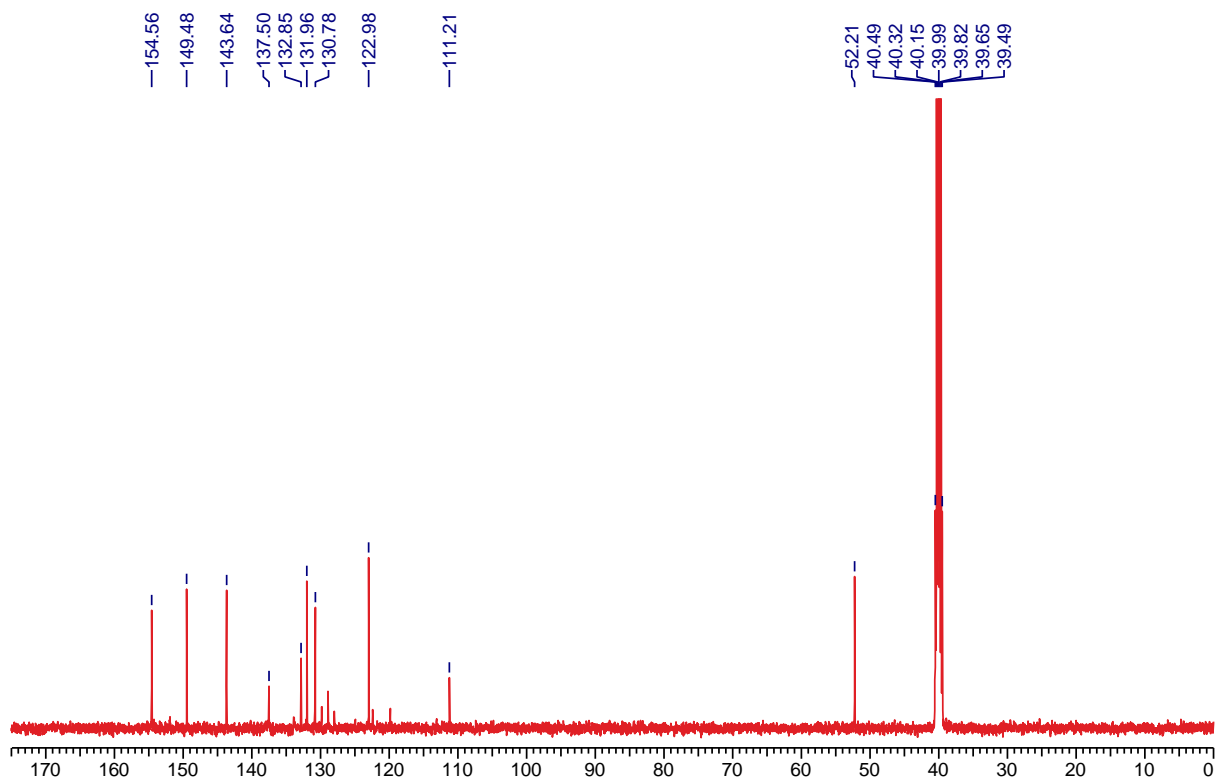


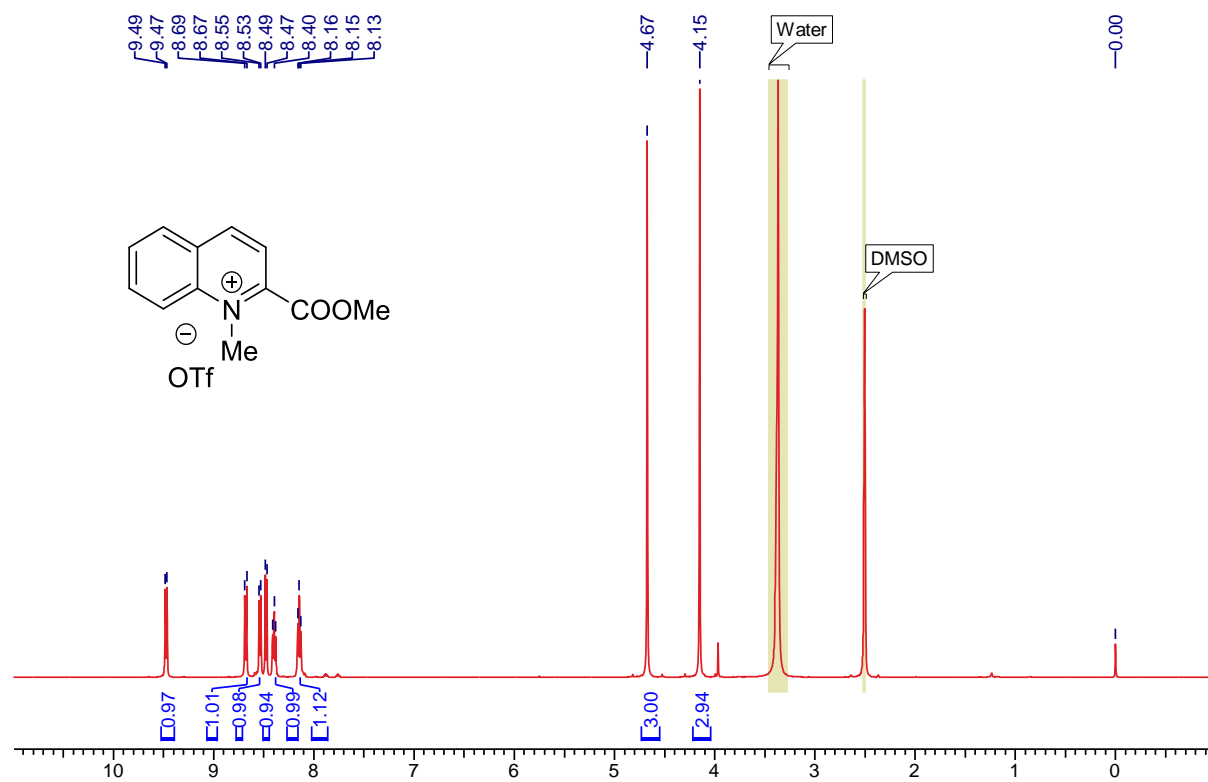
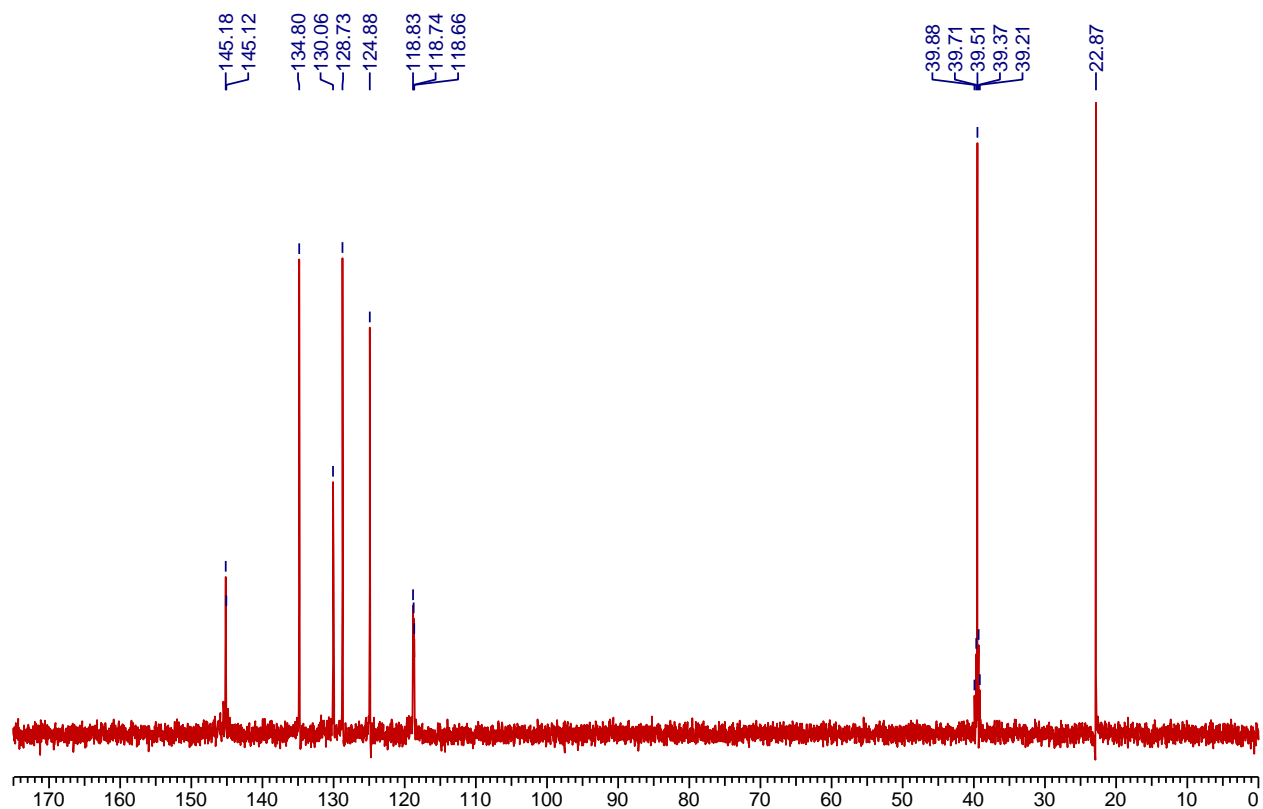


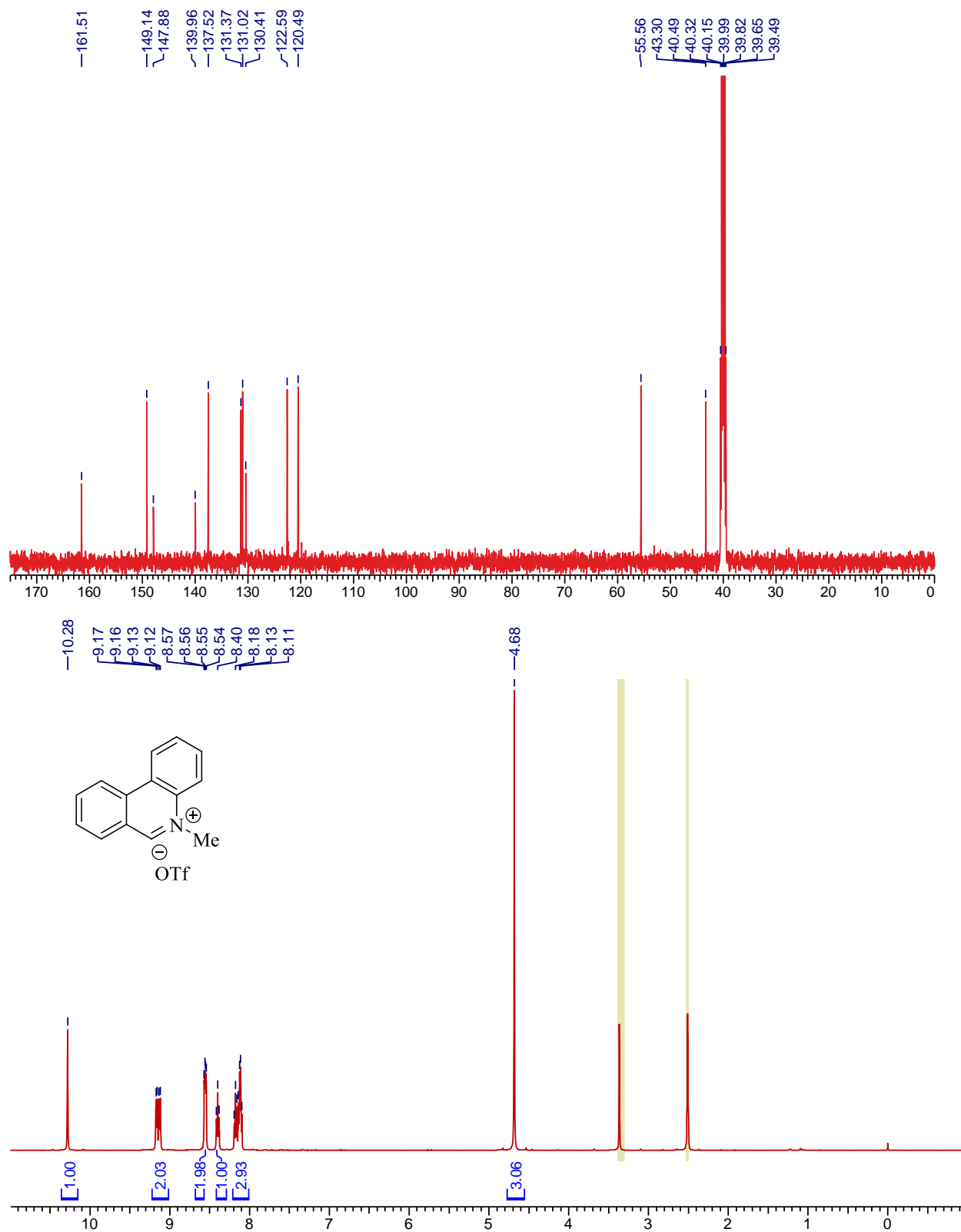


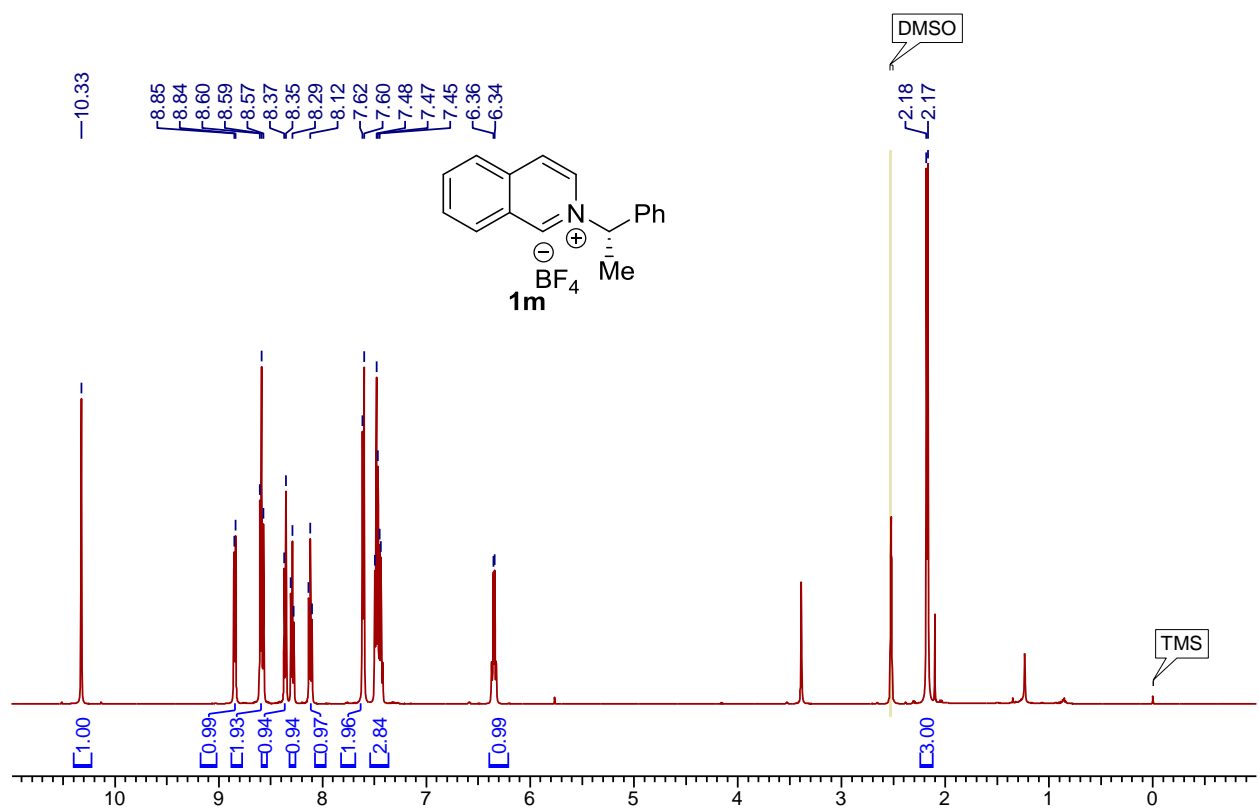
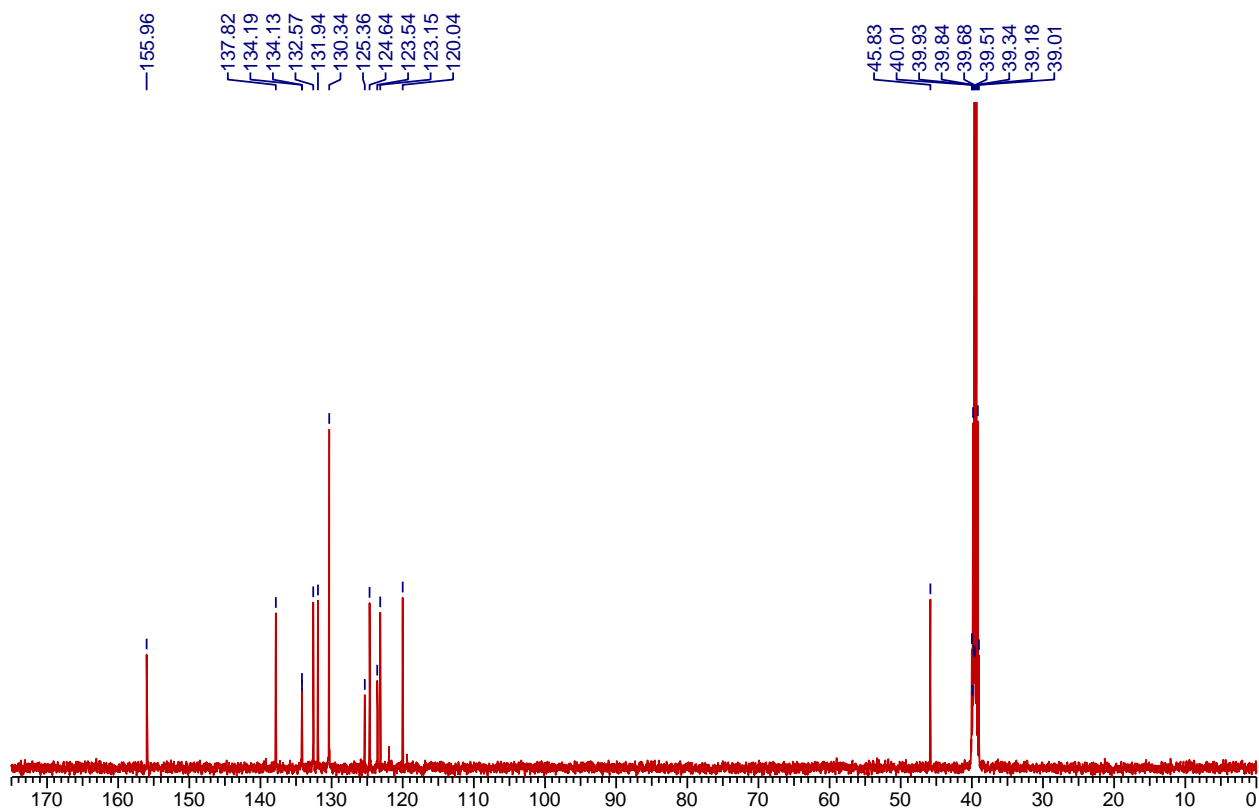


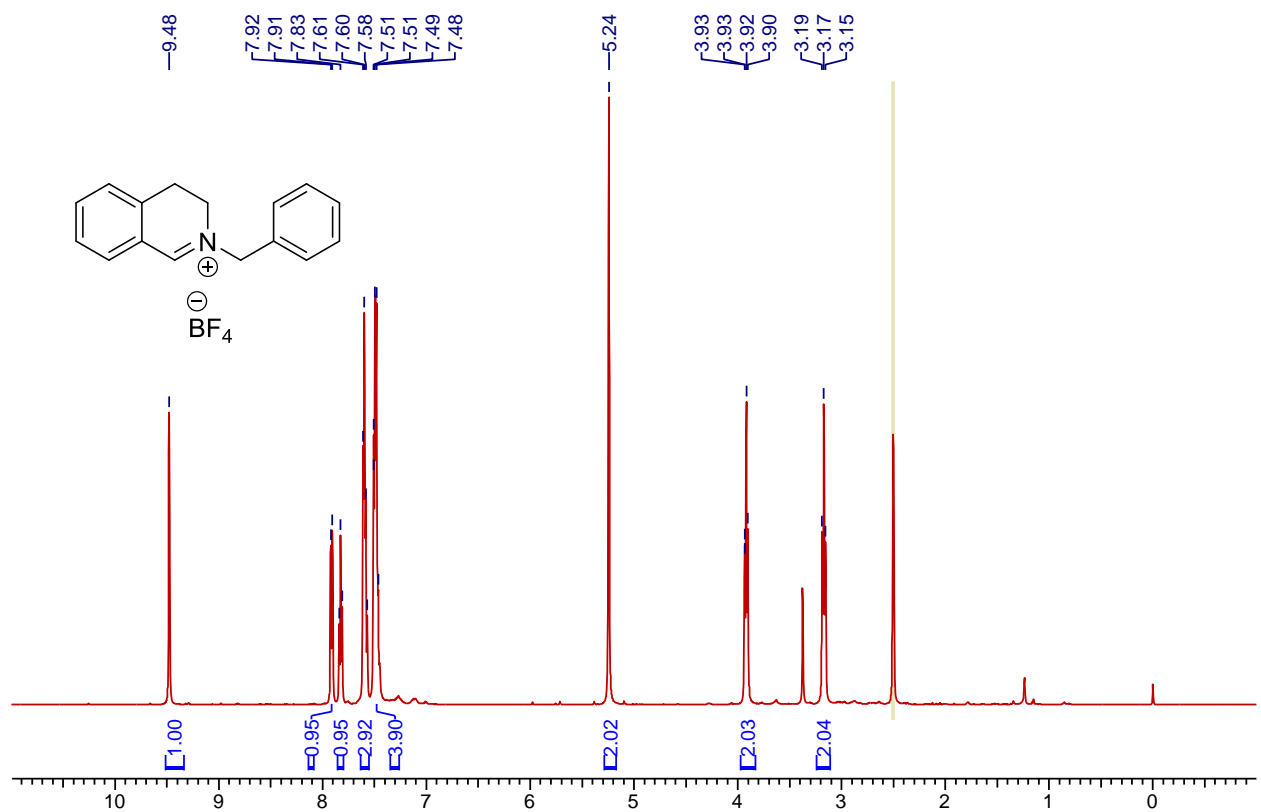
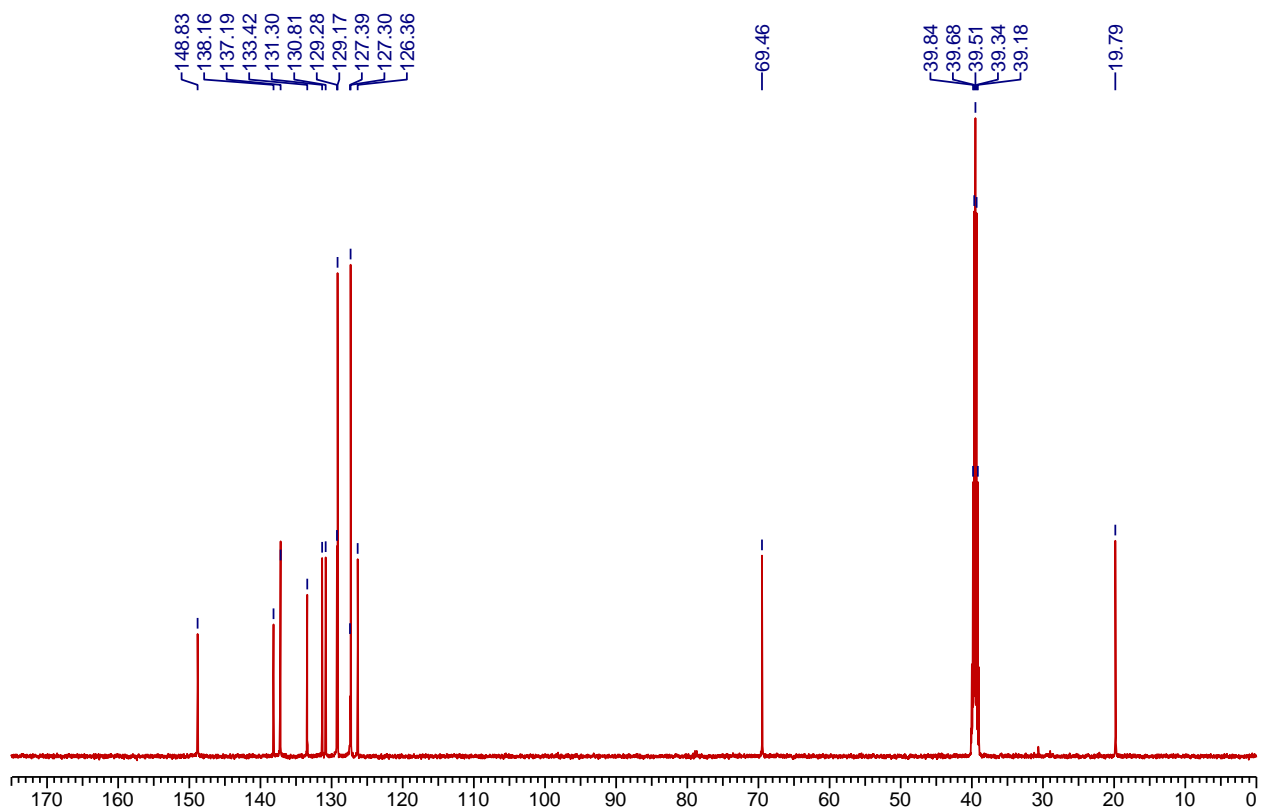


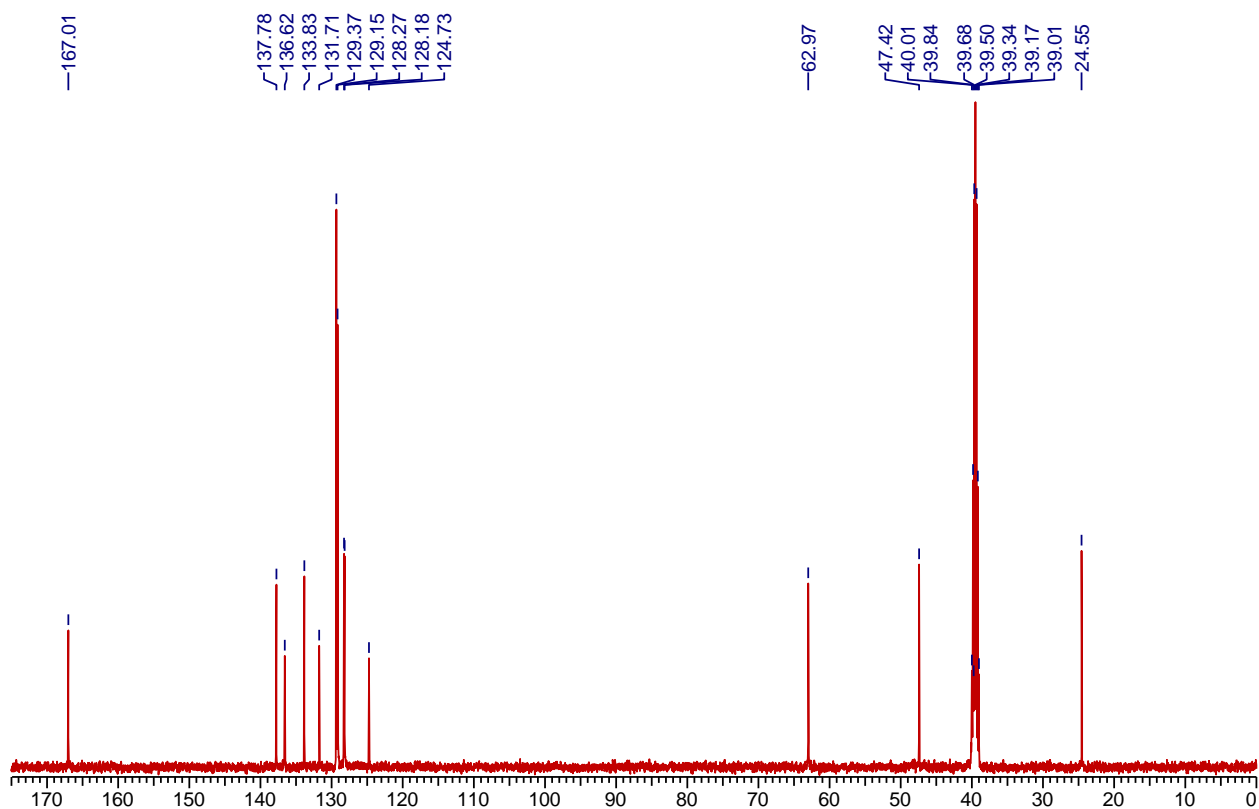




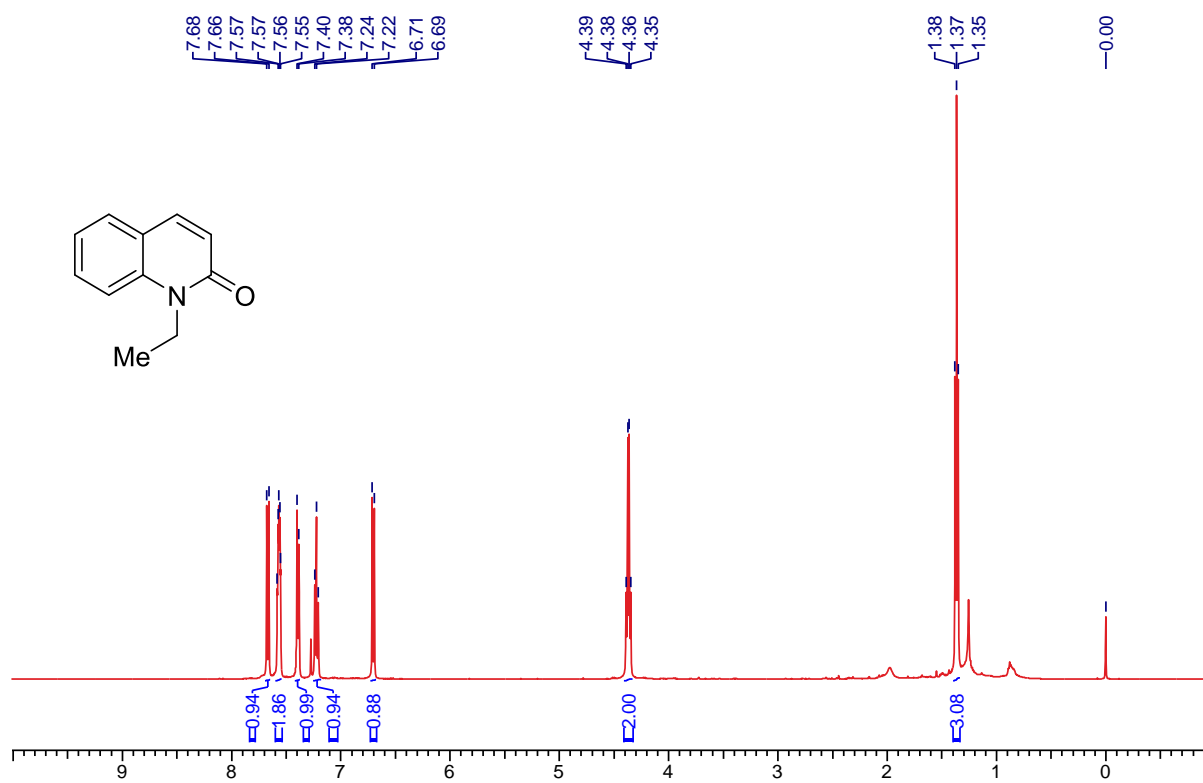


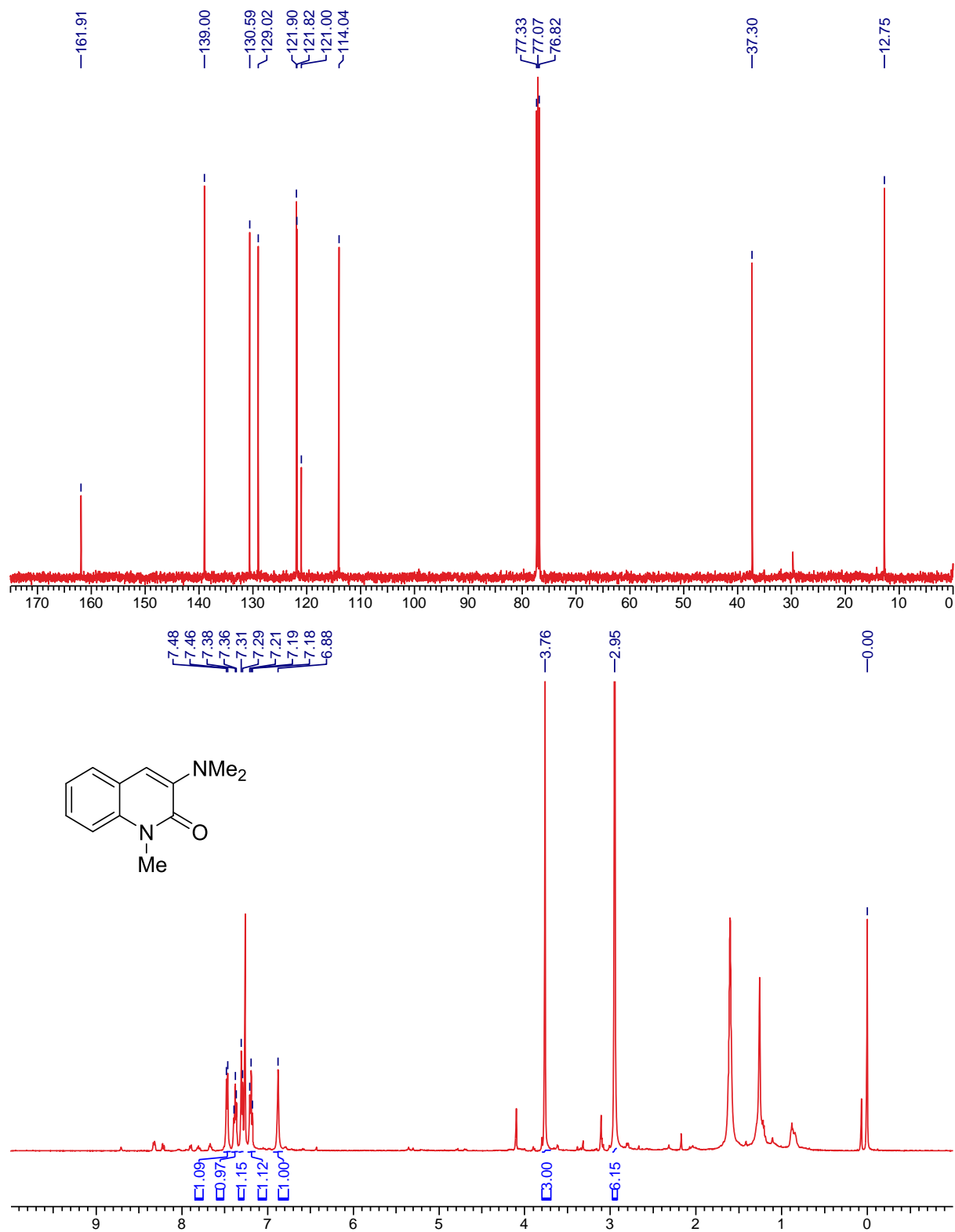


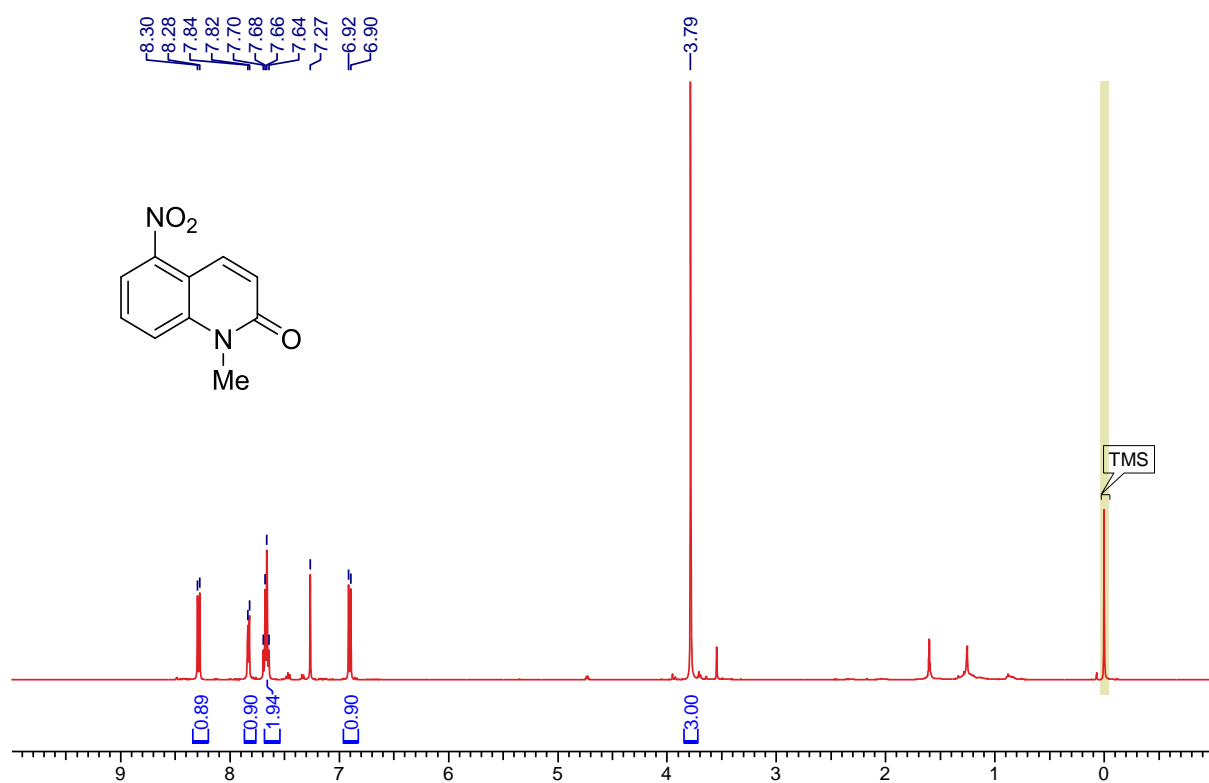
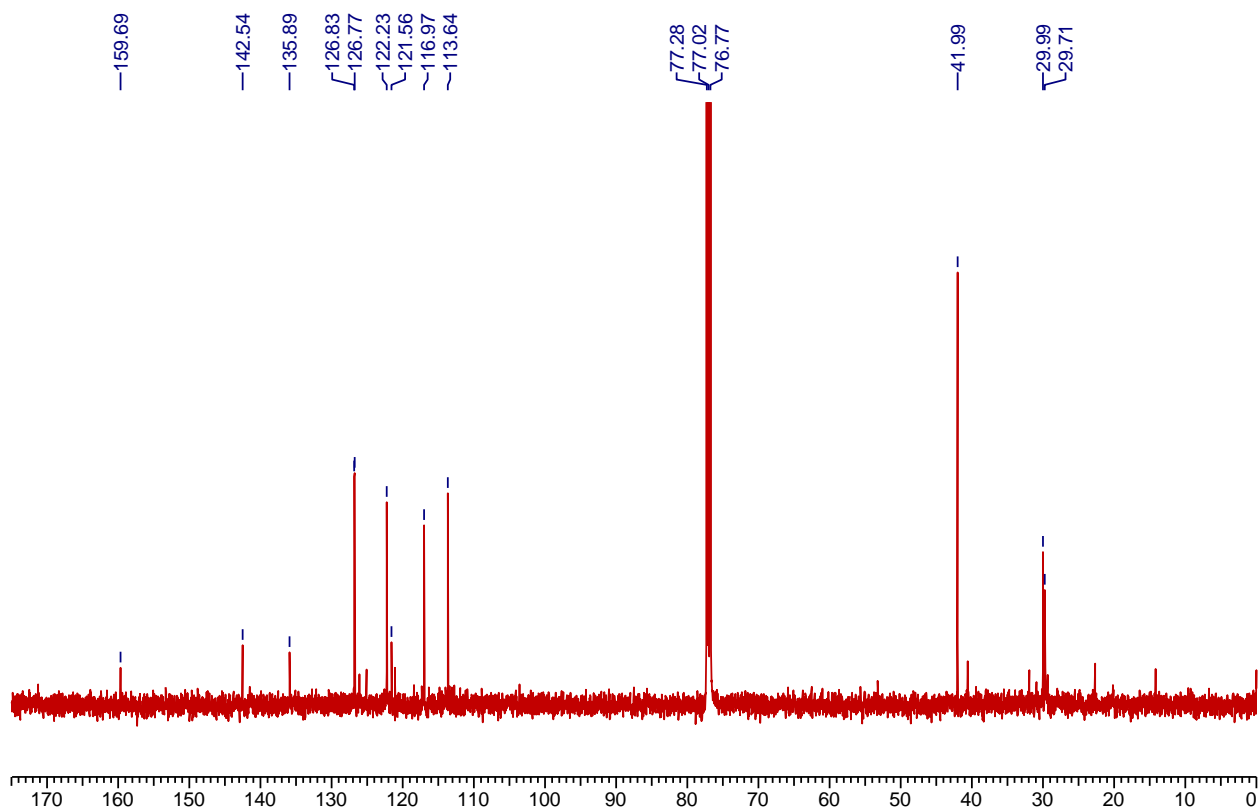


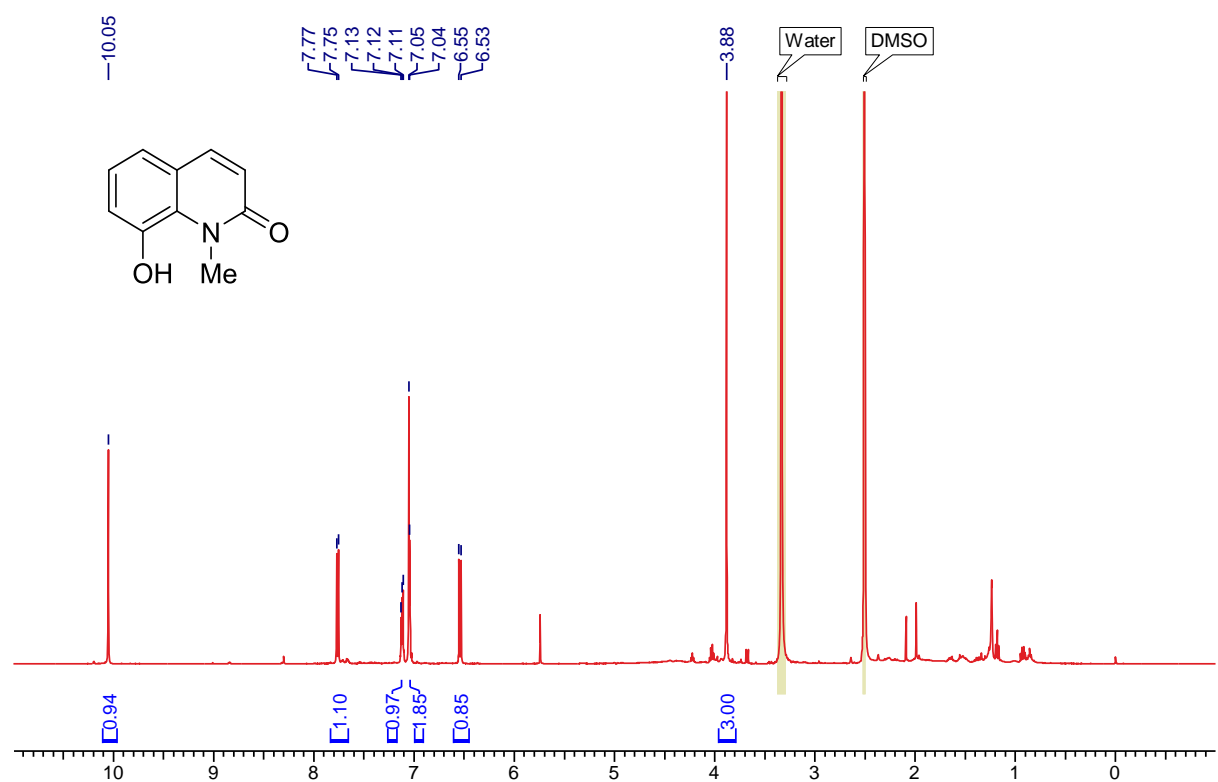
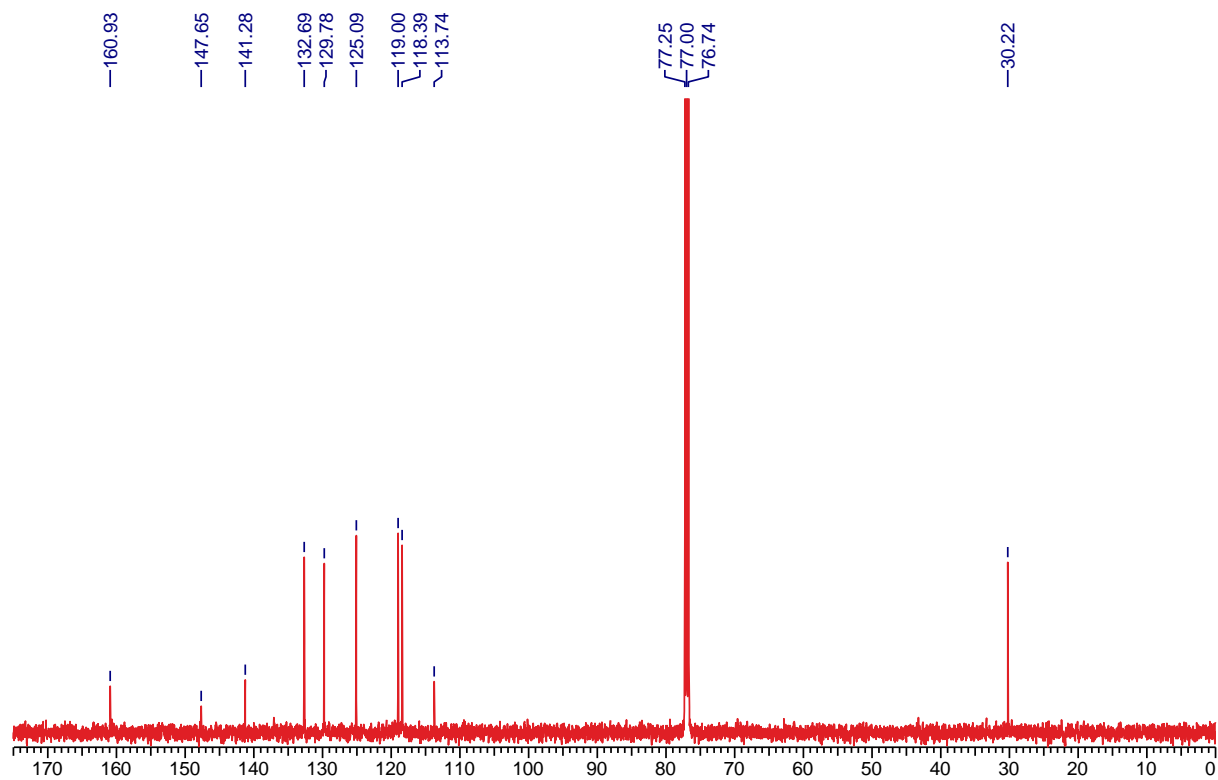


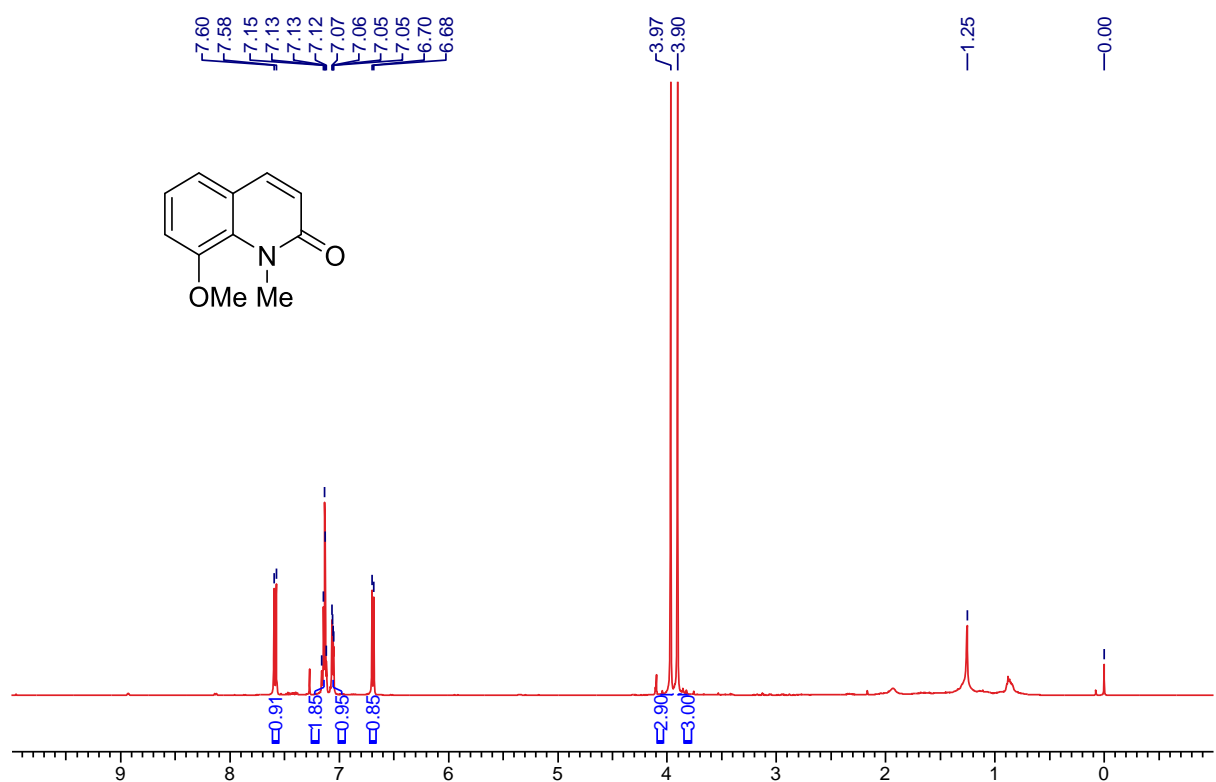
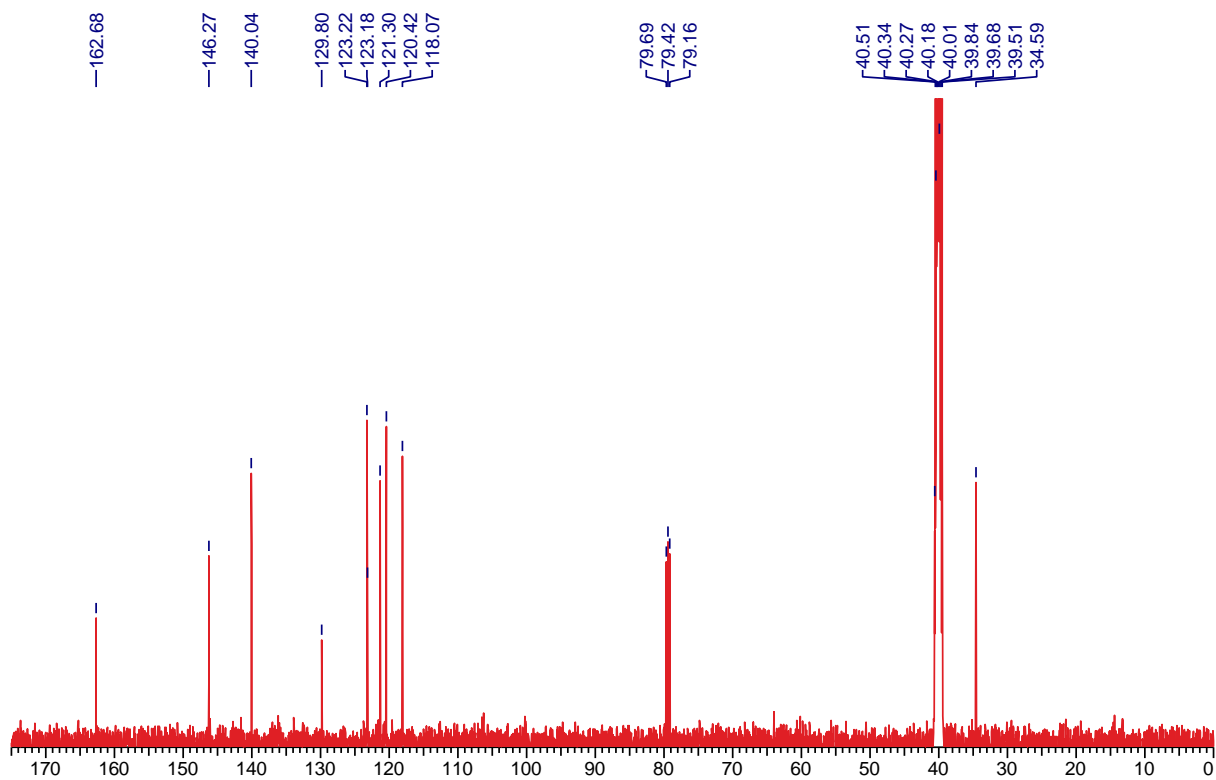
3.15.C NMR of oxo-product

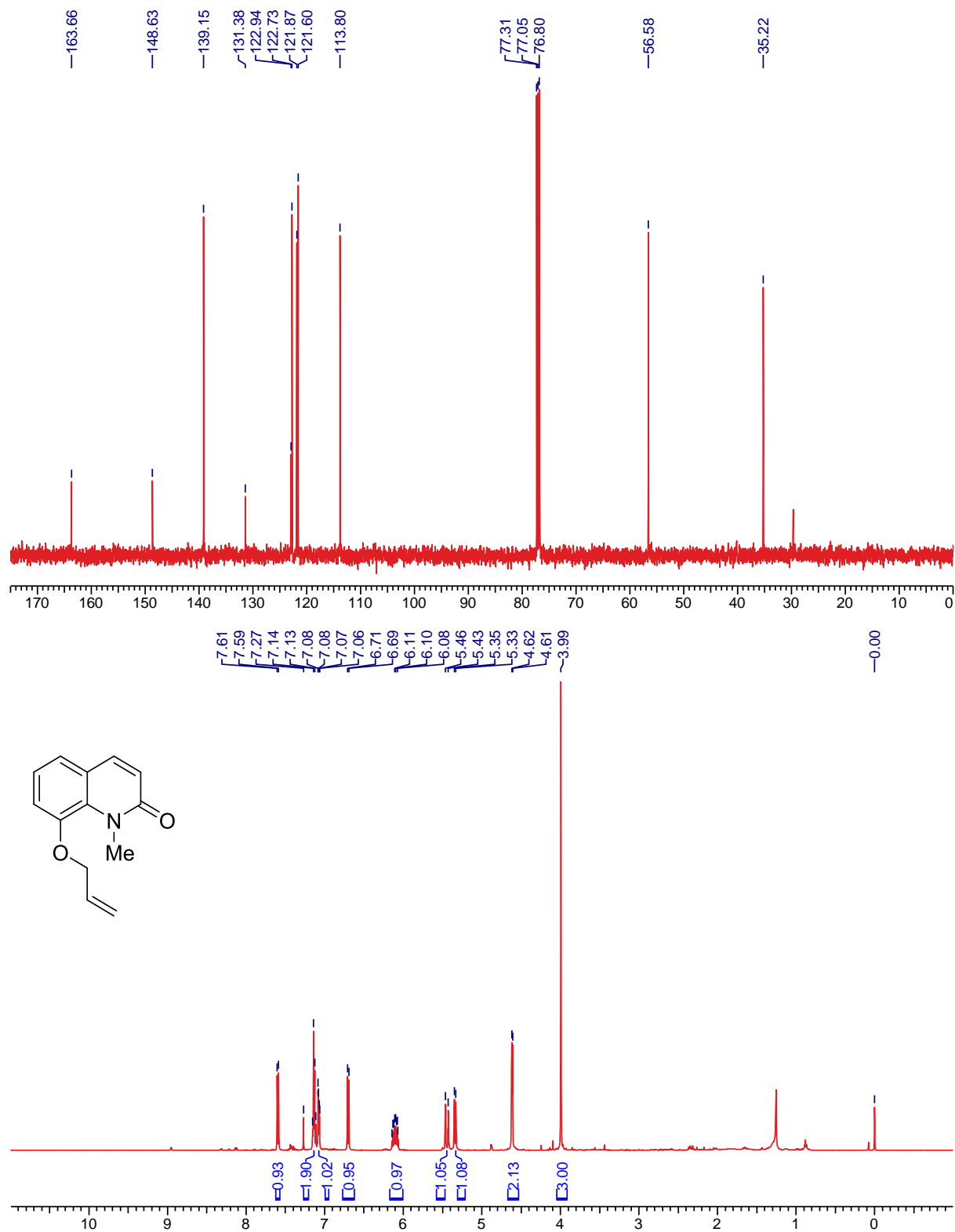


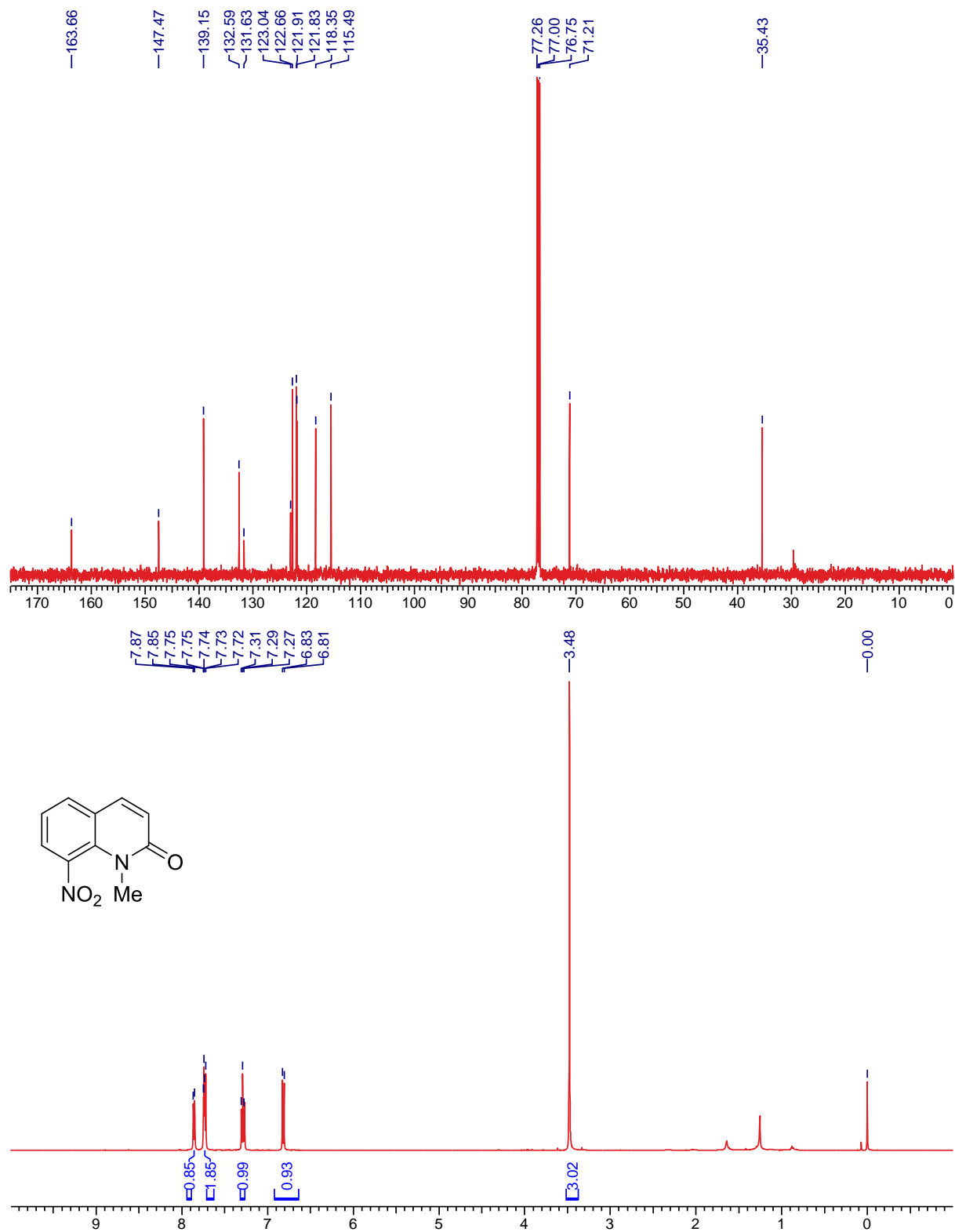


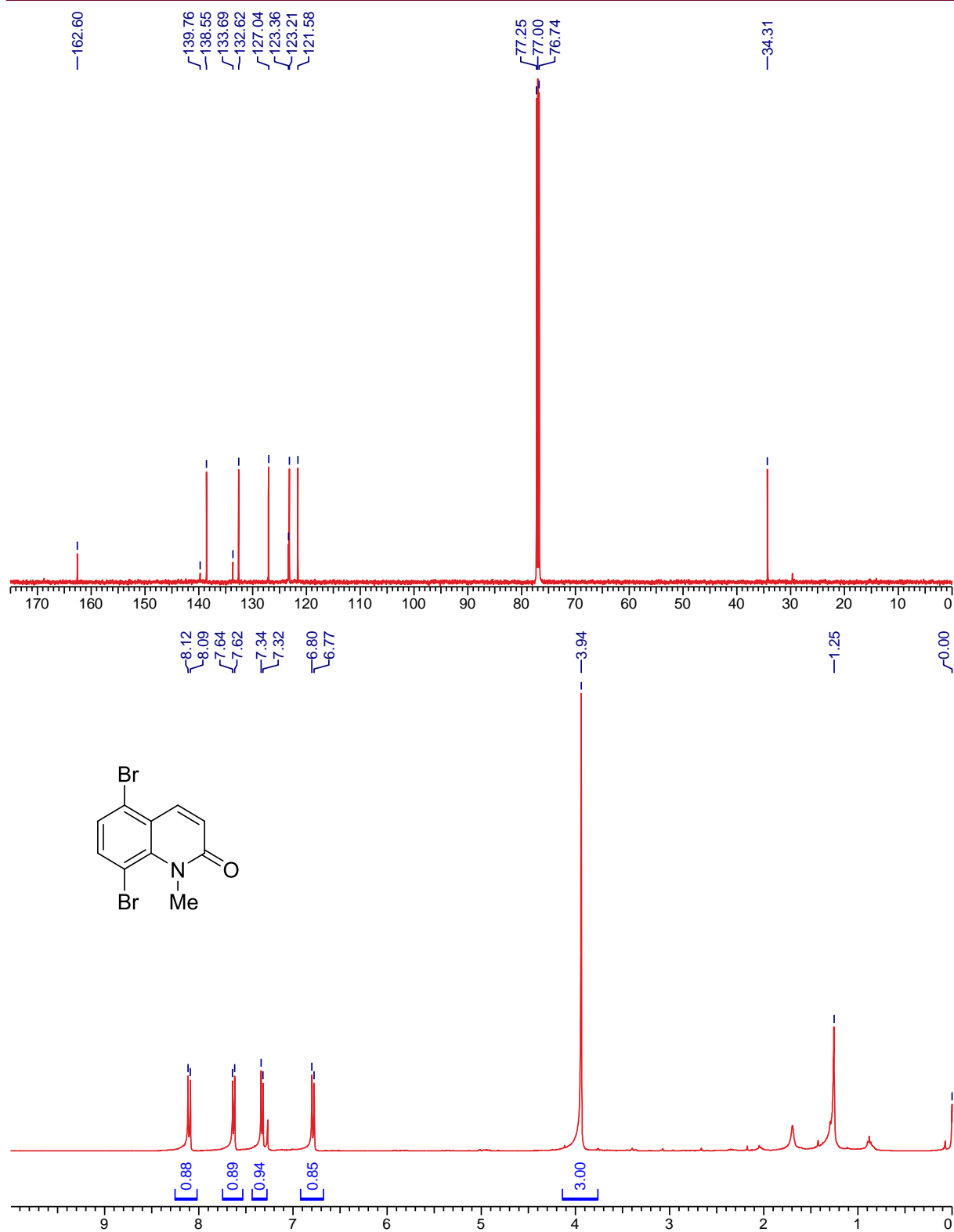


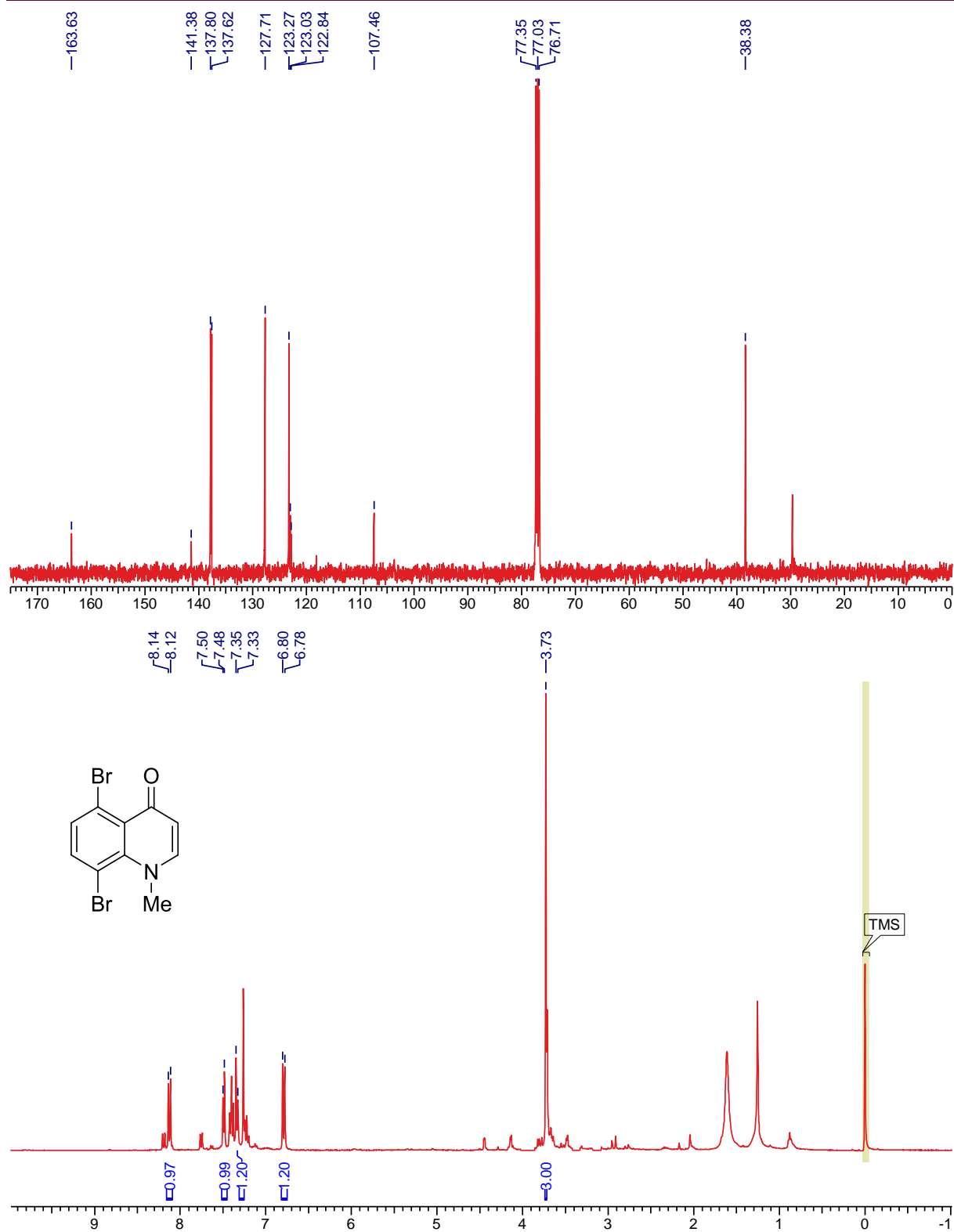


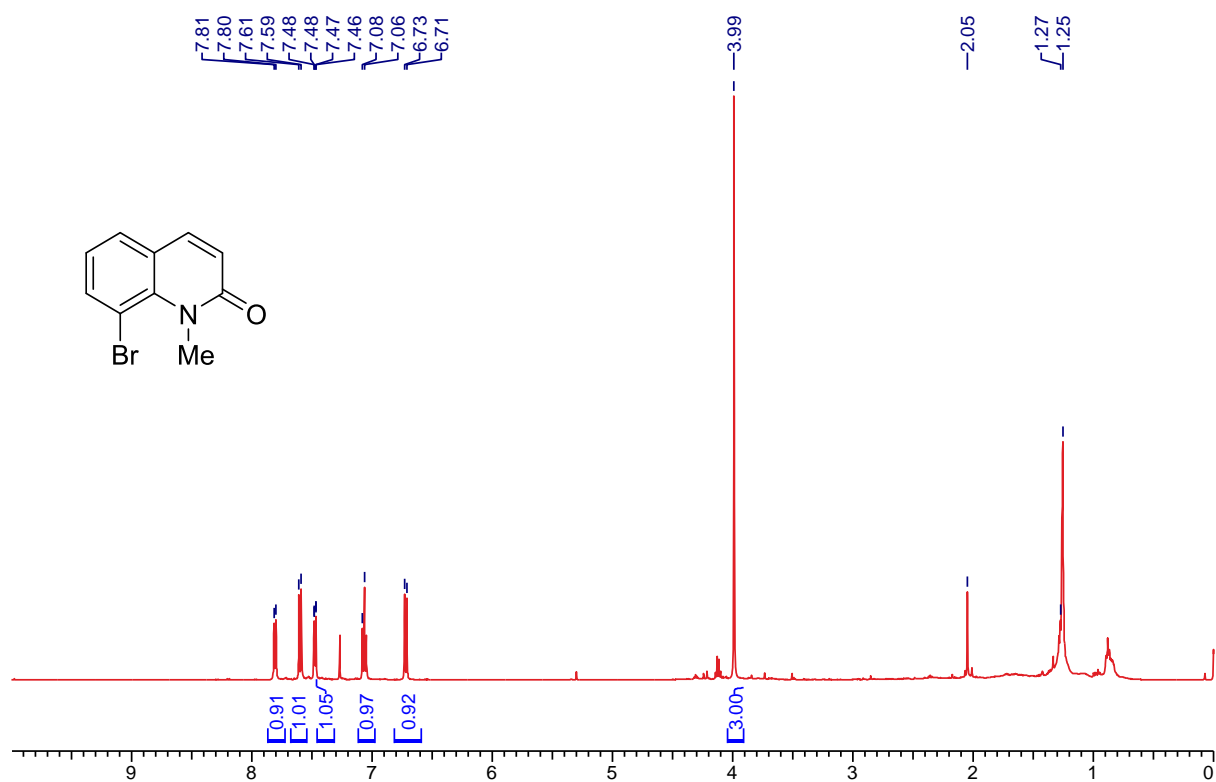
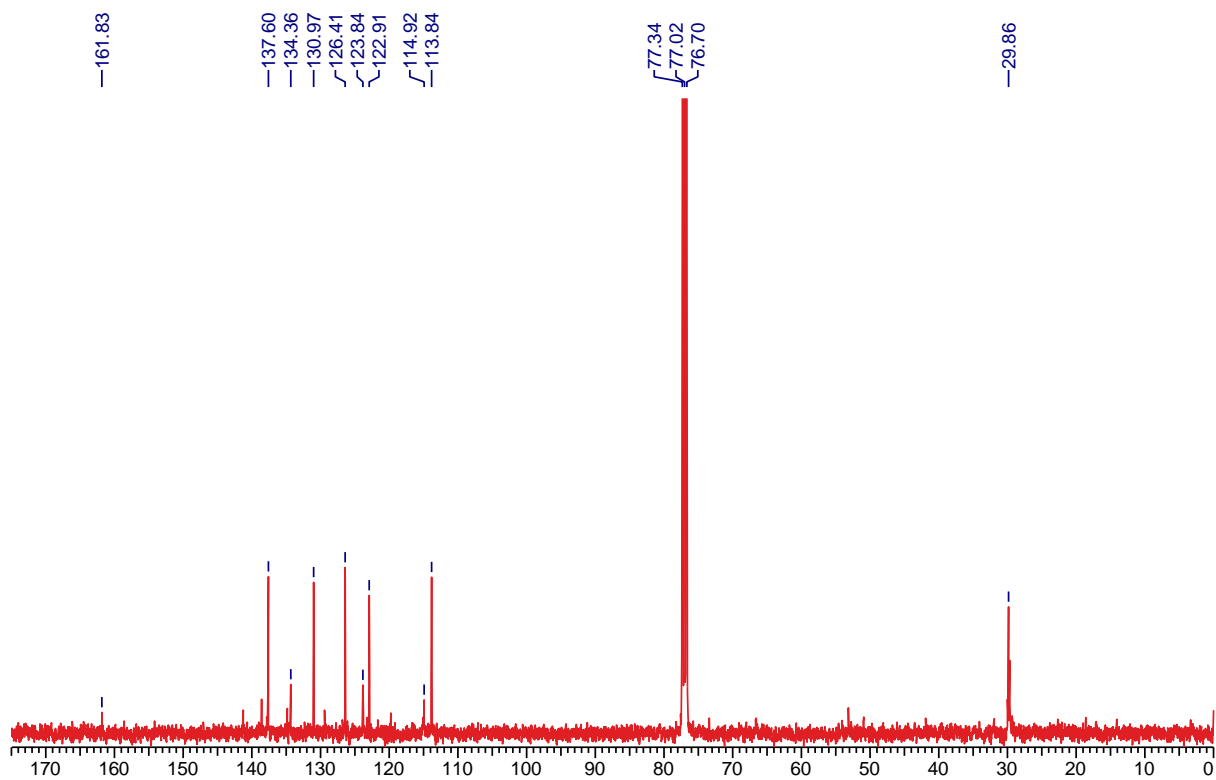


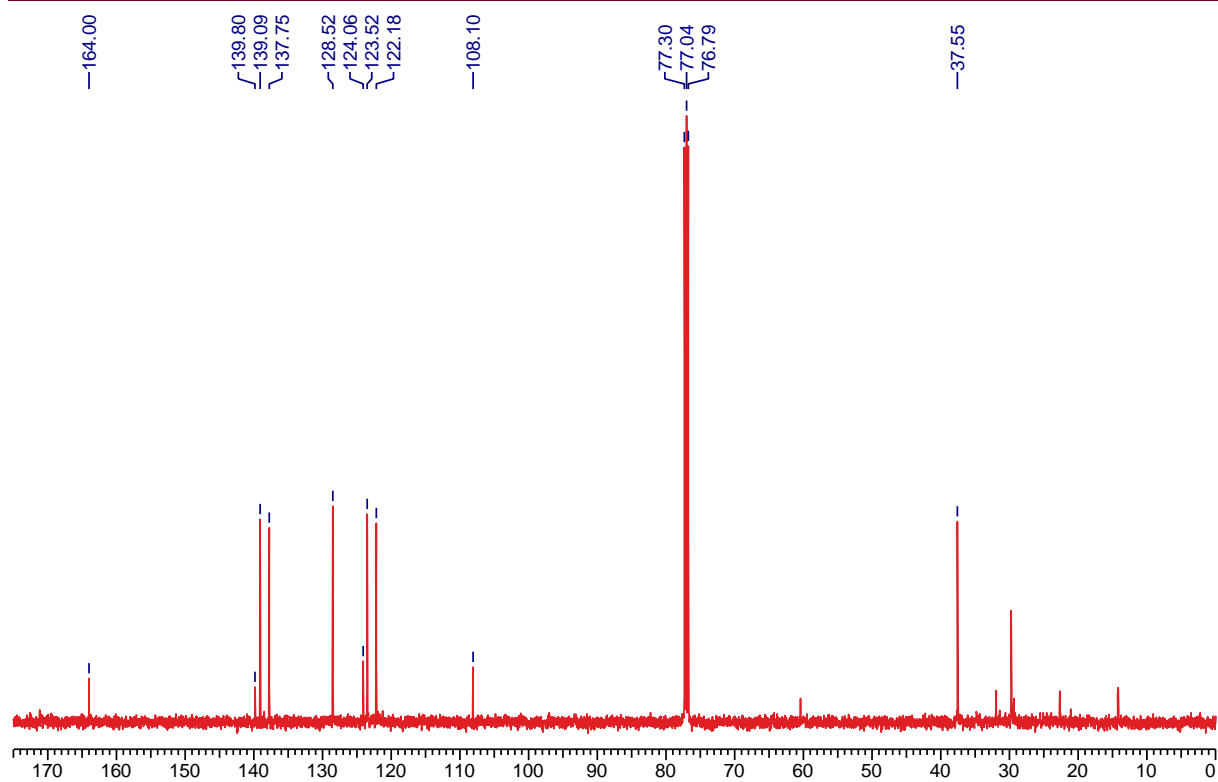




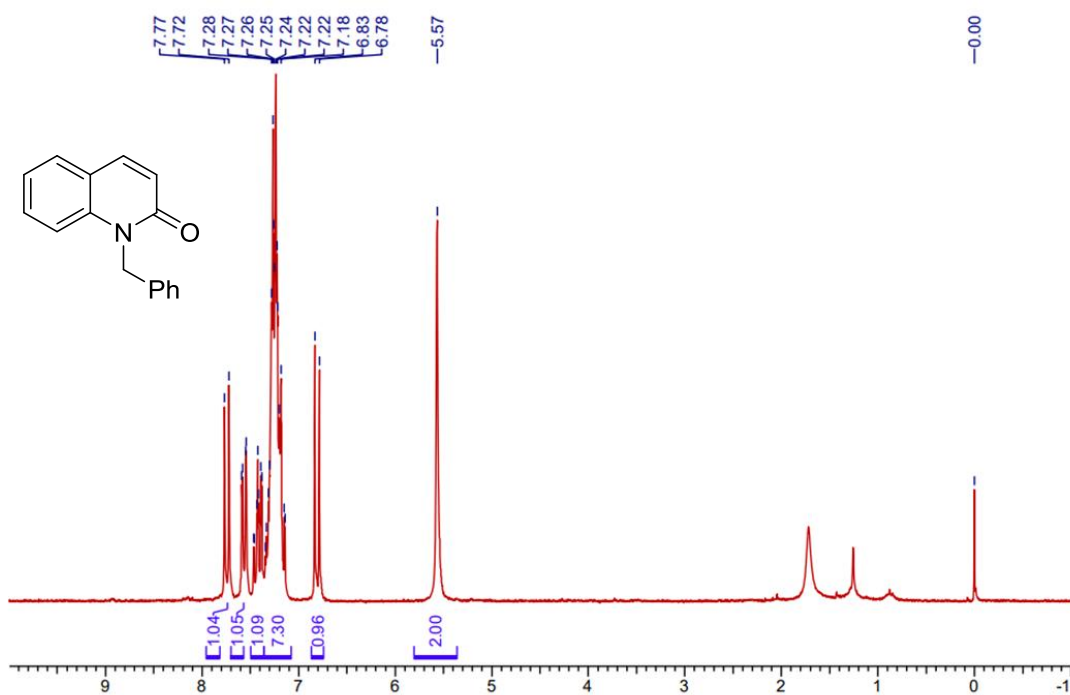
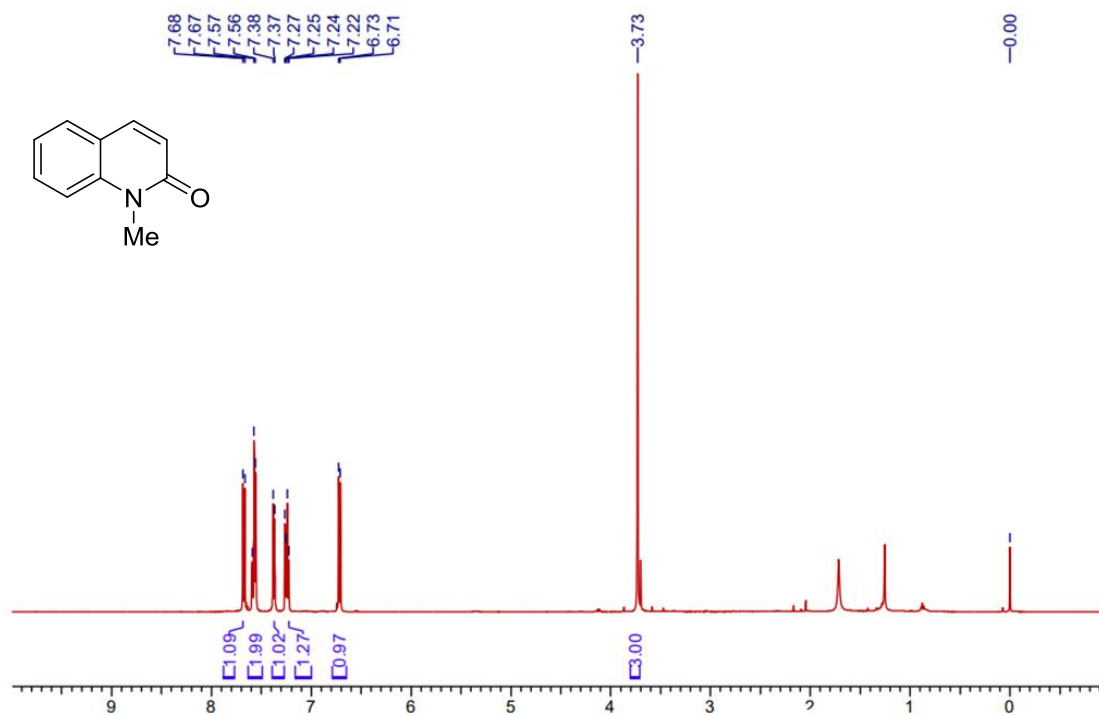


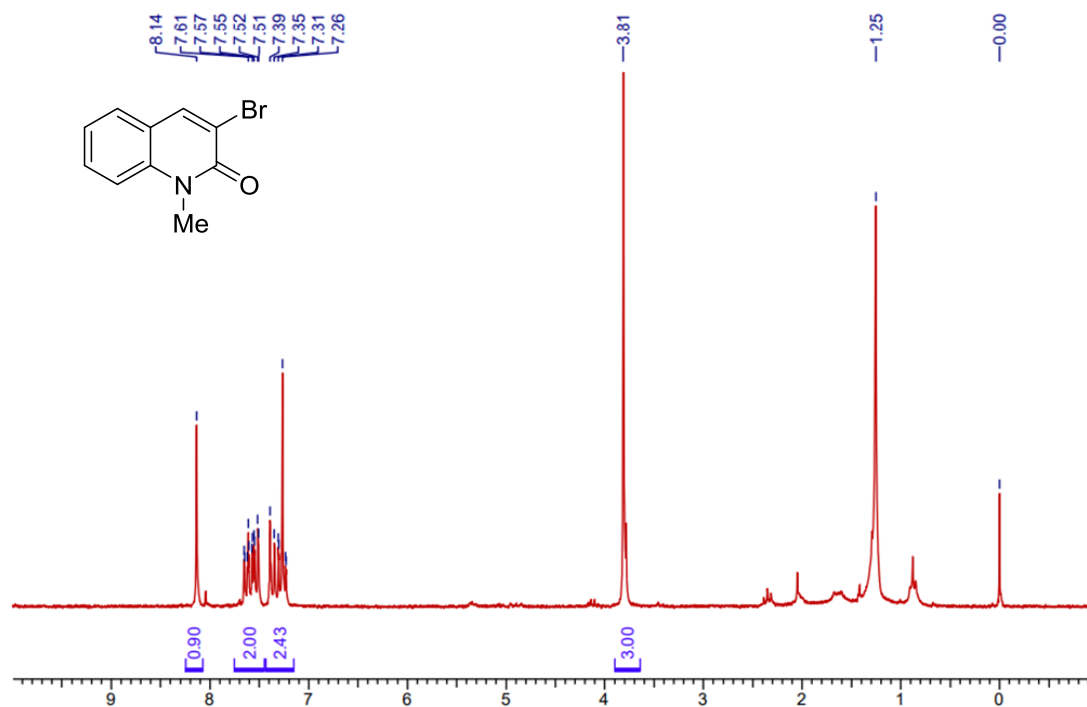
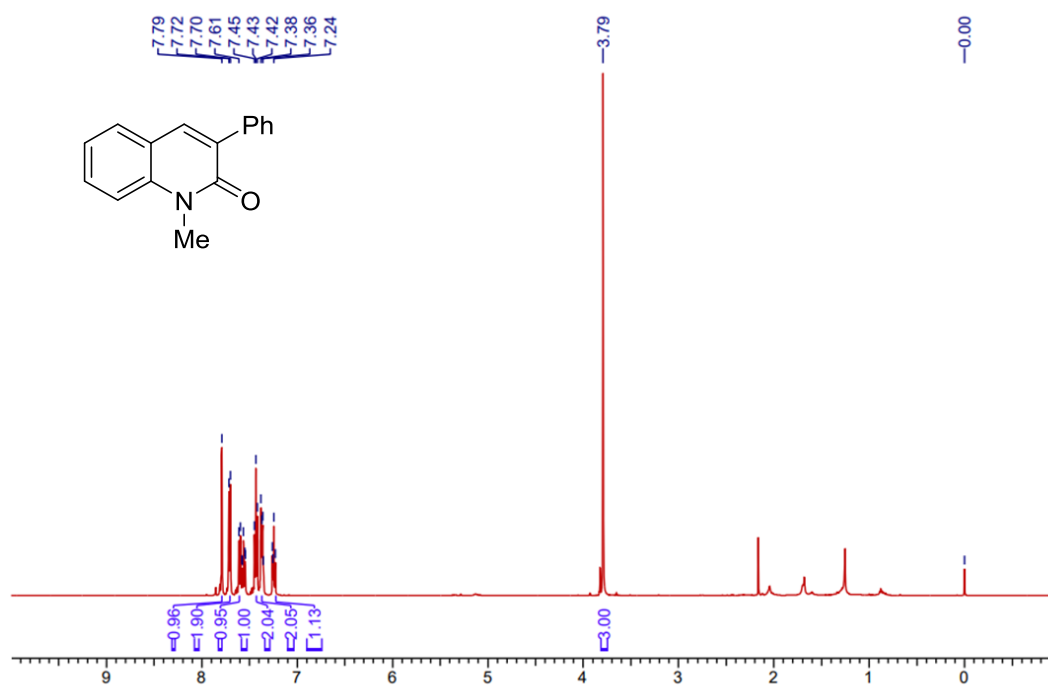


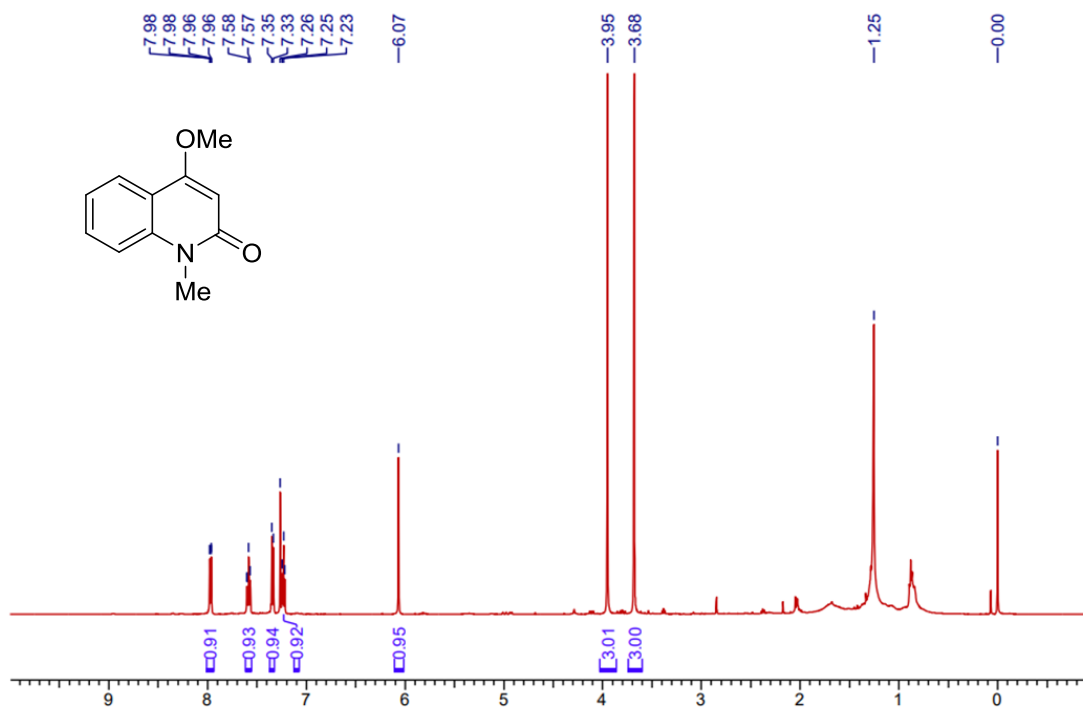
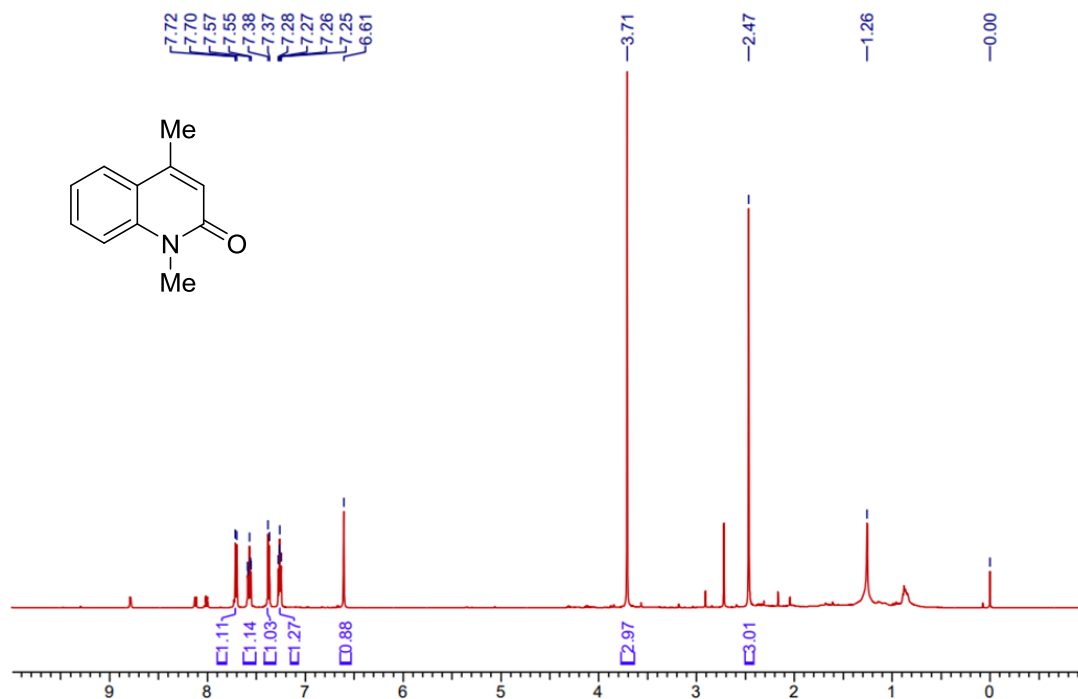


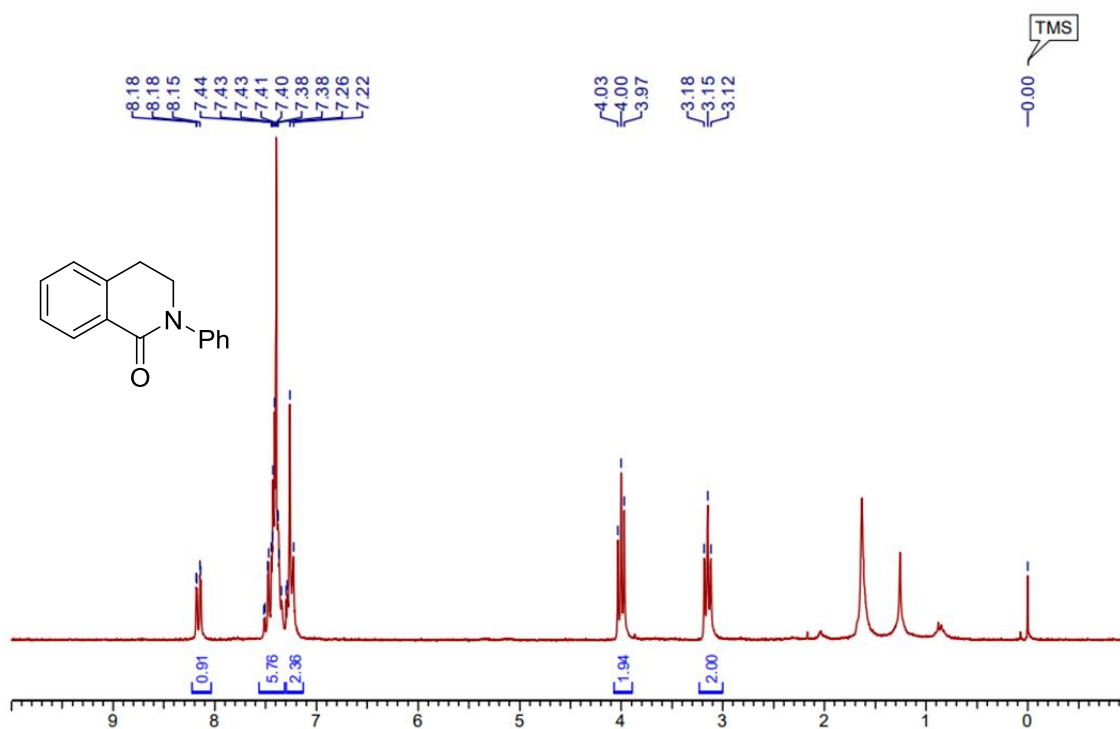
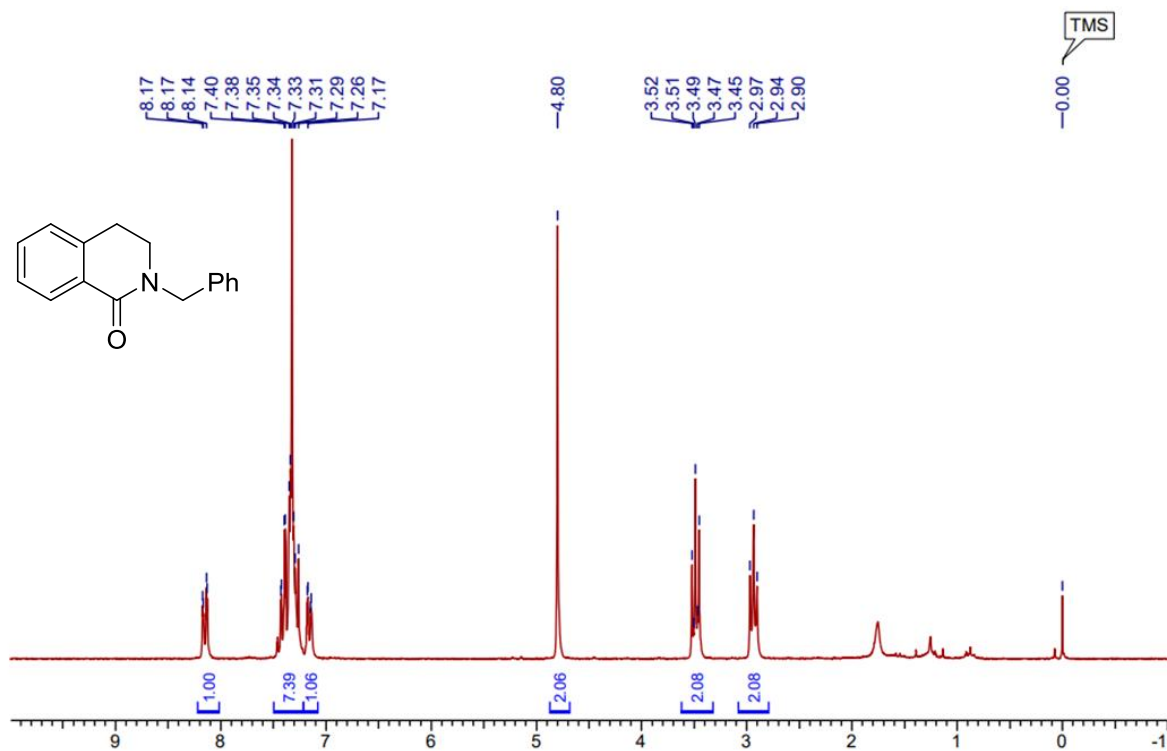


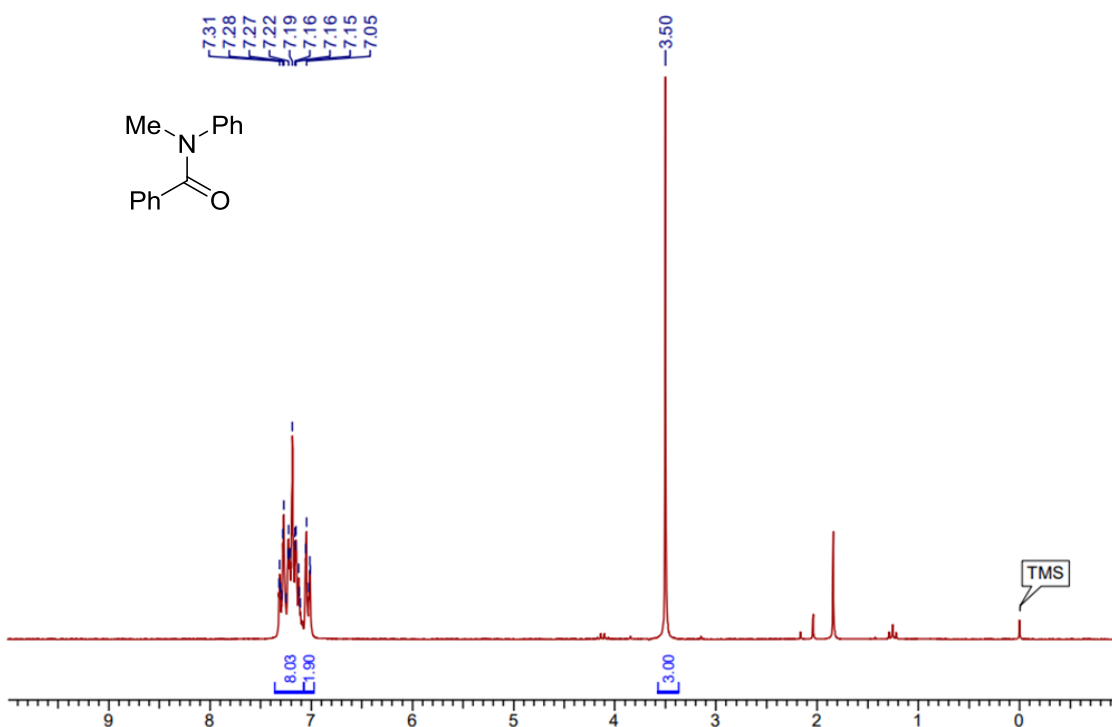
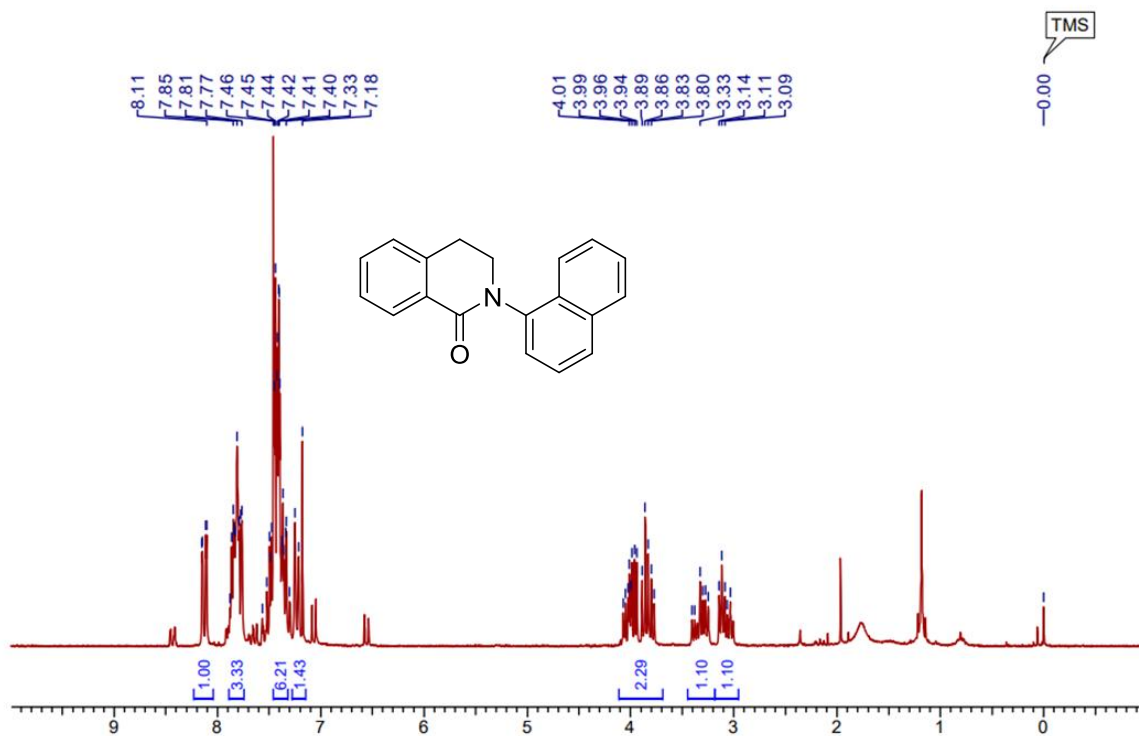
Literature known compound NMR:



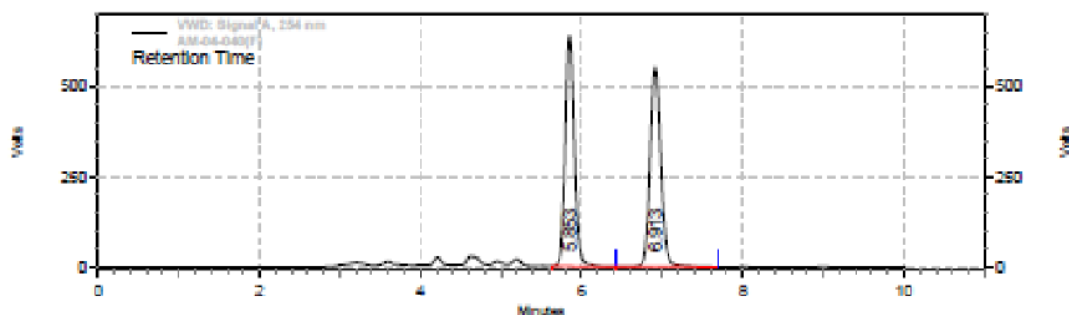








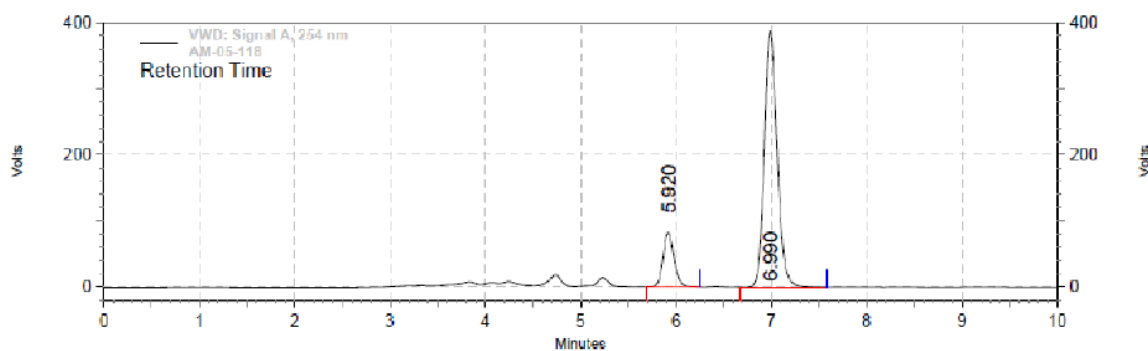
3.16 HPLC for oxidative kinetic resolution of 1m with chiral catalyst 9e



VWD: Signal A, 254 nm Results

Retention Time	Area	Area %
5.853	83231234	49.59
6.913	84615440	50.41
Totals		167846674
		100.00

Column : Chiralpak IA
 Eluent System : 70 : 30 (HEXANE:IPA)
 Flow rate: 1.0 ml/min
 Injection vol.: 10ul
 Wavelength: 254 nm
 Sample Conc.: 1 mg/ml



VWD: Signal A, 254 nm Results

Retention Time	Area	Area %
5.920	10961721	15.20
6.990	61144272	84.80
Totals		72105993
		100.00

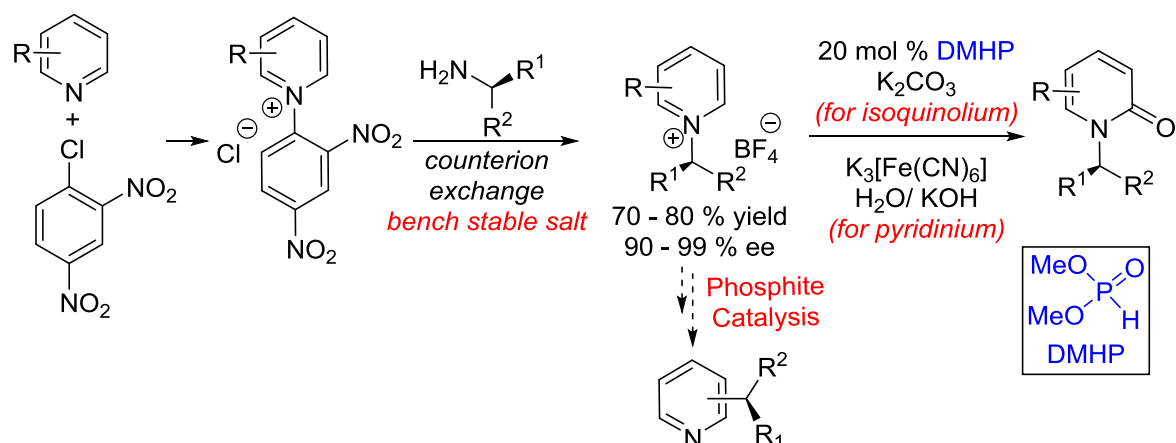
Column : CHIRALPAK-IA
 Eluent System : 70 : 30 (n-HEXANE:IPA)
 Flow rate: 1.0 ml/min
 Injection vol.: 10 ul
 Wavelength: 254 nm
 Sample Conc.: 1.0 mg/ml

Chapter 4

Synthesis of chiral N-alkylpyridinium salts and their
phosphite-catalysed oxidation and rearrangements

4.1 Abstract

This chapter describes the synthesis of chiral and racemic primary amines and their corresponding pyridinium salts. The pyridinium salt synthesis was modified to achieve chiral pyridinium salts without the racemization of chiral amines. The enantioselectivities of both primary amines and their corresponding pyridinium salts were determined. The enantiomeric excess of pyridinium salts was not reported, and we failed to find a suitable chiral HPLC method to separate enantiomers. Therefore, we utilized our phosphite-catalyzed aerobic auto-oxidation for the synthesis of corresponding pyridines. The mild reaction condition avoids any racemizations during the oxidation, and the determination of enantiomeric excess of corresponding pyridones provides us with the % ee of starting N-alkyl pyridines. These N-alkyl pyridinium salts were used for achiral phosphite-catalysed stereoretentive chiral pyridines from the chiral amine-derived salts, as well as chiral phosphite-catalysed asymmetric pyridine synthesis from racemic N-alkyl pyridinium salts.

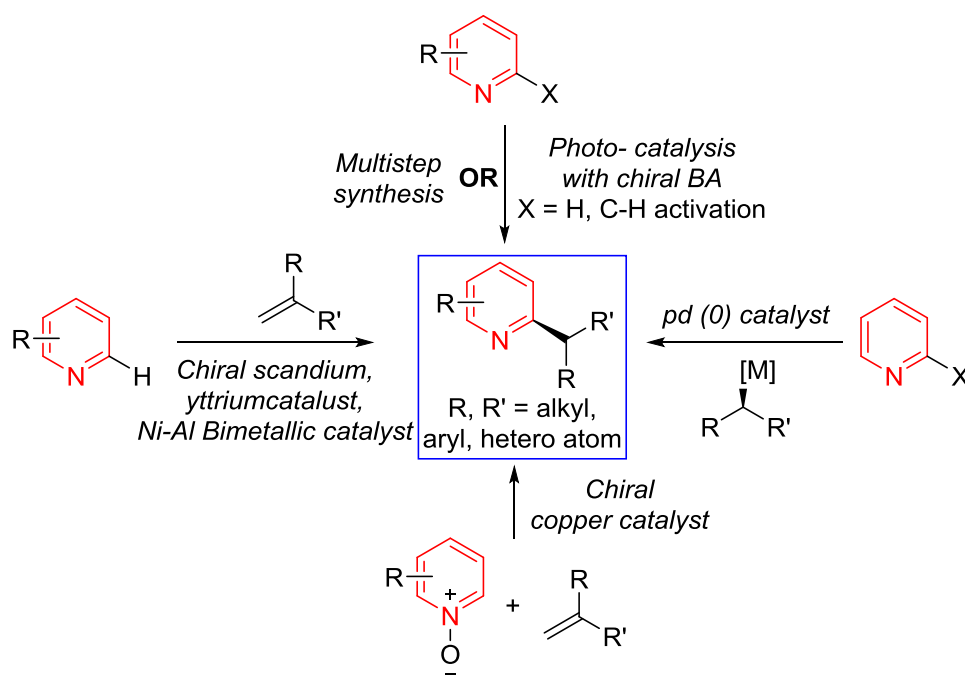


Scheme 4.1: Synthesis of chiral and achiral primary amines, corresponding pyridinium salts & their oxidation

4.2 Introduction

A six-member chiral azaarene scaffold such as isoquinoline, quinoline, and pyridine is found in application for bioactive molecules, in the pharmaceutical industry, as chiral ligands, and sometimes intermediate for drug candidates (chapter 1). Hence, synthesis of these chiral scaffolds, especially for the scaffold having C2 substitution with an α -stereogenic center, remains important and challenging. Regarding this, enormous effort was put by several research groups to develop a synthetic approach for asymmetric transformation via metal catalysis (metal = Pd, Cu, Ni, Sc, Y, etc), by using a stoichiometric amount of chiral reagent

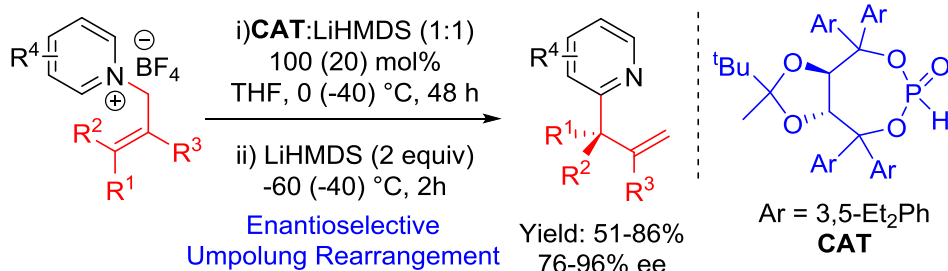
or catalytic amount of chiral ligand with a suitable reacting partner. All the above mentioned methodologies require one extra step and the installation of a functional group leads the methodology more complex. Later on, although photocatalysis developed easy and robust methods for chiral pyridine synthesis still there is no report on asymmetric alkylation of azarenes which can be used further for functionalization as a chiral prevalent backbone (see chapter 1 for details).



Scheme 4.2: Several synthetic routes for chiral Pyridine synthesis

So, the direct and diverse alkylation of imine-embedded pyridine scaffold remains as challenging and demanding and the development of a sustainable approach has encouraged chemists to contribute in this field.

Based on this concept, in 2019 our group achieved successfully established a base-mediated enantioselective aza-[2, 3] Wittig rearrangement to the synthesis of chiral *N*-heterocyclic compounds with good enantioselectivity by using the chiral phosphites (scheme 4.3, also chapter 1).



Scheme 4.3: Phosphite-catalysed asymmetric Aza-[2,3]-rearrangement

4.3 N-alkylpyridinium as alkyl source

Pyridinium salts constitute a privileged class of compounds of both natural and synthetic importance.¹ Over the last century, N-substituted pyridinium scaffolds have been used in organic chemistry as valuable synthetic intermediates or reagents,² oxidants,³ ionic liquids,⁴ phase-transfer catalysts,⁵ as well as in material science⁶ and biology.⁷ Primary alkyl amines have emerged as an inexpensive, stable, abundant, and renewable source⁸ for the generation of reactive salt intermediates and the recent application of its found in alkylation.⁹

¹ Sowmiah, S.; Esperan, S. S. M.; Rebelo, N. P. L.; Afonso, M. A. C. *Org. Chem. Front.* **2018**, *5*, 453.

² a) E. N. Shaw, in *Chemistry of Heterocyclic Compounds*, Interscience Publishers, Inc., New York, **1961**, pp. 1; b) E. Ochiai, *Aromatic Amine Oxides*, Elsevier, Amsterdam, **1967**; c) Kiselyov, S. A. *Chem. Soc. Rev.* **2005**, *34*, 1031.

³ a) Umemoto, T.; Tomita, K.; *Tetrahedron Lett.* **1986**, *27*, 3271; b) Umemoto, T.; Harasawa, K.; Tomizawa, G.; Kawada, K.; Tomita, K. *Bull. Chem. Soc. Jpn.* **1991**, *64*, 1081.

⁴ Welton, T. *Chem. Rev.* **1999**, *99*, 2071.

⁵ Brunelle, J. D.; Singleton, A. D.; *Tetrahedron Lett.* **1984**, *25*, 3383.

⁶ a) Coe, J. B.; Harris, A. J.; Asselberghs, I.; Wostyn, K.; Clays, K.; Persoons, A.; Brunshwig, S. B.; Coles, J. S.; Gelbrich, T.; Light, E. M.; Hursthouse, B. M.; Nakatani, K.; *Adv. Funct. Mater.* **2003**, *13*, 347; b) Madaan, P.; Tyagi, K. V. *J. Oleo Sci.* **2008**, *57*, 197.

⁷ a) Krysinski, J.; *Arch. Pharm.* **1994**, *327*, 247; b) Matos, J. M.; Navo, D. C.; Hakala, T.; Ferhati, X.; Guerreiro, A.; Hartmann, D.; Bernardim, B.; Saar, L. K.; CompaçIn, I.; Corzana, F.; Knowles, J. P. T.; Jimenez-Os8s, G.; Bernardes, L. J. G. *Angew. Chem. Int. Ed.* **2019**, *58*, 6640.; *Angew. Chem.* **2019**, *131*, 6712.

⁸ (a) Froidevaux, V.; Negrell, C.; Caillol, S.; Pascault, P. J.; Boutevin, B. *Chem. Rev.*, **2016**, *116*, 14181; (b) Burn, N.; Hesemann, P.; Esposito, D. *Chem. Sci.*, **2017**, *8*, 4724; (c) Pelckmans, M.; Renders, T.; Vyver, V. S.; Sels, F. B. *Green Chem.*, **2017**, *19*, 5303.

⁹ (a) Crespi, S.; Fagnoni, M. *Chem. Rev.*, **2020**, *120*, 9790; (b) Rossler, L. S.; Jelier, J. B.; Magnier, E.; Fagouset, G.; Carreira, M. E.; Togni, A. *Angew. Chem., Int. Ed.*, **2020**, *59*, 9264; (c) Kong, D.; Moon, J. P.; Lundgren, J. R. *Nat. Catal.*, **2019**, *2*, 473; (d) He, S. F.; Ye, S.; Wu, J. *ACS Catal.*, **2019**, *9*, 8943; (e) Correia, M. T. J.; Fernandes, A. V.; Matsuo, T. B.; Delgado, A. J.; de Souza, C. W.; Paixao, W. M. *Chem. Commun.*, **2020**, *56*, 503; (f) Ouyang, K.; Hao, W.; Zhang, X. W.; Xi, Z. *Chem. Rev.*, **2015**, *115*, 12045.

In 2017, the Watson group developed a nickel catalysed method to generate alkyl radicals from stable N-alkylpyridinium salts, and their coupling with arylboronic acids results in substituted pyridine derivatives. (a).¹⁰ After that, several groups like Rueping,¹¹ Watson,¹² and Martin¹³ was independently worked on nickel catalysis for the reductive cross-coupling reaction of N-alkyl pyridinium salts having C(sp²) halides with suitable coupling partner (a). Parallely, in 2019, Martin and co-workers reported a similar nickel-catalyzed method for the functionalization of unactivated olefins (b).¹⁴ In 2017, Glorius and co-workers explore the radical intermediate formation via a reductive quenching of an excited photocatalyst in the presence of visible light.¹⁵ After that, several groups significantly contribute in this field for the generation of alkyl radicals from N-alkylpyridinium salts and their alkylation with a suitable reacting partner (c).¹⁶ Similarly, in 2019, Molander and co-workers developed a dual catalytic nickel/photoredox cycle for the reductive deamination arylation of N-alkyl pyridinium salts (c).¹⁷ In 2018, Aggarwal *et. al.* and Glorius *et. al.* independently comes up with an approach to EDA chemistry¹⁸ and successively reported deaminating borylation reaction by mixing 1: 1 electron-deficient N-alkyl pyridinium salt and diboron precursor

¹⁰ Basch, H. C.; Liao, J.; Xu, J.; Piane, J. J.; Watson, P. M. *J. Am. Chem. Soc.*, **2017**, *139*, 5313.

¹¹ Yue, H.; Zhu, C.; Shen, L.; Geng, Q.; Hock, J. K.; Yuan, T.; Cavallo, L.; Rueping, M.; *Chem. Sci.* **2019**, *10*, 4430.

¹² Liao, J.; Basch, H. C.; Hoerrner, E. M.; Talley, R. M.; Boscoe, P. B.; Tucker, W. J.; Garnsey, R. M.; Watson, P. M. *Org. Lett.* **2019**, *21*, 2941.

¹³ Martin-Montero, R.; Yatham, R. V.; Yin, H.; Davies, J.; Martin, R. *Org. Lett.* **2019**, *21*, 2947.

¹⁴ Sun, Z. S.; Romano, C.; Martin, R. *J. Am. Chem. Soc.* **2019**, *141*, 16197.

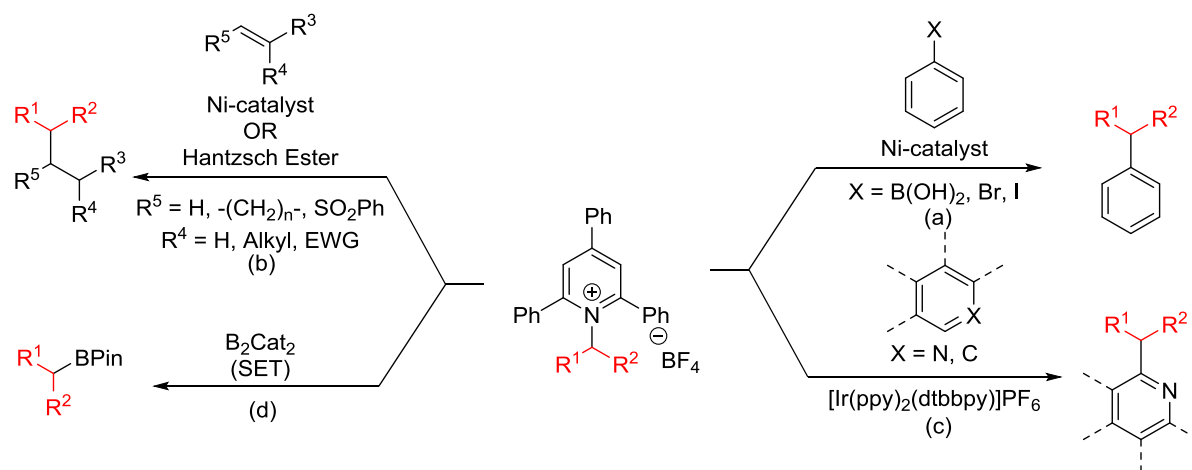
¹⁵ Klauck, R. J. F.; James, J. M.; Glorius, F.; *Angew. Chem. Int. Ed.* **2017**, *56*, 12336; *Angew. Chem.* **2017**, *129*, 12505.; Klauck, R. J. F.; Yoon, H.; James, J. M.; Lautens, M.; Glorius, F. *ACS Catal.* **2019**, *9*, 236.

¹⁶ Ociepa, M.; Turkowska, J.; Gryko, D. *ACS Catal.* **2018**, *8*, 11362.; Jiang, X.; Zhang, M. M.; Xiong, W.; Lu, Q. L.; Xiao, J. W. *Angew. Chem. Int. Ed.* **2019**, *58*, 2402; *Angew. Chem.* **2019**, *131*, 2424.; Yang, K. Z.; Xu, X. N.; Wang, C.; Uchiyama, M.; *Chem. Eur. J.* **2019**, *25*, 5433.; Fu, C. M.; Shang, R.; Zhao, B.; Wang, B.; Fu, Y. *Science*, **2019**, *363*, 1429.; Zhang, M. M.; Liu, F. *Org. Chem. Front.* **2018**, *5*, 3443.

¹⁷ Yi, J.; Badir, O. S.; Kammer, M. L.; Ribagorda, M.; Molander, A. G. *Org. Lett.* **2019**, *21*, 3346.

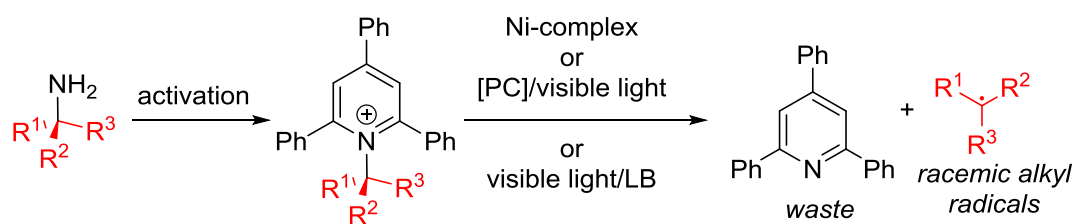
¹⁸ Katritzky, R. A.; de Ville, Z. G.; Patel, C. R. *Tetrahedron Lett.* **1980**, *21*, 1723.; Lee, Y. K.; Kochi, K. J. *J. Chem. Soc. PerkinTrans. 2*, **1992**, *0*, 1011.; Lee, Y. K.; Kochi, K. J. *J. Chem. Soc. Perkin Trans. 2*, **1994**, 237.; Olah, A. G.; Narang, C. S.; Olah, A. J.; Pearson, L. R.; Cupas, A. C. *J. Am. Chem. Soc.* **1980**, *102*, 3507.

having electron-rich aromatic diol ligand attachment (d).¹⁹ Next, in 2019 Aggarwal and co-workers found that the 2, 4, 6-triphenylpyridinium moiety could also form an EDA complex with Hantzsch ester, which upon photoexcitation involved in the SET process to functionalization (b).²⁰



Scheme 4.4: Electrophilic N-alkylpyridinium salts as alkyl source

Overall this approach has become a significant tool for the study of new and elegant deaminative protocols with diverse reaction partners under photoredox and dual catalysis or with redox-active coupling partners. These deaminative processes generate alkyl radicals and are involved in racemic synthesis from both achiral and enantioenriched amines. Additionally, the C–N bond cleavage processes generate triphenyl pyridine as a part of the waste stream. (Scheme X)



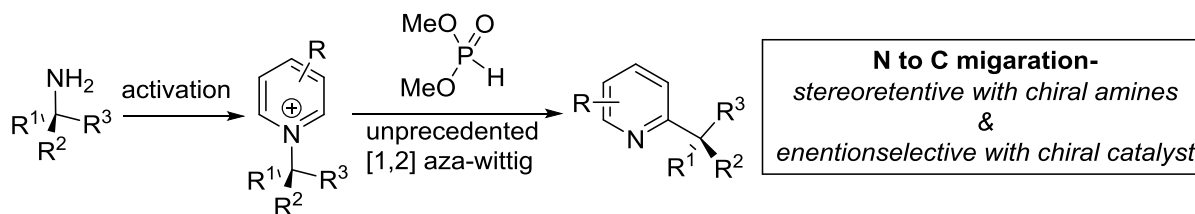
Scheme 4.5: Primary amine as alkylating agents via katritzky pyridinium salts.

4.4 Research Goal

¹⁹ Wu, J.; He, L.; Noble, A.; Aggarwal, K. V. *J. Am. Chem. Soc.* **2018**, *140*, 10700.; Sandfort, F.; Strieth-Kalthoff, F.; Klauk, R. J. F.; James, J. M.; Glorius, F. *Chem. Eur. J.* **2018**, *24*, 17210.

²⁰ Wu, J.; Grant, S. P.; Li, X.; Noble, A.; Aggarwal, K. V. *Angew. Chem. Int. Ed.* **2019**, *58*, 5697; *Angew. Chem.* **2019**, *131*, 5753.

Based on the literature survey and development of phosphite catalysis on aza-[2,3]-rearrangement from our lab, we hypothesized an asymmetric aza-[1,2]-Wittig reaction could be feasible by phosphite catalysis. (scheme 4.6)



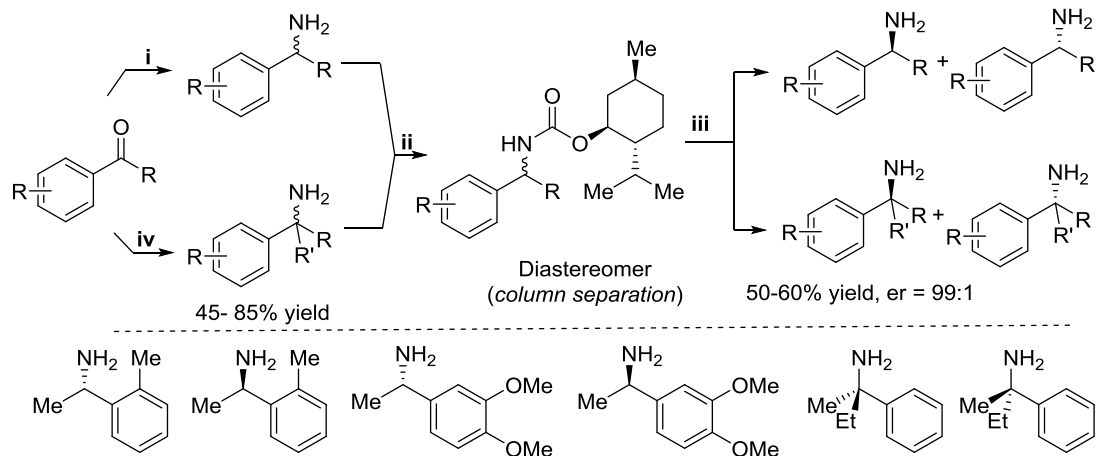
Scheme 4.6: Primary amine as a waste-free chiral alkylating agent: an unprecedented N to C dissociative alkyl migration

4.5 Preparation of chiral amine

The salt-containing maximum amines are laboratory synthesized by using literature-known methods where few are commercially available. For the amine synthesis, we follow the below scheme.²¹ Firstly, we focused to prepared several racemic amines and for the chiral version, a reaction with a compatible chiral auxiliary with this amine form a diastereomeric species (method 1). Further column separation and removal of chiral auxiliary by alkaline hydrolysis give both the chiral amines, R- & S- with less yield with good diastereoselectivity. Based on the project template and requirement of chiral amines, we have looked at the efficient formation of chiral amines. Finally, literature precedent shows the selective formation of chiral amines with good yield and excellent diastereomeric excess (method 2). We also examine the optical rotation of chiral amines and matched them with literature-reported values before using it.

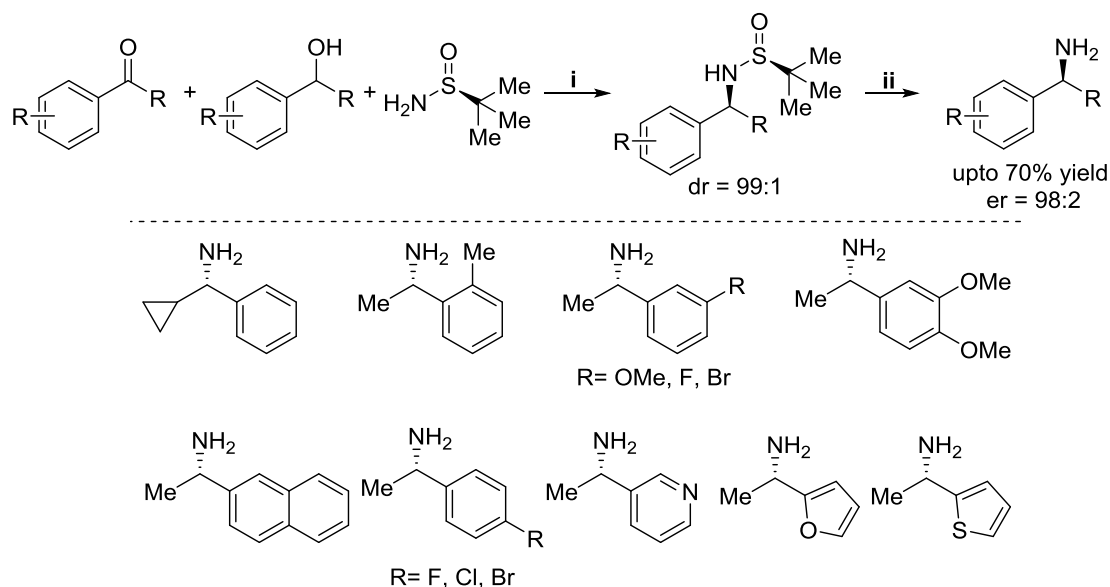
4.5.A Method 1

²¹ Xiao, M.; Yue, X.; Xu, R.; Tang, W.; Xue, D.; Li, C.; Lei, M.; Xiao, J.; Wang, C. *Angew. Chem., Int. Ed.* **2019**, *58*, 10528.; Bagutski, V.; Elford, T. G.; Aggarwal, K. V. *Angew. Chem., Int. Ed.* **2011**, *50*, 1080.; Lawson, C. E.; Luci, K. D.; Ghosh, S.; Kinney, A. W.; Reynolds, H. C.; Qi, J.; Smith, E. C.; Wang, Y.; Minor, K. L.; Haertlein, J. B.; Parry, J. T.; Damiano, P. B.; Maryanoff, E. B. *J. Med. Chem.* **2009**, *52*, 7432.; Nageli, I.; Baud, C.; Serradeil-Albalat, M.; Roussel, C.; Vanthuyne, N.; Vallejos, J.; Wilhelm, D. *Tetrahedron: Asymmetry*, **2008**, *19*, 2682.; Kapoor, M.; Chand-Thakuri, P.; Young, C. M. *J. Am. Chem. Soc.* **2019**, *141*, 7980.; Bernerdinelli, G.; Jacquier, Y.; Moran, M.; Muller, P. *Helv. Chim. Acta.* **1997**, *80*, 1087.



Condition: i) for racemic amine preparation: ketone (1 equiv.), NH_4OAc (10 equiv.), NaBH_3CN (1.2 equiv.), MeOH, r.t.; ii) (-)-(1R)-menthyl chloroformate (1 equiv.), Et_3N (1.5 equiv.), Et_2O , 0 °C-r.t. iii) aq. KOH solution, r.t.; iv) a) $\text{R}'\text{mgBr}$ (1.5 equiv.), THF; (b) NaN_3 (2.2 equiv.), DCM/ TFA; (c) LiAlH_4 (1.1 equiv.), THF

4.5.B Method 2



Condition: i) alcohol (1 equiv.), ketone (0.15 equiv.), chiral amine (1 equiv.), NaOH (0.5 equiv.), toluene, reflux (135 °C), 6 h.; ii) MeOH, HCl (32 %), r.t.

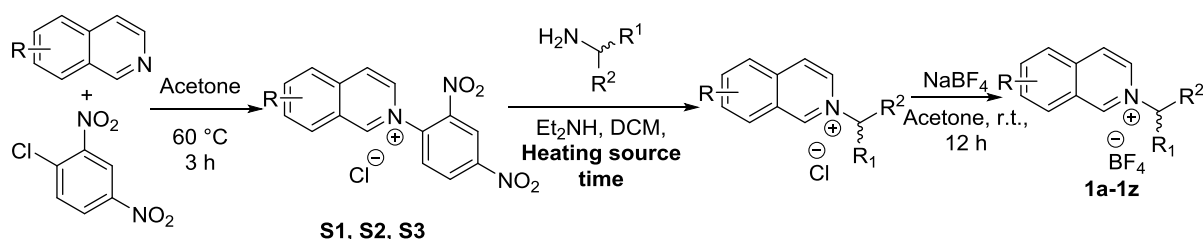
Scheme 4.7: Preparation of amines: Method 1 for both, racemic and chiral & method 2 only for chiral

4.6 Preparation of Substrate

To achieve success, we start to make our design substrate by taking different N-heterocyclic scaffolds with several chiral amines.

4.6.A Isoquinolium salt

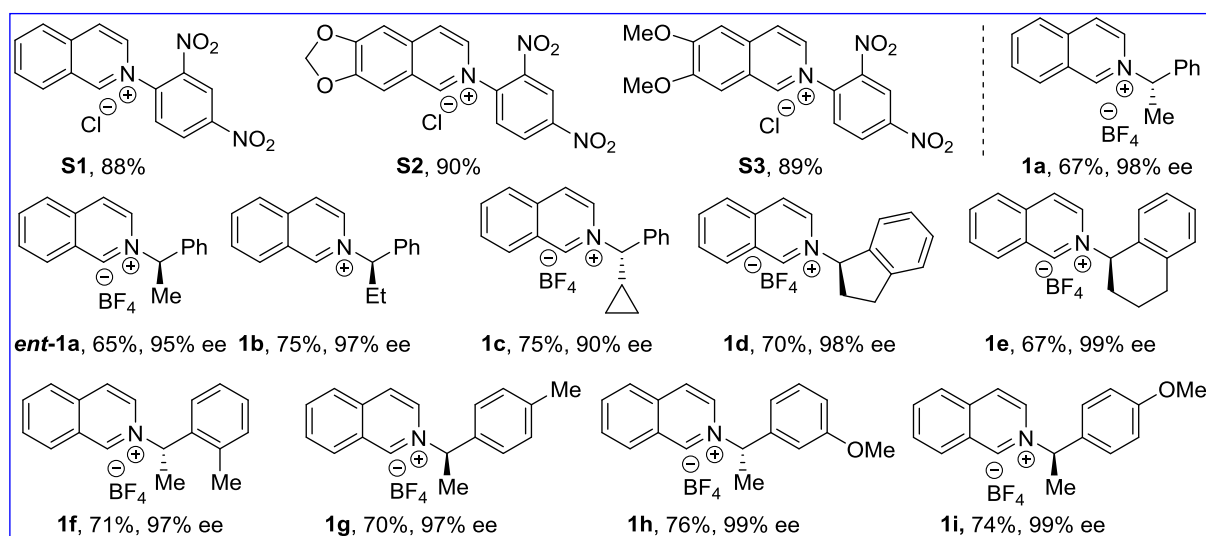
First, we choose isoquinoline moiety, for the preparation of Zincke salt²² and further use of its reaction with different alkylamine derivatives to obtain the expected salt. For that, we developed a method (scheme 4.8). Initial screening to the salt formation with racemic amine from corresponding Zincke salt (S1) in the presence of diethyl amine (Et₂NH) in dichloromethane at room temperature for 48 h works well to provide moderate to good yield. Later on, after getting several chiral amines in our hands (Scheme 4.7), we focused to prepared chiral salt by the same method for the enantioselective phosphite catalysis reaction (Scheme 4.1). The initial success of chiral salt formation and its use under phosphite catalysis resulted in drops of enantiomeric excess occurring in 1,2-alkyl migrated product. Similarly, the salt that is prepared from commercial sources of chiral amines also resulted in stereoselectivity with similar drops of enantiomeric excess. We know it is difficult to check the ee of chiral salt. So, we used chiral salt in the phosphite catalysis reaction by hoping that salt ee should remain the same as in chiral amines. But, probably this is not true as ee drops in reaction outcome. To, figure it out we choose an isoquinolinium chiral salt which is prepared from commercially available chiral amines and oxidized the salt to under mild phosphite catalysis in the presence of oxygen to give isoquinolone (Scheme 4.12). Now HPLC analysis of isoquinolone shows some drops of ee. So, the problem in the chiral salt formation steps as we know oxidation of chiral salt does not hamper the ee too much under phosphite catalysis. To solve this issue, we looked at the very first formation of salt instead of 48 h at room temperature. For this to happen, the microwave is probably the best option, and maintaining the temperature at 35 °C for 30 min by keeping other parameters the same provides a good yield of salt formation. Further, this salt ee is determined by similar oxidation and then use of it for 1,2-alkyl migration via phosphite catalysis to achieve enantioselectivity without drops of ee. So, finally, chiral salt was prepared using a microwave at 35 °C for 30 min and an achiral version was stirred at room temperature for 48 h with chloride anion as a counter ion. Further counteranion exchange in the presence of NaBF₄ gives bench stable salt with BF₄⁻ as counterpart.



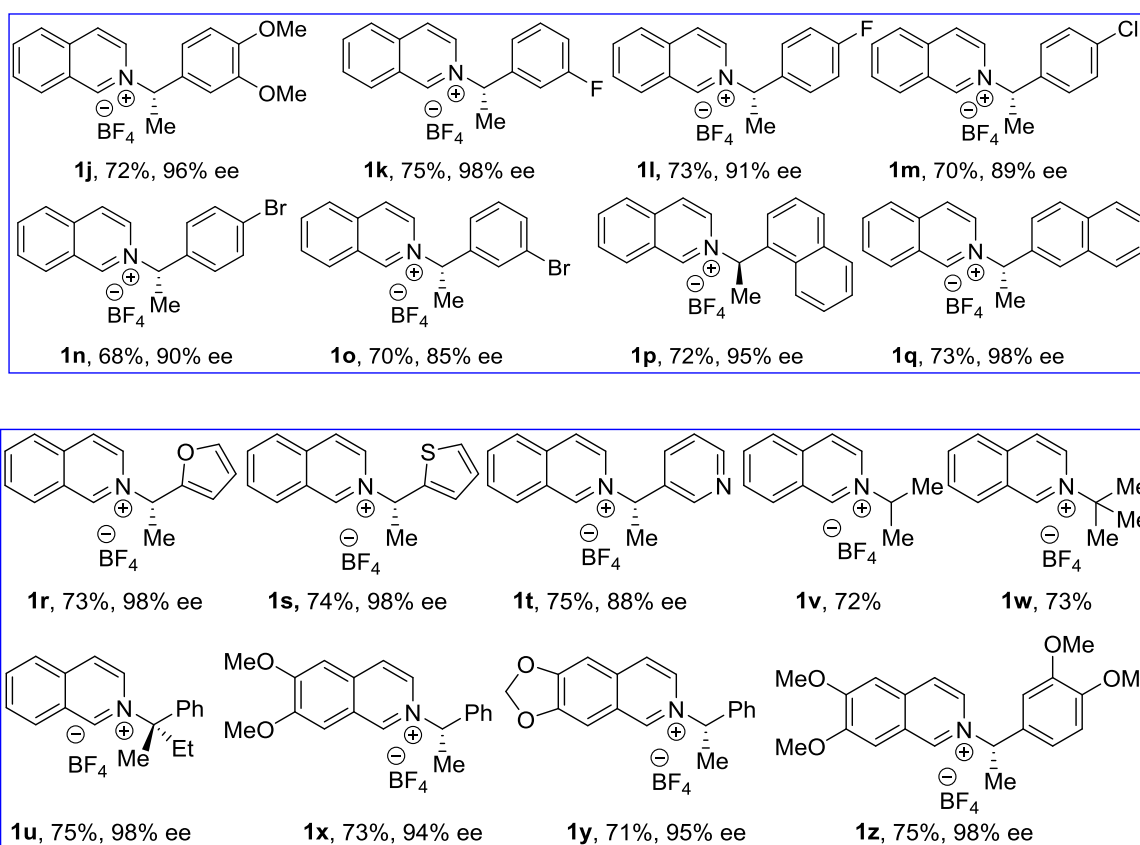
²² Benmekhbi, L.; Louafi, F.; Roisnel, T.; Hurvois, P. J. *J. Org. Chem.* **2016**, *81*, 6721.

Scheme 4.8: General scheme for the preparation of chiral isoquinolinium salt

Initial screening of chiral α -methyl benzylamine with zincky salt gives, corresponding chiral salt I moderate yield (**1a**, *ent-1a*). Changing methyl to ethyl (**1b**), cyclopropyl (**1c**), fused cyclopentyl (**1d**), and cyclohexyl (**1e**) all resulted in moderate yields of salt formation. These salts are prepared to check the influence of the alkyl group at the migrating carbon on the reaction outcome. Especially for the case of α -cyclopropyl group ring-opening happening or not. After that, we varied the aryl groups at the migrating carbon by introducing several groups to show the influence of steric as a well-electronic factor on the reaction outcome (**1f-1o**). Further changing of the aryl group to α -Naphthyl, β -naphthyl provides effective salt formation in good yield (**1p**, **1q**). Then, moving to Heteroaryl groups, such as electron-rich 2-furan (**1r**), 2-thiophene (**1s**), and electron-deficient 3-pyridine (**1t**) also form salt in good yields. Later on, we synthesized an isoquinolinium salt of tertiary and quaternary amine (**1u**, **1v**, & **1w**) with a good yield to check the effect of phenyl stabilization for the reaction to happen. After that to focus on the application of alkyl migrated product, we synthesized salt (**1x**, **1y**, & **1z**) in good yield.²³



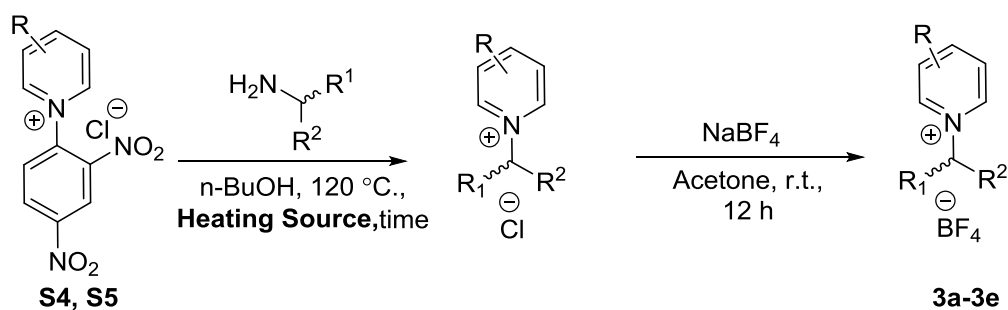
²³ Haiyan, L.; Gaoping, L.; Liu, J. *WO2010075469A1*, **2010**, 2010075469.; Zhou, S.; Tong, R. *Chem. Eur. J.* **2016**, *22*, 7084.; Mengozzi, L.; Gualandi, A.; Cozzi, G. P. *Chem. Sci.*, **2014**, *5*, 3915.; Zhou, S.; Tong, R. *Org. Lett.* **2017**, *19*, 1594.; Yu, J.; Zhang, Z.; Zhou, S.; Zhang, W.; Tong, R. *Org. Chem. Front.*, **2018**, *5*, 242.



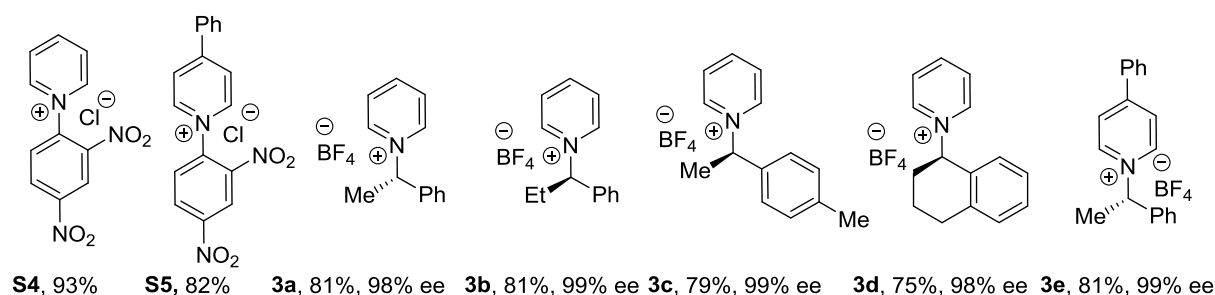
Scheme 4.9: Synthesis of several isoquinolium chiral salts

4.6.B Pyridinium salt

Pyridine was chosen as another moiety for making salt. For that, we prepared Zincke salt first, then use it for reaction with the chiral amine to make the corresponding salt. Using of microwave at 120 °C for 5 min works for the chiral version and achiral synthesis reflux at 120 °C for 12 h works well.



Scheme 4.10: General scheme for the preparation of chiral pyridinium salt



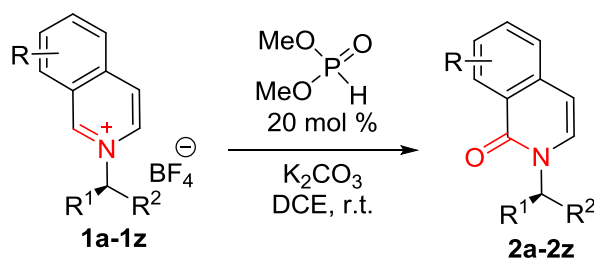
Scheme 4.11: Synthesis of several pyridinium chiral salts

4.7 Oxidation of salt

We used chiral amine to prepare several chiral salts of isoquinolium and pyridinium scaffold. Although we used chiral amine, the chirality of salts could fluctuate after the salt formation reaction. To figure out the exact chirality of the salt, we oxidized the corresponding salt under standard conditions and inject the oxo-product in HPLC to find the enantioselectivity.

4.7.A Oxidation of isoquinolium salt

For the oxidation of isoquinolium salt, we chose our phosphite method (third chapter). Here using 20 mol % dimethyl hydrogen phosphite (DMHP) in the presence of K_2CO_3 as a base in DCE as solvent at room temperature provides 65-85 % yield. After column purification, check the enantioselectivity by the HPLC method.

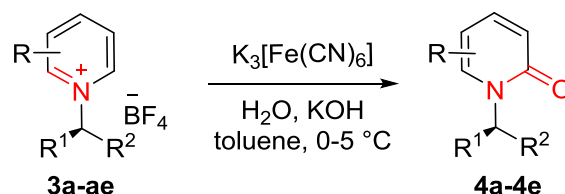


Scheme 4.12: Oxidation of chiral isoquinolium salt by phosphite catalysis

4.7.B Oxidation of pyridinium salt

As we know, our phosphite method for oxidation of the pyridinium system not works under standard conditions, (third chapter). So, we choose a literature-known traditional method for

the oxidation of pyridinium salt by using $K_3[Fe(CN)_6]$ as an oxidant in the presence of aqueous KOH solution in toluene at 0-5 °C.²⁴



Scheme 4.13: Oxidation of chiral pyridinium salt by phosphite catalysis

4.8 Conclusion

In conclusion, we synthesis of chiral and racemic primary amines and their corresponding pyridinium salts. For chiral pyridinium salt synthesis, procedure was modified to achieve chiral pyridinium salts without the racemization of chiral amines. These chiral salt was utilized our phosphite-catalyzed aerobic auto-oxidation for the synthesis of corresponding pyridones to find the ee of salts as the enantiomeric excess of pyridinium salts was not reported, and we failed to find a suitable chiral HPLC method to separate enantiomers. Further, These N-alkyl pyridinium salts were used for enantioselective phosphite catalysis reaction to produce chiral alkyldiarypyridines with out waste of pyridine scaffold.

²⁴ Troster, A.; Bach, T. *Chem. Commun.* **2019**, 55, 302.

4.9 Experimental Procedures

4.9.1 General Information

The rearrangement reactions were carried out with anhydrous solvents in flame-dried glass wares under anhydrous argon and oxygen free conditions. All other reactions were carried out under anhydrous and argon atmosphere. THF was used from MBRAUN (MB-SPS-COMPACT) solvent purification system. All other solvents were purchased anhydrous and stored under argon over 4 Å molecular sieves. Analytical thin-layer chromatography was performed on glass plates pre-coated with silica gel (Silica Gel 60 F254; Merck). Plates were visualized using UV light ($\lambda = 254$ nm) and then stained with either aqueous basic potassium permanganate (KMnO₄) or p-anisaldehyde and developed upon heating in Hitachi heat gun. Flash chromatography was performed using silica gel (Merck and Spectrochem, 230-400 mesh), eluting with solvents as indicated. Flash column was performed using Sebo aquarium air pump (SB-548A). ¹H, ¹³C and ³¹P spectrum were acquired in deuterated solvents at room temperature on Bruker: Ultrashield 400 MHz, Ultrashield 500 MHz and JEOL 400 spectrometer. Chemical shifts (δ) are reported for ¹H NMR in ppm from TMS as internal standard and ¹³C from the residual solvent peak. ¹H NMR spectra are reported as follows: chemical shift (δ ppm), multiplicity, coupling constant (Hz), and integration. Data for ¹³C NMR spectra are reported in terms of chemical shift (δ ppm). Melting points were recorded in Buchi Melting Point B-540 instrument and reported in °C. FT-IR were analyzed in Bruker ALPHA instrument and reported as cm⁻¹. High resolution (HRMS) mass spectral analyses were recorded by High-resolution mass spectrometry using ESI TOF mass analyzer. Chiral HPLC separations were achieved using an Agilent 1260 Infinity series normal phase HPLC unit and HP Chemstation software with Chiralpak® Diacel columns (250 × 4.6 mm). All eluent systems were isocratic. Specific rotations were recorded on JASCO P-2000 Digital Polarimeter. For pyridinium salt synthesis Microwave irradiation experiments were conducted using an Anton Paar microwave 300 single mode microwave reactor. For conducting all microwave irradiation experiments reusable 20 mL pyrex vials were utilized.

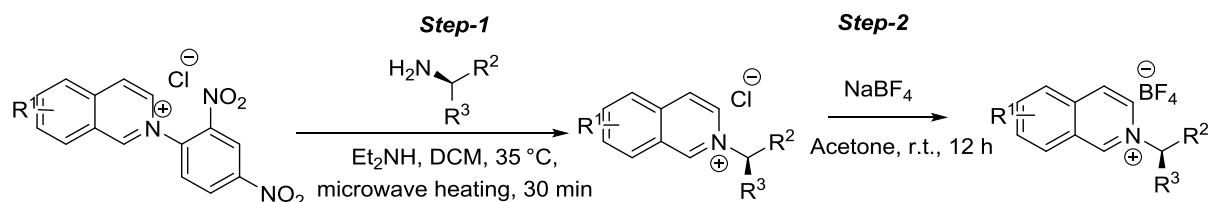
4.9.2 Materials

Commercially available reagents were purchased and used as obtained. Substituted analogs of isoquinoline such as 6,7-dimethoxyisoquinoline¹ and [1,3]dioxolo[4,5-g]isoquinoline² were synthesized following literature procedure. For salt formation all chiral and racemic amines were synthesized following literature procedures.^{3,4,5} Racemic and chiral pyridinium salts were synthesized following the literature procedure.^{6,7} For asymmetric version, chiral

phosphite catalysts were used from the library of catalyst used in our previous report.⁸ The literature reported spectral data were compared favorably with our ¹H NMR spectra of these compounds.

4.9.3 Preparation of chiral salt

A. General procedure for microwave promoted synthesis of N-alkyl Isoquinolinium salts



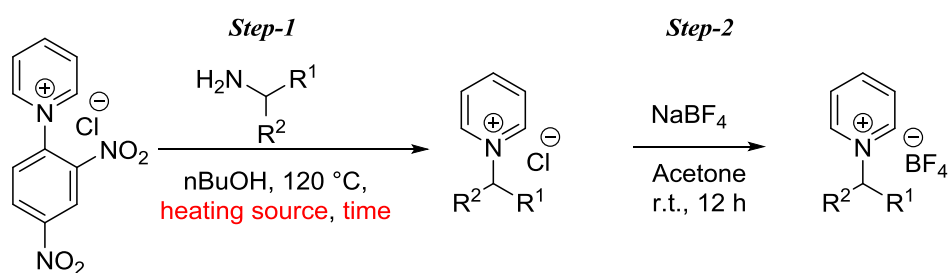
Step-1:

In a flame dried G-20 microwave vial with magnetic bar dinitro-phenyl isoquinolinium salt (3 mmol, 1 equiv.) in dry dichloromethane (9 mL) was taken. To this solution, appropriate chiral amine (3.6 mmol, 1.2 equiv.) was added and the resultant mixture was allowed to react under microwave conditions at 35 °C for 30 min. Upon complete consumption (monitored by TLC), the reaction mixture was directly poured into silica-gel column (3.5 cm in diameter, 40g of silica-gel 230 – 400 mess) and run 100 mL DCM solvent and next we used 5% MeOH/DCM to remove dinitro-phenylamine followed by 10% MeOH/DCM to obtain pure chloride salt.

Step-2:

Acetone (10 mL) was added to a flame dried 50 mL round bottom flask containing pyridinium chloride salt (3 mmol) under argon and stirred at room temperature for 10-15 min until the salt was dissolved. After that sodium tetrafluoroborate (15 mmol, 5 equiv.) was added to the solution and stirred at 30-35 °C. The anion exchange was monitored by TLC (the tetrafluoroborate salt is lower in polarity compare to the corresponding chloride salt). The complete exchange was judged by TLC, and the sodium chloride was filtered off. The solvent was removed under reduced pressure and the residual solid was purified by small silica pad filtration to obtain pure tetrafluoroborate salt.

B. General procedure for microwave promoted synthesis of pyridinium salt

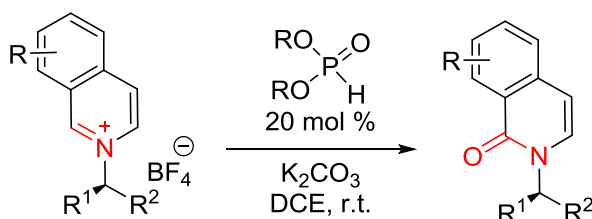


Step-1:

In a flame dried G-20 microwave vial with magnetic bar, dinitro-phenyl pyridinium salt (3 mmol, 1 equiv.) in dry n-BuOH (9 mL) was taken. To this solution, appropriate chiral amine (3.6 mmol, 1.2 equiv.) was added and the resultant mixture was allowed to react under microwave conditions at 120 °C for 5 min. Upon complete consumption (monitored by TLC), the reaction mixture was directly poured into silica-gel column (3.5 cm in diameter, 40g of silica-gel 230 – 400 mesh) and run 250 mL DCM solvent to remove alcohol and next we used 5% MeOH/DCM to remove dinitro-phenylamine) followed by 10% MeOH/DCM to obtain pure chloride salt.

Step-2:

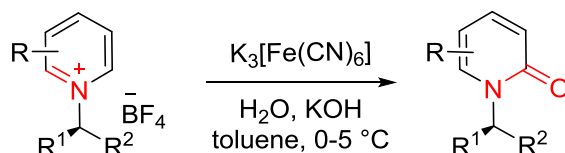
Acetone (10 mL) was added to a flame dried 50 ml round bottom flask containing pyridinium chloride salt (3 mmol) under argon and stirred at room temperature for 10-15 min until the salt dissolved. After that sodium tetrafluoroborate (15 mmol, 5 equiv.) was added to the solution and stirred at 30-35 °C. The anion exchange was monitored by TLC (the tetrafluoroborate salt is lower in polarity compare to the corresponding chloride salt). The complete exchange was judged by TLC, and the sodium chloride was filtered off. The solvent was removed under reduced pressure and the residual solid was purified by small silica pad filtration to obtain pure tetrafluoroborate salt.

4.9.4 Oxidation of chiral salt**C. General procedure for oxidation of isoquinolinium salt**

DCE (2 ml) was added to a dry 10 ml reaction tube containing isoquinolinium salt (0.3 mmol) under air and stirred at room temperature for 10-15 min until the salt dissolved. The reaction tube was closed via an open top cap with septa and cooled to 0 °C under air balloon. To the above mixture dimethyl hydrogen phosphite (DMHP, 20 mol %) was added followed by K_2CO_3 (3 equiv.) and stirred for 2h. Then the reaction tube was slowly brought to room temperature with TLC monitoring for the consumption of starting quinolinium salt. Upon completion, saturated sodium chloride solution (5 ml) was added to quench the reaction, and the organic layer was extracted with ethyl acetate (3 times). The combined organic layer was

dried over anhydrous sodium sulfate, and the solvent was removed under reduced pressure to obtain the crude which was filtered through a 6-inch silica column to get the desired product in pure form.

D. General procedure for oxidation of pyridinium salt

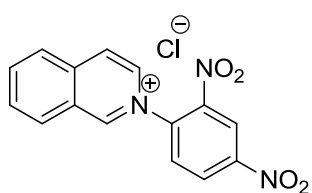


Water (2 ml) was added to a oven dry 10 ml reaction tube containing pyridinium salt (0.3 mmol) under air and stirred at room temperature for 10-15 min until the salt dissolved. The reaction tube was closed via an open top cap with septa and cooled to 0 °C under air balloon. To the above mixture a solution of Potassium hexacyanoferrate (III) (11 equiv.) in water (2 mL) was added dropwise over a period of 10 min. Then a solution of KOH (15.8 equiv.) in water (2 mL) was added dropwise over 5 min with stirred. Finally, Toluene (3 mL) was added to it. Then the reaction tube was slowly brought to room temperature with TLC monitoring for the consumption of starting pyridinium salt. Upon completion, saturated sodium chloride solution (5 ml) was added to quench the reaction, and the organic layer was extracted with ethyl acetate (3 times). The combined organic layer was dried over anhydrous sodium sulfate, and the solvent was removed under reduced pressure to obtain the crude which was filtered through a 6-inch silica column to get the desired product in pure form.

4.10 Compound characterization data

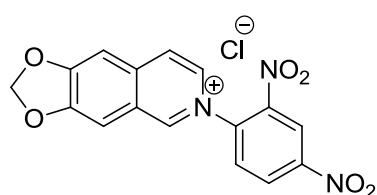
4.10.1 Compound characterization data for zinky's salt

2-(2,4-dinitrophenyl)isoquinolin-2-ium chloride (S1)



The titled compound was prepared following the literature procedure, obtained as a brown solid (1.7 g, 88% yield). R_f (MeOH/DCM; 10:90) = 0.8. The spectral values were matched favourably with previously reported literature values.²⁵

6-(2,4-dinitrophenyl)-[1,3]dioxolo[4,5-g]isoquinolin-6-ium chloride (S2)

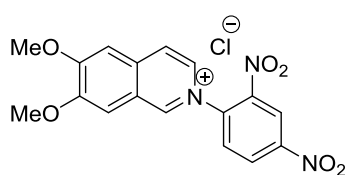


The titled compound was prepared following the literature procedure,²⁵ obtained as a yellowish solid (2.0 g, 90% yield). R_f (MeOH/DCM; 10:90) = 0.10. MP = 223.4 - 224.5 °C. $^1\text{H NMR}$ (400 MHz, DMSO- d_6) δ 10.13 (s, 1H), 9.13 (d, J = 2.50 Hz,

²⁵ Benmekhbi, L.; Louafi, F.; Roisnel, T.; Hurvois, P. J. *J. Org. Chem.* **2016**, *81*, 6721.

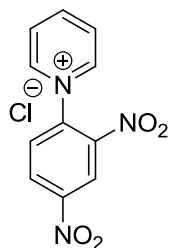
1H), 9.00 (dd, $J = 8.75, 2.50$ Hz, 1H), 8.91 (dd, $J = 6.88, 1.50$ Hz, 1H), 8.60 - 8.49 (m, 2H), 7.94 (d, $J = 3.00$ Hz, 2H), 6.53 (s, 2H). ^{13}C NMR (100 MHz, DMSO- d_6) δ 157.9, 151.8, 148.8, 146.7, 143.4, 139.1, 139.1, 134.5, 132.1, 130.1, 125.0, 123.3, 121.6, 105.0, 104.6, 103.5. FTIR (cm^{-1}): 3111, 3046, 2924, 1607, 1543, 1462, 1350, 1277, 1179, 1031, 967, 918, 740. HRMS (ESI) m/z Calculated for $\text{C}_{16}\text{H}_{10}\text{N}_3\text{O}_6$ $[\text{M}]^+$: 340.0564, found: 340.0572.

2-(2,4-dinitrophenyl)-6,7-dimethoxyisoquinolin-2-ium chloride (S3)



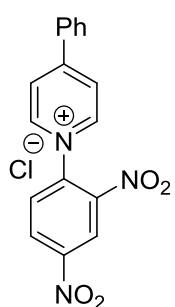
The titled compound was prepared following the literature procedure,²⁵ obtained as a yellowish solid (2.1 g, 89% yield). R_f (MeOH/DCM; 10:90) = 0.10. MP = 133.5 – 135.5 °C. ^1H NMR (400 MHz, DMSO- d_6) δ 10.11 (s, 1H), 9.14 (d, $J = 2.38$ Hz, 1H), 9.00 (dd, $J = 8.63, 2.38$ Hz, 1H), 8.88 (d, $J = 6.75$ Hz, 1H), 8.61 - 8.48 (m, 2H), 8.01 (s, 1H), 7.97 (s, 1H), 4.16 (s, 3H), 4.04 (s, 3H). ^{13}C NMR (100 MHz, DMSO- d_6) δ 59.3, 152.9, 148.9, 146.4, 143.5, 139.3, 136.6, 134.0, 132.1, 130.2, 123.4, 122.8, 121.7, 108.1, 106.4, 57.3, 56.6. FTIR (cm^{-1}): 2077, 1613, 1528, 1489, 1428, 1350, 1270, 1195, 997. HRMS (ESI) m/z Calculated for $\text{C}_{17}\text{H}_{14}\text{N}_3\text{O}_6$ $[\text{M}]^+$: 356.0877, found: 356.0893.

1-(2,4-dinitrophenyl)pyridin-1-ium chloride (S4)



The titled compound was prepared following the literature procedure, obtained as a yellowish solid (1.6 g, 93% yield). R_f (MeOH/DCM; 10:90) = 0.11. The spectral values were matched favourably with previously reported literature values.²⁶

1-(2,4-dinitrophenyl)-4-phenylpyridin-1-ium chloride (S5)



The titled compound was prepared following the literature procedure, obtained as a yellowish solid (1.46 g, 82% yield). R_f (MeOH/DCM; 10:90) = 0.12. The spectral values were matched favorably with previously reported literature values.²⁷

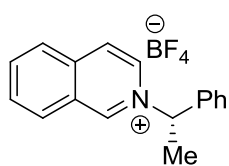
4.13.2 Compound characterization data for pyridinium salts:

The e.r. for each pyridinium salts were confirmed by the HPLC analysis of their oxidation product (pyridone).^{27,28}

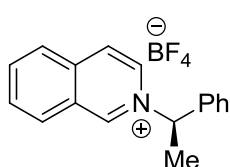
²⁶ Chen, S.; Yamasaki, M.; Polen, S.; Gallucci, J.; Hadad, M. C. *J. Am. Chem. Soc.* **2015**, *137*, 12276.

²⁷ Steinhardt, E. S.; Silverston, S. J.; Vanderwal, D. C. *J. Am. Chem. Soc.* **2008**, *130*, 7560.

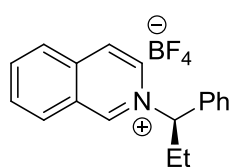
²⁸ Motaleb, A.; Bera, A.; Maity, P.; *Org. Biomol. Chem.* **2018**, *16*, 5081.

(S)-2-(1-phenylethyl)isoquinolin-2-ium tetrafluoroborate (1a)

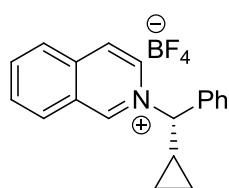
The titled compound was prepared by following the above procedure A, obtained as brown solid (1.3 g, 67% yield, 99.0:1.0 e.r. (98% ee). R_f (MeOH/DCM = 10:90) = 0.6. The spectral values were matched favourably with previously reported literature values.²⁹

(R)-2-(1-phenylethyl)isoquinolin-2-ium tetrafluoroborate (ent-1a)

The titled compound was prepared by following the above procedure A, obtained as brown solid (1.3 g, 68% yield, 2.5:97.5 e.r. (95% ee). R_f (MeOH/DCM = 10:90) = 0.6. The spectral values were matched favourably with previously reported literature values.²⁹

(R)-2-(1-phenylpropyl)isoquinolin-2-ium tetrafluoroborate (1b)

The titled compound was prepared by following the above procedure A, obtained as a yellow solid (1.5 g, 75% yield, 1.5:98.5 e.r. (97% ee). $[\alpha]_D^{25} +1.2$ (c = 1.0, CH₂Cl₂). R_f (MeOH/DCM; 10:90) = 0.4. MP = 116.5 - 117.0 °C. ¹H NMR (500 MHz, DMSO-*d*₆) δ 10.36 (s, 1H), 8.92 (d, *J* = 6.87 Hz, 1H), 8.63 (d, *J* = 6.87 Hz, 1H), 8.58 (d, *J* = 8.39 Hz, 1H), 8.37 (d, *J* = 8.01 Hz, 1H), 8.30 (t, *J* = 7.44 Hz, 1H), 8.13 (t, *J* = 7.63 Hz, 1H), 7.70 (d, *J* = 7.25 Hz, 2H), 7.55 - 7.42 (m, 3H), 6.08 (t, *J* = 7.63 Hz, 1H), 2.68 - 2.62 (m, 2H), 0.94 (t, *J* = 7.06 Hz, 3H). ¹³C NMR (125 MHz, DMSO-*d*₆) δ 148.8, 137.3, 136.8, 133.3, 131.4, 130.8, 129.5, 129.3, 127.8, 127.5, 127.3, 126.7, 75.4, 26.0, 10.4. FTIR (cm⁻¹): 3067, 2977, 2937, 2885, 1643, 1507, 1462, 1399, 1274, 1066, 884, 827, 738. HRMS (ESI) *m/z* Calculated for C₁₈H₁₈N [M]⁺: 248.1433, found: 248.1443.

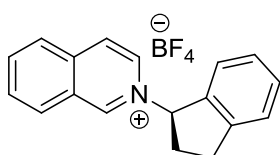
(S)-2-(cyclopropyl(phenyl)methyl)isoquinolin-2-ium tetrafluoroborate (1c)

The titled compound was prepared by following the above procedure A, obtained as a yellow solid (1.5 g, 75% yield, 5.2:94.8 e.r. (90% ee). $[\alpha]_D^{25} -1.5$ (c = 1.0, CH₂Cl₂). R_f (MeOH/DCM; 10:90) = 0.4. MP = 118.2 - 120.5 °C. ¹H NMR (400 MHz, DMSO-*d*₆) δ 10.37 (s, 1H), 8.86 (dd, *J* = 6.94, 1.44 Hz, 1H), 8.63 (dd, *J* = 7.25, 4.50 Hz, 2H), 8.40 (d, *J* = 8.13 Hz, 1H), 8.32 (ddd, *J* = 8.22, 7.04, 1.13 Hz, 1H), 8.14 (ddd, *J* = 8.25, 7.07, 1.06 Hz, 1H), 7.64 - 7.59 (m, 2H), 7.52 - 7.43 (m, 3H), 5.51 (d, *J* = 10.26 Hz, 1H), 2.24 - 2.14 (m, 1H), 1.08 - 1.00 (m, 1H), 0.85 - 0.75 (m, 2H), 0.75 - 0.69 (m, 1H). ¹³C NMR (100 MHz, DMSO-*d*₆) δ 148.8, 137.6, 137.3, 137.3, 133.7, 131.4, 130.9, 129.2, 129.2, 127.5, 127.4, 127.3, 126.4, 78.5, 15.0, 6.5, 4.8. FTIR (cm⁻¹

²⁹ Troster, A.; Bach, T.; *Chem. Commun.* **2019**, 55, 302.

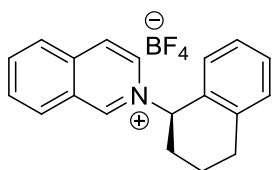
¹): 3072,2923, 1643, 1505, 1462, 1396, 1281, 1064, 881, 828, 735. **HRMS** (ESI) *m/z* Calculated for C₁₉H₁₈N [M]⁺: 260.1434, found: 260.1441.

(R)-2-(2,3-dihydro-1H-inden-1-yl)isoquinolin-2-ium tetrafluoroborate (1d)



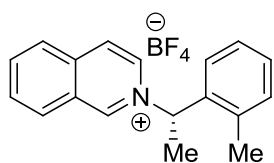
The titled compound was prepared by following the above procedure **B**, obtained as a brown solid (1.4 g, 70% yield, 99.1:0.9 e.r.(98% ee). $[\alpha]_{\text{D}}^{25}$ -1.6 (c = 0.7, CH₂Cl₂). R_f (MeOH/DCM; 10:90) = 0.40. MP = 180.6 – 181.5 °C. ¹H NMR (400 MHz, DMSO-*d*₆) δ 10.08 (s, 1H), 8.64 - 8.48 (m, 3H), 8.38 (d, *J* = 8.25 Hz, 1H), 8.29 (ddd, *J* = 8.22, 7.04, 1.13 Hz, 1H), 8.10 (ddd, *J* = 8.29, 7.04, 1.06 Hz, 1H), 7.52 (d, *J* = 7.63Hz,1H), 7.47 (td, *J* = 7.19, 1.50 Hz, 1H), 7.39 - 7.27 (m, 2H), 6.59 (dd, *J* = 8.38, 5.38 Hz, 1H), 3.44 - 3.34 (m, 1H), 3.19 - 3.09 (m, 1H), 3.07 – 2.98 (m, 1H). 2.53 – 2.62 (m, 1H). ¹³C NMR (100 MHz, DMSO-*d*₆) δ 149.3, 145.0, 138.9, 137.4, 137.1, 133.1, 131.2, 130.8, 130.0, 127.5, 127.6, 127.3, 126.5, 125.5, 125.3, 75.6, 33.7, 30.2. **FTIR** (cm⁻¹): 3075, 2995, 2938, 2867, 1642, 1516, 1467, 1401, 1286, 1179, 1049, 829, 765. **HRMS** (ESI) *m/z* Calculated for C₁₈H₁₆N[M]⁺: 246.1277, found: 246.1288.

(R)-2-(1,2,3,4-tetrahydronaphthalen-1-yl)isoquinolin-2-ium tetrafluoroborate (1e)



The titled compound was prepared by following the above procedure **A**, obtained as a yellow solid (1.4 g, 67% yield, 99.3:0.7 e.r.(99% ee). $[\alpha]_{\text{D}}^{25}$ +1.6 (c = 1.0, CH₂Cl₂). R_f (MeOH/DCM; 10:90) = 0.45. MP = 127.0 – 129.2 °C. ¹H NMR (500 MHz, DMSO-*d*₆) δ 10.10 (s, 1H), 8.67 (dd, *J* = 6.87, 1.14 Hz, 1H), 8.59 (d, *J* = 6.87 Hz, 1H), 8.54 (d, *J* = 8.01 Hz, 1H), 8.38 (d, *J* = 8.01 Hz, 1H), 8.31 - 8.28 (m, 1H), 8.13 - 8.06 (m, 1H), 7.41 - 7.33 (m, 2H), 7.19 - 7.16 (m, 1H), 6.94 (d, *J* = 7.63 Hz, 1H), 6.35 (t, *J* = 7.06 Hz, 1H), 3.02 - 3.12 (m, 1H), 2.91 (dt, *J* = 17.07, 5.39 Hz, 1H), 2.53 - 2.61 (m, 1H), 2.39 - 2.30 (m, 1H), 2.04 - 1.94 (m, 1H), 1.93 - 1.82 (m, 1H). ¹³C NMR (125 MHz, DMSO-*d*₆) δ 150.3, 139.0, 137.4, 137.2, 134.1, 131.7, 131.3, 130.8, 129.7, 129.0, 128.6, 127.4, 127.3, 126.9, 126.3, 69.5, 31.5, 28.4, 19.7. **FTIR** (cm⁻¹): 3067, 2938, 2868, 1644, 1505, 1456, 1401, 1284, 1062, 878, 827, 752. **HRMS** (ESI) *m/z* Calculated for C₁₉H₁₈N [M]⁺: 260.1434, found: 260.1434.

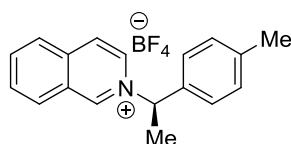
(S)-2-(1-(*o*-tolyl)ethyl)isoquinolin-2-ium tetrafluoroborate (1f)



The titled compound was prepared by following the above procedure **A**, obtained as a brown solid (1.4 g, 71% yield, 98.4:1.6 e.r.(97% ee). $[\alpha]_{\text{D}}^{25}$ -1.8 (c = 1.0, CH₂Cl₂). R_f (MeOH/DCM; 10:90) = 0.41. MP = 118.9 – 119.7 °C. ¹H NMR (400 MHz, DMSO-*d*₆) δ 10.20 (s, 1H),

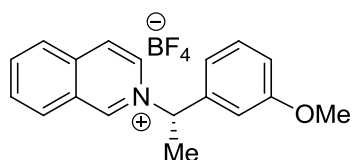
8.81 - 8.67 (m, 1H), 8.65 - 8.55 (m, 2H), 8.40 - 8.33 (m, 1H), 8.33 - 8.24 (m, 1H), 8.11 (t, $J = 7.63$ Hz, 1H), 7.58 - 7.48 (m, 1H), 7.40 - 7.33 (m, 2H), 7.33 - 7.26 (m, 1H), 6.49 (q, $J = 6.80$ Hz, 1H), 2.32 (s, 3H), 2.11 (d, $J = 6.88$ Hz, 3H). ^{13}C NMR (100 MHz, DMSO- d_6) δ 148.7, 137.2, 137.2, 135.8, 133.9, 131.3, 131.2, 130.9, 129.4, 127.4, 127.2, 126.9, 126.7, 126.3, 66.7, 20.6, 18.9. FTIR (cm^{-1}): 3068, 2923, 2857, 1641, 1460, 1395, 1283, 1054, 827, 764. HRMS (ESI) m/z Calculated for $\text{C}_{18}\text{H}_{18}\text{N}$ $[\text{M}]^+$: 248.1434, found: 248.1445.

(R)-2-(1-(p-tolyl)ethyl)isoquinolin-2-ium tetrafluoroborate (1g)



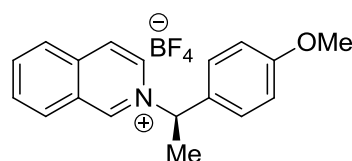
The titled compound was prepared by following the above procedure **A**, obtained as a yellow solid (1.4 g, 70% yield, 1.3:98.7e.r. (97% ee). $[\alpha]_{\text{D}}^{25} -2.1$ ($c = 1.0$, CH_2Cl_2). R_f (MeOH/DCM; 10:90) = 0.4. MP = 123.8 – 124.5 °C. ^1H NMR (400 MHz, DMSO- d_6) δ 10.31 (s, 1H), 8.83 (dd, $J = 7.33$, 1.37 Hz, 1H), 8.60 - 8.56 (m, 2H), 8.41 - 8.33 (m, 1H), 8.33 - 8.24 (m, 1H), 8.16 - 8.08 (m, 1H), 7.51 (d, $J = 7.78$ Hz, 2H), 7.29 (d, $J = 7.78$ Hz, 2H), 6.30 (q, $J = 6.87$ Hz, 1H), 2.32 (s, 3H), 2.15 (d, $J = 6.87$ Hz, 3H). ^{13}C NMR (100 MHz, DMSO- d_6) δ 148.7, 138.9, 137.2, 135.2, 133.4, 131.3, 130.8, 129.7, 127.4, 127.3, 127.3, 126.3, 69.3, 20.7, 19.8. FTIR (cm^{-1}): 3068, 2990, 2926, 1644, 1515, 1461, 1399, 1282, 1064, 879, 828, 734, 694. HRMS (ESI) m/z Calculated for $\text{C}_{18}\text{H}_{18}\text{N}$ $[\text{M}]^+$: 248.1434, found: 248.1445.

(S)-2-(1-(3-methoxyphenyl)ethyl)isoquinolin-2-ium tetrafluoroborate (1h)



The titled compound was prepared by following the above procedure **A**, obtained as a sticky solid (1.6 g, 76% yield, 99.7:0.3 e.r. (99% ee). $[\alpha]_{\text{D}}^{25} -0.5$ ($c = 1.0$, CH_2Cl_2). R_f (MeOH/DCM; 10:90) = 0.37. ^1H NMR (400 MHz, DMSO- d_6) δ 10.35 (s, 1H), 8.91 (dd, $J = 6.87$, 1.37 Hz, 1H), 8.64 - 8.61 (m, 2H), 8.39 (d, $J = 8.24$ Hz, 1H), 8.35 - 8.27 (m, 1H), 8.14 (t, $J = 7.56$ Hz, 1H), 7.43 (t, $J = 8.0$ Hz, 1H), 7.32 - 7.27 (m, 1H), 7.23 (d, $J = 7.79$ Hz, 1H), 7.03 (dd, $J = 8.01$, 2.06 Hz, 1H), 6.34 (q, $J = 6.87$ Hz, 1H), 3.83 (s, 3H), 2.22 (d, $J = 7.33$ Hz, 3H). ^{13}C NMR (100 MHz, DMSO- d_6) δ 159.7, 148.8, 139.6, 137.2, 137.2, 133.4, 131.3, 130.9, 130.5, 127.4, 127.3, 126.4, 119.4, 114.6, 113.4, 69.5, 55.3, 19.7. FTIR (cm^{-1}): 3027, 2937, 2846, 1643, 1518, 1461, 1408, 1259, 1154, 1064, 870, 822, 760. HRMS (ESI) m/z Calculated for $\text{C}_{18}\text{H}_{18}\text{NO}$ $[\text{M}]^+$: 264.1383, found: 264.1390.

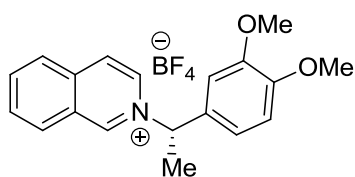
(R)-2-(1-(4-methoxyphenyl)ethyl)isoquinolin-2-ium tetrafluoroborate (1i):



The titled compound was prepared by following the above procedure **A**, obtained as a sticky solid (1.6 g, 74% yield, 0.5:99.5 e.r. (99% ee). $[\alpha]_{\text{D}}^{25} +0.4$ ($c = 1.1$, CH_2Cl_2).

R_f (MeOH/DCM; 10:90) = 0.37. $^1\text{H NMR}$ (400 MHz, $\text{DMSO-}d_6$) δ 10.28 (s, 1H), 8.83 (dd, J = 6.94, 1.44 Hz, 1H), 8.58 (t, J = 8.0 Hz, 2H), 8.39 - 8.33 (m, 1H), 8.31 - 8.26 (m, 1H), 8.12 (ddd, J = 8.19, 7.07, 1.00 Hz, 1H), 7.60 (d, J = 8.75 Hz, 2H), 7.04 (d, J = 8.76 Hz, 2H), 6.30 (q, J = 6.96 Hz, 1H), 3.79 (s, 3H), 2.15 (d, J = 7.13 Hz, 3H). $^{13}\text{C NMR}$ (100 MHz, $\text{DMSO-}d_6$) δ 159.9, 148.6, 137.2, 137.1, 133.2, 131.3, 130.7, 129.9, 129.0, 127.4, 127.3, 126.3, 114.5, 69.2, 55.3, 19.9. **FTIR** (cm^{-1}): 3076, 2972, 2844, 1643, 1514, 1463, 1397, 1256, 1178, 1064, 879, 834, 761. **HRMS** (ESI) m/z Calculated for $\text{C}_{18}\text{H}_{18}\text{NO}[\text{M}]^+$: 264.1383, found: 264.1387.

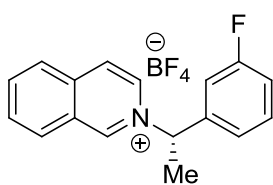
(S)-2-(1-(3,4-dimethoxyphenyl)ethyl)isoquinolin-2-ium tetrafluoroborate (1j)



The titled compound was prepared by following the above procedure A, obtained as a sticky solid (1.6 g, 72% yield, 98.2:1.8 e.r.(96% ee). $[\alpha]_{\text{D}}^{25}$ -1.1 (c = 1.0, CH_2Cl_2).

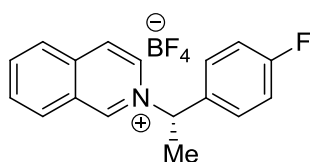
R_f (MeOH/DCM; 10:90) = 0.35. $^1\text{H NMR}$ (400 MHz, $\text{DMSO-}d_6$) δ 10.26 (s, 1H), 8.82 (dd, J = 6.94, 1.31 Hz, 1H), 8.63 - 8.48 (m, 2H), 8.39 - 8.31 (m, 1H), 8.31 - 8.23 (m, 1H), 8.14 - 8.06 (m, 1H), 7.25 (d, J = 2.00 Hz, 1H), 7.20 (dd, J = 8.38, 2.00 Hz, 1H), 7.03 (d, J = 8.50 Hz, 1H), 6.24 (q, J = 6.96 Hz, 1H), 3.78 (s, 3H), 3.76 (s, 3H), 2.12 (d, J = 7.00 Hz, 3H). $^{13}\text{C NMR}$ (100 MHz, $\text{DMSO-}d_6$) δ 149.6, 149.0, 148.5, 137.1, 137.0, 133.2, 131.2, 130.8, 130.0, 127.3, 127.2, 126.2, 120.1, 111.9, 111.4, 69.6, 55.7, 55.5, 19.9. **FTIR** (cm^{-1}): 3074, 2933, 2847, 1643, 1601, 1518, 1461, 1408, 1260, 1155, 1064, 870, 824, 762. **HRMS** (ESI) m/z Calculated for $\text{C}_{19}\text{H}_{20}\text{NO}_2[\text{M}]^+$: 294.1488, found: 294.1495.

(S)-2-(1-(3-fluorophenyl)ethyl)isoquinolin-2-ium tetrafluoroborate (1k):



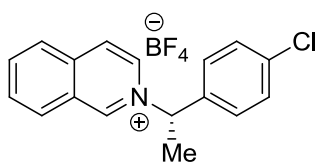
The titled compound was prepared by following the above procedure B, obtained as sticky liquid (762 mg, 75 % yield, 99.1:0.9 e.r.(98% ee). $[\alpha]_{\text{D}}^{25}$ -0.8 (c = 1.0, CH_2Cl_2). R_f (MeOH/DCM; 10:90) = 0.37. $^1\text{H NMR}$ (500 MHz, $\text{DMSO-}d_6$) δ 10.30 (s, 1H), 8.84 (dd, J = 6.87, 1.14 Hz, 1H), 8.62 - 8.56 (m, 2H), 8.40 - 8.34 (m, 1H), 8.33 - 8.27 (m, 1H), 8.16 - 8.08 (m, 1H), 7.59 - 7.48 (m, 2H), 7.44 (d, J = 8.01 Hz, 1H), 7.29 (td, J = 8.49, 2.10 Hz, 1H), 6.36 (q, J = 6.87 Hz, 1H), 2.17 (d, J = 6.87 Hz, 3H). $^{13}\text{C NMR}$ (125 MHz, $\text{DMSO-}d_6$) δ 163.3 (C-F, 1JC-F = 245.09 Hz), 161.4 (C-F, 1JC-F = 245.09 Hz), 149.1, 140.7 (C-F, 4JC-F = 7.63 Hz), 140.6 (C-F, 4JC-F = 7.63 Hz), 137.3, 133.4, 131.3, 131.2, 130.9, 127.4, 127.3, 126.4, 123.7, 116.3 (C-F, 3JC-F = 20.98 Hz), 116.1 (C-F, 3JC-F = 20.98 Hz), 114.7 (C-F, 2JC-F = 22.89 Hz), 114.5 (C-F, 2JC-F = 22.89 Hz), 68.8, 19.7. **FTIR** (cm^{-1}): 3074, 2953, 2923, 2862, 1695, 1644, 1600, 1457, 1397, 1278, 1065, 879, 829, 732. **HRMS** (ESI) m/z Calculated for $\text{C}_{17}\text{H}_{15}\text{NF}[\text{M}]^+$: 252.1183 found: 252.1188.

(S)-2-(1-(4-fluorophenyl)ethyl)isoquinolin-2-ium tetrafluoroborate (1l):



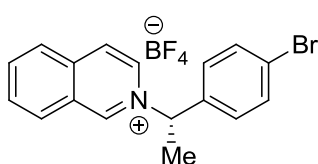
The titled compound was prepared by following the above procedure **A**, obtained as a brown solid (1.4 g, 73 % yield, 95.4:4.6 e.r. (91% ee). $[\alpha]_{\text{D}}^{25}$ -0.6 ($c = 1.0$, CH_2Cl_2). R_f (MeOH/DCM; 10:90) = 0.38. MP = 89.9 – 91.0 °C. $^1\text{H NMR}$ (400 MHz, $\text{DMSO-}d_6$) δ 10.26 (s, 1H), 8.81 (dd, $J = 6.88$, 1.38 Hz, 1H), 8.56 (t, $J = 7.75$ Hz, 2H), 8.37 - 8.28 (m, 1H), 8.24 (td, $J = 7.60$, 1.06 Hz, 1H), 8.08 (ddd, $J = 8.16$, 7.10, 1.00 Hz, 1H), 7.76 - 7.64 (m, 2H), 7.28 (t, $J = 8.88$ Hz, 2H), 6.34 (q, $J = 7.00$ Hz, 1H), 2.15 (d, $J = 7.00$ Hz, 3H). $^{13}\text{C NMR}$ (100 MHz, $\text{DMSO-}d_6$) δ 163.8 (C-F, $1\text{JC-F} = 246.32$ Hz), 161.2 (C-F, $1\text{JC-F} = 246.32$ Hz), 148.8, 137.2, 137.2, 134.3 (C-F, $4\text{JC-F} = 3.63$ Hz), 134.2 (C-F, $4\text{JC-F} = 3.63$ Hz), 133.2, 131.3, 130.8, 130.0 (C-F, $3\text{JC-F} = 8.72$ Hz), 129.9 (C-F, $3\text{JC-F} = 8.72$ Hz), 127.4, 27.3, 126.4, 116.1 (C-F, $2\text{JC-F} = 21.1$ Hz), 115.9 (C-F, $2\text{JC-F} = 21.1$ Hz), 69.9, 19.9. **FTIR** (cm^{-1}): 3081, 2982, 2935, 2868, 1643, 1608, 1512, 1463, 1400, 1283, 1233, 1065, 838, 754. **HRMS** (ESI) m/z . Calculated for $\text{C}_{17}\text{H}_{15}\text{NF}[\text{M}]^+$: 252.1183, found: 252.1183.

(S)-2-(1-(4-chlorophenyl)ethyl)isoquinolin-2-ium tetrafluoroborate (1m)



The titled compound was prepared by following the above procedure **A**, obtained as a sticky liquid (1.5 g, 70% yield, 94.6:5.4 e.r. (89% ee). $[\alpha]_{\text{D}}^{25}$ -0.9 ($c = 1.0$, CH_2Cl_2). R_f (MeOH/DCM; 10:90) = 0.37. $^1\text{H NMR}$ (400 MHz, $\text{DMSO-}d_6$) δ 10.29 (s, 1H), 8.82 (dd, $J = 6.88$, 1.38 Hz, 1H), 8.57 (d, $J = 8.38$ Hz, 1H), 8.59 (d, $J = 7.00$ Hz, 1H), 8.36 (d, $J = 8.13$ Hz, 1H), 8.29 (ddd, $J = 8.16$, 6.97, 1.13 Hz, 1H), 8.12 (ddd, $J = 8.19$, 7.00, 1.06 Hz, 1H), 7.71 - 7.60 (m, 2H), 7.59 - 7.48 (m, 2H), 6.35 (q, $J = 7.00$ Hz, 1H), 2.15 (d, $J = 7.00$ Hz, 3H). $^{13}\text{C NMR}$ (100 MHz, $\text{DMSO-}d_6$) δ 149.0, 137.3, 137.0, 134.1, 133.4, 131.3, 130.9, 129.5, 129.1, 127.4, 127.3, 126.4, 68.7, 19.8. **FTIR** (cm^{-1}): 3070, 2925, 2857, 1644, 1604, 1498, 1462, 1403, 1276, 1064, 881, 832, 737. **HRMS** (ESI) m/z . Calculated for $\text{C}_{17}\text{H}_{15}\text{NCl}[\text{M}]^+$: 268.0887, found: 268.0897.

(S)-2-(1-(4-bromophenyl)ethyl)isoquinolin-2-ium tetrafluoroborate (1n)

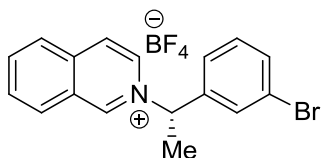


The titled compound was prepared by following the above procedure **A**, obtained as a sticky liquid (1.6 g, 68% yield, 95.1:4.9 e.r. (90% ee). $[\alpha]_{\text{D}}^{25}$ -1.1 ($c = 1.0$, CH_2Cl_2). R_f (MeOH/DCM; 10:90) = 0.33. $^1\text{H NMR}$ (400 MHz, $\text{DMSO-}d_6$) δ 10.28 (s, 1H), 8.81 (dd, $J = 6.87$, 1.37 Hz, 1H), 8.66 - 8.49 (m, 2H), 8.41 - 8.33 (m, 1H), 8.33 - 8.25 (m, 1H), 8.11 (ddd, $J = 8.24$, 6.87, 1.37 Hz, 1H), 7.74 - 7.64 (m, 2H), 7.59 - 7.49 (m, 2H), 6.32 (q, $J = 6.87$ Hz,

1H), 2.13 (d, $J = 6.87$ Hz, 3H). ^{13}C NMR (100 MHz, DMSO- d_6) δ 149.0, 137.4, 137.3, 137.3, 133.4, 132.1, 131.4, 130.9, 129.8, 127.5, 127.3, 126.5, 122.8, 68.8, 19.8.

.FTIR (cm^{-1}): 3073, 2925, 2857, 1644, 1481, 1401, 1277, 1079, 880, 830, 738. HRMS (ESI) m/z Calculated for $\text{C}_{17}\text{H}_{15}\text{NBr}[\text{M}]^+$: 312.0382, found: 312.0390.

(S)-2-(1-(3-bromophenyl)ethyl)isoquinolin-2-ium tetrafluoroborate (1o)

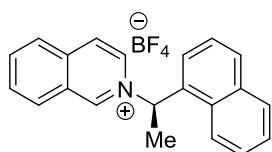


The titled compound was prepared by following the above procedure A, obtained as a sticky liquid (1.7 g, 70% yield, 92.7:7.3 e.r. (85% ee). $[\alpha]_{\text{D}}^{25} -1.2$ ($c = 1.0$, CH_2Cl_2).

$R_f(\text{MeOH}/\text{DCM}; 10:90) = 0.33$. ^1H NMR (400 MHz, DMSO- d_6)

δ 10.31 (s, 1H), 8.84 (d, $J = 6.87$ Hz, 1H), 8.57 (d, $J = 8.24$ Hz, 1H), 8.60 (d, $J = 6.87$ Hz, 1H), 8.36 (d, $J = 7.78$ Hz, 1H), 8.30 (t, $J = 7.33$ Hz, 1H), 8.12 (t, $J = 7.33$ Hz, 1H), 7.90 (s, 1H), 7.68 - 7.56 (m, 2H), 7.51 - 7.38 (m, 1H), 6.33 (q, $J = 6.72$ Hz, 1H), 2.15 (d, $J = 6.87$ Hz, 3H). ^{13}C NMR (100 MHz, DMSO- d_6) δ 148.7, 140.6, 137.4, 132.9, 131.4, 130.8, 128.5, 128.4, 127.7, 127.4, 126.5, 65.1, 21.2. FTIR (cm^{-1}): 3065, 2962, 2928, 2865, 1647, 1467, 1391, 1275, 1198, 1067, 883, 825, 734. HRMS (ESI) m/z Calculated for $\text{C}_{17}\text{H}_{15}\text{BrN}[\text{M}+\text{H}]^+$: 312.0382, found: 312.0383.

(R)-2-(1-(naphthalen-1-yl)ethyl)isoquinolin-2-ium tetrafluoroborate (1p)

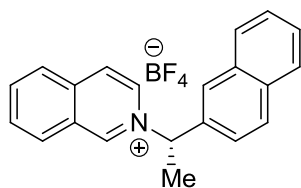


The titled compound was prepared by following the above procedure A, obtained as a sticky solid (1.6 g, 72% yield, 2.5:97.5 e.r. (95% ee).

$[\alpha]_{\text{D}}^{25} -1.7$ ($c = 0.5$, CH_2Cl_2). $R_f(\text{MeOH}/\text{DCM}; 10:90) = 0.55$. ^1H NMR

(500 MHz, DMSO- d_6) δ 10.33 (s, 1H), 8.86 (d, $J = 6.48$ Hz, 1H), 8.58 (d, $J = 7.25$ Hz, 2H), 8.35 (d, $J = 8.01$ Hz, 1H), 8.28 (t, $J = 7.44$ Hz, 1H), 8.17 (d, $J = 8.01$ Hz, 1H), 8.13 - 8.02 (m, 3H), 7.89 (d, $J = 6.87$ Hz, 1H), 7.71 (t, $J = 7.44$ Hz, 1H), 7.65 - 7.54 (m, 2H), 7.18 (q, $J = 6.49$ Hz, 1H), 2.28 (d, $J = 6.49$ Hz, 3H). ^{13}C NMR (125 MHz, DMSO- d_6) δ 148.9, 137.3, 137.2, 133.7, 133.6, 132.5, 131.3, 130.9, 130.5, 130.2, 129.2, 127.6, 127.4, 127.3, 126.5, 126.4, 126.1, 125.7, 122.4, 66.0, 21.1. FTIR (cm^{-1}): 3066, 2964, 1641, 1513, 1461, 1394, 1277, 1063, 876, 792. HRMS (ESI) m/z Calculated for $\text{C}_{21}\text{H}_{18}\text{N}[\text{M}]^+$: 284.1434, found: 284.1444.

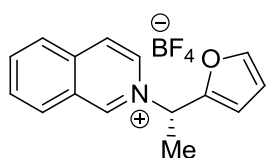
(S)-2-(1-(naphthalen-2-yl)ethyl)isoquinolin-2-ium tetrafluoroborate (1q)



The titled compound was prepared by following the above procedure A, obtained as a sticky solid (1.6 g, 73% yield, 98.9:1.1 e.r. (98% ee). $[\alpha]_{\text{D}}^{25} -2.1$ ($c = 0.5$, CH_2Cl_2). $R_f(\text{MeOH}/\text{DCM}; 10:90) = 0.53$. ^1H NMR (400 MHz, DMSO- d_6) δ 10.36 (s, 1H), 8.95 -

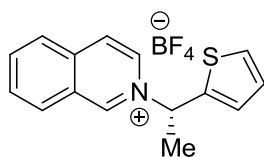
8.79 (m, 1H), 8.58 (d, $J = 6.87$ Hz, 2H), 8.36 (d, $J = 8.39$ Hz, 1H), 8.29 (t, $J = 7.63$ Hz, 1H), 8.20 (s, 1H), 8.15 - 8.07 (m, 1H), 7.92 - 8.03 (m, 3H), 7.55 - 7.66 (m, 3H), 6.51 (q, $J = 6.87$ Hz, 1H), 2.25 (d, $J = 6.87$ Hz, 3H). ^{13}C NMR (100 MHz, DMSO- d_6) δ 148.9, 137.3, 137.2, 133.6, 133.6, 132.5, 131.3, 130.9, 130.4, 130.2, 129.2, 127.5, 127.4, 127.3, 126.5, 126.4, 126.1, 125.6, 122.4, 65.9, 21.1. FTIR (cm^{-1}): 3065, 2986, 2926, 2857, 1643, 1513, 1462, 1395, 1278, 1063, 877, 820, 776, 738. HRMS (ESI) m/z Calculated for $\text{C}_{21}\text{H}_{18}\text{N}$ $[\text{M}]^+$: 284.1433, found: 284.1447.

(S)-2-(1-(furan-2-yl)ethyl)isoquinolin-2-ium tetrafluoroborate (1r)



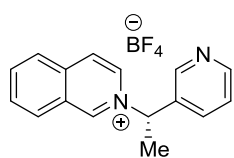
The titled compound was prepared by following the above procedure **B**, obtained as a sticky liquid (681 mg, 73% yield, 99.2:0.8 e.r. (98% ee). $[\alpha]_{\text{D}}^{25}$ -1.9 ($c = 1.0$, CH_2Cl_2). R_f (MeOH/DCM; 10:90) = 0.53. ^1H NMR (400 MHz, DMSO- d_6) δ 10.21 (s, 1H), 8.80 (dd, $J = 6.88$, 1.50 Hz, 1H), 8.63 (d, $J = 6.88$ Hz, 1H), 8.57 (d, $J = 8.26$ Hz, 1H), 8.37 (d, $J = 8.25$ Hz, 1H), 8.30 (ddd, $J = 8.25$, 6.94, 1.19 Hz, 1H), 8.11 (ddd, $J = 8.22$, 6.97, 1.19 Hz, 1H), 7.76 (dd, $J = 1.88$, 0.75 Hz, 1H), 6.93 (dt, $J = 3.38$, 0.81 Hz, 1H), 6.61 (dd, $J = 3.38$, 1.88 Hz, 1H), 6.39 (q, $J = 7.00$ Hz, 1H), 2.10 (d, $J = 7.00$ Hz, 3H). ^{13}C NMR (100 MHz, DMSO- d_6) δ 150.0, 148.9, 144.9, 137.4, 137.4, 132.8, 131.4, 130.8, 127.4, 127.4, 126.6, 111.2, 111.0, 63.6, 18.6. FTIR (cm^{-1}): 3124, 3094, 2992, 2928, 1692, 1644, 1509, 1463, 1398, 1288, 1065, 830, 762. HRMS (ESI) m/z Calculated for $\text{C}_{15}\text{H}_{14}\text{NO}$ $[\text{M}]^+$: 224.1070, found 224.1072.

(S)-2-(1-(thiophen-2-yl)ethyl)isoquinolin-2-ium tetrafluoroborate (1s)



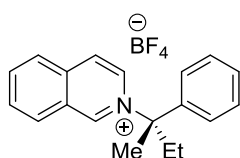
The titled compound was prepared by following the above procedure **B**, obtained as a yellow solid (725 mg, 74% yield, 99.2:0.8 e.r. (98% ee). $[\alpha]_{\text{D}}^{25}$ -2.2 ($c = 0.9$, CH_2Cl_2). R_f (MeOH/DCM; 10:90) = 0.53. MP = 116.5 – 118.9 °C. ^1H NMR (400 MHz, DMSO- d_6) δ 10.29 (s, 1H), 8.90 (d, $J = 6.87$ Hz, 1H), 8.62 (d, $J = 6.87$ Hz, 1H), 8.56 (d, $J = 8.24$ Hz, 1H), 8.37 (d, $J = 8.24$ Hz, 1H), 8.30 (t, $J = 7.56$ Hz, 1H), 8.11 (t, $J = 7.56$ Hz, 1H), 7.71 (d, $J = 5.04$ Hz, 1H), 7.51 (d, $J = 3.21$ Hz, 1H), 7.16 (t, $J = 4.12$ Hz, 1H), 6.59 (q, $J = 6.87$ Hz, 1H), 2.20 (d, $J = 6.87$ Hz, 3H). ^{13}C NMR (100 MHz, DMSO- d_6) δ 148.7, 140.5, 137.4, 132.8, 131.5, 130.8, 128.5, 128.4, 127.7, 127.4, 126.6, 65.3, 21.3. FTIR (cm^{-1}): 3095, 2992, 2931, 2861, 1642, 1516, 1463, 1398, 1284, 1062, 838, 726. HRMS (ESI) m/z Calculated for $\text{C}_{15}\text{H}_{14}\text{NS}$ $[\text{M}]^+$: 240.0841, found: 240.0843.

(S)-2-(1-(pyridin-3-yl)ethyl)isoquinolin-2-ium tetrafluoroborate (1t)



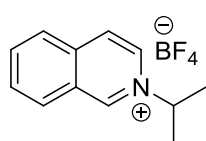
The titled compound was prepared by following the above procedure **A**, obtained as a sticky solid (1.4 g, 75% yield, 5.9:94.1 e.r. (88% ee). $[\alpha]_{\text{D}}^{25}$ -1.4 ($c = 1.1$, CH_2Cl_2). R_f (MeOH/DCM; 10:90) = 0.36. $^1\text{H NMR}$ (400 MHz, $\text{DMSO-}d_6$) δ 10.18 (s, 1H), 8.78 (d, $J = 2.38$ Hz, 1H), 8.74 (dd, $J = 7.00$, 1.50 Hz, 1H), 8.59 (dd, $J = 4.88$, 1.50 Hz, 1H), 8.55 - 8.47 (m, 2H), 8.33 - 8.27 (m, 1H), 8.24 (ddd, $J = 8.22$, 6.91, 1.13 Hz, 1H), 8.07 (ddd, $J = 8.25$, 6.88, 1.25 Hz, 1H), 7.99 (dt, $J = 8.13$, 1.88 Hz, 1H), 7.49 (ddd, $J = 8.04$, 4.85, 0.75 Hz, 1H), 6.34 (q, $J = 7.00$ Hz, 1H), 2.15 (d, $J = 7.00$ Hz, 3H). $^{13}\text{C NMR}$ (100 MHz, $\text{DMSO-}d_6$) δ 150.7, 149.3, 149.0, 137.9, 137.8, 136.0, 134.3, 133.6, 131.9, 131.4, 127.9, 127.8, 127.1, 124.9, 68.0, 20.0. **FTIR** (cm^{-1}): 3235, 2995, 2505, 1642, 1464, 1405, 1292, 1068, 831, 764. **HRMS** (ESI) m/z Calculated for $\text{C}_{16}\text{H}_{15}\text{N}_2$ $[\text{M}]^+$: 235.1229, found: 235.1239.

(S)-2-(2-phenylbutan-2-yl)isoquinolin-2-ium tetrafluoroborate (1u)



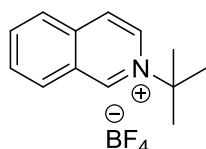
The titled compound was prepared by following the above procedure **B**, obtained as a sticky liquid (0.78 g, 75% yield, 0.9:99.1 e.r. (98% ee). $[\alpha]_{\text{D}}^{25}$ -2.3 ($c = 1.2$, CH_2Cl_2). R_f (MeOH/DCM; 10:90) = 0.36. $^1\text{H NMR}$ (500 MHz, $\text{DMSO-}d_6$) δ 10.28 (s, 1H), 8.70 (d, $J = 8.39$ Hz, 1H), 8.47 (s, 2H), 8.39 - 8.33 (m, 1H), 8.33 - 8.28 (m, 1H), 8.14 (t, $J = 7.63$ Hz, 1H), 7.49 - 7.42 (m, 3H), 7.41 - 7.30 (m, 4H), 2.78 - 2.64 (m, 2H), 2.18 (s, 3H), 0.74 (t, $J = 7.25$ Hz, 3H). $^{13}\text{C NMR}$ (125 MHz, $\text{DMSO-}d_6$) δ 148.7, 142.4, 137.4, 136.8, 133.6, 131.6, 131.1, 129.0, 129.0, 128.7, 128.1, 127.1, 126.5, 125.7, 76.9, 32.1, 25.6, 8.2. **FTIR** (cm^{-1}): 3051, 2965, 2928, 2834, 1610, 1510, 1461, 1300, 1246, 1177, 1032, 826. **HRMS** (ESI) m/z Calculated for $\text{C}_{19}\text{H}_{20}\text{N}$ $[\text{M}]^+$: 262.1590, found 262.1590.

2-isopropylisoquinolin-2-ium tetrafluoroborate (1v)



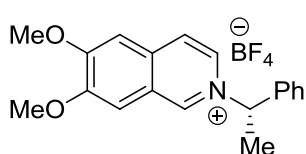
The titled compound was prepared by following the above procedure **A**, obtained as a brown solid (1.1 g, 72% yield). R_f (MeOH/DCM; 10:90) = 0.34. $\text{MP} = 100.7 - 101.9$ °C. $^1\text{H NMR}$ (500 MHz, $\text{DMSO-}d_6$) δ 10.13 (s, 1H), 8.92 (dd, $J = 6.87$, 1.53 Hz, 1H), 8.62 (d, $J = 6.87$ Hz, 1H), 8.51 (d, $J = 7.63$ Hz, 1H), 8.36 (d, $J = 8.39$ Hz, 1H), 8.30 - 8.24 (m, 1H), 8.12 - 8.06 (m, 1H), 5.17 - 5.09 (m, 1H), 1.72 (d, $J = 6.87$ Hz, 6H). $^{13}\text{C NMR}$ (125 MHz, $\text{DMSO-}d_6$) δ 148.5, 137.2, 136.9, 133.0, 131.1, 130.5, 127.4, 127.2, 126.1, 64.0, 22.2. **FTIR** (cm^{-1}): 3391, 3096, 2985, 2858, 2349, 1644, 1515, 1397, 1058, 880, 830, 762. **HRMS** (ESI) m/z Calculated for $\text{C}_{12}\text{H}_{14}\text{N}$ $[\text{M}]^+$: 172.1121, found: 172.1125.

2-(tert-butyl)isoquinolin-2-ium tetrafluoroborate (1w)



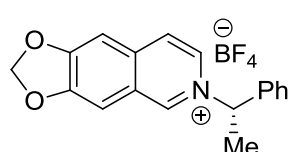
The titled compound was prepared by following the above procedure **A**, obtained as a brown solid (1.2 g, 73% yield). R_f (MeOH/DCM; 10:90) = 0.33. MP = 199.4 – 200.7 °C. $^1\text{H NMR}$ (400 MHz, DMSO- d_6) δ 10.14 (s, 1H), 9.11 (dd, J = 7.25, 1.91 Hz, 1H), 8.65 (d, J = 8.39 Hz, 1H), 8.59 (d, J = 7.63 Hz, 1H), 8.35 (d, J = 7.63 Hz, 1H), 8.27 (t, J = 7.63 Hz, 1H), 8.09 (t, J = 7.63 Hz, 1H), 1.86 (s, 9H). $^{13}\text{C NMR}$ (100 MHz, DMSO- d_6) δ 147.6, 136.9, 131.2, 130.9, 127.2, 126.8, 125.5, 69.1, 29.0. FTIR (cm^{-1}): 3064, 2925, 2856, 1666, 1458, 1394, 1266, 1051, 826, 741. 136.6, 132.2, HRMS (ESI) m/z Calculated for $\text{C}_{13}\text{H}_{16}\text{N} [\text{M}]^+$: 186.1277, found: 186.1286.

(S)-6,7-dimethoxy-2-(1-phenylethyl)isoquinolin-2-ium tetrafluoroborate (1x)



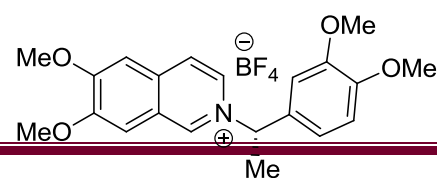
The titled compound was prepared by following the above procedure **A**, obtained as a brown solid (1.7 g, 73% yield, 97.1:2.9 e.r.(94% ee)). $[\alpha]_{\text{D}}^{25} +0.15$ (c = 0.4, CH_2Cl_2). R_f (MeOH/DCM; 10:90) = 0.35. MP = 167.8 – 168.8 °C. $^1\text{H NMR}$ (400 MHz, DMSO- d_6) δ 9.83 (s, 1H), 8.70 (dd, J = 6.82, 1.44 Hz, 1H), 8.31 (d, J = 6.75 Hz, 1H), 7.84 (s, 1H), 7.76 (s, 1H), 7.62 - 7.54 (m, 2H), 7.54 - 7.37 (m, 3H), 6.25 (q, J = 6.96 Hz, 1H), 4.07 (s, 3H), 4.02 (s, 3H), 2.13 (d, J = 7.00 Hz, 3H). $^{13}\text{C NMR}$ (100 MHz, DMSO- d_6) δ 157.8, 152.5, 143.5, 138.6, 135.5, 132.4, 129.2, 127.1, 124.0, 123.7, 107.5, 105.7, 68.6, 56.8, 56.3, 19.9. FTIR (cm^{-1}): 3072, 2940, 2848, 1620, 1498, 1429, 1272, 1214, 1062, 868, 927, 867, 738. HRMS (ESI) m/z Calculated for $\text{C}_{19}\text{H}_{20}\text{NO}_2 [\text{M}]^+$: 294.1489, found: 294.1503.

(S)-6-(1-phenylethyl)-[1,3]dioxolo[4,5-g]isoquinolin-6-ium tetrafluoroborate (1y)



The titled compound was prepared by following the above procedure **A**, obtained as a yellow solid (1.6 g, 71% yield, 97.6:2.4 e.r.(95% ee)). $[\alpha]_{\text{D}}^{25} -2.0$ (c = 0.7, CH_2Cl_2). R_f (MeOH/DCM; 10:90) = 0.40. MP = 161.6 – 163.2 °C. $^1\text{H NMR}$ (400 MHz, DMSO- d_6) δ 9.80 (s, 1H), 8.68 (dd, J = 6.88, 1.50 Hz, 1H), 8.29 (d, J = 6.88 Hz, 1H), 7.78 (s, 1H), 7.71 (s, 1H), 7.59 - 7.51 (m, 2H), 7.51 - 7.39 (m, 3H), 6.45 (s, 2H), 6.22 (q, J = 7.00 Hz, 1H), 2.11 (d, J = 7.00 Hz, 3H). $^{13}\text{C NMR}$ (100 MHz, DMSO- d_6) δ 156.4, 151.3, 144.0, 138.5, 137.8, 132.7, 129.2, 127.1, 125.6, 124.3, 104.5, 104.1, 103.0, 68.6, 19.8. FTIR (cm^{-1}): 3067, 2982, 2927, 1617, 1467, 1271, 1189, 1063, 929, 868, 708. HRMS (ESI) m/z Calculated for $\text{C}_{18}\text{H}_{16}\text{NO}_2 [\text{M}]^+$: 278.1176, found: 278.1180.

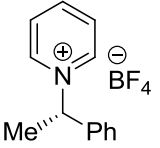
(S)-2-(1-(3,4-dimethoxyphenyl)ethyl)-6,7-dimethoxyisoquinolin-2-ium tetrafluoroborate (1z)



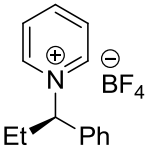
The titled compound was prepared by following the above procedure **A**, obtained as a brown solid (1.9 g, 75%

yield, 99.2:0.8 e.r.(98% ee). $[\alpha]_D^{25}$ -1.0 (c = 0.5, CH₂Cl₂). R_f (MeOH/DCM; 10:90) = 0.35. MP = 178.8 – 180.2 °C. ¹H NMR (400 MHz, DMSO-*d*₆) δ 9.77 (s, 1H), 8.70 (dd, *J* = 6.87, 1.37 Hz, 1H), 8.29 (d, *J* = 6.87 Hz, 1H), 7.82 (s, 1H), 7.75 (s, 1H), 7.23 (d, *J* = 2.29 Hz, 1H), 7.16 (dd, *J* = 8.47, 2.06 Hz, 1H), 7.04 (d, *J* = 8.70 Hz, 1H), 6.14 (q, *J* = 6.87 Hz, 1H), 4.07 (s, 3H), 4.02 (s, 3H), 3.80 (s, 3H), 3.77 (s, 3H), 2.09 (d, *J* = 6.87 Hz, 3H). ¹³C NMR (100 MHz, DMSO-*d*₆) δ 157.7, 152.5, 149.5, 149.0, 143.4, 135.5, 132.2, 130.4, 124.0, 123.6, 119.9, 111.9, 111.2, 107.5, 105.7, 68.7, 56.8, 56.3, 55.7, 55.6, 20.1. FTIR (cm⁻¹): 3080, 2928, 2848, 1612, 1509, 1457, 1430, 1268, 1154, 1063, 924, 867, 738. HRMS (ESI) *m/z* Calculated for C₂₁H₂₄NO₄ [M]⁺: 354.1700, found: 354.1702.

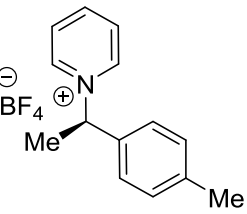
(S)-1-(1-phenylethyl)pyridin-1-ium tetrafluoroborate (3a)

 The titled compound was prepared by following the above procedure **B**, obtained as a sticky liquid (0.66 g, 81% yield, 99.0:1.0 e.r.(98% ee). R_f (MeOH/DCM; 10:90) = 0.35. The spectral values were matched favourably with previously reported literature values.²⁹

(R)-1-(1-phenylpropyl)pyridin-1-ium tetrafluoroborate (3b):

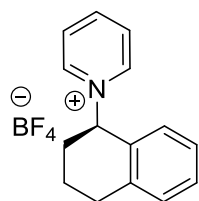
 The titled compound was prepared by following the above procedure **B**, obtained as a sticky liquid (693.5 mg, 81 % yield, 0.9:99.1 e.r. (99% ee). $[\alpha]_D^{25}$ -1.5 (c = 0.6, CH₂Cl₂). R_f (MeOH/DCM; 10:90) = 0.35. ¹H NMR (400 MHz, DMSO-*d*₆) δ 9.28 (d, *J* = 5.50 Hz, 2H), 8.64 (tt, *J* = 7.75, 1.25 Hz, 1H), 8.28 - 8.11 (m, 2H), 7.70 - 7.57 (m, 2H), 7.54 - 7.38 (m, 3H), 5.98 (t, *J* = 7.82 Hz, 1H), 2.60 - 2.51 (m, 2H), 0.86 (t, *J* = 7.25 Hz, 3H). ¹³C NMR (100 MHz, DMSO-*d*₆) δ 146.4, 143.4, 136.6, 129.7, 129.4, 128.8, 127.8, 75.5, 26.1, 10.3. FTIR (cm⁻¹): 3137, 3086, 2974, 2885, 1631, 1488, 1390, 1286, 1060, 846, 773, 694. HRMS (ESI) *m/z* Calculated for C₁₄H₁₆N[M]⁺: 198.1277, found: 198.1283.

(R)-1-(1-(p-tolyl)ethyl)pyridin-1-ium tetrafluoroborate (3c)

 The titled compound was prepared by following the above procedure **B**, obtained as a sticky liquid (675.5 mg, 79 % yield, 0.7:99.3 e.r. (99% ee). $[\alpha]_D^{25}$ +2.1 (c = 0.5, CH₂Cl₂). R_f (MeOH/DCM; 10:90) = 0.34. ¹H NMR (400 MHz, DMSO-*d*₆) δ ppm 9.21 (dd, *J* = 6.82, 1.19 Hz, 2H), 8.61 (tt, *J* = 7.75, 1.31 Hz, 1H), 8.17 (t, *J* = 7.19 Hz, 2H), 7.54 – 7.38 (m, 2H), 7.34 – 7.21 (m, 2H), 6.19 (q, *J* = 7.00 Hz, 1H), 2.31 (s, 3H), 2.04 (d, *J* = 7.13 Hz, 3H). ¹³C NMR (100 MHz, DMSO-*d*₆) δ 146.1, 143.4, 139.1, 134.9, 129.7, 128.5, 127.3, 69.5, 20.6, 19.8. FTIR

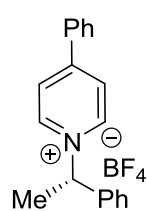
(cm^{-1}): 3138, 3088, 2988, 2931, 1629, 1488, 1387, 1278, 1063, 829, 777, 685. **HRMS** (ESI) m/z Calculated for $\text{C}_{14}\text{H}_{16}\text{N}[\text{M}]^+$: 198.1277, found: 198.1277.

(R)-1-(1,2,3,4-tetrahydronaphthalen-1-yl)pyridin-1-ium tetrafluoroborate (3d)



The titled compound was prepared by following the above procedure **B**, obtained as a brown solid (668.3 mg, 75 % yield, 0.8:99.2 e.r. (98% ee). $[\alpha]_{\text{D}}^{25} +1.1$ ($c = 0.4$, CH_2Cl_2). $R_f(\text{MeOH}/\text{DCM}; 10:90) = 0.32$. $\text{MP} = 161.2 - 163.2$ °C. $^1\text{H NMR}$ (400 MHz, $\text{DMSO}-d_6$) δ ppm 9.00 (dd, $J = 6.69$, 1.19 Hz, 2H), 8.65 (tt, $J = 7.75$, 1.25 Hz, 1H), 8.10 - 8.26 (m, 2H), 7.29 - 7.42 (m, 2H), 7.15 - 7.26 (m, 1H), 6.90 (d, $J = 7.75$ Hz, 1H), 6.25 (t, $J = 6.69$ Hz, 1H), 3.08 - 2.95 (m, 1 H), 2.86 (dt, $J = 16.98$, 5.83 Hz, 1H), 2.48 - 2.42 (m, 1H), 2.30 - 2.15 (m, 1H), 1.93 - 1.77 (m, 2H). $^{13}\text{C NMR}$ (100 MHz, $\text{DMSO}-d_6$) δ 146.2, 144.4, 139.0, 131.2, 129.7, 129.1, 128.5, 128.4, 126.9, 69.3, 31.5, 28.2, 19.1. **FTIR** (cm^{-1}): 3135, 3086, 2932, 2865, 1630, 1490, 1449, 1338, 1273, 1059, 872, 752, 685. **HRMS** (ESI) m/z Calculated for $\text{C}_{15}\text{H}_{16}\text{N}[\text{M}]^+$: 210.1277, found: 210.1277.

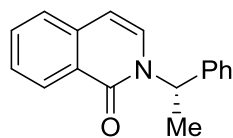
(S)-4-phenyl-1-(1-phenylethyl)pyridin-1-ium tetrafluoroborate (3e)



The titled compound was prepared by following the above procedure **B**, obtained as a yellow solid (843.2 mg, 81 % yield, 99.7:0.3 e.r. (99% ee). $[\alpha]_{\text{D}}^{25} +2.1$ ($c = 0.4$, CH_2Cl_2). $R_f(\text{MeOH}/\text{DCM}; 10:90) = 0.45$. $\text{MP} = 89.4 - 90.4$ °C. $^1\text{H NMR}$ (400 MHz, $\text{DMSO}-d_6$) δ 9.25 (d, $J = 7.00$ Hz, 2H), 8.52 (d, $J = 7.00$ Hz, 2H), 8.11 - 8.06 (m, 2H), 7.69 - 7.59 (m, 5H), 7.52 - 7.44 (m, 3H), 6.24 (q, $J = 7.00$ Hz, 1H), 2.10 (d, $J = 7.00$ Hz, 3H). $^{13}\text{C NMR}$ (100 MHz, $\text{DMSO}-d_6$) δ 155.4, 143.4, 138.1, 134.1, 133.5, 132.2, 129.7, 129.4, 129.2, 128.3, 127.3, 125.0, 68.8, 19.6. **FTIR** (cm^{-1}): 3129, 3068, 2997, 2954, 1635, 1445, 1373, 1285, 1065, 856, 767, 700. **HRMS** (ESI) m/z Calculated for $\text{C}_{19}\text{H}_{18}\text{N}[\text{M}]^+$: 260.1434, found: 260.1434.

4.10.3 Compound characterization data for oxo products

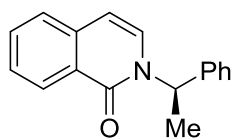
(S)-2-(1-phenylethyl)isoquinolin-1(2H)-one (2a)



The titled compound was prepared by following the above procedure **C** and obtained 99.0:1.0 e.r. (98% ee). $R_f(\text{Ethyl acetate}/\text{Pet. ether} = 20:80) = 0.3$. The spectral values were matched favourably with previously reported literature values.³⁰ **LCMS** (ESI) m/z Calculated for $\text{C}_{17}\text{H}_{16}\text{NO} [\text{M}+\text{H}]^+$: 250.31, found: 250.1.

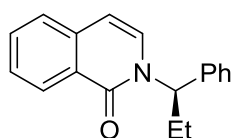
(R)-2-(1-phenylethyl)isoquinolin-1(2H)-one (ent-2a)

³⁰ Clarke, L. S.; McGlacken, P. G. *Tetrahedron*. **2015**, *71*, 2906-2913.



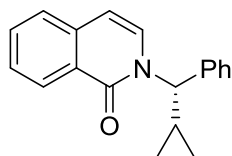
The titled compound was prepared by following the above procedure C, obtained 2.5:97.5 e.r. (95% ee). R_f (Ethyl acetate/Pet. ether = 20.80) = 0.3.. The spectral values were matched favourably with previously reported literature values.³⁰ LCMS (ESI) m/z Calculated for $C_{17}H_{16}NO$ $[M+H]^+$: 250.31, found: 250.1.

(R)-2-(1-phenylpropyl)isoquinolin-1(2H)-one (2b)



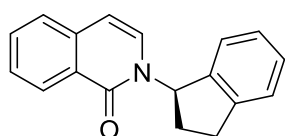
The titled compound was prepared by following the above procedure C, obtained 1.5:98.5 e.r. (97% ee). R_f (Ethyl acetate/Pet. ether = 20.80) = 0.3. 1H NMR (400 MHz, $CDCl_3$) δ 0.99 (t, J = 7.17 Hz, 3 H), 2.06 - 2.17 (m, 1 H), 2.22 - 2.36 (m, 1 H), 6.34 (dd, J = 9.31, 6.56 Hz, 1 H), 6.47 (d, J = 7.63 Hz, 1 H), 6.99 (d, J = 7.63 Hz, 1 H), 7.28 (d, J = 7.32 Hz, 1 H), 7.31 - 7.42 (m, 4 H), 7.44 - 7.53 (m, 2 H), 7.58 - 7.65 (m, 1 H), 8.48 (d, J = 8.24 Hz, 1 H). HRMS (ESI) m/z Calculated for $C_{18}H_{18}NO$ $[M+H]^+$: 264.1388, found: 264.1272.

(S)-2-(cyclopropyl(phenyl)methyl)isoquinolin-1(2H)-one (2c)



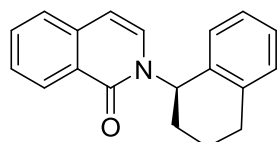
The titled compound was prepared by following the above procedure C, obtained 5.2:94.8e.r.(90% ee). R_f (Ethyl acetate/Pet. ether = 20.80) = 0.3. 1H NMR (500 MHz, $CDCl_3$) δ 0.57 - 0.68 (m, 3 H), 0.80 - 0.86 (m, 1 H), 0.90 - 0.97 (m, 1 H), 5.63 (d, J = 9.76 Hz, 1 H), 6.51 (d, J = 7.74 Hz, 1 H), 7.18 (d, J = 7.74 Hz, 1 H), 7.28 (d, J = 7.41 Hz, 1 H), 7.34 (t, J = 7.49 Hz, 2 H), 7.42 (d, J = 7.57 Hz, 2 H), 7.48 - 7.53 (m, 2 H), 7.62 - 7.67 (m, 1 H), 8.47 (d, J = 8.25 Hz, 1 H). HRMS (ESI) m/z Calculated for $C_{19}H_{18}NO$ $[M+H]^+$: 276.1388, found: 276.1360.

(R)-2-(2,3-dihydro-1H-inden-1-yl)isoquinolin-1(2H)-one (2d)



The titled compound was prepared by following the above procedure C, obtained 99.1:0.9 e.r.(98% ee). 1H NMR (500 MHz, $CDCl_3$) δ 2.04 (dd, J = 13.58, 8.39 Hz, 1 H) 2.73 - 2.86 (m, 1 H) 3.00 - 3.08 (m, 1 H) 3.12 (dd, J = 8.85, 3.97 Hz, 1 H) 6.44 (d, J = 7.63 Hz, 1 H) 6.71 - 6.81 (m, 2 H) 7.09 (d, J = 7.32 Hz, 1 H) 7.23 (t, J = 7.32 Hz, 1 H) 7.28 - 7.33 (m, 1 H) 7.33 - 7.38 (m, 1 H) 7.45 - 7.55 (m, 2 H) 7.62 - 7.68 (m, 1 H) 8.51 (d, J = 7.93 Hz, 1 H). R_f (Ethyl acetate/Pet. ether = 20.80) = 0.3. HRMS (ESI) m/z Calculated for $C_{18}H_{16}NO$ $[M+H]^+$: 262.1231, found: 262.1218.

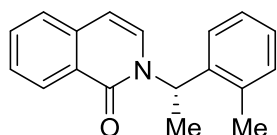
(R)-2-(1,2,3,4-tetrahydronaphthalen-1-yl)isoquinolin-1(2H)-one (2e)



The titled compound was prepared by following the above procedure C, obtained 99.3:0.7 e.r.(99% ee). 1H NMR (500 MHz, $CDCl_3$) δ

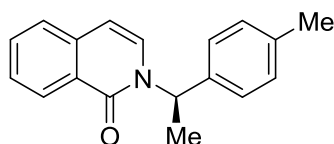
1.86 - 2.03 (m, 3 H), 2.30 (dt, $J = 11.90, 5.95$ Hz, 1 H), 2.81 - 3.03 (m, 2 H), 6.37 - 6.49 (m, 2 H), 6.77 (d, $J = 7.32$ Hz, 1 H), 6.91 (d, $J = 7.63$ Hz, 1 H), 7.11 (t, $J = 6.10$ Hz, 1 H), 7.17 - 7.23 (m, 2 H), 7.45 - 7.57 (m, 2 H), 7.62 - 7.69 (m, 1 H), 8.52 (d, $J = 7.93$ Hz, 1 H). R_f (Ethyl acetate/Pet. ether = 20.80) = 0.3. **HRMS** (ESI) m/z Calculated for $C_{19}H_{18}NO$ $[M+H]^+$: 276.1388, found: 276.1375.

(S)-2-(1-(o-tolyl)ethyl)isoquinolin-1(2H)-one (2f)



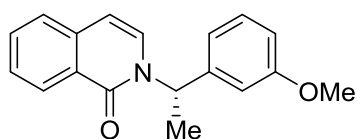
The titled compound was prepared by following the above procedure C, obtained 98.4:1.6 e.r.(97% ee). R_f (Ethyl acetate/Pet. ether = 20.80) = 0.3. 1H NMR (500 MHz, $CDCl_3$) δ 1.74 (d, $J = 6.71$ Hz, 3 H), 2.13 (s, 3 H), 6.39 (d, $J = 7.32$ Hz, 1 H), 6.50 (q, $J = 7.02$ Hz, 1 H), 6.79 (d, $J = 7.32$ Hz, 1 H), 7.19 (d, $J = 7.02$ Hz, 1 H), 7.27 - 7.34 (m, 2 H), 7.44 - 7.57 (m, 3 H), 7.58 - 7.68 (m, 1 H), 8.49 (d, $J = 7.93$ Hz, 1 H). **LCMS** (ESI) m/z Calculated for $C_{18}H_{18}NO$ $[M+H]^+$: 264.34, found: 264.1.

(R)-2-(1-(p-tolyl)ethyl)isoquinolin-1(2H)-one (2g)



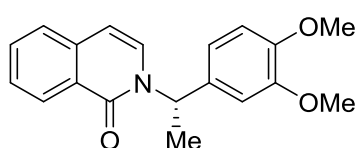
The titled compound was prepared by following the above procedure C, obtained 1.3:98.7e.r. (97% ee). R_f (Ethyl acetate/Pet. ether = 20.80) = 0.3. 1H NMR (500 MHz, $CDCl_3$) δ 1.74 (d, $J = 7.32$ Hz, 3 H), 2.34 (s, 3 H), 6.44 (d, $J = 7.63$ Hz, 1 H), 6.53 (q, $J = 7.22$ Hz, 1 H), 6.91 (d, $J = 7.63$ Hz, 1 H), 7.16 (d, $J = 7.63$ Hz, 2 H), 7.24 (d, $J = 7.93$ Hz, 2 H), 7.44 - 7.53 (m, 2 H), 7.58 - 7.66 (m, 1 H), 8.49 (d, $J = 8.24$ Hz, 1 H). **HRMS** (ESI) m/z Calculated for $C_{18}H_{18}NO$ $[M+H]^+$: 264.1388, found: 264.1369.

(S)-2-(1-(3-methoxyphenyl)ethyl)isoquinolin-1(2H)-one (2h)



The titled compound was prepared by following the above procedure C, obtained 99.7:0.3 e.r. (99% ee). R_f (Ethyl acetate/Pet. ether = 20.80) = 0.3. 1H NMR (500 MHz, $CDCl_3$) δ 1.74 (d, $J = 7.02$ Hz, 3 H), 3.77 (s, 3 H), 6.45 (d, $J = 7.63$ Hz, 1 H), 6.53 (q, $J = 7.02$ Hz, 1 H), 6.81 - 6.86 (m, 1 H), 6.88 (s, 1 H), 6.90 - 6.97 (m, 2 H), 7.27 - 7.30 (m, 1 H), 7.45 - 7.54 (m, 2 H), 7.60 - 7.66 (m, 1 H), 8.49 (d, $J = 7.93$ Hz, 1 H). **LCMS** (ESI) m/z Calculated for $C_{18}H_{18}NO_2$ $[M+H]^+$: 280.34, found: 280.0.

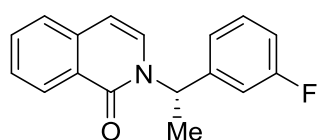
(S)-2-(1-(3,4-dimethoxyphenyl)ethyl)isoquinolin-1(2H)-one (2j)



The titled compound was prepared by following the above procedure C, obtained 98.2:1.8 e.r.(96% ee). R_f (Ethyl acetate/Pet. ether = 20.80) = 0.3. 1H NMR (500 MHz, $CDCl_3$)

δ 1.72 (d, $J = 7.13$ Hz, 3 H), 3.81 (s, 3 H), 3.88 (s, 3 H), 6.44 (d, $J = 7.50$ Hz, 1 H), 6.51 (d, $J = 7.00$ Hz, 1 H), 6.80 (d, $J = 2.00$ Hz, 1 H), 6.86 (d, $J = 8.26$ Hz, 1 H), 6.91 (d, $J = 7.50$ Hz, 1 H), 6.97 (d, $J = 1.63$ Hz, 1 H), 7.51 (d, $J = 7.13$ Hz, 1 H), 7.48 (d, $J = 7.75$ Hz, 1 H), 7.59 - 7.66 (m, 1 H), 8.49 (d, $J = 8.00$ Hz, 1 H). **LCMS** (ESI) m/z Calculated for $C_{19}H_{21}NO_3$ $[M+H]^+$: 311.1521, found: 311.1121.

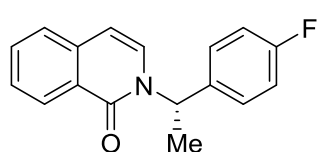
(S)-2-(1-(3-fluorophenyl)ethyl)isoquinolin-1(2H)-one (2k):



The titled compound was prepared by following the above procedure **C**, obtained 99.1:0.9 e.r.(98% ee). **1H NMR (500 MHz, $CDCl_3$)** δ 1.75 (d, $J = 6.71$ Hz, 3 H), 6.49 (d, $J = 7.32$ Hz, 1 H),

6.54 (d, $J = 6.71$ Hz, 1 H), 6.91 (d, $J = 7.02$ Hz, 1 H), 6.95 - 7.02 (m, 1 H), 7.04 (d, $J = 9.46$ Hz, 1 H), 7.12 (d, $J = 7.32$ Hz, 1 H), 7.28 - 7.36 (m, 1 H), 7.44 - 7.57 (m, 2 H), 7.65 (t, $J = 6.87$ Hz, 1 H), 8.48 (d, $J = 7.63$ Hz, 1 H). **R_f** (Ethyl acetate/Pet. ether = 20.80) = 0.3. **LCMS** (ESI) m/z Calculated for $C_{17}H_{15}NF[M+H]^+$: 268.30 found: 268.1.

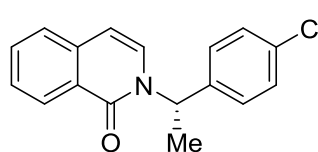
(S)-2-(1-(4-fluorophenyl)ethyl)isoquinolin-1(2H)-one (2l):



The titled compound was prepared by following the above procedure **C**, obtained 95.4:4.6 e.r. (91% ee). **R_f** (Ethyl acetate/Pet. ether = 20.80) = 0.3. **1H NMR (500 MHz, $CDCl_3$)** δ 1.75 (d, $J =$

7.02 Hz, 3 H), 6.47 (d, $J = 7.63$ Hz, 1 H), 6.54 (q, $J = 7.22$ Hz, 1 H), 6.90 (d, $J = 7.63$ Hz, 1 H), 7.04 (t, $J = 8.70$ Hz, 2 H), 7.33 (dd, $J = 8.54, 5.49$ Hz, 2 H), 7.44 - 7.54 (m, 2 H), 7.60 - 7.68 (m, 1 H), 8.48 (d, $J = 8.24$ Hz, 1 H). **LCMS** Calculated for $C_{17}H_{15}NF[M]$: 268.30 found: 268.1.

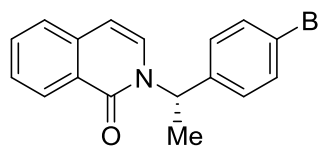
(S)-2-(1-(4-chlorophenyl)ethyl)isoquinolin-1(2H)-one (2m)



The titled compound was prepared by following the above procedure **C**, obtained 94.6:5.4 e.r. (89% ee). **R_f** (Ethyl acetate/Pet. ether = 20.80) = 0.3. **1H NMR (500 MHz, $CDCl_3$)** δ 1.75 (d, $J =$

7.07 Hz, 3 H), 6.47 (d, $J = 7.57$ Hz, 1 H), 6.52 (q, $J = 7.24$ Hz, 1 H), 6.89 (d, $J = 7.57$ Hz, 1 H), 7.28 (d, $J = 8.58$ Hz, 2 H), 7.32 (d, $J = 8.41$ Hz, 2 H), 7.46 - 7.54 (m, 2 H), 7.61 - 7.67 (m, 1 H), 8.48 (d, $J = 8.08$ Hz, 1 H). **LCMS** (ESI) m/z Calculated for $C_{17}H_{15}ClNO[M+H]^+$: 284.76, found: 284.1.

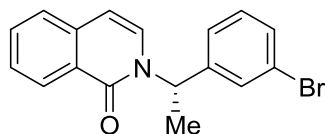
(S)-2-(1-(4-bromophenyl)ethyl)isoquinolin-1(2H)-one (2n)



The titled compound was prepared by following the above procedure **C**, obtained 95.1:4.9 e.r.(90% ee). **R_f** (Ethyl acetate/Pet. ether = 20.80) = 0.3. **1H NMR (500 MHz, $CDCl_3$)** δ 1.74 (d, $J =$

7.07 Hz, 3 H), 6.43 - 6.53 (m, 2 H), 6.89 (d, $J = 7.41$ Hz, 1 H), 7.22 (d, $J = 8.25$ Hz, 2 H), 7.45 - 7.54 (m, 4 H), 7.61 - 7.67 (m, 1 H), 8.48 (d, $J = 7.91$ Hz, 1 H). **LCMS** for $C_{17}H_{15}BrNO[M+1]^-$:328.03, found: 328.0

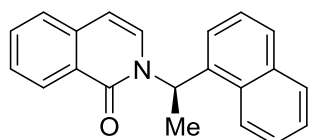
(S)-2-(1-(3-bromophenyl)ethyl)isoquinolin-1(2H)-one (2o)



The titled compound was prepared by following the above procedure **C**, obtained 92.7:7.3 e.r. (85% ee). R_f (Ethyl acetate/Pet. ether = 20.80) = 0.3. 1H NMR (500 MHz, $CDCl_3$) δ 1.73 - 1.78

(m, 3 H), 6.47 (dd, $J = 19.23, 7.32$ Hz, 1 H), 6.57 (d, $J = 7.02$ Hz, 1 H), 6.92 (dd, $J = 7.63, 4.27$ Hz, 1 H), 7.27 - 7.33 (m, 1 H), 7.34 - 7.37 (m, 2 H), 7.45 - 7.54 (m, 3 H), 7.61 - 7.67 (m, 1 H), 8.44 - 8.53 (m, 1 H). **HRMS** (ESI) m/z for $C_{17}H_{15}BrNO[M+H]^+$:328.0337, found: 328.0311.

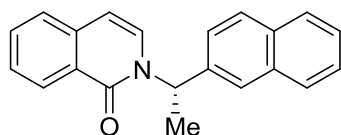
2-((S)-1-(naphthalen-1-yl)ethyl)naphthalen-1(2H)-one (2p)



The titled compound was prepared by following the above procedure **C**, obtained 2.5:97.5 e.r.(95% ee). R_f (Ethyl acetate/Pet. ether = 20.80) = 0.3. 1H NMR (500 MHz, $CDCl_3$) δ 1.87 (d, $J =$

7.02 Hz, 3 H), 6.29 (d, $J = 7.32$ Hz, 1 H), 6.80 (d, $J = 7.63$ Hz, 1 H), 7.15 (q, $J = 6.71$ Hz, 1 H), 7.37 - 7.47 (m, 3 H), 7.47 - 7.66 (m, 3 H), 7.77 (d, $J = 7.32$ Hz, 1 H), 7.82 - 7.92 (m, 2 H), 7.92 - 8.02 (m, 1 H), 8.58 (d, $J = 8.24$ Hz, 1 H).; **HRMS** (ESI) m/z Calculated for $C_{21}H_{17}NO$ $[M+Na]^+$:322.1207, found: 322.1206.

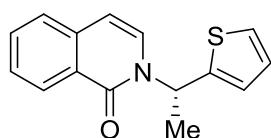
2-((R)-1-(naphthalen-1-yl)ethyl)naphthalen-1(2H)-one (2q)



The titled compound was prepared by following the above procedure **C**, obtained 98.9:1.1 e.r. (98% ee). R_f (Ethyl acetate/Pet. ether = 20.80) = 0.3. 1H NMR (500 MHz, $CDCl_3$) δ

1.87 (d, $J = 7.02$ Hz, 3 H), 6.42 (d, $J = 7.63$ Hz, 1 H), 6.74 (q, $J = 7.12$ Hz, 1 H), 6.92 (d, $J = 7.63$ Hz, 1 H), 7.32 - 7.41 (m, 1 H), 7.43 - 7.55 (m, 4 H), 7.60 - 7.69 (m, 1 H), 7.76 - 7.89 (m, 4 H), 8.52 (d, $J = 8.24$ Hz, 1 H). **HRMS** (ESI) m/z Calculated for $C_{21}H_{17}NO$ $[M+Na]^+$:322.1207, found: 322.1208.

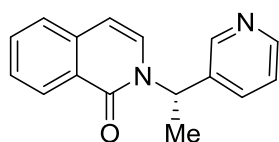
(S)-2-(1-(thiophen-2-yl)ethyl)isoquinolin-1(2H)-one (2s)



The titled compound was prepared by following the above procedure **C**, obtained 99.2:0.8e.r.(98% ee). 1H NMR (500 MHz, $CDCl_3$) δ 1.84 (d, $J = 7.02$ Hz, 3 H), 6.51 (d, $J = 7.63$ Hz, 1 H), 6.76 (q, $J = 7.02$ Hz,

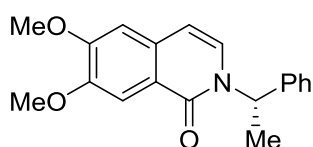
1 H), 7.00 - 7.07 (m, 2 H), 7.11 (d, $J = 3.36$ Hz, 1 H), 7.31 (d, $J = 4.88$ Hz, 1 H), 7.47 - 7.55 (m, 2 H), 7.63 - 7.69 (m, 1 H), 8.51 (d, $J = 7.93$ Hz, 1 H). R_f (Ethyl acetate/Pet. ether = 20.80) = 0.25. **LCMS** (ESI) m/z Calculated for $C_{15}H_{14}NOS$ $[M+H]^+$: 256.34, found: 256.1.

(S)-2-(1-(pyridin-3-yl)ethyl)isoquinolin-1(2H)-one (2t)



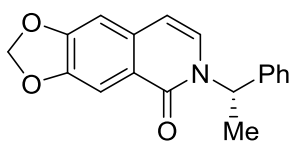
The titled compound was prepared by following the above procedure **C**, obtained 5.9:94.1 e.r. (88% ee). R_f (Ethyl acetate/Pet. ether = 50.50) = 0.2. 1H NMR (500 MHz, $CDCl_3$) δ 1.83 (d, $J = 7.02$ Hz, 3 H), 6.52 (d, $J = 7.63$ Hz, 2 H), 6.96 (d, $J = 7.32$ Hz, 1 H), 7.45 - 7.57 (m, 2 H), 7.67 (d, $J = 8.54$ Hz, 2 H), 8.46 (d, $J = 7.63$ Hz, 1 H), 8.59 (s, $J = 1H$), 8.70 (s, $J = 1H$). **LCMS** (ESI) m/z Calculated for $C_{16}H_{15}N_2O$ $[M+H]^+$: 251.30, found: 251.1.

(S)-6,7-dimethoxy-2-(1-phenylethyl)isoquinolin-1(2H)-one (2x)



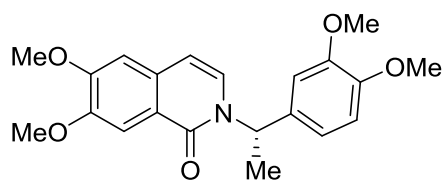
The titled compound was prepared by following the above procedure **C**, obtained 97.1:2.9 e.r.(94% ee). R_f (Ethyl acetate/Pet. ether = 50.50) = 0.3. 1H NMR (500 MHz, $CDCl_3$) δ 1.76 (d, $J = 7.02$ Hz, 3 H), 3.98 (s, 3 H), 4.02 (s, 3 H), 6.38 (d, $J = 7.63$ Hz, 1 H), 6.56 (q, $J = 7.12$ Hz, 1 H), 6.83 - 6.89 (m, 2 H), 7.28 - 7.31 (m, 1 H), 7.32 - 7.37 (m, 4 H), 7.87 (s, 1 H). **LCMS** (ESI) m/z Calculated for $C_{19}H_{20}NO_3$ $[M+H]^+$: 310.1413, found: 310.1432.

(S)-6-(1-phenylethyl)-[1,3]dioxolo[4,5-g]isoquinolin-5(6H)-one (2y)

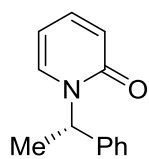


The titled compound was prepared by following the above procedure **C**, obtained 97.6:2.4 e.r.(95% ee). R_f (Ethyl acetate/Pet. ether = 50.50) = 0.3. 1H NMR (500 MHz, $CDCl_3$) δ 1.75 (d, $J = 7.02$ Hz, 3 H), 6.07 (s, 2 H), 6.33 (d, $J = 7.63$ Hz, 1 H), 6.54 (d, $J = 7.02$ Hz, 1 H), 6.80 - 6.85 (m, 2 H), 7.30 - 7.39 (m, 5 H), 7.84 (s, 1 H). **LCMS** (ESI) m/z Calculated for $C_{18}H_{16}NO_3$ $[M+H]^+$: 294.34, found: 294.1.

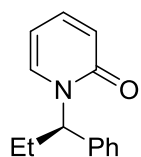
(S)-2-(1-(3,4-dimethoxyphenyl)ethyl)-6,7-dimethoxyisoquinolin-1(2H)-one (2z)



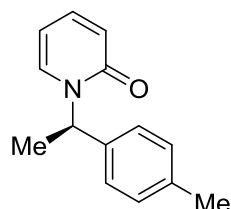
The titled compound was prepared by following the above procedure **C**, obtained 99.2:0.8 e.r. (98% ee). R_f (Ethyl acetate/Pet. ether = 50.50) = 0.2. 1H NMR (500 MHz, $CDCl_3$) δ 1.72 (d, $J = 7.02$ Hz, 3 H), 3.81 (s, 3 H) 3.88 (s, 3 H), 3.98 (s, 3 H), 4.02 (s, 3 H), 6.38 (d, $J = 7.63$ Hz, 1 H), 6.51 (d, $J = 7.02$ Hz, 1 H), 6.79 (s, 1 H), 6.82 - 6.88 (m, 3 H), 6.97 (d, $J = 7.02$ Hz, 1 H), 7.87 (s, 1 H). **LCMS** (ESI) m/z Calculated for $C_{21}H_{23}NO_5$ $[M+Na]^+$: 392.1473, found: 392.1463.

(S)-1-(1-phenylethyl)pyridin-2(1H)-one (4a)

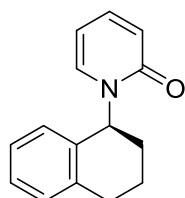
The titled compound was prepared by following the above procedure **D**, obtained 99.0:1.0 e.r.(98% ee). R_f (Ethyl acetate/Pet. ether = 50:50) = 0.3. The spectral values were matched favourably with previously reported literature values.²³ $^1\text{H NMR}$ (500 MHz, CDCl_3) δ 1.72 (d, J = 7.32 Hz, 3 H), 6.06 - 6.15 (m, 1 H), 6.46 (q, J = 7.22 Hz, 1 H), 6.62 (d, J = 9.16 Hz, 1 H), 7.10 (dd, J = 7.02, 1.53 Hz, 1 H), 7.23 - 7.42 (m, 7 H). **LCMS** (ESI) m/z Calculated for $\text{C}_{13}\text{H}_{14}\text{NO}$ $[\text{M}+\text{H}]^+$: 200.25, found: 200.2.

(R)-1-(1-phenylpropyl)pyridin-2(1H)-one (4b)

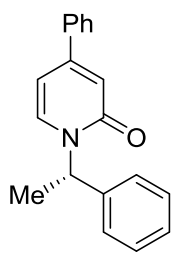
The titled compound was prepared by following the above procedure **D**, obtained 0.9:99.1 e.r. (99% ee). R_f (Ethyl acetate/Pet. ether = 50:50) = 0.3. $^1\text{H NMR}$ (500 MHz, CDCl_3) δ 0.97 (t, J = 7.32 Hz, 3 H), 2.00 - 2.11 (m, 1 H), 2.17 - 2.29 (m, 1 H), 6.13 (t, J = 6.26 Hz, 1 H), 6.25 (dd, J = 8.54, 7.32 Hz, 1 H), 6.61 (d, J = 9.16 Hz, 1 H), 7.17 (dd, J = 6.87, 1.37 Hz, 1 H), 7.23 - 7.33 (m, 4 H), 7.35 (d, J = 4.27 Hz, 4 H). **HRMS** (ESI) m/z Calculated for $\text{C}_{14}\text{H}_{15}\text{NO}$ $[\text{M}+\text{Na}]^+$: 236.1051, found: 236.1043.

(R)-1-(1-(p-tolyl)ethyl)pyridin-2(1H)-one (4c)

The titled compound was prepared by following the above procedure **D**, obtained 0.9:99.1 e.r. (99% ee). $^1\text{H NMR}$ (500 MHz, CDCl_3) δ 1.70 (d, J = 7.02 Hz, 3 H), 2.34 (s, 3 H), 6.04 - 6.15 (m, 1 H), 6.42 (q, J = 7.02 Hz, 1 H), 6.61 (d, J = 9.16 Hz, 1 H), 7.09 (dd, J = 6.87, 1.37 Hz, 1 H), 7.17 (m, J = 8.24 Hz, 2 H), 7.22 (m, J = 8.24 Hz, 2 H), 7.26 - 7.28 (m, 1 H). R_f (Ethyl acetate/Pet. ether = 50:50) = 0.3. **HRMS** (ESI) m/z Calculated for $\text{C}_{14}\text{H}_{16}\text{NO}$ $[\text{M}+\text{H}]^+$: 214.1231, found: 214.1164.

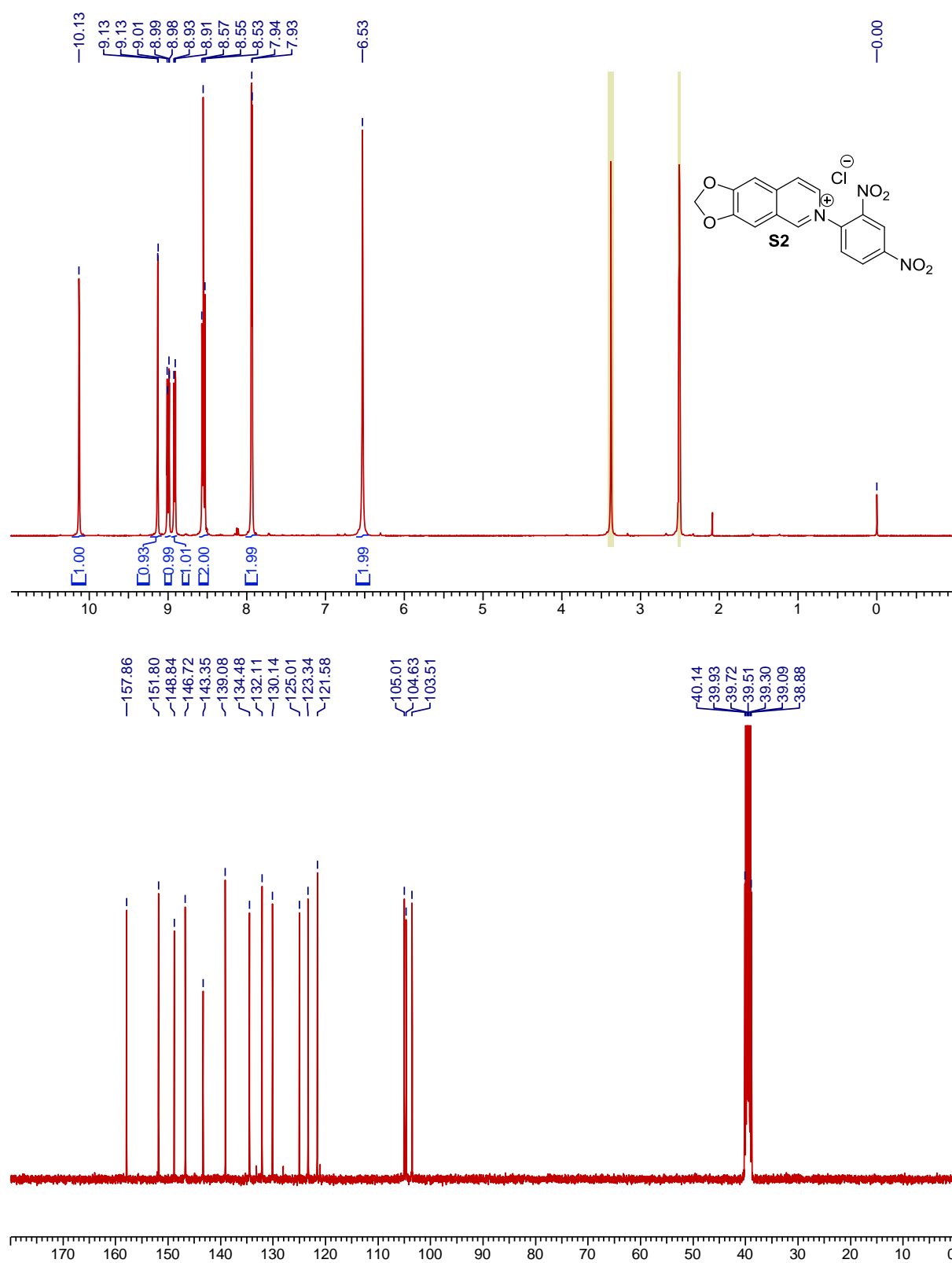
(S)-1-(1,2,3,4-tetrahydronaphthalen-1-yl)pyridin-2(1H)-one (4d)

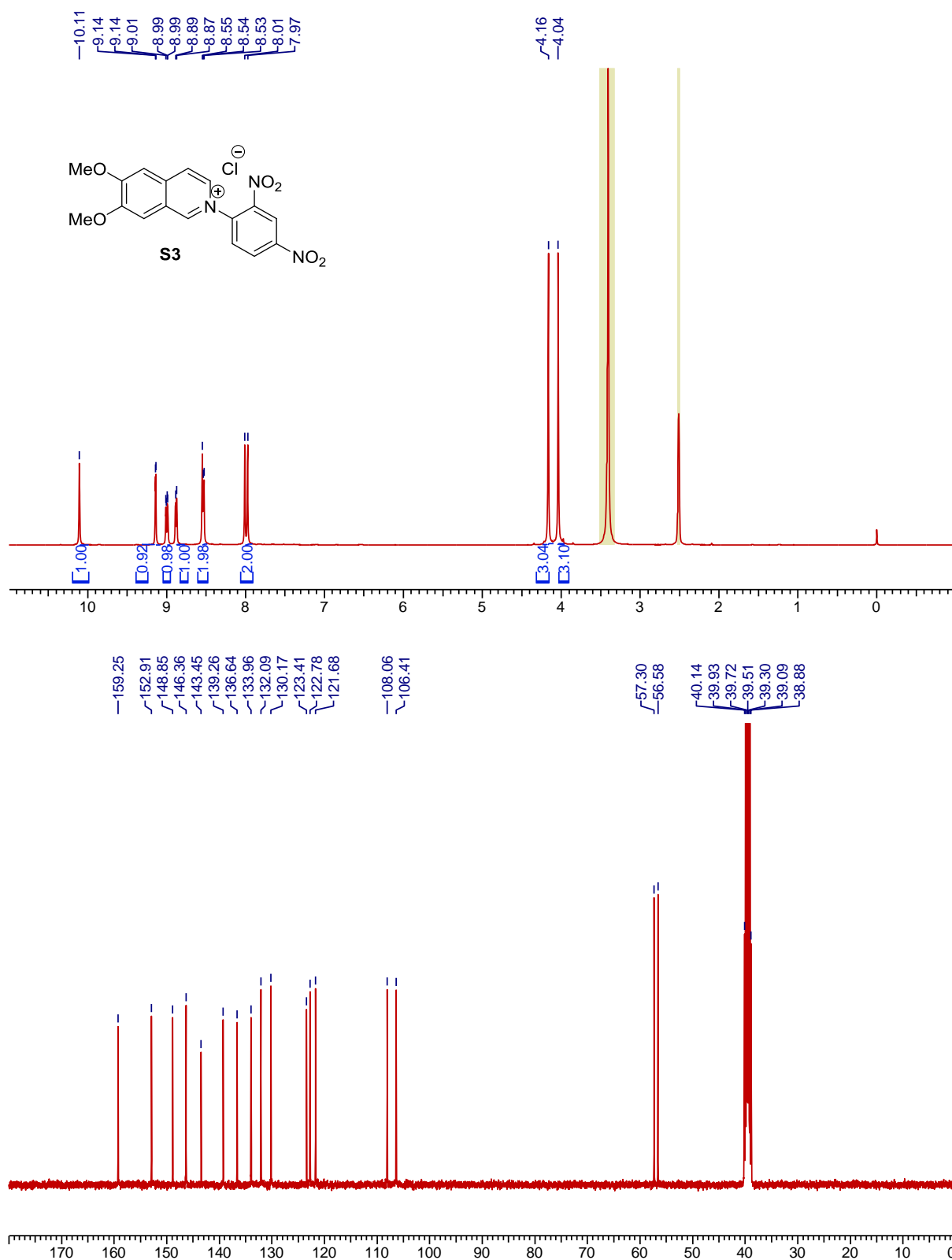
The titled compound was prepared by following the above procedure **D**, obtained 0.9:99.1 e.r. (99% ee). $^1\text{H NMR}$ (500 MHz, CDCl_3) δ 1.84 - 1.99 (m, 3 H), 2.22 - 2.32 (m, 1 H), 2.80 - 3.00 (m, 2 H), 6.07 (t, J = 6.71 Hz, 1 H), 6.31 (t, J = 6.41 Hz, 1 H), 6.63 (d, J = 9.16 Hz, 1 H), 6.86 - 6.99 (m, 2 H), 7.14 (t, J = 7.48 Hz, 1 H), 7.16 - 7.24 (m, 2 H), 7.28 - 7.34 (m, 1 H). R_f (Ethyl acetate/Pet. ether = 50:50) = 0.3. **HRMS** (ESI) m/z Calculated for $\text{C}_{17}\text{H}_{20}\text{NO}$ $[\text{M}+\text{Na}]^+$: 248.1051, found: 248.1037.

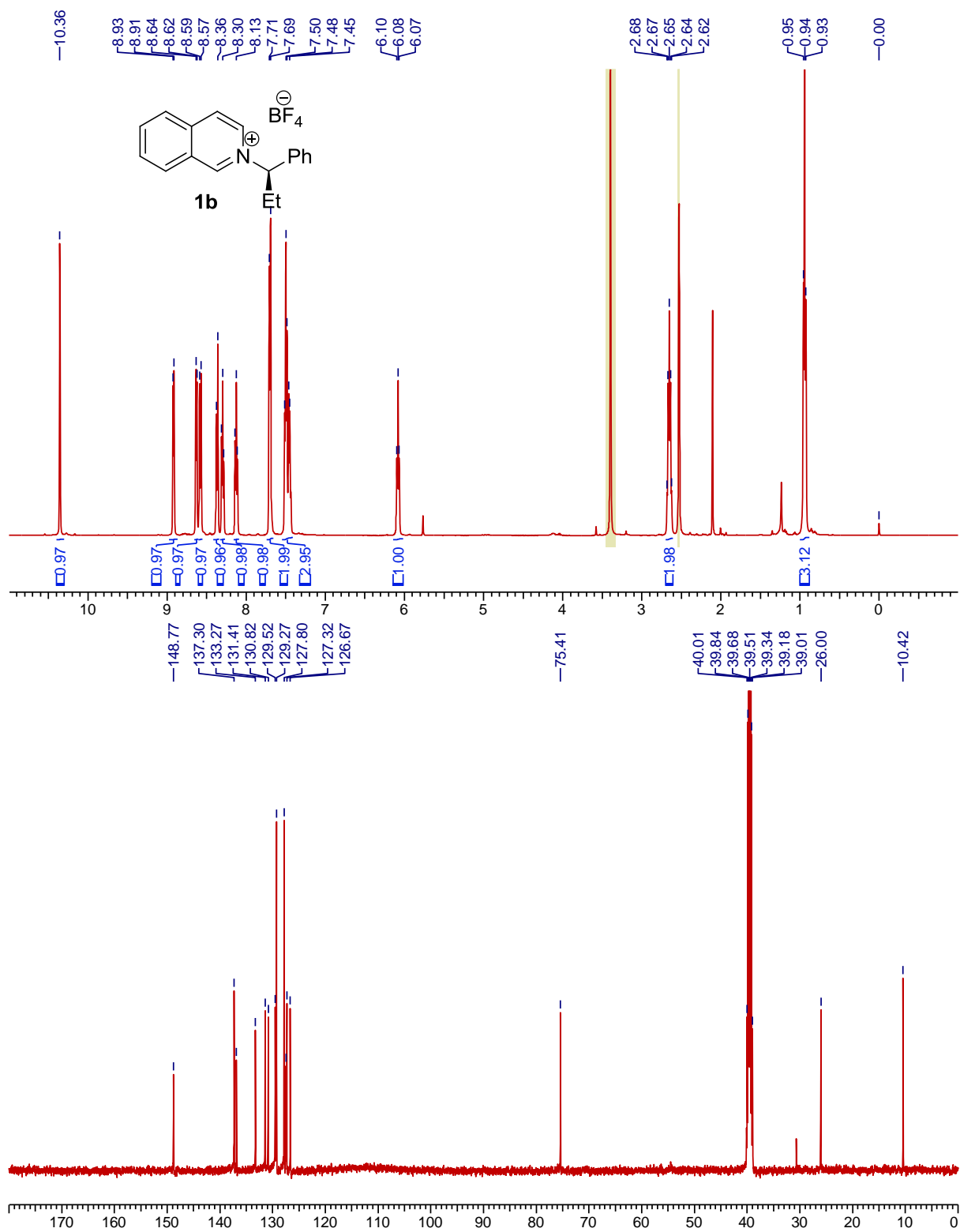
(S)-4-phenyl-1-(1-phenylethyl)pyridin-2(1H)-one (4e)

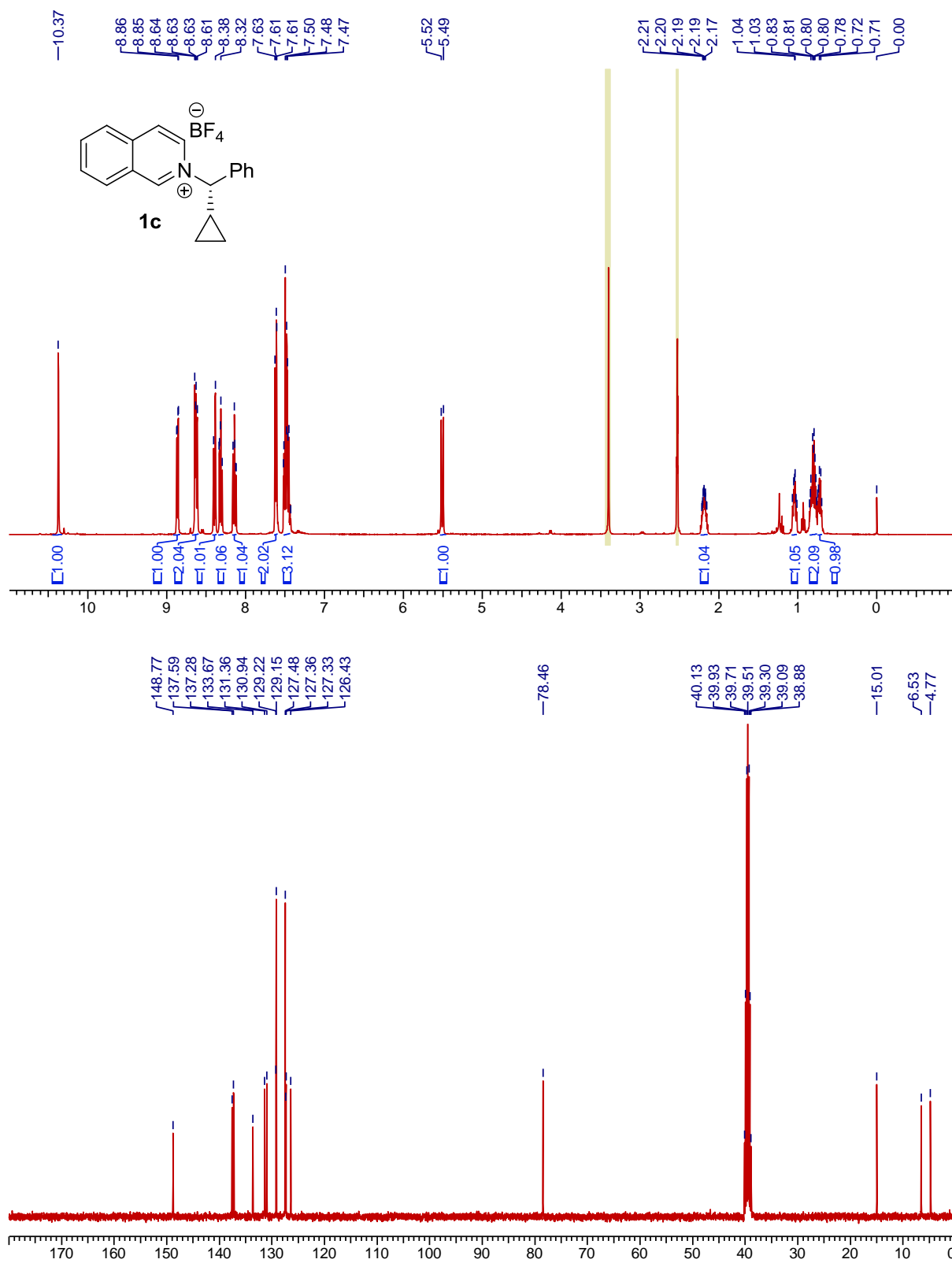
The titled compound was prepared by following the above procedure **D**, obtained 0.9:99.1 e.r. (99% ee). R_f (Ethyl acetate/Pet. ether = 50:50) = 0.35. ^1H NMR (500 MHz, CDCl_3) δ 1.76 (d, $J = 7.32$ Hz, 3 H), 6.39 (dd, $J = 7.32$, 1.83 Hz, 1 H), 6.48 (d, $J = 7.02$ Hz, 1 H), 6.84 (s, 1 H), 7.16 (d, $J = 7.32$ Hz, 1 H), 7.29 - 7.47 (m, 8 H), 7.51 - 7.59 (m, 2 H). HRMS (ESI) m/z Calculated for $\text{C}_{19}\text{H}_{18}\text{NO}[\text{M}+\text{H}]^+$: 276.1388, found: 276.1370.

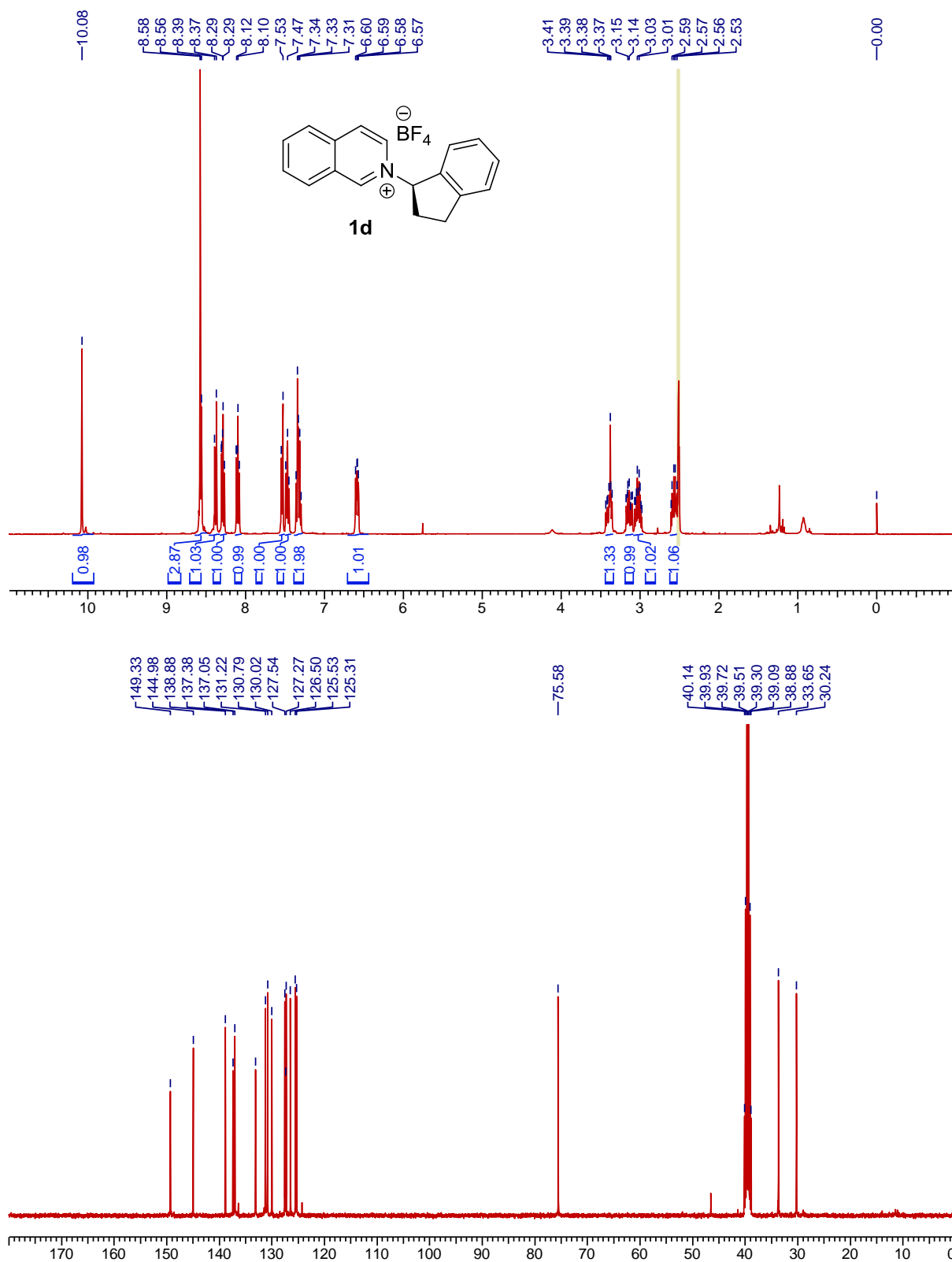
4.11 Spectral data

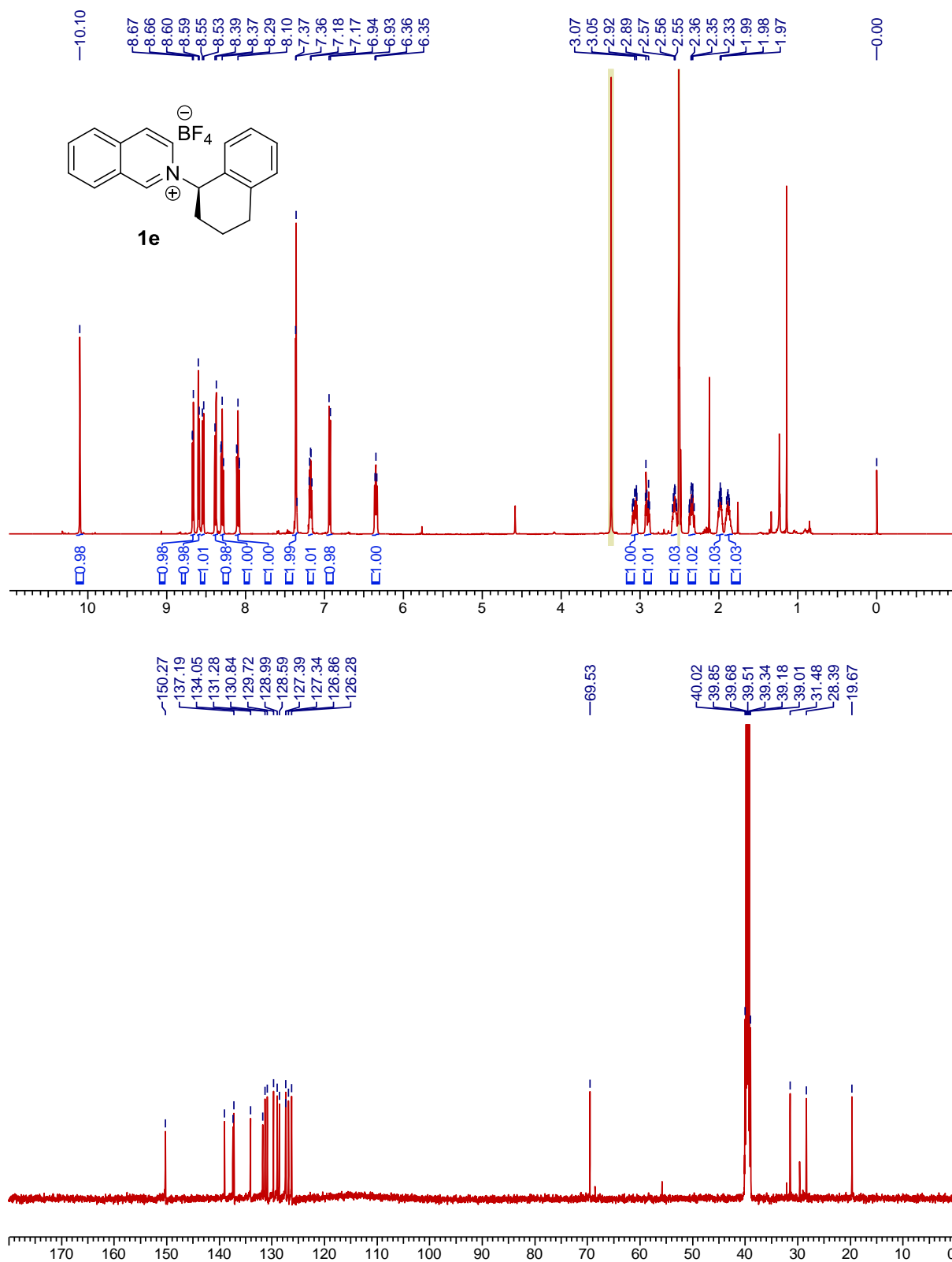


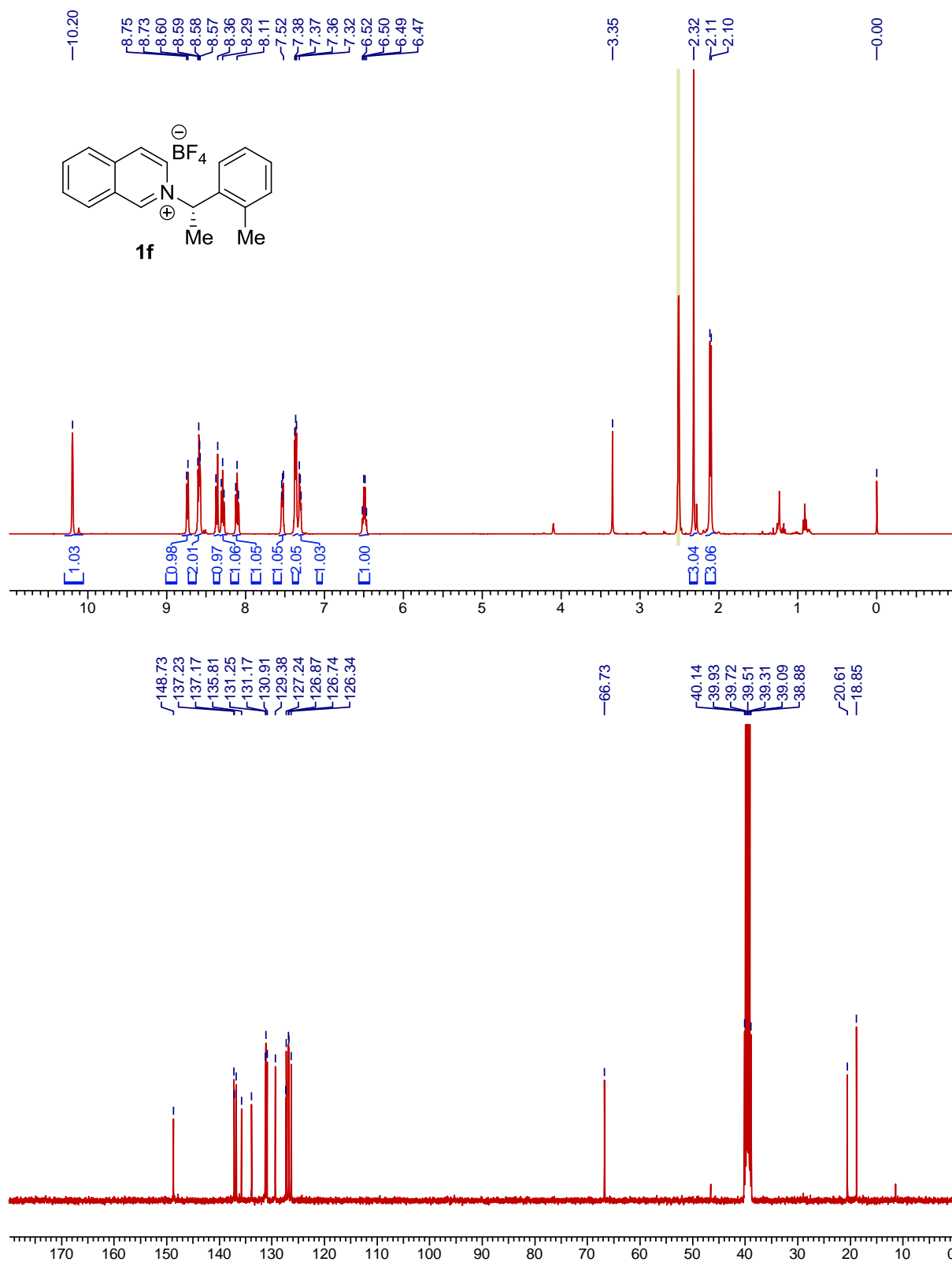


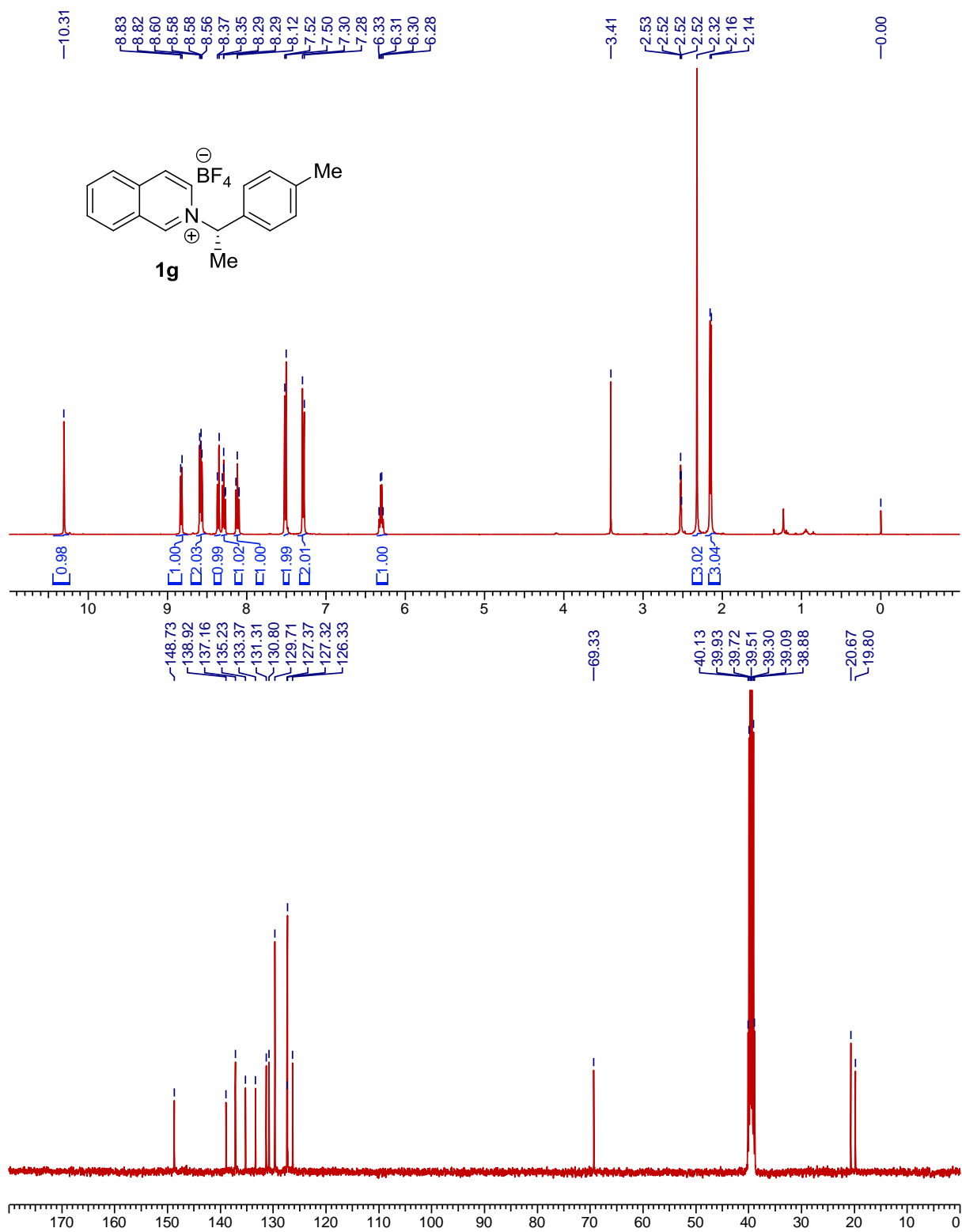


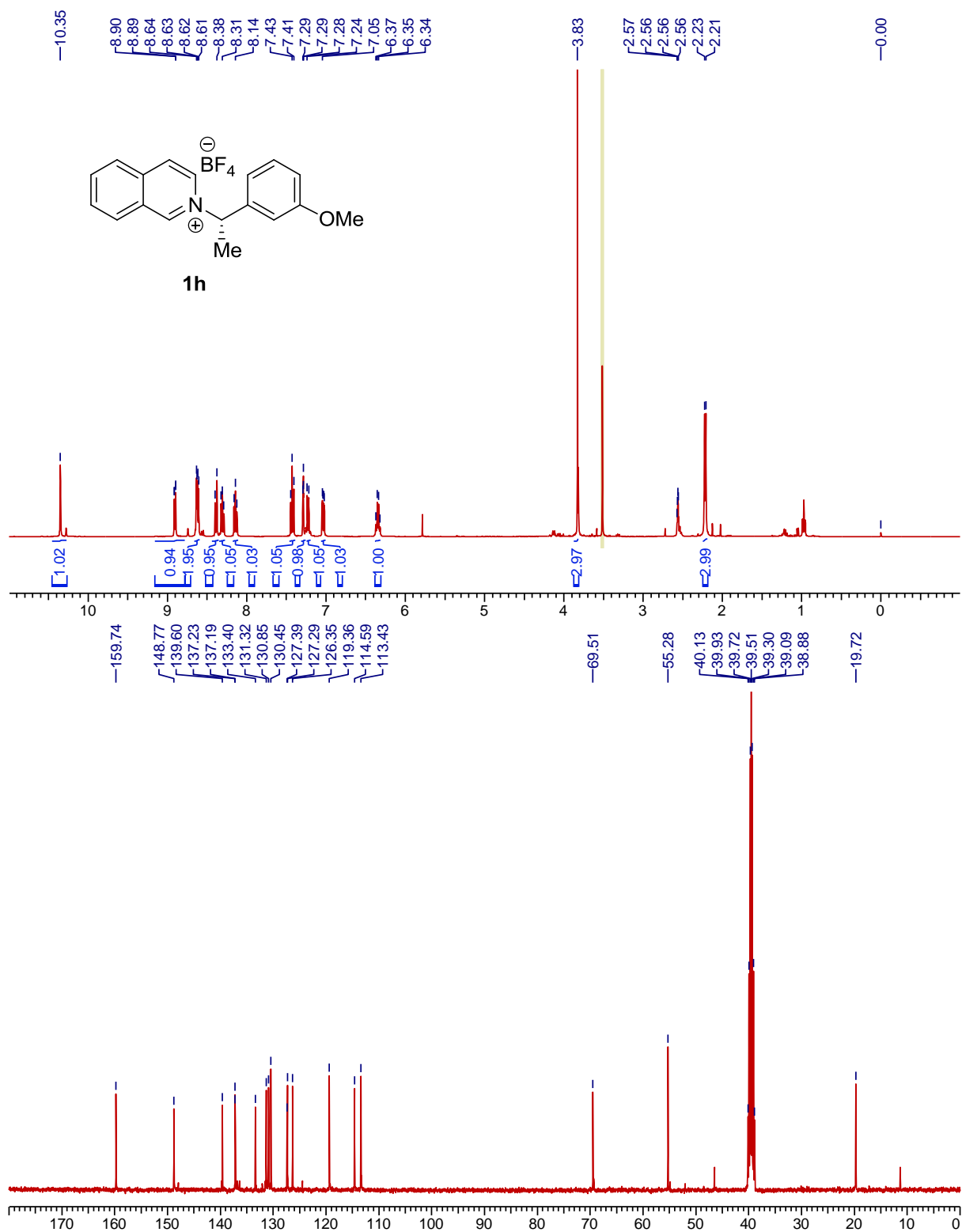


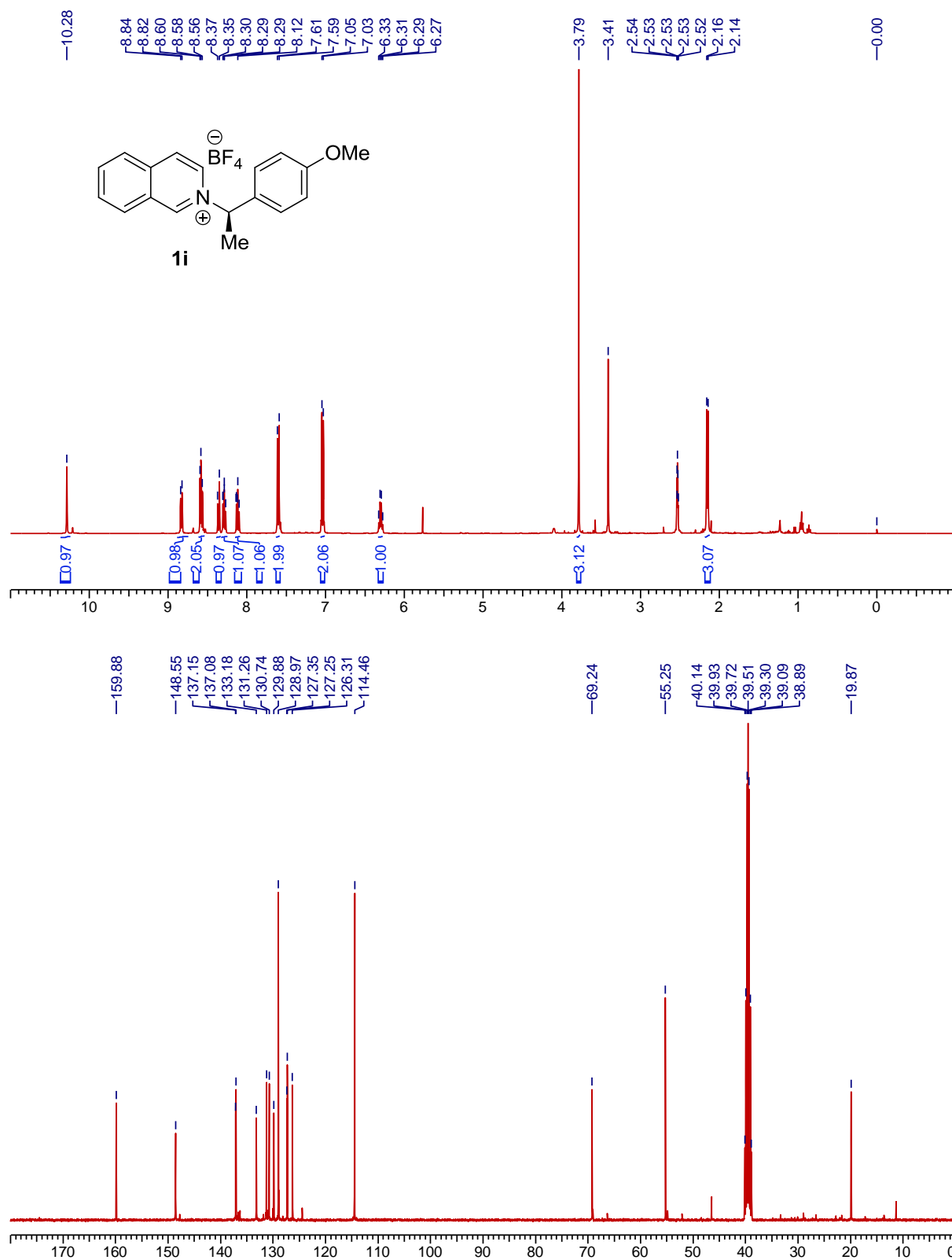


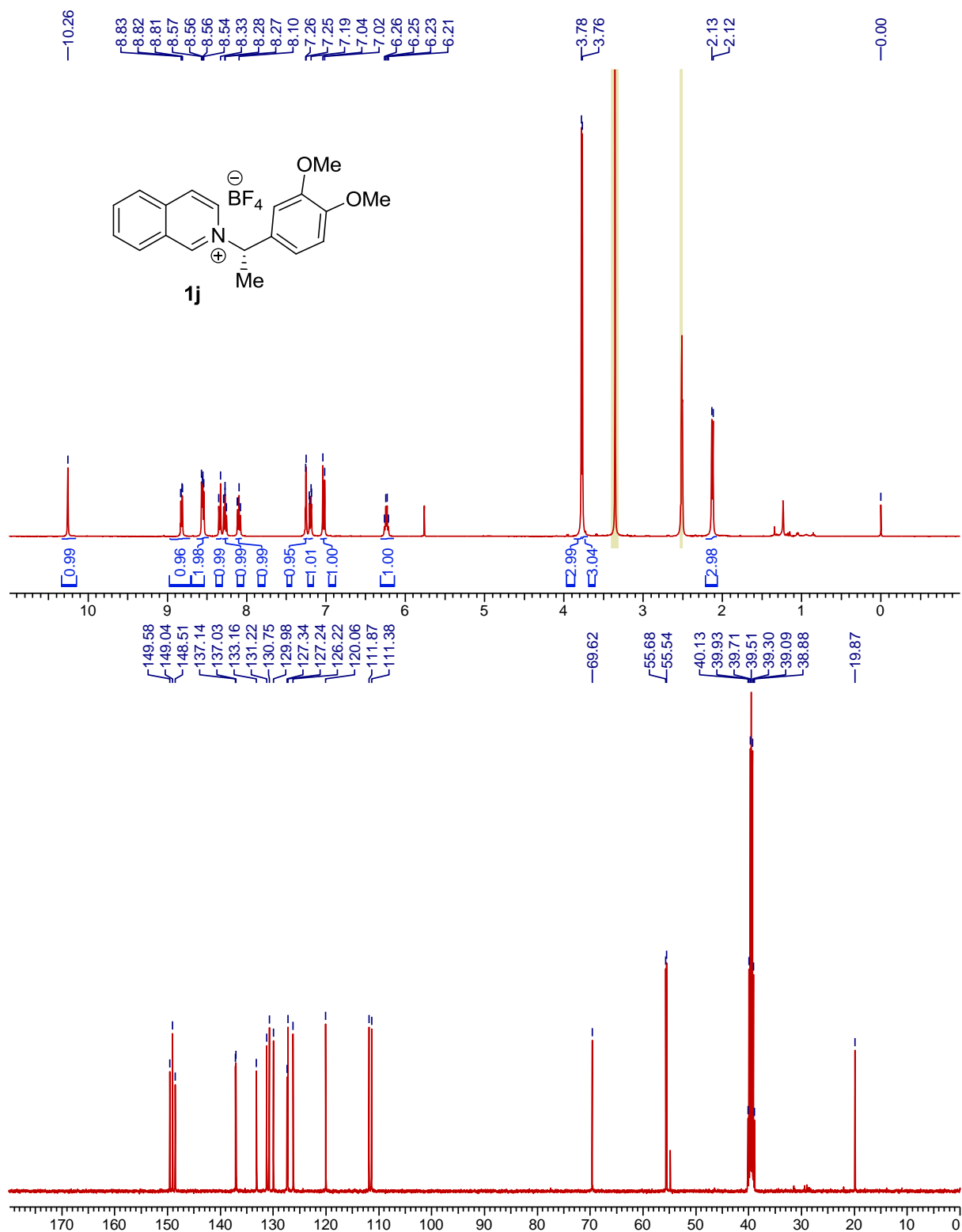


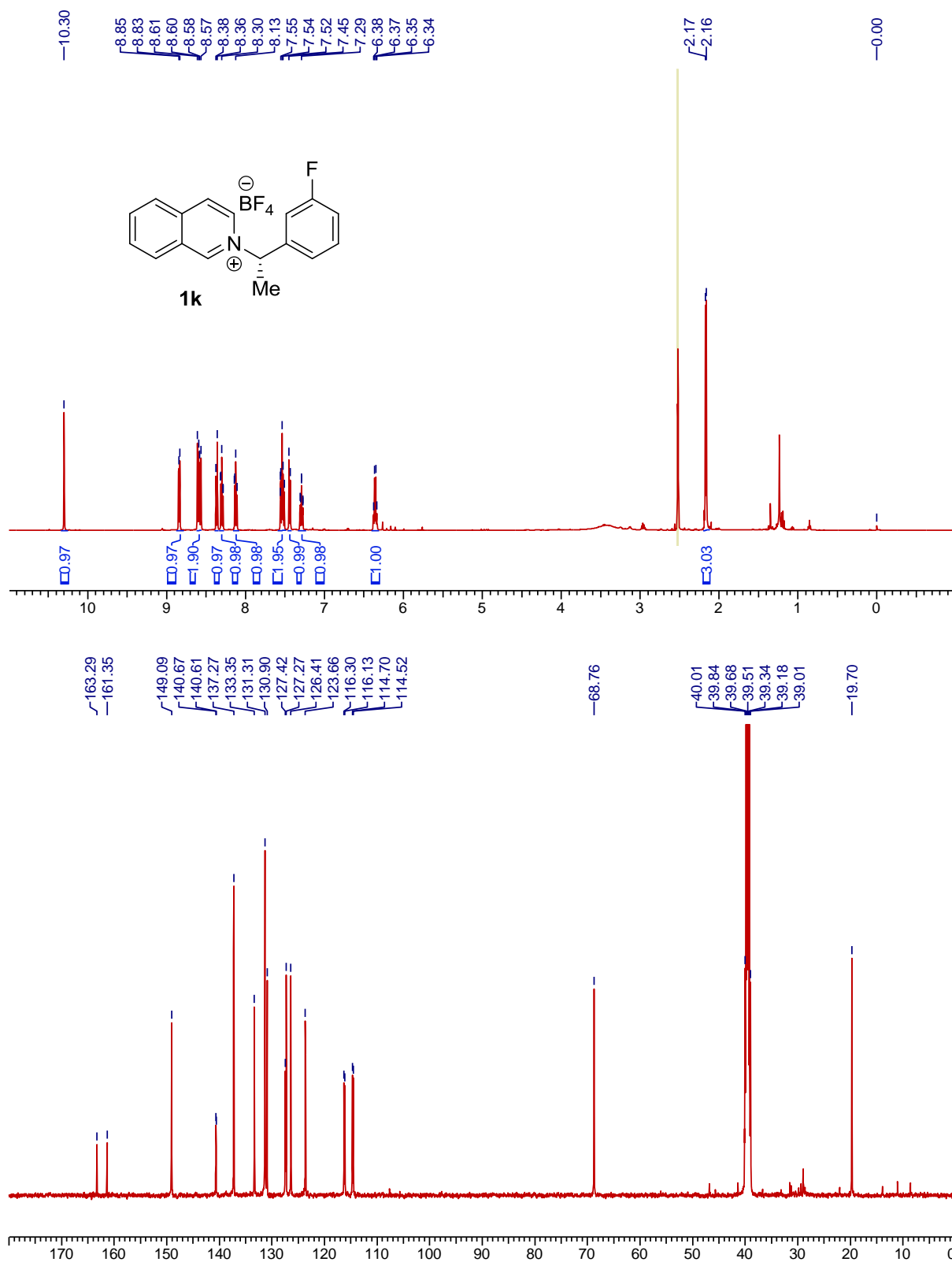


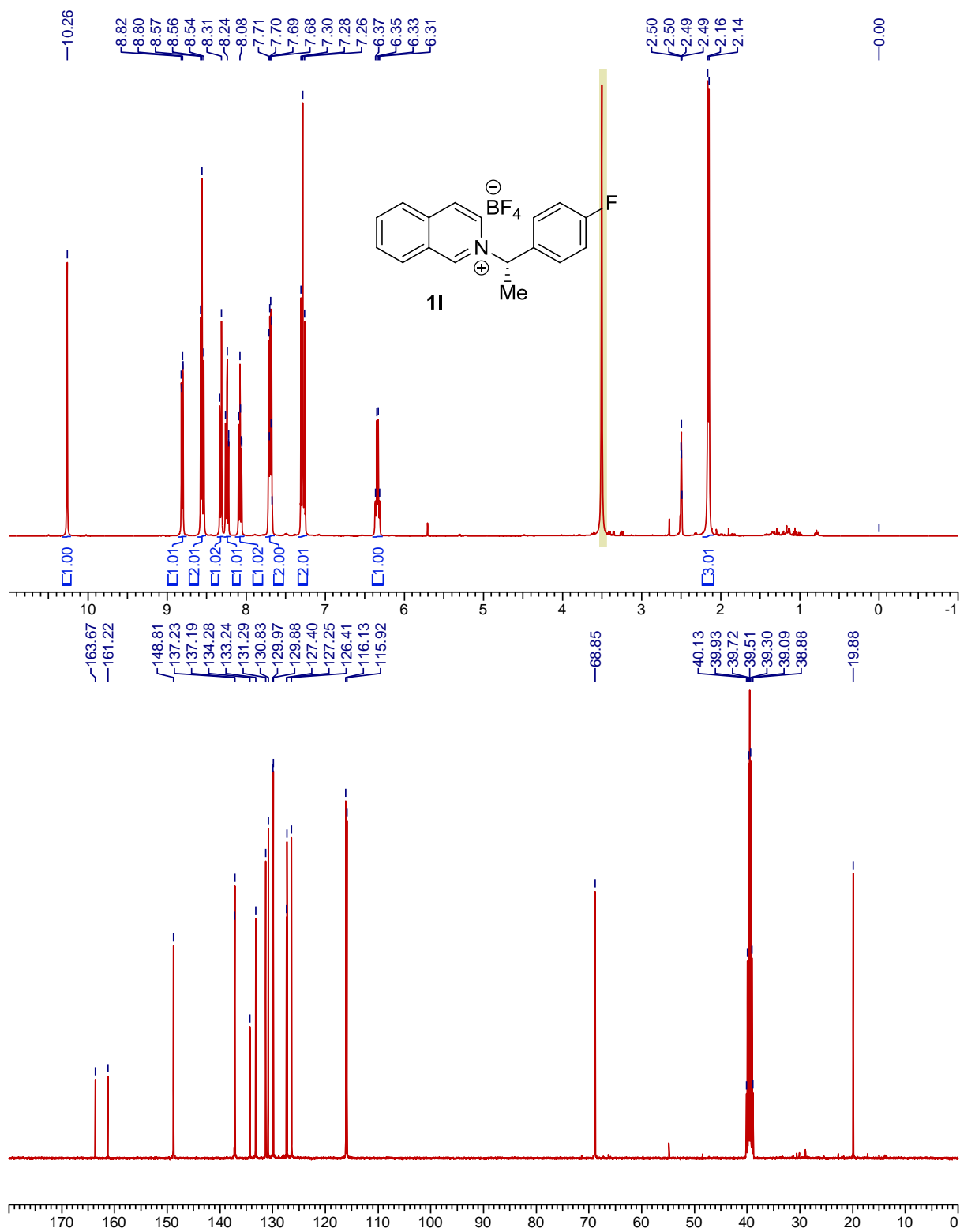


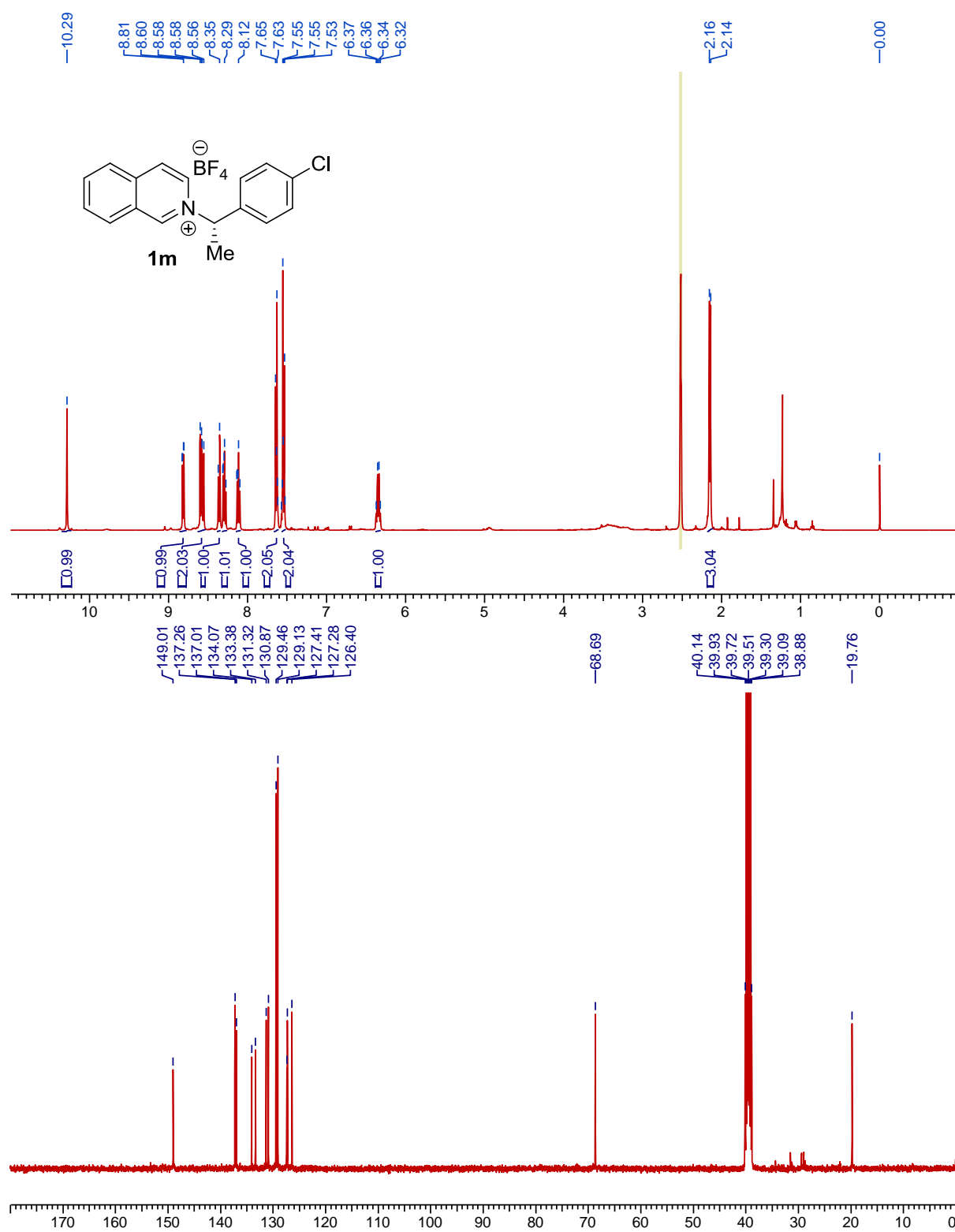


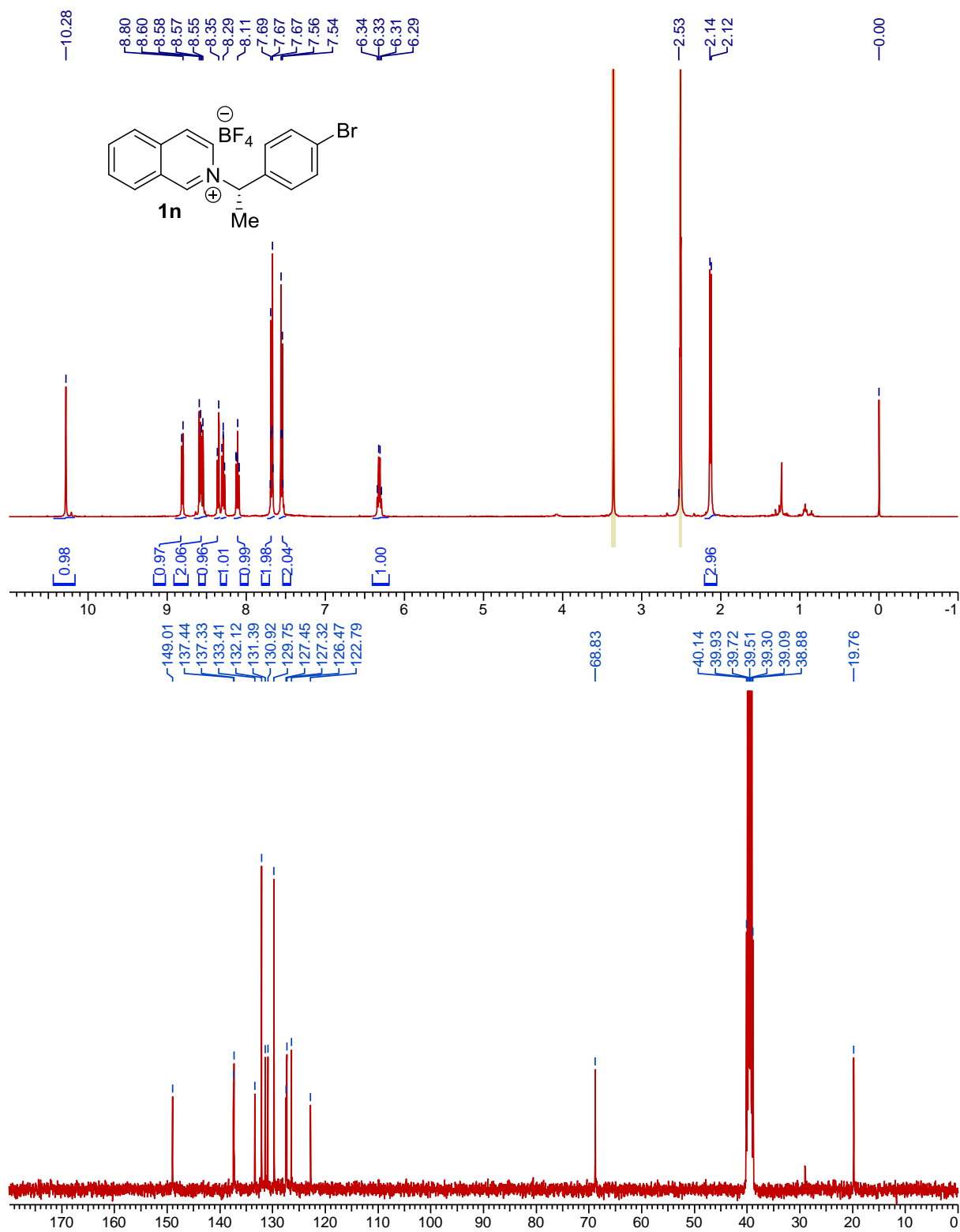


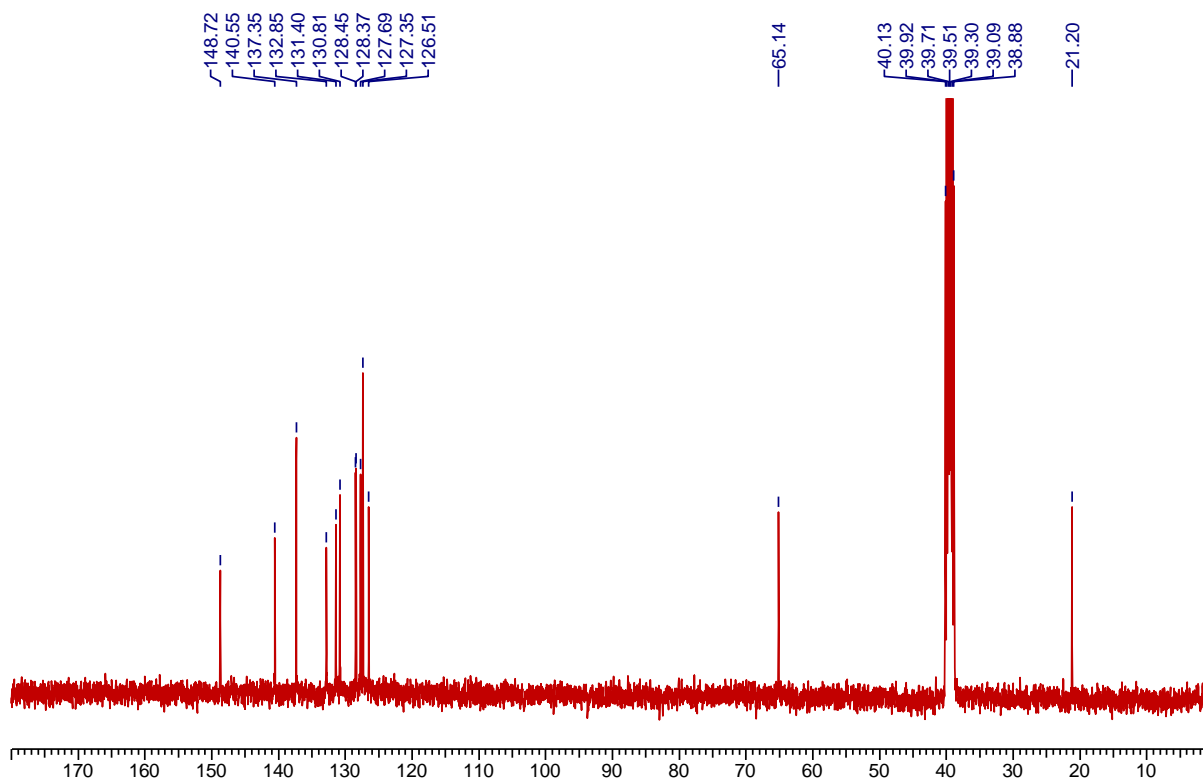
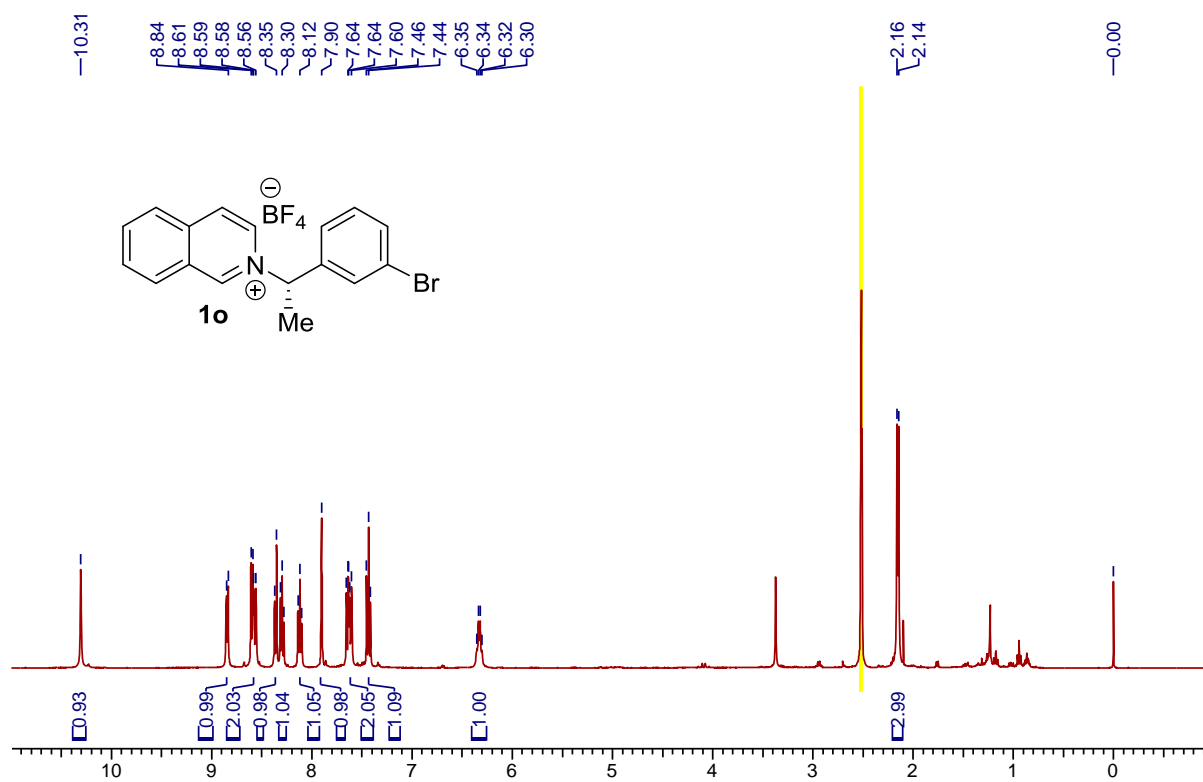


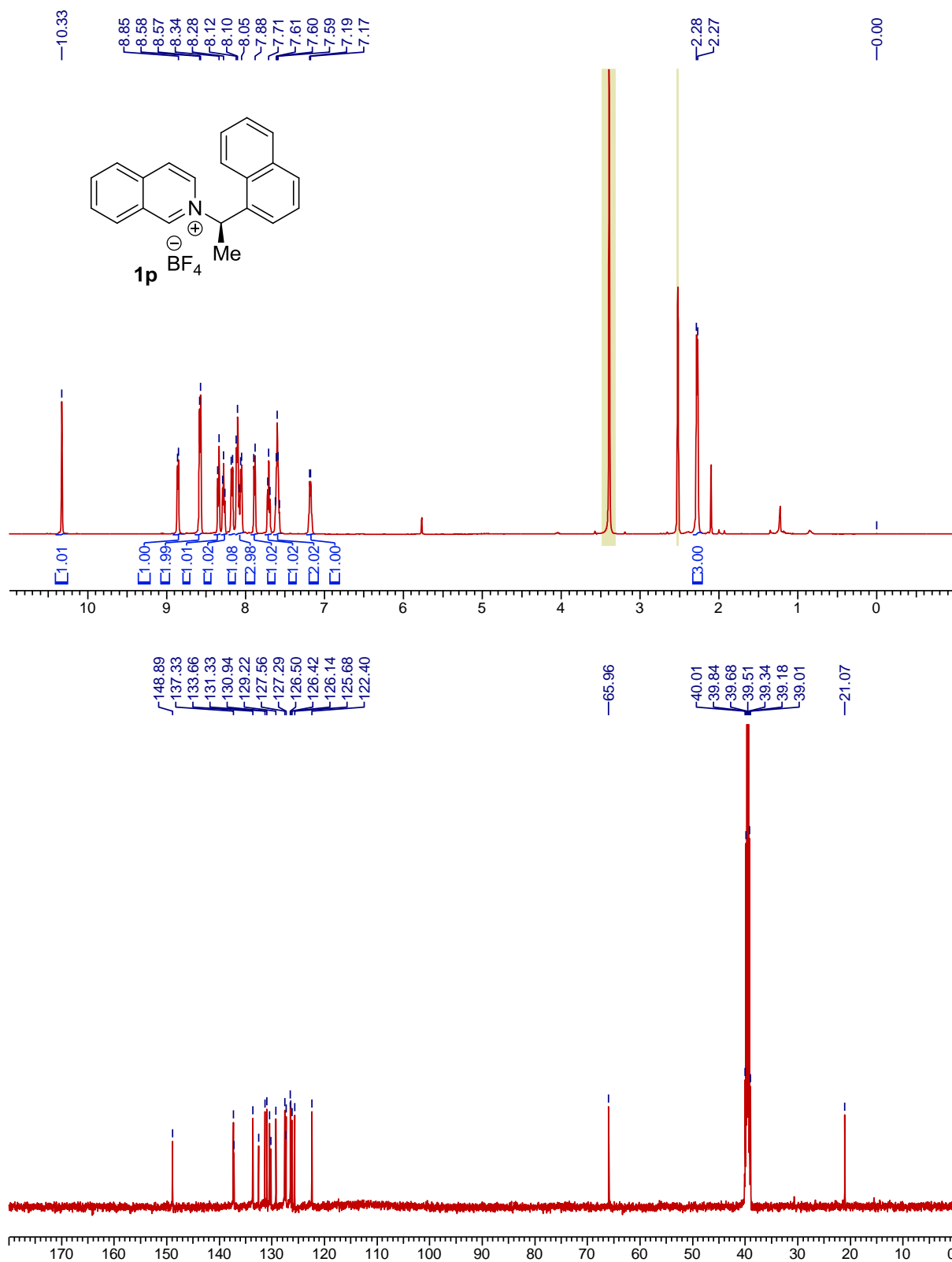


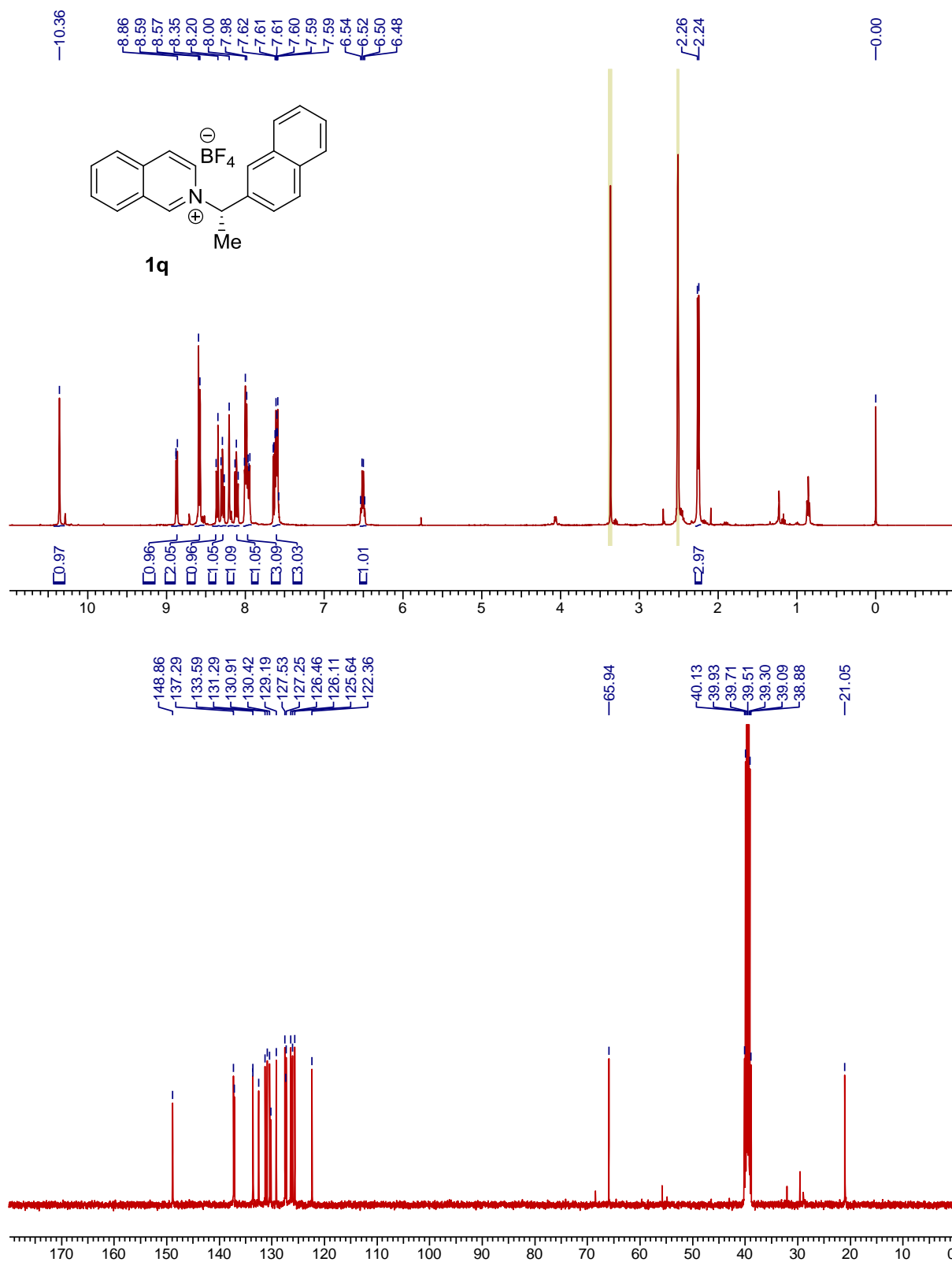


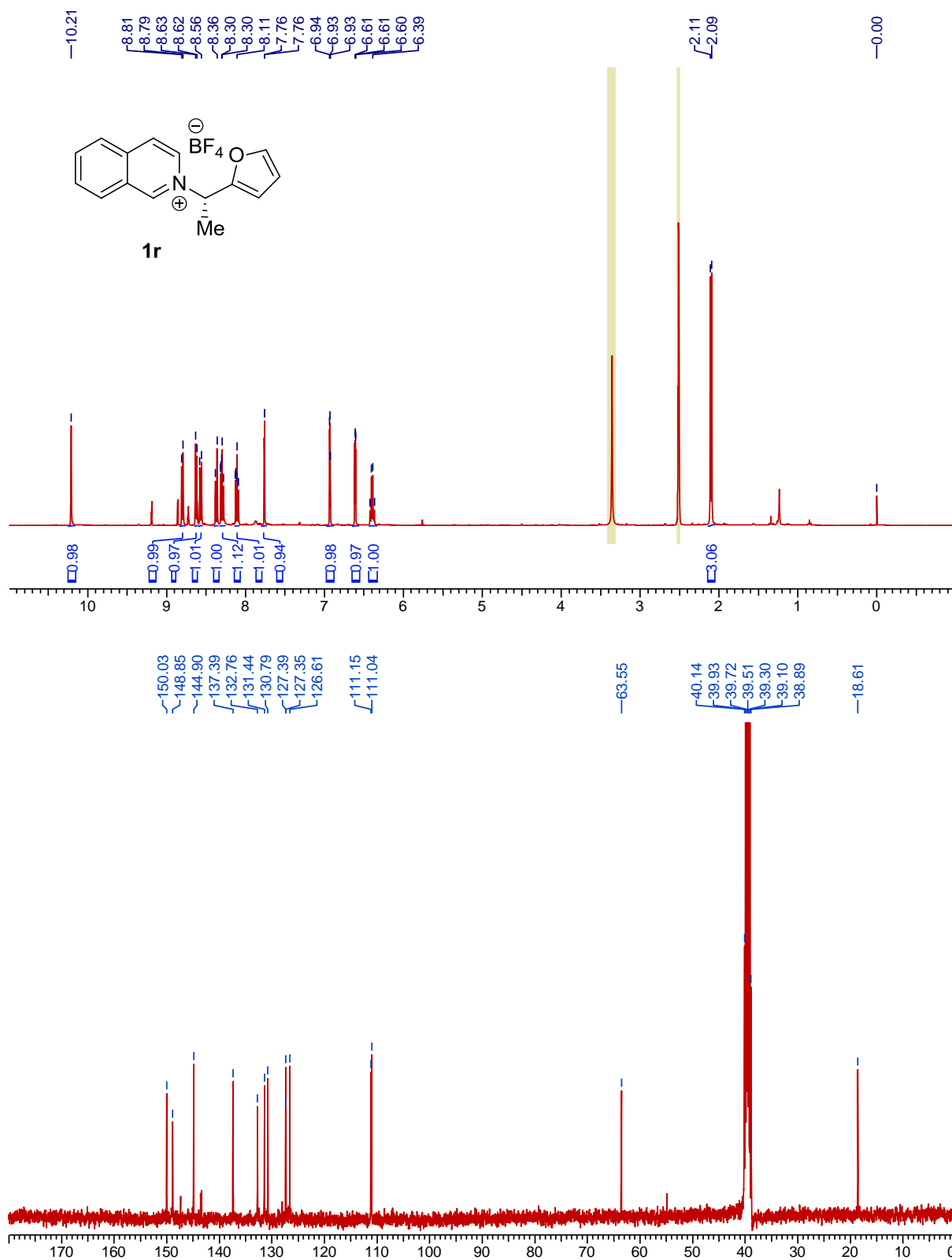


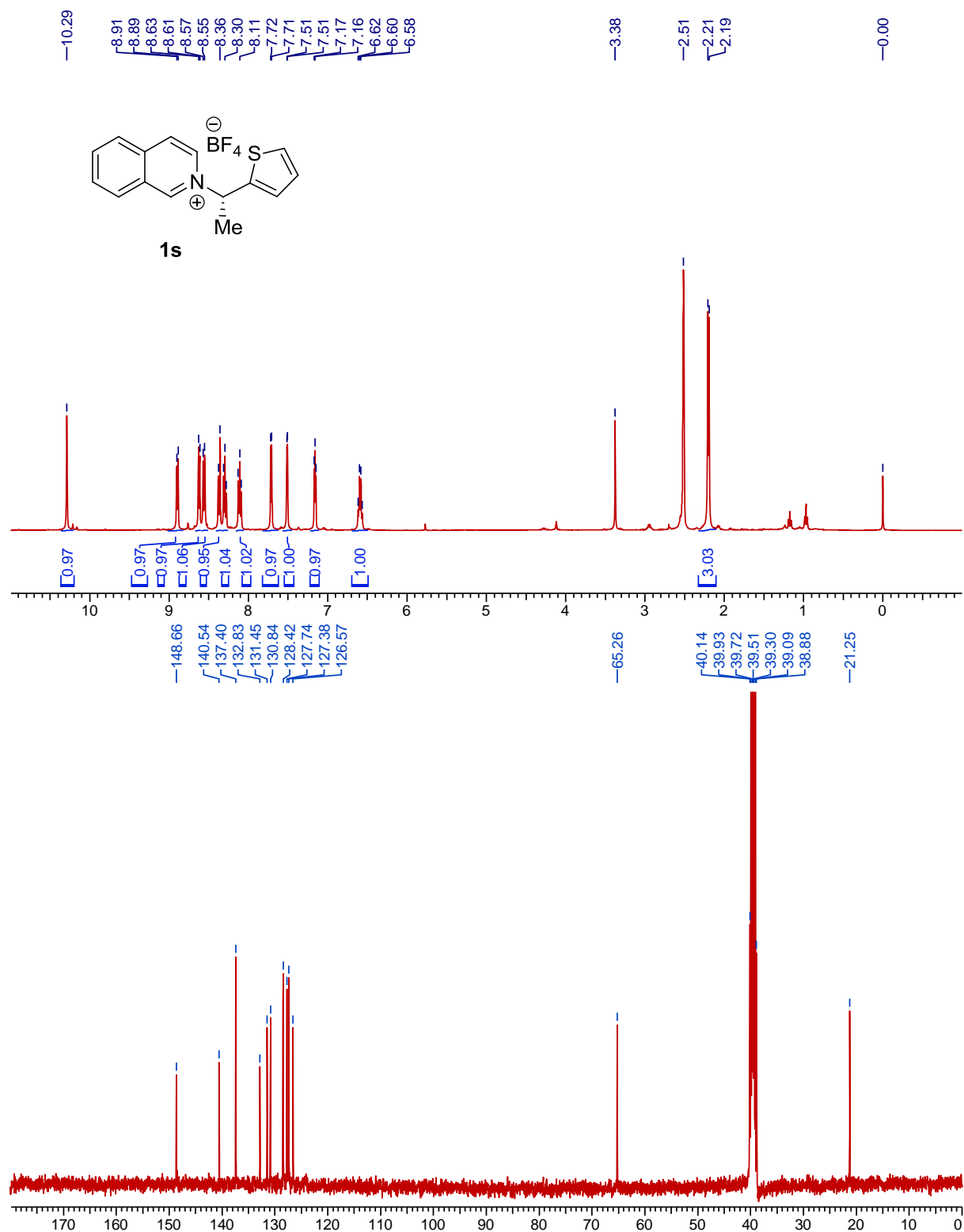


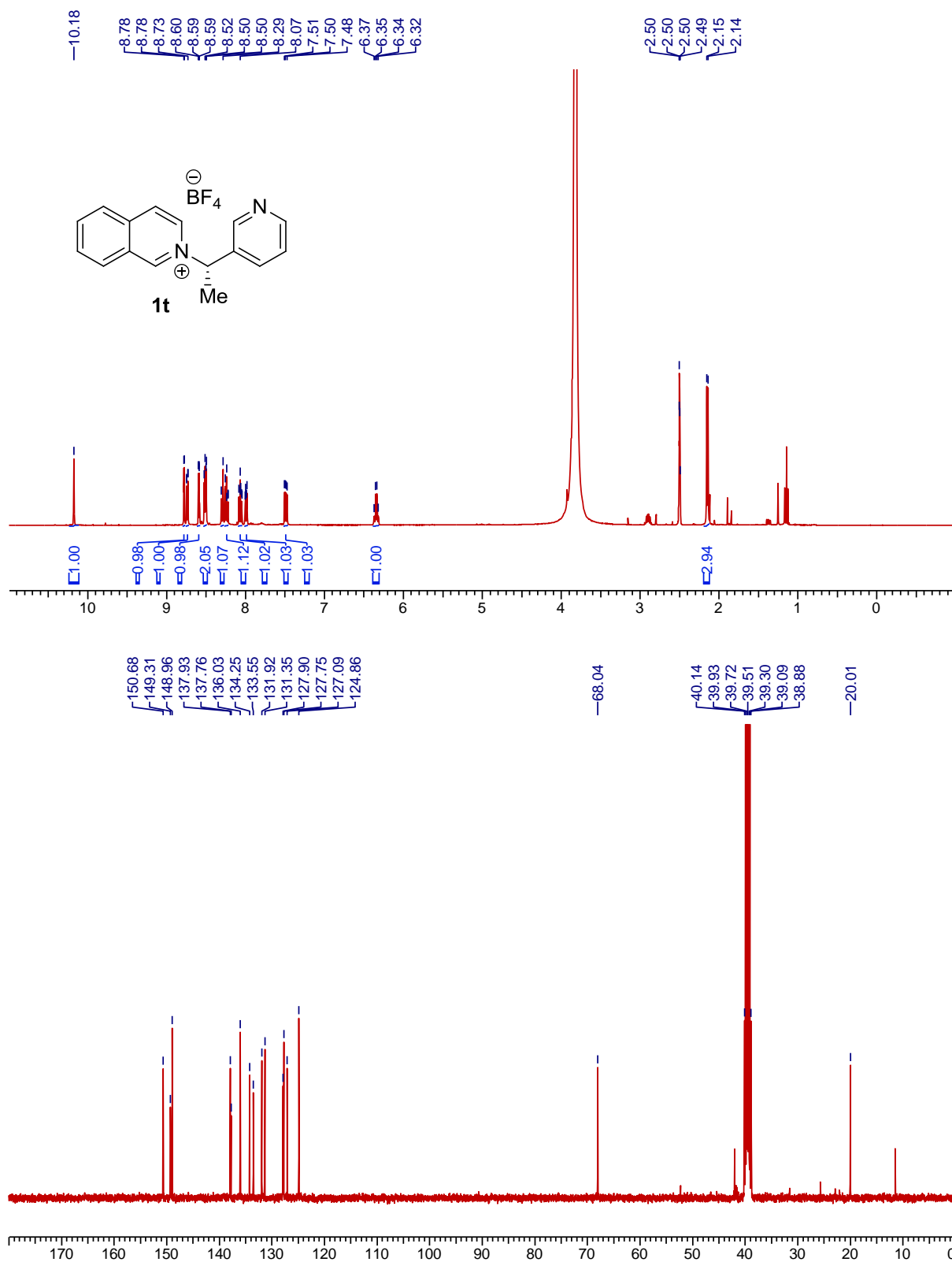


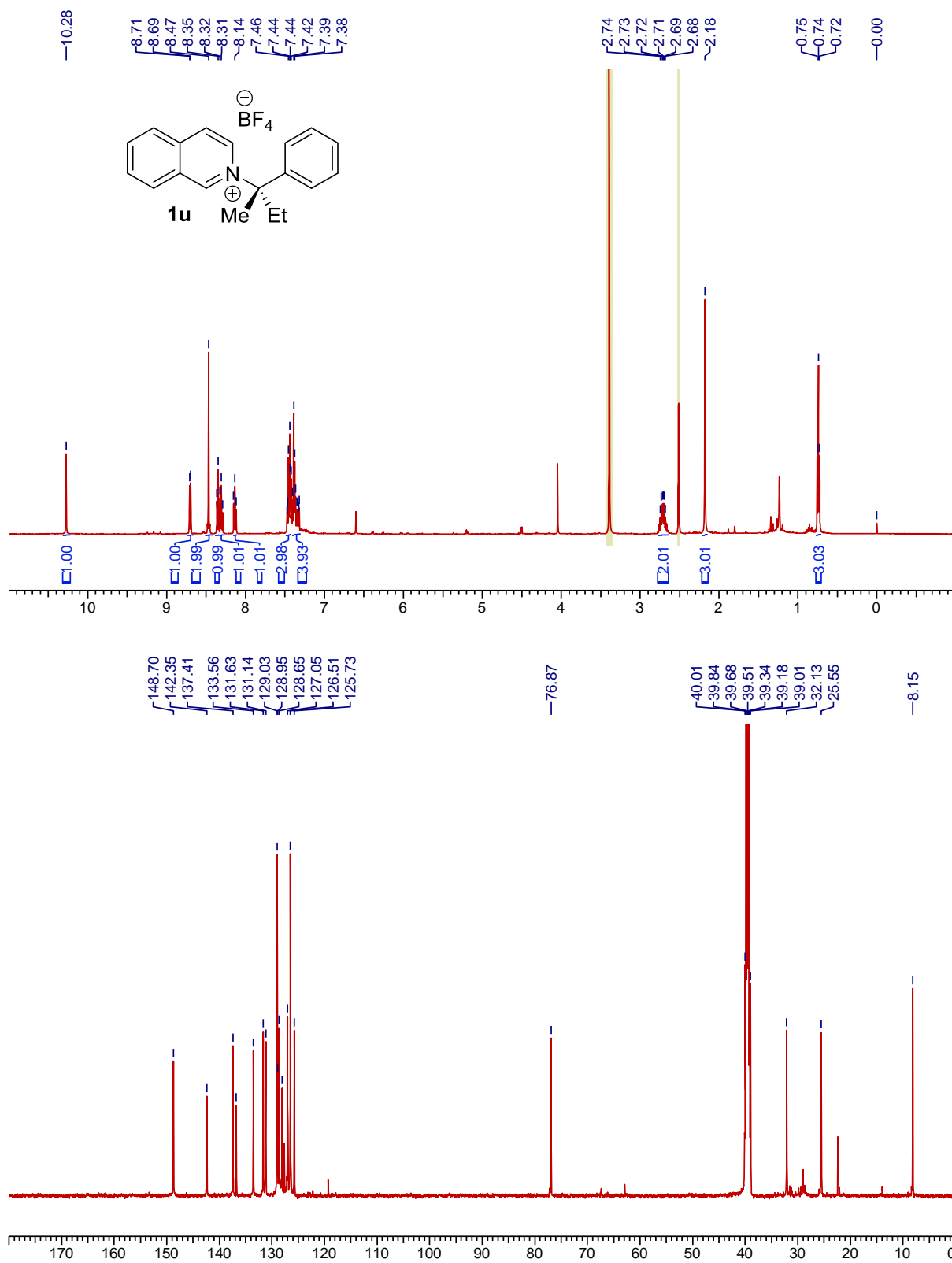


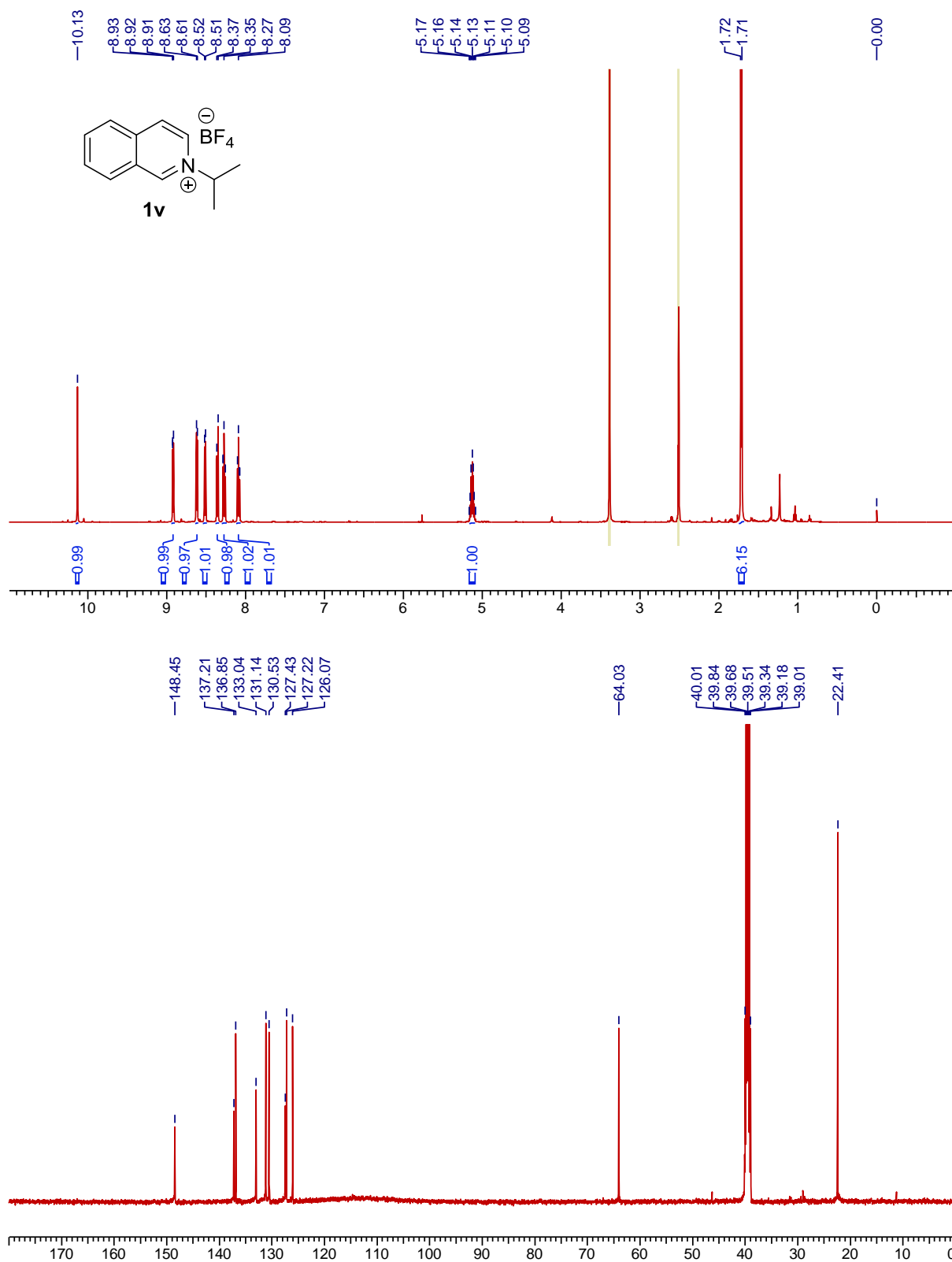


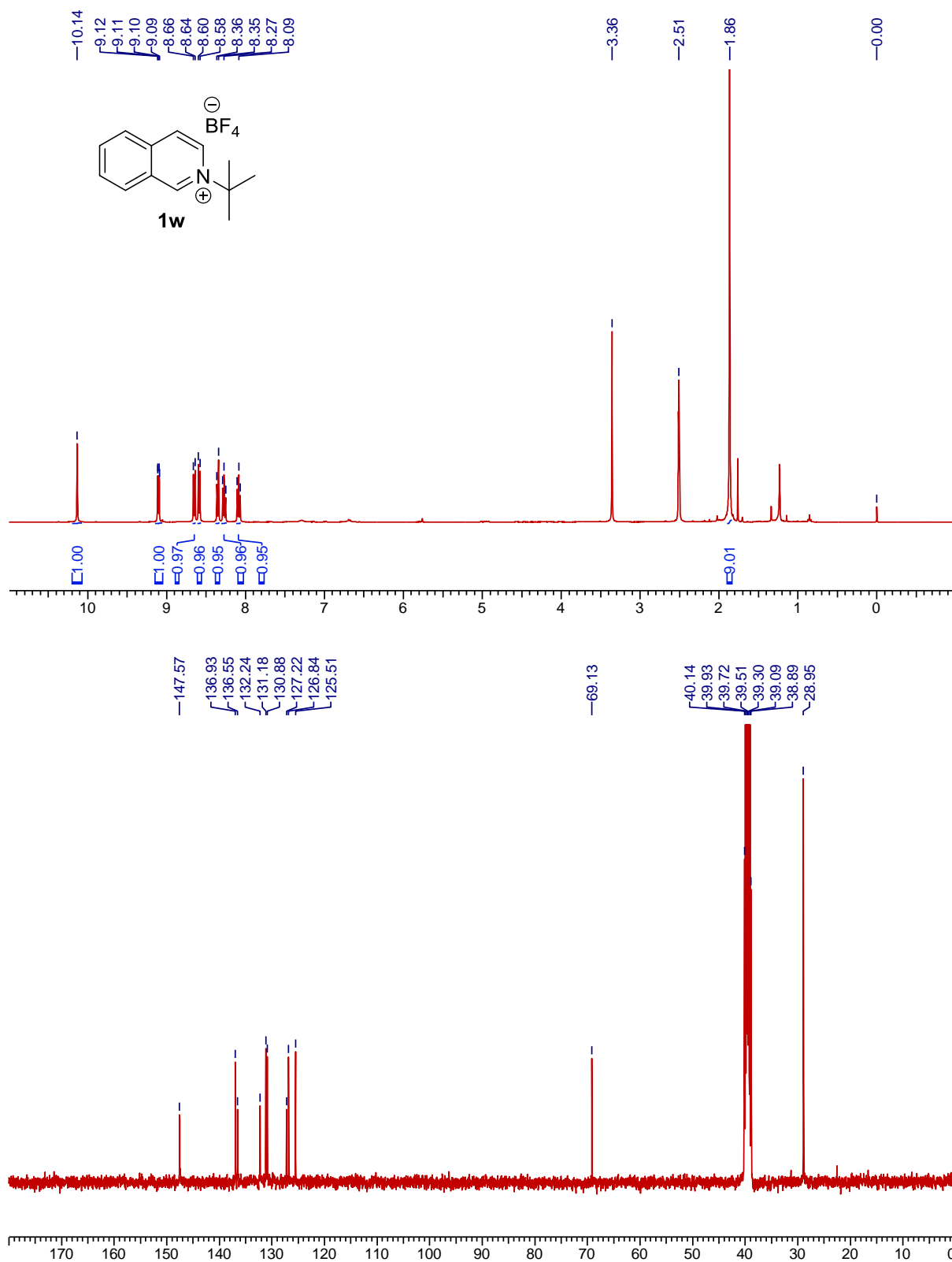


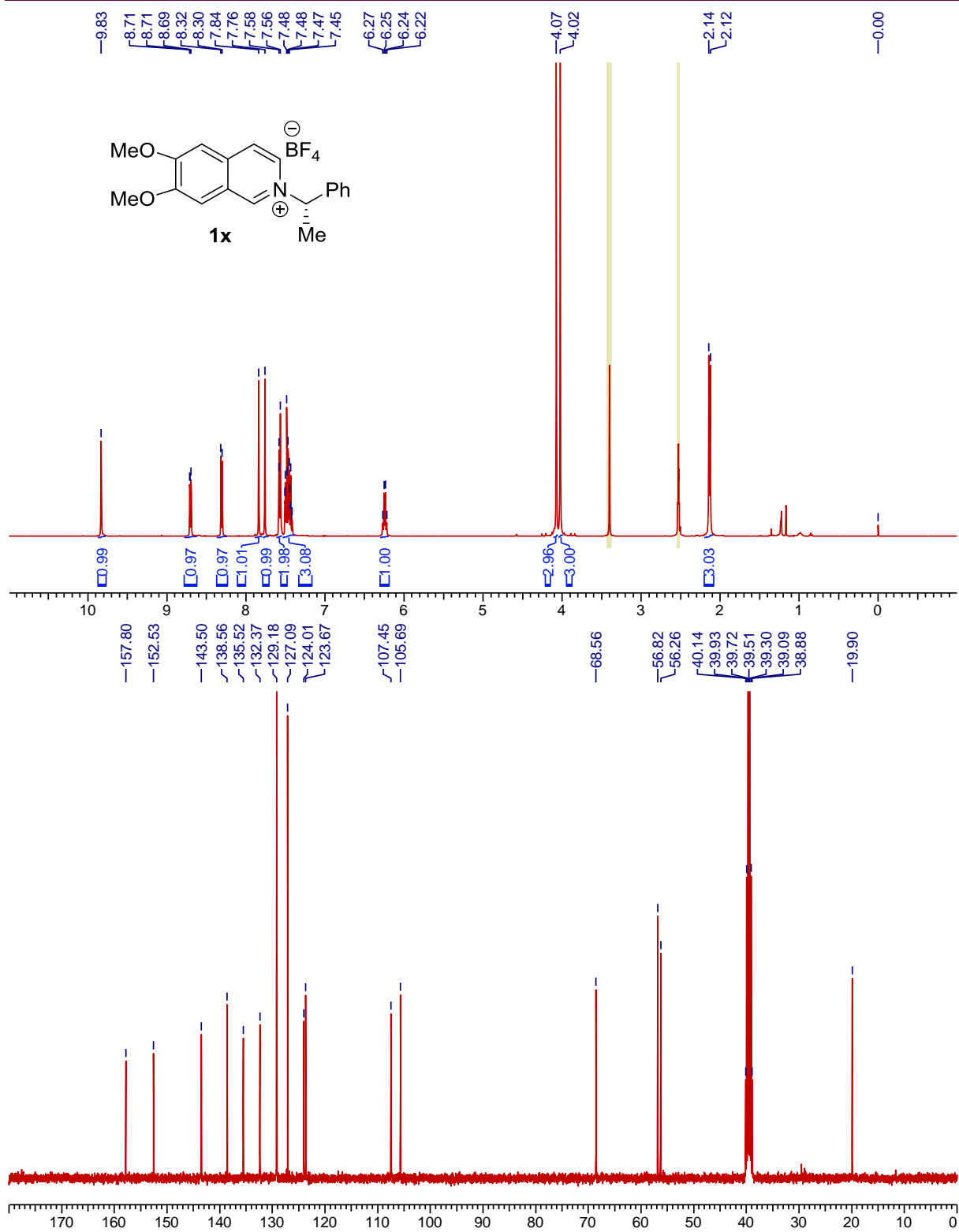


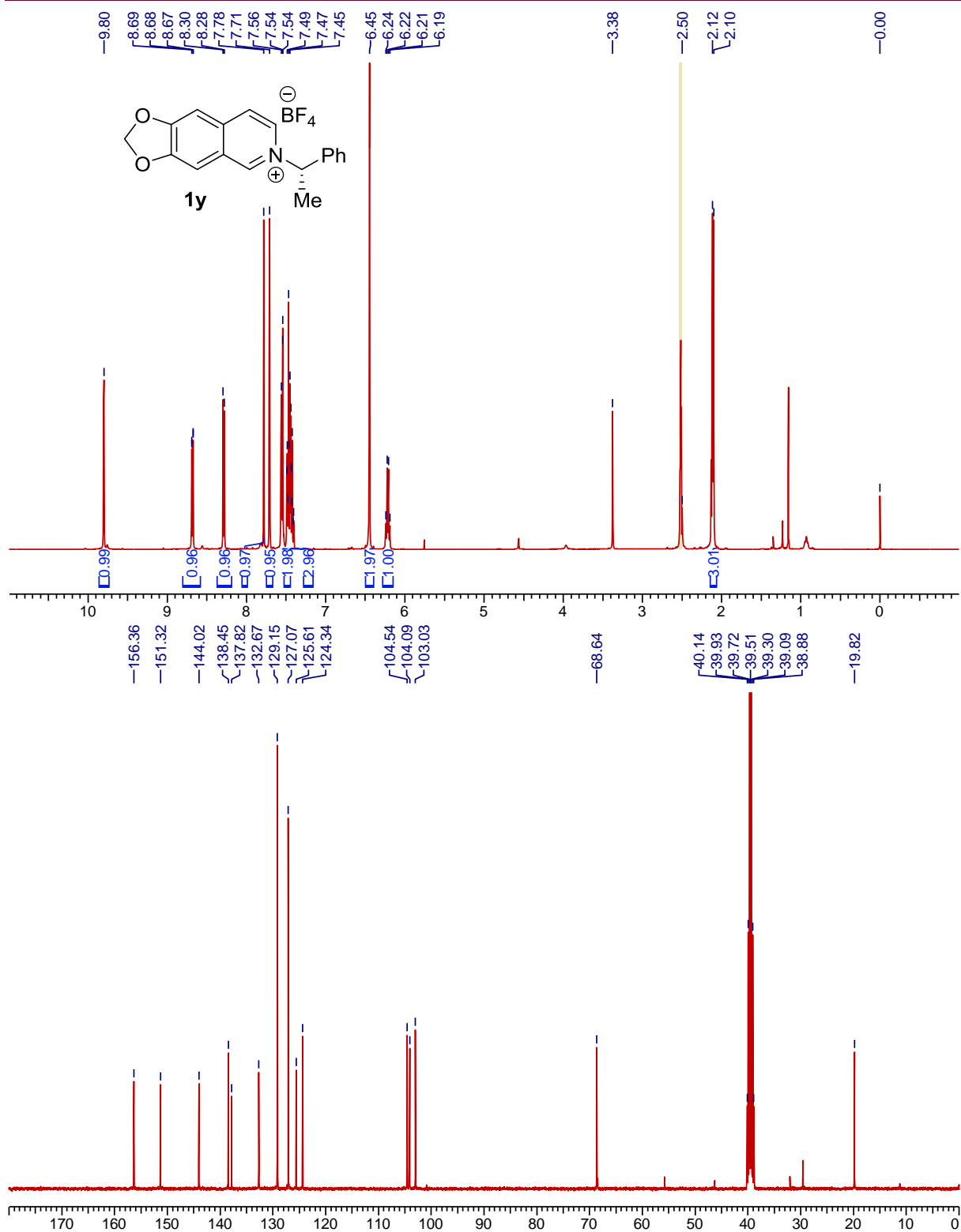


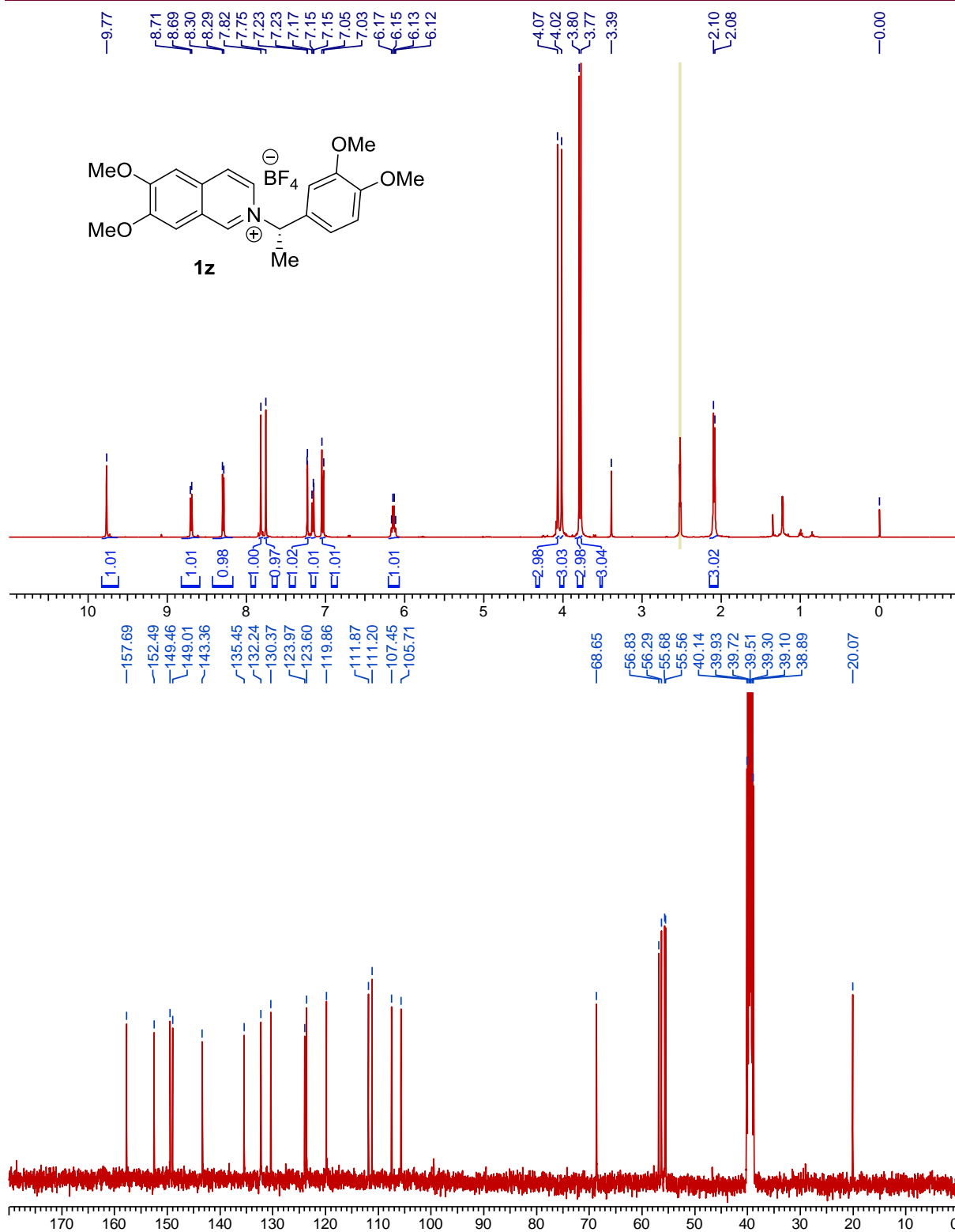


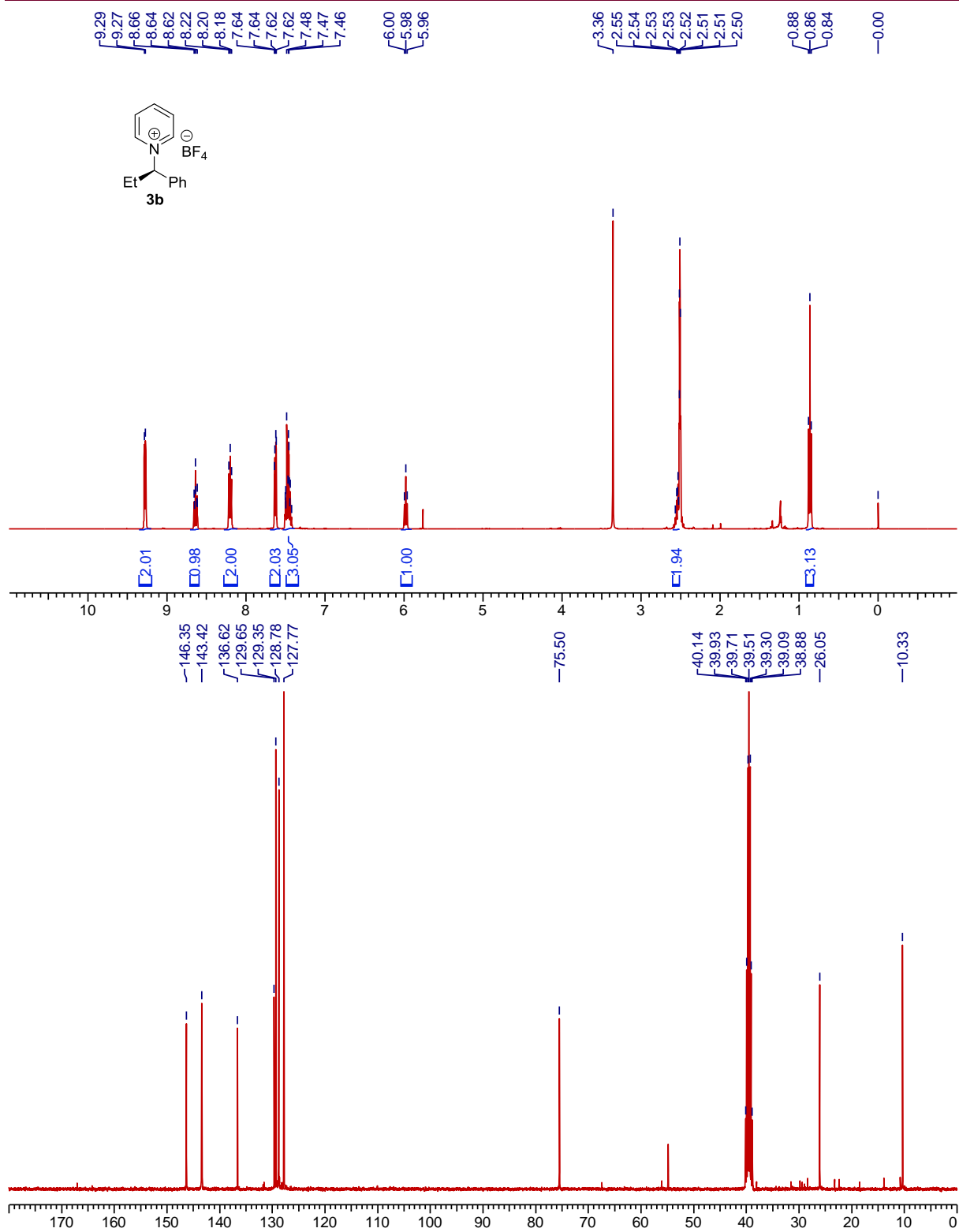


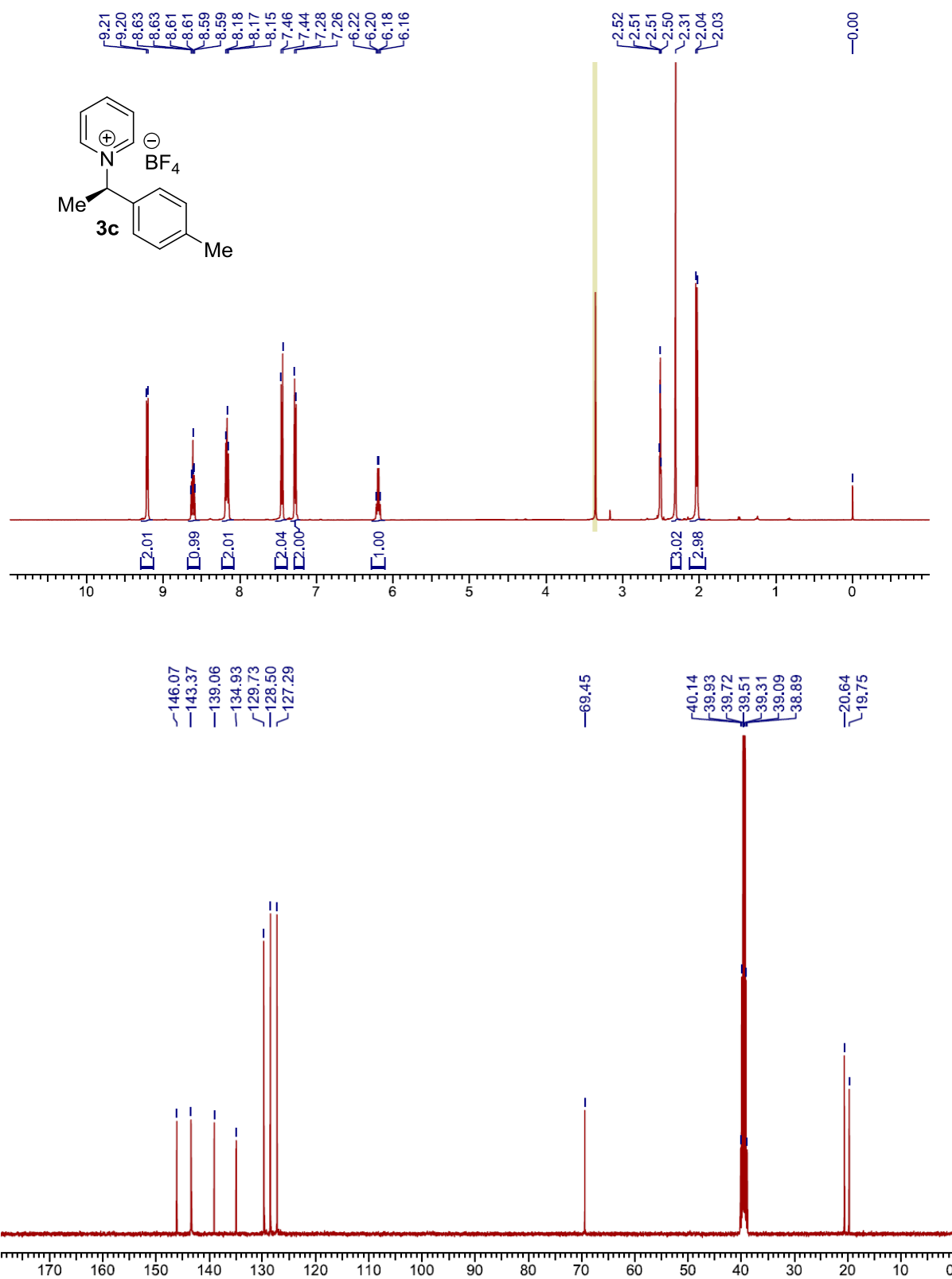


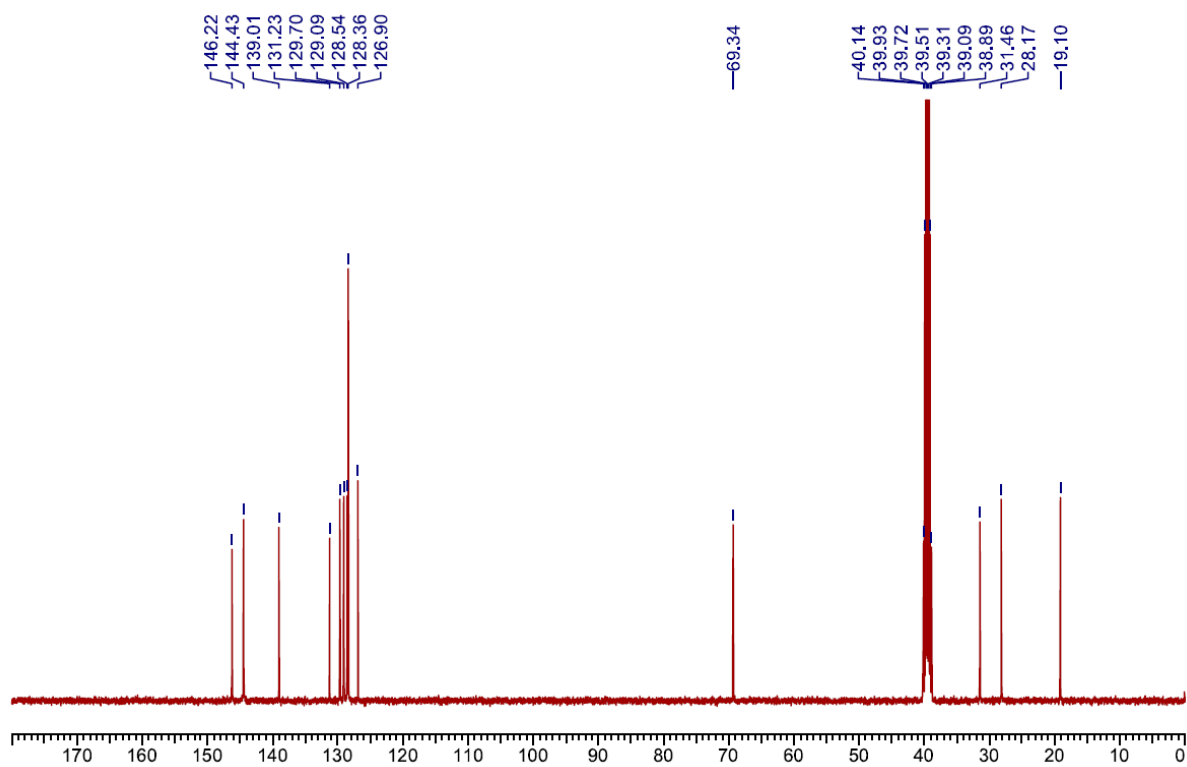
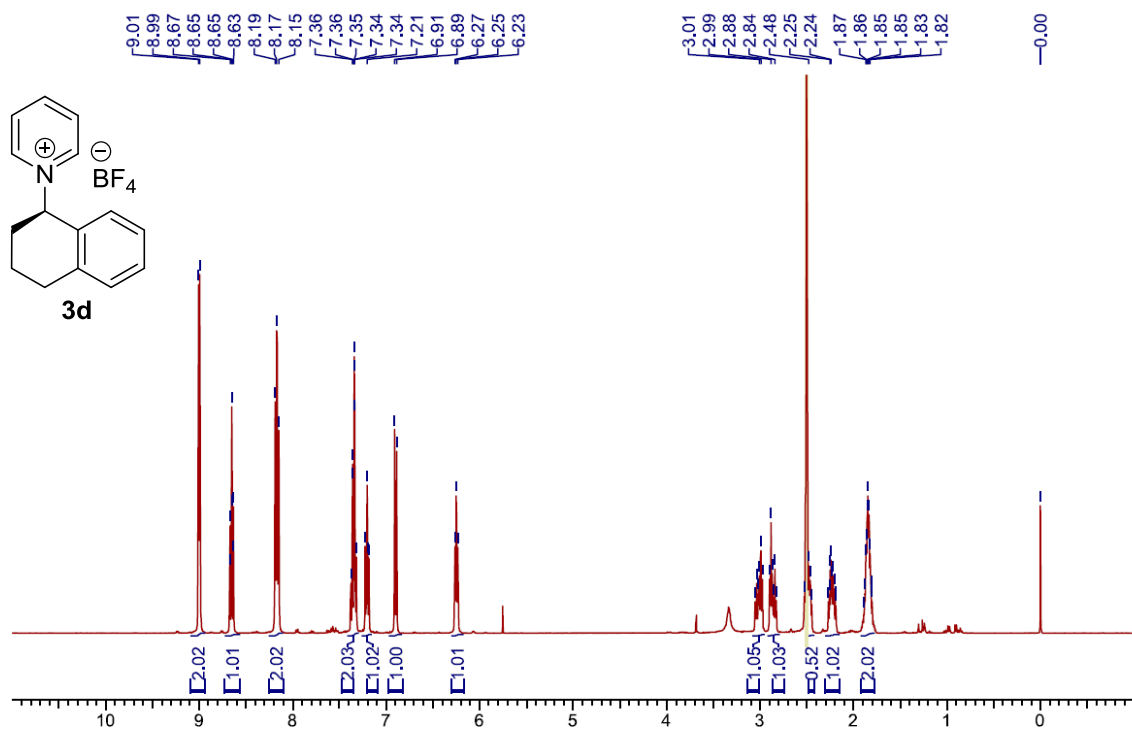


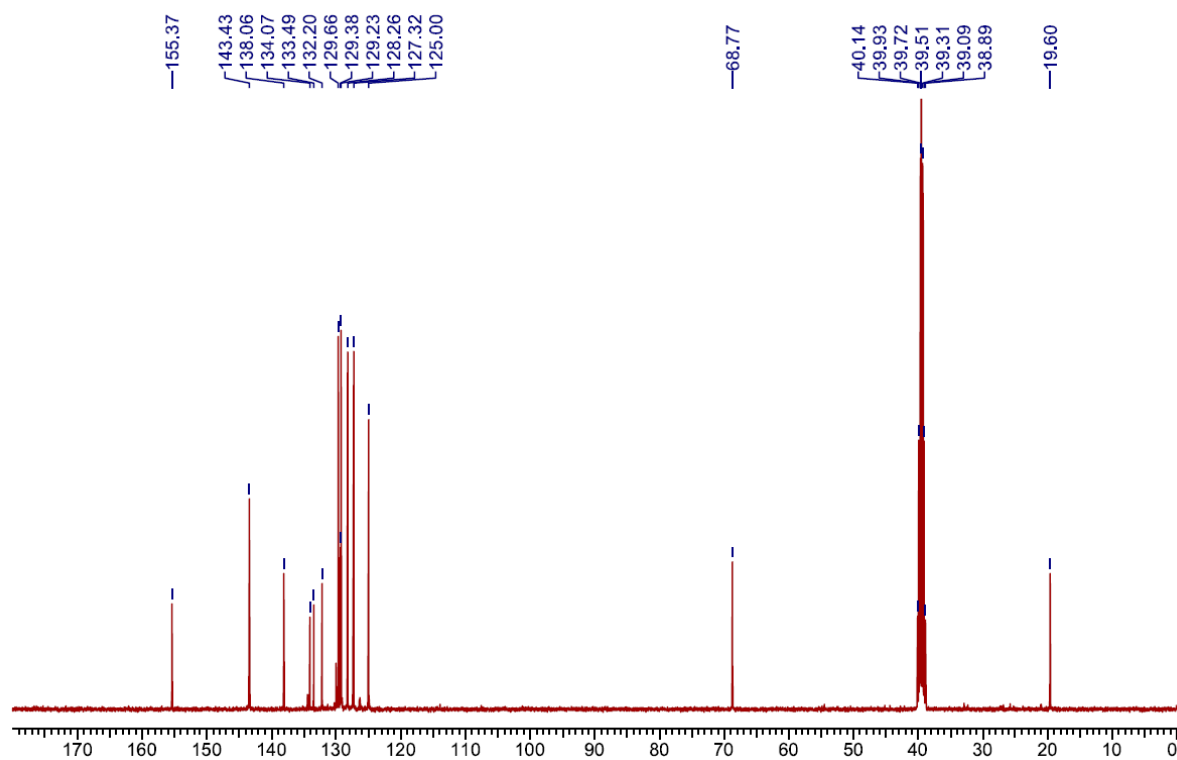
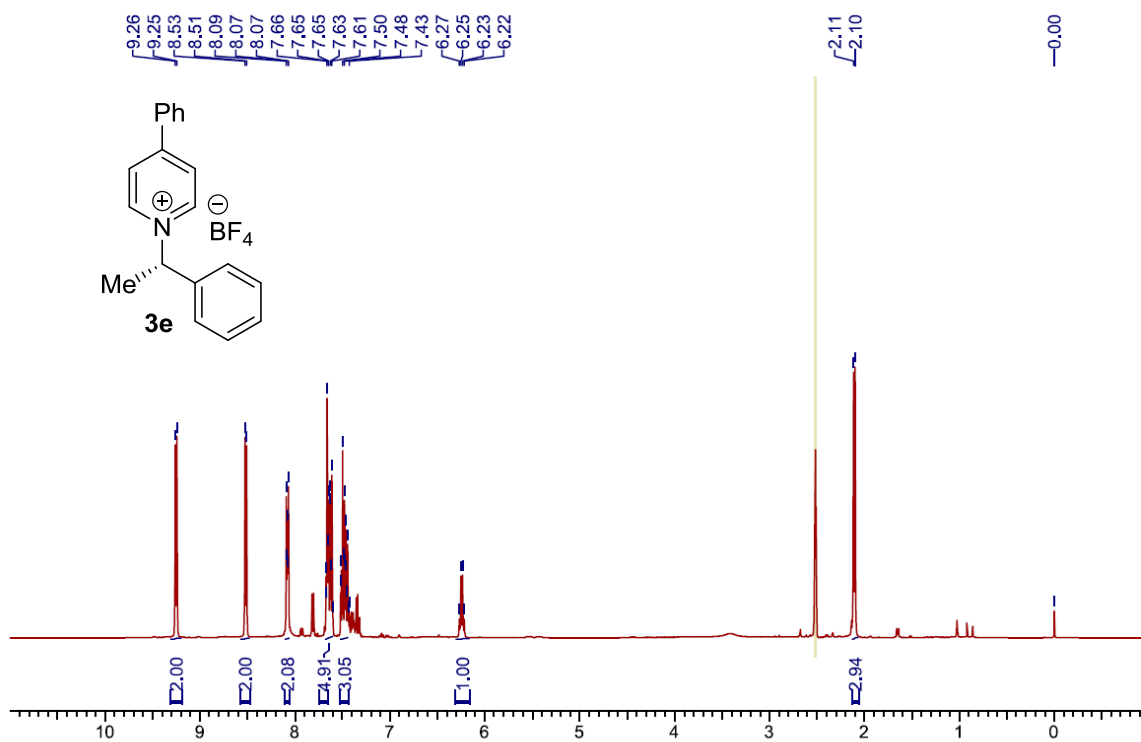


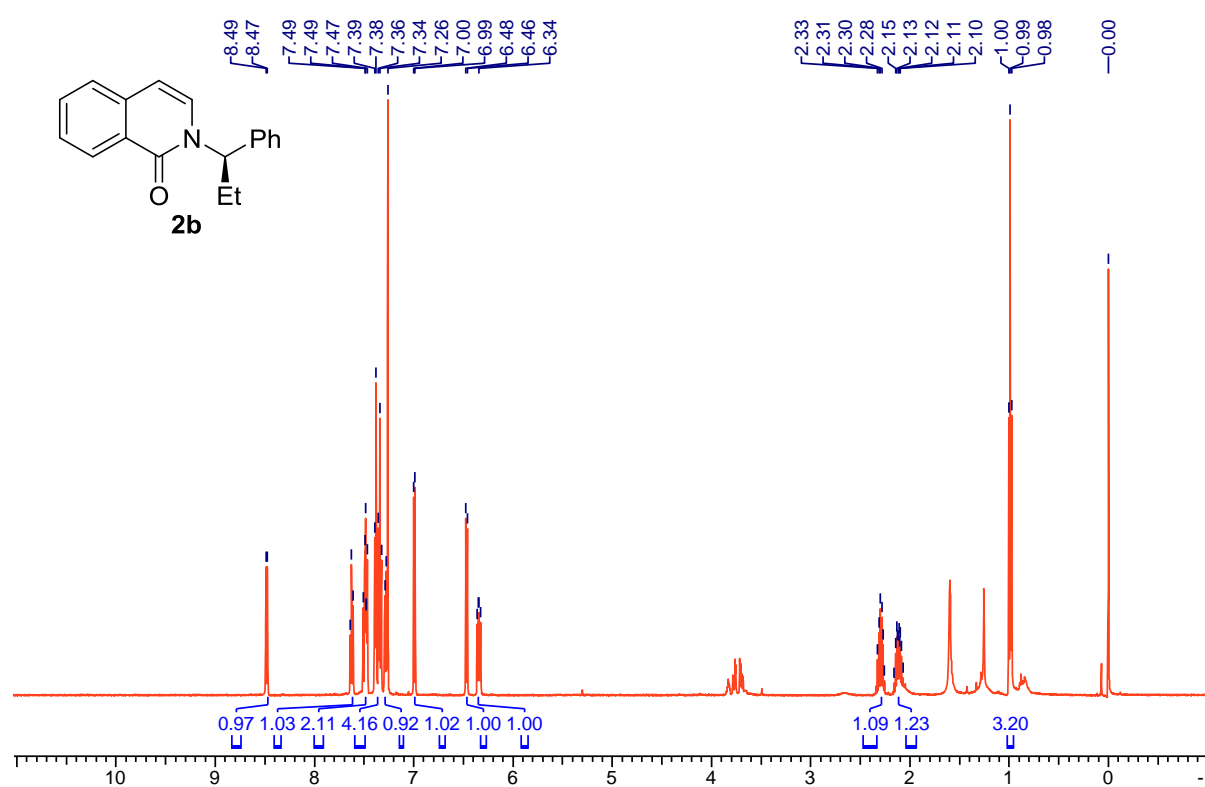
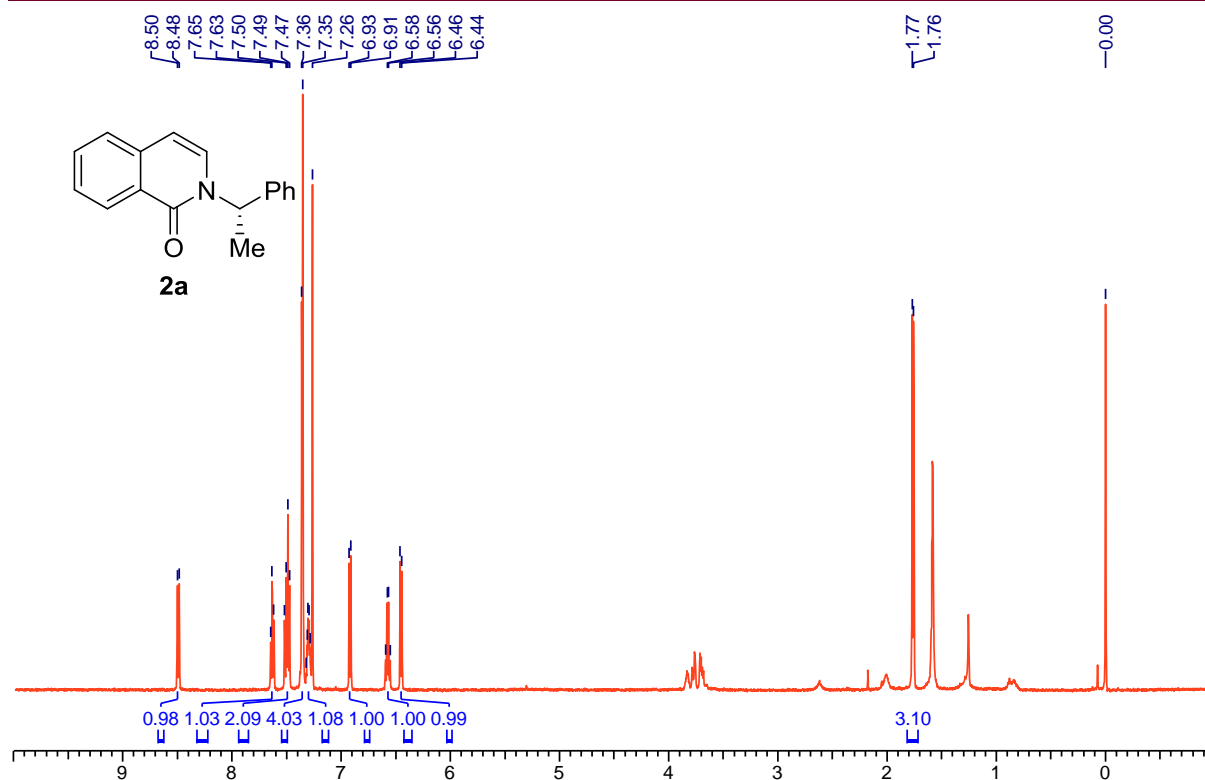


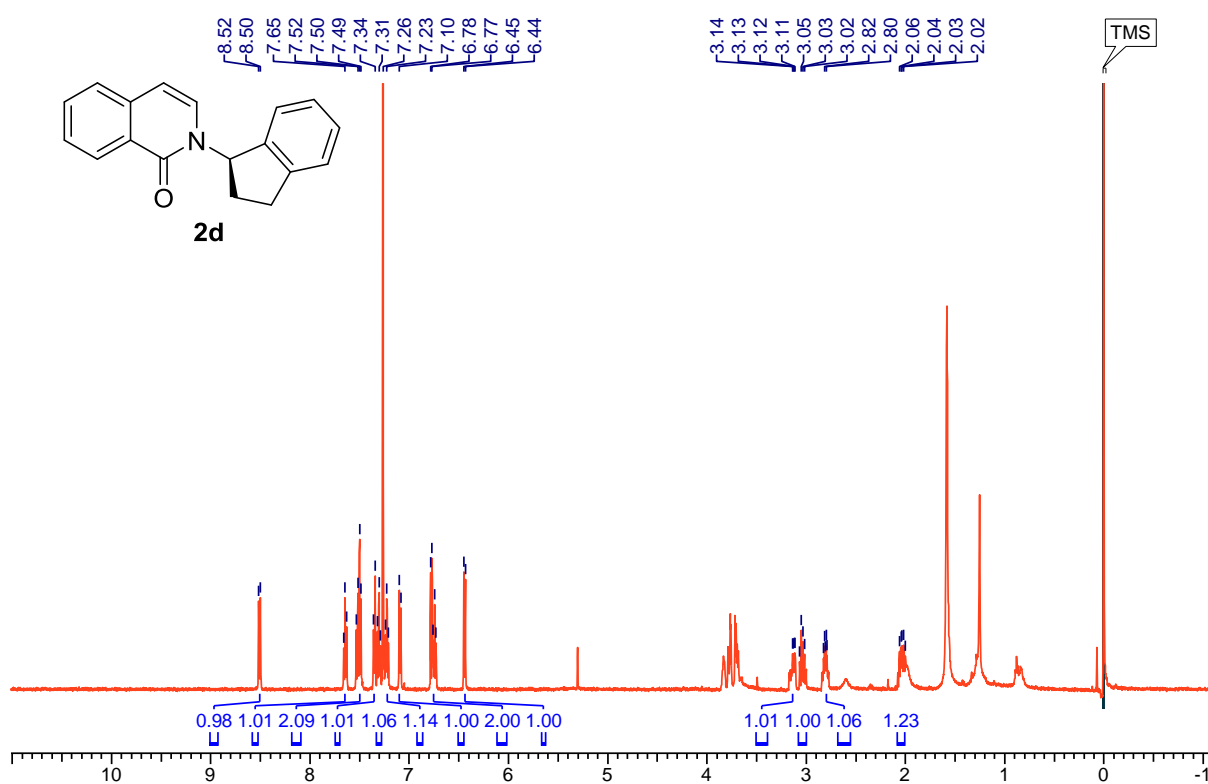
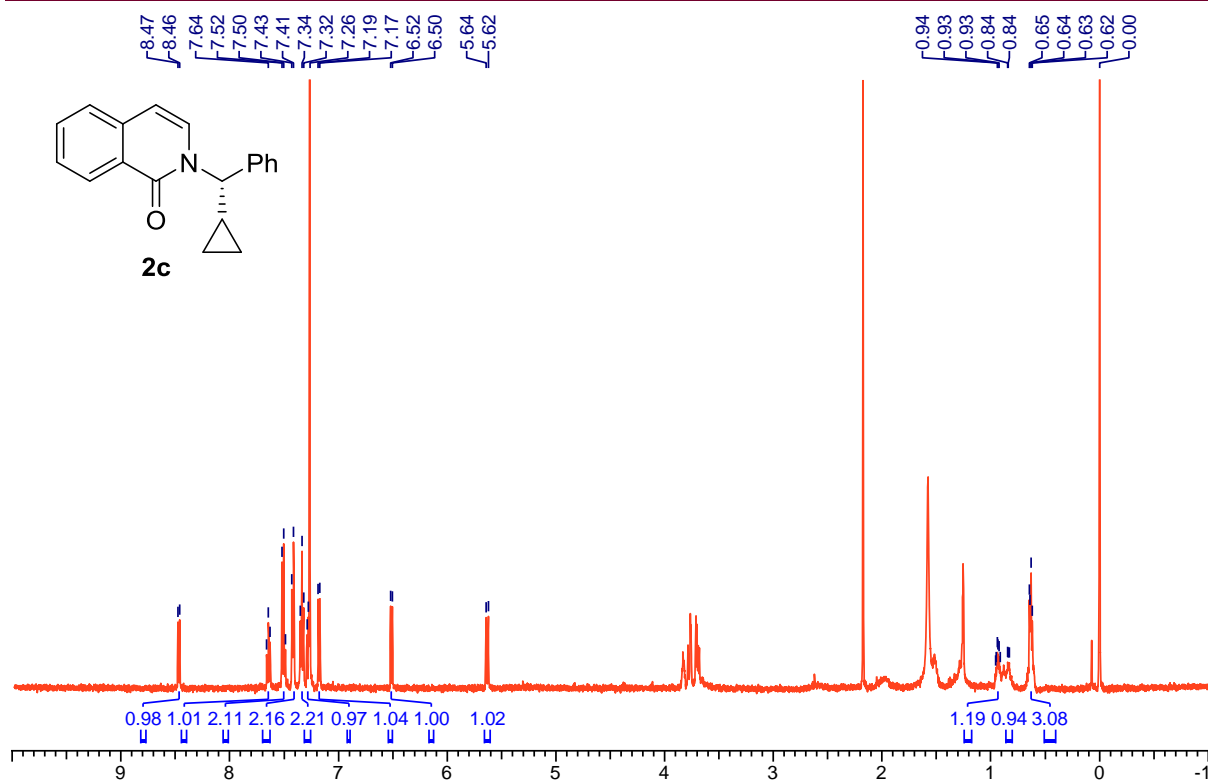


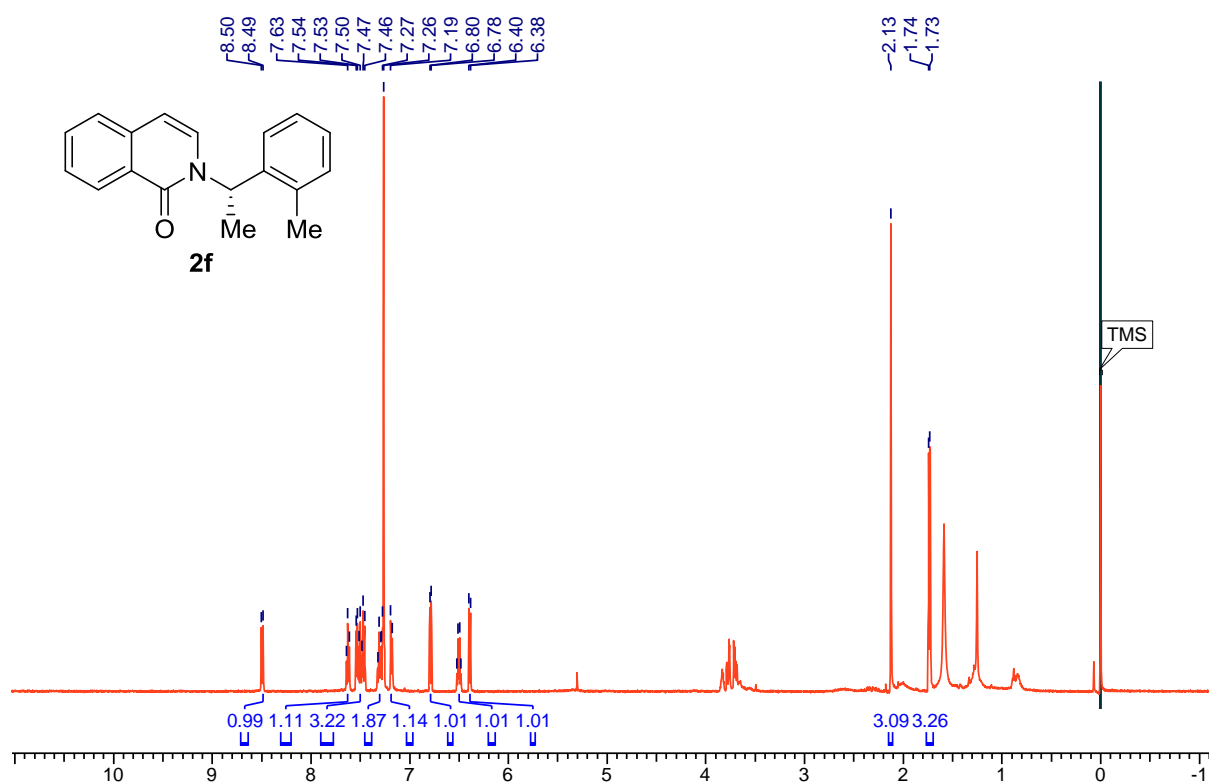
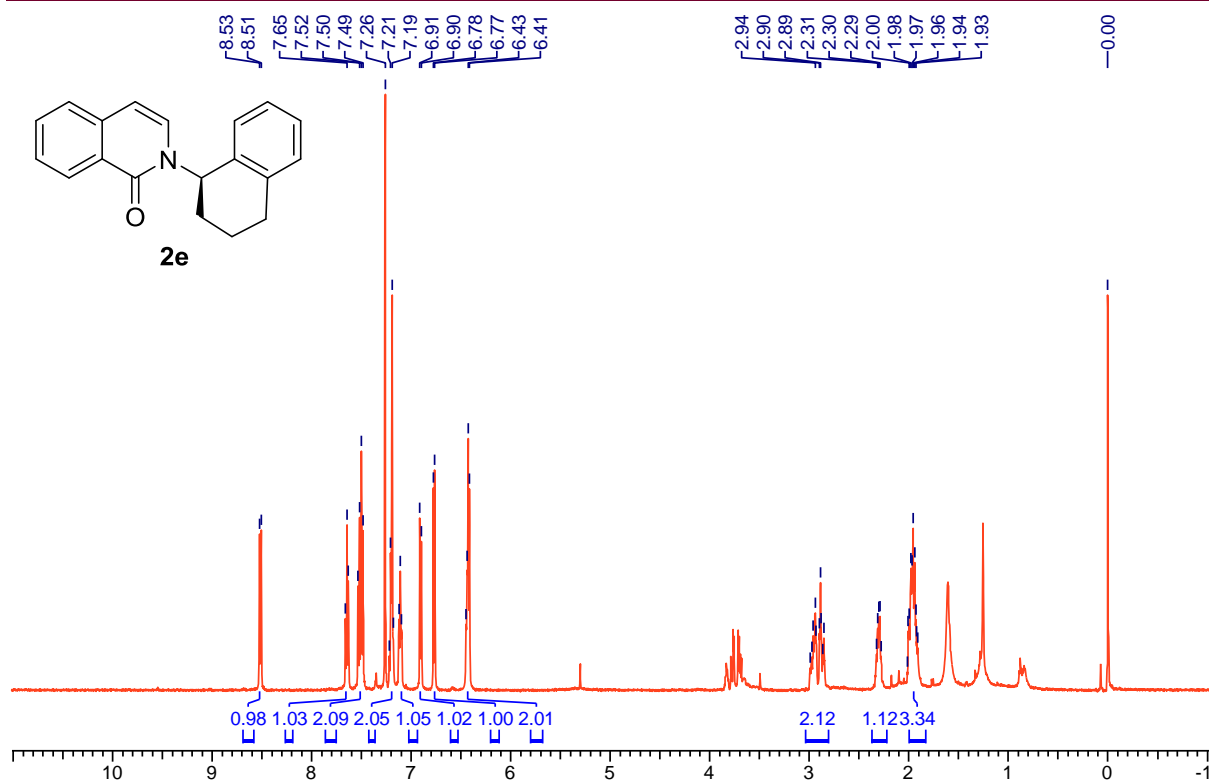


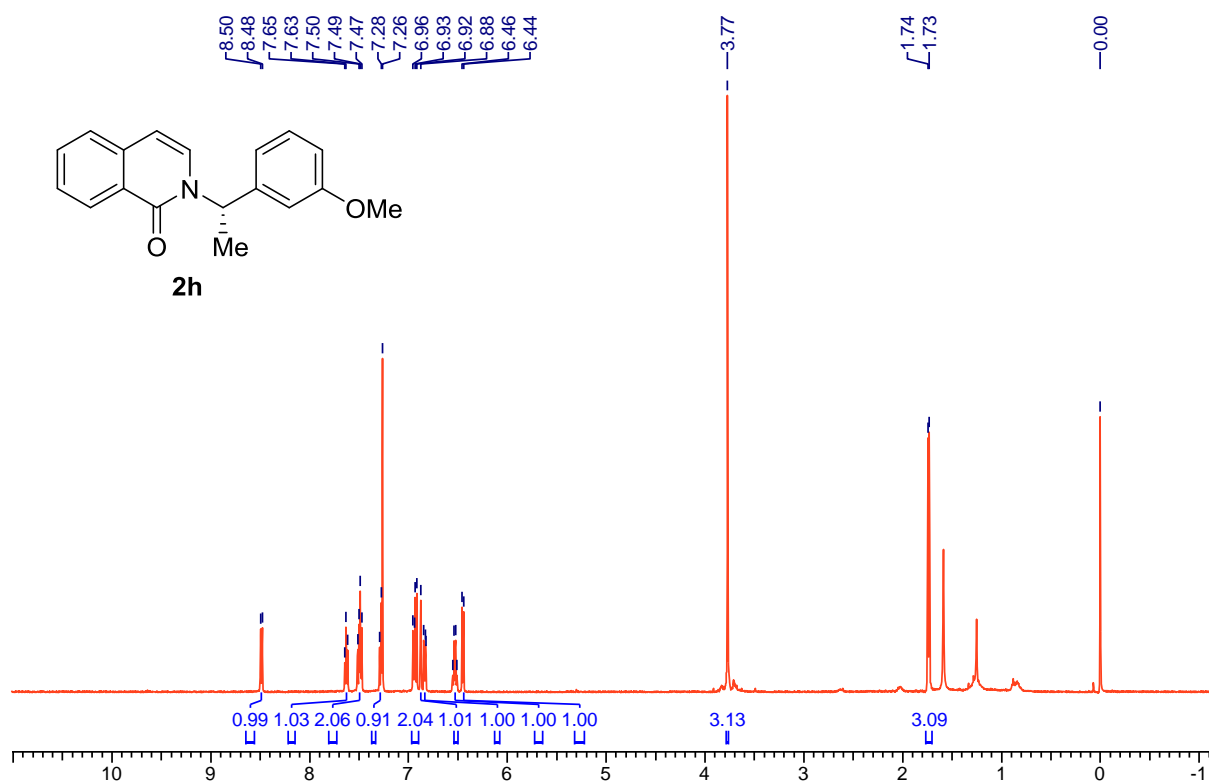
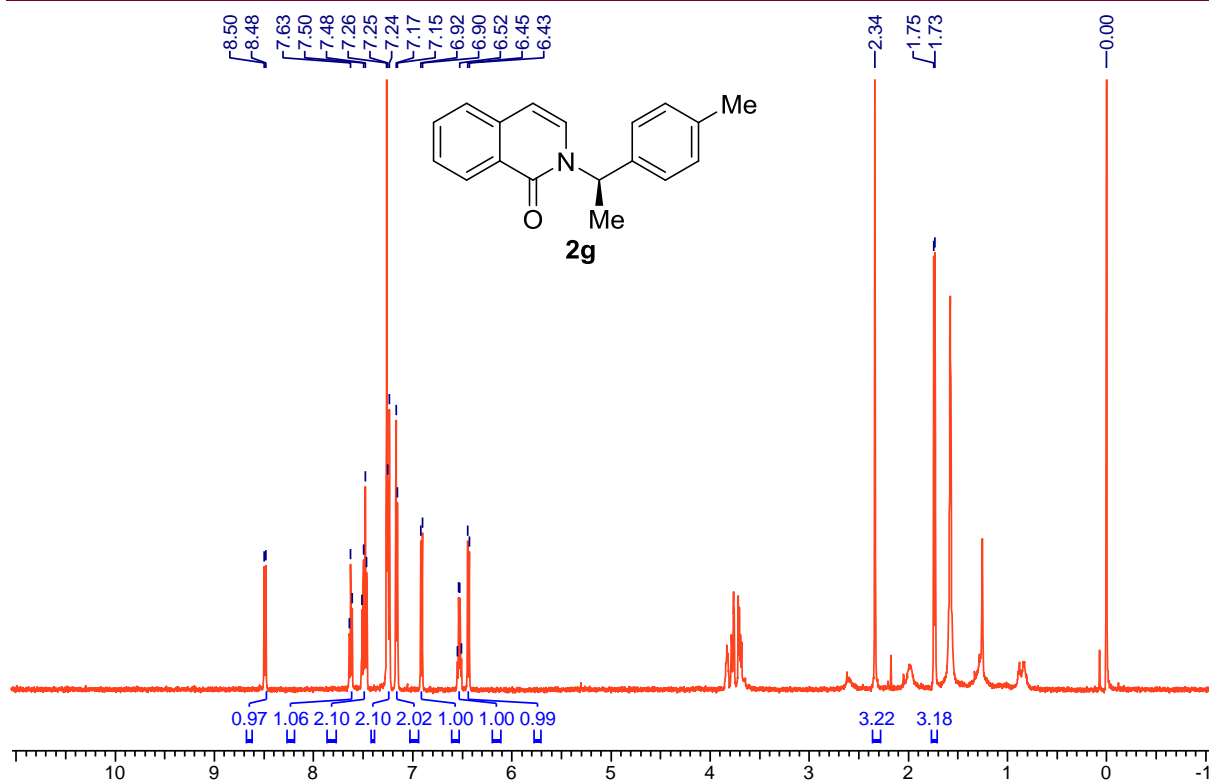


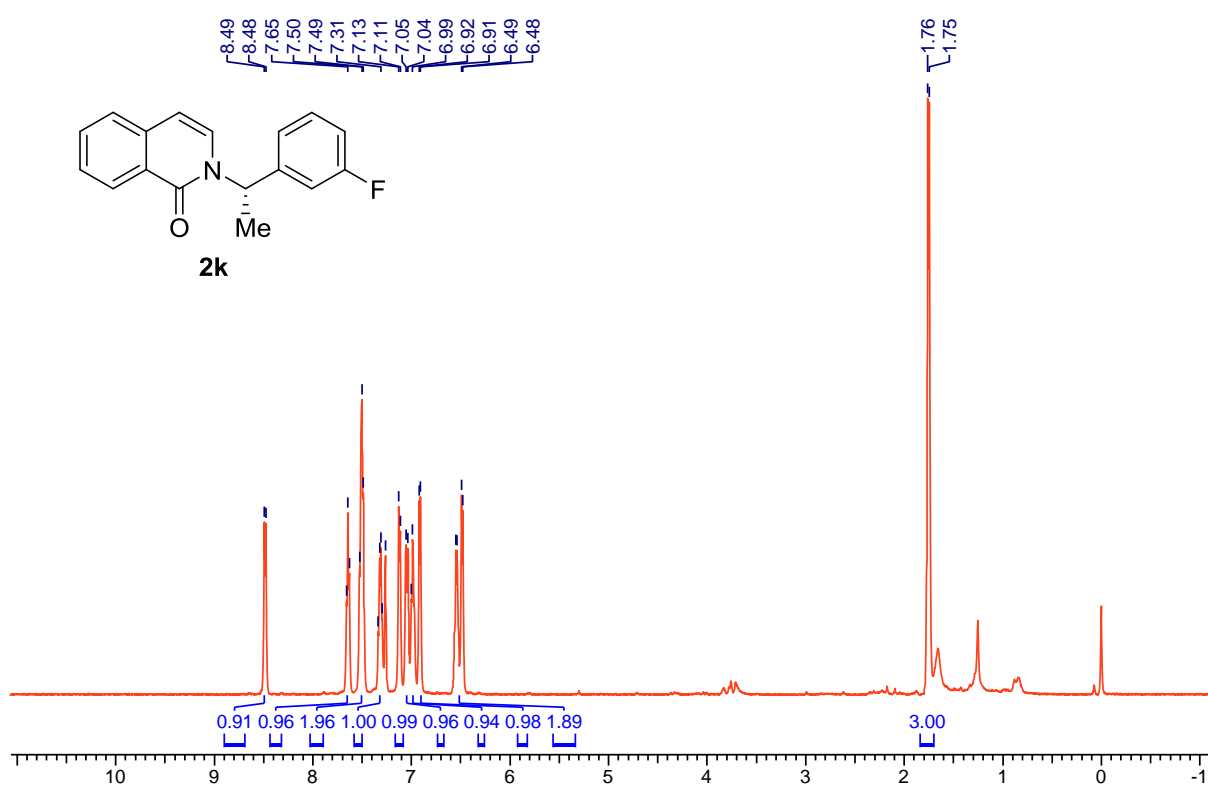
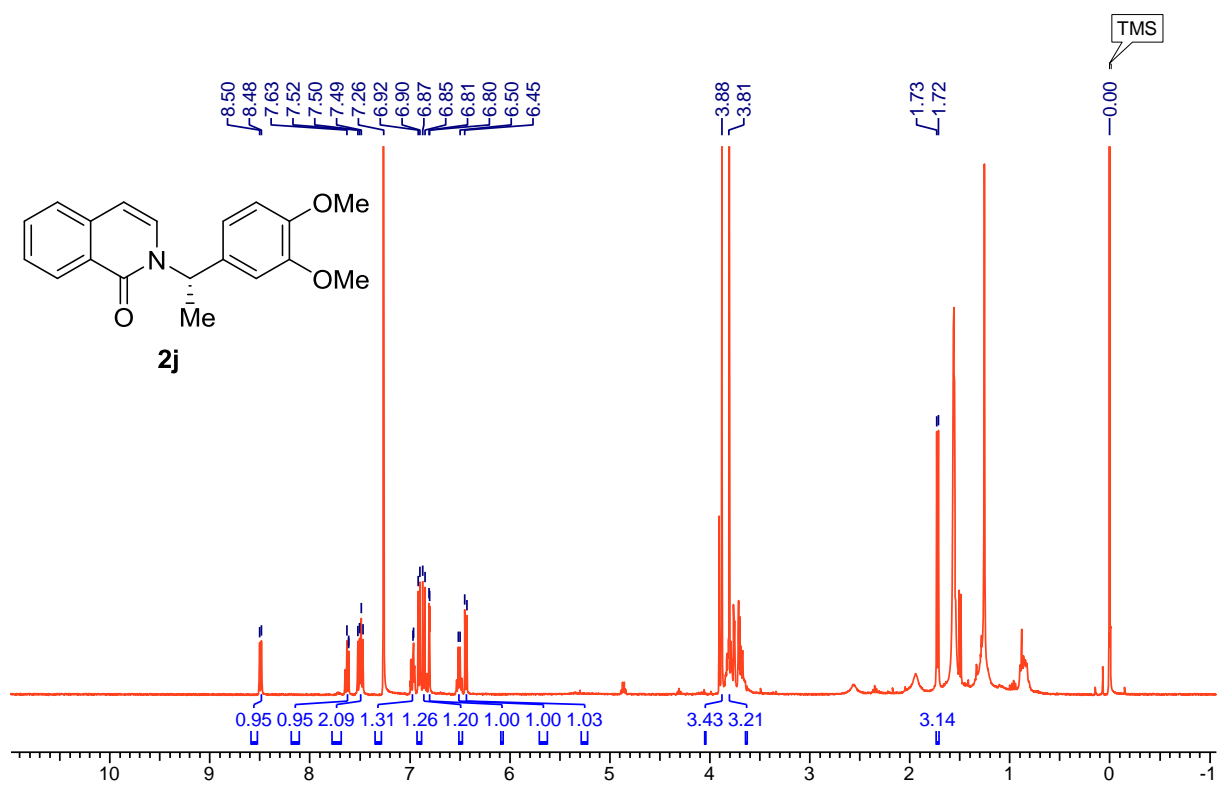


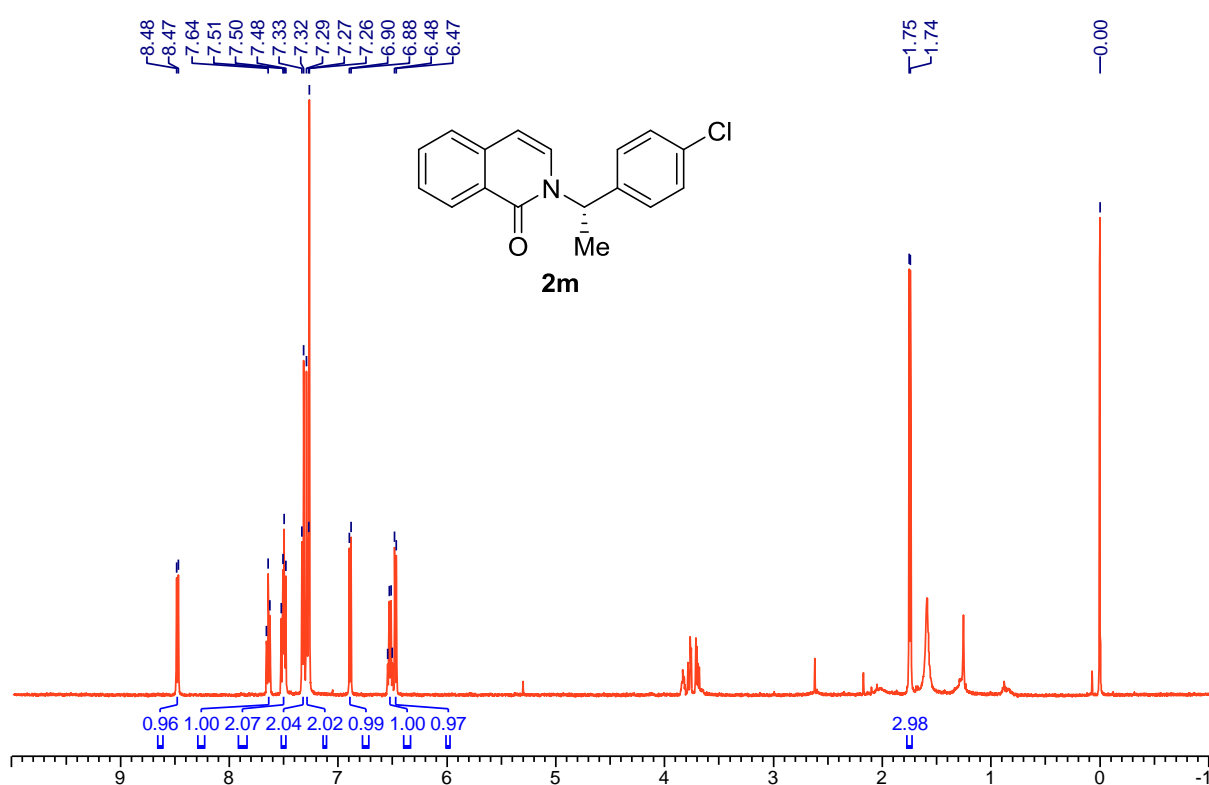
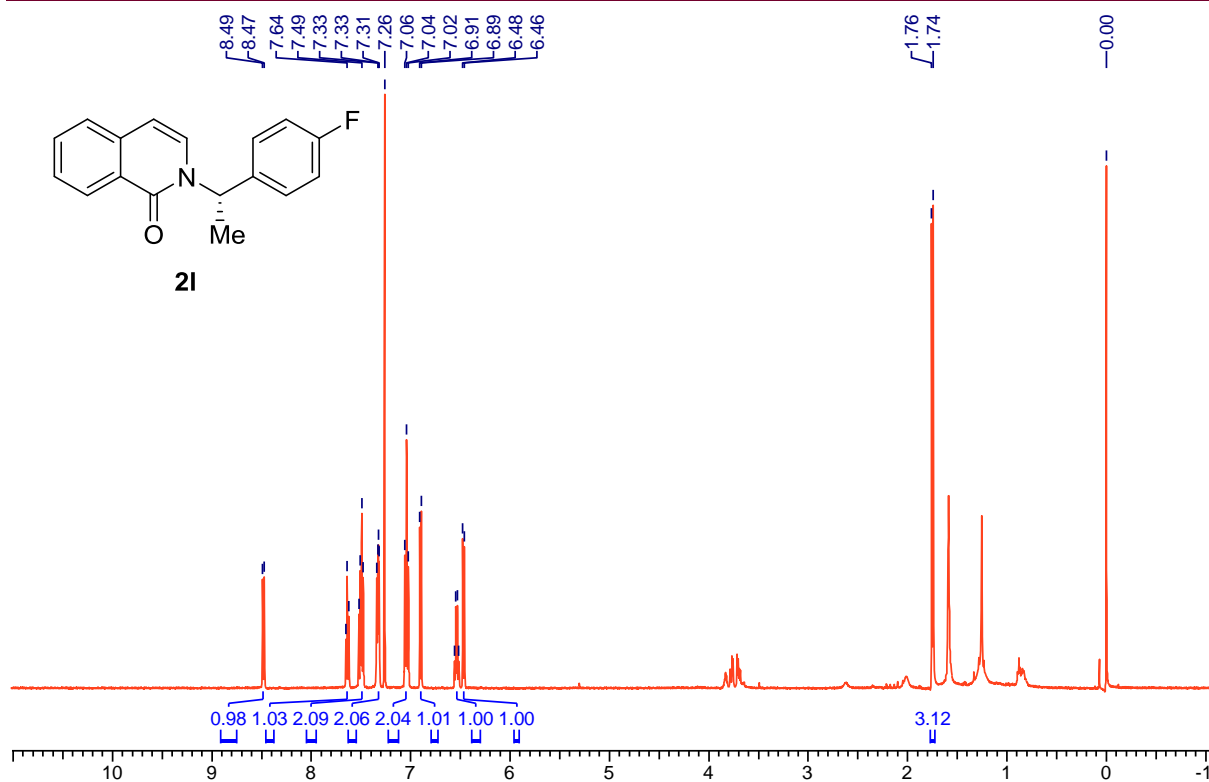


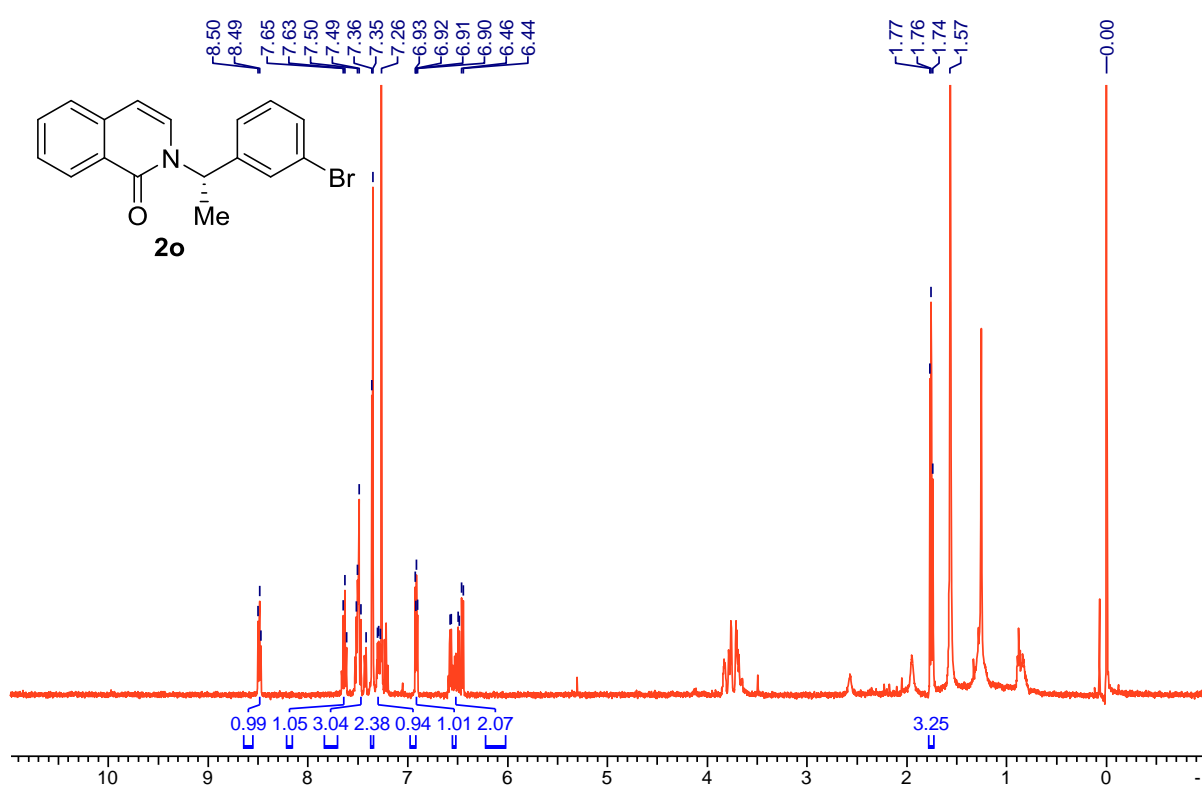
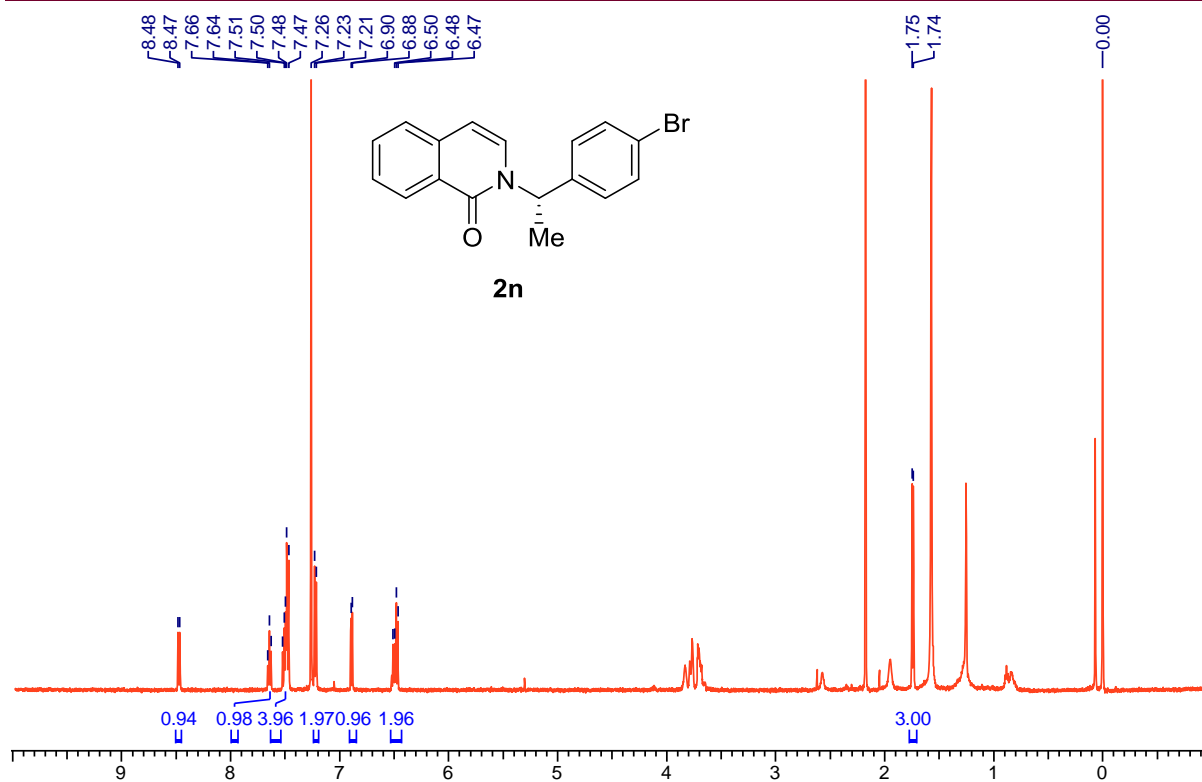


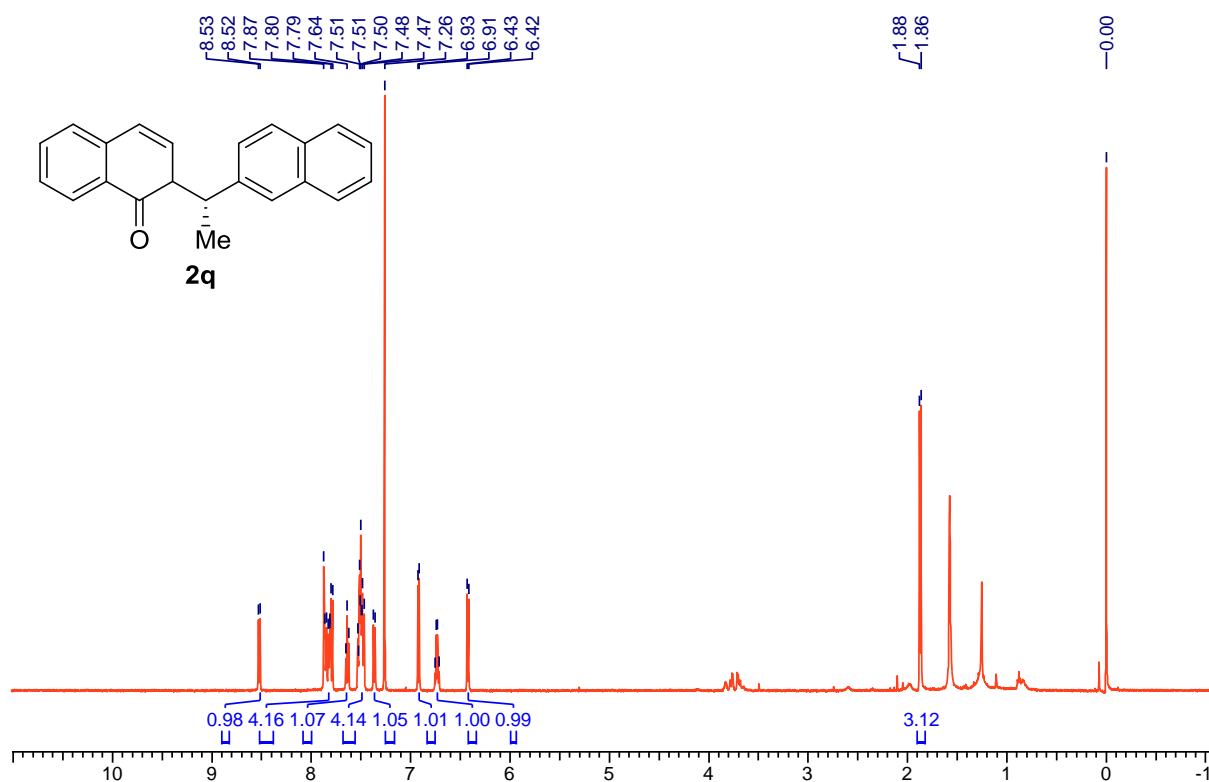
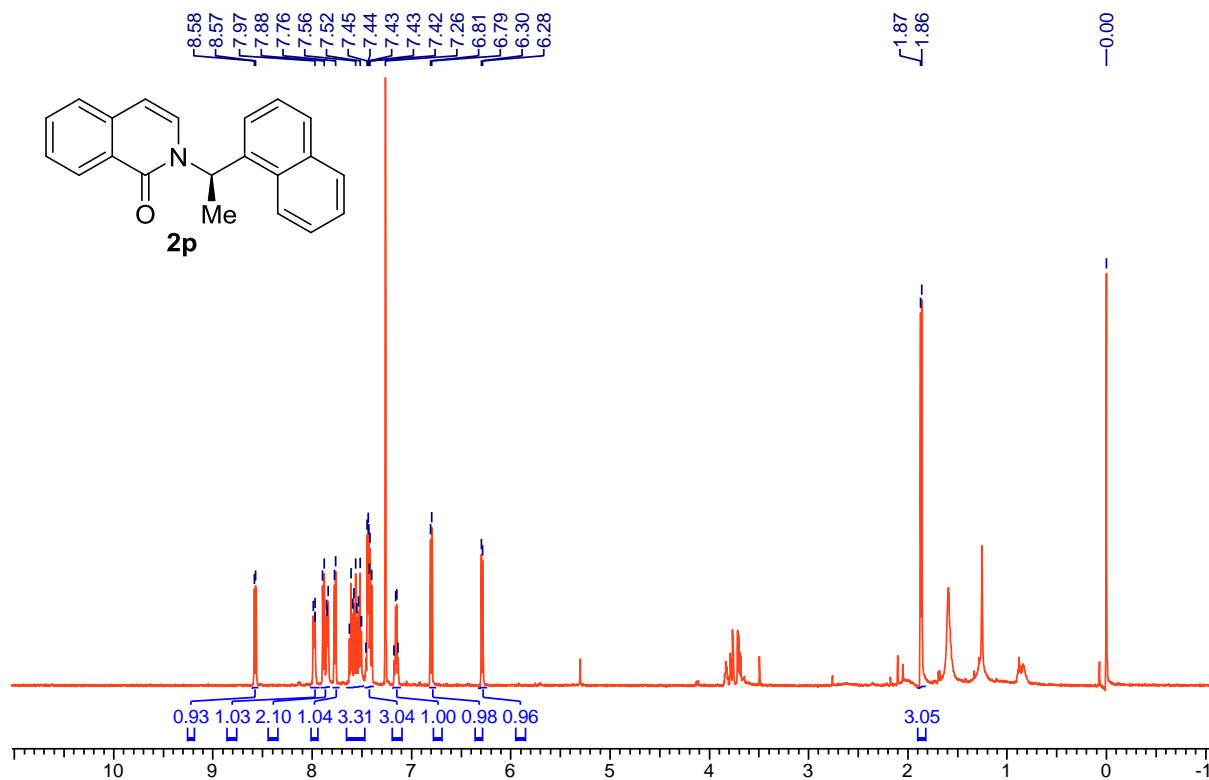


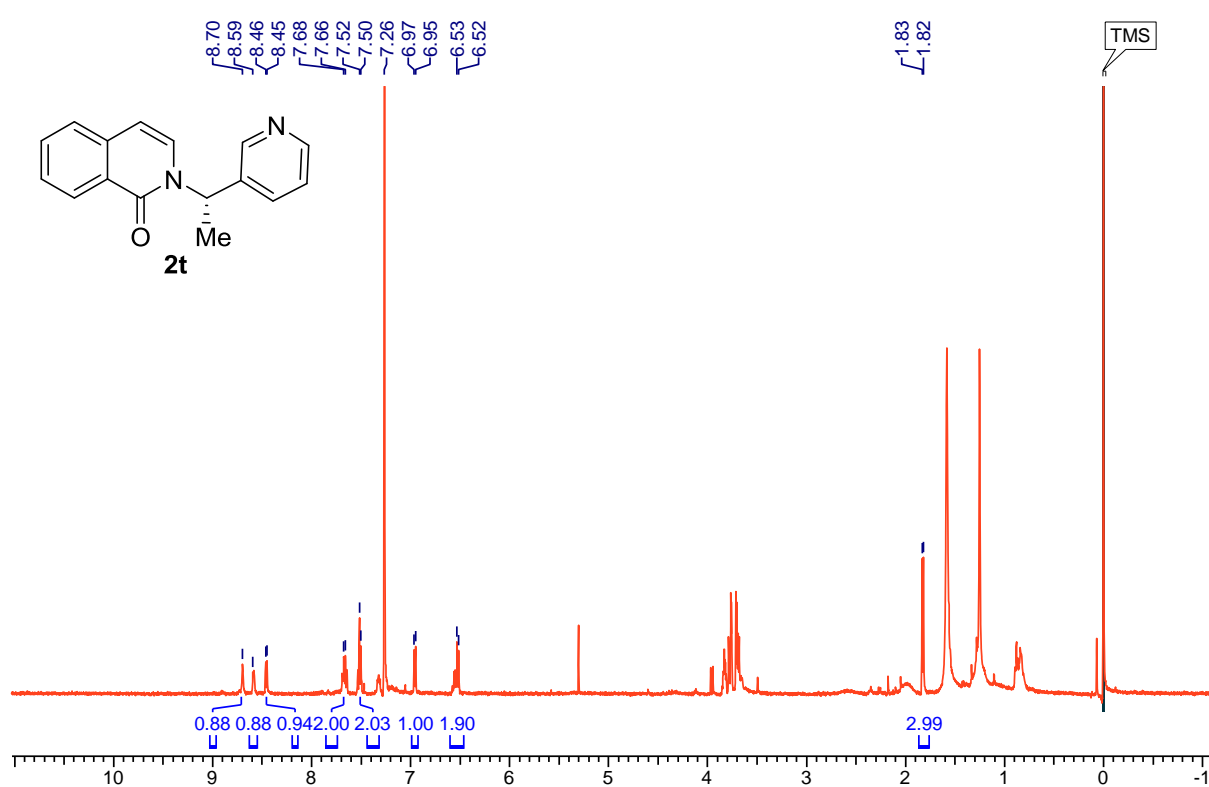
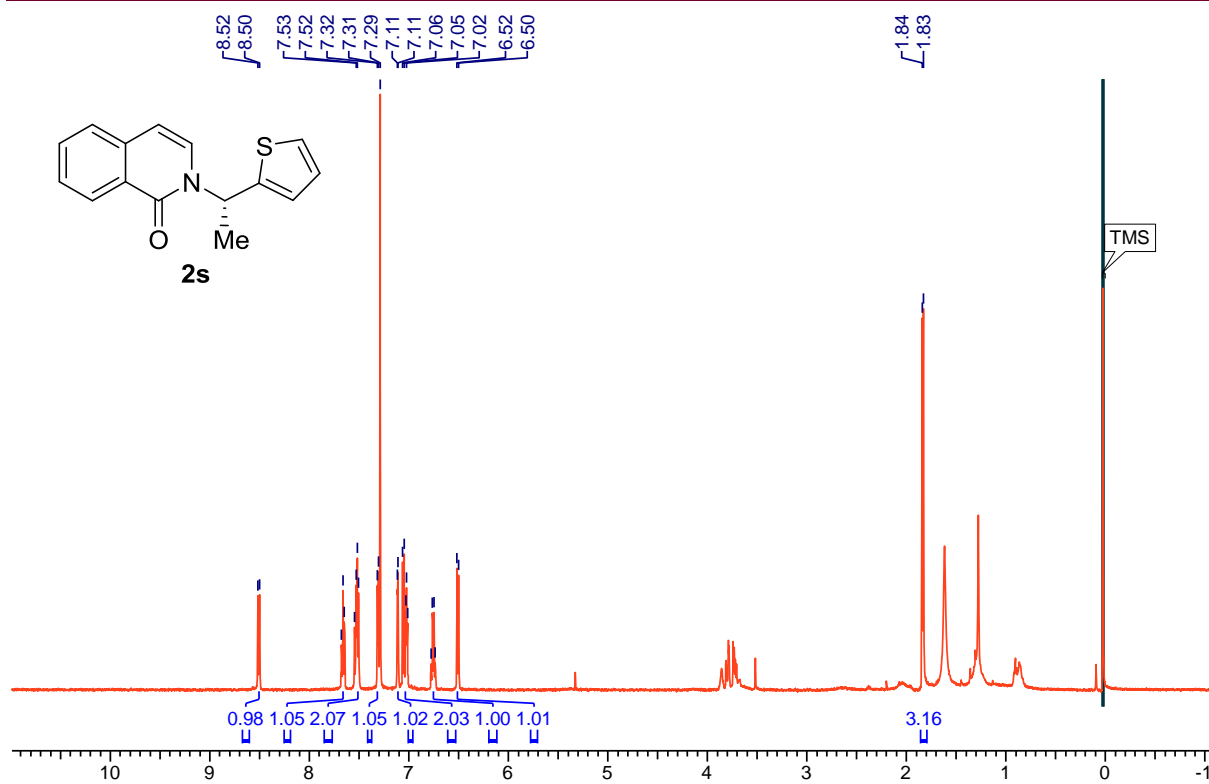


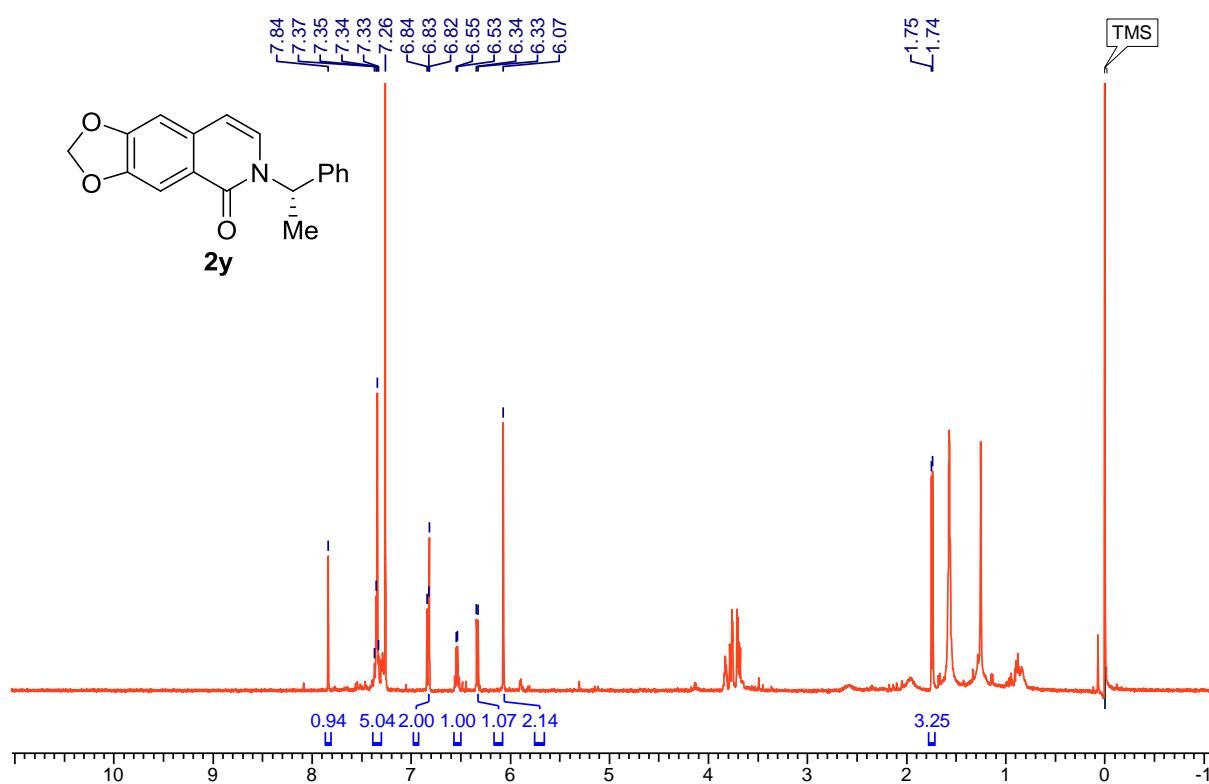
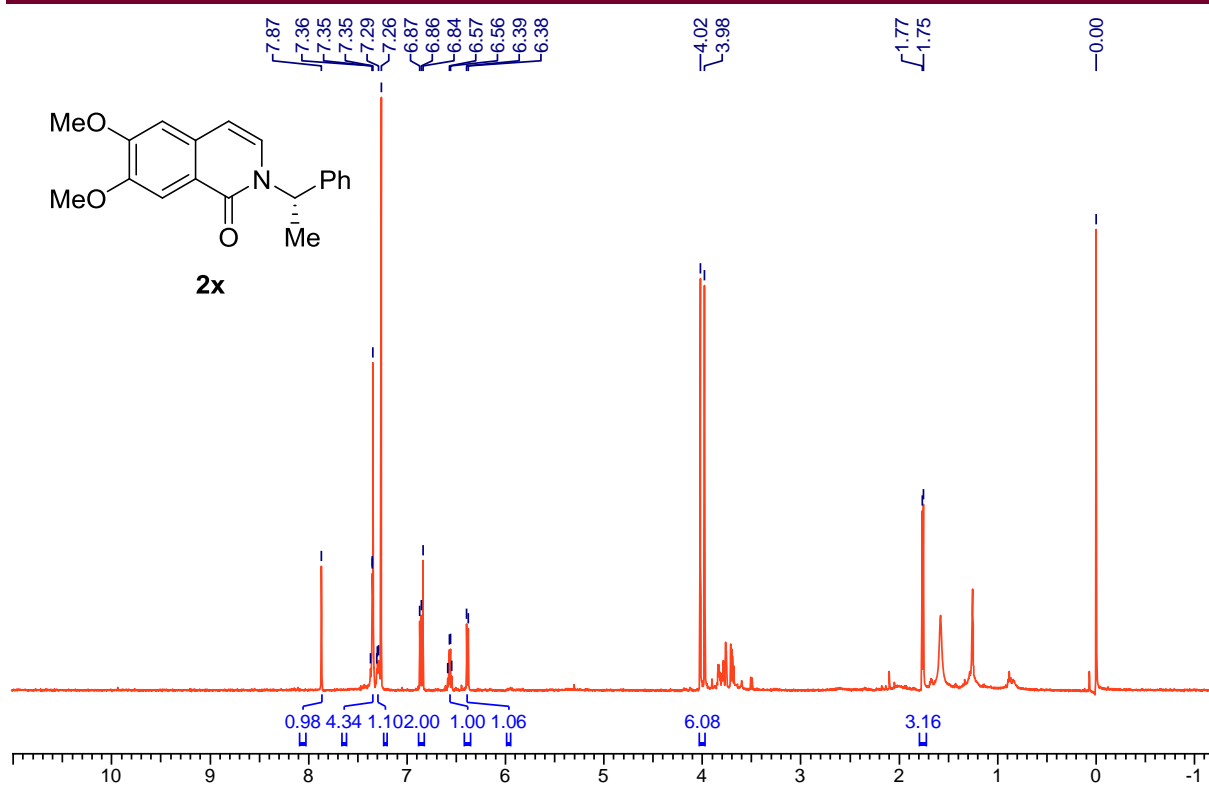


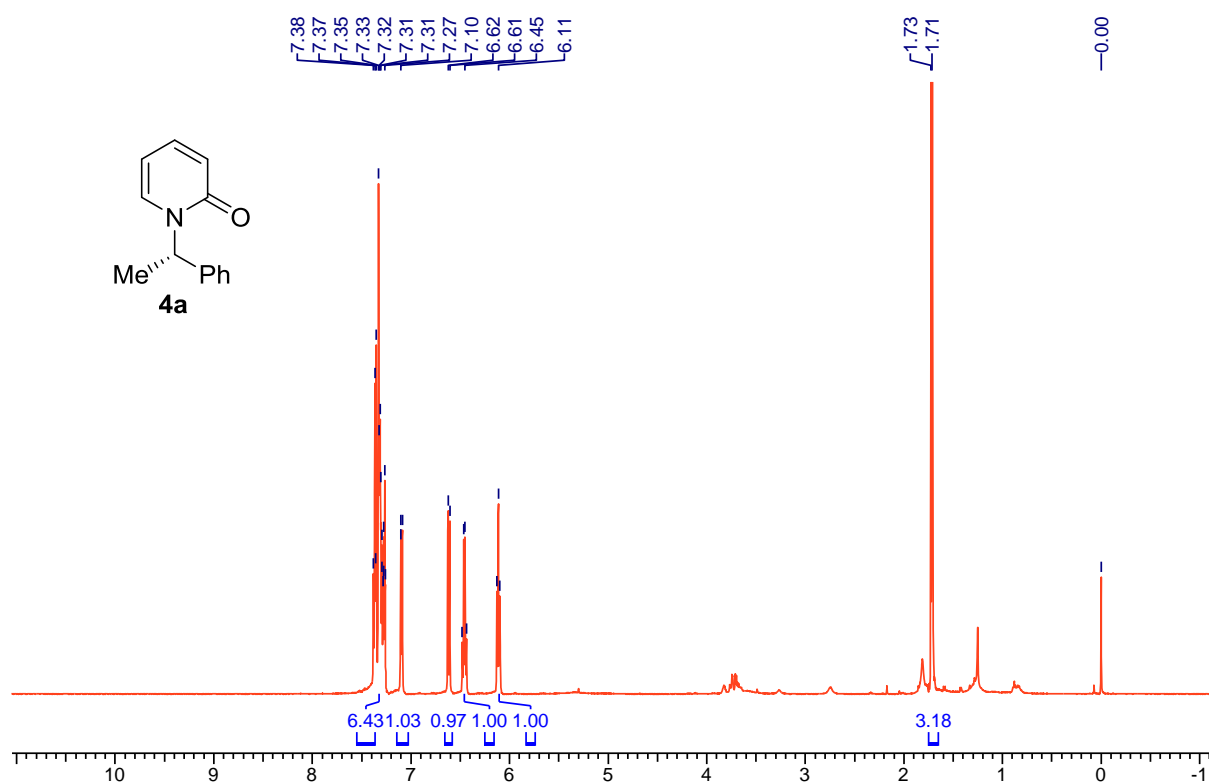
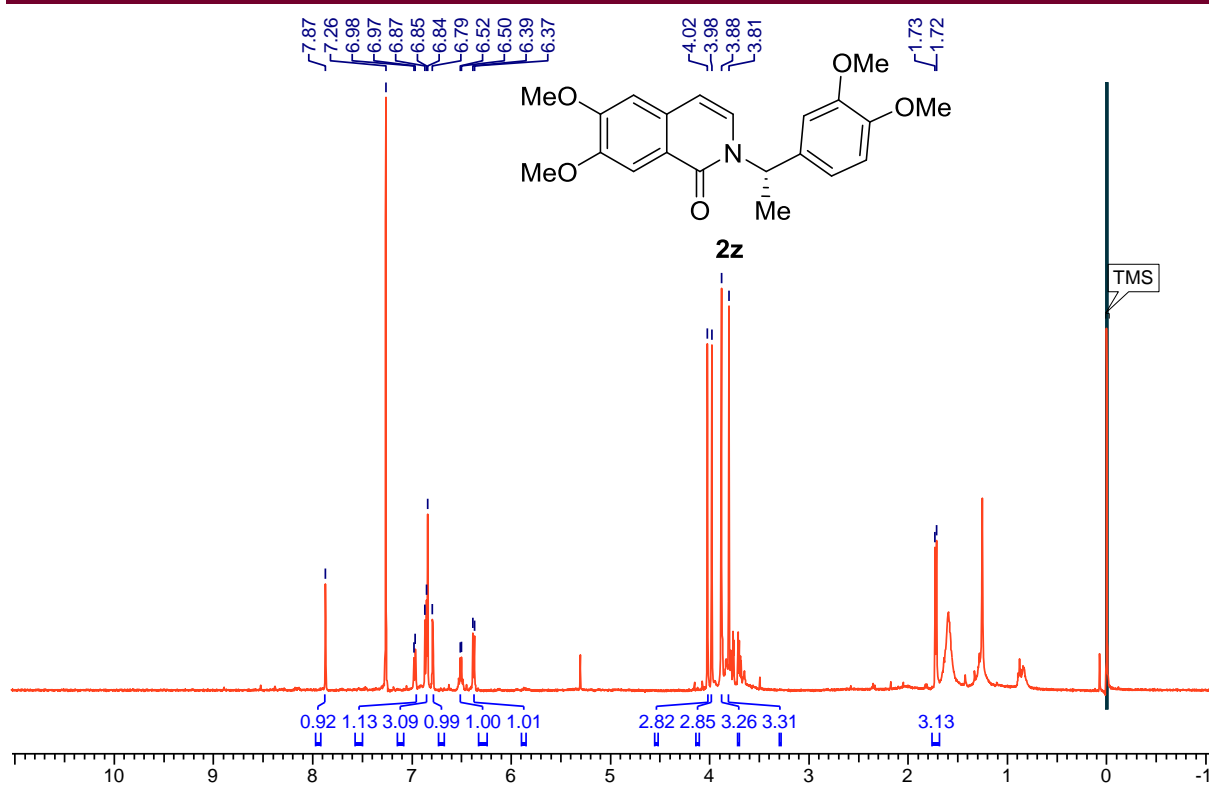


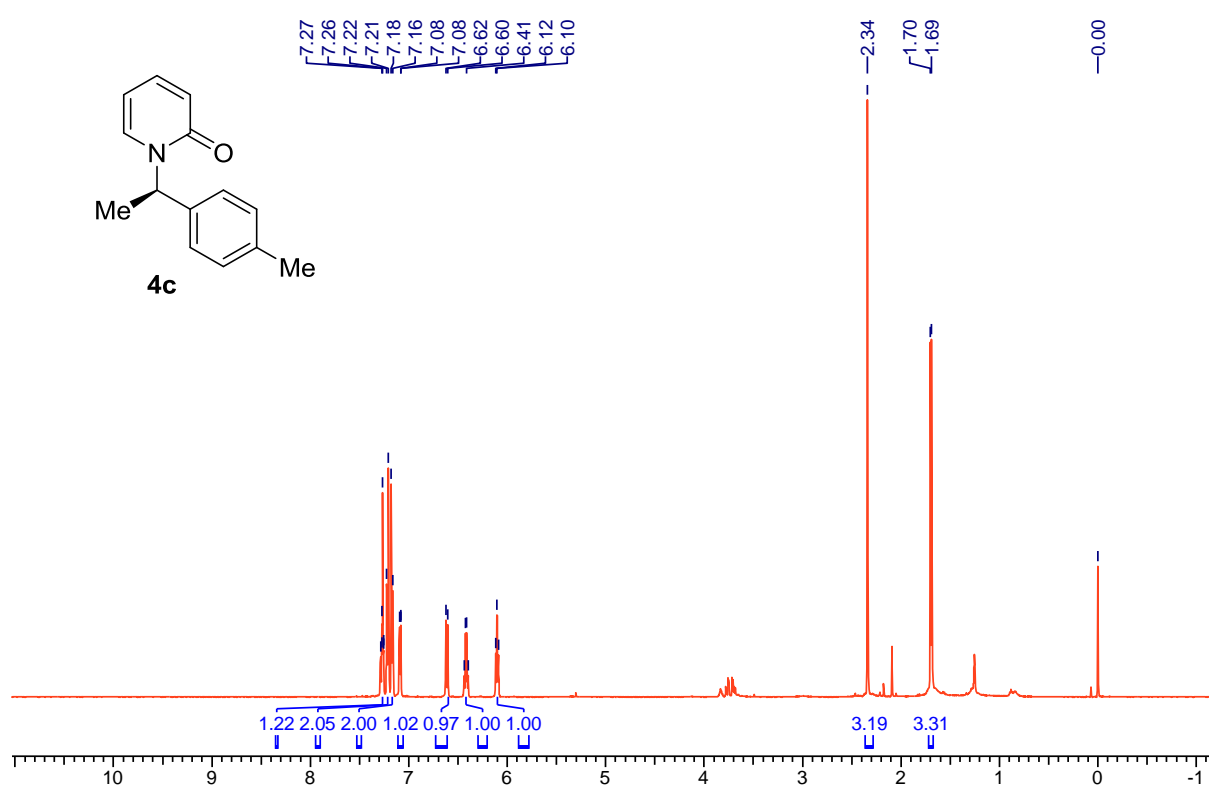
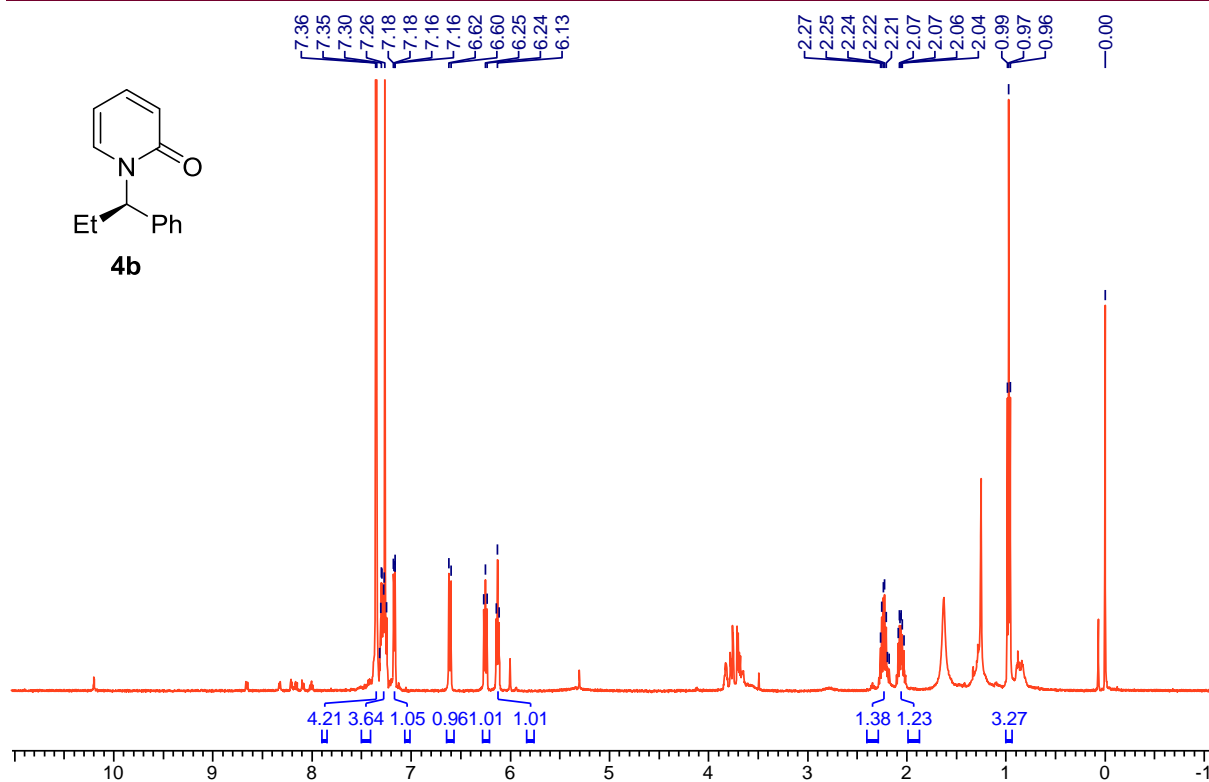


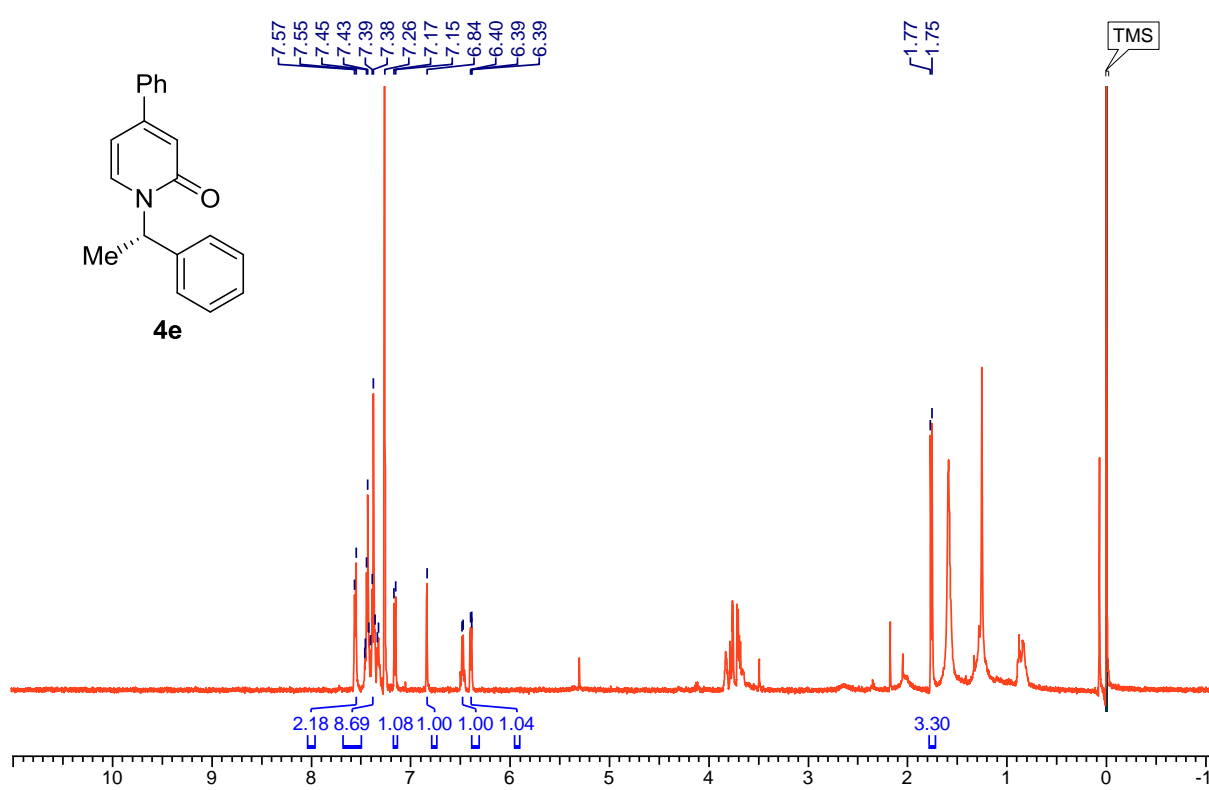
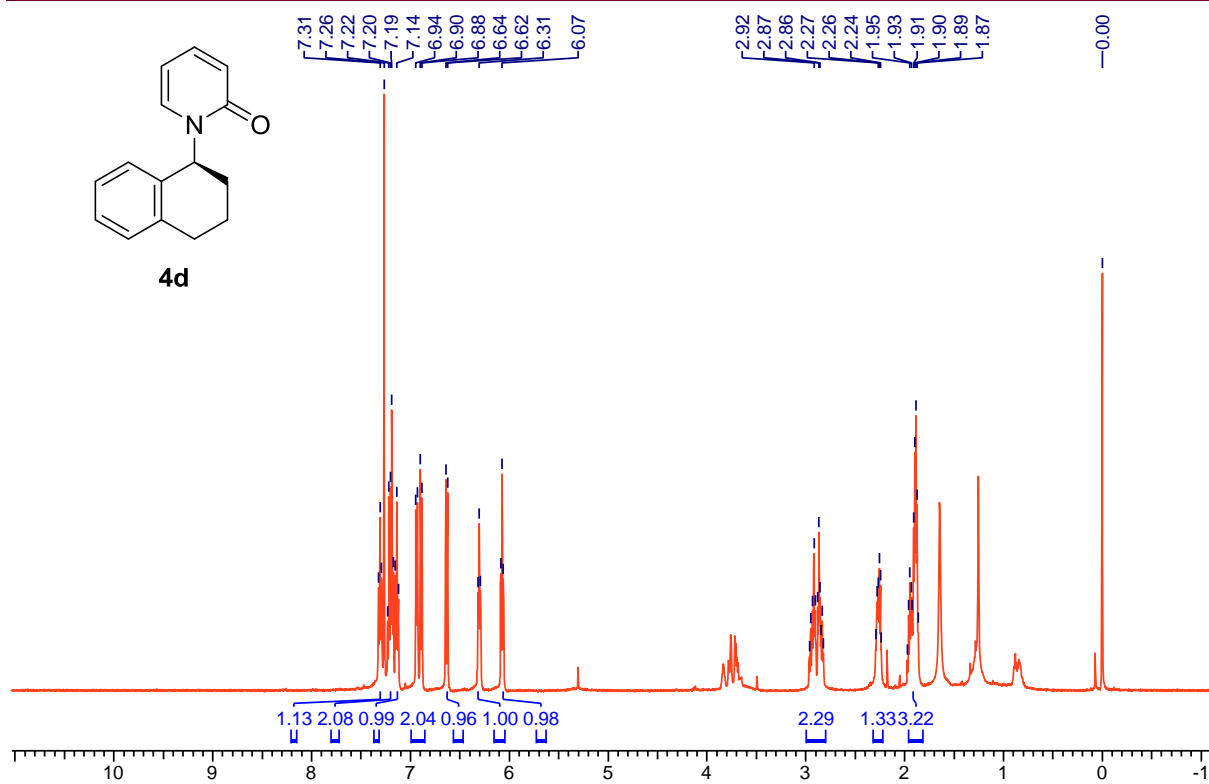






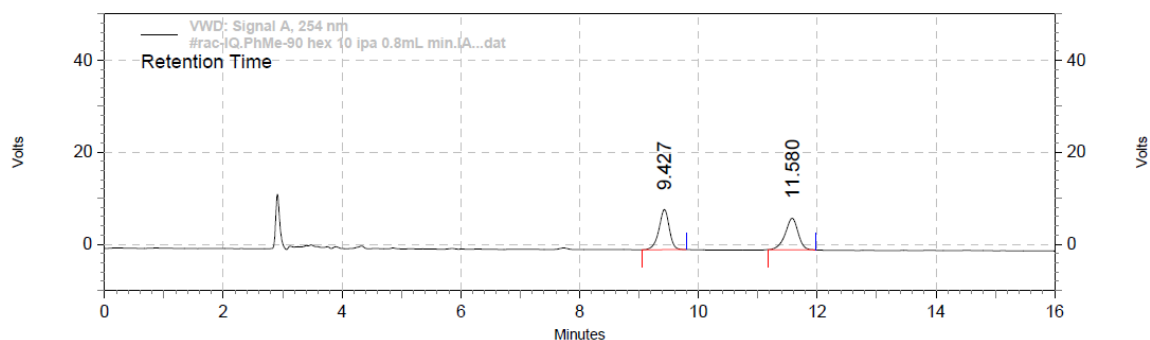






4.12 HPLC data

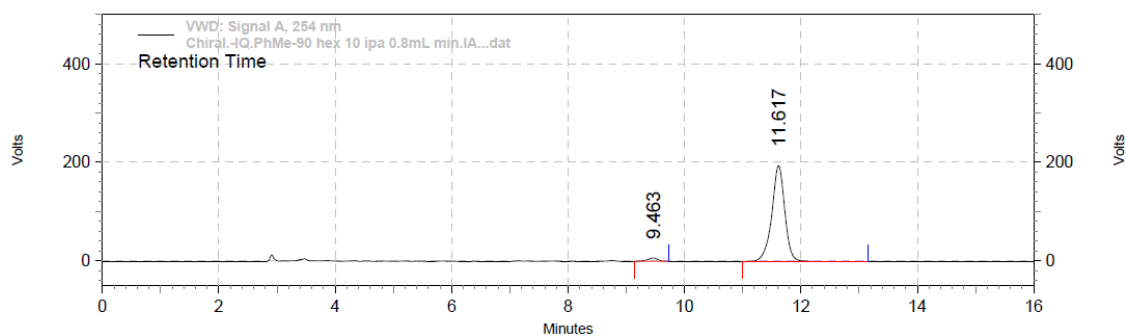
2a



VWD: Signal A, 254 nm Results

Retention Time	Area	Area %
9.427	1778044	50.61
11.580	1735243	49.39
Totals		3513287
		100.00

Column : CHIRALPAK IA
 Eluent System : 90 : 10 (HEXANE:IPA)
 Flow rate: 1.0 ml/min
 Injection vol.: 10ul
 Wavelength: 254 nm
 Sample Conc.: 0.5 mg/ml

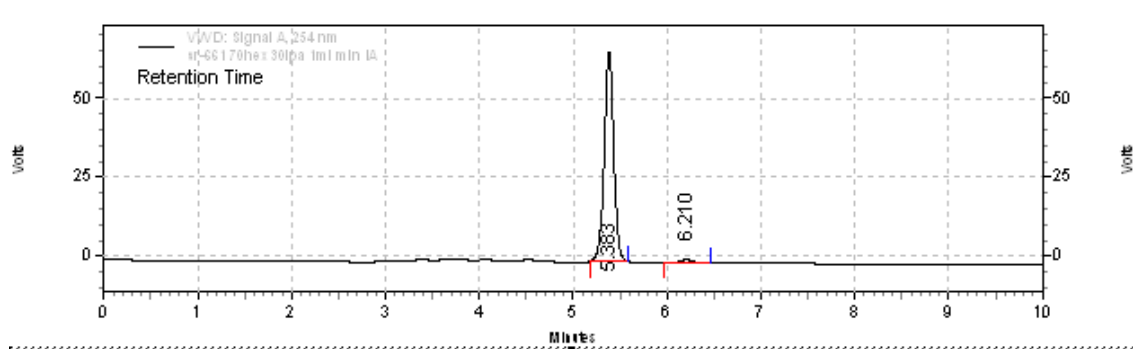


VWD: Signal A, 254 nm Results

Retention Time	Area	Area %
9.463	1425273	2.72
11.617	50931626	97.28
Totals		52356899
		100.00

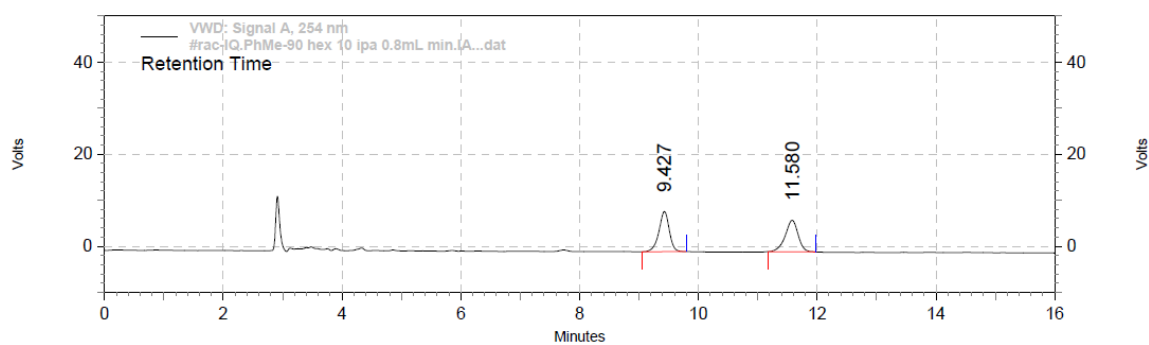
Column : CHIRALPAK IA
 Eluent System : 90 : 10 (HEXANE:IPA)
 Flow rate: 1.0 ml/min
 Injection vol.: 10ul
 Wavelength: 254 nm
 Sample Conc.: 0.5 mg/ml

ent-2a



VWD: Signal A, 254 nm			
Results			
Retention Time	Area	Area %	Height
5.383	7765221	97.97	1109346
6.210	161263	2.03	19128
Totals			
	7926484	100.00	1128474

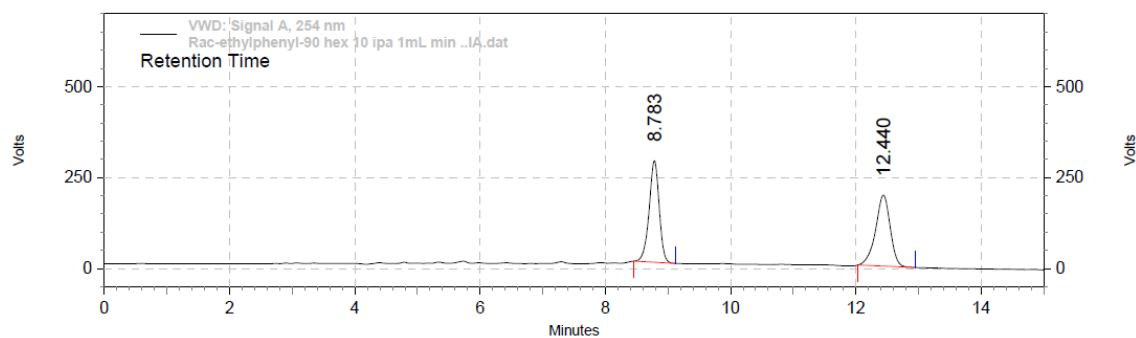
Column: CHIRALPAK IA
 Eluent System: 70 : 30 (HEXANE : IPA)
 Flow Rate: 1 ml / min
 Injection Volume: 10 ul
 Wavelength: 254 nm
 Sample Conc.: 1 mg/ml



VWD: Signal A, 254 nm Results		
Retention Time	Area	Area %
9.427	1778044	50.61
11.580	1735243	49.39
Totals		
	3513287	100.00

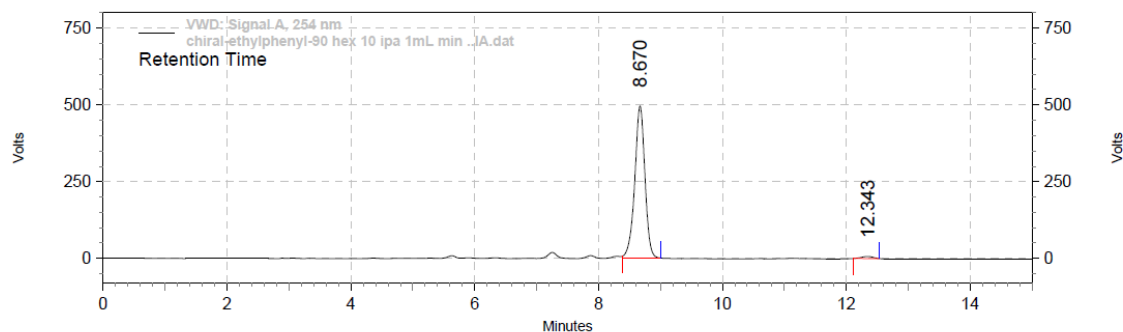
Column : CHIRALPAK IA
 Eluent System : 90 : 10 (HEXANE:IPA)
 Flow rate: 1.0 ml/min
 Injection vol...: 10ul
 Wavelength: 254 nm
 Sample Conc.: 0.5 mg/ ml

2b

**VWD: Signal A, 254 nm Results**

Retention Time	Area	Area %
8.783	52319377	49.65
12.440	53048041	50.35
Totals	105367418	100.00

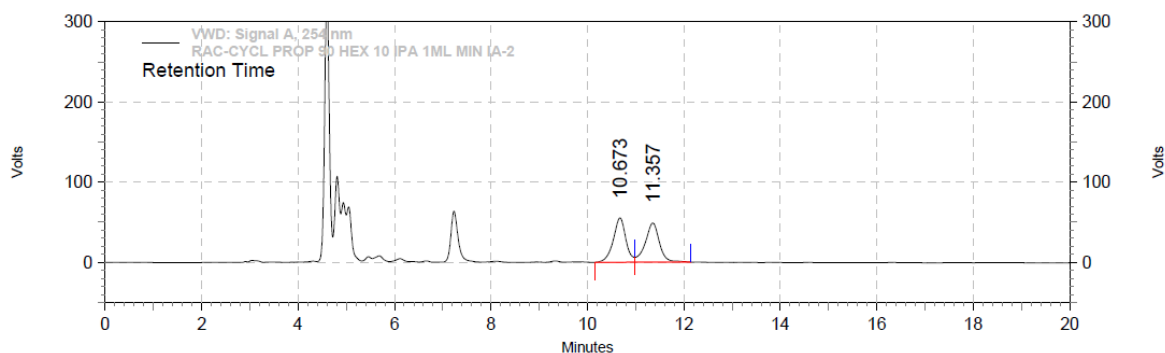
Column : CHIRALPAK IA
 Eluent System : 90 : 10 (HEXANE:IPA)
 Flow rate: 1 ml/min
 Injection vol.: 10ul
 Wavelength: 254 nm
 Sample Conc.: 1 mg/ ml

**VWD: Signal A, 254 nm Results**

Retention Time	Area	Area %
8.670	95097169	98.45
12.343	1497798	1.55
Totals	96594967	100.00

Column : CHIRALPAK IA
 Eluent System : 90 : 10 (HEXANE:IPA)
 Flow rate: 1 ml/min
 Injection vol.: 10ul
 Wavelength: 254 nm
 Sample Conc.: 1 mg/ ml

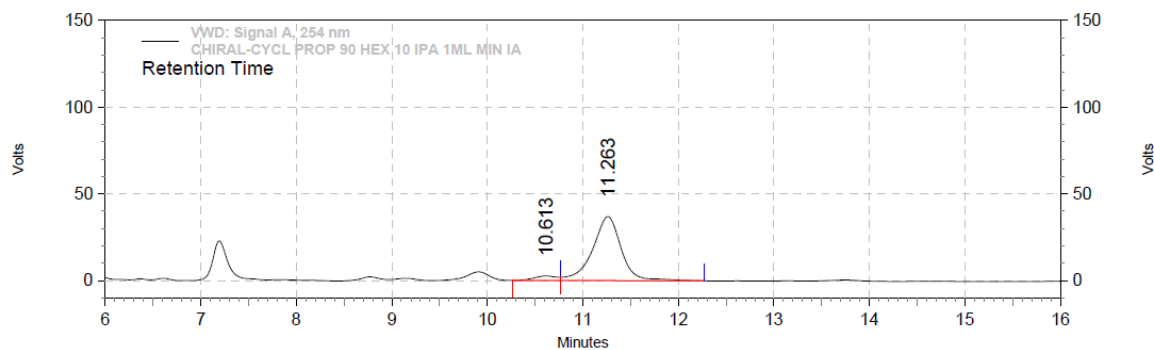
2c



VWD: Signal A, 254 nm Results

Retention Time	Area	Area %
10.673	16737166	50.26
11.357	16562547	49.74
Totals		33299713
		100.00

Column : CHIRALPAK IA
 Eluent System : 90 : 10 (HEXANE:IPA)
 Flow rate: 1.0 ml/min
 Injection vol.: 10ul
 Wavelength: 254 nm
 Sample Conc.: 0.5 mg/ml

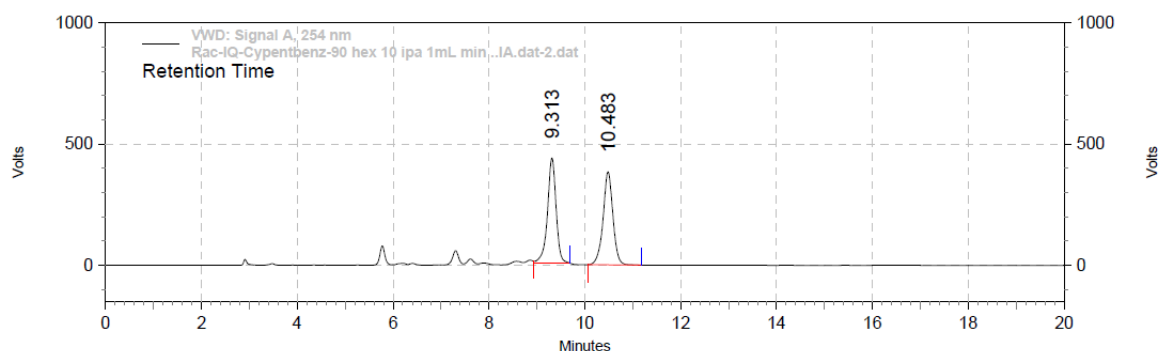


VWD: Signal A, 254 nm Results

Retention Time	Area	Area %
10.613	706497	5.19
11.263	12907188	94.81
Totals		13613685
		100.00

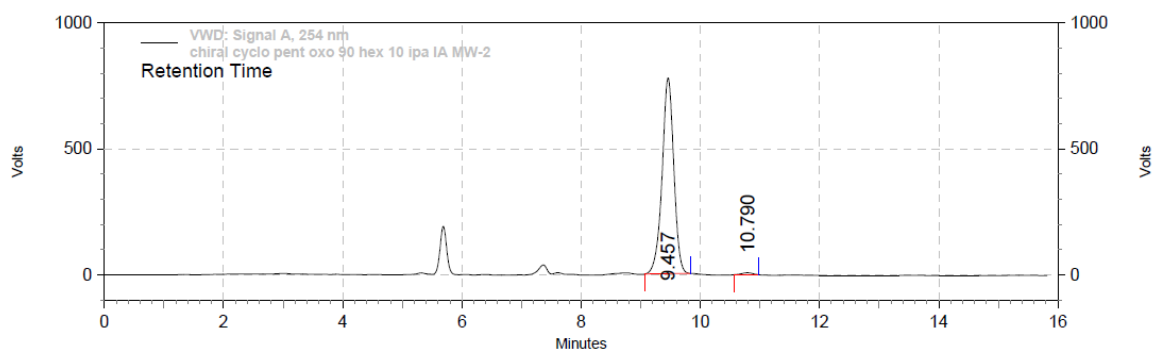
Column : CHIRALPAK IA
 Eluent System : 90 : 10 (HEXANE:IPA)
 Flow rate: 1.0 ml/min
 Injection vol.: 10ul
 Wavelength: 254 nm
 Sample Conc.: 0.5 mg/ml

2d

**VWD: Signal A, 254 nm Results**

Retention Time	Area	Area %
9.313	91350636	49.81
10.483	92063441	50.19
Totals		183414077
		100.00

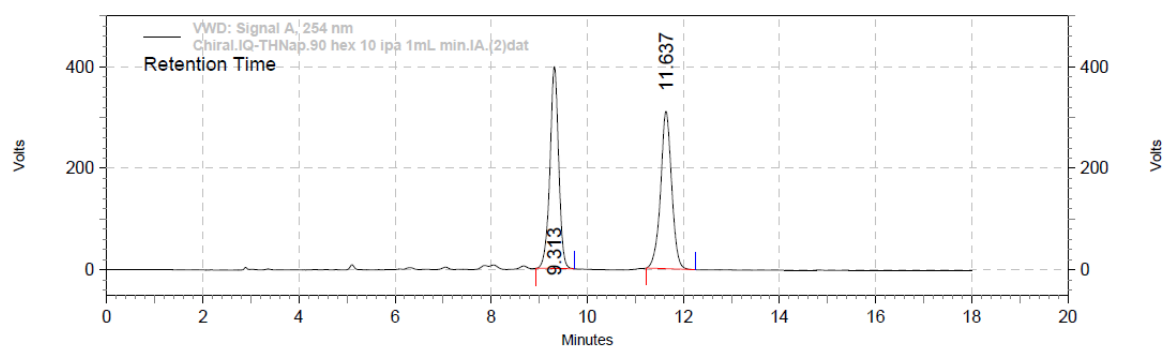
Column : CHIRALPAK IA
 Eluent System : 90 : 10 (HEXANE:IPA)
 Flow rate: 1 ml/min
 Injection vol.: 10ul
 Wavelength: 254 nm
 Sample Conc.: 1 mg/ml

**VWD: Signal A, 254 nm Results**

Retention Time	Area	Area %
9.457	177440649	99.09
10.790	1621788	0.91
Totals		179062437
		100.00

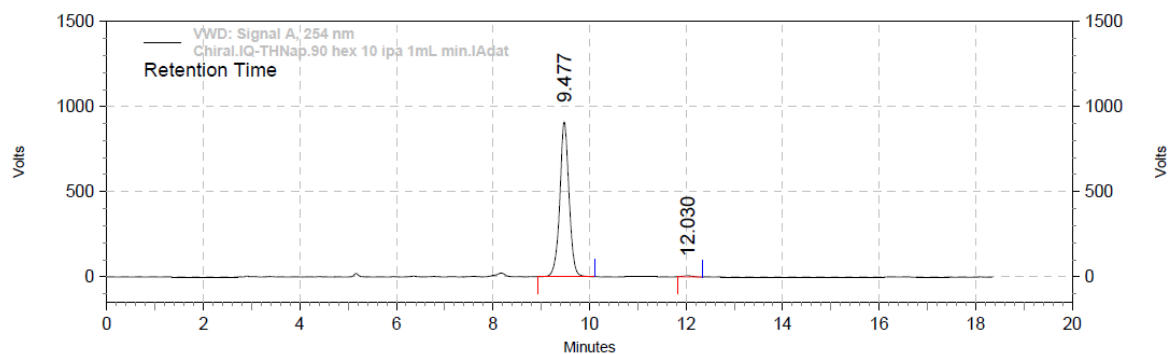
Column : CHIRALPAK IA
 Eluent System : 90 : 10 (HEXANE:IPA)
 Flow rate: 1 ml/min
 Injection vol.: 10 ul
 Wavelength: 254 nm
 Sample Conc.: 1 mg/ml

2e

**VWD: Signal A, 254 nm Results**

Retention Time	Area	Area %
9.313	84306883	50.33
11.637	83202141	49.67
Totals		167509024
		100.00

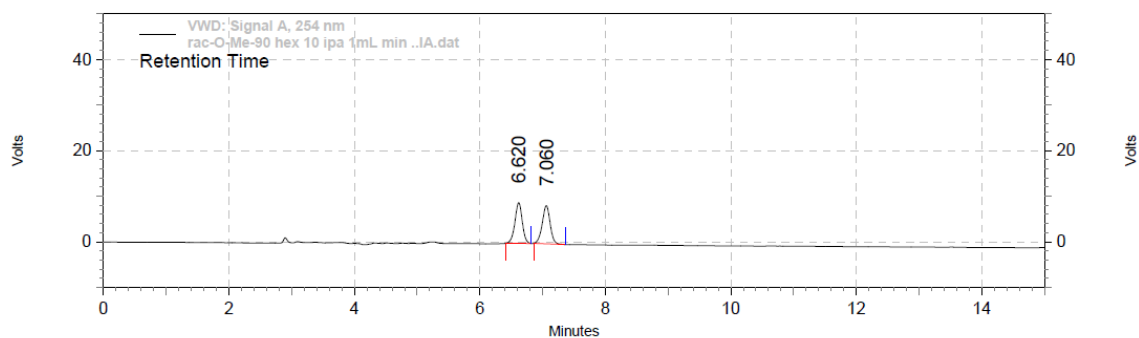
Column : CHIRALPAK IA
 Eluent System : 90 : 10 (HEXANE:IPA)
 Flow rate: 1.0 ml/min
 Injection vol.: 10ul
 Wavelength: 254 nm
 Sample Conc.: 1 mg/ ml

**VWD: Signal A, 254 nm Results**

Retention Time	Area	Area %
9.477	203837567	99.28
12.030	1470663	0.72
Totals		205308230
		100.00

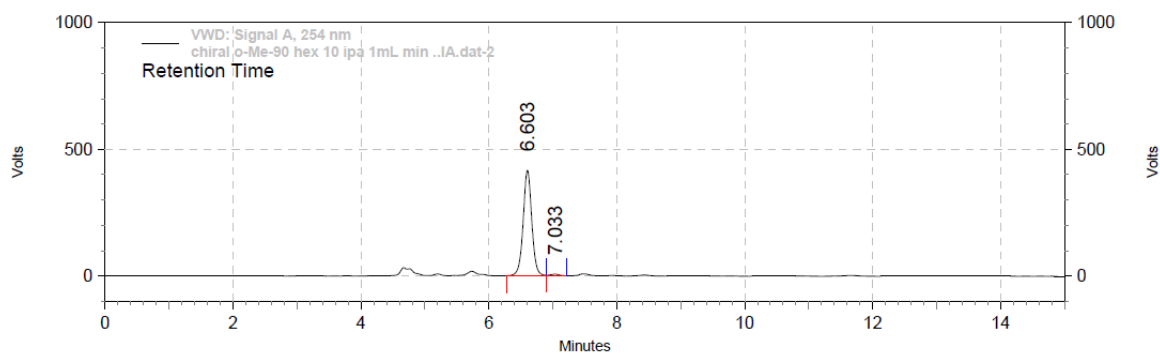
Column : CHIRALPAK IA
 Eluent System : 90 : 10 (HEXANE:IPA)
 Flow rate: 1.0 ml/min
 Injection vol.: 10ul
 Wavelength: 254 nm
 Sample Conc.: 0.5 mg/ ml

2f

**VWD: Signal A, 254 nm Results**

Retention Time	Area	Area %
6.620	1220125	49.82
7.060	1228791	50.18
Totals		2448916
		100.00

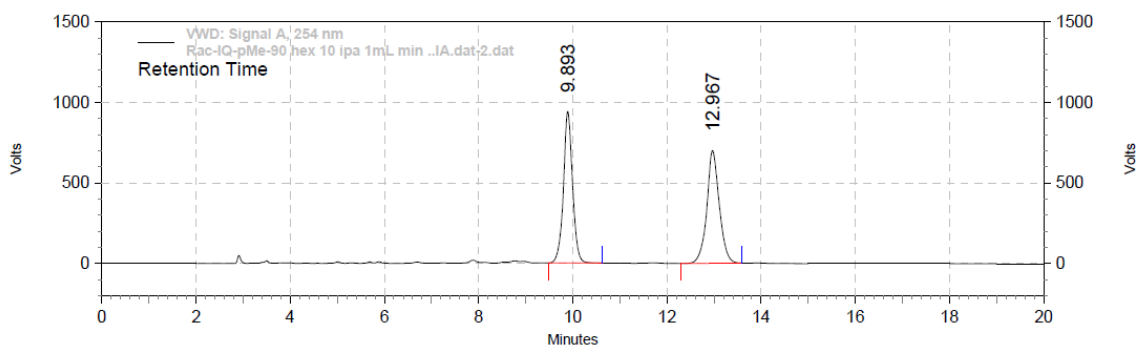
Column : CHIRALPAK IA
 Eluent System : 90 : 10 (HEXANE:IPA)
 Flow rate: 1 ml/min
 Injection vol.: 10ul
 Wavelength: 254 nm
 Sample Conc.: 1 mg/ ml

**VWD: Signal A, 254 nm Results**

Retention Time	Area	Area %
6.603	65272413	98.43
7.033	1042512	1.57
Totals		66314925
		100.00

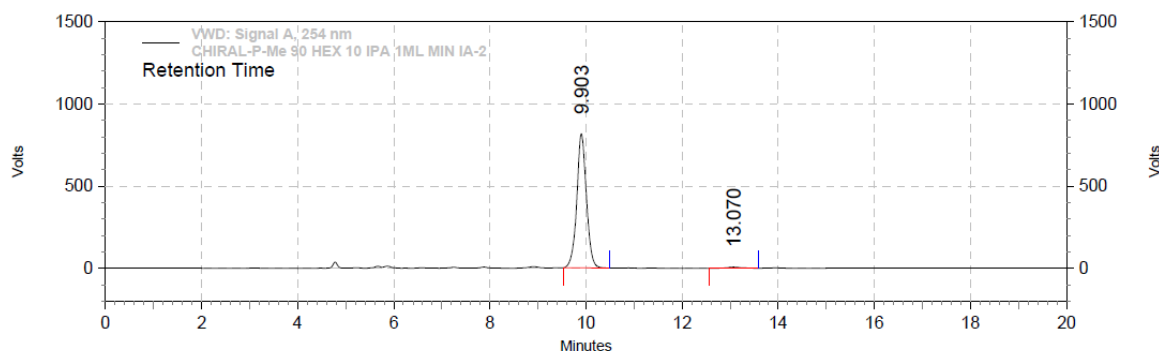
Column : CHIRALPAK IA
 Eluent System : 90 : 10 (HEXANE:IPA)
 Flow rate: 1 ml/min
 Injection vol.: 10ul
 Wavelength: 254 nm
 Sample Conc.: 1 mg/ ml

2g

**VWD: Signal A, 254 nm Results**

Retention Time	Area	Area %
9.893	212400086	49.60
12.967	215788207	50.40
Totals		428188293
		100.00

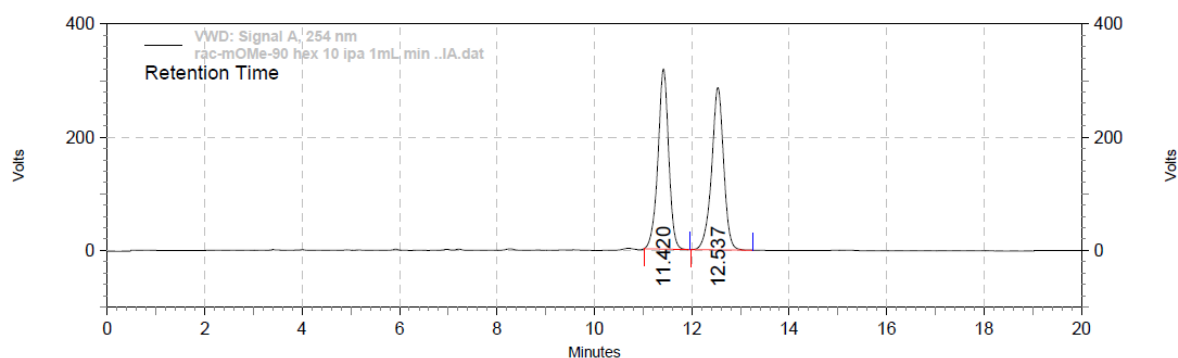
Column : CHIRALPAK IA
 Eluent System : 90 : 10 (HEXANE:IPA)
 Flow rate: 1 ml/min
 Injection vol.: 10ul
 Wavelength: 254 nm
 Sample Conc.: 1 mg/ml

**VWD: Signal A, 254 nm Results**

Retention Time	Area	Area %
9.903	190700802	98.69
13.070	2529266	1.31
Totals		193230068
		100.00

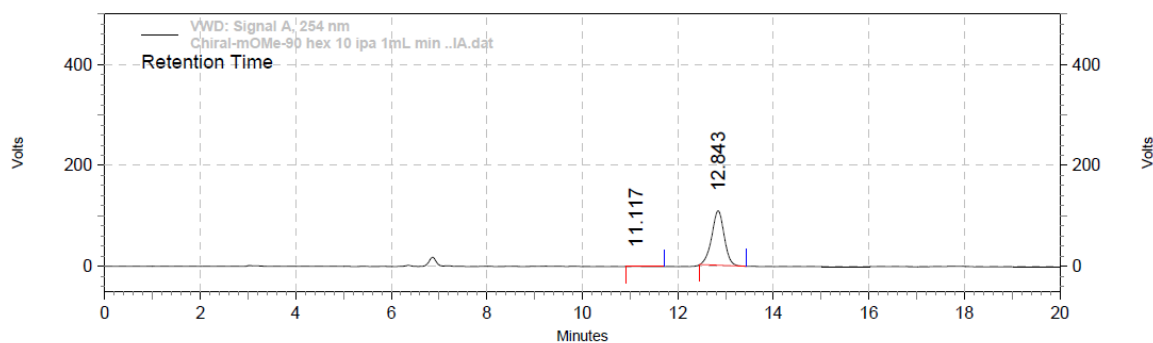
Column : CHIRALPAK IA
 Eluent System : 90 : 10 (HEXANE:IPA)
 Flow rate: 1 ml/min
 Injection vol.: 10ul
 Wavelength: 254 nm
 Sample Conc.: 1 mg/ml

2h


VWD: Signal A, 254 nm Results

Retention Time	Area	Area %
11.420	81779565	49.75
12.537	82609288	50.25
Totals		164388853
		100.00

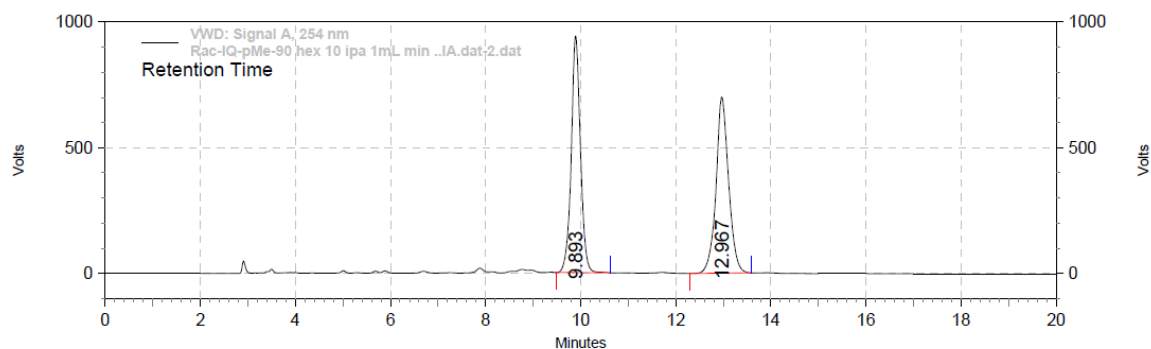
Column : CHIRALPAK IA
 Eluent System : 90 : 10 (HEXANE:IPA)
 Flow rate: 1.0 ml/min
 Injection vol.: 10ul
 Wavelength: 254 nm
 Sample Conc.: 1 mg/ml


VWD: Signal A, 254 nm Results

Retention Time	Area	Area %
11.117	105598	0.32
12.843	32795467	99.68
Totals		32901065
		100.00

Column : CHIRALPAK IA
 Eluent System : 90 : 10 (HEXANE:IPA)
 Flow rate: 1.0 ml/min
 Injection vol.: 10ul
 Wavelength: 254 nm
 Sample Conc.: 1 mg/ml

2i

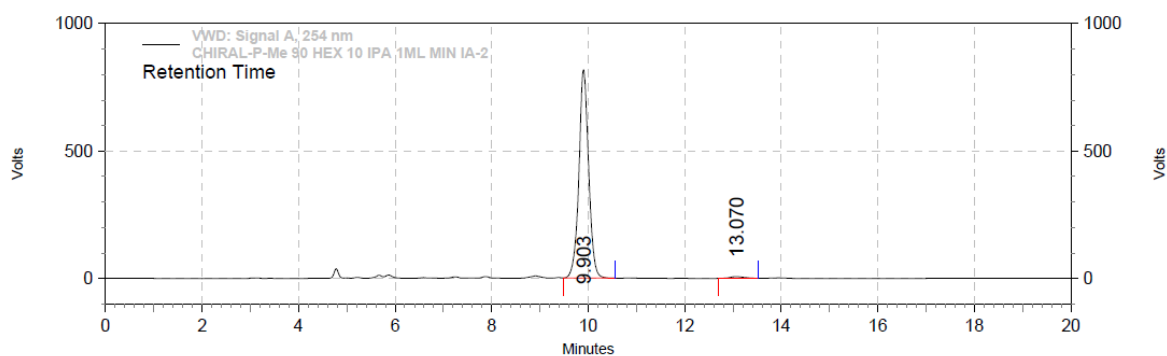


VWD: Signal A, 254 nm Results

Retention Time	Area	Area %
9.893	212400086	49.60
12.967	215788207	50.40

Totals	428188293	100.00
--------	-----------	--------

Column : CHIRALPAK IA
 Eluent System : 90 : 10 (HEXANE:IPA)
 Flow rate: 1.0 ml/min
 Injection vol.: 10ul
 Wavelength: 254 nm
 Sample Conc.: 0.5 mg/ ml



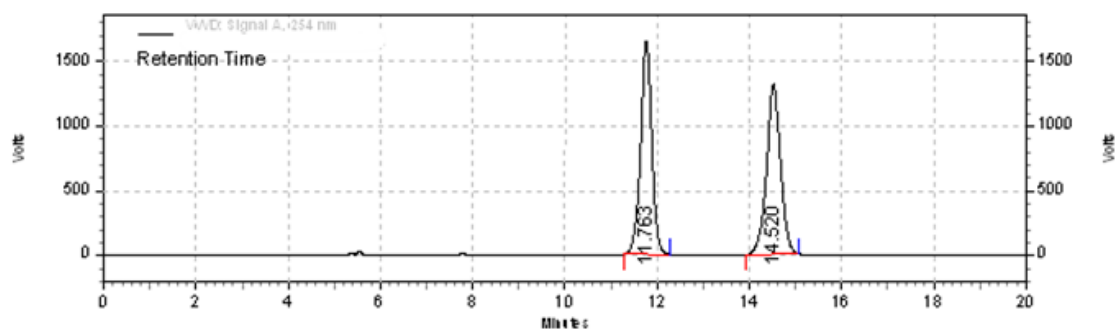
VWD: Signal A, 254 nm Results

Retention Time	Area	Area %
9.903	191757380	98.76
13.070	2401856	1.24

Totals	194159236	100.00
--------	-----------	--------

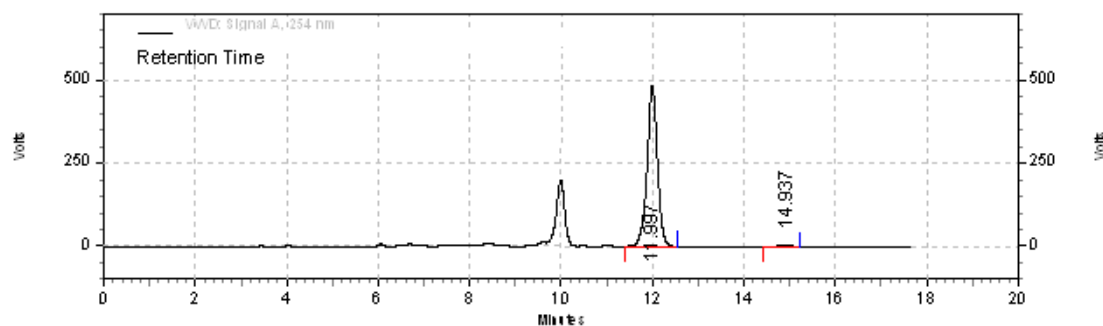
Column : CHIRALPAK IA
 Eluent System : 90 : 10 (HEXANE:IPA)
 Flow rate: 1.0 ml/min
 Injection vol.: 10ul
 Wavelength: 254 nm
 Sample Conc.: 0.5 mg/ ml

2j



VWD: Signal A, 254 nm				
Results				
Retention Time	Area	Area %	Height	
11.763	464624373	49.98	27635394	
14.520	464926691	50.02	22070049	
Totals	929551064	100.00	49705443	

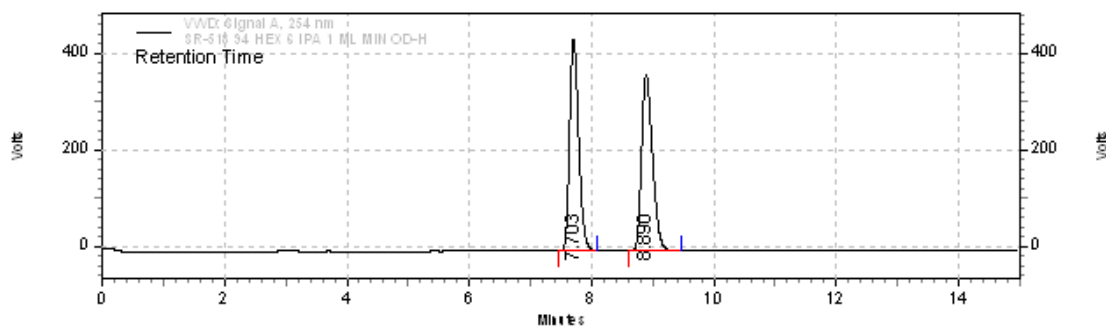
Column: CHIRALPAK IA
 Eluent System: 80: 20 (HEXANE : IPA)
 Flow Rate: 1ml / min
 Injection Volume: 10 ul
 Wavelength: 254 nm
 Sample Conc.: 1mg/ml



VWD: Signal A, 254 nm				
Results				
Retention Time	Area	Area %	Height	
11.997	127519846	98.85	8111532	
14.937	1479659	1.15	62870	
Totals	128999505	100.00	8174402	

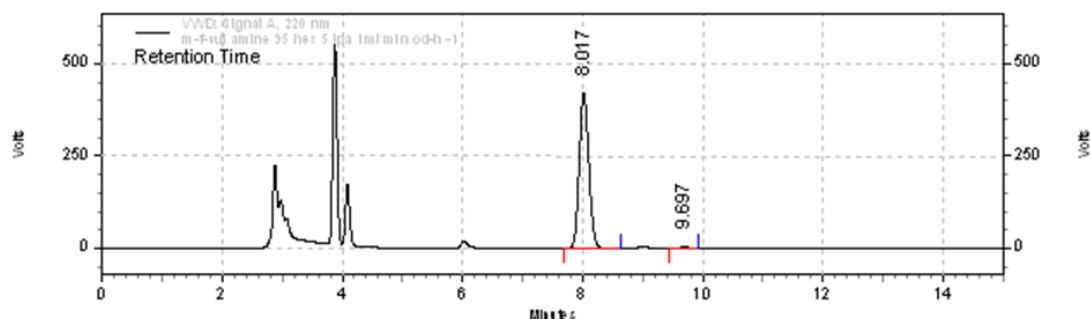
Column: CHIRALPAK IA
 Eluent System: 80: 20 (HEXANE : IPA)
 Flow Rate: 1ml / min
 Injection Volume: 10 ul
 Wavelength: 254 nm
 Sample Conc.: 1mg/ml

2k



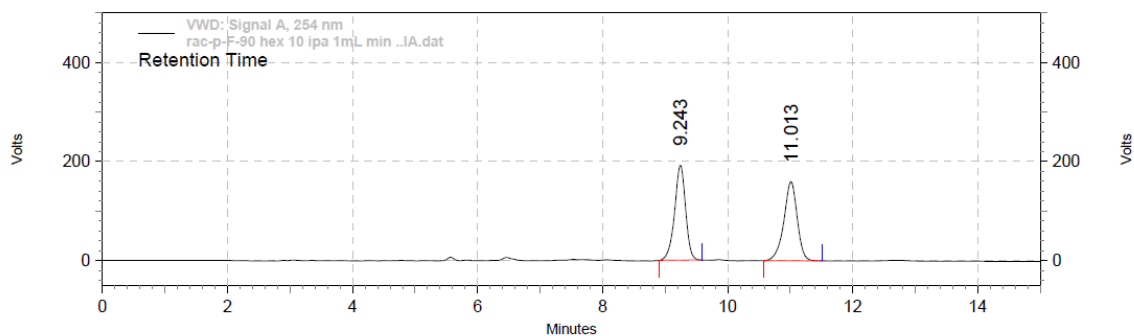
VWD: Signal A, 254 nm			
Results			
Retention Time	Area	Area %	Height
7.703	75936899	49.85	7344962
8.890	76399814	50.15	6104520
Totals	152336713	100.00	13449482

Column: CHIRALPAK OD-H
 Eluent System: 95: 5 (HEXANE : IPA)
 Flow Rate: 1ml / min
 Injection Volume: 10 ul
 Wavelength: 254 nm
 Sample Conc.: 1mg/ml



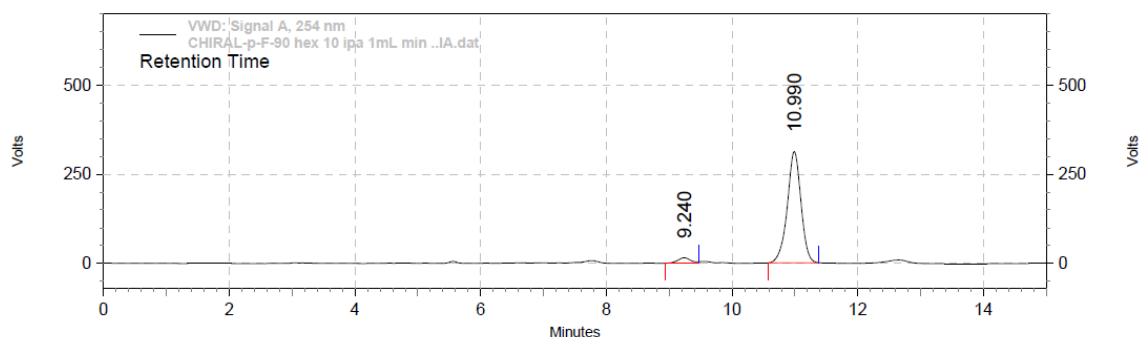
VWD: Signal A, 220 nm			
Results			
Retention Time	Area	Area %	Height
8.017	78160183	99.09	7014424
9.697	715344	0.91	62743
Totals	78875527	100.00	7077167

Column: CHIRALPAK OD-H
 Eluent System: 95: 5 (HEXANE : IPA)
 Flow Rate: 1ml / min
 Injection Volume: 10 ul
 Wavelength: 254 nm
 Sample Conc.: 1mg/ml


VWD: Signal A, 254 nm Results

Retention Time	Area	Area %
9.243	39231548	49.67
11.013	39754617	50.33
Totals		100.00
	78986165	

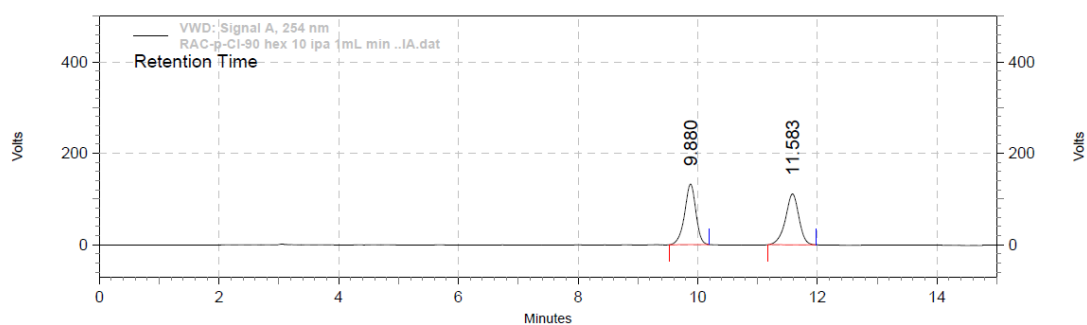
Column : CHIRALPAK IA
 Eluent System : 90 : 10 (HEXANE:IPA)
 Flow rate: 1 ml/min
 Injection vol.: 10ul
 Wavelength: 254 nm
 Sample Conc.: 1 mg/ml


VWD: Signal A, 254 nm Results

Retention Time	Area	Area %
9.240	3817183	4.60
10.990	79244089	95.40
Totals		100.00
	83061272	

Column : CHIRALPAK IA
 Eluent System : 90 : 10 (HEXANE:IPA)
 Flow rate: 1 ml/min
 Injection vol.: 10ul
 Wavelength: 254 nm
 Sample Conc.: 1 mg/ml

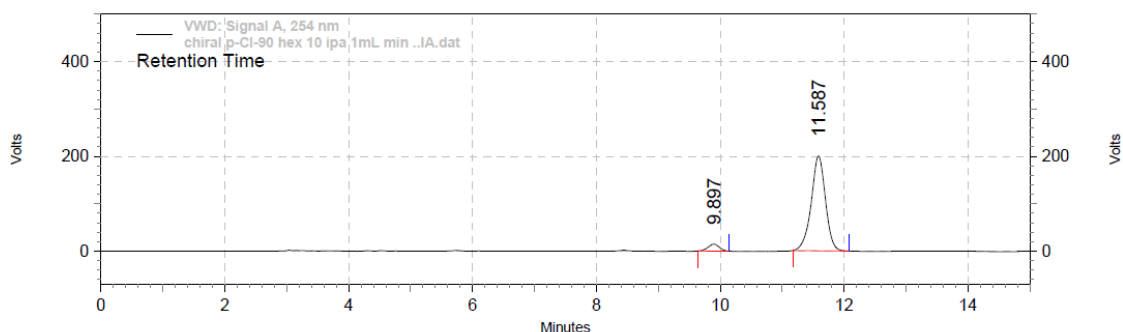
2m

**VWD: Signal A, 254 nm Results**

Retention Time	Area	Area %
9.880	29059585	49.98
11.583	29079432	50.02

Totals	58139017	100.00
--------	----------	--------

Column : CHIRALPAK IA
 Eluent System : 90 : 10 (HEXANE:IPA)
 Flow rate: 1 ml/min
 Injection vol.: 10ul
 Wavelength: 254 nm
 Sample Conc.: 1 mg/ ml

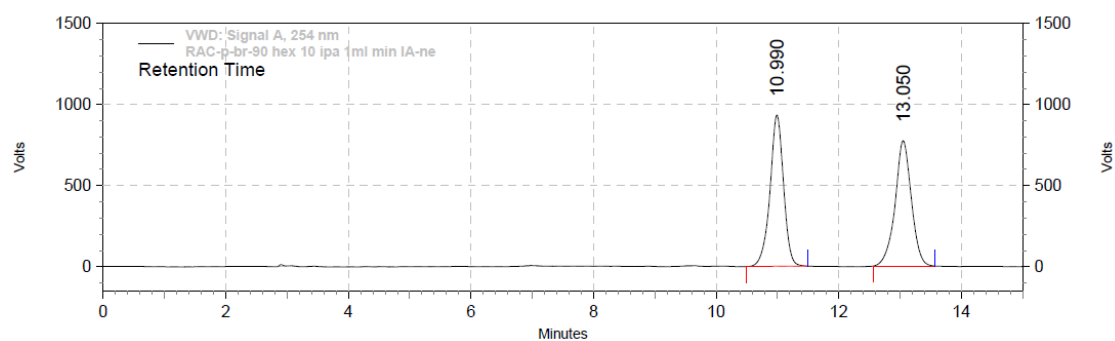
**VWD: Signal A, 254 nm Results**

Retention Time	Area	Area %
9.897	3080453	5.44
11.587	53496580	94.56

Totals	56577033	100.00
--------	----------	--------

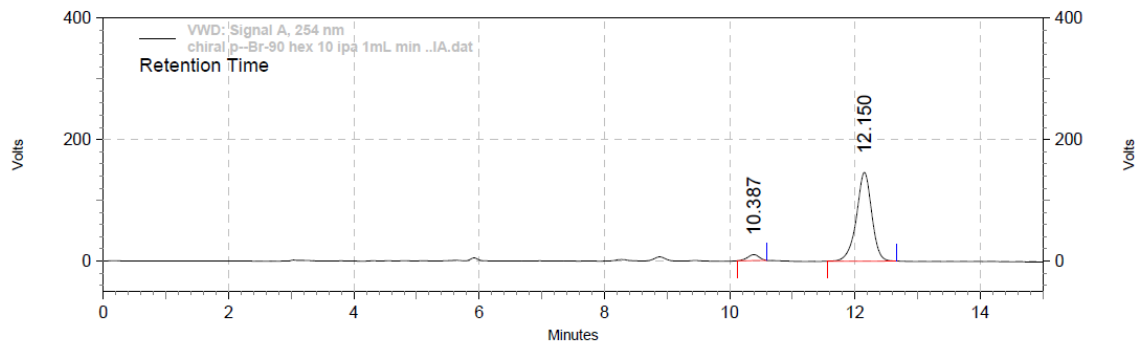
Column : CHIRALPAK IA
 Eluent System : 90 : 10 (HEXANE:IPA)
 Flow rate: 1 ml/min
 Injection vol.: 10ul
 Wavelength: 254 nm
 Sample Conc.: 1 mg/ ml

2n

**VWD: Signal A, 254 nm Results**

Retention Time	Area	Area %
10.990	240479002	50.15
13.050	239007993	49.85
Totals	479486995	100.00

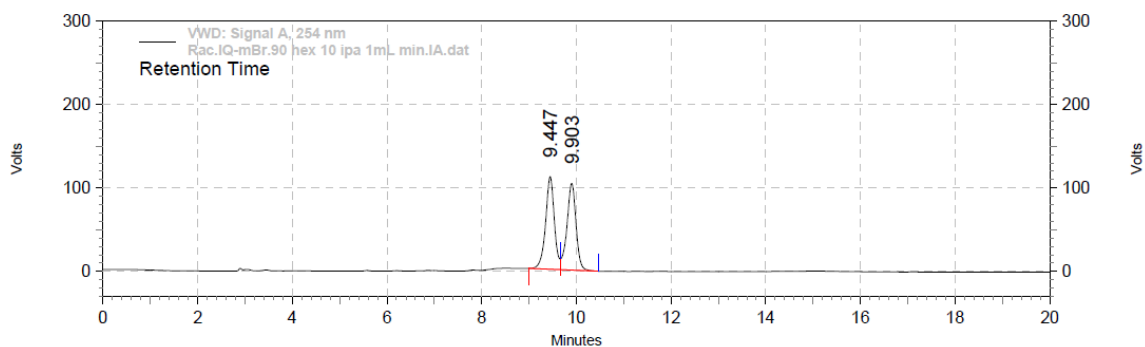
Column : CHIRALPAK IA
 Eluent System : 90 : 10 (HEXANE:IPA)
 Flow rate: 1.0 ml/min
 Injection vol.: 10ul
 Wavelength: 254 nm
 Sample Conc.: 0.5 mg/ ml

**VWD: Signal A, 254 nm Results**

Retention Time	Area	Area %
10.387	2130379	4.86
12.150	41663642	95.14
Totals	43794021	100.00

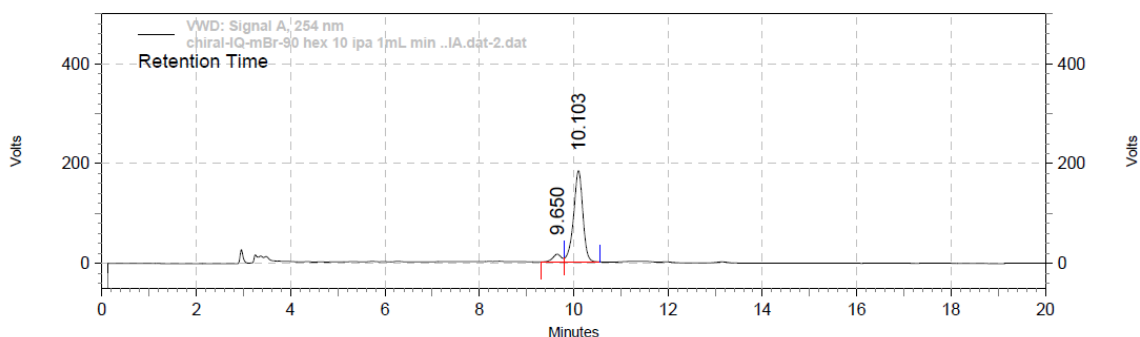
Column : CHIRALPAK IA
 Eluent System : 90 : 10 (HEXANE:IPA)
 Flow rate: 1 ml/min
 Injection vol.: 10ul
 Wavelength: 254 nm
 Sample Conc.: 1 mg/ ml

20

**VWD: Signal A, 254 nm Results**

Retention Time	Area	Area %
9.447	23958925	50.60
9.903	23388479	49.40
Totals		100.00
		47347404

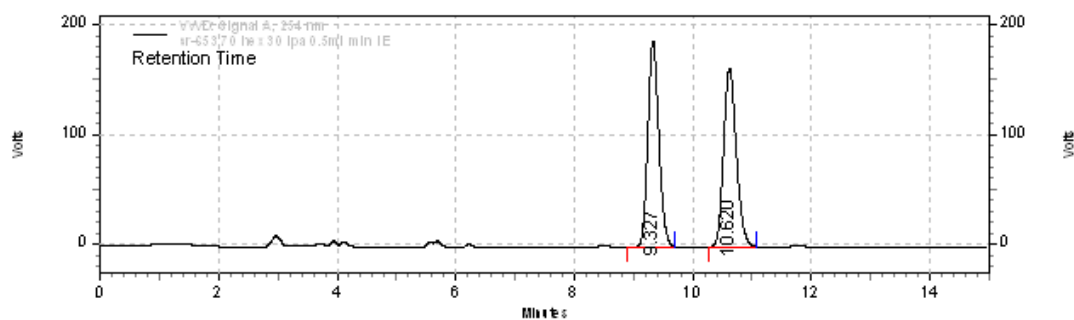
Column : CHIRALPAK IA
 Eluent System : 90 : 10 (HEXANE:IPA)
 Flow rate: 1.0 ml/min
 Injection vol.: 10ul
 Wavelength: 254 nm
 Sample Conc.: 0.5 mg/ ml

**VWD: Signal A, 254 nm Results**

Retention Time	Area	Area %
9.650	3292383	7.29
10.103	41869274	92.71
Totals		100.00
		45161657

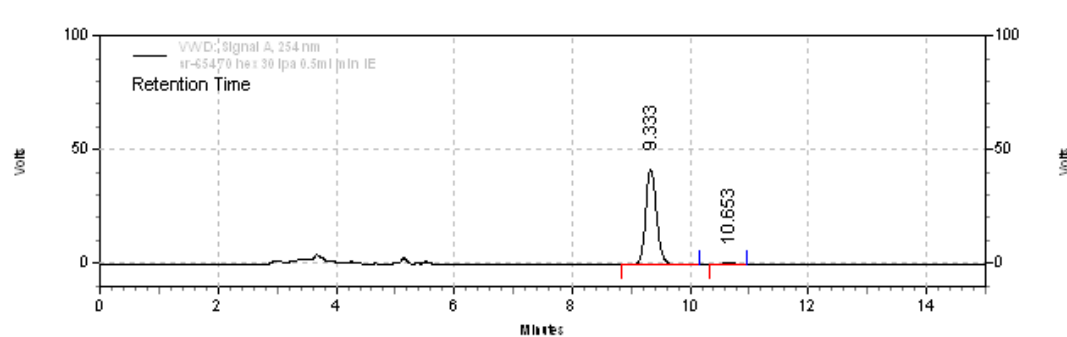
Column : CHIRALPAK IA
 Eluent System : 90 : 10 (HEXANE:IPA)
 Flow rate: 1 ml/min
 Injection vol.: 10ul
 Wavelength: 254 nm
 Sample Conc.: 0.5 mg/ ml

2p



VWD: Signal A, 254 nm			
Results			
Retention Time	Area	Area %	Height
9.327	40678861	49.81	3148006
10.620	40997270	50.19	2738092
Totals	81676131	100.00	5886098

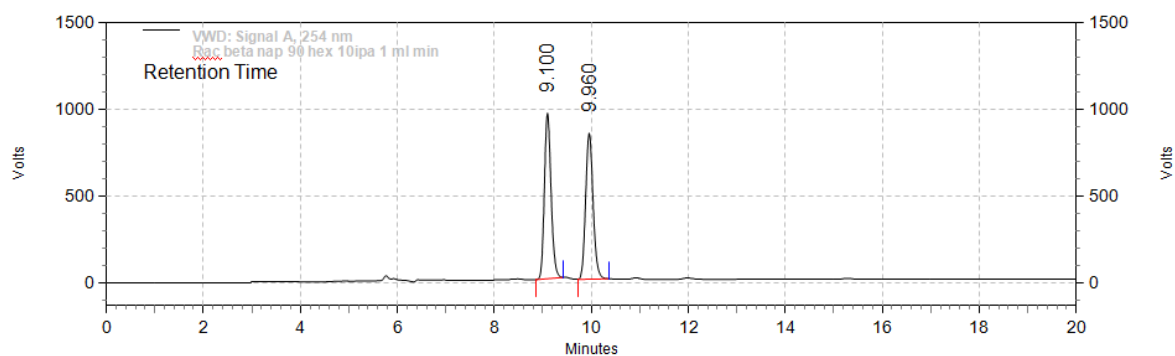
Column: CHIRALPAK IA
 Eluent System: 70:30 (HEXANE : IPA)
 Flow Rate: 0.5 ml/min
 Injection Volume: 10 ul
 Wavelength: 254 nm
 Sample Conc.: 1 mg/ml



VWD: Signal A, 254 nm			
Results			
Retention Time	Area	Area %	Height
9.333	9026611	97.55	702402
10.653	227061	2.45	15680
Totals	9253672	100.00	718082

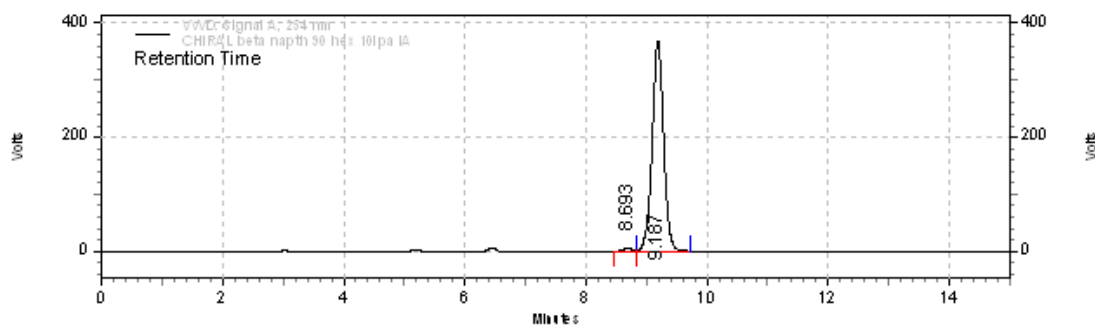
Column: CHIRALPAK IA
 Eluent System: 70:30 (HEXANE : IPA)
 Flow Rate: 1 ml/min
 Injection Volume: 10 ul
 Wavelength: 254 nm
 Sample Conc.: 0.5 mg/ml

2q

**VWD: Signal A, 254 nm Results**

Retention Time	Area	Area %
9.100	153835413	50.48
9.960	150883444	49.52
Totals	304718857	100.00

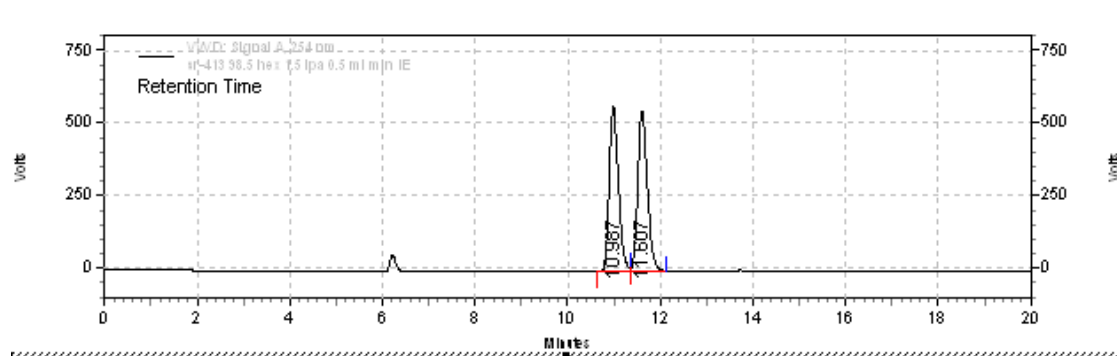
Column : CHIRALPAK IA
 Eluent System : 90 : 10 (HEXANE:IPA)
 Flow rate: 0.5 ml/min
 Injection vol.: 10ul
 Wavelength: 254 nm
 Sample Conc.: 1 mg/ml



VWD: Signal A, 254 nm Results			
Retention Time	Area	Area %	Height
8.693	887115	1.08	80073
9.187	81160871	98.92	6178244
Totals	82047986	100.00	6258317

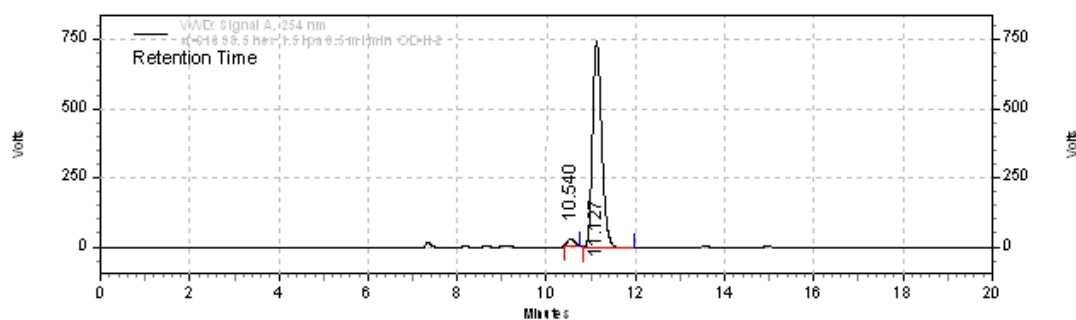
Column: CHIRALPAK IA
 Eluent System: 90:10 (HEXANE:IPA)
 Flow Rate: 1ml/min
 Injection Volume: 10 ul
 Wavelength: 254 nm
 Sample Conc.: 1mg/ml

2r



VWD: Signal A, 254 nm			
Results			
Retention Time	Area	Area %	Height
10.987	131273393	49.49	9542772
11.607	133996249	50.51	9215347
Totals	265269642	100.00	18758119

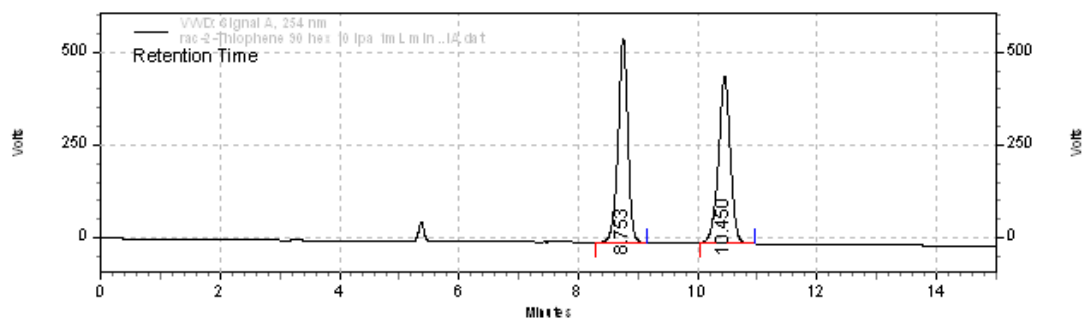
Column: CHIRALPAK IA
 Eluent System: 90: 10 (HEXANE : IPA)
 Flow Rate: 1ml / min
 Injection Volume: 10 ul
 Wavelength: 254 nm
 Sample Conc.: 1mg/ml



VWD: Signal A, 254 nm			
Results			
Retention Time	Area	Area %	Height
10.540	4503042	2.45	427020
11.127	179577154	97.55	12579840
Totals	184080196	100.00	13006860

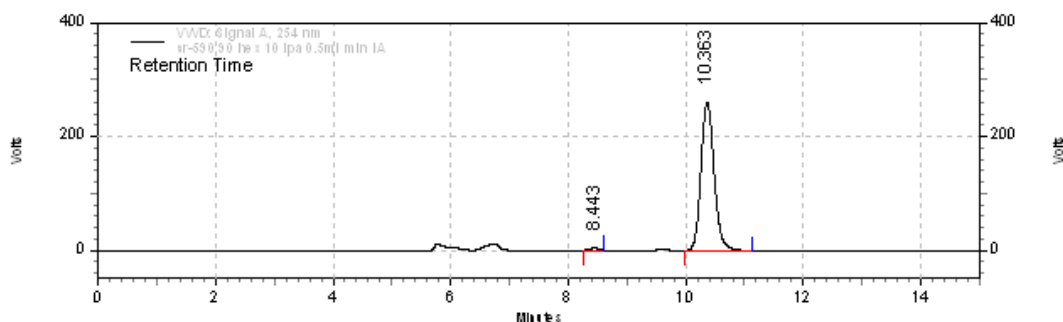
Column: CHIRALPAK IA
 Eluent System: 90: 10 (HEXANE : IPA)
 Flow Rate: 1ml / min
 Injection Volume: 10 ul
 Wavelength: 254 nm
 Sample Conc.: 1mg/ml

2s



VWD: Signal A, 254 nm				
Results				
Retention Time	Area	Area %	Height	
8.753	104567380	50.14	9212711	
10.450	103976387	49.86	7527422	
Totals	208543767	100.00	16740133	

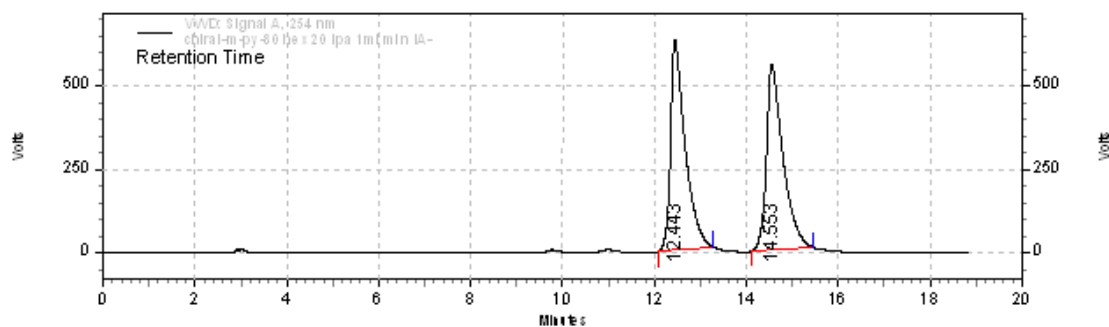
Column: CHIRALPAK IA
 Eluent System: 90: 10 (HEXANE : IPA)
 Flow Rate: 1 ml / min
 Injection Volume: 10 ul
 Wavelength: 254 nm
 Sample Conc.: 1 mg/ml



VWD: Signal A, 254 nm				
Results				
Retention Time	Area	Area %	Height	
8.443	705758	1.02	65479	
10.363	68407330	98.98	4371316	
Totals	69113088	100.00	4436795	

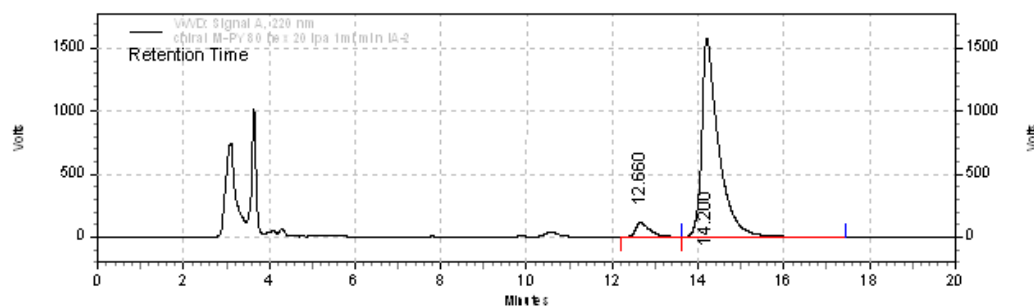
Column: CHIRALPAK IA
 Eluent System: 90: 10 (HEXANE : IPA)
 Flow Rate: 1 ml / min
 Injection Volume: 10 ul
 Wavelength: 254 nm
 Sample Conc.: 1 mg/ml

2t



VWD: Signal A, 254 nm			
Results			
Retention Time	Area	Area %	Height
12.443	232736012	49.92	10581815
14.553	233450471	50.08	9325363
Totals	466186483	100.00	19907178

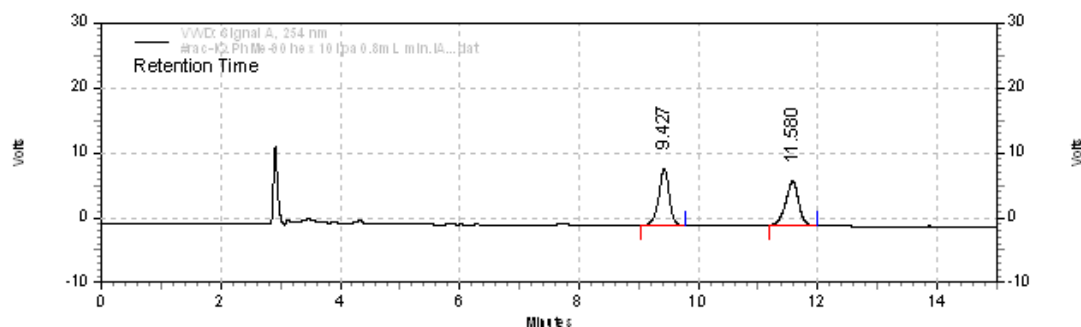
Column: CHIRALPAK IA
 Eluent System: 80: 20 (HEXANE : IPA)
 Flow Rate: 1ml / min
 Injection Volume: 10 ul
 Wavelength: 254 nm
 Sample Conc.: 1mg/ml



VWD: Signal A, 220 nm			
Results			
Retention Time	Area	Area %	Height
12.660	45834696	5.94	1929765
14.200	725759358	94.06	26481437
Totals	771594054	100.00	28411202

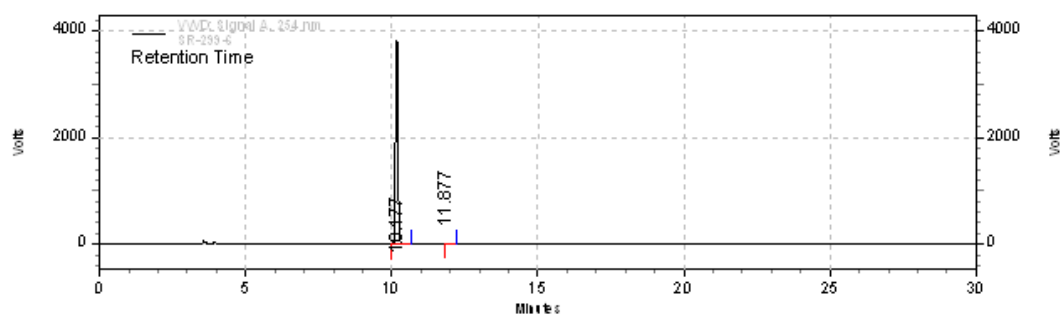
Column: CHIRALPAK IA
 Eluent System: 80: 20 (HEXANE : IPA)
 Flow Rate: 1ml / min
 Injection Volume: 10 ul
 Wavelength: 254 nm
 Sample Conc.: 1mg/ml

2u



VWD: Signal A, 254 nm			
Results			
Retention Time	Area	Area %	Height
9.427	1778044	50.61	146297
11.580	1735243	49.39	114658
Totals	3513287	100.00	260955

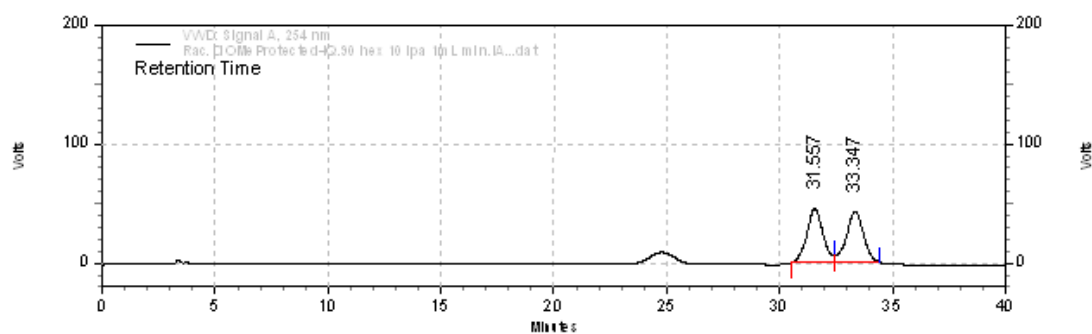
Column: CHIRALPAK IA
 Eluent System: 90: 10 (HEXANE : IPA)
 Flow Rate: 1 ml / min
 Injection Volume: 10 ul
 Wavelength: 254 nm
 Sample Conc.: 0.2mg/ml



VWD: Signal A, 254 nm			
Results			
Retention Time	Area	Area %	Height
10.177	387625983	99.48	63979339
11.877	2039272	0.52	181929
Totals	389665255	100.00	64161268

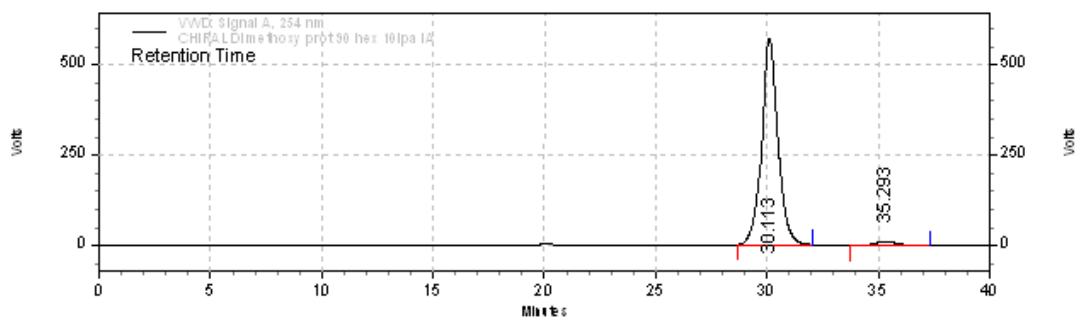
Column: CHIRALPAK IA
 Eluent System: 90: 10 (HEXANE : IPA)
 Flow Rate: 1 ml / min
 Injection Volume: 10 ul
 Wavelength: 254 nm
 Sample Conc.: 2mg/ml

2x



VWD: Signal A, 254 nm			
Results			
Retention Time	Area	Area %	Height
31.557	37369643	49.70	757585
33.347	37824756	50.30	719743
Totals	75194399	100.00	1477328

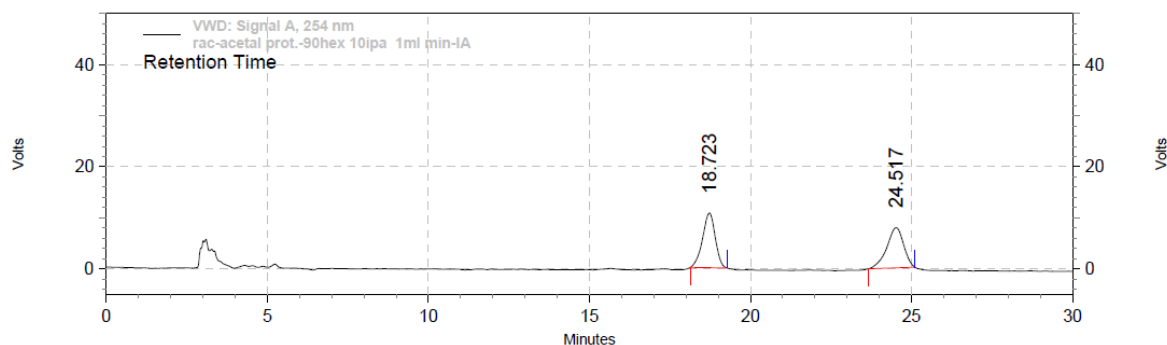
Column: CHIRALPAK IA
 Eluent System: 90:10 (HEXANE : IPA)
 Flow Rate: 1 ml / min
 Injection Volume: 10 ul
 Wavelength: 254 nm
 Sample Conc.: 1 mg/ml



VWD: Signal A, 254 nm			
Results			
Retention Time	Area	Area %	Height
30.113	483627980	97.13	9572830
35.293	14310252	2.87	212314
Totals	497938232	100.00	9785144

Column: CHIRALPAK IA
 Eluent System: 90:10 (HEXANE : IPA)
 Flow Rate: 1 ml / min
 Injection Volume: 10 ul
 Wavelength: 254 nm
 Sample Conc.: 1 mg/ml

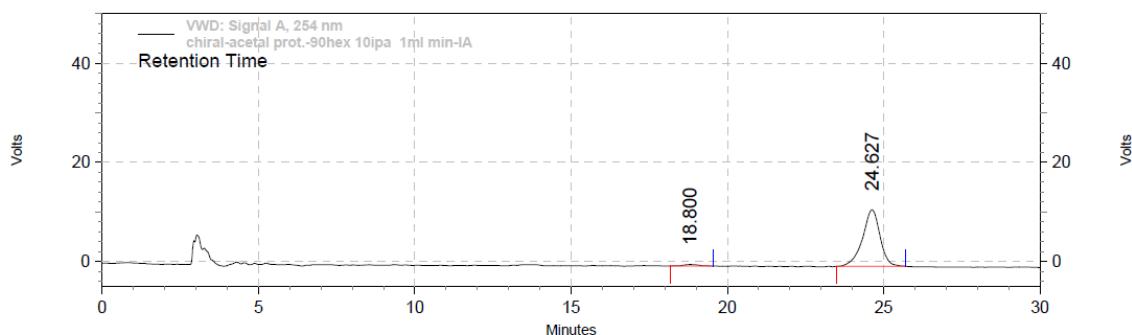
2y



VWD: Signal A, 254 nm Results

Retention Time	Area	Area %
18.723	4901948	50.63
24.517	4780387	49.37
Totals	9682335	100.00

Column : CHIRALPAK IA
 Eluent System : 90 : 10 (HEXANE:IPA)
 Flow rate: 1.0 ml/min
 Injection vol.: 10ul
 Wavelength: 254 nm
 Sample Conc.: 0.5 mg/ml

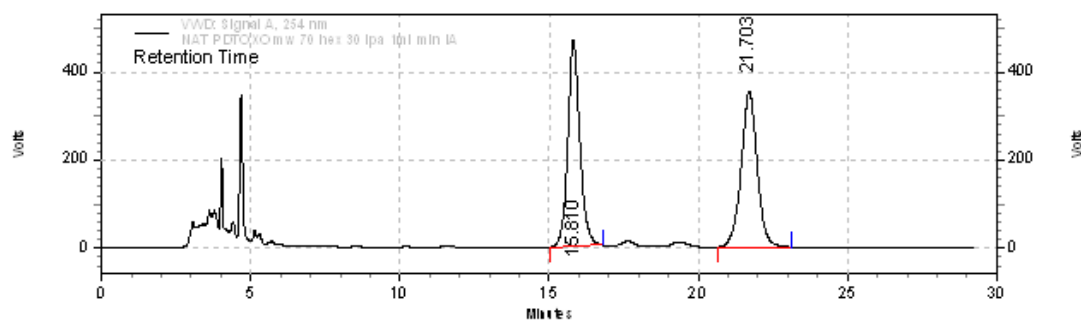


VWD: Signal A, 254 nm Results

Retention Time	Area	Area %
18.800	181757	2.37
24.627	7477339	97.63
Totals	7659096	100.00

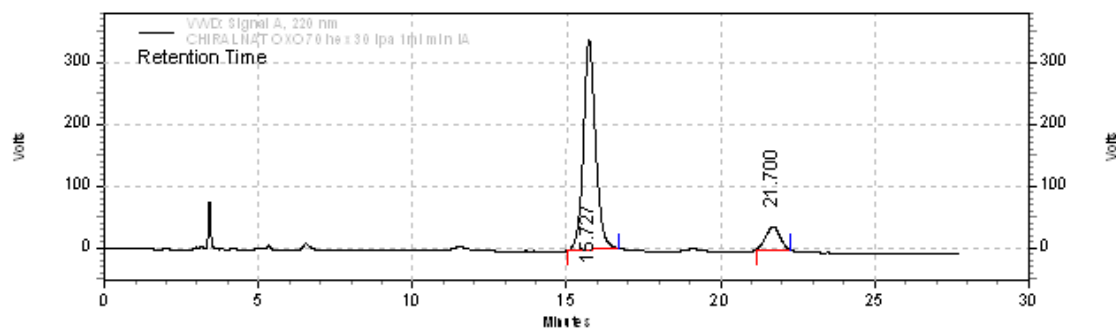
Column : CHIRALPAK IA
 Eluent System : 90 : 10 (HEXANE:IPA)
 Flow rate: 1.0 ml/min
 Injection vol.: 10ul
 Wavelength: 254 nm
 Sample Conc.: 0.5 mg/ml

2z



VWD: Signal A, 254 nm				
Results				
Retention Time	Area	Area %	Height	
15.810	219427772	49.73	7858596	
21.703	221832956	50.27	5937776	
Totals	441260728	100.00	13796372	

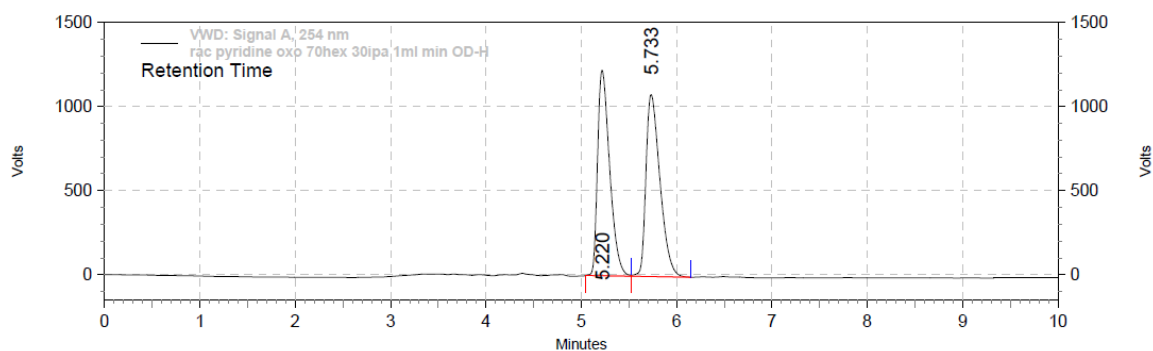
Column: CHIRALPAK IA
 Eluent System: 70:30 (HEXANE : IPA)
 Flow Rate: 1 ml / min
 Injection Volume: 10 ul
 Wavelength: 254 nm
 Sample Conc.: 1 mg/ml



VWD: Signal A, 220 nm				
Results				
Retention Time	Area	Area %	Height	
15.727	154228770	88.76	5686005	
21.700	19523387	11.24	621710	
Totals	173752157	100.00	6307715	

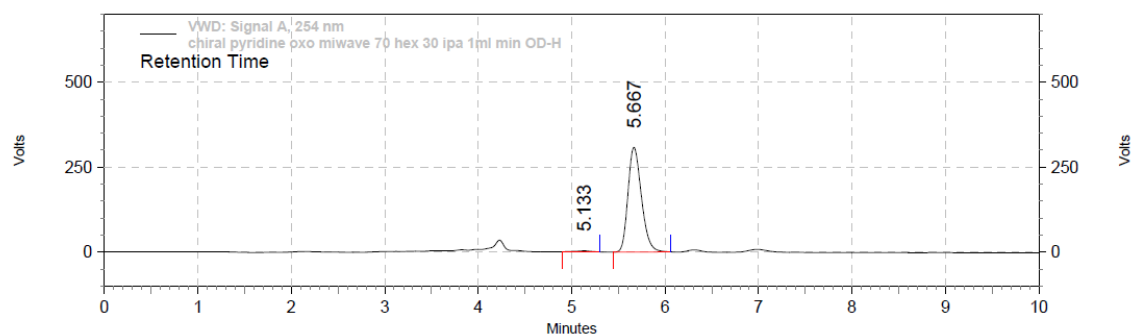
Column: CHIRALPAK IA
 Eluent System: 70:30 (HEXANE : IPA)
 Flow Rate: 1 ml / min
 Injection Volume: 10 ul
 Wavelength: 254 nm
 Sample Conc.: 1 mg/ml

4a

**VWD: Signal A, 254 nm Results**

Retention Time	Area	Area %
5.220	180838025	49.33
5.733	185740862	50.67
Totals	366578887	100.00

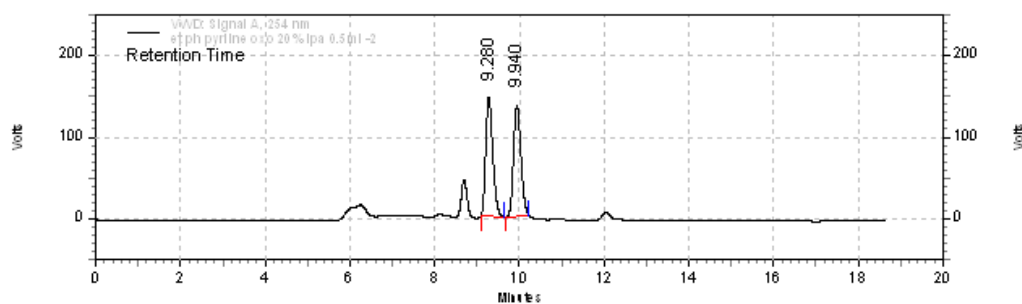
Column : CHIRALPAK OD-H
 Eluent System : 70 : 30 (HEXANE:IPA)
 Flow rate: 1.0 ml/min
 Injection vol.: 10ul
 Wavelength: 254 nm
 Sample Conc.: 1 mg/ml

**VWD: Signal A, 254 nm Results**

Retention Time	Area	Area %
5.133	547136	1.05
5.667	51690324	98.95
Totals	52237460	100.00

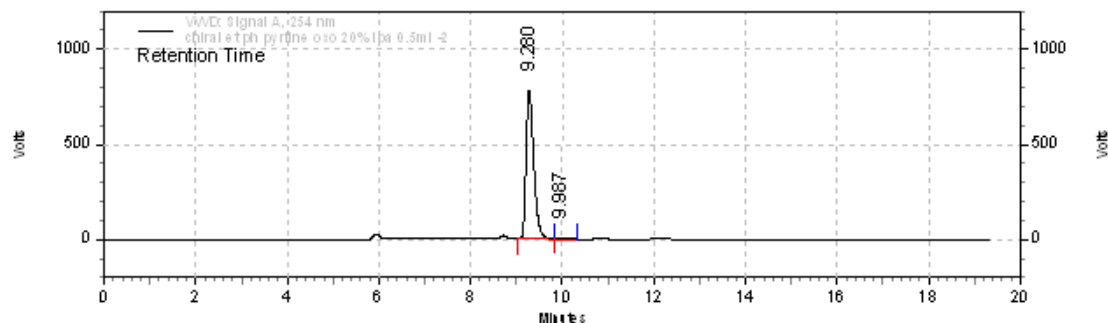
Column : CHIRALPAK OD-H
 Eluent System : 70 : 30 (HEXANE:IPA)
 Flow rate: 1 ml/min
 Injection vol.: 10 ul
 Wavelength: 254 nm
 Sample Conc.: 1 mg/ml

4b



VWD: Signal A, 254 nm				
Results				
Retention Time	Area	Area %	Height	
9.280	28172682	50.62	2430268	
9.940	27484064	49.38	2274699	
Totals	55656746	100.00	4704967	

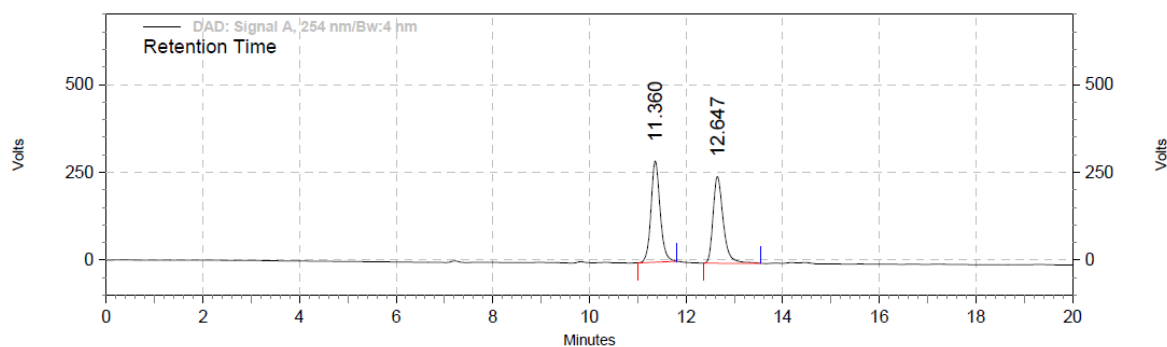
Column: CHIRALPAK IA
 Eluent System: 80: 20 (HEXANE : IPA)
 Flow Rate: 0.5 ml / min
 Injection Volume: 10 ul
 Wavelength: 254 nm
 Sample Conc.: 1mg/ml



VWD: Signal A, 254 nm				
Results				
Retention Time	Area	Area %	Height	
9.280	152236830	98.59	13068739	
9.987	2176765	1.41	152508	
Totals	154413595	100.00	13221247	

Column: CHIRALPAK IA
 Eluent System: 80: 20 (HEXANE : IPA)
 Flow Rate: 0.5ml / min
 Injection Volume: 10 ul
 Wavelength: 254 nm

4c

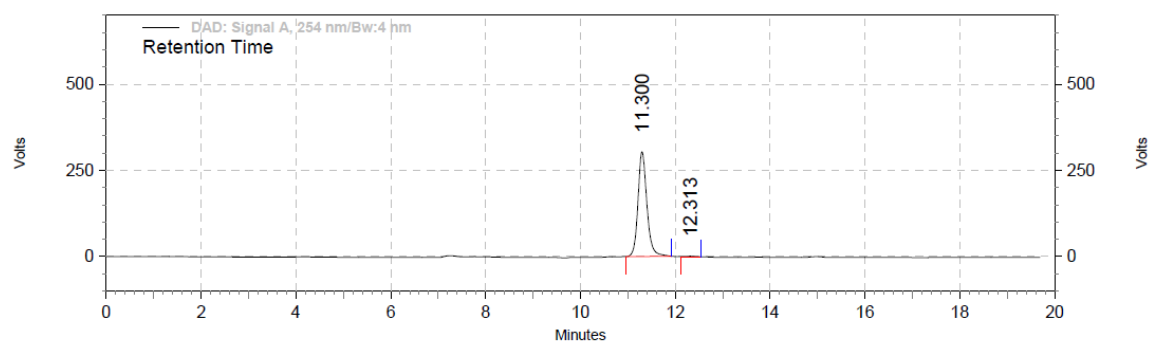


DAD: Signal A, 254 nm/Bw:4 nm

Results

Retention Time	Area	Area %
11.360	7950515	51.08
12.647	7613405	48.92
Totals		100.00
	15563920	

Column: CHIRALPAK OD-H
 Eluent System: 70 : 10 (HEXANE:IPA)
 Flow rate: 0.5 ml/min
 Injection vol.: 10ul
 Wavelength: 254 nm
 Sample Conc.: 1mg/ml



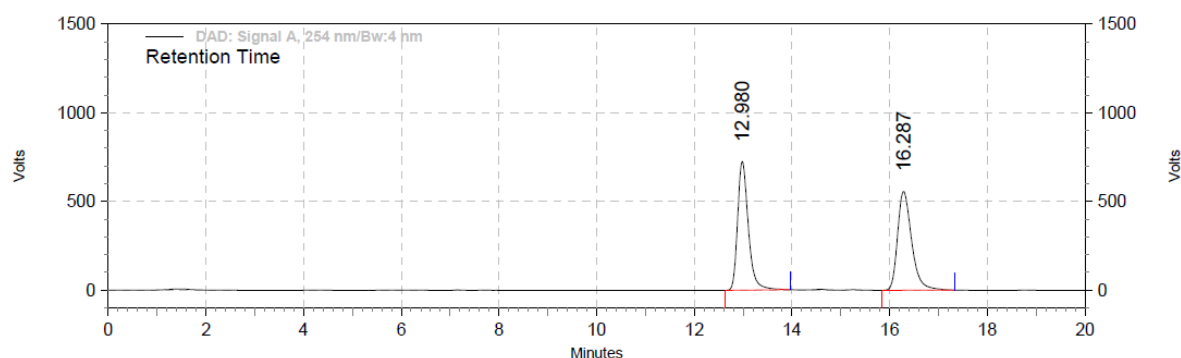
DAD: Signal A, 254 nm/Bw:4 nm

Results

Retention Time	Area	Area %
11.300	8359535	99.31
12.313	58113	0.69
Totals		100.00
	8417648	

Column: CHIRALPAK OD-H
 Eluent System: 70 : 10 (HEXANE:IPA)
 Flow rate: 0.5 ml/min
 Injection vol.: 10ul
 Wavelength: 254 nm
 Sample Conc.: 1mg/ml

4d

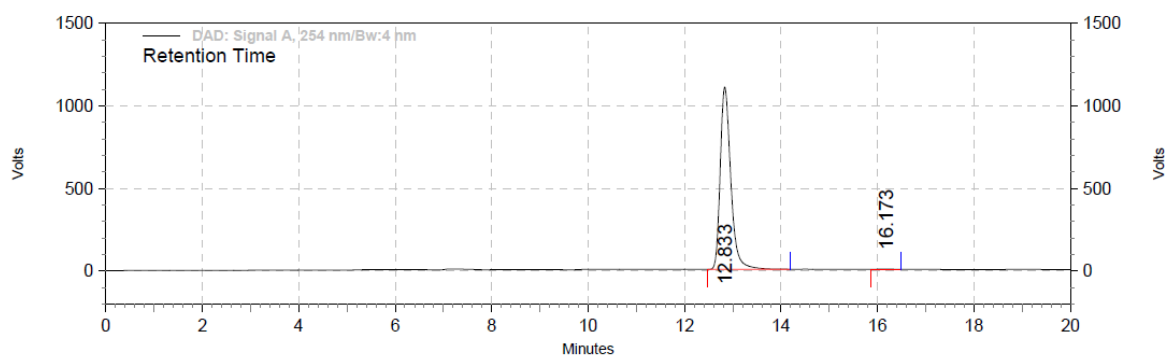


DAD: Signal A, 254 nm/Bw:4 nm

Results

Retention Time	Area	Area %
12.980	23198920	49.78
16.287	23399634	50.22
Totals		
	46598554	100.00

Column: CHIRALPAK OD-H
 Eluent System: 70 : 10 (HEXANE:IPA)
 Flow rate: 0.5 ml/min
 Injection vol.: 10ul
 Wavelength: 254 nm
 Sample Conc.: 1mg/ml



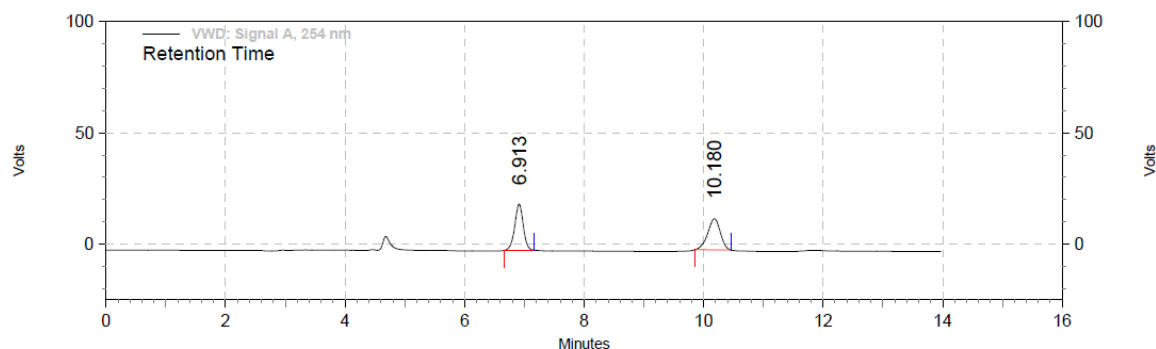
DAD: Signal A, 254 nm/Bw:4 nm

Results

Retention Time	Area	Area %
12.833	35237081	99.79
16.173	74146	0.21
Totals		
	35311227	100.00

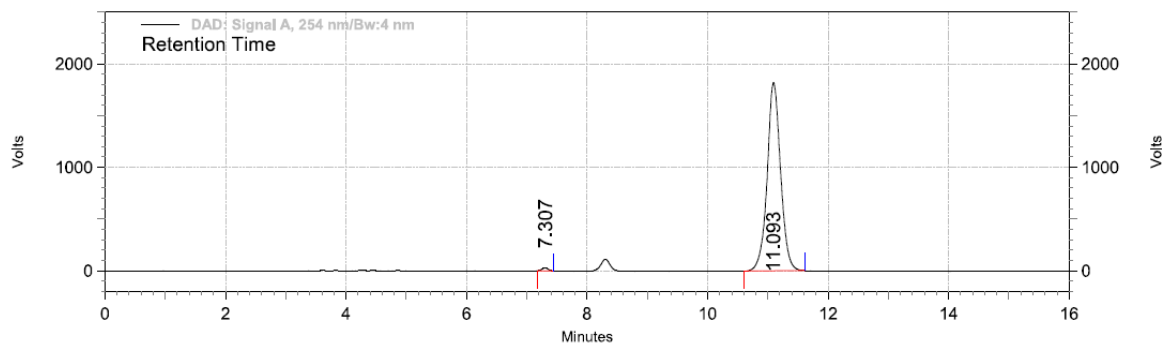
Column: CHIRALPAK OD-H
 Eluent System: 70 : 10 (HEXANE:IPA)
 Flow rate: 0.5 ml/min
 Injection vol.: 10ul
 Wavelength: 254 nm
 Sample Conc.: 1mg/ml

4e

**VWD: Signal A, 254 nm Results**

Retention Time	Area	Area %
6.913	3468500	50.16
10.180	3446770	49.84
Totals	6915270	100.00

Column: CHIRALPAK IA
 Eluent System: 70 : 10 (HEXANE:IPA)
 Flow rate: 1 ml/min
 Injection vol.: 10ul
 Wavelength: 254 nm
 Sample Conc.: 1mg/ml

**DAD: Signal A, 254 nm/Bw:4 nm Results**

Retention Time	Area	Area %
7.307	431101	0.72
11.093	59101123	99.28
Totals	59532224	100.00

Column: CHIRALPAK IA
 Eluent System: 70 : 10 (HEXANE:IPA)
 Flow rate: 1 ml/min
 Injection vol.: 10ul
 Wavelength: 254 nm
 Sample Conc.: 1mg/ml

Chapter 5

Summary

The limited success of transition metal-catalysis for imine (C=N) embedded pyridine C-H functionalization and the initial success of the nucleophilic organocatalysts in umpolung carbonyl (C=O) chemistry suggest to development of a general sustainable nucleophilic catalytic cycle for the functionalization of C=N, an unmet challenge for the synthesis of N-heterocyclic compounds. In this context, the present thesis, entitled “*Phosphite Catalysed Enantioselective Radical Reactions*” describes the development of an organocatalytic cycle to establish a catalyst that could facilitate both ionic and radical functionalization for complementary and broad functionalizations. As the nitrogen on N-heteroaromatic compounds is sufficiently nucleophilic and can form stable quaternary nitrogen salts having N–C bonds. We envision nitrogen to be a docking point to attach various groups on it; and selectively rearrange them catalytically asymmetrically to obtain chiral N-heterocyclic pharmaceuticals, drug intermediates, and chiral ligands (chapter 1). The N-alkyl salts are considered iminium embedded in the Heteroaromatics, and the development of a phosphite catalytic system accepts the challenge for iminium functionalization. In this context, chapter two (chapter 2) describes the synthesis of the TADDOL-based chiral phosphites library as a nucleophilic organocatalyst. These chiral phosphites were successfully utilized for the radical functionalizations of N-alkyl salt of the N-heteroatomic compound. First, we successfully achieved an organocatalyst bound “aza-acyl” radical and anion intermediate for controlled aerobic oxidation of iminium ions and The influence of the catalyst phosphite catalyst found for enantioselective aerobic oxidation (chapter-3). Secondly, the involvement of phosphite catalyst in aza-[1, 2]-Wittig rearrangement suggests an asymmetric N to C migration of the alkyl group via a bis-radical anion intermediate to achieve stereoselectivity. In light of this, chapter four (chapter 4) describes the synthesis of chiral and achiral primary amines and their corresponding N-alkyl salt of N-heteroaromatic compounds. The synthesis of N-alkyl salt was modified to achieve chirality without the racemization of chiral amines. The enantioselectivities of such salts were not reported, and we failed to find a suitable chiral HPLC method to separate enantiomers. So, We utilized our phosphite-catalyzed aerobic auto-oxidation for the synthesis of the corresponding oxo-product. The mild reaction condition avoids any racemizations during the oxidation and the determination of enantiomeric excess of corresponding pyridones. Overall, the work established an organocatalytic activation of C=N embedded in pyridine via “aza-acyl” radical and anionic pathways by using chiral phosphite catalyst and also I believe the establishment of phosphite-catalyzed radical and anion paths for pyridine functionalization has the potential for broader applications.

ABSTRACT

Name of the Student: Asish Bera

Registration No.: 10CC17J26012

Faculty of Study: Chemical Sciences

Year of Submission: 2023

AcSIR Academic Centre / CSIR Lab:
CSIR-National Chemical Laboratory

Name of the Supervisor:
Dr. Pradip Maity

Title of the thesis: Phosphite Catalysed Enantioselective Radical Reactions.

This thesis describes our efforts to functionalize N-heteroaromatic compounds via nucleophilic phosphite organocatalysis. Although transition metal-catalysed pyridine C-H functionalization found some recent successes and On the other hand, umpolung of C=O found great success with nucleophilic organocatalysts, the functionalization of C=N was not reported when we started. Hence, the development of a general sustainable catalytic system for the umpolung of imine embedded in pyridines remains an unmet challenge for the synthesis of N-heterocyclic compounds. We sought to establish a catalyst that could facilitate both ionic and radical functionalization for complementary and broad functionalizations. The nitrogen on N-heteroaromatic compounds is sufficiently nucleophilic and can form stable quaternary nitrogen salts having N-C bonds. We envision nitrogen to be a docking point to attach various groups on it; and selectively rearrange them catalytically asymmetrically to obtain chiral N-heterocyclic pharmaceuticals, drug intermediates, and chiral ligands. For this, the pyridinium salts can be considered as iminium embedded in the Heteroaromatics, and the development of a phosphite catalytic system for iminium functionalization obtains substituted pyridines. In this context, the present thesis, entitled "Phosphite Catalysed Enantioselective Radical Reactions" describes the strategy to address these challenges. This thesis is organized into five different chapters. **The first chapter**, Part I, briefly describes the importance of N-heteroaromatic molecules having chiral pyridine, and pyridone moieties in their core structures and their literature-reported synthesis. In Part II, we discussed the "aza-acyl" anion and the radical equivalent approach for umpolung imine reactivity in nucleophilic catalysis. The last part chronicles the literature reporting phosphite catalysis. **In the second chapter**, we discussed the synthesis of chiral phosphite catalysts for the enantioselective functionalization of imines embedded in pyridines to explore the catalyst structure-activity relationship. **The third chapter** describes an auto-photo redox path with the combination of a phosphite catalyst and household light for imine-embedded pyridine oxidation via catalyst-bound "aza-acyl" radical equivalent. The catalyst bound to the radical intermediate led to catalyst control regioselectivity and kinetic resolution for the first time in the aerobic oxidation of iminium. **In chapter four**, we discussed the synthesis of both racemic and chiral amines for the preparation of racemic and chiral N-alkyl pyridinium salts. The enantiopurity of those salts was determined via their mild aerobic auto-oxidation developed in the third chapter. The chiral N-alkyl pyridinium salts were utilized for the phosphite catalysed asymmetric N-to-C migration to synthesize chiral heterocycles from primary amines via both stereoretentive and enantioselective pathways. **The fifth chapter** deals with summarized work and the future directions related to this field.

List of Publications and Patents Emanating from the Thesis Work

1. Motaleb, A.; **Bera, A.**; Maity, P. “An organocatalyst bound α -aminoalkyl radical intermediate for controlled aerobic oxidation of iminium ions”, *Org. Biomol. Chem.*, **2018**, *16*, 5081.
2. Rani, S.; Dash, R. S.; **Bera, A.**; Alam, N. M.; Vanka, K.; Maity, P. “Phosphite mediated asymmetric N to C migration for the synthesis of chiral heterocycles from primary amines” *Chem. Sci.*, **2021**, *12*, 8996.
3. A catalyst bound α -radical and synthesis of oxo compound using the same. Motaleb, A.; **Bera, A.**; Maity, P.; *PCT/IN2018/050135*
4. Phosphite mediated asymmetric N to C migration for the synthesis of chiral heterocycles from primary amines. Rani, S.; **Bera, A.**; Maity, P. Patent filed.
5. Maity, S.; **Bera, A.**; Bhattacharjya, A.; Maity, P. “C–H functionalization of pyridines”, *Org. Biomol. Chem.*, **2023**, *21*, 5671.

List of participation in national and international conference & presentation

1. Participate in **ICOS 21** (21th International Conference on Organic Synthesis) on Dec, 2016, IIT Bombay, Mumbai, India.
2. Poster presentation on “An organocatalyst bound α -aminoalkyl radical intermediate for controlled aerobic oxidation of iminium ions” in **National Science Day**, NCL Research Foundation, held on Feb 2017 at CSIR-NCL, Pune, India.
3. Poster presentation on “Phosphite mediated asymmetric N to C migration for the synthesis of chiral heterocycles from primary amines” in **National Science Day**, NCL Research Foundation, held on Feb 2018 at CSIR-NCL, Pune, India
4. Participate in ‘**RSC IISER Desktop Seminar with OBC**’ on Nov, 2021 presented by RSC Publishing Webinars.
5. Participate in NCL-Research Foundation Annual Students’ Conference (**NCL-RF, 2021**) Organised by CSIR-NCL Pune NCL Research Foundation & CSIR-National Chemical Laboratory, Pune.
6. Participate in **Photo-Cat Symposium- 2021** (Sustainable Chemistry Lecture Series) Organised by Antwerp University (Prof. S. Das), Leibniz Institute of Catalysis (Prof. R. Ftancke) and Stockholm University (Prof. A. Slabon).
7. Participate in Organic Synthesis Webinar title as ‘**Celebrating Organic Synthesis in Latin America**’ on April, 2022 presented by Science of Synthesis and Organised by Evelyn Hosner.



Cite this: *Org. Biomol. Chem.*, 2018, **16**, 5081

Received 3rd May 2018,
Accepted 15th June 2018

DOI: 10.1039/c8ob01032c

rsc.li/obc

An organocatalyst bound α -aminoalkyl radical intermediate for controlled aerobic oxidation of iminium ions†

Abdul Motaleb,‡ Asish Bera‡ and Pradip Maity *

A catalyst bound α -aminoalkyl radical intermediate from iminium is developed to control its formation and reactivity with aerobic oxygen. The influence of the catalyst was demonstrated *via* the ease of radical intermediate formation and its subsequent reactivity, including the first catalyst-controlled enantioselective aerobic oxidation with a chiral phosphite catalyst.

A diverse pathway to α -aminoalkyl radicals is a major focus for mild amine functionalization.¹ Efficient catalyst systems for radical intermediates have been developed *via* C–H activation of both electron rich^{1,2} and electron poor amines,³ defunctionalization of amino acids⁴ and α -silylamines,⁵ and single electron reduction of imine or iminium.⁶ However, their subsequent reactivity remains largely uncontrolled. MacMillan and others developed an elegant dual catalysis approach with a transition metal (TM), which transforms the initially formed radical into a carbon–TM bond for subsequent cross-coupling reactions.⁷ The Yoon and Ooi groups respectively reported a dual Lewis acid and Brønsted acid catalyzed enantioselective coupling of α -aminoalkyl radicals.⁸

Our interest in finding catalyst control for radical reactions led us to explore a possible organocatalyst bound α -aminoalkyl radical formation and its reactivity. In this communication, we report facile self-photoredox and anionic auto-oxidation processes for the proposed radical (5) formation and its aerobic oxidation. We also demonstrate the first catalyst-controlled enantioselective aerobic oxidation of isoquinolinium with a chiral catalyst (Fig. 1).

We began our study to find a suitable catalyst capable of forming adduct (4) with stable and easy to handle methyl isoquinolinium triflate (1a). The adduct formation was studied in CDCl₃ and analyzed directly by ¹H-NMR, anticipating its reversible formation and instability. Neutral nucleophiles such

as PPh₃, DABCO, and DMAP did not form adducts, but DBU led to complex NMR, indicating a possible formation of the unstable cationic adduct. Among anionic nucleophiles, sulfite did not form an adduct, but phosphites (DMHP and DPHP) and thiophenol with K₂CO₃ led to corresponding adducts, characterized by ¹H-NMR.⁹

The next goal is to explore the feasibility of radical intermediate (5) formation from the adduct (4). We initially chose phosphites as a catalyst since the corresponding radical intermediate should gain synergistic stability *via* the captodative effect.¹⁰ As a result, its formation should be facile and catalyst detachment from the radical intermediate less likely.

Aerobic oxygen was chosen as the coupling partner since a catalyst release pathway similar to Nef oxidation is viable.¹¹ During screening under an air atmosphere, we were pleasantly surprised to observe the oxidation product (6a),^{6b,12} without any radical generating catalyst and specific light (Table 1, entry 1). The reaction under dark conditions did not work (entry 2), indicating that daylight or hood light mediated self-photoredox might be operative.¹³ Optimization of reaction temperature, base, and solvent led to good yield with 3 equivalent K₂CO₃ base in MTBE at 40 °C (entry 8). With quinolone salt (2a), K₂CO₃ did not result in any oxidation, but stronger KOH and KO^tBu led to efficient product formation in acetonitrile solvent (entries 11 and 12).

N-Alkyl salts of isoquinoline, quinoline, and other heteroaromatic compounds were subjected to the optimized reaction

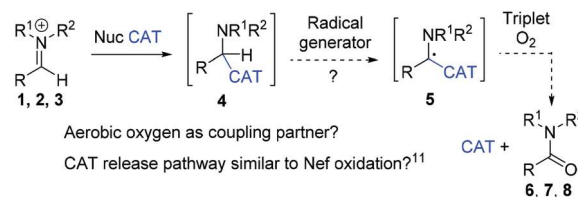


Fig. 1 An organocatalyst bound α -aminoalkyl radical for controlled catalysis: possible formation and reaction course.

Organic Chemistry Division, CSIR-National Chemical Laboratory, Pune-411008, India. E-mail: p.maity@ncl.res.in

†Electronic supplementary information (ESI) available. See DOI: 10.1039/c8ob01032c

‡Equal contribution.

Table 1 Optimization for phosphite catalyzed aerobic oxidation of isoquinoline and quinoline salts

Entry	Starting material	Base	Solvent	Temp (°C)	Time (h)	Yield ^a (%)
1	1a	K ₂ CO ₃	CHCl ₃	r.t.	72	62
2	1a	K ₂ CO ₃	CHCl ₃	r.t.	72	<5 ^b
3	1a	—	CHCl ₃	r.t.	72	<5
4	1a	K ₂ CO ₃	DCM	r.t.	72	60
5	1a	K ₂ CO ₃	MeCN	r.t.	72	56
6	1a	K ₂ CO ₃	THF	r.t.	72	68
7	1a	K ₂ CO ₃	MTBE	r.t.	72	73
8	1a	K ₂ CO ₃	MTBE	40	48	84
9	2a	K ₂ CO ₃	MTBE	0–r.t.	48	<5
10	2a	KOH	THF	0–r.t.	48	25
11	2a	KOH	MeCN	0–r.t.	24	88
12	2a	KO ^t Bu	MeCN	0–r.t.	16	82

^a Isolated yield. ^b Under dark conditions.

conditions to test the generality of our method (Table 2). A methyl, benzyl, and allyl substituent on isoquinoline nitrogen are all equally effective (6a–c). Bromide, phenyl, alkynyl, electron withdrawing nitro, and electron rich methyl are all well tolerated on different positions (6d–i) in moderate to good yields. 5,8-Dibromo substitution resulted in lower yield (6j, 47%). Other isoquinoline type heteroaromatics such as phenanthridinium and dinitrogen phthalazinium salts were also oxidized to the corresponding phenanthridinone (6k) and phthazone (6l) efficiently.

Different *N*-alkyl substitutions on quinoline are also compatible, but the KO^tBu base results in better yield for benzyl substitution (7c). Phenyl at the 3-position works well with the KO^tBu base, but electron rich NMe₂ substitution led to a very slow reaction. Raising the temperature to 50 °C led to moderate yield (7e, 56%). A major debrominated product was obtained along with the minor required product (7f) for 3-bromo substitution. Photoredox debrominations of aryl bromides are known, which might be operating here.¹⁴ Change of base and reaction temperature did not improve the result. 4-Methoxy substitution works well with KO^tBu (7g), but 4-methyl quinolinium gave poor yield (<10%) under standard reaction conditions. We suspect that possible deprotonation of the 4-methyl proton in starting salt under basic reaction conditions could be a problem. To circumvent this, 1.5 equivalent DMHP was added to convert all the salt to the intermediate before base mediated oxidation, which led to 92% yield (7h). Aryl, electron withdrawing as well as electron donating groups on other rings were well tolerated, including a free hydroxyl group at C-8 (7j). Surprisingly, the 8-Br substrate gave required 7n (56%), along with a minor 4-oxo product (23%). A sterically bulky 9a catalyst yielded 7n selectively with good yield (87%). A pyridinium and non-aromatic cyclic iminium salt did not oxidize under our optimized photoredox reaction conditions.

With the successful aerobic oxidation of *N*-alkyl salts of isoquinoline in hand, we eagerly explored the possibility of catalyst controlled oxidative kinetic resolution (Table 3). 1-Phenylethyl salt of isoquinoline (1m) with an α-stereogenic center to nitrogen was chosen,¹⁵ along with TADDOL-based phosphite (9a) as a chiral catalyst.¹⁶ Analysis of the product at ~50% conversion with 10 mol% tetramethyl catalyst 9a did not result in any enantioenrichment (entry 1), but the tetraphenyl catalyst (9b) showed promise (entry 2). Screening of other

Table 2 Substrate scope for household light mediated self-photoredox aerobic oxidation of N-heteroaromatic salts

6a, R = Me, 84%	6d, R = Br, 69%	6f, R = Br 82%	6h, 72%	6i, 81%	6j, 47%	6k, 83%	6l, 85%
6b, R = Bn, 79%	6e, R = Ph, 77%	6g, R = —C≡C—Ph, 73%					
6c, R = Allyl, 78%							
7a, R = Me, 88%	7d, R = Ph, 79% ^a	7g, R = OMe, 89% ^a	7i, 91%	7j, R = OH, 85%	7o, 0%	7n, R = Br, 87% ^d	8a, 0%
7b, R = Et, 78%	7e, R = NMe ₂ , 56% ^{a,b}	7h, R = Me, 92% ^c		7k, R = OMe, 76% ^a			
7c, R = Bn, 83% ^a	7f, R = Br, 10% + 65% ^{7a}			7l, R = OAllyl, 45% ^a			
				7m, R = NO ₂ , 75%			

Conditions: 0.3 mmol scale, for 1 to 6, 2 ml MTBE, K₂CO₃ base, 40 °C, 16 h; for 2 to 7, 2 ml MeCN, KOH or KO^tBu base, 16–48 h. ^a KO^tBu as a base. ^b 50 °C. ^c 1.5 equiv. dimethyl hydrogen phosphite. ^d catalyst 9a.

Table 3 Oxidative kinetic resolution studies with chiral phosphites

$\text{R} = \text{H}, \mathbf{1m}$
 $\text{R} = \text{Me}, \mathbf{1n}$

$\text{R} = \text{H}, \mathbf{6m}$
 $\text{R} = \text{Me}, \mathbf{6n}$

$\mathbf{9a}$, R = Me, $\mathbf{9b}$, R = Ph
 $\mathbf{9c}$, R = 2-Me-Ph
 $\mathbf{9d}$, R = 3,5-Me₂-Ph
 $\mathbf{9e}$, R = α -naphthyl

Entry	SM	Cat.	Base	Solv.	% conv. ^a / _{% yield} ^b	er (R : S)	S factor
1	1m	9a	K ₂ CO ₃	DCE	55/40	50 : 50	0
2	1m	9b	K ₂ CO ₃	DCE	50/30	40 : 60	ND
3	1m	—	K ₂ CO ₃	DCE	10/7	—	—
4	1m	9b	DABCO	DCE	45/30	36 : 64	ND
5	1m	—	DABCO	DCE	<5/—	—	—
6	1m	9c	DABCO	DCE	45/15	34 : 66	ND
7	1m	9d	DABCO	DCE	60/43	42 : 58	ND
8^c	1m	9e	DABCO	DCE	45/32	15 : 85	12.3
9	1m	9e	DABCO	DCM	50/35	15 : 85	ND
10	1m	9e	DABCO	MTBE	55/26	45 : 55	ND
11	1m	9e	DABCO	PhCF ₃	50/25	39 : 61	ND
12^d	1m	DMHP	DABCO	DCE	100/82	1 : 99	—
13^e	1m	DMHP	DABCO	DCE	100/76	66 : 33	ND
14^c	1n	9e	9e	DCE	40/29	18 : 82	9.6

Conditions: 0.2 mmol scale; 2 ml solvent. ^a Based on recovered SM. ^b Isolated yield. ^c % conversion was calculated (CHPLC = ee_{SM}/e_p + ee_{SM}). ^d With chiral **1m** and 20 mol% cat. ^e With recovered **1m** from entry 9 and 20 mol% cat.

tetra-aryl catalysts and reaction conditions (entries 3–11) led to 70% ee at 45% conversion (*s* factor = 12.3) with the α -naphthyl substituted catalyst (**9e**). The recovered enantioenriched SM was also oxidized under photoredox conditions with 20 mol% DMHP catalyst in good yield (entry 13). Optically pure **1m** was oxidized with complete retention of absolute configuration to establish the stability of the chiral center under reaction conditions (entry 12).¹⁷ 6-Methyl substituted salt (**1n**) also resulted in 64% ee at 40% conversion (*s* factor = 9.6, entry 14). These initial results suggest that a suitable catalyst for high kinetic resolution with isoquinoline salt is viable.

To explore the probable mechanistic path, (Fig. 2) we first checked the UV-vis absorption of isoquinoline salt (**1m**) and its adduct with catalyst **9a**. The salt itself does not absorb visible light, but the adduct (**4**) absorbs with fluorescence emission. The Stern–Volmer quenching study showed a concentration- and time-dependent decrease in fluorescence in the presence of **1m**. It indicates a light mediated excitation of the adduct, followed by (Scheme 1) single electron transfer to starting iminium salt (**1**).¹³ The α C–H acidity of the one-electron oxidized intermediate (**4**⁺) would increase greatly,¹⁸ and deprotonation *via* a base led to our proposed catalyst bound α -aminoalkyl radical intermediate (**5**). On the other hand, the reduced salt (**1**[•]) can transfer one electron to oxygen to regenerate the salt and superoxide anion (O₂^{•-}). The reaction of radical **5** with either O₂ or O₂^{•-} can lead to the product formation *via* alternative pathways.^{6b,12} Direct oxidation of the reduced α -aminoalkyl radical (**1**[•]) and oxygen or O₂^{•-} is either not operating or is a minor path at best since we achieved catalyst controlled kinetic resolution.

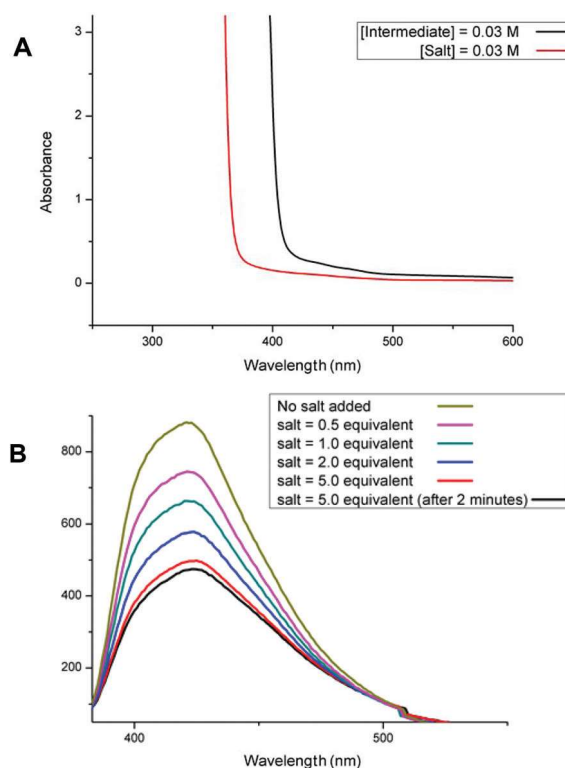
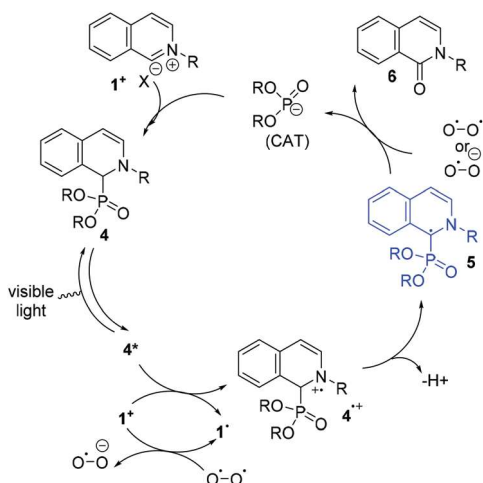


Fig. 2 (a) UV-vis absorption spectrum of **1m** and the corresponding adduct with **9a** at reaction concentration (0.1 M solution in DCM); and (b) emission spectra of the adduct (2×10^{-5} M in DCM, $\lambda_{\text{ex}} = 380$ nm) and its quenching with **1m**.

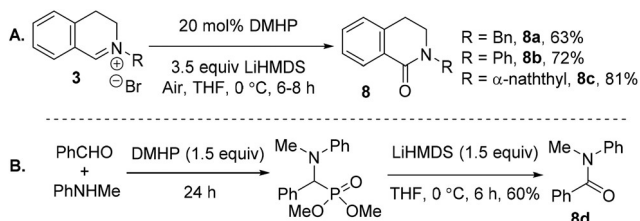


Scheme 1 A proposed catalytic cycle.

No reaction without the presence of iminium salt excludes a direct oxygen activation by the adduct. The oxidation also proceeds in the presence of singlet oxygen quencher DABCO, suggesting that photo-excitation of oxygen is unlikely.

Next, we aim to develop a general method which is not limited to heteroaromatic iminium salts (1, 2; Table 2). Unsuccessful oxidation of a non-aromatic iminium salt (8a) is expected since the salt, or the corresponding phosphite adduct do not absorb visible light. An external photoredox catalyst can oxidize the adduct to initiate the process,² but it has to be compatible with the nucleophilic phosphite catalyst. Instead, we checked a possible Nef type anionic auto-oxidation first to avoid external photoredox catalyst.^{11,12,19} Hydrolytically stable cyclic salts were synthesized (3a–c),²⁰ which were subjected to DMHP catalyzed reaction conditions with a strong LiHMDS base to deprotonate the α C–H bond. To our delight, the corresponding lactams formed in moderate to good yields (Scheme 2A). Acyclic iminium salts were difficult to handle and resulted in poor yield. To check the efficiency of aerobic auto-oxidation, we synthesized a dimethyl hydrogen phosphite adduct for acyclic systems (Scheme 2B),²¹ and which upon treatment with LiHMDS under an air atmosphere led to a good yield of the corresponding amide.

In conclusion, an organocatalyst bound α -aminoalkyl radical formation and its aerobic oxidation was achieved without any other radical generating catalyst. *N*-Alkyl salts of a



Scheme 2 (A) Aerobic auto-oxidation of non-aromatic cyclic iminium salt to lactam; and (B) stepwise oxidation to amide.

variety of heteroaromatic compounds were oxidized in the presence of household light. The catalyst bound α -radical was utilized successfully for an unprecedented oxidative kinetic resolution with racemic isoquinolinium salts. Cyclic and acyclic iminium salts were oxidized *via* an alternative strong base mediated aerobic auto-oxidation. Full mechanistic studies and catalyst controlled stereoselective oxidation are currently underway.

Conflicts of interest

There are no conflicts to declare.

Acknowledgements

The authors gratefully acknowledge the financial support from SERB (EMR/2015/000711) and the CSIR-NCL (MPL030926). A. M. and A. B. thank the UGC for the fellowship.

Notes and references

- (a) K. Nakajima, Y. Miyake and Y. Nishibayashi, *Acc. Chem. Res.*, 2016, **49**, 1946; (b) J. Hu, J. Wang, T. H. Nguyen and N. Zheng, *Beilstein J. Org. Chem.*, 2013, **9**, 1977; (c) J. W. Beatty and C. R. J. Stephenson, *Acc. Chem. Res.*, 2015, **48**, 1474.
- (a) G. Pandey, G. Kumaraswamy and U. T. Bhalerao, *Tetrahedron Lett.*, 1989, **30**, 6059; (b) P. Kohls, D. Jadhav, G. Pandey and O. Reiser, *Org. Lett.*, 2012, **14**, 672.
- M. H. Shaw, V. W. Shurtleff, J. A. Terrett, J. D. Cuthbertson and D. W. C. MacMillan, *Science*, 2016, **352**, 1304.
- Z. Zuo and D. W. C. MacMillan, *J. Am. Chem. Soc.*, 2014, **136**, 5257.
- U. C. Yoon and P. S. Mariano, *Acc. Chem. Res.*, 1992, **25**, 233.
- (a) A. L. F. Arriba, F. Urbitsch and D. J. Dixon, *Chem. Commun.*, 2016, **52**, 14434 and reference herein; (b) Y. Jin, L. Ou, H. Yang and H. Fu, *J. Am. Chem. Soc.*, 2017, **139**, 14237.
- C. K. Prier, D. A. Rankic and D. W. C. MacMillan, *Chem. Rev.*, 2013, **113**, 5322.
- (a) L. R. Espelt, I. S. McPherson, E. M. Wiensch and T. P. Yoon, *J. Am. Chem. Soc.*, 2015, **137**, 2452; (b) D. Uraguchi, N. Kinoshita, T. Kizu and T. Ooi, *J. Am. Chem. Soc.*, 2015, **137**, 13768.
- DMHP = dimethyl hydrogen phosphite; DPHP = diphenyl hydrogen phosphite.
- H. Viehe, Z. D. Anousek and R. Merenyi, *Acc. Chem. Res.*, 1985, **18**, 148.
- (a) S. Umemiya, K. Nishino, I. Sato and Y. Hayashi, *Chem. – Eur. J.*, 2014, **20**, 15753; (b) J. Li, M. J. Lear, Y. Kawamoto, S. Umemiya, A. R. Wong, E. Kwon, I. Sato and Y. Hayashi, *Angew. Chem., Int. Ed.*, 2015, **54**, 12986.

- 12 Base mediated aerobic oxidations with very limited substrate scope are known with a different mechanistic rationale: (a) S. Ruchirawat, S. Sunkul, Y. Thebtaranonth and Y. Thirasasna, *Tetrahedron Lett.*, 1977, **27**, 2335; (b) P. Paira, A. Hazra, K. B. Sahu, S. Banerjee, N. B. Mondal, N. P. Sahu, M. Weber and P. Luger, *Tetrahedron*, 2008, **64**, 4026 and references herein.
- 13 For organic dye catalysed photoredox, see: N. A. Romero and D. A. Nicewicz, *Chem. Rev.*, 2016, **116**, 10075. For direct photoexcitation of the catalyst added substrate (enamine), see: (a) M. Silvi, E. Arceo, I. D. Jurberg, C. Cassani and P. Melchiorre, *J. Am. Chem. Soc.*, 2015, **137**, 6120; (b) A. Bahamonde and P. Melchiorre, *J. Am. Chem. Soc.*, 2016, **138**, 8019.
- 14 J. J. Devery III, J. D. Nguyen, C. Dai and C. R. J. Stephenson, *ACS Catal.*, 2016, **6**, 5962.
- 15 (a) S. G. Bujedo, M. Alcarazo, C. Pichon, E. Alvarez, R. Fernandez and J. M. Lassaletta, *Chem. Commun.*, 2007, **11**, 1180; (b) L. Benmekhbi, F. Loufi, T. Roisnel and J. P. Hurvois, *J. Org. Chem.*, 2016, **81**, 6721.
- 16 (a) X. Linghu, R. J. Potnick and S. J. Johnson, *J. Am. Chem. Soc.*, 2004, **126**, 3070; (b) A. Falk, L. A. Goderz and G. H. Schmalz, *Angew. Chem., Int. Ed.*, 2013, **52**, 1576.
- 17 Chiral isoquinolone of type **6m** was utilized as a chiral auxiliary for the diastereoselective synthesis of chiral natural products: (a) D. T. Chu and L. A. Mitscher, *U.S. Patent*, 4777253, 1998; (b) J.-J. Youte, D. Barbier, A. Al-Mourabit, D. Gnecco and C. Marazano, *J. Org. Chem.*, 2004, **69**, 2737. Bioactive (iso)quinolones have a chiral centre α - to nitrogen: (c) J. Rujirawanich, S. Kim, A. J. Ma, J. R. Butler, Y. Wang, C. Wang, M. Rosen, B. Posner, D. Nijhawane and J. M. Ready, *J. Am. Chem. Soc.*, 2016, **138**, 10561.
- 18 A. Martin de, P. Nicholas and D. R. Arnold, *Can. J. Chem.*, 1982, **60**, 2165.
- 19 Although no clear understanding is presented for the Nef type reaction, we presume that the radical (**5**) stability in comparison to the corresponding carbanion is a key factor. The proposed captodative stability of radical **5** could facilitate this approach.
- 20 (a) V. K. Aggarwal, I. Bae, H.-Y. Lee and D. T. Williams, *Angew. Chem., Int. Ed.*, 2003, **42**, 3274; (b) J. F. Franz, W. B. Krausab and Kirsten Zeitler, *Chem. Commun.*, 2015, **51**, 8280.
- 21 G. Keglevich and E. Bálint, *Molecules*, 2012, **17**, 12821.

Chemical Science

rsc.li/chemical-science



ISSN 2041-6539

Cite this: *Chem. Sci.*, 2021, 12, 8996

All publication charges for this article have been paid for by the Royal Society of Chemistry

Phosphite mediated asymmetric N to C migration for the synthesis of chiral heterocycles from primary amines†

Soniya Rani,^{ab} Soumya Ranjan Dash,^{bc} Asish Bera,^{ab} Md Nirshad Alam,^{ab} Kumar Vanka^{bc} and Pradip Maity^{*,a}

A phosphite mediated stereoretentive C–H alkylation of *N*-alkylpyridinium salts derived from chiral primary amines was achieved. The reaction proceeds through the activation of the *N*-alkylpyridinium salt substrate with a nucleophilic phosphite catalyst, followed by a base mediated [1,2] *aza*-Wittig rearrangement and subsequent catalyst dissociation for an overall N to C-2 alkyl migration. The scope and degree of stereoretention were studied, and both experimental and theoretical investigations were performed to support an unprecedented *aza*-Wittig rearrangement–re-aromatization sequence. A catalytic enantioselective version starting with racemic starting material and chiral phosphite catalyst was also established following our understanding of the stereoretentive process. This method provides efficient access to tertiary and quaternary stereogenic centers in pyridine systems, which are prevalent in drugs, bioactive natural products, chiral ligands, and catalysts.

Received 2nd March 2021

Accepted 27th May 2021

DOI: 10.1039/d1sc01217g

rsc.li/chemical-science

Introduction

The recent focus on sustainable chemistry has encouraged chemists to develop the direct and diverse functionalization of abundant and renewable chemicals.¹ In this context, primary alkyl amines have emerged as an inexpensive, stable, and abundant source for the generation of reactive intermediates. In a recent application of its use as an alkylating agent,² the Watson group in 2017 developed an elegant nickel catalysed method to generate alkyl radicals from stable Katritzky pyridinium salts of primary amines for their coupling with arylboronic acids.³ In the same year, the Glorius group reported an iridium based photoredox catalysed protocol for alkyl radical generation and its coupling with heteroaromatic compounds.⁴ Since then, this approach has become a focus of intensive study *via* new and elegant deaminative protocols with diverse reaction partners under photoredox and dual catalysis or with redox-active coupling partners (Fig. 1a).^{5,6} These deaminative processes to alkyl radicals lead to racemic products from both achiral and enantioenriched amines. Additionally, the C–N bond cleavage processes generate triphenylpyridine as a part of the waste stream.

^aOrganic Chemistry Division, CSIR-National Chemical Laboratory, Pune-411008, India. E-mail: p.maity@ncl.res.in^bAcademy of Scientific and Innovative Research (AcSIR), Ghaziabad-201002, India^cPhysical and Material Chemistry Division, CSIR-National Chemical Laboratory, Pune 411008, India

† Electronic supplementary information (ESI) available. See DOI: 10.1039/d1sc01217g

We reasoned that the unique reactivity of pyridinium salts could be exploited to generate enantioenriched products that retain the pyridine ring system. The synthetic utility of our approach lies in the various simple methods for generating

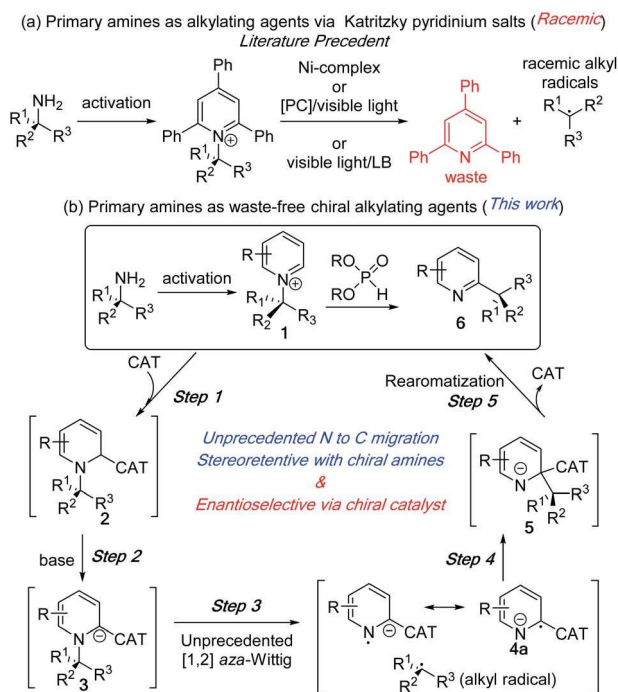


Fig. 1 Primary amines as alkylating reagent. (a) Literature precedents. (b) Proposed N to C dissociative alkyl migration.



alkylpyridinium salts other than Katritzky salts (**1**) from amines.⁷ Despite the prevalence of chiral alkyl pyridines (**6**) and the corresponding saturated heterocycles in numerous pharmaceutical drugs and biologically active compounds,⁸ their enantioselective synthesis *via* catalytic methods remains a challenge.^{9–12} In this communication, we report an intramolecular alkylation process with chirality transfer to synthesize chiral pyridines from enantioenriched pyridinium salts without the loss of pyridines as waste (Fig. 1b). We also report a catalytic enantioselective version of this unprecedented N to C alkyl migration from racemic *N*-alkylpyridinium salt.

The reaction development strategy is based on our experience in various selective molecular rearrangements and radical reactions.^{11e,13} We envisioned that a suitable catalyst adduct (**2**), upon deprotonation could form a reactive carbanion (**3**) and subsequent stable radical anion (**4a**) to reduce the activation energy to effect an [1,2] *aza*-Wittig rearrangement (**3** to **5**, Fig. 1b). To the best of our knowledge, the anionic [1,2] *aza*-rearrangement is not known, presumably due to its high activation energy requirement.¹⁴ The [1,2] alkyl migration (**5**) intermediate would undergo a facile catalyst dissociation to waste-free intramolecular C–H alkylation product (**6**). This subsequent rearomatization exothermic step after the *aza*-Wittig should favour the overall thermodynamics. Although the C–N bond breaks during the rearrangement, the stereochemical outcome of this intramolecular process would be intriguing.¹⁵ A

highly stereoretentive migration or a chiral catalyst controlled stereoselective recombination of radical pair could provide us with multiple pathways to control the stereoselectivity.

To explore the feasibility of alkyl migration, racemic (*S*)-1-phenylethylamine salt of isoquinoline (**1a**) was selected as the substrate. A variety of catalysts were screened based on their nucleophilicity, and subsequent anion and radical stabilization ability (Table 1).^{13,16} NHC catalysts, DBU, and thiophenol were unsuccessful with different bases (entries 1–4). But, to our delight, the addition of stoichiometric diethylphosphite anion at room temperature, followed by treatment with 2.5 equivalents of LiHMDS at 0 °C led to 58% of the migration product **6a** (Table 1, entry 5).¹⁷ With a suitable catalyst in hand, we performed the reaction with enantioenriched **1a** to explore the stereochemical outcome. The chiral pyridinium salt ((*S*)-**1a**) was synthesized from commercially available chiral (*S*)-1-phenylethylamine.^{7b} The migration in THF at 0 °C with (*S*)-**1a** led to an encouraging 86% enantiospecificity (es) with retention of the configuration (entry 6).^{9f} Next, we optimize our stereoretentive method, starting with screening the role of solvent. MTBE instead of THF led to 88% es, while toluene led to 91% es (entries 7 and 8). Cyclohexane as solvent did not improve the stereoretention (90% es, entry 9), but DCM as solvent led to 96% es (entry 10). The counter cation of the HMDS base also plays a significant role, with sodium being more effective than lithium (entry 11).¹⁸ Other phosphites were tested next, which

Table 1 Optimization study for phosphite mediated N to C migration^a

Entry	C (mol%)	T (°C)	Base-1	Base-2	Solvent	6a , yield (%)	6a , % ee (es)
1	C1 (50)	60	Cs ₂ CO ₃	Cs ₂ CO ₃	THF	ND	—
2	C2 (50)	60	Cs ₂ CO ₃	Cs ₂ CO ₃	THF	ND	—
3	C3 (50)	60	Cs ₂ CO ₃	Cs ₂ CO ₃	THF	ND	—
4	C4 (100)	25	K ₂ CO ₃	LiHMDS	THF	ND	—
5	C5 (100)	0	K ₂ CO ₃	LiHMDS	THF	58	—
6	C5 (100)	0	K ₂ CO ₃	LiHMDS	THF	63	69 (86)
7	C5 (100)	0	K ₂ CO ₃	LiHMDS	MTBE	61	73 (88)
8	C5 (100)	0	K ₂ CO ₃	LiHMDS	Toluene	64	80 (91)
9	C5 (100)	0	K ₂ CO ₃	LiHMDS	Cyclohexane	47	78 (90)
10	C5 (100)	0	K ₂ CO ₃	LiHMDS	DCM	67	90 (96)
11	C5 (100)	0	K ₂ CO ₃	NaHMDS	DCM	70	90 (96)
12	C6 (100)	0	K ₂ CO ₃	NaHMDS	DCM	66	88 (95)
13	C7 (100)	0	K ₂ CO ₃	NaHMDS	DCM	55	85 (93)
14	C8 (100)	0	K ₂ CO ₃	NaHMDS	DCM	26	59 (80)
15	C5 (100)	−20	K ₂ CO ₃	NaHMDS	DCM	72	91 (96)
16	C5 (100)	−40	K ₂ CO ₃	NaHMDS	DCM	69	91 (96)
17	C5 (100)	−60	K ₂ CO ₃	NaHMDS	DCM	70	91 (96)
18 ^b	C5 (20)	−60	K ₂ CO ₃	NaHMDS	DCM	67	91 (96)
19 ^c	C5 (100)	−20	K ₂ CO ₃	NaHMDS	DCM	72	92 (97)
20 ^d	C5 (100)	−20	K ₂ CO ₃	NaHMDS	DCM	70	92 (97)

^a Reactions were carried out with 0.3 mmol **1a**, 4 ml solvent, and 1 M THF solution of HMDS base. ^b With catalytic (20 mol%) dimethylphosphite diethylphosphite catalyst (see ESI for procedure). ^c With 2 M NaHMDS in THF. ^d 1 mmol scale.

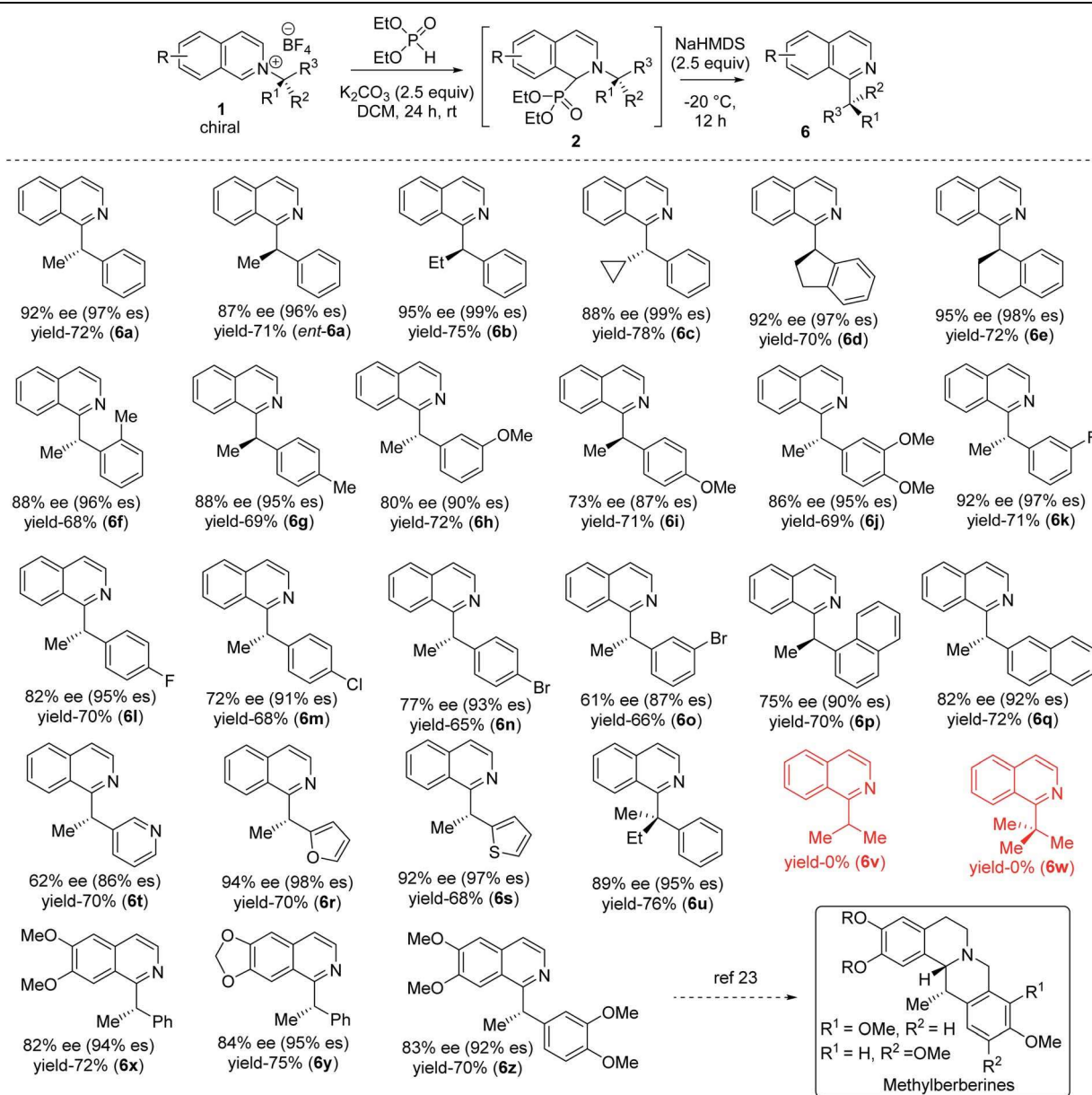


reveals better results with smaller alkoxy groups (entries 12–14). Finally, the optimal reaction temperature was determined to be $-20\text{ }^{\circ}\text{C}$ (entries 15–17). Although the racemic diethylphosphite can be used in catalytic amounts under strict deoxygenated conditions at lower temperature (entry 18), we utilized stoichiometric amounts of the phosphites to simplify the operation to obtain the product at a shorter reaction time, since diethylphosphite is non-toxic and cheaper than the reaction solvents. Since THF is detrimental to the stereoretention (entries 6 vs. 9), we performed the reaction with 2 M THF solution of NaHMDS instead of 1 M, which improved the es to 97% (entry 19), leading to substituted isoquinoline (*S*)-**6a** in 72% yield and 92% ee from

enantioenriched (98% ee) (*S*)-1-phenylethylamine salt (**1a**).¹⁹ The optimized reaction works well on 1 mmol scale, with no change in stereoretention and comparable yield (entry 20).

With optimized reaction conditions in hand, we tested the generality of our stereoretentive method for both chiral amines²⁰ and pyridine derivatives. First, we explored the scope and efficiencies of different chiral amines with isoquinoline (Table 2). Gratifyingly, the enantiomer of **1a** (*ent*-**1a**) led to an efficient synthesis of *ent*-**6a**. Alkyl groups other than methyl at the migrating carbon such as ethyl (**6b**), cyclopropyl (**6c**), fused cyclopentyl (**6d**), and cyclohexyl (**6e**) were all resulted in good yields with almost quantitative chirality transfer. These

Table 2 Isoquinoline substrate scope for stereoretentive alkyl migration^a



^a Conditions: **1** (0.3 mmol) was dissolved in 3 ml DCM and added to diethylphosphite (0.3 mmol) and K_2CO_3 (0.75 mmol) in 1 ml DCM at $25\text{ }^{\circ}\text{C}$ and stirred for 24 h. Then the reaction mixture was cooled to $-20\text{ }^{\circ}\text{C}$ and NaHMDS (2.5 equiv., 2 M in THF) was added and stirred for 12 h.



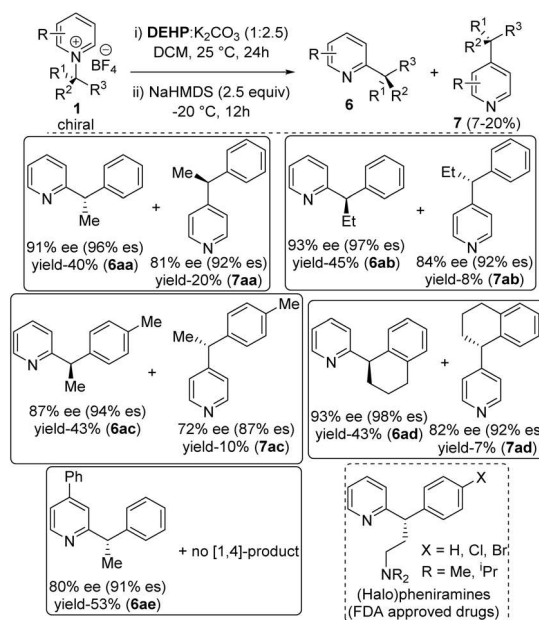
examples showed that the alkyl group at migrating carbon has very little influence on the reaction outcome. The α -cyclopropyl group at migrating carbon is significant with no ring-opening product was observed.²¹ Next, we varied the aryl groups at the migrating carbon. Methyl at *ortho*- (**6f**) and *para*-position (**6g**) of the phenyl ring led to similar results, indicating a minimal steric effect on yield and enantiospecificity. Methoxy substitution at both C-3 (**6h**) and C-4 (**6i**) led to lower stereoretention (90 and 87%), whereas 3,4-dimethoxy substitution (**6j**) led to 95% es. The yields are comparable to that of parent substrate for all methoxyaryl substrates. Halo substituents at C-3 and C-4 positions were well tolerated. Fluoro substituent at C-3 led to 97% es (**6k**), while C-4 fluoro resulted in 95% es (**6l**). Both chloro and bromo substitution resulted in slightly lower chirality transfer (**6m,n,o**). α -Naphthyl instead of phenyl formed product with 90% es (**6p**), and β -naphthyl yielded the corresponding products with 92% es (**6q**). Heteroaryl groups at the migrating center such as electron-rich 2-furan (**6r**) and 2-thiophene (**6s**) both migrated with excellent enantiospecificity (98 & 97% es), while electron-deficient 3-pyridine (**6t**) led to a moderate 86% es. Finally, we synthesized an isoquinolinium salt of quaternary chiral amine (**1u**). Under optimized reaction conditions, it rearranged successfully to the corresponding all carbon quaternary alkyl chiral products with better yield (76%) and very good 95% es (**6u**). Isoquinolinium salts of isopropyl (**6v**) and *tert*-butyl (**6w**) amine did not lead to the product which indicates (hetero) aryl stabilization on migrating alkyl radical is necessary.

A diverse range of substituted pyridines was subjected to the reaction condition to find the generality of our method with azarenes. Electron rich bis-alkoxy groups on isoquinolines were tested first since the corresponding products could be easily converted to the numerous natural products of biological importance.²² 4,5-Bis-alkoxyisoquinoline derivatives of (*S*)-1-phenylethylamine (**6x**, **6y**) resulted in 94 and 95% es with 72 and 75% yields respectively. With 4,5-dimethoxyisoquinoline and 3,4-dimethoxyphenylethylamine, the product **6z** is obtained in 70% yield with 92% es. **6z** and its reduced forms were utilized for the synthesis of various methylberberine alkaloids.^{22a,c}

Finally, the alkyl migration protocol was tested on unsubstituted pyridine substrates, which are common pharmacophores in many approved pharmaceutical drugs.^{7,23} Under standard reaction condition, the C-2 alkyl migrated products formed in moderate yields but with excellent enantiospecificity (Table 3). The stereoretention trend in alkyl migration runs parallel to that in isoquinoline substrates. For 4-unsubstituted pyridines, a minor [1,4] migrated side products **7** also formed with 4–7% lower enantiospecificities. Competitive [1,4] Wittig rearrangements from common radical pair intermediates are known in literature, with a single report by Maleczka Jr group describes stereoretention pattern similar to our findings.²⁴ With pyridinium substrates, either the same C-2 added catalyst or a C-4 added catalyst intermediate can undergo the [1,4] migration.

Quantum chemical calculations (DFT, details in ESI†) were performed to gain insight into the crucial C–N bond breaking (step 3, Fig. 1b) and C–C bond forming (step 4, Fig. 1b) steps of our proposed phosphite catalysed *aza*-Wittig, and subsequent

Table 3 Pyridine substrate scope for stereoretentive alkyl migration



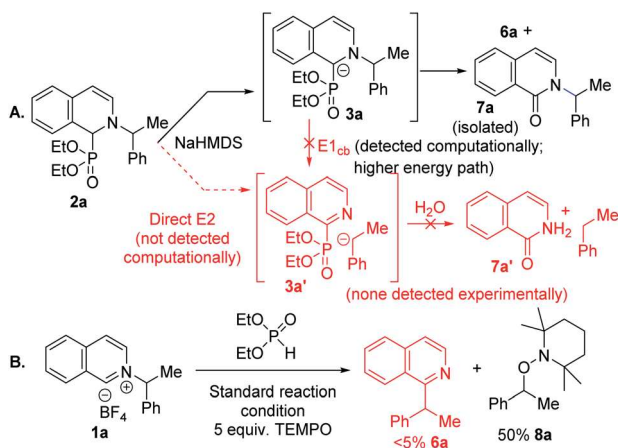
rearromatization protocol.²⁵ First, the C–N bond dissociation energy (BDE) was calculated at the PBE/def-TZVP level of theory. The ΔG for the homolytic C–N bond cleavage was calculated to be exothermic by 0.8 kcal mol⁻¹, supporting the stability of radical **4a** via the catalyst mediated captodative effect and extended conjugation.^{13,16} An alternative heterolytic bond cleavage path with 2.4 kcal mol⁻¹ higher energy via an E2 could also be identified during the calculations. To avoid any bias from the chosen DFT method, and since the difference between homolytic and heterolytic BDE was close, we used different levels of theory to compare the two possibilities.²⁶ In all cases, the homolytic dissociation was found to be favourable (Table 4). We also calculated homolytic and heterolytic dissociation for substrate **1u** with a quaternary migrating group, in which the homolytic cleavage is favoured by 5.7 kcal mol⁻¹ (at the PBE/def-TZVP level of theory).

Experimental mechanistic studies were carried out to support or discredit the alternative paths identified in the computational studies (Scheme 1). We noticed that in the presence of traces of oxygen, the corresponding pyridone side product formed with the C–N bond intact under the N to C

Table 4 Computed homolytic vs. heterolytic C–N bond dissociation energy (ΔG) in kcal mol⁻¹

Substrate	DFT methods	Homo	Hetero	Homo–hetero
1a	PBE/def-TZVP	-0.8	+1.6	-2.4
	B3LYP/def2-TZVPP	-5.0	-1.4	-3.6
	B3LYP/6-31+G**	-16.9	-10.5	-6.4
	M06-2X/6-31+G**	+1.8	+7.2	-5.4
	M06-2X/6-311+G**	+4.1	+8.0	-3.9
1u	PBE/def-TZVP	-6.9	-1.2	-5.7
	B3LYP/def2-TZVPP	-11.1	-3.9	-7.2

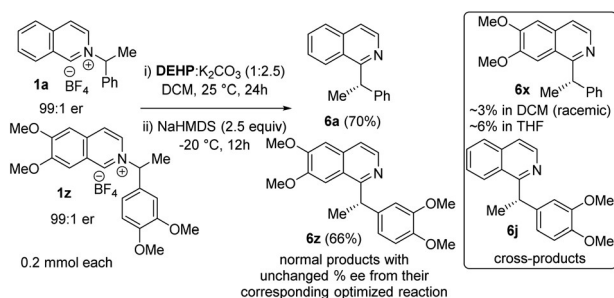




Scheme 1 Mechanistic studies. (A) Homolytic vs. heterolytic paths via intermediate trapping. (B) Radical trap with TEMPO.

migration protocol (Scheme 1a). This result is suggestive of a common carbanionic intermediate **3a** for its competing Nef oxidation *versus* alkyl migration.^{21a} An E1_{cb} pathway would lead to C–N bond cleaved intermediate **3a'**, or its hydrolyzed product **7a'**, which were not detected. A direct base mediated E2 pathway to **3a'** could also be a possibility, but was not detected computationally. To further distinguish between heterolytic E1_{cb}/E2 and homolytic radical pair paths, a radical trapping experiment was conducted with TEMPO. The addition of five equivalents of TEMPO led to a complete shut down of the alkyl migration with 50% TEMPO trapped alkyl product formation (Scheme 1b). No alkyl migration product under excess radical trap reagent along with trapped alkyl product supports a radical pair mechanism.²⁷

Next, we examined the source of high stereoretention for this dissociative alkyl migration (Scheme 2). For [1,2] *oxa*-Wittig rearrangements, the commonly accepted explanation for stereoretention at the migrating centre is that the radical pair formation and recombination occurs within the solvent cage.¹⁵ This solvent-caged radical pair recombination is faster than racemization through solvent-cage escape and recapture. On the other hand, out-of-plane rotation within the solvent cage can also lead to racemization.²⁸ To gain insight, we conducted a crossover experiment with **1a** and **1z** in DCM and THF. The cross-products formations in DCM are ~2–3%, which supports predominantly solvent-caged radical recombination. In THF,

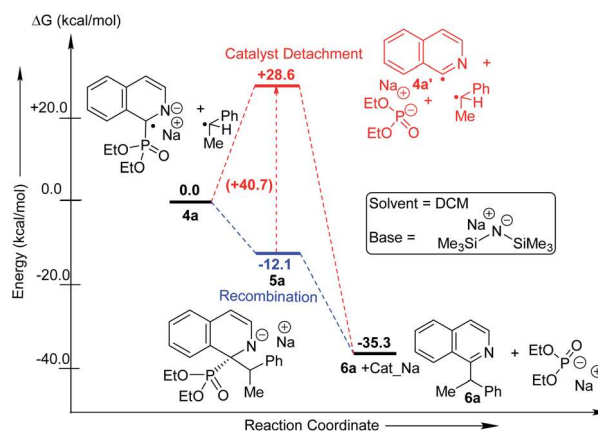


Scheme 2 Crossover experiment & stereoretention.

the cross-products are ~4–6%, which is consistent with less stereoretention in that solvent. The chiral HPLC analysis of cross-products showed that those were rendered almost racemic, supporting solvent cage escape as one possible pathway for racemization. The normal products, which now have less 'solvent-cage escape and recapture' possibility in the crossover experiment, did not result in significantly higher stereoretention. Therefore an out-of-plane rotation within the solvent cage cannot be ruled out.

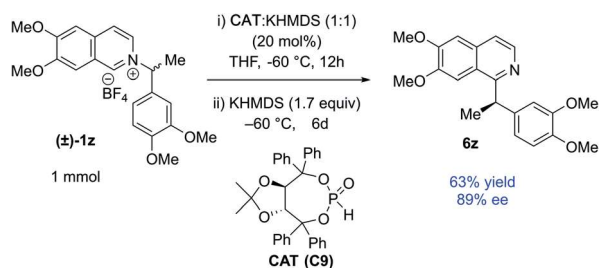
We performed computational studies for radical pair recombination in order to determine the exact juncture of catalyst detachment (step 4, Fig. 1b; Scheme 3). The catalyst detachment from radical **4a** to **4a'**, prior to its recombination with alkyl radical, signifies no catalyst control on the subsequent C–C bond formation. Although we predict radical **4a** formation from anionic intermediate **3a** would be stabilized by captodative effect and extended delocalization, the formation of **4a'** might be feasible owing to the rearomatization of the heterocycle. The calculations reveal that this is highly unlikely, since the ΔG for the corresponding imine radical (**4a'**) formation is endothermic by 28.6 kcal mol⁻¹. The loss of conjugation and captodative stability seems to outweigh the rearomatization in **4a'**. The recombination of the catalyst attached **4a** at C-2 with the alkyl radical could, therefore, be influenced by the catalyst. The subsequent catalyst release from **5a** leading to the rearomatized final product (**6a**) is found to be highly exothermic (23.1 kcal mol⁻¹), which makes the overall transformation favourable.

The catalyst involvement in the C–C bond formation and the possibility of racemization *via* dissociative path led us to speculate if a chiral phosphite catalyst could induce enantioselective transformation starting with racemic pyridinium salts. During reaction optimization, we observed variable degrees of racemization with different catalysts (Table 1). The significant drop in stereoretention with a bulky *tert*-butyl phosphite (80 vs. 96% es, Table 1, entries 12 & 14) could be due to its slower recombination, with racemization paths in play. Therefore, a bigger chiral phosphite catalyst could also slow the recombination for the racemic alkyl radical to allow its rotation to catalyst controlled



Scheme 3 Computed C–C bond formation and subsequent rearomatization energy profile.





Scheme 4 Chiral phosphite catalyzed enantioselective N to C migration.

enantioselection. Since the reaction medium influences the stereoretention (Table 1, entries 7–10), solvents with high racemization might also provide time for the alkyl radical to rotate for the enantioselection. We chose racemic **1z** as a test substrate, since it can be converted to natural products, and its stereoretentive migration generated the product in a modest 83% ee (92% es, Table 2). To our delight, 20 mol% TADDOL-phosphite catalyst (**C9**) generates chiral **6z** with 89% ee in THF (Scheme 4, see ESI† for details). This result represents a proof-of-concept for the chiral phosphite catalyzed enantioselective N to C migration of racemic pyridinium salts.

In conclusion, a phosphite mediated stereoretentive C–H alkylation of *N*-alkylpyridinium salt was developed. Chiral alkylpyridines were obtained from the corresponding chiral amines with a broad range of functional groups. An all-carbon quaternary alkyl group also migrated efficiently. The mechanistic experiments suggest a phosphite catalyzed bis-radical [1,2] aza-Wittig followed by rearomatization *via* catalyst release for product formation. Exploring the source of stereoretention and a variable degree of racemization led us to establish a chiral phosphite catalyzed enantioselective version with racemic alkylpyridinium salt. The dissociative reaction path presents us with the possibility of [1,*n*] alkyl migrations other than the present [1,2] in and around pyridines, which we are exploring currently. Synthesis of natural and bioactive compounds from the chiral alkylpyridines is also under development.

Data availability

The complete data supporting this article have been uploaded as part of the supplementary material.

Author contributions

S. R. and A. B. performed the experiments and developed the method. S. R. D. performed the DFT calculation in consultation with K. V. and P. M.; Md N. A. finalized the data. P. M. directed the project and wrote the manuscript with the feedback from other authors.

Conflicts of interest

There are no conflicts of interest to declare.

Acknowledgements

This research was supported by the SERB (EMR/2015/000711 and CRG/2019/001065). S. R. and A. B. thanks CSIR, and Md. N. A. thanks UGC for a fellowship. The support from central analytical facility, NCL is greatly acknowledged. We thank Dr S. H. Chikkali (NCL, Pune) for experimental help and Prof. U. K. Tambar (UTSW Medical Center, Dallas) for useful discussions and help in writing the manuscript. The support and the resources provided by 'PARAM Brahma Facility' under the National Supercomputing Mission, Government of India at the Indian Institute of Science Education and Research (IISER) Pune are gratefully acknowledged.

Notes and references

- (a) V. Froidevaux, C. Negrell, S. Caillol, J.-P. Pascault and B. Boutevin, *Chem. Rev.*, 2016, **116**, 14181; (b) N. Burn, P. Hesemann and D. Esposito, *Chem. Sci.*, 2017, **8**, 4724; (c) M. Pelckmans, T. Renders, S. V. Vyver and B. F. Sels, *Green Chem.*, 2017, **19**, 5303.
- (a) S. Crespi and M. Fagnoni, *Chem. Rev.*, 2020, **120**, 9790; (b) S. L. Rössler, B. J. Jelier, E. Magnier, G. Fagousset, E. M. Carreira and A. Togni, *Angew. Chem., Int. Ed.*, 2020, **59**, 9264; (c) D. Kong, P. J. Moon and R. J. Lundgren, *Nat. Catal.*, 2019, **2**, 473; (d) F.-S. He, S. Ye and J. Wu, *ACS Catal.*, 2019, **9**, 8943; (e) J. T. M. Correia, V. A. Fernandes, B. T. Matsuo, J. A. Delgado, W. C. de Souza and M. W. Paixao, *Chem. Commun.*, 2020, **56**, 503; (f) K. Ouyang, W. Hao, W.-X. Zhang and Z. Xi, *Chem. Rev.*, 2015, **115**, 12045.
- C. H. Basch, J. Liao, J. Xu, J. J. Piane and M. P. Watson, *J. Am. Chem. Soc.*, 2017, **139**, 5313.
- F. J. R. Klauck, M. J. James and F. Glorius, *Angew. Chem., Int. Ed.*, 2017, **56**, 12336.
- (a) J. Hu, G. Wang, S. Li and Z. Shi, *Angew. Chem., Int. Ed.*, 2018, **57**, 15227; (b) M. Ociepa, J. Turkowska and D. Gryko, *ACS Catal.*, 2018, **8**, 11362; (c) J. Liao, W. Guan, B. P. Boscoe, J. W. Tucker, J. W. Tomlin, M. R. Garnsey and M. P. Watson, *Org. Lett.*, 2018, **20**, 3030; (d) M.-M. Zhang and F. Liu, *Org. Chem. Front.*, 2018, **5**, 3443; (e) F. J. R. Klauck, H. Yoon, M. J. James, M. Lautens and F. Glorius, *ACS Catal.*, 2019, **9**, 236; (f) X. Jiang, M. M. Zhang, W. Xiong, L. Q. Lu and W. J. Xiao, *Angew. Chem., Int. Ed.*, 2019, **58**, 2402; (g) S. Plunkett, C. H. Basch, S. O. Santana and M. P. Watson, *J. Am. Chem. Soc.*, 2019, **141**, 2257; (h) H. Yue, C. Zhu, L. Shen, Q. Geng, K. J. Hock, T. Yuan, L. Cavallo and M. Rueping, *Chem. Sci.*, 2019, **10**, 4430; (i) S.-Z. Sun, C. Romano and R. Martin, *J. Am. Chem. Soc.*, 2019, **141**, 16197; (j) J. Yi, S. O. Badir, L. M. Kammer, M. Ribagorda and G. A. Molander, *Org. Lett.*, 2019, **21**, 3346; (k) S. Ni, C.-X. Li, Y. Mao, J. Han, Y. Wang, H. Yan and Y. Pan, *Sci. Adv.*, 2019, **5**, eaaw9516; (l) M. E. Hoerner, K. M. Baker, C. H. Basch, E. M. Bampo and M. P. Watson, *Org. Lett.*, 2019, **21**, 7356; (m) Z.-K. Yang, N.-X. Xu, C. Wang and M. Uchiyama, *Chem.–Eur. J.*, 2019, **25**, 5433; (n) Z.-F. Zhu, J.-L. Tu and F. Liu, *Chem. Commun.*, 2019, **55**,



- 11478; (o) F. T. Pulikottil, R. Pilli, R. V. Suku and R. Rasappan, *Org. Lett.*, 2020, **22**, 2902; (p) C.-G. Yu and Y. Matsuo, *Org. Lett.*, 2020, **22**, 950; (q) J. Wang, M. E. Hoerner, M. P. Watson and D. J. Weix, *Angew. Chem., Int. Ed.*, 2020, **59**, 13484.
- 6 (a) J. Wu, L. He and V. K. Aggarwal, *J. Am. Chem. Soc.*, 2018, **140**, 10700; (b) F. Sandfort, F. Strieth-Kalthoff, F. J. R. Klauck, M. J. James and F. Glorius, *Chem.–Eur. J.*, 2018, **24**, 17210; (c) J. Wu, P. S. Grant, X. Li, A. Noble and V. K. Aggarwal, *Angew. Chem., Int. Ed.*, 2019, **58**, 5697; (d) M. Yang, T. Cao, T. Xu and S. Liao, *Org. Lett.*, 2019, **21**, 8673; (e) J. Hu, B. Cheng, X. Yang and T.-P. Loh, *Adv. Synth. Catal.*, 2019, **361**, 4902; (f) M. J. James, F. Strieth-Kalthoff, F. Sandfort, F. J. R. Klauck, F. Wagener and F. Glorius, *Chem.–Eur. J.*, 2019, **25**, 8240; (g) Q. Xia, Y. Li, X. Wang, P. Dai, H. Deng and W.-H. Zhang, *Org. Lett.*, 2020, **22**, 7290.
- 7 (a) C. D. Vanderwal, *J. Org. Chem.*, 2011, **76**, 9555; (b) R. S. Paton, S. E. Steinhardt, C. D. Vanderwal and K. N. Houk, *J. Am. Chem. Soc.*, 2011, **133**, 3895; (c) T. M. Nguyen, M. Salvatore, R. S. del, J.-C. Wypych and C. Marazano, *J. Org. Chem.*, 2007, **72**, 5916; (d) Y. Genisson, C. Marazano, M. Mehmandoust, D. Gnecco and B. C. Das, *Synlett*, 1992, **5**, 431.
- 8 (a) E. Vitaku, D. T. Smith and J. T. Njardarson, *J. Med. Chem.*, 2014, **57**, 10257; (b) H. Yang, E. Wang, P. Yang, H. Lv and X. Zhang, *Org. Lett.*, 2017, **19**, 5062; (c) K.-S. Zhou, P. Yi, T. Yang, F.-M. Yanf, K.-H. Lee, B.-Y. Zhao, Y.-H. Wang and C.-J. Tan, *Org. Lett.*, 2019, **21**, 5051; (d) J. Li, Y. Liu, X. Song, T. Wu, J. Meng, Y. Zheng, Q. Qin, D. Zhao and M. Cheng, *Org. Lett.*, 2019, **21**, 7149; (e) S. Varga, P. Angyal, G. Martin, O. Egyed, T. Holczbauer and T. Soos, *Angew. Chem., Int. Ed.*, 2020, **59**, 13547; (f) K. M. Lambert, J. B. Cox, L. Liu, A. C. Jackson, S. Yruegas, K. B. Wiberg and J. L. Wood, *Angew. Chem., Int. Ed.*, 2020, **59**, 9757.
- 9 For stereospecific cross-coupling of C–X with optically pure organometallic reagents: (a) L. Li, C.-Y. Wang, R. Huang and M. R. Biscoe, *Nat. Chem.*, 2013, **5**, 607; (b) T. Ohmura, T. Awano and M. Sugimoto, *J. Am. Chem. Soc.*, 2010, **132**, 13191; (c) G. A. Molander and S. R. Wisniewski, *J. Am. Chem. Soc.*, 2012, **134**, 16856; (d) Q. Zhou, H. D. Srinivas, S. Dasgupta and M. P. Watson, *J. Am. Chem. Soc.*, 2013, **135**, 3307; (e) G. A. Molander, S. R. Wisniewski and M. Hosseini-Sarvari, *Adv. Synth. Catal.*, 2013, **355**, 3037; (f) L. Li, S. Zhao, A. Joshi-Pangu, M. Diane and M. R. Biscoe, *J. Am. Chem. Soc.*, 2014, **136**, 14027; (g) Q. Zhou, K. M. Cobb, T. Tan and M. P. Watson, *J. Am. Chem. Soc.*, 2016, **138**, 12057; (h) K. R. Campos, A. Klapars, J. H. Waldman, P. G. Dormer and C. Chen, *J. Am. Chem. Soc.*, 2006, **128**, 3538; (i) H. M. Wisniewska, E. C. Swift and E. R. Jarvo, *J. Am. Chem. Soc.*, 2013, **135**, 9083; (j) J. Ilveria, D. Leonori and V. K. Aggarwal, *J. Am. Chem. Soc.*, 2015, **137**, 10958.
- 10 For asymmetric C–X alkylation: (a) S. Ge and J. F. Hartwig, *J. Am. Chem. Soc.*, 2011, **133**, 16330; (b) N. T. Kadunce and S. E. Reisman, *J. Am. Chem. Soc.*, 2015, **137**, 10480; (c) D. Wang, L. Wu, F. Wang, X. Wan, P. Chen, Z. Lin and G. Liu, *J. Am. Chem. Soc.*, 2017, **139**, 6811; (d) G. J. Lovinger, M. D. Aparece and J. P. Morken, *J. Am. Chem. Soc.*, 2017, **139**, 3153.
- 11 For asymmetric C–H alkylation: (a) G. Song, W. N. O. Wylie and Z. Hou, *J. Am. Chem. Soc.*, 2014, **136**, 12209; (b) G. A. Molander and S. R. Wisniewski, *J. Am. Chem. Soc.*, 2012, **134**, 16856; (c) S. Yu, H. L. Sang and S. Ge, *Angew. Chem., Int. Ed.*, 2017, **56**, 15896; (d) G. Bertuzzi, D. Pecorari, L. Bernardi and M. Fochi, *Chem. Commun.*, 2018, **54**, 3977; (e) A. Motaleb, S. Rani, T. Das, R. G. Gonnade and P. Maity, *Angew. Chem., Int. Ed.*, 2019, **58**, 14104.
- 12 For racemic and asymmetric C–H aminoalkylation: (a) A. Kundu, M. Inoue, H. Nagae, H. Tsurugi and K. Mashima, *J. Am. Chem. Soc.*, 2018, **140**, 7332; (b) R. S. J. Proctor, H. J. Davis and R. J. Phipps, *Science*, 2018, **360**, 419; (c) X. Liu, Y. Liu, G. Chai, B. Qiao, X. Zhao and Z. Jiang, *Org. Lett.*, 2018, **20**, 6298.
- 13 (a) Md N. Alam, S. R. Dash, A. Mukherjee, S. Pandole, U. K. Marelli, K. Vanka and P. Maity, *Org. Lett.*, 2021, **23**, 890; (b) A. Motaleb, A. Bera and P. Maity, *Org. Biomol. Chem.*, 2018, **16**, 5081; (c) Md N. Alam, K. M. Lakshmi and P. Maity, *Org. Biomol. Chem.*, 2018, **16**, 8922.
- 14 Although these reports by Wolfe group are reported as [1,2] aza-Wittig, excess Lewis acid along with base is required and the authors recognize a possible Stevens pathway via zwitterionic ammonium intermediate: (a) R. K. Everett and J. P. Wolfe, *J. Org. Chem.*, 2015, **80**, 9041; (b) R. K. Everett and J. P. Wolfe, *Tetrahedron Lett.*, 2015, **56**, 3393.
- 15 The corresponding oxa-[1,2] Wittig is a well-known rearrangement, proceeds via a widely accepted dissociative radical pair mechanism, and exhibit substrate and reaction condition dependent variable degrees of chirality transfer: (a) K. Tomooka, H. Yamamoto and T. Nakai, *Liebigs Ann./Recl.*, 1997, 1275; (b) S. L. Schreiber and M. T. Goulet, *Tetrahedron Lett.*, 1987, **28**, 1043; (c) K. Tomoka, M. Kikuchi, K. Igawa, P.-H. Keong and T. Nakai, *Tetrahedron Lett.*, 1999, **40**, 1917; (d) K. Tomoka, H. Yamamoto and T. Nakai, *Angew. Chem., Int. Ed.*, 2000, **39**, 4500; (e) K. Tomoka, M. Kikuchi, K. Igawa, M. Suzuki, P.-H. Keong and T. Nakai, *Angew. Chem., Int. Ed.*, 2000, **39**, 4502; (f) K. Tomooka, H. Yamamoto and T. Nakai, *J. Am. Chem. Soc.*, 1996, **118**, 3317; (g) R. E. Maleczka Jr and F. Geng, *J. Am. Chem. Soc.*, 1998, **120**, 8551.
- 16 For captodative stabilization of radical intermediates, see: (a) H. Viehe, Z. D. Anousek and R. Merenyi, *Acc. Chem. Res.*, 1985, **18**, 148; (b) J. P. Peterson and A. H. Winter, *J. Am. Chem. Soc.*, 2019, **141**, 12901.
- 17 Stoichiometric amount of catalysts were taken for strong MHMDS base at 0 °C to avoid starting material decomposition.
- 18 (a) J. Barluenga, F. J. Fañanás, R. Sanz, C. Marcos and M. Trabada, *Org. Lett.*, 2002, **9**, 1587; (b) F. Gao, B.-S. Kim and P. J. Walsh, *Chem. Sci.*, 2016, **7**, 976.
- 19 The enantiomeric excess of salts **1** was determined by chiral HPLC after converting those to the corresponding pyridones.
- 20 Few chiral amines are commercially available and others were synthesized following a recent literature method: (a)




- M. Xiao, X. Yue, R. Xu, W. Tang, D. Xue, C. Li, M. Lei, J. Xiao and C. Wang, *Angew. Chem., Int. Ed.*, 2019, **58**, 10528; (b) V. Bagutski, T. G. Elford and V. K. Aggarwal, *Angew. Chem., Int. Ed.*, 2011, **50**, 1080.
- 21 Cyclopropanes are known to remain intact in a radical reaction; either *via* reversible ring opening, or faster radical recombination before ring opening: (a) S. Umemiya, K. Nishino, I. Sato and Y. Hayashi, *Chem.–Eur. J.*, 2014, **20**, 15753; (b) X. Gou and O. S. Wenger, *Angew. Chem., Int. Ed.*, 2018, **57**, 2469; (c) J. Li, M. Kong, B. Qiao, R. Lee, X. Zhao and Z. Jiang, *Nat. Commun.*, 2018, **9**, 2445.
- 22 (a) L. Haiyan, L. Gaoping and J. Liu, WO2010075469A1, 2010; (b) S. Zhou and R. Tong, *Chem.–Eur. J.*, 2016, **22**, 7084; (c) L. Mengozzi, A. Gualandi and P. G. Cozzi, *Chem. Sci.*, 2014, **5**, 3915; (d) S. Zhou and R. Tong, *Org. Lett.*, 2017, **19**, 1594; (e) J. Yu, Z. Zhang, S. Zhou, W. Zhang and R. Tong, *Org. Chem. Front.*, 2018, **5**, 242.
- 23 We synthesized pyridinium salts following a modified literature protocol: G. H. R. Viana, I. C. Santos, R. B. Alves, L. Gil, C. M. Marazano and R. P. F. Gil, *Tetrahedron Lett.*, 2005, **46**, 7773.
- 24 For competitive [1,2] & [1,4] *oxa*-[1,4] Wittig rearrangements: F. Wang, J. Wang, Y. Zhang and J. Yang, *Tetrahedron*, 2020, **76**, 130857. For stereoretentive *oxa*-[1,2] & [1,4]: L. M. Mori-Quiroz and R. E. Maleczka Jr, *J. Org. Chem.*, 2015, **80**, 1163.
- 25 (a) J. P. Perdew, K. Burke and M. Ernzerhof, *Phys. Rev. Lett.*, 1996, **77**, 3865; (b) K. Eichkorn, F. Weigend, O. Treutler and R. Ahlrichs, *Theor. Chem. Acc.*, 1997, **97**, 119; (c) R. Ahlrichs, M. Bar, M. Haser, H. Horn and C. Kolmel, *Chem. Phys. Lett.*, 1989, **162**, 165.
- 26 (a) H.-Y. Yoo, K. N. Houk, J. K. Lee, M. A. Scialdone and A. I. Meyers, *J. Am. Chem. Soc.*, 1998, **120**, 205; (b) F. Haeffner, K. N. Houk, S. M. Schulze and J. K. Lee, *J. Org. Chem.*, 2003, **68**, 92310.
- 27 (a) W. Li, W. Xu, J. Xie, S. Yu and C. Zhu, *Chem. Soc. Rev.*, 2018, **47**, 654; (b) X. Wu and C. Zhu, *Acc. Chem. Res.*, 2020, **53**, 1620; (c) Z. Feng and D. J. Tantillo, *J. Am. Chem. Soc.*, 2021, **143**, 088.
- 28 (a) F. D. Greene, M. A. Berwick and J. C. Stowell, *J. Am. Chem. Soc.*, 1970, **92**, 867; (b) S. L. Shevick, C. V. Wilson, S. Kotesova, D. Kim, P. L. Holland and R. Shenvi, *Chem. Sci.*, 2020, **11**, 12401.





Cite this: *Org. Biomol. Chem.*, 2023, **21**, 5671

C–H functionalization of pyridines

Susmita Maity,^{†a} Asish Bera,^{†a,b} Ayantika Bhattacharjya^{†a} and Pradip Maity^{†a,b} 

Pyridine and its reduced form (piperidine) are the most common nitrogen heterocycles in FDA-approved drugs. Additionally, their presence in alkaloids, ligands for transition metals, catalysts, and organic materials with various properties makes them among the most important structural cores. Despite its importance, direct and selective functionalization of pyridine remains scarce due to its electron-poor nature and nitrogen coordination power. Instead, functionalized pyridine rings were primarily constructed from suitably substituted acyclic precursors. The focus on sustainable chemistry with minimum waste generation encourages chemists to develop direct C–H functionalization. This review summarizes different approaches to tackle the reactivity and regio- and stereoselectivity aspects for direct pyridine C–H functionalization.

Received 22nd May 2023,
Accepted 14th June 2023
DOI: 10.1039/d3ob00799e
rsc.li/obc

Six-membered N-heterocyclic (pyridine and piperidines) cores are the first and second most frequent heterocyclic structures that appear in FDA-approved drugs.¹ Besides, pyridines serve as crucial ligands for transition metals,² are present in a large number of alkaloids with biological importance,³ act as organocatalysts,⁴ and feature in many functional materials.⁵ Hence, synthesis of functionalized pyridines attracts considerable attention from synthetic communities.⁶ Traditionally, highly functionalized pyridine rings are built from acyclic precursors. Although many elegant methods were developed over the years, they fundamentally suffer from multi-step synthesis of suitable acyclic precursors and the final elimination reaction sequence to generate waste. With green and sustainable

methods in focus to reduce environmental footprints, regio- and stereoselective direct C–H functionalization becomes one of the most critical approaches.

Aromatic C–H can be directly functionalized by electrophilic aromatic substitutions (S_EAr ; Friedel–Crafts reaction). However, pyridine, an electron-deficient aromatic, needs forced conditions. The Lewis acid activation of electrophiles is also problematic since the nitrogen of pyridine competes *via* coordination with the Lewis acid. As a result, pyridine deactivates the Lewis acid and becomes further electron deficient for the Friedel–Crafts reaction.

In the last few decades, transition metal catalysed regio-selective functionalization of aryl C–H bonds has achieved extraordinary progress.⁷ Electron-deficient pyridines are less reactive for C–H functionalization and are instead used mainly as directing groups owing to their unreactive C–H bonds. The strong coordinating nature of the pyridine nitrogen makes it a good ligand but further deactivates it for C–H activation.

^aOrganic Chemistry Division, CSIR-National Chemical Laboratory, Pune 411008, India. E-mail: p.maity@ncl.res.in

^bAcademy of Scientific and Innovative Research (AcSIR), Ghaziabad 201002, India
†All authors contributed equally.



Susmita Maity

Susmita Maity is currently working as Project Associate-I in the Organic Chemistry Division at the CSIR-National Chemical Laboratory under the supervision of Dr Pradip Maity. She pursued her B.Sc. and M.Sc. from Vidyasagar University in 2020 and 2022, respectively. She is working on catalytic asymmetric aerobic oxidations.



Asish Bera

Asish Bera completed his B.Sc. (Chemistry) in 2012 from Vidyasagar University and his M.Sc. (Chemical Science) in 2014 from IIT Madras, India. In 2016, he joined the CSIR-National Chemical Laboratory (NCL) under the supervision of Dr Pradip Maity. His Ph.D. thesis is based on novel phosphite catalyst synthesis and its application in enantioselective radical reactions.

The lack of reports resulted in only one comprehensive review in 2017 summarizing the C–H functionalization of six-membered N-heteroaromatic compounds, including pyridines.^{6c} The significance of direct pyridine functionalization has led to the development of numerous elegant strategies since then. This review will briefly discuss different approaches based on reactivity patterns and present recent developments for pyridine C–H functionalization.

1. Direct functionalization

This section will discuss the reports for direct C–H functionalization of pyridine without pre-activation of the pyridine nitrogen.

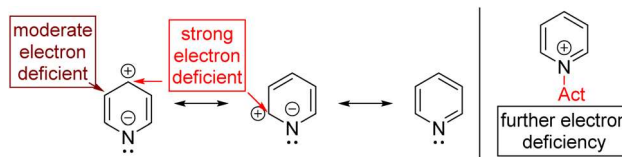
1.1. Friedel–Crafts reaction with electrophiles

S_EAr with electron-deficient pyridine works only at elevated temperatures with C3 selectivity, as C3 is the least deactivated center. Brominations and nitrations are known to work at 300 °C, but acylation with acyl chloride and a Lewis acid does not work.⁸

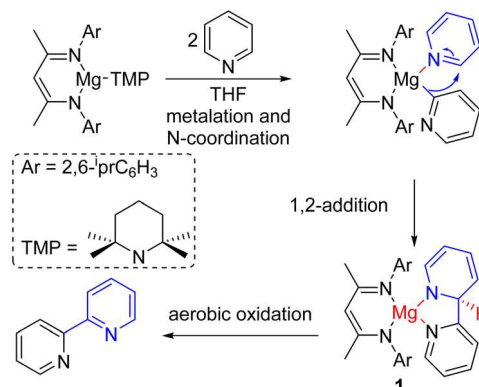
The Lewis acid preferentially coordinates with the pyridine nitrogen over acyl chloride, deactivating the pyridine further (Scheme 1). The functional group tolerance at this high temperature is an issue, and therefore the direct S_EAr approach did not enjoy widespread applications.

1.2. Electrophiles *via* C–H deprotonation

The electron-deficient nitrogen of pyridine makes the C2–H acidic and prone to deprotonation with a strong base. The deprotonated pyridine can react with electrophiles to generate various C2-functionalized pyridines. The Knochel group extensively studied the formation and reactivities of deprotonated pyridines at different positions.⁹ Hevia, McLellan, and



Scheme 1 Electronic nature of pyridine and its deactivation *via* Lewis acid.



Scheme 2 C–H deprotonation followed by its reaction with an electrophile.

co-workers used a strong magnesium amide base for deprotonation (Scheme 2). The monomeric magnesium amide was stabilized by a ligand, and the magnesium coordinates with the pyridine nitrogen for its base-mediated deprotonation. The deprotonated pyridine adds to another pyridine starting material coordinated with the same magnesium Lewis acid. The resulting intermediate (1) oxidized in air to form 2,2'-bipyridine products.¹⁰



Ayantika Bhattacharjya

Ayantika Bhattacharjya obtained her B.Sc. from Vidyasagar University in 2020 and M.Sc. from Midnapore College Autonomous (Vidyasagar University) in 2022. She is currently working as Project Associate-I in the Organic Chemistry Division at the CSIR-NCL under the supervision of Dr Pradip Maity. Her current research interest focuses on the asymmetric functionalization of imines.



Pradip Maity

Dr Pradip Maity received his B.Sc. degree in chemistry from Calcutta University in 2001 and his M.Sc. from IIT Kanpur, India. Then he moved to the US for Ph.D. from Florida Atlantic University in 2006 with Professor Salvatore D. Lepore. After completion, he joined UT Southwestern Medical Center in Dallas as a postdoctoral fellow with Professor Uttam K. Tambar in 2011. He began his independent research career at the CSIR-National Chemical Laboratory, Pune, as a Senior Scientist in 2015. His research group is interested in developing a sustainable catalysis platform for asymmetric pyridine functionalization and medicinal chemistry.

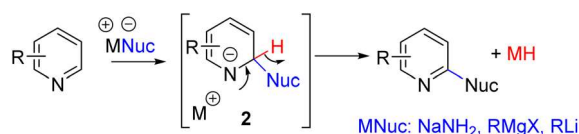
1.3. Nucleophilic substitution

The electron-deficient nature of the pyridine ring also makes it susceptible to nucleophilic addition at C2 and C4. For an overall C–H functionalization, the hydrogen at the nucleophile-added carbon (2) must be removed with its electron pair. S_NAr with hydride as the leaving group was described in 1914 by Chichibabin and co-workers for C2 amination (Scheme 3).¹¹ The addition of sodium amide to the electrophilic C2 position is favorable, but the following hydride elimination is a high-energy step, requiring forced reaction conditions.

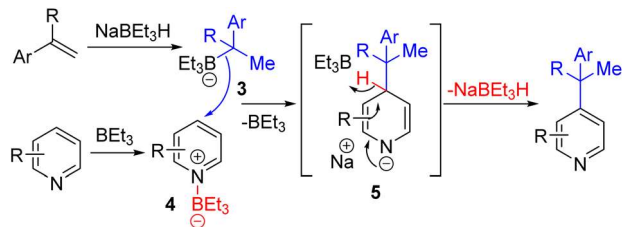
Subsequently, reactions with Grignard reagents by the Evans group and lithiated carbon nucleophiles by the Sarpong group were reported. The formation of a reactive metal hydride as a side product impedes functional group tolerance.

In 2020, Zhang, Xiong, and co-workers reported a trialkylborane-borohydride system for the alkylation of pyridines (Scheme 4). The experimental and computational mechanistic studies suggest initial hydroboration of the alkene. The resulting alkylborane **3** was added to the borane-activated pyridine (**4**) at the C4 position to avoid steric hindrance at C2. Borohydride removal from the corresponding intermediate **5** gives C4 alkylated pyridines. The regeneration of borohydride makes it a sub-stoichiometric reagent, while trialkylborane was used in excess, probably due to product coordination. The reaction occurred at 100 °C in THF with excellent yields and substrate scope.¹²

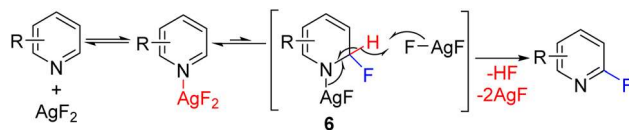
In 2013, the Hartwig group reported C2 fluorination using super-stoichiometric silver difluoride (Scheme 5). The authors planned the reaction in line with the Chichibabin reaction. However, the mechanistic studies suggest that the reaction likely proceeded *via* the nucleophilic addition of fluoride to dihydropyridine (**6**), followed by oxidation with stoichiometric AgF_2 to substituted pyridine with the removal of HF.¹³ The nucleophilic addition at C2/C4 of pyridine leading to dihydropyridine intermediate, followed by its oxidation to rearoma-



Scheme 3 Chichibabin reaction: C2 nucleophilic addition followed by hydride elimination.



Scheme 4 Borohydride catalyzed Chichibabin type C4 alkylation of pyridine with alkenes.



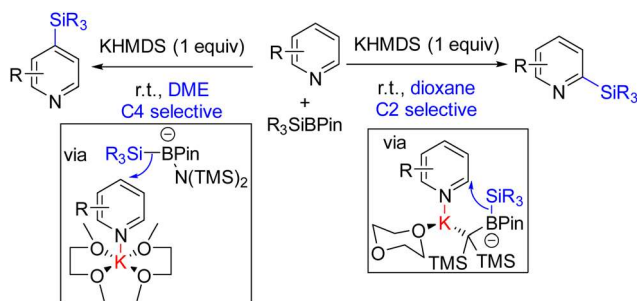
Scheme 5 AgF_2 mediated C2 fluorination *via* silver mediated fluoride addition and subsequent oxidation.

tized substituted pyridine became a general approach for C–H functionalization of pyridines. The initial nucleophile can add to either the C2 or C4 position, leading to the possibility of mixtures of C2 and C4 regioisomers.

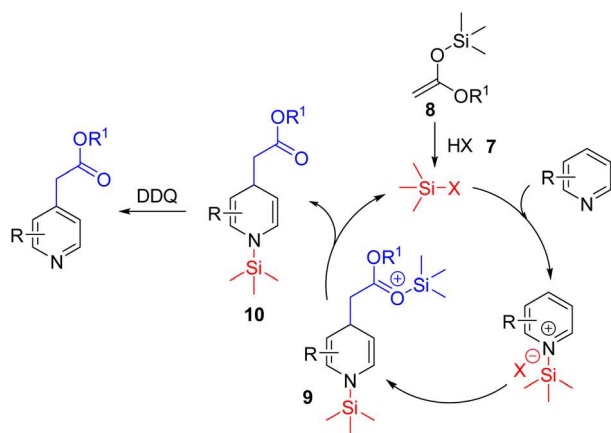
Martin and co-workers in 2019 reported site-selective C2 and C4 silylation of pyridine with $Et_3SiBPin$ and a stoichiometric KHMDS base. Their analysis with different counter-ions and solvents indicated a solvent-separated ion pair for sterically less crowded C4 functionalization. C2 silylation was also achieved through a contact ion-pair intermediate. The mechanistic proposal suggests an initial coordination of the base to the boron of silyl borane. The coordination increases the nucleophilicity of the B–Si bond, which adds to the potassium-coordinated pyridine (Scheme 6). The final product formation from the silylated dihydropyridine is not clear.¹⁴ Either air oxygen during the quench led to oxidative aromatization, or borohydride elimination can lead to product formation.

In 2021, List and Obradors reported a Brønsted acid catalysed C4 nucleophilic functionalization of pyridines with silyl ketene acetals (Scheme 7).¹⁵ In their reaction design, the triflimide Brønsted acid (**7**) acts as a precatalyst which reacts with silyl ketene acetal (**8**) to form the Lewis acidic silylium ($Si-X$). The unprecedented silylium activation of the pyridine nitrogen led to the addition of **8** to the activated pyridine. The corresponding intermediate (**9**) regenerated the silylium Lewis acid and dihydropyridine **10**. The substituted pyridine formed upon subsequent DDQ oxidation. The large silylium led to its enhanced Lewis acidity *via* a longer Si–X bond, and steric hindrance at the pyridine nitrogen resulted in C4 selective nucleophilic addition.

The *in situ* oxidation by various oxidizing reagents compatible with a particular nucleophile became a successful approach for overall pyridine C–H functionalization. When the



Scheme 6 Solvent and base-mediated regio-divergent C2/C4 silylation with $R_3SiBPin$.



Scheme 7 C4 pyridine functionalization of pyridine with silyl ketene acetals.

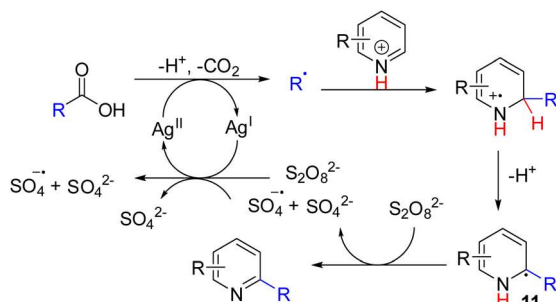
oxidant is not compatible, a one-pot sequential or stepwise oxidation of the dihydropyridine intermediate leads to the substituted pyridine product.¹⁶

1.4. Reaction with radicals

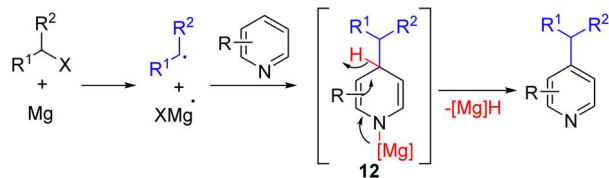
Oxidation of the radical intermediates from nucleophilic radical addition to pyridines became a general C–H activation strategy. In 1971, Minisci and co-workers reported that alkyl radicals generated from silver-mediated decarboxylation were added to pyridines (Scheme 8). The nucleophilic alkyl radicals add to pyridine at either C2 or C4 positions, followed by single-electron oxidation of the radical intermediate **11** to alkylated pyridine.¹⁷ They also discovered that aryl radicals could add to pyridines to give C–H arylation of pyridine.¹⁸

Unlike the anionic nucleophilic addition–oxidation sequence, nucleophilic alkyl radical generation and its addition to pyridine are generally compatible with the stoichiometric oxidant in the Minisci reaction. The advancement of mild alkyl radical generation reignites the Minisci-type C–H functionalization of pyridines. Subsequently, numerous methods for alkyl radical generation and their Minisci-type pyridine substitution were reported and reviewed.¹⁹

The Jingbo Yu group reported nucleophilic radical addition followed by a hydride elimination protocol for C4 alkylation of



Scheme 8 Minisci reaction: radical alkylation and arylation with an *in situ* oxidant.



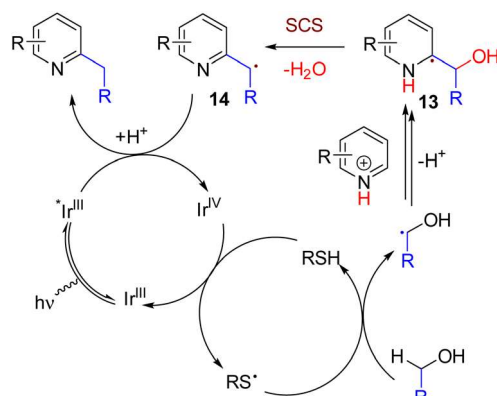
Scheme 9 C4 alkylation of pyridine with an alkyl halide and mechanochemically activated magnesium metal.

pyridine (Scheme 9). Alkyl halide and magnesium metal initially reacted to form an alkyl radical and radical Mg(I) species which was stabilized by the *N,N'*-di-*tert*-butylethane-1,2-diamine (DTEDA) ligand. The Mg(I) species reduces the magnesium coordinated pyridine. The radical–radical recombination led to dihydropyridine **12**, and subsequent [Mg]–H elimination led to the C4 alkylated product.²⁰

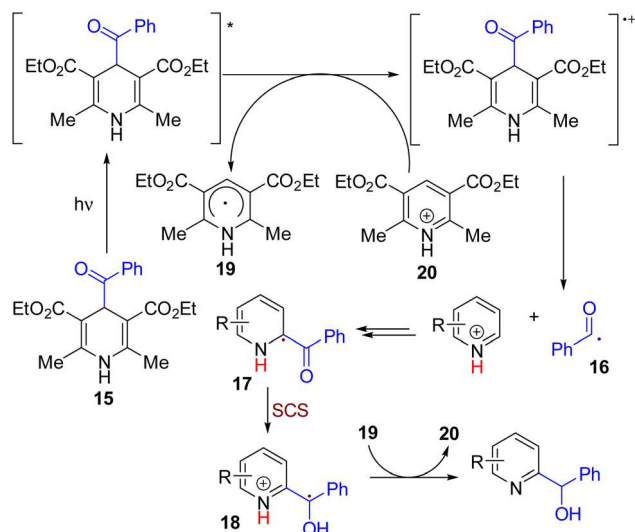
In 2015, the MacMillan group showed that alcohol could be used as an alkylating reagent under photoredox reaction conditions. The removal of OH *via* a biologically relevant spin center shift (SCS) enables an inexpensive and abundant alcohol as the alkylating agent without the requirement of an oxidant (Scheme 10). The method resulted in both C2 and C4 alkylated products, which can be controlled by substrate substitution patterns.²¹ The reaction works *via* dual photoredox and HAT catalysis for the formation of an α -hydroxyalkyl radical. The addition of this radical to protonated pyridine results in the formation of the radical intermediate **13** after facile deprotonation. This radical with an α -hydroxyl group undergoes an SCS to eliminate water and generate the benzylic radical (**14**). The photoexcited iridium catalyst reduces this electron-deficient benzyl radical, and subsequent protonation leads to the formation of alkylpyridine.

UV light-mediated photocatalyst-free methylation and ethylation using the corresponding alcohol were reported later under acidic conditions by Li and co-workers.²²

In 2019, the Melchiorre group reported C–H hydroxyalkylation of quinolines and isoquinolines. The reaction between acyl dihydropyridine as an acyl radical generator and pyridine resulted in hydroxyalkylation products (Scheme 11).



Scheme 10 Alcohol as the radical alkylating reagent for pyridine alkylation without an oxidant.

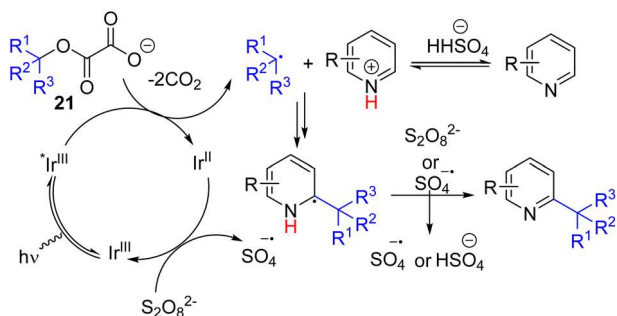


Scheme 11 Acyl dihydropyridine as a dual hydroxyalkyl reagent and oxidant for pyridine C–H functionalization.

Both C2 and C4 products were formed based on the substitution pattern. The reaction proceeded under 460 nm light irradiation and acidic conditions without any photocatalyst.²³ The theoretical and experimental studies suggested that a light-mediated single electron reduction of acyl dihydropyridine (15) initiates the reaction. The acyl radical (16) formed was added to the protonated pyridine followed by deprotonation to form the radical intermediate 17. This intermediate undergoes an SCS to rearomatize the pyridine ring with a radical center shift to the α carbon (18). The benzylic radical undergoes single electron reduction by the pyridyl radical to form the corresponding carbanion, which protonates to yield the final product.

The Overman group introduced oxalate intermediates 21 from alcohol which undergoes one-electron oxidation to generate alkyl radicals with the loss of two CO₂. Reaction with the cesium salt of oxalate from a tertiary alcohol and pyridine under light and the iridium photocatalyst resulted in C2 alkylated product formation with two equivalents of ammonium persulfate as the oxidant (Scheme 12).²⁴

The method was applied to many other N-heteroaromatic compounds with embedded imines. Zard's research group developed an efficient alkylation starting with different thiol



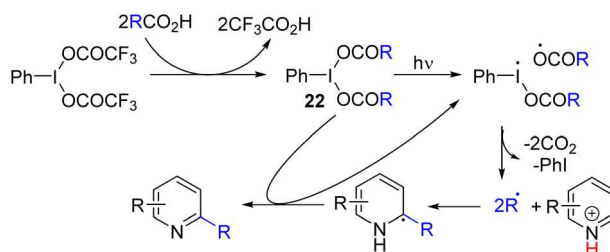
Scheme 12 Alcohol derivative as a radical alkylating reagent of pyridine.

derivatives, including tertiary thiols, for the formation of quaternary alkylated pyridines.²⁵ Dilauroyl peroxide (DLP) was used for light-mediated radical initiation and subsequent oxidation of the alkyl-added pyridine intermediates.

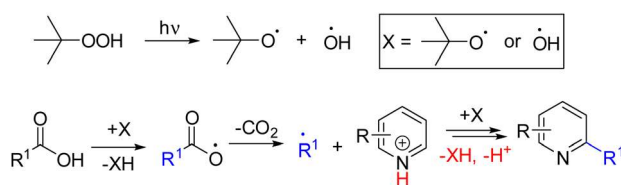
Zhang, Yang, and co-workers, and later Poole and co-workers reported a carboxylic acid-derived hypervalent iodine (III) reagent (22) as an alkyl generation and oxidizing reagent under visible light irradiation (Scheme 13). The hypervalent iodine-carboxylate bond cleaves homolytically under light, which initiates the C–H alkylation and acylation of pyridine, quinoline, and isoquinoline.²⁶

In 2023, Zhang's group discovered that *tert*-butyl hydroperoxide can homolytically cleave upon irradiation with 395 nm light. The alkoxy or hydroxyl radical generated undergoes HAT with carboxylic acid to form an alkyl radical *via* CO₂ expulsion. The same alkoxy/hydroxy radical then undergoes another HAT with the radical-pyridine adduct for the synthesis of alkylated pyridines (Scheme 14).^{27a} In the same year, Wang, Niu, and co-workers developed a desulfonative radical pyridylation with glycosyl sulfonates as the glycosyl radical precursor.^{27b} In this case, excess *tert*-butyl hydroperoxide generates the *tert*-butyl hydroxyl radical that accepts a single electron from the sulfonate anion. The corresponding radical intermediate generates a glycosyl radical after SO₂ expulsion, similar to decarboxylation. The rest of the reaction pathway runs parallel to Scheme 14.

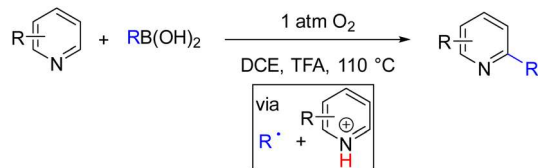
In 2017, Liu and Zhang reported the Minisci alkylation of pyridines using alkylboronic acid as an alkyl radical precursor under 1 atm oxygen (Scheme 15).²⁸ The authors proposed aerobic oxidative alkyl radical formation from boronic acid that adds to pyridine in the DCE solvent and TFA additive. The alkyl added pyridine intermediate was subsequently oxidized by oxygen or an oxygen-derived oxidant to generate alkylpyridines. Primary and secondary alkylation was shown to work well with a variety of pyridine derivatives.



Scheme 13 Carboxylic acid and PIDA for the decarboxylating radical alkylation of pyridine.



Scheme 14 TBHP as a photoactive oxidant for decarboxylating alkylation.

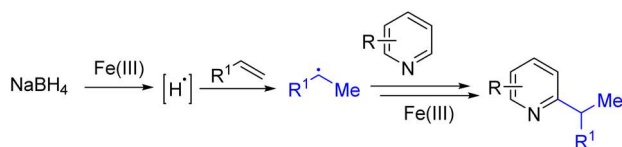


Scheme 15 Boronic acid under air for alkyl radical generation and oxidation for pyridine functionalization.

Another approach for generating an alkyl radical is to add a hydrogen radical to an alkene. The Herzon group used Co(II)/TBHP, and the Baron group used Fe(III)/BF₃·OEt₂ to generate alkyl radicals from alkene and silanes. Subsequently, Liu and co-workers reported sodium borohydride and Fe(III) mediated radical alkylation of pyridines (Scheme 16). Fe(III) was proposed to oxidize hydride to a hydrogen radical that adds an alkene to form the alkyl radical. The alkyl radical added pyridine intermediate was oxidized further with Fe(III) to generate the final product.^{29a} The reaction scope was broad, and the dialkylation product forms when multiple C2/C4 hydrogens are available for functionalization. Although inexpensive iron, borohydride, and alkenes were used for this transformation, excess reagents were necessary to obtain a good yield, and therefore the monoalkylated product was difficult to obtain.

Similarly, radical addition of an azide to an alkene generated alkyl radicals which were added to pyridine for the synthesis of β-azido alkylpyridines. Here, two equivalents of (diacetoxyiodo)benzene (DIB) were used as an oxidant to generate an azide radical from TMSN₃.^{29b} The reaction steps are similar to that of Zhang and Yang (Scheme 14). Later, Zhou, Li, and co-workers reacted alkene with alcohol in the presence of pyridine and persulfate to generate a β-alkoxy radical under visible light (390–400 nm LED). It is proposed that the pyridine derivative gets excited under visible light. The excited pyridine engages in a single-electron reduction reaction with the persulfate anion to form a sulfate radical anion. Alternatively, a sulfate radical anion may form *via* homolytic cleavage of persulfate under light irradiation. The alkene is oxidized by SO₄^{•-} and reacts with alcohol to form a β-alkoxy radical. This radical adds to the pyridine, followed by its single electron oxidation leading to product formation.^{29c}

Huang, Chen, and co-workers reported alkyl radical formation from bulky and inert C_{sp³}–C_{sp³} bond cleavage from alcohol 23. The alcohol OH undergoes photoredox catalysed HAT to form reactive alkoxide radical 24, which forms an alkyl radical *via* expulsion of the carbonyl compound. The sub-

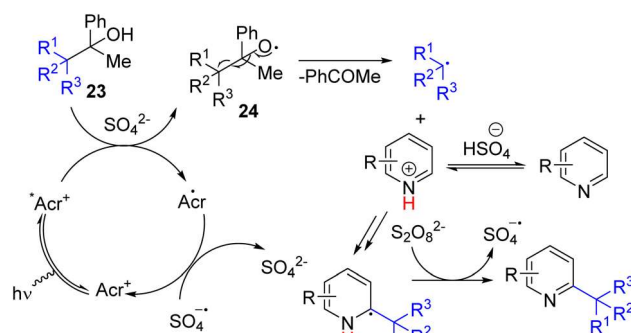


Scheme 16 Radical alkene hydrogenation mediated alkyl radical generation for pyridine alkylation.

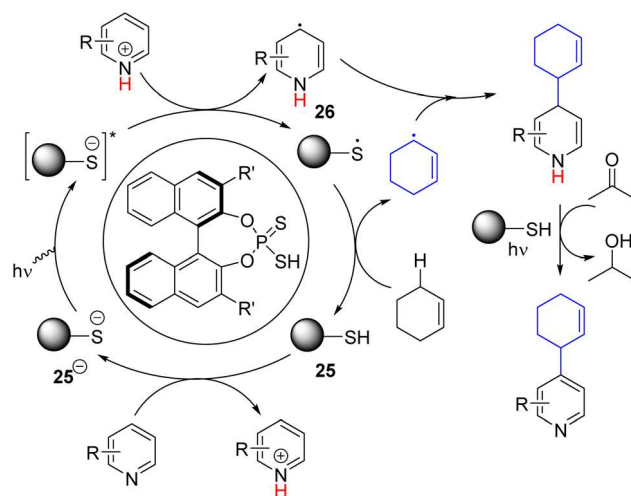
sequent reaction of the alkyl radical with electron-deficient systems, including pyridines, led to C–H functionalization (Scheme 17).³⁰

Ammonium persulfate was used as a stoichiometric oxidant. Finally, alkyl radicals were also generated from C(sp³)–H, followed by their addition to pyridines for substituted pyridines.³¹ In line with the initial reports by the MacMillan group for alkylation from the ether, Togo reported the UV light-mediated α-alkylation of amide which needed excess amide for its success.³² Berthelot and co-workers use MacMillan conditions under visible light to improve the yield and efficiencies with a secondary amine.³³ The reaction was shown to work with pyridine, quinoline, and isoquinolines, and substrates were chosen with either C2 or C4 sites blocked for selective product formation. Acyl radicals, being highly nucleophilic, are also suitable for the Minisci-type acylation of pyridines. Fluoroalkyl radicals are also compatible with the C2/C4 functionalization of pyridines.

In 2023, the Melchiorre group reported the photochemical organocatalytic C2/C4 allylation and benzylation of pyridine (Scheme 18).³⁴ They found a suitable dithio-derivative of the



Scheme 17 Photochemical oxidative C_{sp³}–C_{sp³} bond cleavage for alkyl radical generation for pyridine alkylation.

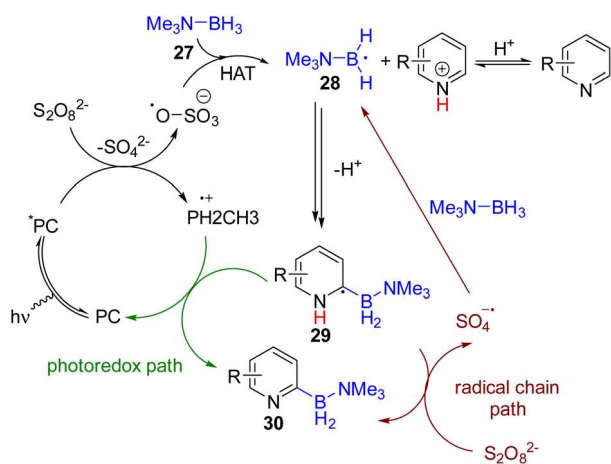


Scheme 18 Photochemical organocatalytic allylation and benzylation of pyridine *via* double C–H activation.

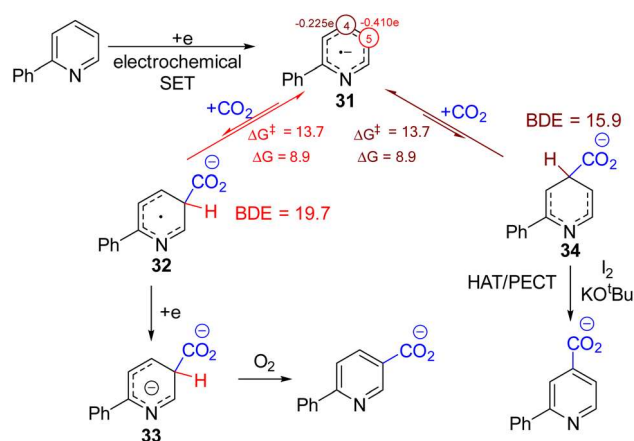
phosphate anion (25^-) organocatalyst that absorbs 365 nm light to generate a highly reducing excited state. The excited catalyst 25^{*-} reduced the protonated pyridine to form a pyridinyl radical (26). The corresponding thiophosphate radical (25^{\cdot}) undergoes HAT with allylic and benzylic C–H to form the corresponding radical. Hetero-coupling of these two radicals gave the alkylated dihydropyridine intermediate. The following oxidative rearomatization to product formation occurred without any oxidizing agent. The authors speculated a photochemical oxidation path in which acetone solvent acts as an oxidant.

In 2021, the Leonori group utilized the Minisci-type C2 borylation of pyridines *via* the photocatalytic generation of nucleophilic boryl radicals (Scheme 19). The photocatalyst 4CzIPN, under blue light, gets excited and reduces ammonium persulfate to a sulfate radical anion. The radical anion undergoes HAT with B–H of borane-triethylamine (27) to form the boryl radical 28 that was added to the pyridine at the C2 position. The resulting intermediate (29) oxidized to the stable 2-borylpyridine product (30) by ammonium persulfate. The sulfate radical anion formed in the last step led to the radical chain borylation process, which was applicable to pyridine, quinoline, isoquinoline, and other electron-deficient heterocycles.^{35a} In 2023, the Banerjee group synthesized a β -keto-enamine-based COF photocatalyst with suitable redox properties to achieve the same C2 borylation. Several catalytic cycles were performed to establish COF catalysts' high photostability and recyclability.^{35b}

Recently, Lin, Yu, and co-workers developed a tuneable C3 and C4 and electrochemical carboxylation of pyridine with CO_2 .³⁶ The tuneable regioselectivity was achieved using either divided or undivided electrochemical cells (Scheme 20). The authors studied the reaction extensively *via* experiments and DFT calculation to suggest the reasons for this regiodivergent carboxylic acid formation. The reaction starts with the cathodic reduction of the pyridine substrate. The spin density of this radical-anion intermediate 31 is maximum at C5 carbon,



Scheme 19 Photoredox C2 borylation of pyridines with ammonia-borane.



Scheme 20 Electrochemical regiodivergent C3 and C4 carboxylation with CO_2 .

and therefore it is the most nucleophilic carbon to attack electrophilic CO_2 . C5 nucleophilic attack to CO_2 formed intermediate 32 , which transformed into the dianionic 33 upon a second electron reduction. Aerobic oxidation of 33 forms the C3 carboxylate product. The spin density also suggests that the electron density at C4 is the second best, and both the C5 and C4 addition to CO_2 is endothermic. Their DFT also showed that the subsequent C–H bond dissociation energy for the C4 intermediate (34) is lower than that of the C5 intermediate 32 . Therefore, they speculated if tandem HAT catalysis could react faster with the C4 intermediate 34 to the C4 carboxylated product. It may shift the overall CO_2 addition step in favor of C4 carboxylation. Different HAT reagents failed, presumably due to their facile reduction over the substrate pyridine at the cathode. On the other hand, running the reaction in an undivided cell serendipitously gave them the major C4 carboxylate product. They reason that iodine from the electrolyte $n\text{Bu}_4\text{I}$ undergoes HAT or proton-coupled electron transfer (PCET) to abstract C4–H, leading to the regiodivergent formation of the C4 product. The iodine could also reduce at the cathode, but it can consistently regenerate at the anode oxidation of iodide, providing a constant source of iodine.

One of the challenging aspects of radical reactions is its stereocontrol. The Minisci type alkylation was mainly proposed to proceed with protonated pyridines as the activated coupling partner with alkyl radicals. In 2018, the Phipps group established that a sub-stoichiometric amount of acid was sufficient to catalyse the alkylation. Chiral phosphoric acid was tested for reductive aminoalkylation from *N*-acyloxyphthalimides with an iridium photocatalyst under a dual catalysis system.

The presence of NH at the aminoalkyl radical was essential to achieve significant enantioselectivity. Multiple coordination with chiral phosphoric acid was proposed for effective stereoinduction.³⁷ Jiang and co-workers were working on the photoredox and chiral phosphoric acid dual catalysis for asymmetric radical reactions and reported an asymmetric Minisci reaction of isoquinoline and *N*-acyloxyphthalimides later in 2018.³⁸ Subsequently, the Phipps group extended their work to show

that alcohol is compatible under dual catalysis to yield the corresponding chiral alcohols.³⁹ In 2023, the Wang group extended its application to β -carbolines (**35**) using the same redox-active ester as the alkylating agent.⁴⁰ The cooperative photoredox iridium and chiral phosphoric acid catalysis gave the 2-aminoalkylation product (**36**) with good yields and high enantioselectivities (Scheme 21).

1.5. Transition metal catalysis

The Jordan group reported the early examples of C–H alkylation of pyridines with alkenes using a cationic zirconium catalyst system.⁴¹ The alkylation was shown to work with 2-substituted pyridines for C6 alkylation. A follow-up report by the Jordan group and later the Hou group with a scandium catalyst reports asymmetric induction *via* chiral catalysts. However, those were reported with a limited substrate scope, similar to the 1989 report.⁴² It was speculated that the unsubstituted pyridine and quinoline nitrogen coordinate strongly with the catalyst, leading to catalyst arrest. In successful cases, the coordination power of pyridine nitrogen led to transition metal catalyst binding to the nitrogen, directing the metal center for selective C2–H activation. However, strong bonding with the substrate led to catalyst arrest, which limits the substrate scope.

The acyl-directed alkylation of pyridine *via* a ruthenium catalyst was reported by Grigg and Savic in 1997.⁴³ The preferential coordination of ruthenium to carbonyl over pyridine was proposed under heating conditions in toluene. The reaction failed with 2-acetyl pyridine, presumably due to double coordination mediated catalyst poisoning.

Other lanthanide complexes were reported for the C2 functionalization of pyridines. Marks, Kratish, Motta, and co-workers reported C2 borylation with HBpin (**36**) using a Cp*₂LuCH(TMS)₂ catalyst (**37a**).⁴⁴ The catalyst coordinates with pyridine nitrogen to increase the acidity of the C2 proton,

which was deprotonated by the alkyl group on the catalyst. The hydride of borane (**39**) coordinates with the catalyst after it loses the alkyl ligand, leading to C2 borylation (**40**) with catalyst–H formation (**37b**) (Scheme 22).

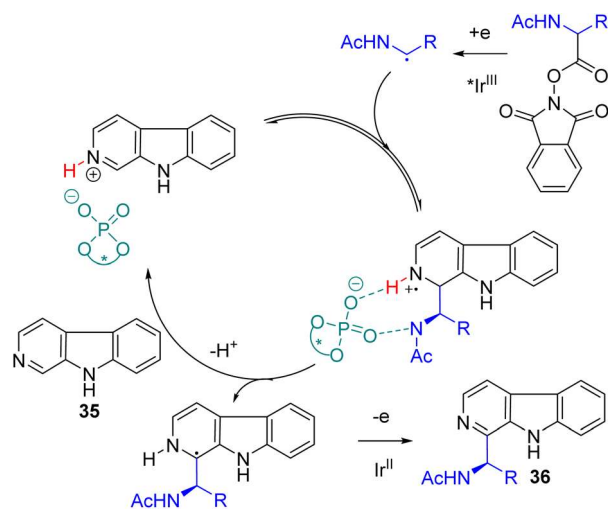
Coordination with another substrate releases the product, and Lu–H (**37b**) acts as an effective catalyst for the subsequent catalytic cycle. The hydride of the catalyst reacts with acidic C2 proton this time, releasing H₂ as a by-product during C–H metallated intermediate formation. This protocol was shown to work with substituted pyridines, but isoquinoline led to hydroborylation product formation rather than C2 borylation.

The Xu group also reported C2 selective borylation with pinacol borane in the same year. An alkyl ytrocene catalyst undergoes a similar reaction path for C2 borylation.⁴⁵

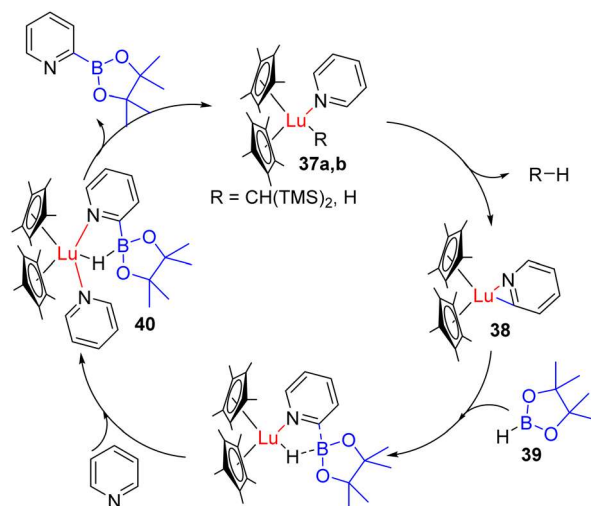
The dehydrogenative pyridine dimerization was known with RANEY® nickel or palladium on charcoal. The dimerization of 4-substituted pyridines with ruthenium or ruthenium/cobalt catalysis was also reported previously with hydrogen evolution. Those methods were generally narrow in the substrate scope. In 2019, Itami, Murakami, and co-workers reported the dehydrogenative synthesis of 2,2'-bipyridyls *via* C2–H activation and coupling of two pyridine molecules (Scheme 23).

They used Pd(OAc)₂ as the catalyst, with a stoichiometric silver salt as an oxidant with an acid additive. The reaction occurred in cyclopropyl methyl ether (CPME) at 140 °C. Pd(II) acetate was proposed to undergo C2–H activation with pyridine (**41**) *via* loss of one acetic acid, followed by a second C–H activation to bipyridyl Pd(II) intermediate **42**. The reductive coupling led to the formation of the product along with a reduced Pd(0) catalyst, in which the silver salt oxidized back to the Pd(II). The reaction is effective with a variety of pyridine substitutions at different positions.⁴⁶

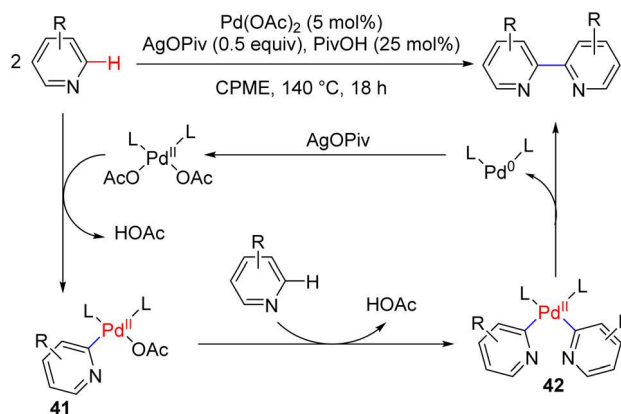
Few other functionalizations were reported with an electron withdrawing group attached pyridines and aryl halide. Here, a transition metal undergoes oxidative addition with an aryl halide, followed by ligand exchange with C–H deprotonated



Scheme 21 Photoredox and chiral phosphoric acid dual catalysis for asymmetric C2 aminoalkylation.



Scheme 22 Lanthanide catalysed C2 functionalization of pyridines.



Scheme 23 Pd(II) catalyzed deprotonative C–H activation of pyridines for their reductive coupling.

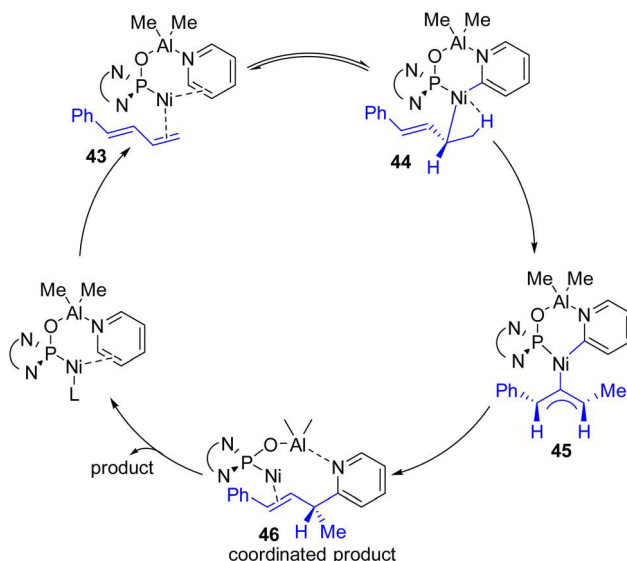
pyridine and subsequent reductive coupling to product formation. A concerted metalation–deprotonation (CMD) was proposed for the catalytic process.⁴⁷ Therefore, this is not technically a transition metal catalyzed C–H activation, and the deprotonation of electron-deficient pyridine is crucial for this approach.

The Hiya group used Lewis acid to coordinate the pyridine nitrogen, followed by nickel-catalyzed C–H alkenylation with alkynes. The Lewis acid activation increases the acidity of the C2 hydrogen for nickel insertion, which leads to C2 functionalization under mild reaction conditions.⁴⁸ The role of Lewis acid was proposed to be more than just sacrificial coordination to pyridine for its activation, but it enhances the C–H activation step. The combination of Lewis acid and transition metal seems a general solution to tackle the pyridine C–H activation, including its asymmetric alkylations at the C2 position.

Ye, Huang, and co-workers reported a Ni–Al bimetallic catalyst system for the C2–H allylation of pyridines with 1,3-dienes (Scheme 24).⁴⁹ Phosphine oxides (phosphites) with chiral diamine backbones were effective for asymmetric induction. The bimetallic catalyst synthesis was not required prior to the reaction. All reagents, metal salts, and the ligand were mixed in toluene, and heating at 135 °C resulted in a product with high enantioselectivity.

The reaction was shown to work with aryl-substituted dienes (43), whereas an alkyl-substituted diene resulted in the formation of a major linear product. This bimetallic catalyst system does not need C2 alkylated sterically suitable pyridines for its success. Simple unsubstituted pyridines and a variety of substituents at different positions were successful substrates. The method was successfully applied to quinoline and quinoxaline with moderate yields and enantioselectivities. However, heterocycles such as bipyridines, terpyridines, pyridazines, and imidazoles did not work. It was reasoned that the stronger coordination of Lewis acidic aluminium with these substrates probably inhibited the bimetallic catalyst regeneration.

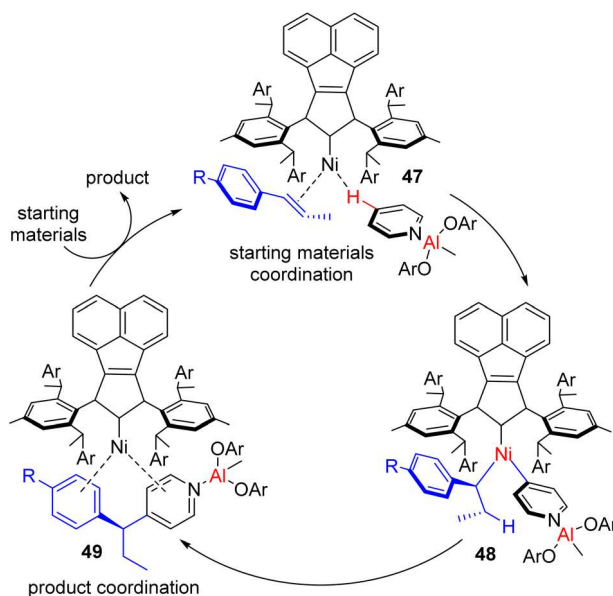
Shi and co-workers synthesized a bulky N-heterocyclic carbene ligand for Ni(0) (47), which undergoes C–H activation of pyridine and its insertion into an intramolecular alkene



Scheme 24 Ni–Al bimetallic complex with the chiral phosphine oxide ligand on nickel for asymmetric C2 allylation.

(Scheme 25). The combination of stoichiometric bulky Lewis acid and the bulky ligand on nickel led to C–H activation far from the pyridinic nitrogen to give excellent regiocontrol. The C2-symmetric chiral NHC ligand also resulted in high enantioselectivity.^{50a}

Shi, Zhang, and co-workers followed up with C4 selective alkylation with intermolecular substituted styrene. Pyridine, 2-substituted pyridine, and quinolines were functionalized with moderate yields and high enantioselectivities. The reaction with a terminal styrene was less efficient and mainly generated a linear product.^{50b} The computational mechanistic



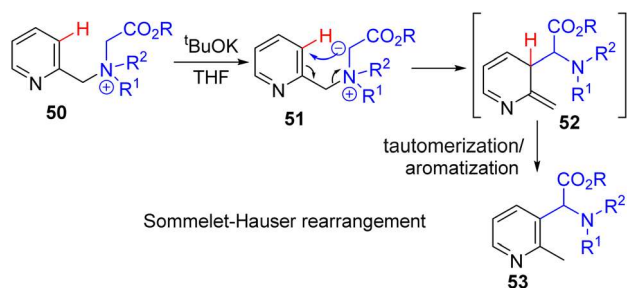
Scheme 25 Lewis acid-transition metal bimetallic complex for pyridine C–H functionalization.

studies suggest that pyridine C–H activation and hydrometalation of alkene occur simultaneously without a distinct metal-hydride intermediate formation. The strong π – π stacking of styrene and aryl fragments of the NHC ligand is crucial for reaction efficiencies and enantioselectivity.

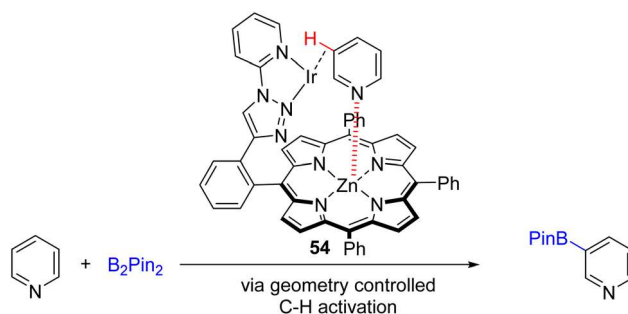
The Nakao group developed C2 selective silylation with silyl hydride as a reagent using a rhodium–aluminum bimetallic complex catalyst.⁵¹ The Lewis acidic aluminum coordinates to the pyridine nitrogen, bringing the rhodium catalyst in close proximity to the C2–H. The C–H-activated Rh–H intermediate cannot react with Si–H, and therefore a sacrificial alkene is needed. The alkene coordinates with Rh–H for its hydrometalation and reacts with Si–H to release alkane. The reductive coupling from the pyridine and silyl coordinated Rh intermediate generated the C2 silylpyridine product with the catalyst regeneration.

Tayama and co-workers reported a base-mediated Sommelet Hauser rearrangement of *N*-(pyridinylmethyl) tetraalkylammonium salts (Scheme 26). The ester stabilized acidic proton of ammonium substitution at C2 of pyridine (**50**) was deprotonated with a *tert*-butoxide base, which led to a [2,3] rearrangement. The electron-deficient pyridine ring facilitates the carbanion attack at the C3 position to the non-aromatic intermediate **52**. A proton shift to aromatization gave the final C3 substituted product **53** in good yields.⁵²

In 2021, the Doria group developed an enzyme-like supramolecular iridium catalyst system for C3 borylation (Scheme 27).⁵³ The designed catalyst geometry of the supramolecular ligand **54** binds both zinc and iridium. The coordi-



Scheme 26 [2,3] rearrangement from 2-pyridine ammonium salt for C3 functionalization.



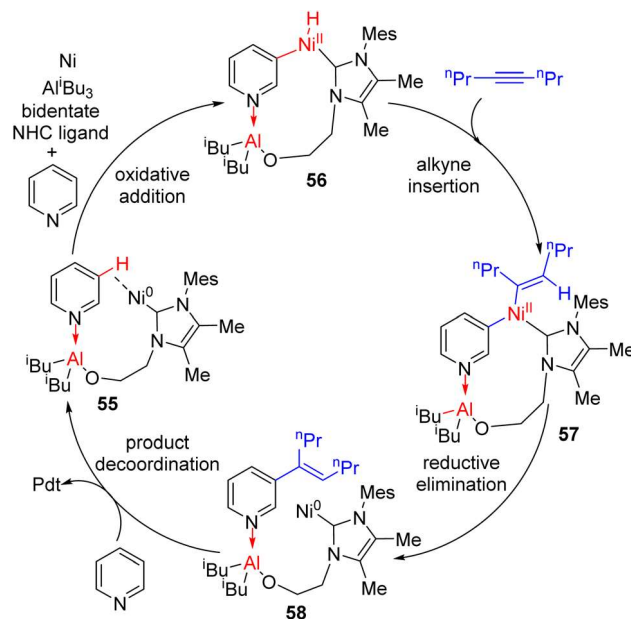
Scheme 27 Bimetallic catalyst with an enzyme-like ligand to coordinate both the Lewis acid and iridium for C3 borylation.

nation of the pyridine substrate to zinc brings the C3–H in close proximity to the iridium catalyst for its activation and borylation. The substrate scope is relatively limited, with iodide, electron-deficient acid, and amide at the C3 position of pyridine did not give a borylation product. The C4 alkylated substrates were also unsuccessful.

The Yu group focused on the transition metal catalysed direct C3 functionalization of pyridines. The direct C3–H metalation generally proceeds *via* an electrophilic activation pathway, and the nitrogen coordination of electron-deficient pyridine makes it even harder to achieve. In 2011, they developed a strongly coordinating bidentate ligand for palladium which prevents the metal from being poisoned by pyridine coordination. However, this approach only works with a large excess of pyridines and at a higher concentration.⁵⁴ Conversely, C2/C4–H functionalization *via* Lewis acid-transition metal catalysis was developed *via* an oxidative addition pathway. In 2021, the Yu group utilized the oxidative addition pathway rather than the electrophilic activation mode to achieve C3 alkenylation efficiently (Scheme 28).⁵⁵

The inherent C2/C4 reactivity was circumvented *via* a bifunctional ligand design which coordinated both the transition metal and Lewis acid simultaneously. The aluminum Lewis acid coordination to pyridine directs the nickel (0) to C3–H for metalation (intermediate **55**). The bifunctional ligand complex formation was achieved *in situ* to generate alkenylation products in good yields.

The Ackermann group in 2021 reported a reusable heterogeneous manganese catalyst system for C3 arylation and alkylation of C2-amide pyridines. The bipyridine ligand on the manganese catalyst was anchored on the solid support SBA-15. Both alkylation and arylation were achieved with the corresponding Grignard reagent at 70 °C.⁵⁶



Scheme 28 Bimetallic ligand-directed C3 alkenylation with alkynes.

2. Functionalization via a dual activator and reactive partner

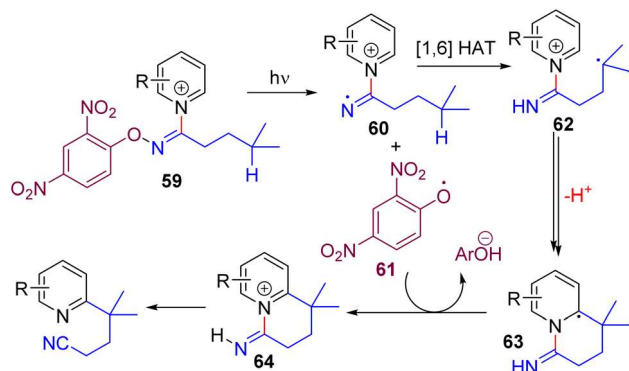
Although pyridine is electron deficient, the loss of aromaticity during nucleophilic addition makes it relatively challenging. As a result, a strong nucleophile is needed for successful addition at an elevated temperature. The nitrogen lone pair of pyridine is not part of the aromaticity and therefore acts as a strong electron donor. Donating nitrogen lone pairs to an activator makes the ring more electron deficient, and nucleophilic addition becomes facile.

N-Activated pyridines for radical reactions were well developed mainly due to their dual roles. Stephenson and co-workers treated pyridine *N*-oxide with acetyl chloride to generate an *N*-acyloxy pyridinium salt. The *in situ* generated salt undergoes single electron reduction and decarboxylation to generate an alkyl radical that couples with the pyridine ring for the C2 alkylated product.⁵⁷ Starting with oxidized pyridine makes this alkylation a redox neutral process.

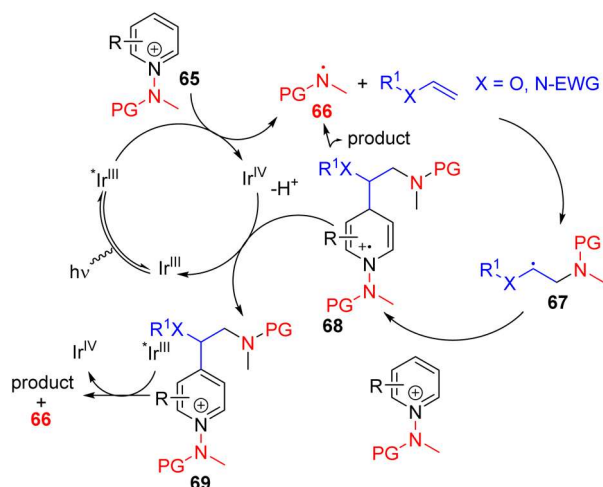
In 2021, the Hong group discovered that an *O*-aryl oxime pyridinium salt with a photoactive aryloxy group (59) homolytically cleaves under visible light. The generated imine radical (60) undergoes 1,6-intramolecular HAT to form the carbon radical 62, which was added intramolecularly to the pyridinium. The resulting intermediate (63) loses a proton and subsequently oxidizes with an aryloxy radical (61) to form the C2 alkylated pyridinium intermediate 64. Finally, the base mediated C–N bond cleavage led to the alkyl pyridine product (Scheme 29).⁵⁸

Hong, Baik, and co-workers later utilized the *N*-aminopyridinium salt 65 in which the amino group acts as both the activator of pyridine and a radical reagent for β -aminoalkylation of pyridines (Scheme 30). The reaction starts with an electron-deficient aminopyridinium salt (65) undergoing single electron reduction *via* a photoredox catalyst under visible light.

The resulting intermediate gives rise to pyridine after the expulsion of the amine radical 66. The electrophilic amine radical adds to an electron rich alkene, and the resulting



Scheme 29 Intramolecular C2 alkylation of the photoactive *O*-aryl oxime pyridinium salt.

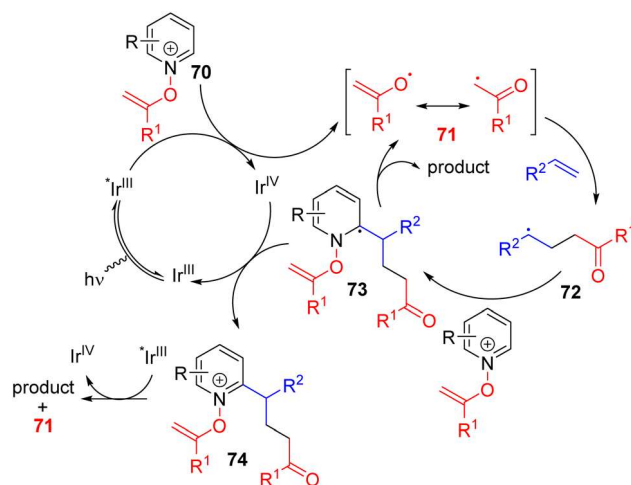


Scheme 30 *N*-Aminopyridinium as a pyridine activator and radical generator for photoredox C4 alkylation.

nucleophilic alkyl radical (67) attacks the electrophilic C4 position of another pyridinium salt. This radical cation adduct (68) led to the product after deprotonation and expulsion of the amine radical for a radical chain reaction.⁵⁹ Alternatively, intermediate 68 could be oxidized by Ir(IV) to form intermediate 69. Photocatalytic reduction of 69 by excited Ir(III) led to product formation with the regeneration of an amine radical for reaction progression. The C4 selectivity observed was proposed on the basis of the steric hindrance at C2.

The Hong group continued their dual activation and alkylating reagent strategy with other activators for photoredox functionalization. In 2020, they reported C2 and C4 alkylation using *N*-alkenoxy pyridinium salts and alkenes (Scheme 31).⁶⁰ The pyridinium salts were synthesized from pyridine *N*-oxide and terminal alkyne, which acts as a bifunctional reagent.

In 2020, the Hong group used a similar strategy for radical three-component coupling to obtain C4 β -trifluoromethyl alkyl



Scheme 31 *N*-Alkenoxy pyridinium as a pyridine activator and acyl radical generator for photoredox C2 alkylation.

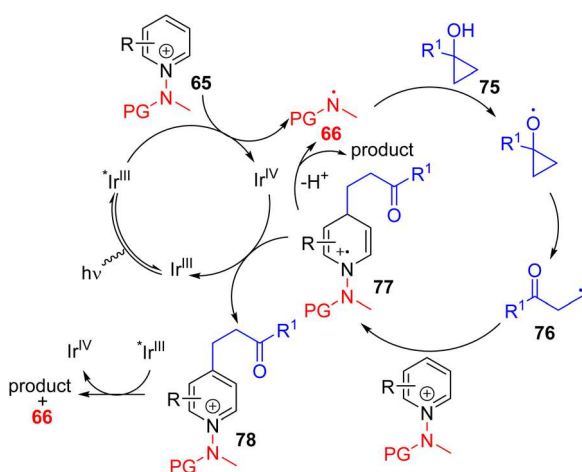
pyridines and quinolines. Trifluoromethanesulfonic anhydride was used to activate pyridine, which undergoes single electron reduction by photoexcited eosin Y. The reduced form generates a trifluoromethane radical after the removal of pyridine and SO₂. The CF₃ radical was added to the alkene, and the following nucleophilic radical was added to another pyridinium triflate.⁶¹

In 2022, the Hong group utilized the *N*-aminopyridinium salt **65** to generate the amine radical **66** that undergoes HAT with alcohol **75** to generate an alkyl radical coupling partner (**76**). The generated alkyl radical was added to another pyridinium salt. The resulting intermediate (**77**) was proposed to oxidize by the oxidized photocatalyst (Ir^{IV}) for the formation of a C4 alkylated pyridinium salt (**78**). This salt undergoes reductive elimination to form the amine radical **66** and the final product.⁶² The scope of the reaction is broad, with a variety of functional groups shown to be tolerated (Scheme 32).

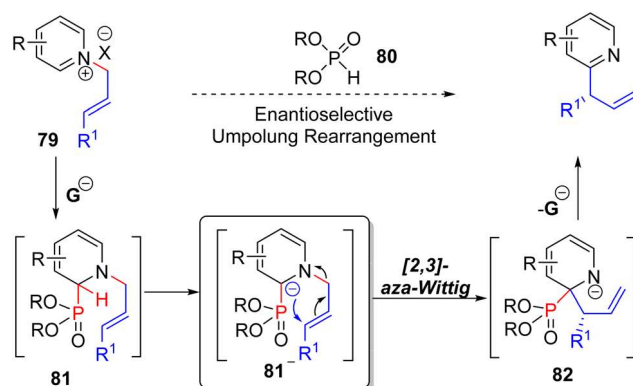
Maity's research group, in 2019, developed a phosphite catalysed C2 allylation strategy starting with an *N*-allylpyridinium salt (**79**).⁶³ The *N*-allylation activated the pyridine ring for phosphite catalyst (**80**) addition at C2 to form adduct **81**. The subsequent base mediated [2,3] aza-Wittig rearrangement of anionic **81** transferred the allyl group from nitrogen to C2 (**82**).

The anionic nitrogen intermediate **82** releases the catalyst to form branched allyl pyridines. The use of chiral TADDOL-based phosphite led to high enantioselective product formation. Using this methodology, isoquinoline, quinoline, and 4-substituted pyridine substrates successfully formed branched allylation products (Scheme 33). The enantioselectivities were very good for most of the substrates, including fully substituted terminal alkene substrates to all-carbon quaternary centers.

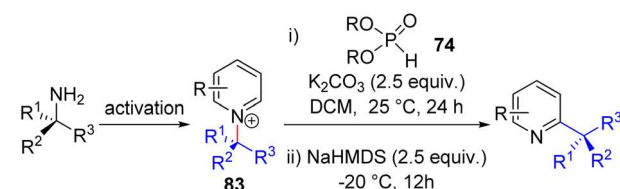
In 2021, they followed up with the phosphite catalysed C–H alkylation of pyridines (Scheme 34). The *N*-alkylpyridiniums (**83**) were synthesized from the Zincke salt and amine, and a base-mediated protocol similar to their allylation method gave



Scheme 32 *N*-Aminopyridinium as a pyridine activator and HAT reagent for photoredox C4 alkylation.



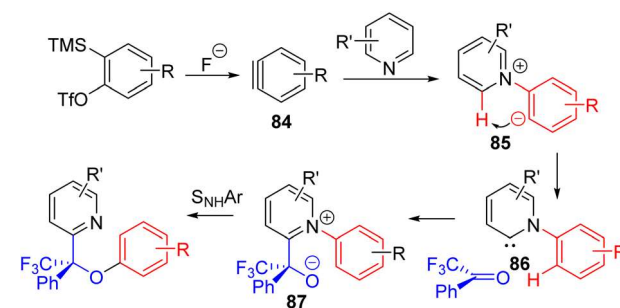
Scheme 33 *N*-Allylpyridinium as a pyridine activator and branched C2-allylation reagent.



Scheme 34 *N*-Alkylpyridinium as a pyridine activator and d C2 and C4 alkylation reagent.

alkylpyridines. The tandem [1,2] aza-Wittig rearrangement proceeded *via* solvent-caged radical pair formation and predominantly intramolecular recombination to product formation. As a result, the reaction starting with a chiral amine led to the chiral product with high stereoretention. The stereoretention is solvent dependent, and a racemic starting material with a chiral phosphite catalyst in THF led to the establishment of a catalytic enantioselective version.⁶⁴ Pyridines with both C2 and C4 positions free for catalyst addition led to minor C4 alkylated products along with major C2 alkylpyridines.

The Biju group developed a unique three-component strategy using reactive aryne to functionalize C2–H of pyridine (Scheme 35). The pyridine nitrogen donates electron pairs to aryne (**84**), and the following anion of the zwitterion (**85**) was



Scheme 35 Pyridine C–H functionalization *via* aryne three-component coupling.

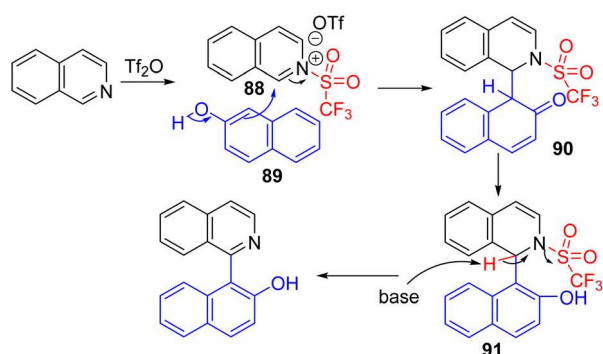
proposed to abstract C2–H to generate carbene species **86**. The nucleophilic carbene reacts with the carbonyl compounds, followed by intramolecular S_NAr for overall C2 functionalization.⁶⁵ The method was shown to be applicable to pyridines and electron-rich pyridines.

3. Functionalization *via* a sacrificial activator

The dual role of the pyridine activator in C–H activation is elegant but not applicable to all functionalization types. A mild and general approach is to quaternize the pyridine nitrogen to make it a better electrophile. After nucleophile addition, the C–H and the group on nitrogen have to leave to regenerate the pyridine ring. If the activator becomes a good leaving group upon the addition of nucleophiles, then base-mediated E2 elimination reinstalls the pyridine core. The success of this approach depends on selective nucleophile addition to C2 or C4 carbon rather than the electrophilic center of the activator. In the case of certain nucleophiles, such as amines, ring-opening product formation could dominate over the C–H functionalization path. The oxidation of pyridine to its *N*-oxide, followed by its activation with an activator enjoys a better outcome due to its less electrophilicity and better leavability, but suffers from step and atom economy. Additionally, functional groups on pyridine prone to oxidative decomposition are not compatible. A variety of functionalization dependent activators starting from pyridine *N*-oxide have been developed and reviewed recently.⁶⁶

The Corey group reported triflic anhydride as a direct activator, but the efficiencies highly depend on the nature of the nucleophile. For example, electron-rich aromatics as nucleophiles gave moderate to good yields for intermediate formation, but cyanide resulted in a poor yield. The nucleophile-added intermediate to product formation was achieved *via* a *t*-BuOK base in DMSO with quantitative yields.⁶⁷

Following Corey's lead, Tan, Li, and co-workers used triflic anhydride as the activator and β -naphthol (**89**) as a nucleophile to obtain C2 arylation of isoquinolines (Scheme 36). The tauto-



Scheme 36 Triflic anhydride activation for nucleophilic arylation of isoquinoline with β -naphthols.

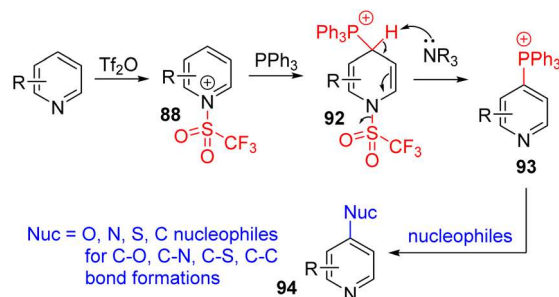
merization of β -naphthol after nucleophilic addition and *in situ* K_2CO_3 mediated triflic acid removal gave the final product in good yields.⁶⁸

The Anders group in 1987 reported that pyridine was converted to 4-phosphonium or 2,4-diphosphonium salts upon treatment with triflic anhydride and triphenylphosphine in the presence of trimethylamine base.⁶⁹ In 2016, the McNally group re-examined the triphenylphosphonium pyridine (**93**) synthesis.⁷⁰ They found that the *N*-triflyl salt undergoes a selective C4 nucleophilic addition to differently substituted pyridines. The choice of the solvent and organic base for subsequent base-mediated triflic acid removal was important to obtain good results. The phosphonium substitution occurred at C2 when the C4 position was blocked. McNally and co-workers studied the subsequent transformations of this phosphonium pyridine **93** for various C–C and C–heteroatom bond formations at the pyridine C4 position (**94**). In their 2016 report, they treated the phosphonium salt with alcohols in the presence of sodium hydride, which led to the formation of C4 alkoxy pyridines. The substitution of other nucleophiles, such as sulfur, nitrogen, and halides, was reported subsequently (Scheme 37).⁷¹

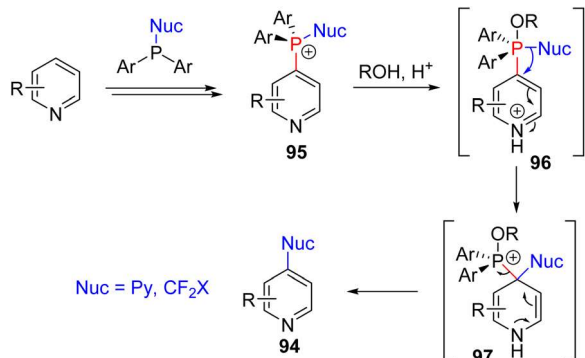
The mechanistic examination of the nucleophilic substitution reactions of phosphonium pyridine revealed that the reaction proceeds *via* the P(v) intermediate **96** rather than direct S_NAr substitution for most nucleophiles.^{71d,e} Cross-coupling from P(v) was proposed for product formation, similar to transition metal cross-coupling reactions. With that knowledge, they continued their exploration with phosphonium containing a nucleophile (**95**) for intramolecular coupling. The suitable second nucleophile, less prone to cross-coupling, assisted the intramolecular cross-coupling product *via* the P(v) intermediate. Heteroaryl and fluoroalkyl nucleophiles were shown to be effective (Scheme 38).⁷²

In 2018, they reported the carbonate assisted incorporation of deuterium and tritium at C4 of pyridine *via* the intermediate of C4 phosphonium **93** (Scheme 39).⁷³ The carbonate is a poor nucleophile for cross-coupling, and the expulsion of CO_2 from carbonate-bound phosphonium **98** led to strong P=O mediated electrophilic substitution.

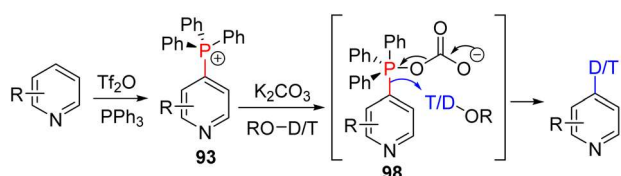
The Manolikakes group used triflic anhydride as the pyridine activating group, followed by the addition of sulfinate salt



Scheme 37 Triflic anhydride activation C4 phosphonium salts for their subsequent functionalization.



Scheme 38 Nucleophilic substitution of pyridine phosphonium via phosphorus ligand couplings.

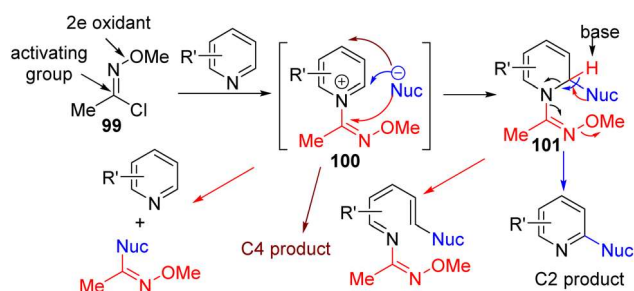


Scheme 39 Carbonate assisted electrophilic substitution of pyridine phosphonium with deuterium and tritium.

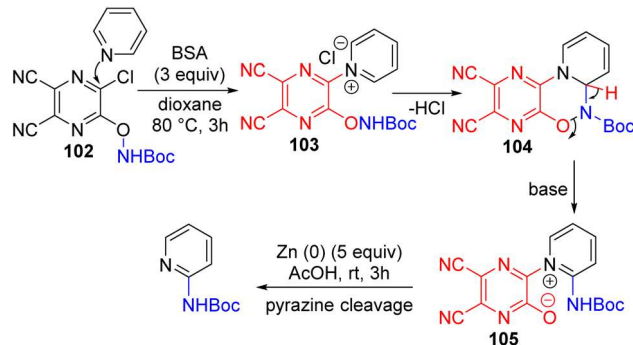
and base-mediated elimination of triflic acid for C–H sulfonylation. In their first publication, they achieved moderate selectivity for C4 functionalization over C2 with DABCO as the base. In a subsequent report, *N*-methypiperidine as a base led to improved regiocontrol for C4 sulfonylation. They proposed that a base lone pair interacts with the electrophilic pyridinium intermediate and therefore has an additional role in controlling the regioselectivity of nucleophilic addition.⁷⁴

In 2017, Fier developed chlorooxime **99** as an *in situ* activator for C–H functionalization with nucleophiles at C2.⁷⁵ The chlorooxime is generally good with the cyanide nucleophile but gave poor results with oxygen and carbon nucleophiles (Scheme 40). Amine as a nucleophile did not produce the required product.

The Fier group came up with an explanation for the poor yields or no product formation with certain nucleophiles.



Scheme 40 Chlorooxime activating group for direct pyridine C2–H functionalization with nucleophiles.

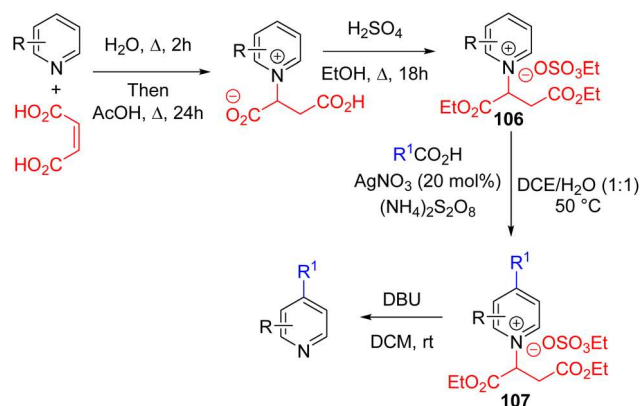


Scheme 41 A multifunctional pyridine activating group with a nucleophile for C2–H amination of pyridines.

They subsequently developed a bifunctional activator **102** that contains the amine nucleophile in it for effective C2 amination (Scheme 41).⁷⁶

The Phil Baran group in 2021 reported C4 selective Minisci-type alkylation with a stable *N*-alkyl salt (**106**) derived from fumaric acid. Its subsequent Minisci reaction with a carboxylic acid in the presence of a silver nitrate catalyst and ammonium persulfate oxidant gave the C4 alkylated pyridinium salt **107**. The *N*-alkyl group was removed under ambient conditions by treating it with excess DBU in dichloromethane to form the final product (Scheme 42).^{77a} The already activated pyridinium salt (**106**) does not require typical acid activation for the Minisci reaction.

Following the lead from Baran's work, the Noel group utilized the same activator for the radical C4 alkylation of pyridines with alkane as the radical source.^{77b} Benzophenone under 365 nm light irradiation acts as a HAT catalyst for alkane C–H abstraction to form the alkyl radical. The rest of the catalytic cycle is identical to that of Baran's work. The Noel group developed a continuous-flow process for the synthesis of alkylated pyridine from the pyridinium salt **106** in a single set-up. In 2022, Zhang, Yang, and co-workers used redox active *N*-(acyloxy)phthalimides as the radical coupling partner for the



Scheme 42 A Minisci-type C4 alkylation from fumaric acid derived *N*-alkylpyridinium salt.

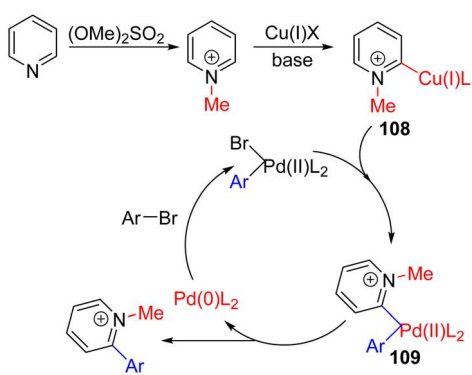
alkylation of **106** using photoredox catalysis under oxidant free conditions.^{77c}

Chen, Fu, and co-workers reported the mono- and di-arylation of *N*-methylated pyridinium using copper and palladium catalysis. All the reagents, including methylating reagents, aryl bromide coupling partners, and catalysts, were added together with the pyridine and carbonate base for a one-pot process. The reaction was carried out in dimethylacetamide solvent at 150 °C.

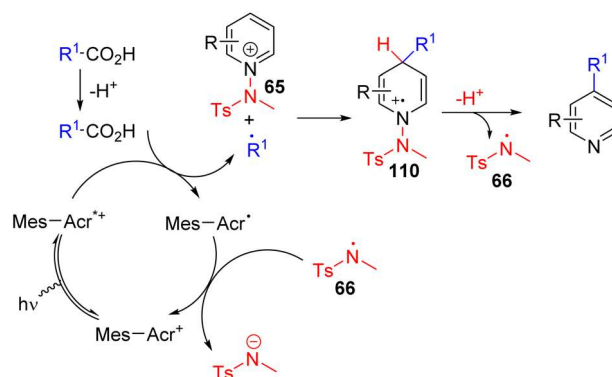
In a subsequent report, Fu, Zheng, and co-workers conducted a detailed computational and experimental study to provide a plausible mechanism (Scheme 43).⁷⁸ Initial *N*-methylation of pyridine activates it for C2–H insertion by the copper catalyst (**108**). In parallel, the oxidative insertion of palladium into aryl bromide generated an arylpalladium(II) intermediate. *trans*-Metallation of pyridyl from copper to palladium to **109**, followed by its reductive elimination formed the C2 arylated *N*-methylpyridinium intermediate. The demethylation also occurred under the reaction conditions *via* S_N2 demethylation with a methyl sulfonate counter anion. The stoichiometry of aryl halide led to either mono or 2,6-diaryl pyridine formation.

Hong and co-workers, in 2022, started with a sacrificial amine activator on pyridine (**65**) for its decarboxylative alkylation with carboxylic acid.^{79a} The photoexcited acridinium oxidized the carboxylic acid to generate an alkyl radical. The alkyl radical reacts with activated aminopyridinium salt (**65**). The corresponding intermediate **110** loses a proton and amine radical (**66**) to yield the 4-alkylated pyridine product. The amine radical **66** undergoes single electron reduction with the reduced photocatalyst to regenerate acridinium (Scheme 44).

Zhang, Neu, and co-workers found that *N*-methoxy pyridinium salts can form an EDA complex with alkyl sulfoxide in the presence of potassium fluoride. The 455 nm light irradiation of LED light to this EDA complex led to methoxy radical formation, which reacts with an alkyl sulfoxide to form an alkyl radical and sulfinate by-product. The following reaction of the alkyl radical with the *N*-methoxy pyridinium salt gave C2 alkylated pyridine with methoxy radical generation for the radical chain reaction.^{79b} In 2021, Zipse, Renaud, and



Scheme 43 Copper and palladium catalysed mono- and di-arylation of methylpyridinium salt.

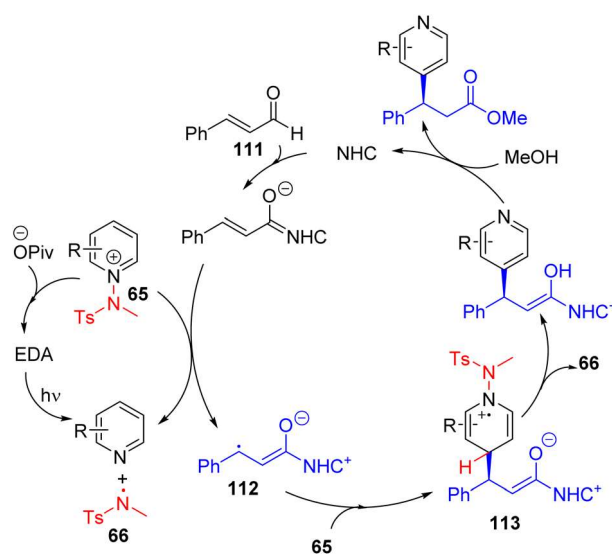


Scheme 44 Photocatalytic decarboxylative alkylation of *N*-aminopyridinium salt.

co-workers reported alkyl radical addition to *N*-methoxy pyridinium salts for C2 alkylated pyridine formation.^{79c}

In 2022, the Hong group utilized the same sacrificial activator for asymmetric C4 alkylation with chiral NHC catalysis under blue light irradiation (Scheme 45).⁸⁰ Sodium pivalate hydrate was used as an additive, and forms an EDA complex with the aminopyridinium salt (**65**) that could generate an amine radical (**66**). The NHC added intermediate of enal (**111**) undergoes single electron oxidation with **65** to form radical intermediate **112**. The reaction of **112** with activated pyridine **65** formed **103**, and the elimination of the proton and amine radical from it resulted in the final product. The chiral NHC catalyst determines the stereochemistry.

When the *N*-activating group is not a good leaving group, oxidation of the corresponding *N*-substituted dihydropyridine is required. For example, the acyl activation of pyridine allows soft organocuprate and silylcuprate to add under mild conditions with C4 selectivity. The corresponding intermediate is stable, and oxidation with elemental sulfur in boiling toluene



Scheme 45 Enantioselective C4 functionalization of *N*-aminopyridinium salts *via* NHC catalysis.

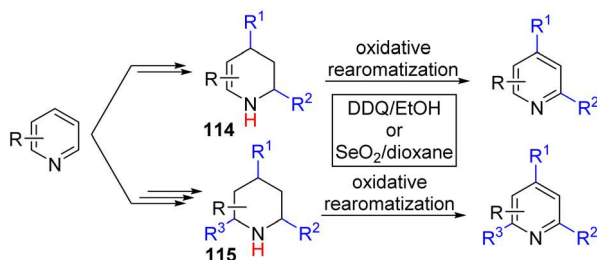
was required for the oxidation and removal of *N*-acyl to C4 functionalized pyridines.⁸¹

Kanai, Kuninobu, and co-workers showed that a stoichiometric amount of triarylborane Lewis acid could activate the pyridines for nucleophilic addition by trifluoroalkylsilanes. The corresponding intermediate was shown to be oxidized with different oxidants for trifluoroalkylpyridines. In 2023, the Lakhdar group reported that $\text{BF}_3 \cdot \text{OEt}_2$ can be a compatible stoichiometric activator for C2 and C4 phosphonation of pyridines with phosphites. Chloronil was used as the subsequent oxidant.⁸²

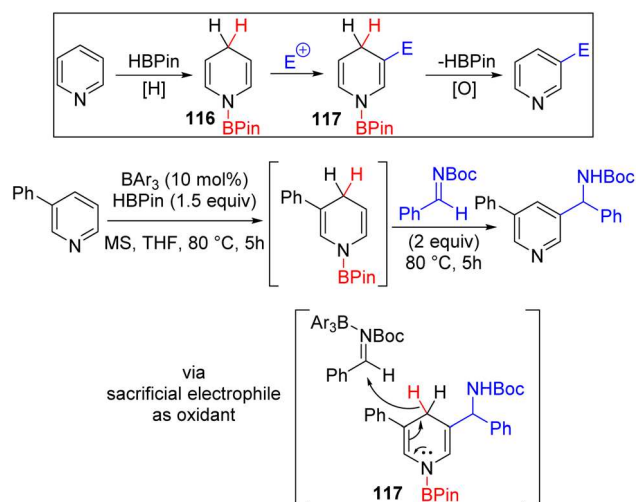
The Wang group, in 2022, disclosed an overall double and triple nucleophile substitution in a stepwise fashion (Scheme 46).⁸³

Initial activation of pyridine with stoichiometric $\text{BF}_3 \cdot \text{OEt}_2$ and Grignard addition led to the formation of 4-substituted dihydropyridine. Then dihydropyridine was treated with trifluoroacetic acid for the formation of enamine-iminium, and trapping the iminium with an *N*-substituted indole for the formation of C2 added tetrahydropyridine intermediate (**114**). The authors established that DDQ oxidation of tetrahydropyridine could double oxidize it back to 2,4-substituted pyridines. With excess TFA and indole, the other enamine can also react similarly to form a 2,4,6-trifunctionalized piperidine intermediate (**115**). The piperidine intermediate was also oxidized with DDQ to generate trisubstituted pyridines.

The C2/C4 C–H functionalization of pyridine predominates over C3, which remains difficult to achieve. The Lewis acid catalysed hydroboration and hydrosilylation of pyridines were known and generally functionalized further for substituted tetrahydropyridine or piperidine synthesis.⁸⁴ Wang and co-workers utilized the nucleophilic reactivity of 1,4-dihydropyridine to react it with an electrophile and subsequent oxidative aromatization for the formation of C3 functionalized pyridines (Scheme 47).⁸⁵ The one-pot tandem reaction sequence was conducted sequentially to avoid the reduction of the electrophile rather than the pyridine itself and the oxidation of dihydropyridine in the last step rather than borane. The mechanistic studies reveal that the triarylborane Lewis acid catalyses both the hydroboration of pyridine and its subsequent reaction with the imine and ketone electrophile. The initial hydroboration is reversible, and thermodynamic equilibrium was reached between 1,2- and 1,4-dihydropyridines. Since 1,2-dihydropyridines are also nucleophilic at C3 and C5 positions, they



Scheme 46 Double and triple functionalization of pyridine via sequential functionalization and final oxidative aromatization.



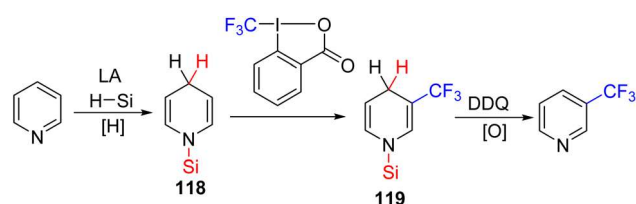
Scheme 47 Lewis acid catalysed HBpin mediated C3 functionalization of pyridines with C=X electrophiles.

can also react with the electrophile to generate C3 functionalized pyridines. Two equivalent electrophiles were used, where the second equivalent oxidized the C3 functionalized dihydropyridine **117** to the product. C4 substituted pyridines did not work with imines and ketones, although initial hydroboration led to 1,2-dihydropyridine. The authors suspect that steric hindrance might be the reason for this failure, and a smaller and stronger iminium electrophile led to successful C3 substitution.

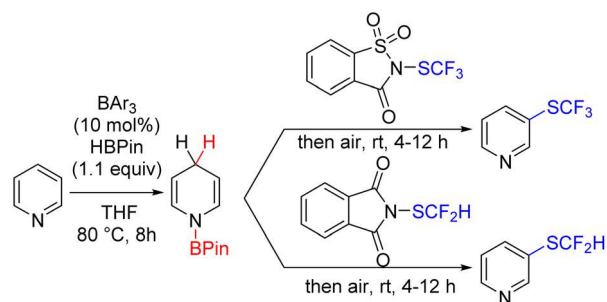
The Kuninobu group developed the C3 trifluoromethylation of pyridines using reduction to dihydropyridine **118**, followed by reacting it with an electrophilic trifluoromethylating reagent for C3 functionalization (**119**). Finally, oxidation of the C3 functionalized dihydropyridine **119** led to the formation of the product.⁸⁶ The whole sequence was achieved in a single-pot reaction with a single solvent (Scheme 48).

Wang's group reported a conceptually similar approach for C3 fluorothiolation. The reaction is versatile for mono- and difunctionalization of a variety of pyridine, quinoline, and isoquinoline derivatives (Scheme 49).⁸⁷

In 2023, Wang, Xu, and co-workers reported C3 cyanation with an electrophilic cyanation reagent following similar tandem processes.^{88a} In this case, most of the electrophilic cyanation reagents failed to give good yields. The authors reasoned that the oxidizing power of the cyanation reagent could oxidize the dihydropyridine intermediate rather than



Scheme 48 Lewis acid catalysed silane mediated C3 trifluoromethylation of pyridines with a DDQ oxidant.

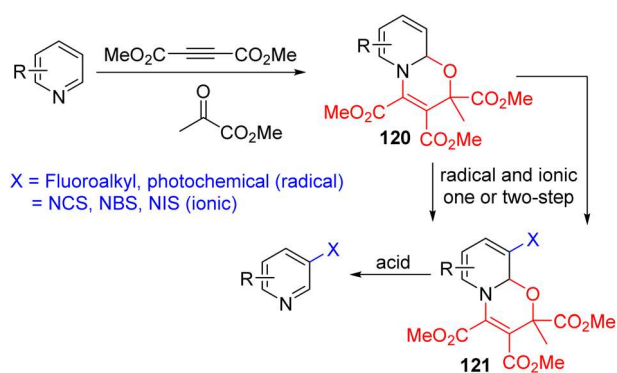


Scheme 49 Lewis acid catalysed hydroborane mediated C3 fluorothiolation of pyridines under aerobic oxidation.

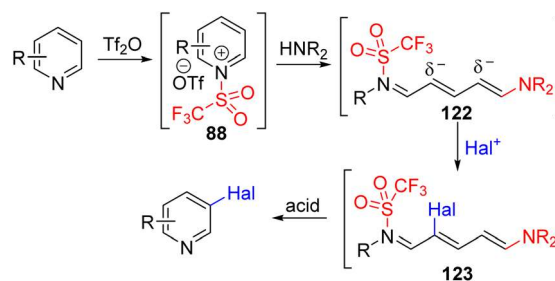
provide “CN⁺”. To circumvent this problem, they screened a variety of reagents and the reaction with 2,2-bis-(4-cyanatophenyl) propane with the lowest oxidation potential led to good results. The final oxidation of cyano-substituted dihydropyridine was achieved with DIAD. A large variety of 3-cyano products were formed from substituted pyridine, quinoline, and isoquinolines.

Very recently, the Wang group developed a dual catalysis mode to form asymmetric C3 allylation of pyridines.^{88b} Their BAR₃ catalysed hydroboration forms **116**, as reported earlier. In this report, they found that the nucleophilic **116** can react with an Ir- π -allyl electrophile to form C3 allylated dihydropyridine **117**. The crude reaction mixture was stirred under air at room temperature, which oxidized the intermediate to the pyridine product. The well-developed chiral BINOL derived phosphoramidate ligand on iridium induces high enantioselectivity in the product.

In 2022, both the Studer group and McNally, Paton, and co-workers separately came up with their redox neutral strategies, which avoid the reductive dearomatization–oxidative rearomatization protocol. The Studer group used the three-component coupling of pyridines with dimethyl acetylenedicarboxylate (DMAD) and methyl pyruvate (MP) to form an oxazinopyridine intermediate (**120**).⁸⁹ This intermediate, **120**, behaves as a dienamine and reacts with ionic and radical electrophiles. The C3 functionalized intermediate **121** could be converted back to the C3 functionalized pyridine under acidic removal of activating groups (Scheme 50). This protocol used fluoroalkyl



Scheme 50 Pyridine activation and its radical and ionic C3 functionalization.



Scheme 51 Triflic anhydride mediated C3 halogenation of pyridines via a Zincke imine intermediate.

iodides for fluoroalkylation under blue light irradiation. The electron-rich oxazinopyridine (**120**) forms an EDA complex with electron-deficient iodide, which initiates radical functionalization.

Additionally, ionic electrophilic halogenation with NCS, NBS, and NIS led to the C3 halogenation product. Functionalization at C3 and C5 of the dienamine-type intermediate is feasible, and the sequential addition of different electrophiles led to the formation of a regioselective difunctionalization product.

McNally and co-workers utilized the Zincke salt ring opening type reactivity of pyridinium with an amine to generate an electron-rich acyclic intermediate.⁹⁰ They reacted pyridine with triflic anhydride to pyridinium salt and treated it with a secondary amine to the ring opening intermediate (**122**). The ring-opening intermediate is electron-rich and reacts with NCS, NBS, and NIS for its halogenation at C3 and/or C5 positions. The removal of triflate from nitrogen and ring-closure were achieved under acidic conditions to reinstall the pyridine ring with 3 and 3,5-disubstitution (Scheme 51). Like the Studer approach, sequential electrophilic substitution led to the formation of regioisomeric dihalogenation product.

4. Conclusions

In this review, we classified various types of pyridine C–H activation modes. Owing to its electro-deficient nature and coordination ability, S_EAr at C3 occurred only at higher temperatures with a limited scope. S_NAr for C–H activation requires hydride as a leaving group and, although discovered a century ago, it did not find widespread application. Transition metal catalysed C–H functionalization of pyridine is generally difficult compared to other aryl C–H functionalizations. Lanthanide complexes turned out to be very effective for pyridine C2–H activation. A combination of dual Lewis acid-transition metal catalysis was recently developed for effective and regioselective C–H activation. Catalytic or stoichiometric pyridine nitrogen activation is the most common and efficient approach for its C–H reactivity. The choice of ligands and metals proved effective in functionalizing all 2, 3, and 4 positions regioselectively. The radical reaction in line with the Minisci reaction, or with activated pyridinium substrates, became one of the most

frequently used techniques for various C2 and C4 functionalizations. Many pyridine activating functional groups were chosen that act as dual reagents for activation, followed by subsequent functionalization. Very recently, the conversion of pyridine to dihydropyridine, followed by its C3 functionalization and rearomatization, led to overall C3 functionalization. Significant progress has been made in the last five years, and it is expected to grow faster owing to the importance of functionalized pyridines.

Author contributions

Susmita Maity, Asish Bera, and Ayantika Bhattacharjya researched the relevant papers. Susmita drafted the direct functionalization part, Asish drafted the functionalization *via* the dual activator and reactive partner part, and Ayantika drafted the part on functionalization *via* sacrificial activators. Pradip Maity: conceptualization, resources, supervision, funding acquisition, and writing – review & editing.

Conflicts of interest

There are no conflicts to declare.

Acknowledgements

This research was supported by the SERB (CRG/2019/001065 and SCP/2022/000465). Susmita and Ayantika thank the SERB for a fellowship and Asish thanks the CSIR for a fellowship. We greatly acknowledge the CSIR-NCL for providing infrastructure facilities.

References

- 1 E. Vitaku, D. T. Smith and J. T. Njardarson, *J. Med. Chem.*, 2014, **57**, 10257–11027.
- 2 S. Pal, *Pyridine*, 2018, ch. 5, ISBN 978-1-78923-423-7. DOI: [10.5772/intechopen.76986](https://doi.org/10.5772/intechopen.76986).
- 3 (a) P. Patil, S. P. Sethy, T. Sameera and K. Shailaja, *Asian J. Res. Chem.*, 2013, **6**, 888–899; (b) D. O'Hagan, *Nat. Prod. Rep.*, 2000, **17**, 435–446.
- 4 R. Gujjarappa, N. Vodnala and C. C. Malakar, *ChemistrySelect*, 2020, **5**, 8745–8758.
- 5 S. Shimizu, N. Watanabe, T. Kataoka, T. Shoji, N. Abe, S. Morishita and H. Ichimura, *Pyridine and Pyridine Derivatives*, *Ullmann's Encyclopedia of Industrial Chemistry*, Wiley-VCH, Weinheim, 2000.
- 6 (a) A. V. Gulevich, A. S. Dudnik, N. Chernyak and V. Gevorgyan, *Chem. Rev.*, 2013, **113**(5), 3084–3213; (b) C. Allais, J. M. Grassot, J. Rodriguez and T. Constantieux, *Chem. Rev.*, 2014, **114**(21), 10829–10868; (c) K. Murakami, S. Yamada, T. Kaneda and K. Itami, *Chem. Rev.*, 2017, **117**, 9302–9332; (d) X. L. Liu, L. B. Jiang, M. P. Luo, Z. Ren and S. G. Wang, *Org. Chem. Front.*, 2022, **9**, 265–280.
- 7 (a) H. M. L. Davies, J. Du Bois and J. Q. Yu, *Chem. Soc. Rev.*, 2011, **40**, 1855–1856; (b) L. Guillemard, N. Kaplaneris, L. Ackermann and M. J. Johansson, *Nat. Rev. Chem.*, 2021, **5**, 522–545.
- 8 (a) D. E. Pearson, W. W. H. Judith, K. T. Chaw and B. R. Suthers, *J. Org. Chem.*, 1961, **26**, 789–792; (b) L. I. Belen'kii, *Chem. Heterocycl. Compd.*, 1986, **22**, 587–608.
- 9 S. H. Wunderlich and P. Knochel, *Angew. Chem., Int. Ed.*, 2007, **46**, 7685.
- 10 (a) L. Davin, W. Clegg, A. R. Kennedy, M. R. Probert, R. McLellan and E. Hevia, *Chem. – Eur. J.*, 2018, **24**, 14830–14835; (b) M. Balkenhohl, H. Jangra, I. S. Makarov, S.-M. Yang, H. Zipse and P. Knochel, *Angew. Chem., Int. Ed.*, 2020, **59**, 14992–14999.
- 11 A. E. Chichibabin and O. A. Zeide, *J. Russ. Phys.-Chem. Soc.*, 1914, **46**, 1216–1236.
- 12 Y. Wang, R. Li, W. Guan, Y. Li, X. Li, J. Yin, G. Zhang, Q. Zhang, T. Xiong and Q. Zhang, *Chem. Sci.*, 2020, **11**, 11554–11561.
- 13 P. S. Fier and J. F. Hartwig, *Science*, 2013, **342**, 956–960.
- 14 Y. Gu, Y. Shen, C. Zarate and R. Martin, *J. Am. Chem. Soc.*, 2019, **141**, 127–132.
- 15 C. Obradors and B. List, *J. Am. Chem. Soc.*, 2021, **143**, 6817–6822.
- 16 Q. Chen, X. M. Jourdin and P. Knochel, *J. Am. Chem. Soc.*, 2013, **135**, 4958–4961.
- 17 F. Minisci, R. Bernardi, F. Bertini, R. Galli and M. Perchinnamo, *Tetrahedron*, 1971, **27**, 3575–3579.
- 18 F. Minisci, E. Vismara, F. Fontana, G. Morini, M. Serravalle and C. Giordano, *J. Org. Chem.*, 1986, **51**, 4411–4416.
- 19 R. S. J. Proctor and R. J. Phipps, *Angew. Chem., Int. Ed.*, 2019, **58**, 13666–13699.
- 20 C. Wu, T. Ying, H. Fan, C. Hu, W. Su and J. Yu, *Org. Lett.*, 2023, **25**, 2531–2536.
- 21 J. Jin and D. W. C. MacMillan, *Nature*, 2015, **525**, 87–90.
- 22 W. Liu, X. Yang, Z. Z. Zhou and C. J. Li, *Chem*, 2017, **2**, 688–702.
- 23 B. Bieszczad, L. A. Perego and P. Melchiorre, *Angew. Chem., Int. Ed.*, 2019, **58**, 16878–16883.
- 24 S. P. Pitre, M. Muuronen, D. A. Fishman and L. E. Overman, *ACS Catal.*, 2019, **9**, 3413–3418.
- 25 (a) M. G. Braun, G. Castanedo, L. Qin, P. Salvo and S. Z. Zard, *Org. Lett.*, 2017, **19**(15), 4090–4093; (b) V. L. Revil-Baudard, J. P. Vors and S. Z. Zard, *Org. Lett.*, 2018, **20**(12), 3531–3535.
- 26 (a) X. Y. Zhang, W. Z. Weng, H. Liang, H. Yang and B. Zhang, *Org. Lett.*, 2018, **20**, 4686–4690; (b) J. M. Anderson, N. D. Measom, J. A. Murphy and D. L. Poole, *Org. Lett.*, 2023, **25**, 2053–2057.
- 27 (a) J. Xu, C. Liang, J. Shen, Q. Chen, W. Li and P. Zhang, *Green Chem.*, 2023, **25**, 1975–1981; (b) S. Xu, W. Zhang, C. Li, Y. Li, H. Zeng, Y. Wang, Y. Zhang and D. Niu, *Angew. Chem., Int. Ed.*, 2023, **62**, e202218303.

- 28 L. Zhang and Z. Q. Liu, *Org. Lett.*, 2017, **19**, 6594–6597.
- 29 (a) B. Liang, Q. Wang and Z. Q. Liu, *Org. Lett.*, 2017, **19**, 6463–6465; (b) Z. Liu and Z. Q. Liu, *Org. Lett.*, 2017, **19**, 5649–5652; (c) C. Wang, S. Song, Z. Chen, D. Shen, Z. Wang, J. Zhou, J. Guo and J. Li, *J. Org. Chem.*, 2022, **87**, 16794–16806.
- 30 K. Liao, F. Wu, J. Chen and Y. Huang, *Cell Rep. Phys. Sci.*, 2022, **3**, 100763.
- 31 A. Ghosh, P. Pyne, S. Ghosh, D. Ghosh, S. Majumdar and A. Hazra, *Green Chem.*, 2022, **24**, 3056–3080.
- 32 (a) J. Jin and D. W. C. MacMillan, *Angew. Chem., Int. Ed.*, 2015, **54**, 1565; (b) N. Okugawa, K. Moriyama and H. Togo, *J. Org. Chem.*, 2017, **82**, 170–178.
- 33 C. Bosset, H. Beucher, G. Bretel, E. Pasquier, L. Queguiner, C. Henry, A. Vos, J. P. Edwards, L. Meerpoel and D. Berthelot, *Org. Lett.*, 2018, **20**, 6003–6006.
- 34 E. L. Saux, E. Georgiou, I. A. Dmitriev, W. C. Hartley and P. Melchiorre, *J. Am. Chem. Soc.*, 2023, **145**, 47–52.
- 35 (a) K. J. Kim, T. Constantin, M. Simonetti, J. Llaveria, N. S. Sheikh and D. Leonori, *Nature*, 2021, **595**, 677–683; (b) A. Basak, S. Karak and R. Banerjee, *J. Am. Chem. Soc.*, 2023, **145**, 7592–7599.
- 36 G. Q. Sun, P. Yu, W. Zhang, Y. Wang, L. L. Liao, Z. Zhang, L. Li, Z. Lu, D. G. Yu and S. Lin, *Nature*, 2023, **615**, 67–73.
- 37 (a) R. S. J. Proctor, H. J. Davis and R. J. Phipps, *Science*, 2018, **360**, 419–422; (b) R. S. J. Proctor, P. Chuentragool, A. C. Colgan and R. J. Phipps, *J. Am. Chem. Soc.*, 2021, **143**, 4928–4934.
- 38 X. Liu, Y. Liu, G. Chai, B. Qiao, X. Zhao and Z. Jiang, *Org. Lett.*, 2018, **20**, 6298–6301.
- 39 A. C. Colgan, R. S. J. Proctor, D. C. Gibson, P. Chuentragool, A. S. K. Lahdenpera, K. Ermanis and R. J. Phipps, *Angew. Chem., Int. Ed.*, 2022, **61**, e202200266.
- 40 M. P. Luo, Y. J. Gu and S. G. Wang, *Chem. Sci.*, 2023, **14**, 251–256.
- 41 R. F. Jordan and D. F. Taylor, *J. Am. Chem. Soc.*, 1989, **111**, 778–779.
- 42 (a) S. Rodewald and R. F. Jordan, *J. Am. Chem. Soc.*, 1994, **116**, 4491–4492; (b) B. T. Guan and Z. Hou, *J. Am. Chem. Soc.*, 2011, **133**, 18086–18089; (c) G. Song, W. N. O. Wylie and Z. Hou, *J. Am. Chem. Soc.*, 2014, **136**, 12209–12212.
- 43 R. Grigg and V. Savic, *Tetrahedron Lett.*, 1997, **38**, 5737–5740.
- 44 J. O. Rothbaum, A. Motta, Y. Kratish and T. J. Marks, *J. Am. Chem. Soc.*, 2022, **144**, 17086–17096.
- 45 Y. Luo, S. Jiang and X. Xu, *Angew. Chem., Int. Ed.*, 2022, **61**, e202117750.
- 46 S. Yamada, T. Kaneda, P. Steib, K. Murakami and K. Itami, *Angew. Chem., Int. Ed.*, 2019, **58**, 8341–8345.
- 47 (a) H. Q. Do and O. Daugulis, *J. Am. Chem. Soc.*, 2008, **130**, 1128–1129; (b) X. Zhang, S. Fan, C. Y. He, X. Wan, Q. Q. Min, J. Yang and X. Z. Jiang, *J. Am. Chem. Soc.*, 2010, **132**, 4506–4507; (c) P. Guo, J. M. Joo, S. Rakshit and D. Sames, *J. Am. Chem. Soc.*, 2011, **133**, 16338–16341; (d) O. Rene and K. Fagnou, *Org. Lett.*, 2010, **12**, 2116–2119; (e) C. Z. Wu, C. Y. He, Y. Huang and X. Zhang, *Org. Lett.*, 2013, **15**, 5266–5269.
- 48 Y. Nakao, K. S. Kanyiva and T. Hiyama, *J. Am. Chem. Soc.*, 2008, **130**, 2448–2449.
- 49 J.-F. Li, D. Pan, H.-R. Wang, T. Zhang, Y. Li, G. Huang and M. Ye, *J. Am. Chem. Soc.*, 2022, **144**, 18810–18816.
- 50 (a) W. B. Zhang, X. T. Yang, J. B. Ma, Z. M. Su and S. L. Shi, *J. Am. Chem. Soc.*, 2019, **141**, 5628–5634; (b) J. B. Ma, X. Zhao, D. Zhang and S. L. Shi, *J. Am. Chem. Soc.*, 2022, **144**(30), 13643–13651.
- 51 N. Hara, N. Uemura and Y. Nakao, *Chem. Commun.*, 2021, **57**, 5957–5960.
- 52 E. Tayama, G. Shimizu and R. Nakao, *Tetrahedron*, 2022, **111**, 132721.
- 53 J. Trouve, P. Zardi, S. Al-Shehimi, T. Roisnel and R. G. Doria, *Angew. Chem., Int. Ed.*, 2021, **60**, 18006–18013.
- 54 M. Ye, G.-L. Gao and J.-Q. Yu, *J. Am. Chem. Soc.*, 2011, **133**, 6964–6967.
- 55 T. Zhang, Y.-X. Luan, N. Y. S. Lam, J.-F. Li, Y. Li, M. Ye and J.-Q. Yu, *Nat. Chem.*, 2021, **13**, 1207–1213.
- 56 I. Choi, Z. Shen, E. Ronge, V. Karius, C. Jooss and L. Ackermann, *Chem. – Eur. J.*, 2021, **27**, 12737–12741.
- 57 A. C. Sun, E. J. McClain, J. W. Beatty and C. R. J. Stephenson, *Org. Lett.*, 2018, **20**, 3487–3490.
- 58 B. Kweon, C. Kim, S. Kim and S. Hong, *Angew. Chem., Int. Ed.*, 2021, **60**, 26813–26821.
- 59 Y. Moon, B. Park, I. Kim, G. Kang, S. Shin, D. Kang, M.-H. Baik and S. Hong, *Nat. Commun.*, 2019, **10**, 4117.
- 60 G. R. mathi, Y. Jeong, Y. Moon and S. Hong, *Angew. Chem., Int. Ed.*, 2020, **59**, 2049–2054.
- 61 K. Lee, S. Lee, N. Kim, S. Kim and S. Hong, *Angew. Chem., Int. Ed.*, 2020, **59**, 13379–13384.
- 62 M. Vellakkaran, T. Kim and S. Hong, *Angew. Chem., Int. Ed.*, 2022, **61**, e202113658.
- 63 A. Motaleb, S. Rani, T. Das, R. G. Gonnade and P. Maity, *Angew. Chem., Int. Ed.*, 2019, **58**, 14104–14109.
- 64 S. Rani, S. R. Dash, A. Bera, M. N. Alam, K. Vanka and P. Maity, *Chem. Sci.*, 2021, **12**, 8996–9003.
- 65 A. Guin, S. Bhattacharjee and A. T. Biju, *Chem. – Eur. J.*, 2021, **27**, 13864–13869.
- 66 D. Wang, L. Desaubry, G. Li, M. Huang and S. Zheng, *Adv. Synth. Catal.*, 2021, **363**, 2–39.
- 67 E. J. Corey and Y. Tian, *Org. Lett.*, 2005, **7**(24), 5535–5537.
- 68 P.-Y. Jiang, K.-F. Fan, S. Li, S.-H. Xiang and B. Tan, *Nat. Commun.*, 2021, 2384.
- 69 E. Anders and F. Markus, *Tetrahedron Lett.*, 1987, **28**, 2675–2676.
- 70 M. C. Hilton, R. D. Dolewski and A. McNally, *J. Am. Chem. Soc.*, 2016, **138**, 13806.
- 71 (a) R. D. Dolewski, M. C. Hilton and A. McNally, *Synlett*, 2018, **29**, 8–14; (b) R. G. Anderson, B. M. Jett and A. McNally, *Tetrahedron*, 2018, **74**, 3129–3136; (c) C. Patel, M. Mohnik, M. C. Hilton and A. McNally, *Org. Lett.*, 2018, **20**, 2607–2610; (d) R. G. Anderson, B. M. Jett and A. McNally, *Angew. Chem., Int. Ed.*, 2018, **57**, 12514; (e) J. N. Levy, J. V. Alegre-Requena, R. Liu, R. S. Paton and

- A. McNally, *J. Am. Chem. Soc.*, 2020, **142**, 11295; (f) R. D. Dolewski, P. J. Fricke and A. McNally, *J. Am. Chem. Soc.*, 2018, **140**, 8020.
- 72 (a) M. C. Hilton, X. Zhang, B. T. Boyle, J. V. Alegre-Requena, R. S. Paton and A. McNally, *Science*, 2018, **362**, 799; (b) B. T. Boyle, M. C. Hilton and A. McNally, *J. Am. Chem. Soc.*, 2019, **141**, 15441; (c) X. Zhang, K. G. Nottingham, C. Patel, J. V. Alegre-Requena, J. N. Levy, R. S. Paton and A. McNally, *Nature*, 2021, **594**, 217.
- 73 J. L. Koniarczyk, D. Hesk, A. Overgard, I. W. Davies and A. McNally, *J. Am. Chem. Soc.*, 2018, **140**, 1990.
- 74 (a) M. Friedrich and G. Manolikakes, *Eur. J. Org. Chem.*, 2022, e202200915; (b) M. Friedrich, L. Schluz, K. Hofman, R. Zangl, N. Morgner, S. Shaaban and G. Manolikakes, *Tetrahedron Chem.*, 2022, **1**, 100003.
- 75 P. S. Fier, *J. Am. Chem. Soc.*, 2017, **139**, 9499–9502.
- 76 P. S. Fier, S. Kim and R. D. Cohen, *J. Am. Chem. Soc.*, 2020, **142**, 8614–8618.
- 77 (a) J. Choi, G. Laudadio, E. Godineau and P. S. Baran, *J. Am. Chem. Soc.*, 2021, **143**, 11927–11933; (b) J. S. Orduna, R. C. Silva, F. Raymenants, B. Reus, J. Thaens, K. T. de Oliveira and T. Noel, *Chem. Sci.*, 2022, **13**, 12527–12532; (c) Z. Zhang, Q. He, X. Zhang and C. Yang, *Org. Biomol. Chem.*, 2022, **20**, 1969–1973.
- 78 (a) C. Lin, D. Li, B. Wang, J. Yao and Y. Zhang, *Org. Lett.*, 2017, **19**, 1970–1973; (b) F. Jia, C. Yin, Y. Zheng, R. Sun, Y.-C. Ge, D. Xu, R. Li, H. Chen, C. Zheng and H. Fu, *J. Org. Chem.*, 2018, **83**, 10389–10397.
- 79 (a) C. Kim, J. Jeong, M. Vellakkaran and S. Hong, *ACS Catal.*, 2022, **12**, 13225–13233; (b) D. Xie, Y. Wang, X. Zhang, Z. Fu and D. Niu, *Angew. Chem., Int. Ed.*, 2022, **61**, e202204922; (c) S. Rieder, C. Melendez, F. Denes, H. Jangra, K. Mulliri, H. Zipse and P. Renaud, *Chem. Sci.*, 2021, **12**, 15362–15373.
- 80 H. Choi, G. R. Mathi, S. Hong and S. Hong, *Nat. Commun.*, 2022, **13**, 1776.
- 81 D. L. Comins, L. S. King, E. D. Smith and F. C. Fevrier, *Org. Lett.*, 2005, **7**, 5059–5062.
- 82 (a) M. Nagase, Y. Kuninobu and M. Kanai, *J. Am. Chem. Soc.*, 2016, **138**, 6103–6106; (b) V. Quint, T. H. V. Nguyen, G. Mathieu, S. Chelli, M. Breugst, J.-F. Lohier, A.-C. Gaumont and S. Lakhdar, *ACS Org. Inorg. Au*, 2023, **3**, 151–157.
- 83 D. Wang, L. Xu, S. Zheng and X. Yang, *Adv. Synth. Catal.*, 2022, **364**, 2720–2728.
- 84 (a) X. Fan, J. Zheng, Z. H. Li and H. Wang, *J. Am. Chem. Soc.*, 2015, **137**, 4916–4919; (b) N. Gandhamsetty, S. Park and S. Chang, *J. Am. Chem. Soc.*, 2015, **137**, 15176–15184; (c) Z.-Y. Liu, Z.-H. Wen and X.-C. Wang, *Angew. Chem., Int. Ed.*, 2017, **56**, 5817–5820; (d) J.-J. Tian, Z.-Y. Yang, X.-S. Liang, N. Liu, C.-Y. Hu, X.-S. Tu, X. Li and X.-C. Wang, *Angew. Chem., Int. Ed.*, 2020, **59**, 18452–18456.
- 85 Z. Liu, J.-H. He, M. Zhang, Z.-J. Shi, H. Tang, X.-Y. Zhou, J.-J. Tian and X.-C. Wang, *J. Am. Chem. Soc.*, 2022, **144**, 4810–4818.
- 86 R. Muta, T. Torigoe and Y. Kuninobu, *Org. Lett.*, 2022, **24**, 8218–8222.
- 87 X.-Y. Zhou, M. Zhang, Z. Liu, J.-H. He and X.-C. Wang, *J. Am. Chem. Soc.*, 2022, **144**, 14463–14470.
- 88 (a) M. Zhang, Q. Zhou, H. Luo, Z.-L. Tang, X. Xu and X.-C. Wang, *Angew. Chem., Int. Ed.*, 2023, **62**, e202216894; (b) Z. Liu, Z.-J. Shi, L. Liu, M.-C. Zhang, H.-Y. Guo and X.-C. Wang, *J. Am. Chem. Soc.*, 2023, **145**, 11789–11797.
- 89 H. Cao, Q. Cheng and A. Studer, *Science*, 2022, **378**, 779–785.
- 90 B. T. Boyle, J. N. Levy, L. de Lescure, R. S. Paton and A. McNally, *Science*, 2022, **378**, 773–779.